Discrete and Continuum Models for Complex Metamaterials

Edited by Francesco dell'Isola
and David Steigmann

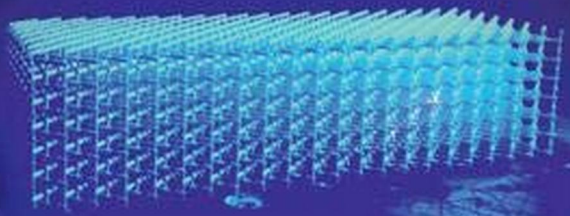

CAMBRIDGE

MRS MATERIALS RESEARCH SOCIETY®
Advancing materials. Improving the quality of life.

Discrete and Continuum Models for Complex Metamaterials

Bringing together contributions on a diverse range of topics, this text explores the relationship between discrete and continuum mechanics as a tool to model new and complex metamaterials. Providing a comprehensive bibliography and historical review of the field, it covers mechanical, acoustic, and pantographic metamaterials, discusses naive model theory and Lagrangian discrete models, and their applications, and presents methods for pantographic structures and variational methods for multidisciplinary modeling and computation. The relationship between discrete and continuous models is discussed from both mathematical and engineering viewpoints, making the text ideal for those interested in the foundation of mechanics and computational applications, and innovative viewpoints on the use of discrete systems to model metamaterials are presented for those who want to go deeper into the field.

An ideal text for graduate students and researchers interested in continuum approaches to the study of modern materials, in mechanical engineering, civil engineering, applied mathematics, physics, and materials science.

Francesco dell'Isola is Professor of Structural Mechanics at the Sapienza University of Rome, and Director of the International Research Centre of Mathematics and Mechanics of Complex Systems (M&MoCS) at the University of L'Aquila.

David J. Steigmann is a professor in the Department of Mechanical Engineering at the University of California, Berkeley.

Discrete and Continuum Models for Complex Metamaterials

Edited by

FRANCESCO DELL'ISOLA

Università degli Studi di Roma, La Sapienza

DAVID J. STEIGMANN

University of California, Berkeley

MRS MATERIALS RESEARCH SOCIETY®
Advancing materials. Improving the quality of life.

CAMBRIDGE
UNIVERSITY PRESS

CAMBRIDGE
UNIVERSITY PRESS

University Printing House, Cambridge CB2 8BS, United Kingdom

One Liberty Plaza, 20th Floor, New York, NY 10006, USA

477 Williamstown Road, Port Melbourne, VIC 3207, Australia

314–321, 3rd Floor, Plot 3, Splendor Forum, Jasola District Centre, New Delhi – 110025, India

79 Anson Road, #06–04/06, Singapore 079906

Cambridge University Press is part of the University of Cambridge.

It furthers the University's mission by disseminating knowledge in the pursuit of education, learning, and research at the highest international levels of excellence.

www.cambridge.org
Information on this title: www.cambridge.org/9781107087736
DOI: 10.1017/9781316104262

First published 2020

Printed in the United Kingdom by TJ International Ltd., Padstow Cornwall

A catalogue record for this publication is available from the British Library.

ISBN 978-1-107-08773-6 Hardback

Contents

List of Contributors

Ugo Andreaus
Department of Structural and Geotechnical Engineering, Sapienza University of Rome.

Emilio Barchiesi
Department of Structural and Geotechnical Engineering, Sapienza University of Rome.
International Research Center M&MoCS, University of L'Aquila.

Francesco dell'Isola
Department of Structural and Geotechnical Engineering, Sapienza University of Rome.
International Research Center M&MoCS, University of L'Aquila.
Department of Civil, Construction-Architectural and Environmental Engineering, University of L'Aquila.

Alessandro Della Corte
International Research Center M&MoCS, University of L'Aquila.
Department of Civil, Construction-Architectural and Environmental Engineering, University of L'Aquila.

Fabio Di Cosmo
International Research Center M&MoCS, University of L'Aquila.
Department of Civil, Construction-Architectural and Environmental Engineering, University of L'Aquila.

Justin Dirrenberger
Process and Engineering in Mechanics and Materials laboratory (PIMM), Ensam, CNRSC, CNAM, Paris.

Corinne Dupuy
Process and Engineering in Mechanics and Materials laboratory (PIMM), Ensam, CNRSC, CNAM, Paris.

Ivan Giorgio
International Research Center M&MoCS, University of L'Aquila.

François Hild
LMT, ENS Paris-Saclay/ CNRS/ University of Paris-Saclay.

Marco Laudato
Department of Information Engineering, Computer Science and Mathematics, University of L'Aquila.

Tomasz Lekszycki
Warsaw University of Technology, Institute of Mechanics and Printing, Department of Construction Engineering and Biomedical Engineering.

Anil Misra
Department of Civil, Environmental and Architectural Engineering, University of Kansas, Lawrence, USA
International Research Center M&MoCS, University of L'Aquila.

Patrice Peyre
Process and Engineering in Mechanics and Materials laboratory (PIMM), Ensam, CNRSC, CNAM, Paris.

Luca Placidi
Faculty of Engineering, International Telematic University Uninettuno, Rome.
International Research Center M&MoCS, University of L'Aquila.

Pierre Seppecher
International Research Center M&MoCS, University of L'Aquila.
Mathematics Institute of Toulon, University of Toulon and Var.

Mario Spagnuolo
International Research Center M&MoCS, University of L'Aquila.
CNRS, LSPM UPR3407, University Paris 13, Sorbonne Paris Cité.

David J. Steigmann
Department of Mechanical Engineering, University of California, Berkeley.

Emilio Turco
Department of Architecture, Design and Urban Planning, Alghero.
International Research Center M&MoCS, University of L'Aquila.

Part I

Designing Complex (Meta)Materials: Results and Perspectives

1 Metamaterials: What Is Out There and What Is about to Come

F. dell'Isola, D. J. Steigmann, A. Della Corte, E. Barchiesi, M. Laudato

1.1 Technology and Science: A Two-way Interaction

Developing[1] *new science produces technological benefits*: this is so often repeated it is a commonplace nowadays. In our opinion the converse statement, i.e. that cutting-edge technology provides substantial stimuli for scientific innovation, has not to be underestimated either. Hence, the interaction between science and technology has not to be regarded as unilateral/one-way. In fact (as summarized in Fig. 1.1), the investigation of theoretical models describing some known phenomena can lead to the development of new *scientifically designed* devices which, in turn, might unveil some not-yet-discovered phenomena. This process of scientific modeling, designing and experimental discoveries could in principle keep going indefinitely. Of note, the process leads to the discovery of progressively "higher order" phenomena, which become accessible only after some necessary "lower order" modeling and discoveries. Apparent examples of very high-order phenomena are easily found in current research (to mention a recent and widely known case) in quantum gravity, concerning the discovery of gravitational waves.

It is a matter of fact that emerging technologies and development of the exact sciences have a close relation. Actually, it is a *leitmotiv* in the History of Science that new technological possibilities lead to new phenomenological evidences, putting in crisis any existing paradigm and gradually leading to a totally new one. The birth of scientific technology in the Hellenistic World, the rise of modern mechanics in the age of Galileo, and the development of thermodynamics in the early nineteenth century are relevant examples of this phenomenon. In all these cases, it is by now well-established among historians of science that a significant conceptual revolution occurred driven by technological reasons. The main goal of these successful new ideas, that nowadays after a long and troublesome process we call *classical physics*, was to design and describe new technology (as for example bombards, steam engines, or catapults). Let us examine in more detail one of the above-mentioned examples: the revolution in the conception of mechanics due to the results of Galileo and his school. Simplifying necessarily a complex matter, we can say that, while within the Peripatetic school (the philosophic tradition based on Aristotle) the motion of objects like the projectiles of bombards does not obey the same laws that govern celestial mechanics. Galileo managed to include phenomena

[1] The present Introduction is based, with large additions and significant updating, on the papers [1, 2].

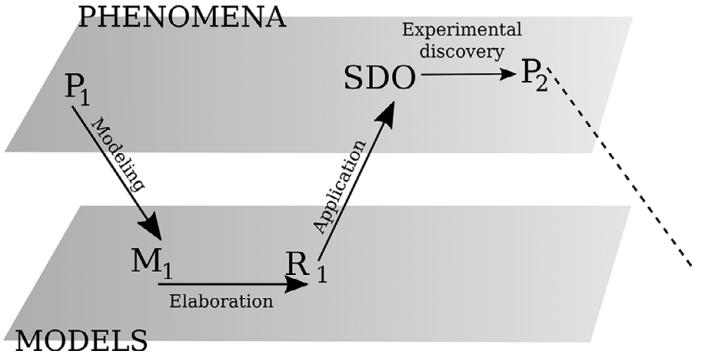

Figure 1.1 A graphical representation of the two-way interaction between science and technology in time. A phenomenon (P_1) appears which is not yet scientifically described; a theoretical model (M_1) is built; theoretical results (R_1) come from the study of (M_1); the application of (R_1) leads to a *Scientifically Designed Object* (SDO); a new phenomenon (P_2) is discovered as a byproduct of (SDO).

which were previously deemed to be completely separate (i.e. those characterising the Celestial World and the Terrestrial World) in the same conceptual framework. Therefore, he established the fundamental uniqueness of Nature regarding its division in Celestial and Terrestrial World, and concerning the latter in natural and man-made objects [3].

In our opinion, the new technological possibilities in controlling the micro- and nano-scale of materials, which are capable of producing objects that, at the macro-level, display properties that are not found (or very rarely found) in nature, are leading mechanics to a similar conceptual revolution. Indeed, these methods often produce objects with peculiar behaviors that cannot be explained by using the classical point of view and therefore new theoretical models have to be developed.

Moreover, due to the technical manufacturing advancements experienced in the last years, we are forced to consider again the whole relation between theoretical (and applied) mechanics and technology. Indeed, thanks to advancement of manufacturing processes it is now possible to design and develop materials, the so-called metamaterials, with properties that cannot be found directly in nature, while for thousand of years these properties have been considered as something which existed but could not be exploited. Several scientific questions which demand an answer are now arising due to the advancement of techniques like electrospinning, self-assembly and 3D printing. We are living today, as in the history of science sometimes happens, in an historical moment in which the scientific modeling is behind the technological advancement. The multi-scale (and multi-physics) description of such materials shows a wide range of exotic behaviors which hides, in their inner organization, a high level of complexity. Therefore, an effort in the development of mechanics and physics of solids and fluids, of computer-aided technology, and of mathematical and numerical modeling is now required. The challenge of design and construction of metamaterials is calling for a stronger theoretical foundation and a pragmatic understanding of what is feasible today.

1.2 The Importance of a Universal Terminology

A common feature of novel research topics and emerging fields is the lack of a general order based on well-established language and concepts. The main problem to which a confused terminology gives rise is the creation of barriers complicating scientific communication between researcher from different topics, which is a serious problem in every branch of modern science. The research on design and manufacturing of metamaterials precisely exemplifies this phenomenon.

We incidentally recall that (modern) scientific biology started with establishing some precise taxonomy criteria (eventually to be updated according to our genetic knowledge) which unequivocally determine the scientific name of each species (once discovered). Although Aristotle (*De Partibus Animalium*) had already started such systematization of biological knowledge, it is only with Linnaeus (*Systema Naturae*, 1758, 10th edition) that taxonomical classification displayed its full descriptive power.

It is generally accepted that every part of hard science (including of course mechanics) should have at least the same level of exactness of biological taxonomy in its terminology. Actually, since hard science deals with a theoretical universe in which there are virtually infinite objects susceptible of meaningful definitions, this requirement is even more strict here than when studying sets of objects which are in principle finite (as biology does).

One of the frontiers of research in mechanics must be situated at the border separating the models introduced for describing "standard materials" and those for "exotic materials." There are many difficulties in recognizing where such a frontier is located, especially because the adjectives "standard" and "exotic" are very difficult to make precise. In what follows, we will consider as "exotic material" a system constituted at micro level by matter distributed in a refined and complex microstructure where, for instance, micro gaps divide different deformable micro parts which in some cases may undergo large localized micro relative displacement. With respect to this definition, a critical reader may even start discussing initially the most fundamental concept of "material" and the difficulties involving in its definition. Indeed, if there is a material at all in such a system one has to find it at the micro level, that is at the level in which the characteristic length is a fraction of the dimensions of the elements of the microstructure. To this reader, another one, even more critical, may object that, by magnifying the image further another microstructure may appear: this microstructure is constituted, for example, by the partially melted and partially agglomerated grains of the polyamide powder which has been used as initial input of the 3D printing process used to produce the considered specimens. These critical remarks, in different contexts and in different situations, have often been repeated to try to understand the ultimate nature of physical phenomena (see e.g. Democritus [4–6]).

Therefore, in an effort to be precise, we shall use the term *homogeneous material* as follows:

We assume that it is possible to choose a length scale L and a corresponding Representative Elementary Volume (REV) (a cubic volume whose sides are L) such that, by moving the REV in the specimen the overall (macro) mechanical response of the material included in it does not change and can be described exclusively in terms of overall (macro) kinematical descriptors which can be assumed to be constant for every REV.

A polyamide, when considering a REV including a group of grains, is a material in the sense of the previous definition. A pantographic sheet (that we will discuss in detail in following sections), when considering a REV including a group of cells is another material, although it consists ultimately, at a lower length scale, of another material, i.e. polyamide. We refrain here from any other philosophical consideration, which may cause us to go back to Heraclitus and Democritus, to discuss Epicureans and Boltzmann, ending with modern Truesdellism (see for more details e.g. [7, 8]).

After having specified what we mean by the concept of material, we observe that also the standard definition of "metamaterial" as given for instance by the statement (reformulating the corresponding entry of Wikipedia as read on 6 Dec. 2017) can be discussed:

> Metamaterials (a combination of the Greek word $\mu\epsilon\tau\acute{\alpha}$, meaning "beyond" and the Latin word *materialis*) are materials engineered to have property that is not found in nature. They are made from assemblies of multiple elements fashioned from materials such as metals or plastics. The constituting materials are *usually [our italic]* arranged in repeating patterns, at scales that are smaller than the wavelengths of the phenomena they influence. Metamaterials derive their property not from the properties of the base materials, but from their newly designed structures.

It is also clearly not fully correct. We are particularly surprised by:

- the occurrence of the adverb *usually*,
- the final statement which seems to underestimate the possibility to design very interesting metamaterials by considering many base materials which can show large differences in physical properties,
- by the obscure use of the expression "in nature."

Indeed, nobody can claim that either iron or stainless steel is a natural material. Humans needed many thousands of years to develop such "artificial" materials. However, nobody designates them "metamaterials." We would like to avoid considering something as "natural" simply because we are accustomed to its use and its existence.

Tentatively we propose here to call *metamaterial*:

> *A material which has been designed to meet a specific purpose, by combining more elementary materials (characterized by a smaller micro length scale) and by shaping them with geometrical structures and mechanical interactions (what we call a* ***microstructure****) characterized by the same micro length scale.*

We will call *micro* the level at which the considered structure shows all its (geometrical and mechanical) inhomogeneity and complexity and call *macro* the level where it behaves as a homogeneous material.

Note (see [9, 10]) that the more interesting cases, i.e. the cases in which the macro metamaterial shows a completely different behavior when compared with the micro behavior, is represented by micro structures in which an extremely marked contrast of mechanical and geometrical properties occurs.

One of the main goals of this introduction is to show how different research fields are addressing, by means of several approaches and maybe not in an obvious way, different

points of view of the same general problem. At the same time, we want to provide a reasonable (of course far from being exhaustive) coverage of the relevant literature.

In the current research in applied mechanics, what we call here metamaterials, according to the previous definition, have been labeled as:

- **Metamaterials** [11–15],
- **Multi-scale Materials** [16–19],
- **Multi-physics Materials** [20–34],
- **Complex Materials** [35–41]
- **Architectured Materials** [42–45, 45–48],
- **Optimized Materials** [49–51],
- **Negative Mechanical Constitutive Coefficients Materials** (Poisson ratio, modulus, stiffness, etc.) [52–56]
- **Smart Materials** [57–61],
- **Advanced Materials** [62–65],
- **Composite Materials** [66–70]).

As for the theoretical aspects, we may find, for example:

- **Generalized Continua** [71–79],
- **Higher Gradient Continua** [80–87],
- **Continua with Microstrains** [88, 89]
- **Cosserat Continua** [90–97],
- **Micro-structured Continua** [98–114],
- **Micropolar Continua** [115–118].

Apart from some cases of almost exact equivalence (the identification of the overlapping between some of the previous fields are studied in some dedicated work, we refer to [4, 74, 119–124]) these labels do not exactly refer to the same scientific content. Rather, what they share are goals and *motivations* behind their origins.

The real challenge, in the opinion of the authors, for both applied and theoretical mechanics can be summarized in the following:

MISSION STATEMENT – to choose the governing equations of a material describing its desired behaviour, and successively to design and produce a complex micro-structure (or a multi-physics system) whose behavior is suitably described by the chosen equations.

This mission statement is the common foundation of all the research lines indicated by the previous labels. This point of view, in our opinion, may provide a useful guide in this spectrum of complicated problems. Indeed, by keeping clear this final aim we do not distract attention from the useful scientific content by focusing on cumbersome technicalities and subtleties. Thus we simplify the transfer of information about tools and methods from different areas of science, providing us with a stronger arsenal for dealing with the challenges.

The authors dare to share the opinion of Richard Toupin (private communication at *4th Canadian Conference on Nonlinear Solid Mechanics*, Montreal, 2012) about the reasons behind the dangerous proliferation of names for the same physical or mathematical

concepts. While referring to a famous quote by Poincaré,[2] Toupin declared that often mechanicians, simply to distinguish themselves among others and in order to have more chances of financial support, rename "clouds" of concepts, collected in existing literature, with new terminology. Of course, Toupin blamed this attitude, considering it detrimental for the advancement of knowledge [2].

1.3 The Relation between Mechanics' Fundamental Hypotheses and Existing Technology

The technologies of every advanced society have been based on mathematical modeling capabilities [125]. The Archimidean mathematical description of engineering artifacts and phenomena characterized the Western civilization. The great technological and economical development of the Age of Enlightenment was based on solid mathematical foundations. However, in this period, and in particular in the following Industrial Revolution, engineering was based on the limiting (but simplifying) assumption that mathematical modeling merely had to be focused on the description of pre-existing materials in order to allow selection of materials in structural design (an introduction to material selection can be found in [126]). Of course, this idea and the hypothesis assumed by the fathers of engineering science as it is known today (Poisson, Navier, Cauchy, Piola, Maxwell, etc.) was based on the observation of (natural) phenomenology, but the whole scientific and technological thought founded on this paradigm became basic doctrine. Indeed, in the mind of engineers and scientists, it was deeply established.

As we have already mentioned, however, "higher order" phenomena, discovered by means of technological innovation, cannot be neglected without limiting our scientific prospects. In fact, several interesting investigations have seen their evolution stopped precisely because of the automatic (and erroneous) distinction between natural phenomena and phenomenological reality *tout-court*, even if the brand-new technology of computer-aided manufacturing has made this distinction completely outdated (see [127]).

To give our reasoning a more concrete character, let us consider a specific example, concerning the concept of external contact action. If we deal with deformation energy depending on the objective part of the first gradient of the displacement field, i.e. if we consider classical Cauchy continua, we are essentially limiting external contact actions only to surface forces. However, complex microstructures may give rise, in their homogenized limit, to models based on higher gradients (see above in the previous section) which are able to describe also other possible external contact actions, such as double forces, line forces, concentrated forces and higher order objects [128]. In other words, since 3D printing, electrospinning, or other kinds of technical possibility allow you to manufacture objects and materials whose microstructures in a continuum limit can sustain higher order forces (for instance, double forces), the theoretical model that we are considering cannot neglect them any more. Therefore, to enrich the set of

[2] "*Mathematics is the art of giving different things the same name*."

behaviors that your theoretical model can describe, you have to reconsider its assumptions. This is what the title of the present section aims to mean: the most appropriate set of assumptions for the theoretical mechanical construction (and in fact, for science in general) has to be determined by the technological possibilities. Therefore, during the formulation of the theoretical model it is not sufficient to consider only purely abstract reasons without including in the picture also the effects of novel technologies – a notable example where the description of unusual response of materials to elastic waves required an appropriate extension of elementary dynamics' concepts can be found in [129].

One of the most recent conceptual revolutions caused by the emergence of new technology happened around 1940 due to the development of the first prototypes of digital computers based on Turing–von Neumann machines. In particular, the possibility to compute solutions to complex partial or ordinary differential equations for the design of large-scale production [130] and for scientific experiments [131] by using digital machines became concrete. Since people working in engineering and science could not wait for the final establishment of the superiority of digital computers, the supporters of analog computing, inspired by the new paradigm, started to synthesize analogous electric circuits described by different mathematical equations. The aforementioned mission statement has several methodological analogies with this example. Indeed also in this case, once the equations governing the desired macroscopic behavior of the material have been chosen, its microstructure (or a complex multi-physics system) has to be synthesized, giving rise to the behavior described by the chosen equations. However, the main difference between the competition between analog and digital computers (that was historically important in the development of computing) and the case of metamaterials is the wider generality of the latter in the relevant applications and systems and which therefore gives rise to demands for a greater effort and sophistication in theoretical tools.

1.4 Three Approaches to Accomplish the Objective

The beginning of material technology can be traced back to non-sapiens hominids. This audacious journey can be summarized in the following basic steps [44]:

1. the on site available materials (e.g. bone, wood, or native metals) were used;
2. the optimization of particular kind of materials (e.g. empirical metallurgy techniques) based on empirical attempts started;
3. the birth of approaches based on science (e.g. scientific metallurgy and later the study of polymers, etc.) occurred;
4. the so-called *hyperchoice of materials*. Here we mean the development of scientific tools and methods in order to select and compare different classes of materials which, individually considered, had already optimized applications in the engineering science;
5. study of the multi-functionality of materials, with increasingly ambitious requirements for materials capable of fulfilling conflicting needs.

Of course, mathematical modeling plays an increasingly important role passing from one step to another and today the available theoretical tools are not enough to fulfill the multi-functionality requirements coming from technical possibilities and industry [42, 132].

In the following subsections we will outline three possible ways to achieve the mission statement.

1.4.1 Trial and Error

In this approach a conjecture on the structure of a system exhibiting a given behavior is based on experience and on physical intuition. The validity of such a conjecture has then to be proved by means of experimental evidence on prototypes. Of course, numerical simulations, in this approach, play a fundamental role in orienting the trial conjectures toward the right one. Among the powerful methods available today, Finite Element Analysis allows us to rapidly get information on the main quantitative properties of complex mechanical systems. Indeed, its flexibility allows an effective description of the complex geometry of systems like metamaterials (recent applications can be found in [133–137], while an historical reference is [138]). Some interesting applications are the modeling of fracture phenomena by using finite elements with particular interfaces (see for instance [139, 140]) and isogeometric analysis (see e.g. [141–147]) performed by introducing elements with high regularity properties.

Another powerful computational tool is the so-called Molecular Dynamics that is particularly feasible to numerically study systems consisting of a huge number of particles. It employs equations of motion of classical mechanics to numerically compute the trajectories of N particles in the phase-space, i.e. the $6N$-dimensional space of positions and momenta (see e.g. [148] for an introduction). Finally, computational methods based on scale-bridging like DDD, QC, CADD, MADD (see [149] for a discussion by means of an example of the comparison of these models and other general problems) which were initially developed to describe small-scale systems in terms of classical physics, can be useful to describe inelastic mechanical systems.

1.4.2 Generalized Continua Models

The previous approach is the most suitable when only a simple refining is needed after the achievement of major advancements. However, this is not the most general scenario and, if we want to achieve technological progress by means of completely new concepts, we may need to consider a drastic change of paradigm by reconsidering a considerable part of engineering science. An effective way to achieve this end may be to re-examine a research line started by Gabrio Piola [150] about the foundation of continuum mechanics. Actually, maybe even in an unconscious way, a revival of the ideas of Piola has already started and one of the most fruitful examples is the field of Peridynamics (for an historical perspectives see [4], while relevant results may be found in [151–155]). Basically, Peridynamics is the modern term for the most general formulation of continuum mechanics initiated by Piola, initially introduced to describe

the mechanics of deformable bodies. It is considered now a very active field also because standard continuum mechanics, which has provided us with very useful conceptual tools, seems to be inadequate for the modern open challenges, at least when macro-modeling is concerned. Indeed, the only way to describe the smaller-scale structure, once a continuum model has been introduced, is by means of numerical analysis which is naturally discrete. In fact, apart from some academic exercises solvable in a (semi-) analytical way, which are not of particular interest for technological application, the only way to obtain useful forecasting of the phenomena occurring in the system is by means of discrete numerical methods. However, the main role of continuum mechanics in this framework is to give rise to numerical code benchmarks. Let us clarify this point by considering the particular example of the synthesis of second gradient metamaterials. It was confronted and solved with homogenization methodologies involving continuous descriptions both at macro and micro level. One has to remark that the need to synthesize a second gradient (meta) material (i.e. to design a suitable microstructure showing second gradient behavior at macro level) was formulated in a purely theoretical context in which even the consistency of mathematical theories was seriously questioned.

This scientific controversy is not modern: already Gabrio Piola [156], when attacked about the soundness of his continuum models and about the true physical content of his theories, resorted to the study of a homogenization problem. Indeed he proved the validity of his macroscopic continuous models by:

i) basing them on the study of a micro structured mechanical system characterized by simply interacting elementary constituents and a well- specified geometry,
ii) describing such a micro system with a Lagrangian discrete finite dimensional model,
iii) finally homogenizing said micro models (via what we can call Piola Ansatz) to get the corresponding macro higher gradient ones (see peridynamics).

The postulation format for higher gradient theories, as understood and formulated by Piola, is not the format chosen by Cauchy and his successors, and it is definitively more complex from a mathematical point of view. This should not surprise anybody: more complicated structures demand more complicated models! On the other hand Cauchy continua became a standard in engineering sciences: their wide range of applicability did allow for great advancements in technology and in the understanding of mechanical phenomena. In a sense engineering sciences became prisoners of the success of such a particular theory, which was erroneously presented as being the most general possible. Clearly, also with the impetus of the need to invent new metamaterials, the paradigm set up by Cauchy seems to need further development, as already demanded by Piola in 1825 even before Cauchy's full formulation of his ideas. Actually there is no reason why one should look for Cauchy metamaterials only.

1.4.3 Dimension Reduction of Discrete Models

One of the most important steps in modeling metamaterials is to represent them by means of a discrete model which is able to describe the relevant phenomenology of the

identified small-scale substructure. Usually this discrete system is useful to understand the conceptual basis of the theoretical description of the system. However, due to its huge number of degrees of freedom, apart from some applications of academic interest made by means of very powerful supercomputers, it is not feasible for application to engineering problems. It is therefore useful to look for another discrete model which is able to capture the most important phenomenological properties of the small-scale structure but defined on a lower dimensional configurations space. In other words, say q_i, $(i = 1, \ldots, N)$, the degrees of freedom of the small-scale structure and Q_h, $(h = 1, \ldots, n \quad \text{with} \quad n << N)$, those of the lower dimensional discrete model, we look for a kinematic map (which in multi-scale modeling is usually called "handshake step") which allows us to determine all the q_i once the Q_h are given (see [157] for some interesting results). Since this procedure depends on the particular problem under consideration, its success depends only on the ability of the modeler to maximize the fidelity of the handshake map. In some particular cases, it is possible to prove in a rigorous mathematical way that when some of the parameters of the small-scale structure vanish in the procedure, the resulting discrete system yields a good approximation. From this point of view, an interesting situation arises when both discrete systems are Lagrangian. Indeed, in this case the reduction map yields the Lagrangian function of the reduced system (which may include also a Hamilton–Rayleigh dissipation potential) and several useful computational tools are available.

1.4.4 An Overview of the Three Approaches

In most cases, scientific progress in terms of the Archimedean–Galilean method requires the synergistic interaction of the aforementioned approaches according to their intrinsic merits. A concrete way to realize this purpose by using the methods briefly described in the previous subsections is to produce 3D printed specimens, like the ones in Fig. 1.2 (for details, see below). The literature about architectured materials ([44, 114, 126, 158]) and the fiber-reinforced composites technology available today may inspire the small-scale structure of the printed prototype. Measures on the mechanical properties of the 3D specimen are useful to test tentative modifications of the parameters. Moreover, it is possible to exploit a multi-physics approach to obtain the desired behavior at macro-scale. For instance, one may consider the possibility of introducing some piezo-electromechanical systems with smaller actuators with respect to the ones considered in [159–161] at the level of the microstructure of the material. However, due to technological limitations, it is not possible to achieve a description with a characteristic length-scale of nanometers with the aforementioned methods (for instance, the fact that by means of electrospinning it is not possible to produce complex fabrics at nano-scale is well known). However, once a suitable theoretical rescaling procedure is available, it could be possible to obtain interesting insights from the nano-scale on the effectiveness of the fabric concept at macro-level (size-related surface effects are discussed in Section 1.8).

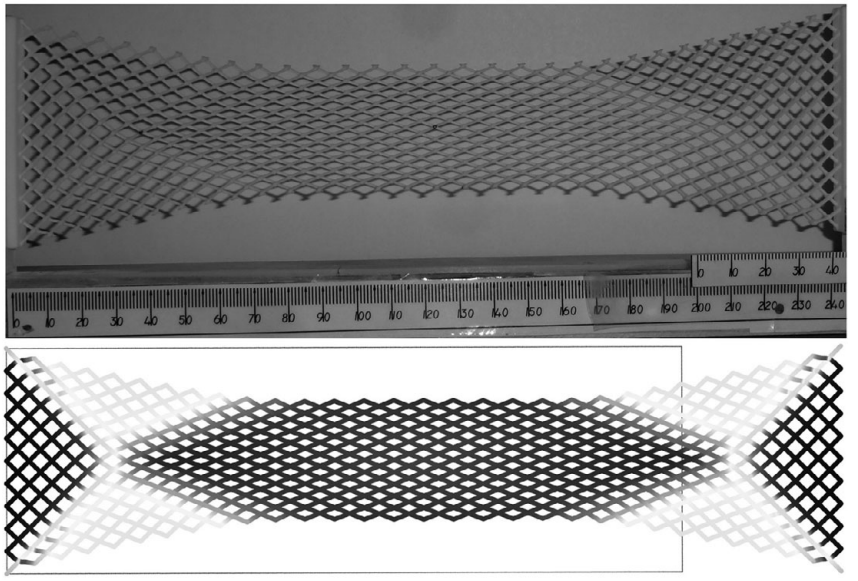

Figure 1.2 Bias test on a 3D printed pantographic sheet (top) and simulation; the curves (straight lines in the reference configuration) are the result of a continuum simulation and therefore they represent a set of materials points.

1.5 Discrete and Continuous: An Attempt at a Twenty-First-Century Methodological Position

Most of the longstanding discussion regarding favoring either the continuous or the discrete approach in the description of reality, and in particular of material behavior, can nowadays be put in perspective, thanks to the power of today's theoretical developments and computation tools.

While at the time of Cauchy and Navier there was still the ambition of capturing all the features of molecular behavior by means of the tools provided by classical physics, it has been clear, since at least a hundred years ago, that this is not possible. Still, continuum models are employed regularly and keep posing challenging problems. Their philosophical meaning, however, has changed, as they represent in most cases "just" a useful simplified reformulation of problems that would find their "full" formulation in terms of Schrödinger equations (or rather Klein–Gordon equations, or rather string dynamics equations, or anything that will deserve a Nobel Prize in Physics in the next years). In other terms, continuum models can be judged as suitable (or not) to describe reality *once a certain phenomenological observation scale has been chosen*.

Keeping this in mind, it should appear clear that the very concepts of "discrete" and "continuous," at least from a phenomenological point of view, have a relative character rather than an absolute one. It is remarkable that this idea is already expressed by Gabrio Piola, in his 1845 work *Intorno alle equazioni fondamentali del movimento di corpi qualsivogliono, considerati secondo la naturale loro forma e costituzione* (see [5]):

Therefore it results that the same quantities which are asserted to be negligible for us without being afraid of going wrong, could be great and not at all negligible quantities for beings which could be, for instance, capable to perceive the proportions which characterized the structure of microorganisms. For those beings those bodies which appear to us to be continuous could appear as bunches of sacks: water, which for us is a true liquid, could appear as for us [appears] millet or a flowing bunch of lead shots. But also for these beings there would exist true fluids, relative to which the same consequences, which we deduce relatively to water, should hold true for them. There are therefore quantities which are null absolutely for all orders of beings, as the analytical elements used in the Integral Calculus, and there are quantities which are null only for beings of a certain order, and these quantities would not be null for other beings, as some elements which are considered in Mechanics.

The point of view expressed here by Piola is intrinsically multi-scale, and fully aware of the possibility of using different scientific models to describe the same elements of reality according to the specific needs and limitations of the selected observation scale. This kind of awareness is very close to much more recent ideas developed in the philosophy of science (Duhem–Quine thesis, see e.g. [162]). This awareness is very important, in the opinion of the authors, especially when dealing with the design of materials aimed at going beyond the behaviors observed in nature, since it avoids the risk of confusing complex phenomena with the models traditionally employed for similar (but simpler) ones.

Finally, in the opinion of the authors there is still another feature that makes continuum models important and will always do so, no matter what level of advancement in computation power is available in the future: their simplicity. To make the point clear, let us imagine that in the future it will be possible to devise a mathematically perfect description of any living being once its genetic code and sufficient information about the surrounding environment are known; let us also suppose that a very powerful computer will be able to compute the model. Knowing the output of the computation will mean knowing everything possible about that living being – say, a lion. Still, it would not be the same as observing it running, or roaring or hunting its prey. As Poincaré once wrote about an elephant, *could you say that a biologist knows it well if he has only observed it at the microscope?* Just like direct observation of the lion and of the elephant, continuum models give us the simplicity of the overall understanding of a scientific model/problem. Since among the ultimate goals of science there is a general progress in the understanding of reality, this feature is by no means of lesser importance. You can refine the mesh as much as you want, but will never get a horizontal tangent in the origin for a piece-wise linear interpolation of a graph of $y = x^2$ centered at zero; however, no one would deny that the parabola "actually has" a horizontal tangent in zero. We do not want to give up the simplicity of this statement (that we can prove in a continuous ideal model) just because our computation tool is intrinsically discrete, and rightly so. Especially in our age of hyper-specialization, the power of simplicity has to be taken strongly into consideration to avoid the fragmentation of science in a multitude of narrow and non-communicating directions (for some more reflections on this point, see [2]).

1.6 Mission Statement: Examples of Possible Implementations

The aforementioned general form of the mission statement can be realized in different ways. One of the crucial challenges is to look for materials with optimized/prescribed constitutive features (e.g. strength, dispersion relations, stiffness toughness, etc.). Furthermore, nowadays several interesting problems can be of interest, in the opinion of the authors:

1. To find a material exhibiting a large ratio between weight and fracture toughness, at least in some directions ([163–172]).
2. To find an adaptive material in which a built-in sensing system can activate some changes in constitutive mechanical parameters; as an example, let us consider a beam endowed with sensors, activated for instance by an electrical signal or by mechanical wave propagation, which can modify its moment of inertia, or different metamaterials aimed to repair bone fracture ([173, 174, 174–187]).
3. To design a material whose microstructure is made of nearly inextensible fibers, whose main feature is to resist elongation and shear by storing deformation energy in fiber bending energy [188].
4. To design a granular microstructured material which aimed to damp mechanical oscillations [189] or a material able to transform, via piezoelectric transduction, mechanical energy into electromagnetic energy ([159, 190–194]).
5. To find a porous deformable material able to control magneto- or electro- wave propagation by enhancing Darcy dissipation by means of the presence of a magnetically or electrically active nematic fluid, ([195–198]).
6. To find a multi-scale material theoretically described by a deformation energy which depends on the nth gradient of a displacement field. A possible way is to consider a beam-like substructure in order to obtain, by means of these structural elements, fabrics which exhibit non-standard dispersion effects, which may also include frequency band gaps.

The provided references are only a partial overview of some tools and potentially useful results which are available in the literature. Moreover, it should be noted also that the (elementary) theory of the beam is still crucial in almost all considered problems. Indeed, the study of metamaterials often pushes the development of suitable generalizations of classical beam models to more complex theories (on generalized beam theory see e.g. [199–202]).

It should also be pointed out that the beam model already possesses an intrinsic scaling, being a 1D model in which the mechanical effects of certain lengths (characterizing the cross-section) are driven by scalar coefficients (stiffnesses). Therefore, any mechanical system employing the beam model as an atomic constituent is intrinsically multi-scale, displaying (at least) either micro-, meso- or macro-scale effects.

1.7 Standard Methods and Related Challenges in Material Designing

The mathematical modeling of new technology, in particular in the case of micro-structured objects, usually follows a procedure consisting of the following steps:

1. To conceive, by means of predictable or already existing manufacturing techniques, a promising and actually realizable microstructure; the main tools in this case are experience, intuition, or the methods of structural optimization [44, 114, 126].
2. To identify, at least in principle, the smallest length scale at which it is possible to introduce a field theory. Such a model, depending on the particular identified length scale of the structure and on the accuracy of the description, can be based both on classical and molecular dynamics. Usually, the main shortcoming of this field theory is that, due to the enormous computational effort required, it cannot be used to make predictions on the system.
3. To overcome this difficulty, an approximate description of the behavior of the considered complex system can be pursued by introducing a discrete meso-scale model. Such a model has to be able to describe the interesting overall behavior of the model on the smallest length-scale introduced in the previous step.
4. To build, by considering a set of simplifying assumptions, an averaged (continuous) macro-model. The main tools are asymptotic expansions, perturbative analyses and appropriate homogenization processes, as for instance was done in [169] for the pantographic structures case (see below for more details); other interesting general results based on perturbative methods can be found in [203–206]).
5. To study by means of numerical methods the continuous model, i.e. to consider a discretization of the model by means of one of the well-established techniques, like finite element methods (FEM), finite difference methods (FDM), isogeometric methods, etc.
6. To compare experimental data with solutions obtained via numerical methods and accordingly refine the model.

Of course, this micro- to macro-scale scheme is far from being the only possible one and other interesting approaches have been developed in the literature (e.g. the so-called scale-bridging scheme, in which a coarser and a finer scale are considered and used to describe the system [207]). Therefore, it is reasonable to question if the aforementioned scheme is universally valid. For instance, a possible conjecture could be that the steps 3–5 may be condensed to avoid introducing the intermediate continuum model.

Let us focus on this point. Nowadays it is possible to produce structures with a high degree of complexity and therefore it is very rare to find (semi-) analytical solutions for the equation of motion of the micro-model (the one discussed in the second step). Indeed, numerical analysis (discussed in the fifth step) has become gradually the only way to make a model that relates to experiments. In engineering science, during the previous two (or more) centuries, the most appropriate description of reality has been realized in terms of continuous models. Currently, however, a novel epistemological picture has emerged, driven by the awareness of the discrete nature of both the used

computational tools and of matter itself. Of course, the use of continuous modeling and of homogenization techniques still plays a fundamental role (recent relevant results can be found in [122, 208–212], some useful general references are [213–215], while on related numerical methods we recommend [216]) but what is changing is the motivation: to save computational time, continuous models are very effective. Indeed, by means of homogenization methods, it is possible to:

1. Capture the main features of the given discrete system [217].
2. Neglect phenomena which are characteristic of a length scale too small to give some contribution to the behavior of the structure as a whole.
3. Select for the system only the characteristics which are interesting for the considered class of applications.

Usually, this procedure leads to simpler equations than those obtained by means of discrete modeling, and often they can be solved by already existing numerical methods. Therefore, the steps

(a) microstructure (discrete) $\longrightarrow$ (b) macrostructure (continuous) $\longrightarrow$(c) numerical formulation (discrete)

can reveal for the considered structure (as discussed in Section 1.8) all the fundamental physical features.

The relationship between classical and more sophisticated mechanical models characterizes in a complementary and complex way the identification of the micro-meso-macro scale, and is crucial to actually understanding both the homogenized models and the meso-scale with respect to the micro-model. Let us clarify this point by discussing it in more detail. As long as we consider a length-scale large enough to neglect quantum effects, it is possible in principle to model the micro-level of a structure by using the usual Cauchy continuum model (see Section 1.8, for a discussion about effects at a classical nanoscale). Of course, as we have already discussed, the main shortcoming of such an approach is the huge computational cost that it requires. Quite often, during the run of a numerical analysis of the micro-model of a complex structure, it happens that even the most advanced computational possibilities of software and hardware available today are overwhelmed, and that even a physical breakdown of a powerful workstation may occur (as has actually happened in the authors' research experience!). A meso-model, instead, dealing with simpler objects (like chords, beams, cylinders, cylinders of Saint-Venant, etc.) replacing Cauchy continua, is usually more convenient from the computational point of view, and therefore can be very useful once it is successfully established on simplifying *right* assumptions, where by right we mean that they do not lead to loss of relevant physical information (that usually is not a trivial task). In this framework, the adaptation/generalization of already existing models is often required (consider for instance [76, 218, 219] in which a suitable nonlinear model for the beam is introduced). The reward for this effort is a computational advantage of several orders of magnitude, reducing weeks of computational times to a few hours or minutes. Even better results can be achieved by correctly choosing the homogenized model for the considered system. Usually in such cases, new and more sophisticated

generalized continuum models are used, in place of trying to adjust already existing models. Finally, we should note that in general it is far from being a trivial task to prove that the chosen micro-model actually converges to the desired homogenized one, and quite often it is difficult even to choose the particular suitable mode of convergence [78, 220].

1.7.1 Perspectives for Generalization and Extension of Available Results

Both finite and infinite dimensional systems can be described in terms of Lagrangian mechanics, which is founded on stationary principles, exemplified by the principle of virtual works. However, if we want to produce predictions by means of an (intrinsically discrete) Turing–von Neumann machine to be compared with experimental evidence, infinite dimensional Lagrangian systems must also be approximated to discrete ones. The search for simplified discrete Lagrangian systems which are able to approximate more complex ones and can be obtained without dealing with homogenized continuous field models is becoming a critical field in research. Although some general results are available in this framework, they have never been considered for studying structural and material mechanics and this may be a new field of application for the advance of discrete mathematics.

An in-depth investigation is needed, from a historical viewpoint, for the reason behind the choice of the fathers of analytical mechanics, like Poisson, Piola, Cauchy, Navier, Boltzmann, and all their successors (despite the fact that they were deeply persuaded by the real discrete nature of matter!), for describing deformable bodies by means of continuous models. A simple answer may be that such a choice was induced by the ingrained habit of seeking analytical solutions by means of classical mathematical analysis methods, or by means of every kind of series expansion developed to produce semi-analytical solutions. However, it cannot be ruled out that these founders, when dealing with the investigation of the global behavior of a structure, had clearly in mind the importance of continuous models. This epistemological point of view may be supported by the standard classification of partial differential equations into hyperbolic, parabolic, and elliptic. Let us for instance consider a possible chaotic and extremely unlikely (so not relevant from the macroscopic point of view) time evolution of a set of masses connected by non-linear springs. By proving that the hyperbolic D'Alembert wave equation governs this system in a small deformations regime, we gain a deep understanding of their total behavior. We expect that the main results of forthcoming researches will be obtained by simply considering the interconnection between elementary structural elements. In particular, it is possible to generalize the results obtained for 1D systems [121] by synthesizing microstructures associated to a continuous model exhibiting wave propagation band-gab frequencies [221], the onset of trapping boundary layers or energy trapping at the microscopic level and consequent enhanced damping [222, 223]. The model for fabrics described in [224] exemplifies such a multi-scale structure, however, concerning static problems only. Some other generalizations of these research lines involve:

1. The introduction, at a smaller scale, of kinetic effects.
2. The generalization to higher dimensional structures (2D (see [122]) and 3D).
3. The study of multiphysics effects, such as those based on the piezoelectric effect, by introducing suitable transducers [225–227].

Newly arisen technological possibilities also require new results in the framework of the study of instabilities. Indeed, it is predictable that, in a complex system, microstructure instabilities can lead to various kinds of "macro" effects, including for instance phase transitions [228, 229] and other kinds of bulk behavior. It is therefore crucial to deeply study and understand the complex instabilities to fully exploit the microstructure's potential. In the literature, it is possible to find in this regard relevant results concerning both specific issues related to the behavior of the microstructure [230–233] and more general aspects [234–247].

1.7.2 Experimental Features

The evolution of mechanics, as already discussed, has been deeply influenced by the emergence of computer-aided manufacturing, in both theoretical and numerical investigations. Among many methodological novelties, it is particularly remarkable that, in computer-aided manufacturing, the same code (or compatible version in different software of the same code) can be employed to produce both a sample and to establish the topology for performing numerical simulations. The methodological consequences of such a feature are very deep and they involve also the epistemological nature of the problem. Indeed, the power of the whole concept of "describing reality by means of a theoretical model" seems to increase as we sidestep the approximate nature of numerical simulations by this model identification between the one realizing the object and the one used for the numerical analysis.

As for the experimental side, some remarks have to be made about the differences between the various computer-aided manufacturing techniques. Indeed, while the technology of 3D printing allows for a high quality control precision (at least of the order of 10^{-2} mm) to produce specific multi-scale fabrics (see for instance [127, 248, 249]), electrospinning technology admits a more limited precision (see for instance [250–254]) but it is able to allow the construction of micro- (and even nano-) structures. Control capability improvement of electrospinning techniques is, in this context, a very important problem. For example, it could be useful to design new devices which are able to exploit the dependence of surface tension on the curvature of the outer interface of the injected filament [255]. Furthermore, another task of great interest that could give rise to new applications among the several that electrospinning has already in several fields (for instance, see [256] for tissue engineering applications), is analysis of the sensitivity to estimate the effect on the global behavior of the considered fabrics of micro- and nano-imperfections. A remarkable example of such applications is the construction of polyurethane biomimetic scaffolds which are able to drive the growth of cell tissues. In particular, in [257] it has been shown how a thin pre-stretched elastic polyurethane

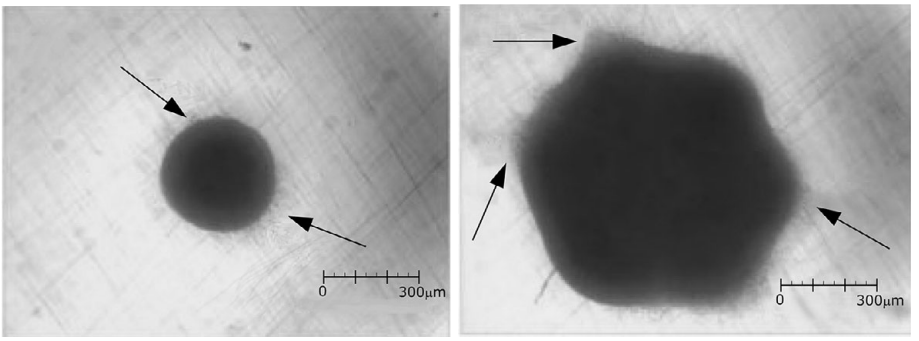

Figure 1.3 An electrospun pre-stretched polyurethane metamaterial is used as a scaffold for tissue growth; left: single spheroid tissue on the electrospun scaffold; right: seven tissue spheroids fused together, on the scaffold. The areas of tissue spreading and attachment-dependent cell are indicated by the arrows; scale-bar 300 μm.

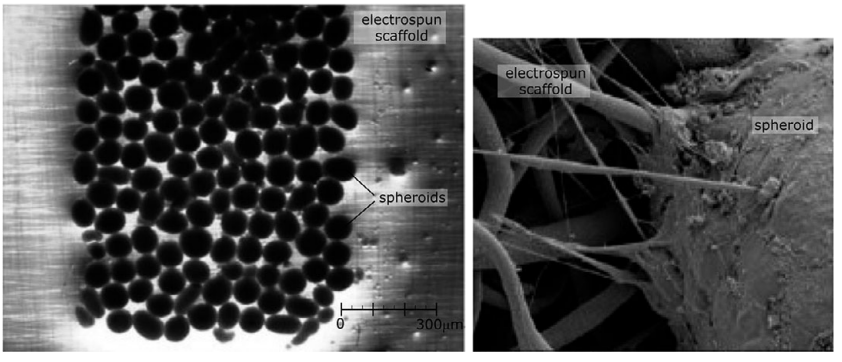

Figure 1.4 Left: tissue spheroids adherent to the electrospun scaffold; right: the adhesion to the electrospun matrix of tissue spheroids tissue is shown by the SEM image.

electrospin scaffold can be exploited as a supporting template to rapidly biofabricate thick tissue-engineered constructs (see Fig. 1.3 and 1.4).

Apart from the technical difficulties that one has to overcome to achieve the desired accuracy degree at nanoscale, deeper problems arise related to size effects of nano-sized objects, which do not appear at macro- and micro-scales. Of course, some of these problems arise due to the intrinsic quantum nature of physical laws which govern phenomena at a small enough length-scale; moreover, other effects that can be fully described even using a classical approach, but which become more and more relevant as the length-scale decreases, also appear well before the need of quantum mechanics. These kind of effects have a crucial importance for the theoretical and experimental study of metamaterials and for the full exploitation of their behaviors. We will provide an overview of them in Section 1.8.

We will end this section by noting that, apart these advanced computer-aided manufacturing procedures and techniques, there are several others that are producing new

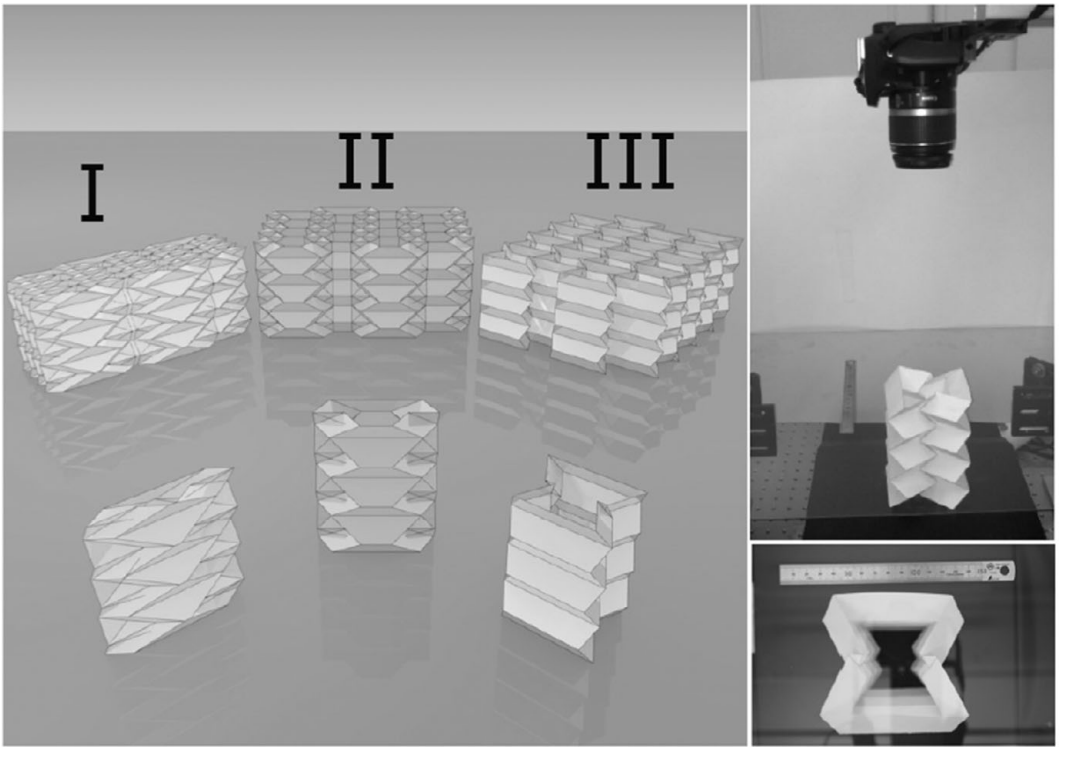

Figure 1.5 Handicraft metamaterial with exotic mechanical properties (negative stiffness, high damping, snap-through, etc.): paper made Tachi-Miura polyhedron realized by means of origami structures. Left: digital image of the prototypes; right: the top of the prototype (original pictures by the authors).

interesting micro-structured materials. Indeed, by means of ordinary industrial procedures and handicraft methods (at least for the realization of prototypes), many interesting metamaterials exhibiting new promising behaviors have been realized. As an example of this, one can consider the one discussed in [258], in which a Tachi-Miura paper polyhedron is studied and realized (see Fig. 1.5).

In particular, the cross-sectional area of the structure was measured by the authors and they have studied the dependence of the mechanical properties of the structure on it. In the right panel of Fig. 1.6 is represented the ratio of the normalized (i.e. divided by the density of torsional stiffness) applied force versus the folding ratio. Under certain dynamical circumstances hysteresis effects can arise, as shown by its loading and unloading behaviors, and can be used to design materials characterized by interesting damping properties. In Fig. 1.6 (left panel), the system is seen to reach three different configurations under the same value of the normalized force with significantly different folding ratio.

An interesting example of handicraft metamaterials is the one studied and realized by Becot and Boutin in [259]. The acoustic properties of a rigid porous medium, saturated

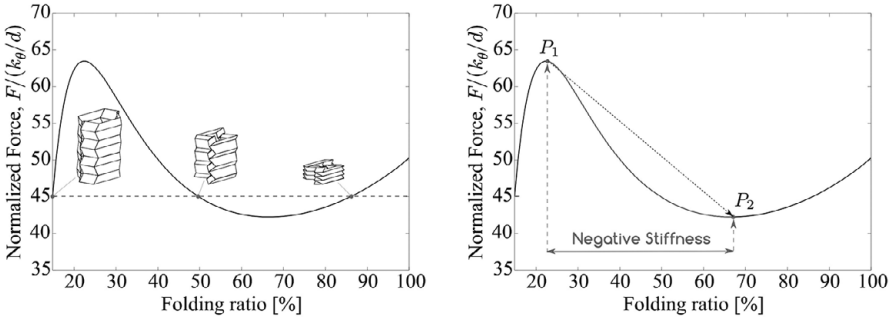

Figure 1.6 Left: The paper Tachi-Miura polyhedron is shown, under the same normalized force, in three different configurations; right: snap-through response and force-folding ratio relationship (original rendering of pictures provided by the authors).

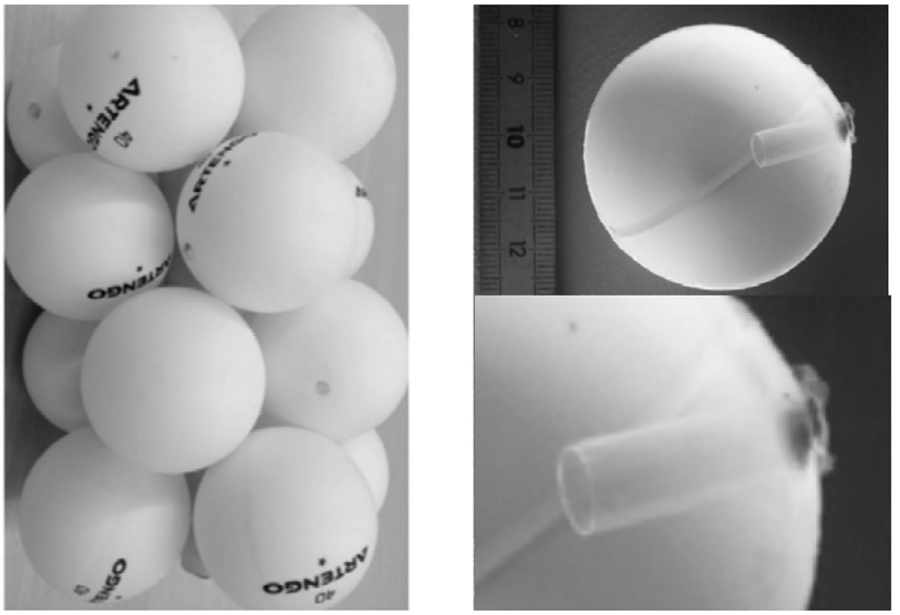

Figure 1.7 Another example of a handicraft metamaterial: hollow plastic spheres (138 mm high) with a central impervious cylinder. These spheres can be both resonators or impervious hollow spheres (for details, see Table 1 in the reference paper). The space between the spheres can be either filled by a granular medium or occupied by air. Left: prototype geometry; upper right: a prototype; lower right: cut of the two kinds of Helmholtz resonators (original pictures by Professor Claude Boutin).

by a gas, with inner resonance effects were investigated by the authors both theoretically and experimentally. They have realized a prototype made by packing in an approximately cubic geometry a set of cut hollow plastic spheres (see Fig. 1.7), and they have experimentally confirmed that the medium effective bulk modulus was modified by the resonators, inducing high attenuation and strong velocity dispersion in the frequency

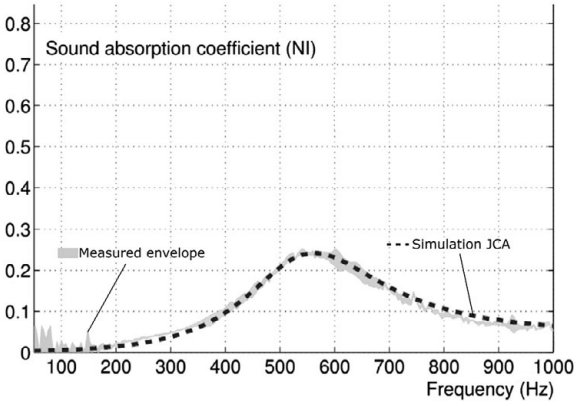

Figure 1.8 For the system represented in Fig. 1.7, sound absorption coefficient at ambient conditions of pressure and temperature is shown. Thick lines represent measurements, while dashed lines represent simulations (original picture by Professor Claude Boutin).

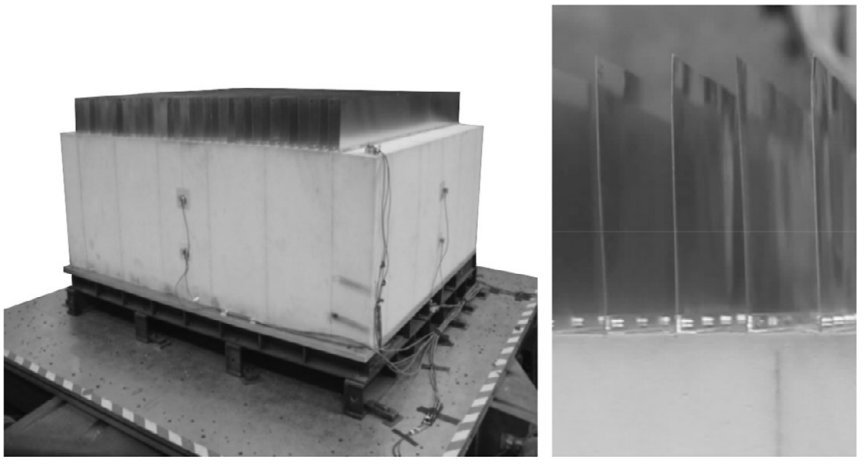

Figure 1.9 Left: Aluminum sheets acting as resonators by means of a shaking table (Bristol Laboratory for Advanced Dynamics Engineering); right: zoom on the sheets (original pictures by Professor Claude Boutin).

range of the theoretical band gaps. At ambient condition of pressure and temperature of the sphere packing shown in Fig. 1.7, the coefficient of sound absorption is shown in Fig. 1.8. Simulations are represented by the dashed line and measurement by the thick one. An analogous investigation is reported in [260] (for similar researches see also [261–264]) concerning an analysis of the bulk modulus effects of microstructure resonance with respect to resonators made of aluminum sheets on a shaking table (see Fig. 1.9). In Fig. 1.10 is shown the effect of the addition of 1 and 37 sheets on resonance. This research line is only one example of the big efforts that researchers are applying to so-called locally resonant mechanical metamamaterial frameworks (see for instance [265, 266]).

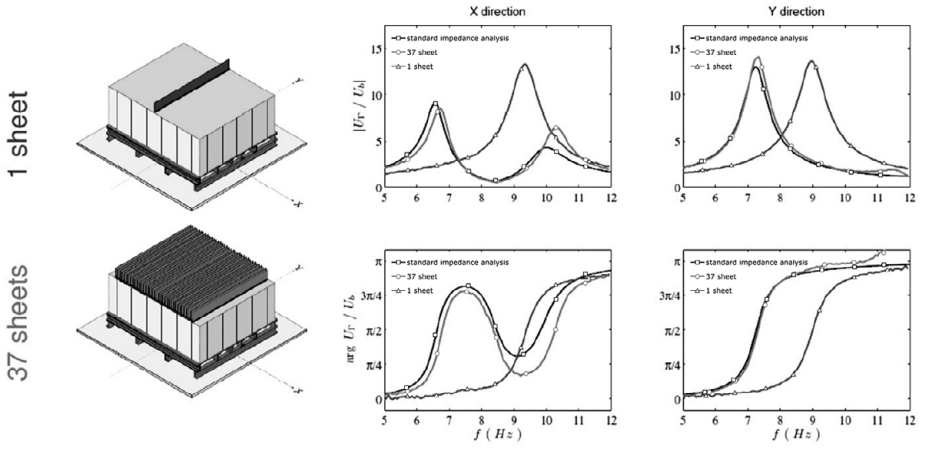

Figure 1.10 Changes in spectrum surface/table for the system shown in Fig. 1.9. Triangular dots, 1 resonator: very close to the usual layer's resonance; circular dots, 37 resonators: layer's resonance in x resonant direction drastically changes while in y inert direction the usual resonance peak appears; square dots: standard impedance analysis; U_b and U_Γ are respectively the displacement to the base of the sample and of the material points belonging to the upper surface (original picture by Professor Claude Boutin).

1.8 Surface-Related Effects in Micro- and Nano-structured Materials

Surface- and interface-related effects in the microstructure can have significant effects on the behavior of a mechanical system (see for instance [267, 268]). For this topic, a comprehensive and general theoretical framework is still lacking and researchers from different fields are making big efforts in order to develop one, or at least to make the puzzle clearer. In what follows, we will briefly discuss what is already known and which open problems have to be still understood.

The main idea is that size-related behaviors strongly depend on the presence of surface effects in the complex micro- or nano-structures. It is possible to find several examples in the literature of new complex-microstructured materials which are able to exploit surface-related effects and their consequences, and this rapid development of micro- and nano-technology is applying a strong impetus for new theoretical developments. It is possible to made a distinction between "intrinsic" and "extrinsic" size effects (see for instance [269]), i.e. between the dependence of the bulk properties on the micro- and nano-structure or on the size of a sample, respectively. Interesting examples can be found in [270, 271] and [272–276], respectively.

Let us start by considering the geometry of surfaces in the simplest case, i.e. "perfect" surfaces. Differential geometry is the main tool able to describe them, and one then has to take care in considering the special physical properties of the system (for instance, the ZnO nanotubes and nanocrystals studied in [277] and shown in Fig. 1.11).

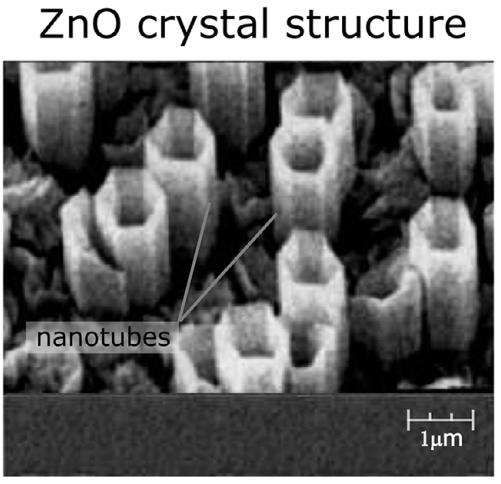

Figure 1.11 ZnO crystal and ZnO nanotubes.

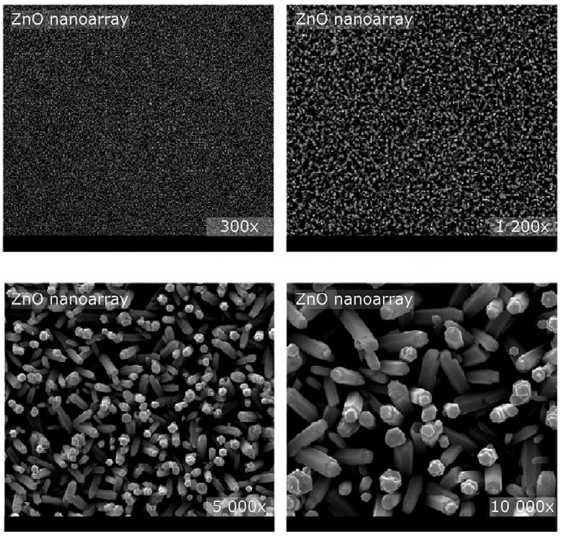

Figure 1.12 ZnO nanoarray (respectively 300x, 1200x, 5000x and 10000x from top left to bottom right).

Of course, a perfect surface is just a particular case. Indeed, geometries showing large irregularities appear in several cases, even if the microstructure is formed by nanocrystals or nanotubes, because, as shown in Fig. 1.12 (see [278]), they may admit quite complicated and non-uniform spatial configurations. This kind of material has several applications and can be exploited to produce the elementary building blocks of micro- and nano-electromechanical systems, like actuators or sensors (see e.g. [278–284]). A detailed mathematical description of this kind of surface is completely pointless, and it is preferable to aim instead to develop a suitable averaged model and,

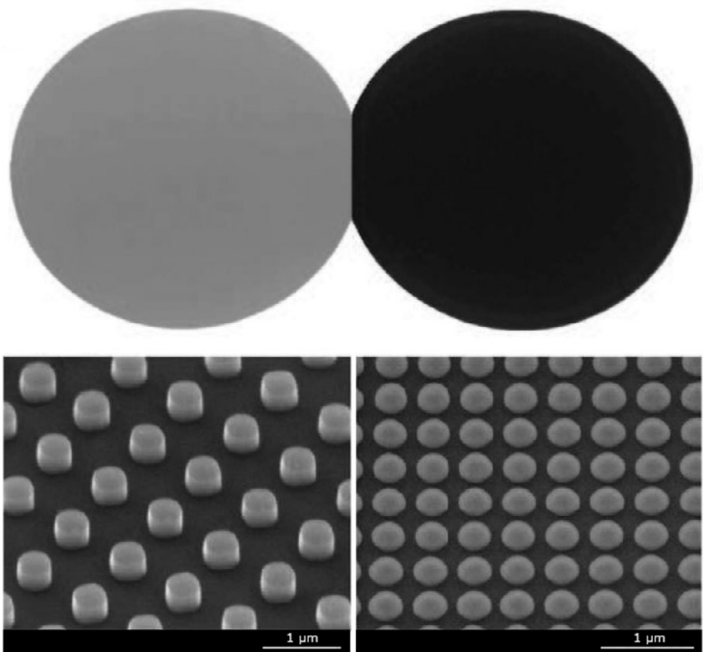

Figure 1.13 Black silicon for solar cells.

in the authors' opinion, this research direction could lead to promising results. An interesting research line in the same spirit is the theory of layered shells and plates developed in [285] and which has interesting applications to photovoltaic technology. Another example is the so-called black silicon, which has important applications to development of energetically efficient solar cells (see Fig. 1.13 and [284]). Other examples of specific properties obtained by exploiting highly irregular surfaces are provided by bactericide and self-cleaning coatings [286–293]).

A still active research field is the study of the concept, introduced by Gibbs [294], of surface tension for solids (in [295, 296] and in the works there cited is coverage of recent literature). A non-linear elastic solid which is able to take the surface tension into account by means of a pre-stressed membrane on the surface was studied by Murdoch and Gurtin in [297, 298]. This model is able to describe differences in mechanical properties related to the size (see e.g. [299]), and has therefore applications in micro- and nano-mechanics [300–302]. The success of this model is measured by considering the several proposed generalizations which are able to take into account thermoelasticity or fracture or also the external membrane bending stiffness [303–308]. Providing solutions to IVPs (initial value problems) and BVPs (boundary value problems) which are met in surface elasticity is of course very useful in this framework; related results are provided in [309–312]. An interesting general result is that the presence of surface stresses leads, in linear surface elasticity, to a stiffening of the material (see for instance [311, 313–317]). This theoretical result allows us to understand that surface reinforcements, in

fracture mechanics, can influence the behavior of solutions near singularities like holes and cracks (see for example [307, 308]).

We conclude this section about surface stresses and effects by listing other recently developed related topics that it is possible to find in the literature:

1. in the Gurtin–Murdoch model framework, finite deformations of elastic solids are studied in [318–321];
2. studies of bodies with surface stresses based on finite element methods can be found in [322–324];
3. investigations on surface energy written in terms of bulk energy excess are provided in [325];
4. studies on how free vibrations of materials influence surface stresses can be found in [326–330];
5. a study of linear elasticity of BVPs with surface stresses is discussed in [309–312, 331];
6. atomistic simulations and other *ab initio* methods are covered in [332–335];
7. higher gradient continuum models including surface stresses are discussed in [295, 336–339].

1.9 An Example: Pantographic Structures

In this section, as an example, we will briefly discuss 3D printed pantographic structures, that can be considered as a model case of the approaches proposed in Section 1.4 to study a structure. A pantographic sheet is a structure consisting of long fibers set in parallel arrays, orthogonal to each other. By means of internal pivots, fibers of different arrays are connected (see Fig. 1.2). These fibers are modeled, depending on the particular application under study, as Euler or Timoshenko beams, or by even more general models [167, 340]). Although this system may appear to have a simple geometry and mechanics of its microstructure, it is nevertheless able to exhibit a very rich and exotic macroscopic behavior that poses difficult challenges to describe its theoretical characterization. The main reasons are primarily: i) inextensibility has to be taken into account; ii) there are macroscopic configurations, the so-called floppy-modes, not associated with any strain energy; iii) due to the four different length scales which characterize its microstructure (namely the fiber diameters, the fiber spacing, the closest pivots distance, and the pivots size) it has clearly a multi-scale nature that has to be considered in the theoretical model.

Pantographic sheets are a perfect example of the synthesis problem of second gradient materials (see the final discussion in Section 1.4.2) using architectured microstructures. One must remark that the problem was solved with a double scale homogenization process (see [83, 224]). Indeed in the cited papers one first considers "slender" continua then obtains, after homogenization, some beam elements and subsequently interconnects such beams with ideal pivots and performs a second homogenization. Already, in the particular synthesis process just cited, ideal pivots seem to represent a kind of preferred constraints in the chosen class of beams, micro lattices, which

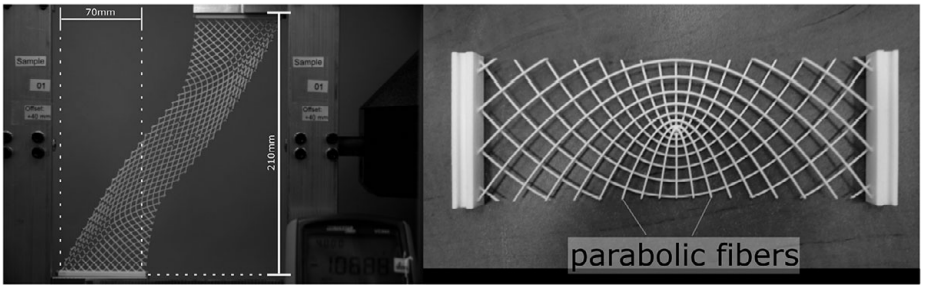

Figure 1.14 Left: shear test with a hard device on a polyamide 3D printed pantographic sheet. Right: a sample with parabolic fibers.

appear to be essential to produce second gradient macro continua. In is noteworthy that the obtained homogenized macro equations (see [341, 342]) actually show some pathologies which reflect the exotic behavior of the considered meta materials. These mathematical pathologies are of interest by themselves (see the detailed discussion again in [342]) as the theoretical issues that they raise represent an intellectual challenge and also a means for revealing potentially interesting new phenomena. One can see therefore that the construction and the study of pantographic sheets with perfect pivots were driven by the need to verify the consequences of some theoretical considerations involving continuum models, their mutual relationships, the logical consistency of their formulation and their physical meaning.

One of the most interesting features of pantographic structures is that they show a very favorable strength/weight ratio, and there are experimental proofs of their particularly safe behavior in fracture [343]. Indeed, such structures have been shown to firmly sustain load long after the beginning of a rupture: the stored elastic deformation energy is comparable to that accumulated by the fibers from the end of the elastic regime to the final failure (a shear experimental test is shown in Fig. 1.14, left panel). This particular feature suggests promising applications in the aerospace and aeronautical industries (for numerical investigations see [344, 345], for micro-macro identification see [346] and for experimental results see [347]). The structure can be generalized to curved fibers (see [348] for some numerical results), which can allow us to exploit different promising mechanical effects, such as an arch-like response to traction (a 3D printed sample is shown in Fig. 1.14, right panel).

For health-monitoring purposes, flexible bio-inspired electronics were recently developed, for instance by Nanshu Lu and collaborators (see for example [349]), and can be considered as a possible ambitious application of pantographic structures. Indeed, a generalization of pantographic structures has been proposed (see Fig. 1.15) which is able to mechanically conform to skin tissue, in the sense that if the epidermis deforms, the electronic systems remain congruent to it (for coverage of the results in this topic, see [350–356]). This kind of mechanical behavior can be exploited also with other soft-tissue biomimetic applications (for the employment for vascular prosthesis of similarly architectured materials see Fig. 1.16). A deeper understanding of the mechanics of these

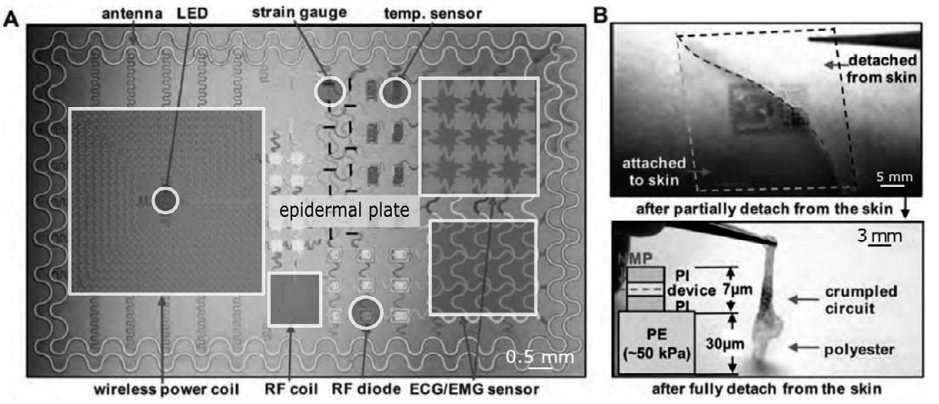

Figure 1.15 Epidermal flexible plate.

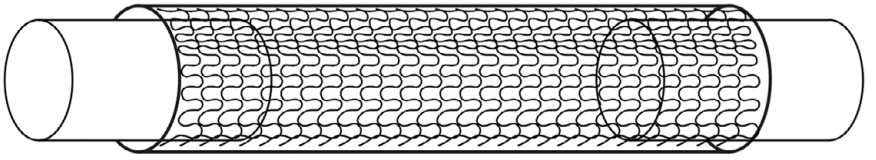

Figure 1.16 Scheme of an architectured material employed for a vascular implant inserted in a silicone elastomer and made of NiTi knitted fabric.

kinds of structures, together with a deeper knowledge of the skin mechanophysiology, is crucial and will lead to other ways to exploit the potential of pantographic structures.

1.10 Final Thoughts before Moving On

The present scientific understanding of Nature can be considered as the most detailed and the deepest ever attained by humankind. The production of unexpected and wonderful mechanisms, tools, devices, and solutions to the problems for which people have been seeking since the dawn of humankind is pushing modern technology toward tumultuous growth. From the historical point of view, this is quite similar to what happened during the Renaissance era, when scientists, by exploiting technological transfer, innovation, and scientific knowledge (also due to a general rediscovery of Western science, in particular Hellenistic and Italian, see again [125]), were increasingly able to shape modern human society, and ultimately the quality of life.

Following this historical comparison, it is therefore reasonable even nowadays to recognize the stream of innovation and the methodological considerations which animated all Renaissance men, Galileo Galilei being first among them. We can read in Galileo's *Il Saggiatore* ([357], p.232):

La filosofia è scritta in questo grandissimo libro che continuamente ci sta aperto innanzi a gli occhi (io dico l'universo) ma non si può intendere se prima non s'impara a intender la lingua,

e conoscer i caratteri, ne' quali è scritto. Egli è scritto in lingua matematica, e i caratteri son triangoli, cerchi ed altre figura geometriche, senza i quali mezzi è impossibile a intenderne umanamente parola; senza questi è un aggirarsi vanamente per un oscuro laberinto.

Which was translated by Stillman Drake (in [3]) as:

Philosophy is written in this grand book, the universe, which stands continually open to our gaze. But the book cannot be understood unless one first learns to comprehend the language and read the letters in which it is composed. It is written in the language of mathematics, and its characters are triangles, circles, and other geometric figures without which it is humanly impossible to understand a single word of it; without these, one wanders about in a dark labyrinth.[3]

These words should not lead the reader to believe that Galilei is part of the "Platonistic" philosophical vision, at least in the way in which people nowadays interpret it. For Galilei (and ourselves), mathematics is not a reality outside our mind: in his words, "Philosophy" is written in a mathematical language and the only way to understand the universe is by means of a philosophy which exploits the tools and the scientific logical-deductive methods given to us by mathematics. Any investigation in engineering science, aimed to exploit a phenomenon for developing its applications, has to be founded on a preparatory deep understanding of the nature of this phenomenon. Therefore, in engineering mathematical formulation of predictive models has to play an essential role. Moreover, the lucid observer can discover that mathematical knowledge has shaped (and is shaping nowadays) our environment, our "ecological niche," and our world by means of the technology and the engineering applications which mathematics ultimately makes possible. The world is not written in mathematical terms: mathematical symbols are the fundamental tools which our mind exploits to shape the world, to control and predict its phenomena, and to design the artifacts which surround us. From this point of view, it is natural that human minds are able to recognize the mathematics behind the artifacts. Let us clarify our point by means of an example: Navier's project to design a suspension bridge, starting from mathematical modeling, failed due to the poor knowledge of the mechanical behavior of foundations which people had at that time (in any case, this attempt pushed the subsequent development of geotechnics). However, the mathematical approach by Navier to the study of this project led to the techniques used to cross large distances, without intermediate pillars, changing forever our highways, railways, and cities (see for instance [358], and [359]). Similarly, a highly mathematically based study on tube-frame structural systems allowed Fazlur Rahman Khan, among others, to project and to realize the twin towers and, after that, many other skyscrapers were built following these lines. Furthermore, the role played by failure in mathematical problems is as important as success in developing our technology. As an instance, among many possible structures, the Warren truss was mainly chosen due to the fact that it has concentrated loads on the nodes, modeled as ideal hinges. This feature was able to make the problem solvable, heavily cutting computational costs at a time when computers were not readily available; today this is the main reason why, even

[3] It is unfortunate, in the opinion of the authors, that a complete translation into English of the whole works of Galileo is not easily found.

if our software is generally able to solve computational problems involving distributed bending loads, this kind of structure is so often employed.

The main take-home point of this Introduction is that mathematical modeling is now able to shape "exotic" novel fabric materials. Their physical behavior is chosen a priori by mathematical equations which, in turn, will determine the structure of the fabric material. The only limit in the conception and design process is the amount of mathematical knowledge which we are able to handle. The limits of mechanical and mathematical theories and models nowadays, exactly like the lack of knowledge in the previous example of Navier's bridge, are at risk of holding back the development of our technological capabilities, by imposing in particular restrictions on the materials which can be exploited in any engineering application. Only the development of more powerful mechanical, numerical, and mathematical methods will allow us to develop materials with better features and to improve their capacity to sustain electrical, thermal, or mechanical external actions. In this sense, one of the most useful and practical tools available in engineering is certainly mathematics. Finally, it has to be remarked that, in order to inform and validate any of the developed models and theories, new experimental techniques are nowadays needed in the field of novel engineered materials.

The authors of this book hope that it will give an effective overview of what has already been achieved and what has still to be investigated in the vast field of complex mechanical metamaterials design, prototyping, and modeling. It has therefore been unavoidable, in order to reach such objectives, to provide the reader with extensive literature lists throughout the book.

Bibliography

[1] Francesco dell'Isola, David Steigmann, and Alessandro Della Corte. Synthesis of fibrous complex structures: Designing microstructure to deliver targeted macroscale response. *Applied Mechanics Reviews*, 67(6):21 pages, 2016.

[2] Francesco dell'Isola, Sara Bucci, and Antonio Battista. Against the fragmentation of knowledge: The power of multidisciplinary research for the design of metamaterials. In *Advanced Methods of Continuum Mechanics for Materials and Structures*, pages 523–545. Springer, 2016.

[3] Stillman Drake. *Discoveries and Opinions of Galileo*. Doubleday New York, 1957.

[4] Francesco dell'Isola, Ugo Andreaus, and Luca Placidi. At the origins and in the vanguard of peridynamics, non-local and higher-gradient continuum mechanics: An underestimated and still topical contribution of Gabrio Piola. *Mathematics and Mechanics of Solids*, page 1081286513509811, 2014.

[5] Francesco dell'Isola, Giulio Maier, Umberto Perego, Ugo Andreaus, Raffaele Esposito, and Samuel Forest. *The Complete Works of Gabrio Piola: Volume I*. Cham, Switzerland: Springer, 2014.

[6] Richard P Feynman, Robert B Leighton, and Matthew Sands. *The Feynman Lectures on Physics Including Feynman's Tips on Physics: The Definitive and Extended Edition*. Addison-Wesley, 2005.

[7] Simon R Eugster *et al.* Exegesis of the introduction and Sect. i from "Fundamentals of the mechanics of continua" by E. Hellinger. *ZAMM-Journal of Applied Mathematics and Mechanics/Zeitschrift für Angewandte Mathematik und Mechanik*, 97(4):477–506, 2017.

[8] Simon R Eugster *et al.* Exegesis of Sect. ii and iii. a from "Fundamentals of the mechanics of continua" by E. Hellinger. *ZAMM-Journal of Applied Mathematics and Mechanics/Zeitschrift für Angewandte Mathematik und Mechanik*, 98(1):31–68, 2018.

[9] Catherine Pideri and Pierre Seppecher. A second gradient material resulting from the homogenization of an heterogeneous linear elastic medium. *Continuum Mechanics and Thermodynamics*, 9(5):241–257, 1997.

[10] F dell'Isola, P Seppecher, and A Della Corte. The postulations á la d'Alembert and á la Cauchy for higher gradient continuum theories are equivalent: A review of existing results. *Proc. R. Soc. A*, 471(2183):20150415, 2015.

[11] Nikolay I Zheludev. The road ahead for metamaterials. *Science*, 328(5978):582–583, 2010.

[12] Jaehyung Ju, Joshua D Summers, John Ziegert, and George Fadel. Design of honeycomb meta-materials for high shear flexure. In *Proceedings of the ASME International Design Engineering Technical Conferences, San Diego, CA, Paper No. DETC2009-87730*, pages 805–813, 2009.

[13] Nader Engheta and Richard W Ziolkowski. *Metamaterials: Physics and Engineering Explorations*. John Wiley & Sons, 2006.

[14] D. Del Vescovo and I. Giorgio. Dynamic problems for metamaterials: Review of existing models and ideas for further research. *International Journal of Engineering Science*, 80:153–172, 2014.

[15] Graeme Milton and Pierre Seppecher. A metamaterial having a frequency dependent elasticity tensor and a zero effective mass density. *Physica Status Solidi (B)*, 249(7): 1412–1414, 2012.

[16] Franck Vernerey, Wing Kam Liu, and Brian Moran. Multi-scale micromorphic theory for hierarchical materials. *Journal of the Mechanics and Physics of Solids*, 55(12):2603–2651, 2007.

[17] François Nicot, Félix Darve, and RNVO Group. A multi-scale approach to granular materials. *Mechanics of Materials*, 37(9):980–1006, 2005.

[18] D. P. Bentz. Influence of silica fume on diffusivity in cement-based materials: Ii. Multi-scale modeling of concrete diffusivity. *Cement and Concrete Research*, 30(7):1121–1129, 2000.

[19] Tony Fast, Stephen R Niezgoda, and Surya R Kalidindi. A new framework for computationally efficient structure–structure evolution linkages to facilitate high-fidelity scale bridging in multi-scale materials models. *Acta Materialia*, 59(2):699–707, 2011.

[20] Su Hao, Brian Moran, Wing Kam Liu, and Gregory B Olson. A hierarchical multi-physics model for design of high toughness steels. *Journal of Computer-Aided Materials Design*, 10(2):99–142, 2003.

[21] René de Borst. Challenges in computational materials science: Multiple scales, multi-physics and evolving discontinuities. *Computational Materials Science*, 43(1):1–15, 2008.

[22] Robert Hamilton, Donald MacKenzie, and Hongjun Li. Multi-physics simulation of friction stir welding process. *Engineering Computations*, 27(8):967–985, 2010.

[23] V. A. Eremeyev and Wojciech Pietraszkiewicz. Phase transitions in thermoelastic and thermoviscoelastic shells. *Archives of Mechanics*, 61(1):41–67, 2009.

[24] V. A. Eremeyev and W. Pietraszkiewicz. Thermomechanics of shells undergoing phase transition. *Journal of the Mechanics and Physics of Solids*, 59(7):1395–1412, 2011.

[25] Wojciech Pietraszkiewicz, Victor Eremeyev, and Violetta Konopińska. Extended non-linear relations of elastic shells undergoing phase transitions. *Zeitschrift für angewandte Mathematik und Mechanik*, 87(2):150–159, 2007.

[26] G Piccardo and G Solari. 3D wind-excited response of slender structures: Closed-form solution. *Journal of Structural Engineering*, 126(8):936–943, 2000.

[27] Giuseppe Piccardo. A methodology for the study of coupled aeroelastic phenomena. *Journal of Wind Engineering and Industrial Aerodynamics*, 48(2):241–252, 1993.

[28] Roberto Guzmán de Villoria, Namiko Yamamoto, Antonio Miravete, and Brian L. Wardle. Multi-physics damage sensing in nano-engineered structural composites. *Nanotechnology*, 22(18):185502, 2011.

[29] S. Alessandroni, U. Andreaus, F. dell'Isola, and M. Porfiri. Piezo-Electromechanical (PEM) Kirchhoff–Love plates. *European Journal of Mechanics-A/Solids*, 23(4):689–702, 2004.

[30] L. Placidi and Hutter K. Thermodynamics of polycrystalline materials treated by the theory of mixtures with continuous diversity. *Continuum Mechanics and Thermodynamics*, 17:409–451, 2006.

[31] U. Andreaus and M. Porfiri. Effect of electrical uncertainties on resonant piezoelectric shunting. *Journal of Intelligent Material Systems and Structures*, 18(5):477–485, 2007.

[32] Dae-Hyeong Kim, Jizhou Song, Won Mook Choi, *et al.* Materials and noncoplanar mesh designs for integrated circuits with linear elastic responses to extreme mechanical deformations. *Proceedings of the National Academy of Sciences*, 105(48):18675–18680, 2008.

[33] Stefan C. B. Mannsfeld, Benjamin C. K. Tee, Randall M. Stoltenberg, *et al.* Highly sensitive flexible pressure sensors with microstructured rubber dielectric layers. *Nature Materials*, 9(10):859–864, 2010.

[34] Corrado Maurini, Joël Pouget, and Francesco dell'Isola. On a model of layered piezoelectric beams including transverse stress effect. *International Journal of Solids and Structures*, 41(16):4473–4502, 2004.

[35] Craig B Arnold, Pere Serra, and Alberto Piqué. Laser direct-write techniques for printing of complex materials. *MRS Bulletin*, 32(01):23–31, 2007.

[36] Yuriy V. Pershin and Massimiliano Di Ventra. Memory effects in complex materials and nanoscale systems. *Advances in Physics*, 60(2):145–227, 2011.

[37] Th. Proffen, S. J. L. Billinge, T. Egami, and D. Louca. Structural analysis of complex materials using the atomic pair distribution function—a practical guide. *Zeitschrift für Kristallographie/International Journal for Structural, Physical, and Chemical Aspects of Crystalline Materials*, 218(2/2003):132–143, 2003.

[38] A. Grillo, S. Federico, and G. Wittum. Growth, mass transfer, and remodeling in fiber-reinforced, multi-constituent materials. *International Journal of Non-Linear Mechanics*, 47(2):388–401, 2012.

[39] A. Grillo, S. Federico, G. Wittum, *et al.* Evolution of a fibre-reinforced growing mixture. *Nuovo Cimento C*, 32C(1):97–119, 2009.

[40] A. Grillo and G. Wittum. Growth and mass transfer in multi-constituent biological materials. *AIP Conference Proceedings*, 1281(1):355–358, 2010.

[41] Hakime Seddik, Ralf Greve, Thomas Zwinger, and L. Placidi. A full Stokes ice flow model for the vicinity of Dome fuji, Antarctica, with induced anisotropy and fabric evolution. *The Cryosphere*, 5(2):495–508, 2011.

[42] N.A. Fleck, V.S. Deshpande, and M.F. Ashby. Micro-architectured materials: Past, present and future. In *Proceedings of the Royal Society of London A: Mathematical, Physical and Engineering Sciences*, 466(2121), 2495–2516. The Royal Society, 2010.

[43] John W.C. Dunlop and Peter Fratzl. Multilevel architectures in natural materials. *Scripta Materialia*, 68(1):8–12, 2013.

[44] Y. Brechet and J.D. Embury. Architectured materials: Expanding materials space. *Scripta Materialia*, 68(1):1–3, 2013.

[45] O. Bouaziz, Y. Brechet, and J.D. Embury. Heterogeneous and architectured materials: A possible strategy for design of structural materials. *Advanced Engineering Materials*, 10(1–2):24–36, 2008.

[46] Pierre Bollen, Nicolas Quiévy, Isabelle Huynen, *et al.* Multifunctional architectured materials for electromagnetic absorption. *Scripta Materialia*, 68(1):50–54, 2013.

[47] Mike Ashby. Designing architectured materials. *Scripta Materialia*, 68(1):4–7, 2013.

[48] M.F. Ashby and Y.J.M. Brechet. Designing hybrid materials. *Acta Materialia*, 51(19):5801–5821, 2003.

[49] Erika Griesshaber, Wolfgang W. Schmahl, Rolf Neuser, *et al.* Crystallographic texture and microstructure of terebratulide brachiopod shell calcite: An optimized materials design with hierarchical architecture. *American Mineralogist*, 92(5-6):722–734, 2007.

[50] Rainer Bruchhaus, Matthias Honal, Ralf Symanczyk, and Michael Kund. Selection of optimized materials for cbram based on ht-xrd and electrical test results. *Journal of The Electrochemical Society*, 156(9):H729–H733, 2009.

[51] O. Vetterl, F. Finger, R. Carius, *et al.* Intrinsic microcrystalline silicon: A new material for photovoltaics. *Solar Energy Materials and Solar Cells*, 62(1):97–108, 2000.

[52] Roderic Lakes. Advances in negative poisson's ratio materials. *Advanced Materials*, 5(4):293–296, 1993.

[53] R.S. Lakes and W.J. Drugan. Dramatically stiffer elastic composite materials due to a negative stiffness phase? *Journal of the Mechanics and Physics of Solids*, 50(5):979–1009, 2002.

[54] T. Jaglinski, D. Kochmann, D. Stone, and R.S. Lakes. Composite materials with viscoelastic stiffness greater than diamond. *Science*, 315(5812):620–622, 2007.

[55] Katia Bertoldi, Pedro M Reis, Stephen Willshaw, and Tom Mullin. Negative poisson's ratio behavior induced by an elastic instability. *Advanced materials*, 2010.

[56] Lia Kashdan, Carolyn Conner Seepersad, Michael Haberman, and Preston S Wilson. Design, fabrication, and evaluation of negative stiffness elements using sls. *Rapid Prototyping Journal*, 18(3):194–200, 2012.

[57] Inpil Kang, Yun Yeo Heung, Jay H Kim, *et al.* Introduction to carbon nanotube and nanofiber smart materials. *Composites Part B: Engineering*, 37(6):382–394, 2006.

[58] Zhong Lin Wang. *Functional and Smart Materials*. Wiley Online Library, 1998.

[59] Victor Giurgiutiu. Review of smart-materials actuation solutions for aeroelastic and vibration control. *Journal of Intelligent Material Systems and Structures*, 11(7):525–544, 2000.

[60] Yujun Song, Weili Wei, and Xiaogang Qu. Colorimetric biosensing using smart materials. *Advanced Materials*, 23(37):4215–4236, 2011.

[61] I. Chopra. Review of state of art of smart structures and integrated systems. *AIAA Journal*, 40(11):2145–2187, 2002.

[62] Chang Liu, Feng Li, Lai-Peng Ma, and Hui-Ming Cheng. Advanced materials for energy storage. *Advanced Materials*, 22(8):E28–E62, 2010.

[63] Frank Caruso. Nanoengineering of particle surfaces. *Advanced Materials*, 13(1):11–22, 2001.

[64] Jonathan N Coleman, Umar Khan, and Yurii K Gun'ko. Mechanical reinforcement of polymers using carbon nanotubes. *Advanced Materials*, 18(6):689–706, 2006.

[65] Paula T. Hammond. Form and function in multilayer assembly: New applications at the nanoscale. *Advanced Materials*, 16(15):1271–1293, 2004.

[66] Graeme W. Milton. *The Theory of Composites (Cambridge Monographs on Applied and Computational Mathematics)*. Cambridge University Press, 2002.

[67] H. Nikopour and A.P.S. Selvadurai. Torsion of a layered composite strip. *Composite Structures*, 95:1–4, 2013.

[68] H. Nikopour and A.P.S. Selvadurai. Concentrated loading of a fibre-reinforced composite plate: Experimental and computational modeling of boundary fixity. *Composites Part B: Engineering*, 60:297–305, 2014.

[69] Luca Placidi and Kolumban Hutter. An anisotropic flow law for incompressible polycrystalline materials. *Zeitschrift für angewandte Mathematik und Physik ZAMP*, 57(1):160–181, 2005.

[70] A.P.S. Selvadurai and H. Nikopour. Transverse elasticity of a unidirectionally reinforced composite with an irregular fibre arrangement: Experiments, theory and computations. *Composite Structures*, 94(6):1973–1981, 2012.

[71] Alexey V. Porubov, Eron L. Aero, and B.R. Andrievsky. Dynamic properties of essentially nonlinear generalized continua. In *Mechanics of Generalized Continua*, pages 161–168. Springer, 2010.

[72] Samuel Forest. Mechanics of generalized continua: Construction by homogenizaton. *Le Journal de Physique IV*, 8(PR4):Pr4–39, 1998.

[73] Gérard A. Maugin and Andrei V. Metrikine. Mechanics of generalized continua. *Advances in Mechanics and Mathematics*, 21, 2010.

[74] Cihan Tekoğlu and Patrick R Onck. Size effects in two-dimensional voronoi foams: A comparison between generalized continua and discrete models. *Journal of the Mechanics and Physics of Solids*, 56(12):3541–3564, 2008.

[75] Samuel Forest and Duy Khanh Trinh. Generalized continua and non-homogeneous boundary conditions in homogenisation methods. *ZAMM*, 91(2):90–109, 2011.

[76] Claude Boutin, Stéphane Hans, and Céline Chesnais. Generalized beams and continua. Dynamics of reticulated structures. In *Mechanics of Generalized Continua*, pages 131–141. Springer, 2010.

[77] Frédéric Feyel. A multilevel finite element method (FE 2) to describe the response of highly non-linear structures using generalized continua. *Computer Methods in Applied Mechanics and Engineering*, 192(28):3233–3244, 2003.

[78] S. Forest. Mechanics of generalized continua: Construction by homogenization. *Le Journal de Physique IV*, 8(PR4):4–39, 1998.

[79] A.E. Green and P.M. Naghdi. A unified procedure for construction of theories of deformable media. ii. Generalized continua. In *Proceedings of the Royal Society of London A: Mathematical, Physical and Engineering Sciences*, 448(1934), 357–377. The Royal Society, 1995.

[80] Yang Yang and Anil Misra. Micromechanics based second gradient continuum theory for shear band modeling in cohesive granular materials following damage elasticity. *International Journal of Solids and Structures*, 49(18):2500–2514, 2012.

[81] Yang Yang, W.Y. Ching, and Anil Misra. Higher-order continuum theory applied to fracture simulation of nanoscale intergranular glassy film. *Journal of Nanomechanics and Micromechanics*, 1(2):60–71, 2011.

[82] P Seppecher. Second-gradient theory: Application to Cahn-Hilliard fluids. In *Continuum Thermomechanics*, pages 379–388. Springer, 2002.

[83] Jean-Jacques Alibert, Pierre Seppecher, and Francesco dell'Isola. Truss modular beams with deformation energy depending on higher displacement gradients. *Mathematics and Mechanics of Solids*, 8(1):51–73, 2003.

[84] Patrizio Neff, Krzysztof Chełmiński, and Hans-Dieter Alber. Notes on strain gradient plasticity: Finite strain covariant modelling and global existence in the infinitesimal rate-independent case. *Mathematical Models and Methods in Applied Sciences*, 19(02):307–346, 2009.

[85] L. Placidi, G. Rosi, I. Giorgio, and A. Madeo. Reflection and transmission of plane waves at surfaces carrying material properties and embedded in second-gradient materials. *Mathematics and Mechanics of Solids*, 19(5):555–578, 2014.

[86] H. Askes, A.S.J. Suiker, and L.J. Sluys. A classification of higher-order strain-gradient models–linear analysis. *Archive of Applied Mechanics*, 72(2-3):171–188, 2002.

[87] A. Rinaldi and L. Placidi. A microscale second gradient approximation of the damage parameter of quasi-brittle heterogeneous lattices. *ZAMM - Zeitschrift für Angewandte Mathematik und Mechanik/Journal of Applied Mathematics and Mechanics*, 2013.

[88] T Leismann and R Mahnken. Comparison of micromorphic, micropolar and microstrain continua. *Book of Abstracts-Extract*, page 58, 2015.

[89] D.G. Kim, J.B. Brunski, and D.P. Nicolella. Microstrain fields for cortical bone in uniaxial tension: optical analysis method. *Proceedings of the Institution of Mechanical Engineers, Part H: Journal of Engineering in Medicine*, 219(2):119–128, 2005.

[90] Maria-Magdalena Iordache and Kaspar Willam. Localized failure analysis in elastoplastic cosserat continua. *Computer Methods in Applied Mechanics and Engineering*, 151(3):559–586, 1998.

[91] Djordje Perić, Jianguo Yu, and D.R.J. Owen. On error estimates and adaptivity in elasto-plastic solids: Applications to the numerical simulation of strain localization in classical and cosserat continua. *International Journal for Numerical Methods in Engineering*, 37(8):1351–1379, 1994.

[92] W. Ehlers, E. Ramm, S. Diebels, and G.A. d'Addetta. From particle ensembles to cosserat continua: Homogenization of contact forces towards stresses and couple stresses. *International Journal of Solids and Structures*, 40(24):6681–6702, 2003.

[93] H. Neuber. On the general solution of linear-elastic problems in isotropic and anisotropic cosserat continua. In *Applied Mechanics*, pages 153–158. Springer, 1966.

[94] Andreas Dietsche and Kaspar Willam. Boundary effects in elasto-plastic cosserat continua. *International Journal of Solids and Structures*, 34(7):877–893, 1997.

[95] D. Ieşan. A theory of thermoviscoelastic composites modelled as interacting cosserat continua. *Journal of Thermal Stresses*, 30(12):1269–1289, 2007.

[96] W. Pietraszkiewicz and V.A. Eremeyev. On vectorially parameterized natural strain measures of the non-linear cosserat continuum. *International Journal of Solids and Structures*, 46(11):2477–2480, 2009.

[97] Johannes Altenbach, Holm Altenbach, and Victor A Eremeyev. On generalized cosserat-type theories of plates and shells: A short review and bibliography. *Archive of Applied Mechanics*, 80(1):73–92, 2010.

[98] A. Cemal Eringen. Theory of micropolar fluids. Technical report, DTIC Document, 1965.

[99] A. Cemal Eringen and E.S. Suhubi. Nonlinear theory of simple micro-elastic solids—I. *International Journal of Engineering Science*, 2(2):189–203, 1964.

[100] A. Cemal Eringen. Theory of micropolar elasticity. In *Microcontinuum Field Theories*, pages 101–248. Springer, 1999.

[101] Roberto Serpieri, Alessandro Della Corte, Francesco Travascio, and Luciano Rosati. Variational theories of two-phase continuum poroelastic mixtures: A short survey. In *Generalized Continua as Models for Classical and Advanced Materials*, pages 377–394. Springer, 2016.

[102] R. D. Mindlin. Micro-structure in linear elasticity. *Archive for Rational Mechanics and Analysis*, 16(1):51–78, 1964.

[103] A. Cemal Eringen. *Microcontinuum Field Theories: I. Foundations and Solids*. Springer Science & Business Media, 2012.

[104] P. Neff, I.-D. Ghiba, A. Madeo, L. Placidi, and G. Rosi. A unifying perspective: The relaxed linear micromorphic continuum. *Continuum Mechanics and Thermodynamics*, pages 1–43, 2013.

[105] Patrizio Neff. On material constants for micromorphic continua. *Trends in Applications of Mathematics to Mechanics, STAMM Proceedings, Seeheim*, pages 337–348, 2004.

[106] A. Misra and V. Singh. Micromechanical model for viscoelastic-materials undergoing damage. *Continuum Mechanics and Thermodynamics*, 25:1–16, 2013.

[107] A. Misra and Y. Yang. Micromechanical model for cohesive materials based upon pseudo-granular structure. *International Journal of Solids and Structures*, 47:2970–2981, 2010.

[108] Paul Germain. The method of virtual power in continuum mechanics. Part 2: Microstructure. *SIAM Journal on Applied Mathematics*, 25(3):556–575, 1973.

[109] Loredana Contrafatto, Massimo Cuomo, and Francesco Fazio. An enriched finite element for crack opening and rebar slip in reinforced concrete members. *International Journal of Fracture*, 178(1-2):33–50, 2012.

[110] D Scerrato, I Giorgio, A Della Corte, A Madeo, and A Limam. A micro-structural model for dissipation phenomena in the concrete. *International Journal for Numerical and Analytical Methods in Geomechanics*, 39(18):2037–2052, 2015.

[111] Daria Scerrato, Ivan Giorgio, Angela Madeo, Ali Limam, and Félix Darve. A simple non-linear model for internal friction in modified concrete. *International Journal of Engineering Science*, 80:136–152, 2014.

[112] Claude Boutin. Microstructural effects in elastic composites. *International Journal of Solids and Structures*, 33(7):1023–1051, 1996.

[113] A. Cemal Eringen. *Mechanics of Micromorphic Continua*. Springer, 1968.

[114] Yves Bréchet. *Microstructures, Mechanical Properties and Processes*. Wiley-Vch, 2000.

[115] P. Steinmann and E. Stein. A unifying treatise of variational principles for two types of micropolar continua. *Acta Mechanica*, 121(1-4):215–232, 1997.

[116] Victor A. Eremeyev and Wojciech Pietraszkiewicz. Material symmetry group and constitutive equations of micropolar anisotropic elastic solids. *Mathematics and Mechanics of Solids*, page doi: 1081286515582862, 2015.

[117] Victor A. Eremeyev and Wojciech Pietraszkiewicz. Material symmetry group of the non-linear polar-elastic continuum. *International Journal of Solids and Structures*, 49(14):1993–2005, 2012.

[118] W. Pietraszkiewicz and V.A. Eremeyev. On natural strain measures of the non-linear micropolar continuum. *International Journal of Solids and Structures*, 46(3):774–787, 2009.

[119] Ralf Jänicke, Stefan Diebels, Hans-Georg Sehlhorst, and Alexander Düster. Two-scale modelling of micromorphic continua. *Continuum Mechanics and Thermodynamics*, 21(4):297–315, 2009.

[120] Samuel Forest and Rainer Sievert. Nonlinear microstrain theories. *International Journal of Solids and Structures*, 43(24):7224–7245, 2006.

[121] Antonio Carcaterra, F dell'Isola, R Esposito, and M Pulvirenti. Macroscopic description of microscopically strongly inhomogenous systems: A mathematical basis for the synthesis of higher gradients metamaterials. *Archive for Rational Mechanics and Analysis*, pages 1–24, 2015.

[122] J. J. Alibert and A. Della Corte. Second-gradient continua as homogenized limit of pantographic microstructured plates: A rigorous proof. *Zeitschrift für angewandte Mathematik und Physik DOI: 10.1007/s00033-015-0526-x*, 2015.

[123] I. Giorgio, L. Galantucci, A. Della Corte, and D. Del Vescovo. Piezo-electromechanical smart materials with distributed arrays of piezoelectric transducers: Current and upcoming applications. *International Journal of Applied Electromagnetics and Mechanics*, 47(4):1051–1084, 2015.

[124] Duy Khanh Trinh, Ralf Janicke, Nicolas Auffray, Stefan Diebels, and Samuel Forest. Evaluation of generalized continuum substitution models for heterogeneous materials. *International Journal for Multiscale Computational Engineering*, 10(6), 2012.

[125] Lucio Russo. The forgotten revolution. How science was born in 300 BC and why it had to be reinvented. *Übersetzung aus dem Italienischen von Silvio Levy*. Springer, Berlin, 2004.

[126] Michael F. Ashby and D. Cebon. Materials selection in mechanical design. *Le Journal de Physique IV*, 3(C7):C7–1, 1993.

[127] C. Elanchezhian and G. Shanmuga Sundar. *Computer Aided Manufacturing*. Firewall Media, 2007.

[128] N. Auffray, Francesco dell'Isola, V.A. Eremeyev, A. Madeo, and Giuseppe Rosi. Analytical continuum mechanics à la Hamilton–Piola least action principle for second gradient continua and capillary fluids. *Mathematics and Mechanics of Solids*, 20(4):375–417, 2015.

[129] Graeme W. Milton and John R. Willis. On modifications of Newton's second law and linear continuum elastodynamics. In *Proceedings of the Royal Society of London A: Mathematical, Physical and Engineering Sciences*, 463(2079), 855–880. The Royal Society, 2007.

[130] Harvey H. Happ and Gabriel Kron. *Gabriel Kron and Systems Theory*. Union College Press, 1973.

[131] Nicholas Metropolis. The beginning of the Monte Carlo method. *Los Alamos Science*, 15(584):125–130, 1987.

[132] Y. Bréchet. *Euromat 99, Microstructures, Mechanical Properties and Processes: Computer Simulation and Modelling*, Volume 3. John Wiley & Sons, 2000.

[133] L Greco and M Cuomo. Consistent tangent operator for an exact Kirchhoff rod model. *Continuum Mechanics and Thermodynamics*, pages 1–17, 2014.

[134] Luigi Carassale and Giuseppe Piccardo. Non-linear discrete models for the stochastic analysis of cables in turbulent wind. *International Journal of Non-Linear Mechanics*, 45(3):219–231, 2010.

[135] Ali Javili and Paul Steinmann. A finite element framework for continua with boundary energies. Part I: The two-dimensional case. *Computer Methods in Applied Mechanics and Engineering*, 198(27):2198–2208, 2009.

[136] A. Javili and P. Steinmann. A finite element framework for continua with boundary energies. Part II: The three-dimensional case. *Computer Methods in Applied Mechanics and Engineering*, 199(9):755–765, 2010.

[137] E. Turco and P. Caracciolo. Elasto-plastic analysis of Kirchhoff plates by high simplicity finite elements. *Computer Methods in Applied Mechanics and Engineering*, 190(5–7):691–706, 2000.

[138] Olgierd Cecil Zienkiewicz, Robert Leroy Taylor, P. Nithiarasu, and J.Z. Zhu. *The Finite Element Method*, volume 3. McGraw-hill London, 1977.

[139] Daniela Ciancio, Ignacio Carol, and Massimo Cuomo. Crack opening conditions at 'corner nodes' in FE analysis with cracking along mesh lines. *Engineering Fracture Mechanics*, 74(13):1963–1982, 2007.

[140] Daniela Ciancio, Ignacio Carol, and Massimo Cuomo. On inter-element forces in the FEM-displacement formulation, and implications for stress recovery. *International Journal for Numerical Methods in Engineering*, 66(3):502–528, 2006.

[141] Thomas J.R. Hughes, John A. Cottrell, and Yuri Bazilevs. Isogeometric analysis: CAD, finite elements, nurbs, exact geometry and mesh refinement. *Computer Methods in Applied Mechanics and Engineering*, 194(39):4135–4195, 2005.

[142] A. Cazzani, M. Malagù, and E. Turco. Isogeometric analysis of plane-curved beams. *Mathematics and Mechanics of Solids*, 2014. DOI: 10.1177/1081286514531265.

[143] L. Greco and M. Cuomo. An implicit G1 multi patch B-spline interpolation for Kirchhoff–Love space rod. *Computer Methods in Applied Mechanics and Engineering*, 269(0):173–197, 2014.

[144] Antonio Cazzani, Marcello Malagù, and Emilio Turco. Isogeometric analysis: A powerful numerical tool for the elastic analysis of historical masonry arches. *Continuum Mechanics and Thermodynamics*, pages 1–18, 2014.

[145] Antonio Cazzani, Marcello Malagù, Emilio Turco, and Flavio Stochino. Constitutive models for strongly curved beams in the frame of isogeometric analysis. *Mathematics and Mechanics of Solids*, page 1081286515577043, 2015.

[146] Massimo Cuomo, Loredana Contrafatto, and Leopoldo Greco. A variational model based on isogeometric interpolation for the analysis of cracked bodies. *International Journal of Engineering Science*, 80:173–188, 2014.

[147] E. De Luycker, D.J. Benson, T. Belytschko, Y. Bazilevs, and M.C. Hsu. X-fem in isogeometric analysis for linear fracture mechanics. *International Journal for Numerical Methods in Engineering*, 87(6):541–565, 2011.

[148] Michael P. Allen. Introduction to molecular dynamics simulation. *Computational Soft Matter: From Synthetic Polymers to Proteins*, 23:1–28, 2004.

[149] J. Tinsley Oden, Serge Prudhomme, Albert Romkes, and Paul T. Bauman. Multiscale modeling of physical phenomena: Adaptive control of models. *SIAM Journal on Scientific Computing*, 28(6):2359–2389, 2006.

[150] Gabrio Piola. *The Complete Works of Gabrio Piola: Commented English Translation*, Volume 38. Springer, 2014.

[151] Stewart A. Silling, M. Epton, O. Weckner, J. Xu, and E. Askari. Peridynamic states and constitutive modeling. *Journal of Elasticity*, 88(2):151–184, 2007.

[152] S.A. Silling and R.B. Lehoucq. Peridynamic theory of solid mechanics. *Advances in Applied Mechanics*, 44(1):73–166, 2010.

[153] E. Askari, F. Bobaru, R.B. Lehoucq, *et al.* Peridynamics for multiscale materials modeling. In *Journal of Physics: Conference Series*, volume 125(1), page 012078. IOP Publishing, 2008.

[154] Stewart A. Silling and Ebrahim Askari. A meshfree method based on the peridynamic model of solid mechanics. *Computers & Structures*, 83(17):1526–1535, 2005.

[155] Michael L. Parks, Richard B. Lehoucq, Steven J. Plimpton, and Stewart A. Silling. Implementing peridynamics within a molecular dynamics code. *Computer Physics Communications*, 179(11):777–783, 2008.

[156] Gabrio Piola. *Sull'applicazione de'principj della meccanica analitica del Lagrange ai principali problemi. Memoria di Gabrio Piola presentata al concorso del premio e coronata dall'IR Istituto di Scienze, ecc. nella solennità del giorno 4 ottobre 1824*. dall'Imp. Regia stamperia, 1825.

[157] Sigrid Leyendecker, Sina Ober-Blöbaum, Jerrold E Marsden, and Michael Ortiz. Discrete mechanics and optimal control for constrained systems. *Optimal Control Applications and Methods*, 31(6):505–528, 2010.

[158] Manuel Ferretti, Angela Madeo, Francesco dell'Isola, and Philippe Boisse. Modeling the onset of shear boundary layers in fibrous composite reinforcements by second-gradient theory. *Zeitschrift für angewandte Mathematik und Physik*, 65(3):587–612, 2014.

[159] Ugo Andreaus, Francesco dell'Isola, and Maurizio Porfiri. Piezoelectric passive distributed controllers for beam flexural vibrations. *Journal of Vibration and Control*, 10(5):625–659, 2004.

[160] Corrado Maurini, Joël Pouget, and Francesco dell'Isola. Extension of the Euler–Bernoulli model of piezoelectric laminates to include 3D effects via a mixed approach. *Computers & Structures*, 84(22):1438–1458, 2006.

[161] Francesco dell'Isola, Corrado Maurini, and Maurizio Porfiri. Passive damping of beam vibrations through distributed electric networks and piezoelectric transducers: Prototype design and experimental validation. *Smart Materials and Structures*, 13(2):299, 2004.

[162] Stathos Psillos. Underdetermination thesis, Duhem-Quine thesis. 2006.

[163] A.C. Pipkin. Plane traction problems for inextensible networks. *The Quarterly Journal of Mechanics and Applied Mathematics*, 34(4):415–429, 1981.

[164] R.S. Rivlin. Plane strain of a net formed by inextensible cords. In *Collected Papers of RS Rivlin*, pages 511–534. Springer, 1997.

[165] M. V. D'Agostino, I. Giorgio, L. Greco, A. Madeo, and P. Boisse. Continuum and discrete models for structures including (quasi-) inextensible elasticae with a view to the design and modeling of composite reinforcements. *International Journal of Solids and Structures*, 59:1–17, 2015.

[166] F. dell'Isola, M.V. D'Agostino, Madeo A., Boisse P., and Steigmann D. Minimization of shear energy in two dimensional continua with two orthogonal families of inextensible fibers: the case of standard bias extension test. *Journal of Elasticity*, 122(2):131–155, 2016.

[167] Francesco dell'Isola, Ivan Giorgio, and Ugo Andreaus. Elastic pantographic 2D lattices: A numerical analysis on static response and wave propagation. *Proceedings of the Estonian Academy of Sciences*, 2015.

[168] B. Descamps. *Computational Design of Lightweight Structures: Form Finding and Optimization*. John Wiley & Sons, 2014.

[169] Francesco dell'Isola, Alessandro Della Corte, Leopoldo Greco, and Angelo Luongo. Plane bias extension test for a continuum with two inextensible families of fibers: A variational treatment with Lagrange multipliers and a perturbation solution. *International Journal of Solids and Structures*, 81:1–12, 2016.

[170] Francesco dell'Isola and David Steigmann. A two-dimensional gradient-elasticity theory for woven fabrics. *Journal of Elasticity*, 118(1):113–125, 2015.

[171] N. Hamila and P. Boisse. Tension locking in finite-element analyses of textile composite reinforcement deformation. *Comptes Rendus Mécanique*, 341(6):508–519, 2013.

[172] N. Hamila and P. Boisse. Locking in simulation of composite reinforcement deformations. analysis and treatment. *Composites Part A: Applied Science and Manufacturing*, 53:109–117, 2013.

[173] U. Andreaus and M. Colloca. Prediction of micromotion initiation of an implanted femur under physiological loads and constraints using the finite element method. *Proc. Inst. Mech. Eng. H*, 223(5):589–605, Jul 2009.

[174] U. Andreaus, M. Colloca, and D. Iacoviello. *Modeling of Trabecular Architecture as Result of an Optimal Control Procedure*, Volume 4 of *Lecture Notes in Computational Vision and Biomechanics*. Springer Netherlands, 2013.

[175] U. Andreaus, M. Colloca, D. Iacoviello, and M. Pignataro. Optimal-tuning PID control of adaptive materials for structural efficiency. *Structural and Multidisciplinary Optimization*, 43(1):43–59, 2011.

[176] U. Andreaus, I. Giorgio, and T. Lekszycki. A 2-D continuum model of a mixture of bone tissue and bio-resorbable material for simulating mass density redistribution under load slowly variable in time. *ZAMM - Zeitschrift für Angewandte Mathematik und Mechanik / Journal of Applied Mathematics and Mechanics*, 94(12):978–1000, 2014.

[177] Jong-Gu Park, Qiang Ye, Elizabeth M. Topp, *et al.* Dynamic mechanical analysis and esterase degradation of dentin adhesives containing a branched methacrylate. *Journal of Biomedical Materials Research Part B: Applied Biomaterials*, 91(1):61–70, 2009.

[178] U. Andreaus, I. Giorgio, and A. Madeo. Modeling of the interaction between bone tissue and resorbable biomaterial as linear elastic materials with voids. *Zeitschrift fur Angewandte Mathematik und Physik*, 66(1):209–237, 2014.

[179] Jean-François Ganghoffer. A contribution to the mechanics and thermodynamics of surface growth. Application to bone external remodeling. *International Journal of Engineering Science*, 50(1):166–191, 2012.

[180] I. Giorgio, U. Andreaus, and A. Madeo. The influence of different loads on the remodeling process of a bone and bio-resorbable material mixture with voids. *Continuum Mechanics and Thermodynamics*, doi: 10.1007/s00161-014-0397-y, 2014.

[181] C.P. Laurent, D. Durville, C. Vaquette, R. Rahouadj, and J.F. Ganghoffer. Computer-aided tissue engineering: Application to the case of anterior cruciate ligament repair. *Biomechanics of Cells and Tissues*, 9:1–44, 2013.

[182] C.P. Laurent, D. Durville, D. Mainard, J-F. Ganghoffer, and R. Rahouadj. Designing a new scaffold for anterior cruciate ligament tissue engineering. *Journal of the Mechanical Behavior of Biomedical Materials*, 12:184–196, 2012.

[183] C.P. Laurent, D. Durville, X. Wang, J-F. Ganghoffer, and R. Rahouadj. Designing a new scaffold for anterior cruciate ligament tissue engineering. *Computer Methods in Biomechanics and Biomedical Engineering*, 13(S1):87–88, 2010.

[184] Anil Misra, Paulette Spencer, Orestes Marangos, Yong Wang, and J Lawrence Katz. Parametric study of the effect of phase anisotropy on the micromechanical behaviour of dentin–adhesive interfaces. *Journal of The Royal Society Interface*, 2(3):145–157, 2005.

[185] Paulette Spencer, Qiang Ye, Jonggu Park, *et al.* Adhesive/dentin interface: The weak link in the composite restoration. *Annals of Biomedical Engineering*, 38(6):1989–2003, 2010.

[186] David J. Steigmann and Francesco dell'Isola. Mechanical response of fabric sheets to three-dimensional bending, twisting, and stretching. *Acta Mechanica Sinica*, DOI:10.1007/s10409-015-0413-x.

[187] Qiang Ye, Paulette Spencer, Yong Wang, and Anil Misra. Relationship of solvent to the photopolymerization process, properties, and structure in model dentin adhesives. *Journal of Biomedical Materials Research Part A*, 80(2):342–350, 2007.

[188] Liangbing Hu, Mauro Pasta, Fabio La Mantia, *et al.* Stretchable, porous, and conductive energy textiles. *Nano Letters*, 10(2):708–714, 2010.

[189] G. Gantzounis, M. Serra-Garcia, K. Homma, J.M. Mendoza, and C. Daraio. Granular metamaterials for vibration mitigation. *Journal of Applied Physics*, 114(9):093514, 2013.

[190] S. Alessandroni, U. Andreaus, F. dell'Isola, and M. Porfiri. A passive electric controller for multimodal vibrations of thin plates. *Computers & Structures*, 83(15):1236–1250, 2005.

[191] T. Bailey and J. E. Ubbard. Distributed piezoelectric-polymer active vibration control of a cantilever beam. *Journal of Guidance, Control, and Dynamics*, 8(5):605–611, 1985.

[192] S. Behrens, A. J. Fleming, and S. O. R. Moheimani. A broadband controller for shunt piezoelectric damping of structural vibration. *Smart Materials and Structures*, 12(1):18, 2003.

[193] L. R. Corr and W. W. Clark. A novel semi-active multi-modal vibration control law for a piezoceramic actuator. *Journal of Vibration and Acoustics*, 125(2):214–222, 2003.

[194] E. K. Dimitriadis, C. R. Fuller, and C. A. Rogers. Piezoelectric actuators for distributed vibration excitation of thin plates. *Journal of Vibration and Acoustics*, 113(1):100–107, 1991.

[195] S. Federico. On the linear elasticity of porous materials. *International Journal of Mechanical Sciences*, 52(2):175–182, 2010.

[196] S. J. Hollister. Porous scaffold design for tissue engineering. *Nature Materials*, 4(7):518–524, 2005.

[197] Francesca Serra, Krishna C. Vishnubhatla, Marco Buscaglia, *et al.* Topological defects of nematic liquid crystals confined in porous networks. *Soft Matter*, 7(22):10945–10950, 2011.

[198] Takeaki Araki, Marco Buscaglia, Tommaso Bellini, and Hajime Tanaka. Memory and topological frustration in nematic liquid crystals confined in porous materials. *Nature Materials*, 10(4):303–309, 2011.

[199] Giuseppe Piccardo, Gianluca Ranzi, and Angelo Luongo. A complete dynamic approach to the generalized beam theory cross-section analysis including extension and shear modes. *Mathematics and Mechanics of Solids*, 19(8):900–924, 2014.

[200] Giuseppe Piccardo and Federica Tubino. Dynamic response of Euler–Bernoulli beams to resonant harmonic moving loads. *Structural Engineering and Mechanics*, 44(5):681–704, 2012.

[201] A. Luongo, D. Zulli, and G. Piccardo. A linear curved-beam model for the analysis of galloping in suspended cables. *Journal of Mechanics of Materials and Structures*, 2(4):675–694, 2007.

[202] Holm Altenbach, Mircea Bîrsan, and Victor A. Eremeyev. On a thermodynamic theory of rods with two temperature fields. *Acta Mechanica*, 223(8):1583–1596, 2012.

[203] Angelo Luongo and Giuseppe Piccardo. Non-linear galloping of sagged cables in 1: 2 internal resonance. *Journal of Sound and Vibration*, 214(5):915–940, 1998.

[204] Angelo Luongo, Daniele Zulli, and Giuseppe Piccardo. Analytical and numerical approaches to nonlinear galloping of internally resonant suspended cables. *Journal of Sound and Vibration*, 315(3):375–393, 2008.

[205] A. Luongo, G. Rega, and F. Vestroni. Planar non-linear free vibrations of an elastic cable. *International Journal of Non-Linear Mechanics*, 19(1):39–52, 1984.

[206] A. Luongo. Perturbation methods for nonlinear autonomous discrete-time dynamical systems. *Nonlinear Dynamics*, 10(4):317–331, 1996.

[207] Wing Kam Liu, Harold S. Park, Dong Qian, *et al.* Bridging scale methods for nanomechanics and materials. *Computer Methods in Applied Mechanics and Engineering*, 195(13):1407–1421, 2006.

[208] F. Dos Reis and J.F. Ganghoffer. Equivalent mechanical properties of auxetic lattices from discrete homogenization. *Computational Materials Science*, 51:314–321, 2012.

[209] Francisco Dos Reis and Jean-François Ganghoffer. Construction of micropolar continua from the homogenization of repetitive planar lattices. In *Mechanics of Generalized Continua*, pages 193–217. Springer, 2011.

[210] Pierre Ladeveze and Anthony Nouy. On a multiscale computational strategy with time and space homogenization for structural mechanics. *Computer Methods in Applied Mechanics and Engineering*, 192(28):3061–3087, 2003.

[211] S. Federico, A. Grillo, and W. Herzog. A transversely isotropic composite with a statistical distribution of spheroidal inclusions: A geometrical approach to overall properties. *Journal of the Mechanics and Physics of Solids*, 52(10):2309–2327, 2004. DOI: 10.1016/j.jmps.2004.03.010.

[212] I. Goda, M. Assidi, S. Belouettar, and J.F. Ganghoffer. A micropolar anisotropic constitutive model of cancellous bone from discrete homogenization. *Journal of the Mechanical Behavior of Biomedical Materials*, 16:87–108, 2012.

[213] Christian Miehe, Jörg Schröder, and Jan Schotte. Computational homogenization analysis in finite plasticity simulation of texture development in polycrystalline materials. *Computer Methods in Applied Mechanics and Engineering*, 171(3):387–418, 1999.

[214] M. Brun, O. Lopez-Pamies, and P. Ponte Castaneda. Homogenization estimates for fiber-reinforced elastomers with periodic microstructures. *International Journal of Solids and Structures*, 44(18):5953–5979, 2007.

[215] G.W. Milton. Modelling the properties of composites by laminates. In *Homogenization and Effective Moduli of Materials and Media*, pages 150–174. Springer, 1986.

[216] T. Ebinger, H. Steeb, and S. Diebels. Modeling macroscopic extended continua with the aid of numerical homogenization schemes. *Computational Materials Science*, 32(3):337–347, 2005.

[217] Sina Ober-Blöbaum, Oliver Junge, and Jerrold E Marsden. Discrete mechanics and optimal control: An analysis. *ESAIM: Control, Optimisation and Calculus of Variations*, 17(02):322–352, 2011.

[218] Angelo Luongo, Giuseppe Rega, and Fabrizio Vestroni. On nonlinear dynamics of planar shear indeformable beams. *Journal of Applied Mechanics*, 53(3):619–624, 1986.

[219] Mircea Bîrsan, Holm Altenbach, Tomasz Sadowski, V.A. Eremeyev, and Daniel Pietras. Deformation analysis of functionally graded beams by the direct approach. *Composites Part B: Engineering*, 43(3):1315–1328, 2012.

[220] Chiang C Mei and Bogdan Vernescu. *Homogenization Methods for Multiscale Mechanics*. World scientific, 2010.

[221] Angela Madeo, Patrizio Neff, Ionel-Dumitrel Ghiba, Luca Placidi, and Giuseppe Rosi. Wave propagation in relaxed micromorphic continua: Modeling metamaterials with frequency band-gaps. *Continuum Mechanics and Thermodynamics*, pages 1–20, 2013.

[222] Arkadi Berezovski, Ivan Giorgio, and Alessandro Della Corte. Interfaces in micromorphic materials: Wave transmission and reflection with numerical simulations. *Mathematics and Mechanics of Solids*, page 1081286515572244, 2015.

[223] A. Madeo, A. Della Corte, L. Greco, and P. Neff. Wave propagation in pantographic 2D lattices with internal discontinuities. *arXiv:1412.3926*, 2014.

[224] Pierre Seppecher, Jean-Jacques Alibert, and Francesco dell'Isola. Linear elastic trusses leading to continua with exotic mechanical interactions. In *Journal of Physics: Conference Series*, Volume 319, page 012018. IOP Publishing, 2011.

[225] I. Giorgio, A. Culla, and D. Del Vescovo. Multimode vibration control using several piezoelectric transducers shunted with a multiterminal network. *Archive of Applied Mechanics*, 79(9):859–879, September 2009.

[226] S. O. R. Moheimani. A survey of recent innovations in vibration damping and control using shunted piezoelectric transducers. *Control Systems Technology, IEEE Transactions on*, 11(4):482–494, 2003.

[227] M. Porfiri, F. dell'Isola, and F.M.F. Mascioli. Circuit analog of a beam and its application to multimodal vibration damping, using piezoelectric transducers. *International Journal of Circuit Theory and Applications*, 32(4):167–198, 2004.

[228] V.A. Eremeev, A.B. Freidin, and L.L. Sharipova. Nonuniqueness and stability in problems of equilibrium of elastic two-phase bodies. In *Doklady Physics*, Volume 48, pages 359–363. Springer, 2003.

[229] V.A. Yeremeyev, A.B. Freidin, and L.L. Sharipova. The stability of the equilibrium of two-phase elastic solids. *Journal of Applied Mathematics and Mechanics*, 71(1):61–84, 2007.

[230] J.C. Knight, T.F. Page, and H.W. Chandler. Thermal instability of the microstructure and surface mechanical properties of hydrogenated amorphous carbon films. *Surface and Coatings Technology*, 49(1):519–529, 1991.

[231] En Ma. Nanocrystalline materials: Controlling plastic instability. *Nature Materials*, 2(1): 7–8, 2003.

[232] T. Konkova, S. Mironov, A. Korznikov, and S.L. Semiatin. Microstructure instability in cryogenically deformed copper. *Scripta Materialia*, 63(9):921–924, 2010.

[233] Hanliang Zhu, K. Maruyama, D.Y. Seo, and P. Au. Effect of initial microstructure on microstructural instability and creep resistance of xd TiAL alloys. *Metallurgical and Materials Transactions A*, 37(10):3149–3159, 2006.

[234] N.L. Rizzi, V. Varano, and S. Gabriele. Initial postbuckling behavior of thin-walled frames under mode interaction. *Thin-Walled Structures*, 68:124–134, 2013.

[235] N.L. Rizzi and V. Varano. On the postbuckling analysis of thin-walled frames. In B.H.V. Topping, Y. Tsompanakis, (Editors), *Proceedings of the Thirteenth International Conference on Civil, Structural and Environmental Engineering Computing*, Civil-Comp Press, Stirlingshire, UK, Paper 43, 2011. doi:10.4203/ccp.96.43

[236] N.L. Rizzi and V. Varano. The effects of warping on the postbuckling behaviour of thin-walled structures. *Thin-Walled Structures*, 49(9):1091–1097, 2011.

[237] M. Pignataro, G. Ruta, N. Rizzi, and V. Varano. Effects of warping constraints and lateral restraint on the buckling of thin-walled frames. In ASME 2009 *International Mechanical Engineering Congress and Exposition* (pp. 803–810). American Society of Mechanical Engineers, 2009.

[238] M. Pignataro, N. Rizzi, G. Ruta, and V. Varano. The effects of warping constraints on the buckling of thin-walled structures. *Journal of Mechanics of Materials and Structures*, 4(10):1711–1727, 2009.

[239] G.C. Ruta, V. Varano, M. Pignataro, and N.L. Rizzi. A beam model for the flexural-torsional buckling of thin-walled members with some applications. *Thin-Walled Structures*, 46(7-9):816–822, 2008.

[240] Marcello Pignataro, N. Rizzi, and A. Luongo. *Stability, Bifurcation, and Postcritical Behaviour of Elastic Structures*. Elsevier, 1991.

[241] Angelo Luongo. Mode localization in dynamics and buckling of linear imperfect continuous structures. *Nonlinear Dynamics*, 25(1-3):133–156, 2001.

[242] Angelo Luongo and Giuseppe Piccardo. Linear instability mechanisms for coupled translational galloping. *Journal of Sound and Vibration*, 288(4):1027–1047, 2005.

[243] Angelo Luongo and Daniele Zulli. Dynamic instability of inclined cables under combined wind flow and support motion. *Nonlinear Dynamics*, 67(1):71–87, 2012.

[244] Angelo Luongo and Daniele Zulli. Aeroelastic instability analysis of nes-controlled systems via a mixed multiple scale/harmonic balance method. *Journal of Vibration and Control*, 20(13): 1985–1998, 2014.

[245] Angelo Luongo. A unified perturbation approach to static/dynamic coupled instabilities of nonlinear structures. *Thin-Walled Structures*, 48(10):744–751, 2010.

[246] Angelo Di Egidio, Angelo Luongo, and Achille Paolone. Linear and non-linear interactions between static and dynamic bifurcations of damped planar beams. *International Journal of Non-Linear Mechanics*, 42(1):88–98, 2007.

[247] Fabrizio Vestroni, Angelo Luongo, and Monica Pasca. Stability and control of transversal oscillations of a tethered satellite system. *Applied Mathematics and Computation*, 70(2):343–360, 1995.

[248] Hod Lipson and Melba Kurman. *Fabricated: The New World of 3D Printing*. John Wiley & Sons, 2013.

[249] L.A. Hockaday, K.H. Kang, N.W. Colangelo, *et al.* Rapid 3D printing of anatomically accurate and mechanically heterogeneous aortic valve hydrogel scaffolds. *Biofabrication*, 4(3):035005, 2012.

[250] Andreas Greiner and Joachim H. Wendorff. Electrospinning: A fascinating method for the preparation of ultrathin fibers. *Angewandte Chemie International Edition*, 46(30):5670–5703, 2007.

[251] Travis J. Sill and Horst A. von Recum. Electrospinning: Applications in drug delivery and tissue engineering. *Biomaterials*, 29(13):1989–2006, 2008.

[252] Nandana Bhardwaj and Subhas C. Kundu. Electrospinning: A fascinating fiber fabrication technique. *Biotechnology Advances*, 28(3):325–347, 2010.

[253] Daniela Di Camillo, Vito Fasano, Fabrizio Ruggieri, *et al.* Near-field electrospinning of conjugated polymer light-emitting nanofibers. *arXiv preprint arXiv:1310.5101*, 2013.

[254] Daniela Di Camillo, Fabrizio Ruggieri, S Santucci, and Luca Lozzi. N-doped TiO2 nanofibers deposited by electrospinning. *The Journal of Physical Chemistry C*, 116(34):18427–18431, 2012.

[255] Ramiro Dell'Erba, Francesco dell'Isola, and Giacomo Rotoli. The influence of the curvature dependence of the surface tension on the geometry of electrically charged menisci. *Continuum Mechanics and Thermodynamics*, 11(2):89–105, 1999.

[256] Seema Agarwal, Joachim H. Wendorff, and Andreas Greiner. Progress in the field of electrospinning for tissue engineering applications. *Advanced Materials*, 21(32-33):3343–3351, 2009.

[257] Vince Beachley, Vladimir Kasyanov, Agnes Nagy-Mehesz, *et al.* The fusion of tissue spheroids attached to pre-stretched electrospun polyurethane scaffolds. *Journal of Tissue Engineering*, 5:2041731414556561, 2014.

[258] H. Yasuda and J. Yang. Reentrant origami-based metamaterials with negative poisson's ratio and bistability. *Physical Review Letters*, 114(18):185502, 2015.

[259] Claude Boutin and François Xavier Becot. Theory and experiments on poro-acoustics with inner resonators. *Wave Motion*, 54:76–99, 2015.

[260] C. Boutin, L. Schwan, and M.S. Dietz. (2015). Elastodynamic metasurface: Depolarization of mechanical waves and time effects. *Journal of Applied Physics*, 117(6): 064902, 2015.

[261] C. Boutin and J.L. Auriault. Rayleigh scattering in elastic composite materials. *International Journal of Engineering Science*, 31(12):1669–1689, 1993.

[262] Claude Boutin, Antoine Rallu, and Stephane Hans. Large scale modulation of high frequency acoustic waves in periodic porous media. *The Journal of the Acoustical Society of America*, 132(6):3622–3636, 2012.

[263] C. Boutin, P. Royer, and J.L. Auriault. Acoustic absorption of porous surfacing with dual porosity. *International Journal of Solids and Structures*, 35(34):4709–4737, 1998.

[264] Céline Chesnais, Stéphane Hans, and Claude Boutin. Wave propagation and diffraction in discrete structures: Effect of anisotropy and internal resonance. *PAMM*, 7(1):1090, 2007.

[265] Vladimir Fokin, Muralidhar Ambati, Cheng Sun, and Xiang Zhang. Method for retrieving effective properties of locally resonant acoustic metamaterials. *Physical Review B*, 76(14):144302, 2007.

[266] Pai Wang, Filippo Casadei, Sicong Shan, James C Weaver, and Katia Bertoldi. Harnessing buckling to design tunable locally resonant acoustic metamaterials. *Physical Review Letters*, 113(1):014301, 2014.

[267] Holm Altenbach, Victor A. Eremeyev, and Nikita F. Morozov. Mechanical properties of materials considering surface effects. In *IUTAM Symposium on Surface Effects in the Mechanics of Nanomaterials and Heterostructures*, pages 105–115. Springer, 2013.

[268] V.F. Nesterenko, Chiara Daraio, E.B. Herbold, and Sungho Jin. Anomalous wave reflection at the interface of two strongly nonlinear granular media. *Physical review letters*, 95(15):158702, 2005.

[269] Victor A. Eremeyev. On effective properties of materials at the nano-and microscales considering surface effects. *Acta Mechanica*, DOI:10.1007/s00707-015-1427-y, 2015.

[270] Julia R. Greer and Jeff Th. M. De Hosson. Plasticity in small-sized metallic systems: Intrinsic versus extrinsic size effect. *Progress in Materials Science*, 56(6):654–724, 2011.

[271] Julia R. Greer and William D. Nix. Size dependence of mechanical properties of gold at the sub-micron scale. *Applied Physics A*, 80(8):1625–1629, 2005.

[272] Stéphane Cuenot, Christian Frétigny, Sophie Demoustier-Champagne, and Bernard Nysten. Surface tension effect on the mechanical properties of nanomaterials measured by atomic force microscopy. *Physical Review B*, 69(16):165410, 2004.

[273] C.Q. Chen, Y. Shi, Y.S. Zhang, J. Zhu, and Y.J. Yan. Size dependence of Young's modulus in ZnO nanowires. *Physical Review Letters*, 96(7):075505, 2006.

[274] Xiaohua Liu, Jun Luo, and Jing Zhu. Size effect on the crystal structure of silver nanowires. *Nano Letters*, 6(3):408–412, 2006.

[275] G. Y. Jing, H. L. Duan, X. M. Sun, *et al.* Surface effects on elastic properties of silver nanowires: Contact atomic-force microscopy. *Physical Review B*, 73(23):235409–6, 2006.

[276] Jin He and Carmen M. Lilley. Surface effect on the elastic behavior of static bending nanowires. *Nano Letters*, 8(7):1798–1802, 2008.

[277] Ü. Özgür, Ya I. Alivov, C. Liu, *et al.* A comprehensive review of ZnO materials and devices. *Journal of Applied Physics*, 98(4):041301, 2005.

[278] Xingfa Ma, Aiyun Liu, Huizhong Xu, *et al.* A large-scale-oriented ZnO rod array grown on a glass substrate via an in situ deposition method and its photoconductivity. *Materials Research Bulletin*, 43(8):2272–2277, 2008.

[279] B. Bhushan, editor. *Handbook of Nanotechnology*. Springer, Berlin, 2007.

[280] Anatoli Vasilievich Melechko, Vladimir I. Merkulov, Timothy E. McKnight, *et al.* Vertically aligned carbon nanofibers and related structures: Controlled synthesis and directed assembly. *Journal of Applied Physics*, 97(4):041301, 2005.

[281] Silko Grimm, Reiner Giesa, Kornelia Sklarek, *et al.* Nondestructive replication of self-ordered nanoporous alumina membranes via cross-linked polyacrylate nanofiber arrays. *Nano Letters*, 8(7):1954–1959, 2008.

[282] Lee Kheng Tan, Manippady K Kumar, Wen Wen An, and Han Gao. Transparent, well-aligned TiO2 nanotube arrays with controllable dimensions on glass substrates for photocatalytic applications. *ACS Applied Materials & Interfaces*, 2(2):498–503, 2010.

[283] Shelby B. Hutchens, Alan Needleman, and Julia R. Greer. Analysis of uniaxial compression of vertically aligned carbon nanotubes. *Journal of the Mechanics and Physics of Solids*, 59(10):2227–2237, 2011.

[284] P. Spinelli, M.A. Verschuuren, and A. Polman. Broadband omnidirectional antireflection coating based on subwavelength surface Mie resonators. *Nature Communications*, 3:692, 2012.

[285] Konstantin Naumenko and Victor A. Eremeyev. A layer-wise theory for laminated glass and photovoltaic panels. *Composite Structures*, 112:283–291, 2014.

[286] Xu Kang, Wei-Wei Zi, Zhu-Guo Xu, and Hao-Li Zhang. Controlling the micro/nanostructure of self-cleaning polymer coating. *Applied Surface Science*, 253(22):8830–8834, 2007.

[287] P.F. Rios, H. Dodiuk, S. Kenig, S. McCarthy, and A. Dotan. Transparent ultra-hydrophobic surfaces. *Journal of Adhesion Science and Technology*, 21(5-6):399–408, 2007.

[288] Subhash Latthe Sanjay, Basavraj Gurav Annaso, Shridhar Maruti Chavan, and Shrikant Vhatkar Rajiv. Recent progress in preparation of superhydrophobic surfaces: a review. *Journal of Surface Engineered Materials and Advanced Technology*, 2(02): 76, 2012.

[289] Roya Dastjerdi and Majid Montazer. A review on the application of inorganic nano-structured materials in the modification of textiles: Focus on anti-microbial properties. *Colloids and Surfaces B: Biointerfaces*, 79(1):5–18, 2010.

[290] Cintia B. Contreras, Gabriela Chagas, Miriam C. Strumia, and Daniel E Weibel. Permanent superhydrophobic polypropylene nanocomposite coatings by a simple one-step dipping process. *Applied Surface Science*, 307:234–240, 2014.

[291] Xiaoping Tian, Lingmin Yi, Xiaomei Meng, *et al.* Superhydrophobic surfaces of electrospun block copolymer fibers with low content of fluorosilicones. *Applied Surface Science*, 307:566–575, 2014.

[292] Saara Heinonen, Elina Huttunen-Saarivirta, Juha-Pekka Nikkanen, *et al.* Antibacterial properties and chemical stability of superhydrophobic silver-containing surface produced by sol–gel route. *Colloids and Surfaces A: Physicochemical and Engineering Aspects*, 453:149–161, 2014.

[293] Ana M. Escobar and Nuria Llorca-Isern. Superhydrophobic coating deposited directly on aluminum. *Applied Surface Science*, 305:774–782, 2014.

[294] W. R. Longley and R. G. Van Name, editors. *The Collected Works of J. Willard Gibbs, PhD., LL.D. Vol. I Thermodynamics*. Longmans, New York, 1928.

[295] J. S. Rowlinson and B. Widom. *Molecular Theory of Capillarity*. Dover, New York, 2003.

[296] P. G. de Gennes, F. Brochard-Wyart, and D. Quéré. *Capillarity and Wetting Phenomena: Drops, Bubbles, Pearls, Waves*. Springer, New York, 2004.

[297] M. E. Gurtin and A. I. Murdoch. A continuum theory of elastic material surfaces. *Archive for Rational Mechanics and Analysis*, 57(4):291–323, 1975.

[298] M. E. Gurtin and A. I. Murdoch. Addenda to our paper "A continuum theory of elastic material surfaces." *Archive for Rational Mechanics and Analysis*, 59(4):389–390, 1975.

[299] J. Wang, H. L. Duan, Z. P. Huang, and B. L. Karihaloo. A scaling law for properties of nano-structured materials. *Proceedings of the Royal Society A*, 462(2069):1355–1363, 2006.

[300] H. L. Duan, J. Wang, and B. L. Karihaloo. Theory of elasticity at the nanoscale. In *Advances in Applied Mechanics*, Volume 42, pages 1–68. Elsevier, 2008.

[301] J. Wang, Z. Huang, H. Duan, *et al.* Surface stress effect in mechanics of nanostructured materials. *Acta Mechanica Solida Sinica*, 24:52–82, 2011.

[302] A. Javili, A. McBride, and P. Steinmann. Thermomechanics of solids with lower-dimensional energetics: On the importance of surface, interface, and curve structures at the nanoscale. A unifying review. *Applied Mechanics Reviews*, 65:010802–1–31, 2012.

[303] D. J. Steigmann and R. W. Ogden. Elastic surface-substrate interactions. *Proceedings of the Royal Society A* , 455(1982):437–474, 1999.

[304] A. Javili and P. Steinmann. On thermomechanical solids with boundary structures. *International Journal of Solids and Structures*, 47(24):3245–3253, 2010.

[305] Yu. Povstenko. Mathematical modeling of phenomena caused by surface stresses in solids. In H. Altenbach and N. F. Morozov, editors, *Surface Effects in Solid Mechanics*, pages 135–153. Springer, 2013.

[306] M.B. Rubin and Y. Benveniste. A Cosserat shell model for interphases in elastic media. *Journal of the Mechanics and Physics of Solids*, 52(5):1023–1052, 2004.

[307] C. I. Kim, P. Schiavone, and C.-Q. Ru. Effect of surface elasticity on an interface crack in plane deformations. *Proceedings of Royal Society A*, 467(2136):3530–3549, 2011.

[308] C.I. Kim, C.-Q. Ru, and P. Schiavone. A clarification of the role of crack-tip conditions in linear elasticity with surface effects. *Mathematics and Mechanics of Solids*, 18(1):59–66, 2013.

[309] P. Schiavone and C.-Q. Ru. Solvability of boundary value problems in a theory of plane-strain elasticity with boundary reinforcement. *International Journal of Engineering Science*, 47(11):1331–1338, 2009.

[310] Holm Altenbach, Victor A. Eremeyev, and Leonid P. Lebedev. On the existence of solution in the linear elasticity with surface stresses. *ZAMM-Journal of Applied Mathematics and Mechanics/Zeitschrift für Angewandte Mathematik und Mechanik*, 90(3):231–240, 2010.

[311] Holm Altenbach, Victor A. Eremeyev, and Leonid P. Lebedev. On the spectrum and stiffness of an elastic body with surface stresses. *ZAMM-Journal of Applied Mathematics and Mechanics/Zeitschrift für Angewandte Mathematik und Mechanik*, 91(9):699–710, 2011.

[312] A. Javili, A. McBride, P. Steinmann, and B.D. Reddy. Relationships between the admissible range of surface material parameters and stability of linearly elastic bodies. *Philosophical Magazine*, 92(28-30):3540–3563, 2012.

[313] J. G. Guo and Y. P. Zhao. The size-dependent elastic properties of nanofilms with surface effects. *Journal of Applied Physics*, 98(7):074306–11, 2005.

[314] Z. Q. Wang, Y.-P. Zhao, and Z.-P. Huang. The effects of surface tension on the elastic properties of nano structures. *International Journal of Engineering Science*, 48(2): 140–150, 2010.

[315] Victor A. Eremeyev, Holm Altenbach, and Nikita F. Morozov. The influence of surface tension on the effective stiffness of nanosize plates. *Doklady Physics*, 54(2):98–100, 2009.

[316] Holm Altenbach, Victor A. Eremeyev, and Nikita F. Morozov. Surface viscoelasticity and effective properties of thin-walled structures at the nanoscale. *International Journal of Engineering Science*, 59:83–89, 2012.

[317] Holm Altenbach and Victor A. Eremeyev. On the shell theory on the nanoscale with surface stresses. *International Journal of Engineering Science*, 49(12):1294–1301, 2011.

[318] Z. Huang and J. Wang. A theory of hyperelasticity of multi-phase media with surface/interface energy effect. *Acta Mechanica*, 182:195–210, 2006.

[319] Z. Huang and L. Sun. Size-dependent effective properties of a heterogeneous material with interface energy effect: From finite deformation theory to infinitesimal strain analysis. *Acta Mechanica*, 190:151–163, 2007.

[320] H. X. Zhu, J. X. Wang, and B. L. Karihaloo. Effects of surface and initial stresses on the bending stiffness of trilayer plates and nanofilms. *Journal of Mechanics of Materials and Structures*, 4(3):589–604, 2009.

[321] Z. Huang and J. Wang. Micromechanics of nanocomposites with interface energy effect. In S. Li and X.-L. Gao, editors, *Handbook on Micromechanics and Nanomechanics*, pages 303–348. Pan Stanford Publishing, 2012.

[322] A. Javili and P. Steinmann. A finite element framework for continua with boundary energies. Part I: The two-dimensional case. *Computer Methods in Applied Mechanics and Engineering*, 198(27–29):2198–2208, 2009.

[323] A. Javili and P. Steinmann. A finite element framework for continua with boundary energies. Part III: The thermomechanical case. *Computer Methods in Applied Mechanics and Engineering*, 200(21):1963–1977, 2011.

[324] A. Javili, A. McBride, and P. Steinmann. Numerical modelling of thermomechanical solids with mechanically energetic (generalised) Kapitza interfaces. *Computational Materials Science*, 65:542–551, 2012.

[325] Harald Ibach. The role of surface stress in reconstruction, epitaxial growth and stabilization of mesoscopic structures. *Surface Science Reports*, 29(5):195–263, 1997.

[326] J. Lagowski, H. C. Gatos, and E. S. Sproles. Surface stress and normal mode of vibration of thin crystals: GaAs. *Applied Physics Letters*, 26(9):493–495, 1975.

[327] M. E. Gurtin, X. Markenscoff, and R. N. Thurston. Effect of surface stress on natural frequency of thin crystals. *Applied Physics Letters*, 29(9):529–530, 1976.

[328] G.-F. Wang and X.-Q. Feng. Effects of surface elasticity and residual surface tension on the natural frequency of microbeams. *Applied Physics Letters*, 90(23):231904, 2007.

[329] E. Kampshoff, E. Hahn, and K. Kern. Correlation between surface stress and the vibrational shift of CO chemisorbed on Cu surfaces. *Physical Review Letters*, 73(5):704–707, 1994.

[330] G. F. Wang and X. Q. Feng. Effect of surface stresses on the vibration and buckling of piezoelectric nanowires. *EPL – A Letters Journal Exploring the Frontiers of Physics*, 91(5):56007, 2010.

[331] Victor A. Eremeyev and Leonid P. Lebedev. Existence of weak solutions in elasticity. *Mathematics and Mechanics of Solids*, 18(2):204–217, 2013.

[332] Marino Arroyo and Ted Belytschko. An atomistic-based finite deformation membrane for single layer crystalline films. *Journal of the Mechanics and Physics of Solids*, 50(9):1941–1977, 2002.

[333] D. Sfyris, G.I. Sfyris, and C. Galiotis. Curvature dependent surface energy for a free standing monolayer graphene: Some closed form solutions of the non-linear theory. *International Journal of Non-Linear Mechanics*, 67:186–197, 2014.

[334] Ronald E. Miller and Vijay B. Shenoy. Size-dependent elastic properties of nanosized structural elements. *Nanotechnology*, 11(3):139, 2000.

[335] Vijay B. Shenoy. Atomistic calculations of elastic properties of metallic fcc crystal surfaces. *Physical Review B*, 71(9):094104, 2005.

[336] P. G. De Gennes. Some effects of long range forces on interfacial phenomena. *Journal de Physique Lettres*, 42(16):377–379, 1981.

[337] P. Seppecher. *Les Fluides de Cahn–Hilliard*. Mémoire d'habilitation à diriger des recherches, Université du Sud Toulon, 1996.

[338] F. dell'Isola and P. Seppecher. Edge contact forces and quasi-balanced power. *Meccanica*, 32(1):33–52, 1997.

[339] F. dell'Isola and P. Seppecher. The relationship between edge contact forces, double forces and interstitial working allowed by the principle of virtual power. *Comptes rendus de l'Académie des sciences. Série 2*, 321(8):303–308, 1995.

[340] Ivan Giorgio, Roman Grygoruk, Francesco dell'Isola, and David J Steigmann. Pattern formation in the three-dimensional deformations of fibered sheets. *Mechanics Research Communications*, 69:164–171, 2015.

[341] Claude Boutin, Ivan Giorgio, Luca Placidi, *et al.* Linear pantographic sheets: Asymptotic micro-macro models identification. *Mathematics and Mechanics of Complex Systems*, 5(2):127–162, 2017.

[342] Victor A. Eremeyev, Francesco dell'Isola, Claude Boutin, and David Steigmann. Linear pantographic sheets: Existence and uniqueness of weak solutions. *Journal of Elasticity*, pages 1–22, 2017.

[343] Francesco dell'Isola, Tomasz Lekszycki, Marek Pawlikowski, Roman Grygoruk, and Leopoldo Greco. Designing a light fabric metamaterial being highly macroscopically tough under directional extension: First experimental evidence. *Zeitschrift für angewandte Mathematik und Physik*, 66(6):3473–3498, 2015.

[344] I. Giorgio. Numerical identification procedure between a micro-Cauchy model and a macro-second gradient model for planar pantographic structures. *Zeitschrift fur Angewandte Mathematik und Physik*, 67(4), 2016.

[345] E. Turco, F. dell'Isola, A. Cazzani, and N.L. Rizzi. Hencky-type discrete model for pantographic structures: Numerical comparison with second gradient continuum models. *Zeitschrift fur Angewandte Mathematik und Physik*, 67(4):1–28, 2016.

[346] F. dell'Isola, I. Giorgio, M. Pawlikowski, and N.L. Rizzi. Large deformations of planar extensible beams and pantographic lattices: Heuristic homogenization, experimental and numerical examples of equilibrium. *Proceedings of the Royal Society A: Mathematical, Physical and Engineering Sciences*, 472(2185), 2016.

[347] E. Turco, K. Barcz, and N.L. Rizzi. Non-standard coupled extensional and bending bias tests for planar pantographic lattices. Part II: Comparison with experimental evidence. *Zeitschrift fur Angewandte Mathematik und Physik*, 67(5), 2016.

[348] Ivan Giorgio, Alessandro Della Corte, Francesco dell'Isola, and David J. Steigmann. Buckling modes in pantographic lattices. *Comptes rendus Mecanique*, 344(7):487–501, 2016.

[349] Dae-Hyeong Kim, Nanshu Lu, Rui Ma, *et al.* Epidermal electronics. *Science*, 333(6044):838–843, 2011.

[350] V. Arumugam, M.D. Naresh, and R. Sanjeevi. Effect of strain rate on the fracture behaviour of skin. *Journal of Biosciences*, 19(3):307–313, 1994.

[351] Peter Elsner, Enzo Berardesca, and Klaus-Peter Wilhelm. *Bioengineering of the Skin: Skin Biomechanics*, Volume 5. Taylor & Francis US, 2001.

[352] Marion Geerligs, Lambert Van Breemen, Gerrit Peters, *et al.* In vitro indentation to determine the mechanical properties of epidermis. *Journal of Biomechanics*, 44(6):1176–1181, 2011.

[353] Alain Goriely, Michel Destrade, and M. Ben Amar. Instabilities in elastomers and in soft tissues. *The Quarterly Journal of Mechanics and Applied Mathematics*, 59(4):615–630, 2006.

[354] Stephanie P. Lacour, Joyelle Jones, Sigurd Wagner, Teng Li, and Zhigang Suo. Stretchable interconnects for elastic electronic surfaces. *Proceedings of the IEEE*, 93(8):1459–1467, 2005.

[355] C. Pailler-Mattei, S. Bec, and H. Zahouani. In vivo measurements of the elastic mechanical properties of human skin by indentation tests. *Medical Engineering & physics*, 30(5):599–606, 2008.

[356] Tsuyoshi Sekitani, Yoshiaki Noguchi, Kenji Hata, *et al.* A rubberlike stretchable active matrix using elastic conductors. *Science*, 321(5895):1468–1472, 2008.

[357] Galileo Galilei. *Opere: Edizione nazionale sotto gli auspicii di Sua Maestà il re d'Italia*, Volume 6. Barbèra, 1894.

[358] Marco Cannone and Susan Friedlander. Navier: Blow-up and collapse. *Notices of the AMS*, 50(1):7–13, 2003.

[359] Antoine Picon. Navier and the introduction of suspension bridges in France. *Construction History*, pages 21–34, 1988.

2 A Review of Some Selected Examples of Mechanical and Acoustic Metamaterials

E. Barchiesi, F. Di Cosmo, M. Laudato

2.1 Mechanical Metamaterials

2.1.1 Introduction

Recent improvements in manufacturing techniques together with developments in the capability of manipulating materials at the scale of micro- and nano-meters, have enormously accelerated the production of new scientifically designed materials with extraordinary acoustical and mechanical behaviours (we will call them metamaterials). Among the several manufacturing techniques which are widely used, we can mention, for instance, 3D-printing [2–6], roll-to-roll processing [7, 8], optical litography [9], electrospinning [10, 11], dry and wet etching, micromolding, wet bulk micromachining, etc. The main reason for these exotic behaviours, observed at a macro-level, can be found in the particular microstructure underlying the metamaterial, while the physical and chemical properties of the constituents play a very marginal role. It is appropriate to note here that the prefixes macro- and micro- are not referred to a given absolute length scale (in particular micro does not mean micro-meters [1]). According to the usual nomenclature used in the metamaterial framework, with the prefix macro- we will denote, generally, the scale at which a certain phenomenon is observed, whereas the prefix micro- is related to the characteristic length of the structure underlying the metamaterial, which is usually determined during the design phase and is limited by the relevant manufacturing process.

Traditional materials are not able to satisfy the continuous quest for extreme performance and, as a natural consequence, metamaterials with tailored extreme properties have attracted the attention of many scientists.

This section will present a survey of the state of the art in the field of metameterials which primarily involve mechanical phenomena. Metamaterials, indeed, have been introduced from the very beginning, as materials whose macroscopic exotic behaviour is determined by microstructures designed to exploit coupled interactions of different nature (multi-physics phenomena). For instance, there exist metamaterials, also called smart materials, whose microstructures are controlled by means of electromagnetic devices. Here we will focus only on one family of metamaterials, the one which involves only mechanical processes both at the micro- and macro-scale.

This section is divided into two parts, each one comprising several sub-sections. The first part is mainly a survey of promising microstructures, subdivided into four

smaller groups: extremal metamaterials [17–25], metamaterials with negative constitutive parameters [26–28], pantographic structures [29–34] and metamaterials with foldable microstructures [22, 35, 36].

The second part will focus on more general theoretical discussions: the goal of this part is to show how (sufficiently general) models can drive the design and manufacturing of new materials [25, 37–39] and help in accomplishing the metamaterials mission statement.

2.1.2 A Survey of Existing Microstructures

In this sub-section we will present the main features characterizing some classes of mechanical microstructures which have proved to be promising and are the most widespread in the literature.

We first require the introduction of some standard nomenclature. For instance, central properties to which we will often refer are so-called engineering material constants: bulk modulus (or compressibility), elastic Young's modulus, shear modulus (also known as modulus of rigidity), and Poisson's ratio provide useful information within the paradigm of Cauchy mechanics. For the sake of completeness, before discussing the properties of specific microstructures, we will briefly introduce the definitions of these physical quantities.

The bulk modulus, B, describes the resistance of a material with respect to compression and it is defined as the ratio of pressure variation to that in volume. It is positive if the volume of the relevant material decreases to correspond with a pressure increase. The elastic Young's modulus, E, is defined as the ratio between the force per unit area exerted on a material along a specific axis divided by the strain along that same axis (given a material segment, the strain is the ratio of its deformed length to the initial one). The shear modulus, G, measures the resistance of a material to actions which are parallel to the surface of the material. Finally, given a specific axis, the Poisson's ratio, ν, is defined as the ratio of the transverse strain to the corresponding axial strain.

Extremal Metamaterials

Extremal metamaterials were introduced by Milton and Cherkaev in 1995 while they were trying to understand how to build a material with a specific elasticity tensor [37]. Indeed, composites made up of these extremal metamaterials can reproduce any desired elasticity tensor, as we will see later in this section. The main feature of an extremal metamaterial is that it is very stiff when undergoing some modes of deformation, whereas it is very compliant in others. Roughly speaking, the corresponding elasticity tensor possesses only very large or very small eigenvalues. Since in 3D-elasticity the strain tensor has six independent components, we can collect three-dimensional extremal metamaterials into seven groups, according to the number of deformation modes with respect to which the metamaterial is compliant: null-mode, uni-mode, bi-mode, tri-mode, quadra-mode, penta-mode and hexa-mode (these modes will be called *easy modes*). We are going to illustrate only the microstructure corresponding to a penta-mode material, since the combination of penta-mode metamaterials with different

easy modes makes it possible to build all the intermediate materials [37] mentioned above. On the other hand, null-mode and hexa-mode materials are simply isotropic stiff and compliant materials.

Pentamode Materials

According to the previous classification, penta-mode materials possess five easy modes, which means that five eigenvalues of the elasticity tensor (in the Voigt representation) are very small with respect to the last one. From an experimental point of view, penta-mode metamaterials preserve their volume when they are subject to a deformation. From a theoretical point of view, if one describes the behaviour of such metamaterials by introducing a continuum model, this property can be modelled by requiring that the gradient of the placement field has a determinant, i.e. the Jacobian, equal to one. According to Cauchy linear elasticity theory, this implies a very large bulk modulus with respect to the corresponding shear modulus and, consequently (by looking at formulas relating different material parameters for materially linear isotropic Cauchy continua; a useful table is reported in *https://en.wikipedia.org/wiki/Elastic_modulus* as retrieved on 19 July 2019), Poisson's ratio has to be close to $\nu = 0.5$. Such a behaviour, where shearing effects are negligible, is typical of incompressible fluids. This is the reason why penta-mode metamaterials are also sometimes referred to as meta-fluids or meta-liquids.

A specific periodic microstructure, which behaves as a penta-mode metamaterial, has been designed by Milton and Cherkaev and is proposed in [37]. The fundamental cell is composed of identical beams arranged in a diamond-type lattice geometry (see Fig. 2.1). The beam elements forming the cell have a peculiar variable cross section: they are made up of two cones joined at their bases and the four beam elements constituting the unit cell are connected through one tip at the centre of a tetrahedral lattice, while the remaining tips form the vertices of the unit cell. The realization of any kind of microstructure is

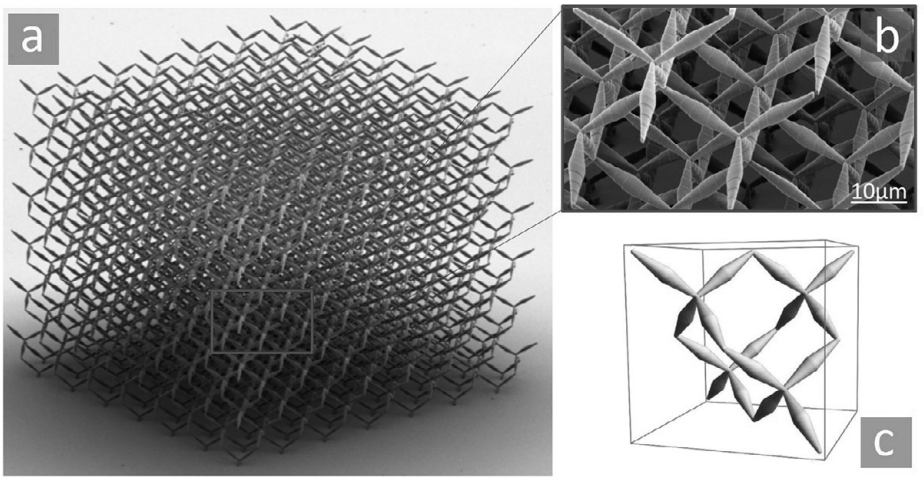

Figure 2.1 A penta-mode metamaterial. The four beam elements are arranged to form a diamond-like fundamental cell.

clearly limited by the resolution of the relevant manufacturing process. Approaching 10 years ago, in 2012, Wegener and collaborators realized such a microstructure [17] at the micro-meters scale.

Because of the specific variable cross-section, which presents an apex, the stiffness of this metamaterial is not affected by the radius of the base of the cones constituting the beams. On the other hand, by varying this parameter the mass can be significantly changed. In other words, this microstructure permits us to modify its stiffness and its mass density independently. Because of their properties, penta-mode extremal metamaterials could be used as elastic and acoustic cloaks, or they could be employed in designing porous tissue engineering scaffolds, where the possibility of changing stiffness and mass density independently could be exploited to improve cell adhesion or tissue regeneration rate. In order to fruitfully build cloaks using metamaterials, it is fundamental to choose properly the length of the unit cell. Indeed, it is well known that the ratio of the wavelength of the external action to the lattice constant deeply affects the behaviour of the metamaterial. There have also been some proposals aimed at making the previous microstructure anisotropic, that is, e.g. that the velocity of longitudinal waves will depend on the direction of propagation. For instance, Kadic *et al.* [41] have built a similar microstructure where the point in the fundamental cells where the four beam elements meet has been shifted. The role of different types of lattices have also been investigated [42] in the achievement of penta-mode metamaterials.

Dilational and Auxetic Behaviours

The term 'auxetic' was first suggested by Evans *et al.* [43] to name those materials characterized by an increase of the transverse dimension when subject to a longitudinal tensile load along a certain axis. Indeed, this word comes from the Greek adjective $\alpha\nu\xi\eta\tau\iota\kappa\zeta$, 'auxetikos', whose meaning, 'which tends to increase', perfectly agrees with the behaviour of these materials.

A quantity which gives information about auxetic behaviours is the Poisson's ratio, ν, which we have already introduced. Note that, for an isotropic material described in the context of the Cauchy theory, the value of the Poisson's ratio ranges between -1 and 0.5, in order to get a stable elastic material. However, this limit can be exceeded when the material is not isotropic. When discussing the properties of penta-mode metamaterials, we saw that they were characterized by $\nu = 0.5$, since they were subject to change of shape whereas the variation of volume was negligible. In this section, on the contrary, we will give an account of materials which possess a negative Poisson's ratio: these are auxetic materials [23, 44–49].

Let us start with a particular family of isotropic auxetic materials which are called dilational metamaterials. Their characterizing property lies in the fact that their Poisson's ratio is equal to -1, with the immediate consequence that the ratio of the bulk modulus to the shear modulus is close to 0. Therefore, their volume can be easily modified without altering their shape: this is the reason for the name dilational metamaterials. From a certain point of view, they show an opposite behaviour with respect to penta-mode metamaterials which we have previously introduced. Indeed, they can be considered as uni-mode extremal metamaterials where dilation is the easy

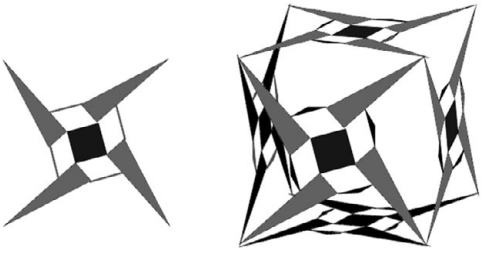

Figure 2.2 Left: the fundamental cell constituting a dilational metamaterial, sketched on the right. It is composed of several elastic and rigid elements interconnected by hinges. Relative movements of these elements produce the global dilational behaviour.

deformation mode. One of the first microstructures with a Poisson's ratio close to the value $\nu = -1$ was proposed by Almgren in 1985 [50] and it was composed of a sequence of sliding collars interconnected by springs. Later, in 2013, Milton [25] proposed a microstructure for a planar uni-mode dilational metamaterial made up of a central square plaquette whose vertices are connected by pivots to four rigid bars (see Fig. 2.2). By assembling six planar cells to form a cube, one gets a fundamental cell which can be arranged in a three-dimensional array behaving as a dilational metamaterial. Bückmann *et al.* [24] have investigated the properties of this structure both from a theoretical and an experimental point of view. Experimental evidence has confirmed theoretical predictions, showing an isotropic Poisson's ratio consistent with the expected one.

Dilational metamaterials are also known as 'ideal' auxetic materials, since transverse strain and axial strain have the same sign and the same value. However, it is not yet clearly understood if microstructures with a dilational behaviour can be obtained via a prescribed limiting procedure starting with an auxetic metamaterial with negative Poisson's ratio different from -1.

In the rest of this section, we shall present an overview of the vast landscape of proposed microstructures which are available in the literature[51, 52]. In particular, one can collect these models into three families: re-entrant structures [53, 54], chiral structures [55, 56], and assembly of rigid and semi-rigid rotating elements [57, 58].

Let us start with the structure proposed by Gibson *et al.* in 1982 [53]: it is a bi-dimensional array made up of re-entrant honeycombs (see Fig. 2.3). The auxetic behaviour is due to the fact that, under a tensile load, the re-entrant hexagons composing this microstructure, tend to increase their areas since the ribs delimitating the cell are forced to align. This kind of pattern can also be extended to the three-dimensional case [20]. After this pioneering work, other re-entrant honeycombs have been investigated such as, for instance, cellular structures with arrow-shaped or star-shaped building blocks. Also in this case, the motion of the cell ribs under a tensile load generates a positive variation of the transverse strain, resulting in a metamaterial with a negative Poisson's ratio.

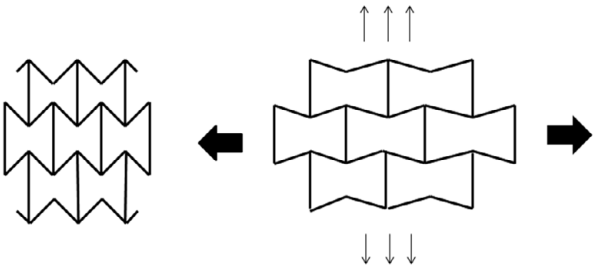

Figure 2.3 Re-entrant honeycomb lattice. Under a tensile load, the movement of the ribs forming the cells produces an increment of dimension in the directions transverse to the one of the load.

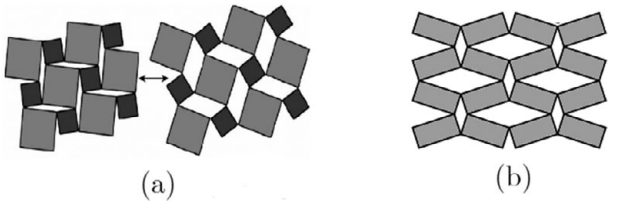

Figure 2.4 Microstructures made up of rigid rotating constituents: different types of squares (a) and rectangles (b).

Some years after the work by Gibson, in 1987, Lakes investigated the auxetic behaviour of manufactured polyurethane foams [18]. The realization procedure of these foams is very involved and requires several steps. First of all, a thermo-mechanical process compresses the open cell foam into a mould; then the mould is heated to a temperature just above its softening point; finally, the foam is cooled down and undergoes a controlled relaxation up to the final form. Also in this case, the unit cell composing the foam has some re-entrant ribs which tend to move out when the elements of the neighbouring cells are subject to tension. However, for this kind of structure, geometrical arguments are not sufficient to explain their auxetic behaviour and one has to take into account the mechanical properties of the constituents, such as flexure and stretching.

A second class of microstructures which has been investigated to create auxetic metamaterials consists in an assembly of rigid or semi-rigid units [59] which can rotate around some connecting pivots, as shown in Fig. 2.4. A lot of different element shapes have been proposed, such as triangles, rhombs, squares and parallelograms [60–63]. These structures show a plethora of possible Poisson's ratio depending on the arrangement of components: in some cases one can obtain ideal dilational metamaterials, in other cases one can obtain a highly variable Poisson's ratio, ranging from negative to positive values. Generalizations in which the rigidity hypothesis is relaxed have been also proposed, see [64, 65].

So far we have limited discussion to bi-dimensional designs. A three-dimensional model which also takes account of out-of-plane deformations has been proposed by Alderson and Evans [66]. They extended the planar model with rotating rigid squares

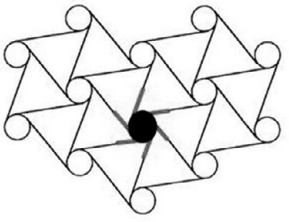

Figure 2.5 An example of chiral microstructure: circles represent cylinders, whereas curves interconnecting the circles are flexible ligaments. When the cylinders rotate, the ligaments move producing a global auxetic behaviour.

and rectangles to the three-dimensional case, in order to model the auxetic behaviour of α-cristobalite.

The third family of microstructures we are going to illustrate are called chiral structures. The name is suggested by the presence of axes of rotation which give to the fundamental units a clockwise or counterclockwise orientation.

A typical cell of an auxetic chiral structure is shown in Fig. 2.5: it is made up of cylinders set at the vertices of a bi-dimensional lattice. These cylinders are interconnected by means of flexible elements, which are called ligaments. Cylinders start to rotate when subject to external loads and, consequently, the ligaments wrap around them producing a transverse strain of the same sign as the axial one. Different lattices and ligaments have been investigated (see [55, 67, 68]): the most studied structure involves hexachiral elements,, where the lattice has hexagonal symmetry.

From the manufacturing point of view, one has to remark that it is possible to realize these structures not only by means of additive systems, like 3D-printing, but also by gluing ligaments to cylinders: the glue seems to influence only the Young's modulus of the resulting metamaterial, while the Poisson's ratio does not depend on it [69]. Recently, three-dimensional chiral structures have also been proposed, see for instance [70].

Mechanisms Determining Negative Constitutive Parameters

The majority of books presenting classical Cauchy continuum models, stress that stability arguments dictate that the elasticity tensor is positive definite. Consequently, the constitutive coefficients which we have already introduced, bulk and shear modulus, should be positive. Even if these positivity requirements have been considered as a fundamental pillar of first gradient elasticity, some experimental evidence has recently shown the existence of materials, which, under special circumstances, behave in a way which can be better described using models with negative constitutive parameters. In particular, in the context of Cauchy elasticity, constraints can deeply affect this positivity property. Lakes and Wojciechowski, for instance, have shown that constrained materials can be stable in spite of negative moduli [71]. Indeed, when constraints are present, a stable and unique solution exists if the problem is strongly elliptic, a condition which is satisfied for the following ranges of constitutive parameters [71]:

$$-\infty < E < \infty \qquad -\frac{4}{3}G < B < \infty .$$

For the sake of completeness it has also to be noted that there are some research groups working on possible unconstrained materials which can be described using negative moduli.

Negative Stiffness

Springs are one-dimensional mechanical elements which tend to come back to their stable undeformed configuration after the imposition of some displacement in both extension and compression. Stiffness is the ratio of the force needed to impose a displacement to the displacement itself and this definition can be extended to higher dimensional elasticity theories. Indeed, if one considers a three-dimensional continuum body, the Young's modulus, which we have already introduced as the ratio of the force per unit area to the axial strain, is a measure of the axial stiffness, whereas the shear modulus is a measure of the torsional (around an axis) stiffness (these properties in general depending on the axes chosen for their computation).

We are now going to introduce a very simple mechanical system which exemplifies one of the mechanisms which leads to negative stiffness (see [72, 73]). This system is called a Von Mises truss and it comprises two rods of length d_0 interconnected via a hinge to a vertical spring, whose undeformed length is x and stiffness is K (see Fig. 2.6). We call β_0 the angle formed by the rods and the horizontal axis in the undeformed configuration. By applying a force P to the connecting node along the vertical direction, the spring undergoes a vertical displacement u whereas the new configuration of the rods is characterized by a length d and an angle β with respect to the horizontal axis. In this configuration the force P can be computed and one obtains the following expression:

$$P = 2\sigma A \sin\beta + Ku\,, \tag{2.1}$$

where σ is the tension and A is the area of the cross-section of the rod. By assuming linear elastic behaviour for the rod, we have that $\sigma = E\epsilon$ (Fig. 2.7(left)), where E denotes the Young's modulus of the rod, and ϵ is the axial strain, which is related to the parameters of the current configuration via the following expression:

$$\epsilon = \frac{d_0 - d}{d_0} = 1 - \frac{\cos\beta_0}{\cos\beta}. \tag{2.2}$$

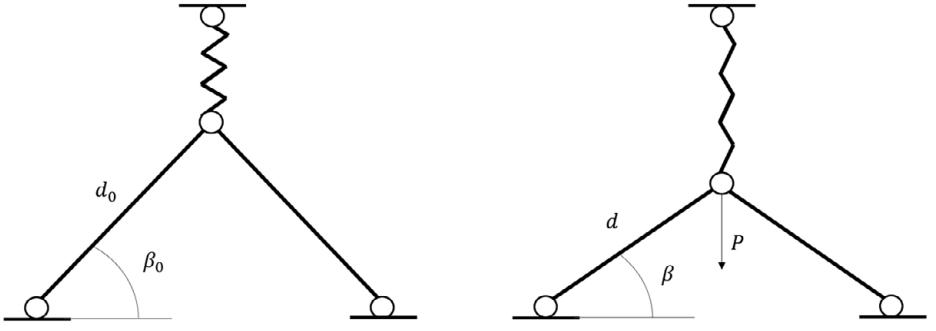

Figure 2.6 A Von Mises truss.

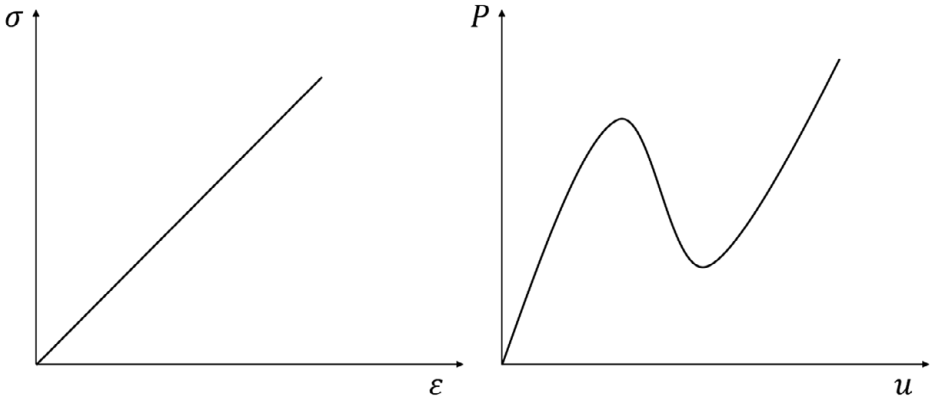

Figure 2.7 Left: the relation between the stress, σ, and the strain ϵ; right: the load, G, vs displacement, u.

Using the relation $u = d_0 \cos\beta_0 (\tan\beta_0 - \tan\beta)$, one can replace β with a certain function of u and β_0 which can be inserted in the equation for P. Eventually, one obtains the following result:

$$P = 2EA\,(d_0 \sin\beta_0 - u)\left(\frac{1}{\sqrt{b^2 + (d_0 \sin\beta_0 - u)^2}} - \frac{1}{d_0}\right) + Ku\,, \qquad (2.3)$$

where $b = d_0 \cos\beta$. One can plot the function P using the displacement u as the independent variable and, for typical values of the constitutive parameters d_0, β_0, K, one gets diagrams resembling that shown in Fig. 2.7(right).

Microstructures which try to exploit this snap-through mechanism have been proposed, for instance, in [76]. The unit cells are honeycombs which can suddenly undergo a buckling under a compressional load, because some non-straight elements delimiting cells suddenly pass to a buckled configuration.

As a final remark, note that it is possible to build composite structures comprising materials with both positive and negative stiffness. By choosing a suitable design, where a matrix made up of a material with positive stiffness constrains an embedded negative stiffness material component, one can realize metamaterials with the main advantage of being characterized by concurrent high values of stiffness and damping ratio [75, 78, 79]. The damping ratio is a parameter which gives information about the capability of a dynamical system to damp its oscillatory motions following a disturbance around an equilibrium configuration. Stiffness and damping ratio are two properties which are crucial to designing performance structures in engineering applications. Indeed, a high value of the stiffness reduces deformation whilst a high value of the damping ratio is necessary to control the dynamical response of the system. However, for materials which are usually used in present day engineering, these two properties seem to be mutually exclusive: as the stiffness increases, the damping ratio decreases and vice versa. Therefore, these positive–negative stiffness composite materials could be fruitfully exploited in engineering applications for vibration isolation and seismic protection [80–82].

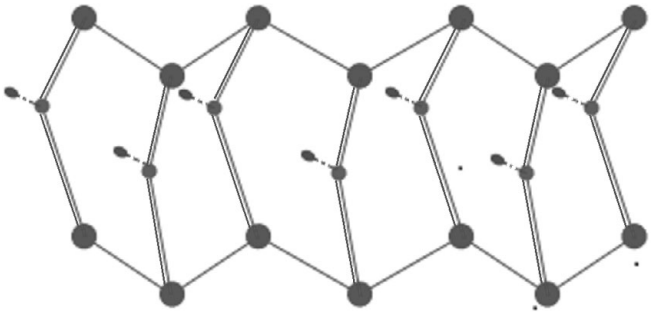

Figure 2.8 A representation of the lattice formed by methanol monohydrate after crystallization. The elements of a water chain are interconnected by single lines, whereas the hydrogen bonds between two water chains are represented by two lines.

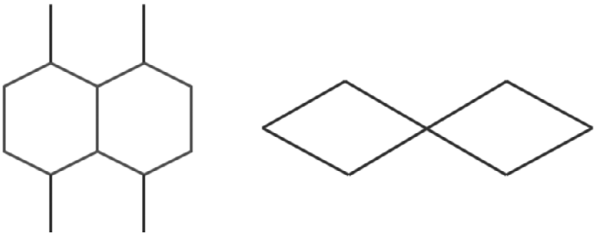

Figure 2.9 Two microstructures which produce metamaterials possessing negative compressibility: on the left a hexagon lattice, on the right a wine rack lattice.

Negative Compressibility

Negative compressibility has also been investigated in the literature [26, 71, 83, 84]. Negative compressibility is exhibited by crystalline methanol monohydrate, which has been studied by Fortes *et al.* [85], but has not been purposely designed for having such property. Methanol monohydrate crystallizes in an orthorhombic lattice with four molecules per unit cell. The structure consists of water–water chains, linked by ordered hydrogen bonds, which cross-link methanol–water chains via disordered hydrogen bonds (a schematic diagram of the structure is shown in Fig. 2.8). This material shows not only negative compressibility, but also negative and anisotropic thermal expansion.

Attempts have been made to synthesise microstructures which exhibit a global behaviour described by means of negative compressibility. Some lattices showing this property have been proposed in literature. Two of the easiest examples realizing such behaviour, which have been presented in [86], are bi-dimensional lattices with hexagonal and wine rack unit cells, see Fig. 2.9. These microstructures could be realized via networks of beams interconnected through suitable mechanical elements, such as (flexural) hinges. The authors also extended their considerations to three-dimensional solids, proposing a structure which exhibits both negative Poisson's ratio and negative compressibility [87]. A different approach has been followed in [88]. Here the authors show that negative compressibility can be obtained in specific body-centered or face-centered tetragonal networks of vertices interconnected by beams. In order to

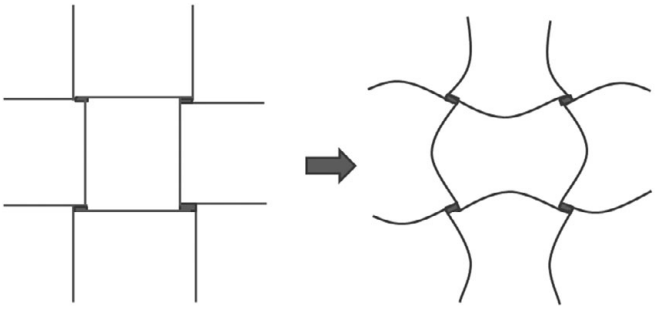

Figure 2.10 A porous microstructure formed by beams made up of materials with different properties. The combination of these different behaviours produces a global structure characterized by negative compressibility.

show this property, both simulations based on finite element techniques and analytical computations have been performed. Finally, it is worth mentioning also the work in [89], where negative compressibility has been studied in systems comprising materials with different mechanical properties. These materials are arranged in order to form a porous microstructure, which is shown in Fig. 2.10. This example is interesting since the proposed material has negative constitutive coefficients even if it is unconstrained. The basic mechanism is simple: beams made up of two different materials glued together connects the vertices of a lattice. Under pressure these bimaterial beams tend to bend, and the material undergoes a global expansion, showing negative compressibility.

Tissue-inspired Metamaterials: Mechanical Behaviour of Fabric Microstructures

One of the tissue-inspired microstructures which have been recently proposed, and whose mechanical properties seem promising for engineering purposes, is the so-called pantographic lattice [29]. This material possesses a characteristic microstructure arrangement which strongly determines its global mechanical properties. A pantographic lattice is made up of two parallel layers of rectilinear (this property can be relaxed, parabolic fibres have been considered in the literature for instance) parallel fibres with different orientation: the fibres in one layer are orthogonal to fibres in the other. Hinges[1] connect fibres belonging to different layers at their intersection points, resulting in a highly compliant structure with mechanical properties which cannot be described at macro-scale by means of traditional Cauchy continuum theory. An SLS 3D printed polyamide specimen is shown in Fig. 2.11.

One of the possible applications involving tissue-inspired microstructures is fibre-reinforcement for structural matrices and the development of biologically compatible tissues.

Foldable Microstructures and Origami-based Metamaterials

The word origami denotes the ancient Japanese art of folding sheets of paper in order to produce three-dimensional objects with a given shape, for instance a bird. During the

[1] Or small cylinders which are meant to mainly twist about their axes; clearly there are situations in which shearing of such cylinders might be non-negligible.

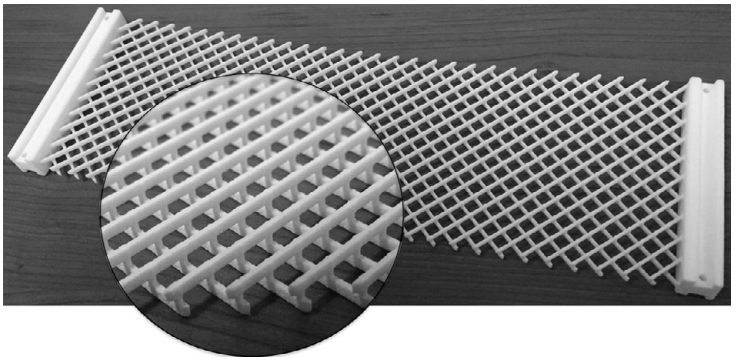

Figure 2.11 A plastic pantographic sheet manufactured via a 3D-printing process: the magnified area shows more clearly the tissue-inspired microstructure. There are two families of fibres interconnected via small cylinders called pivots.

80s, a proposal to create materials based on foldable unit cells using typical origami techniques was put forward [94] and then further developed [95–97]. One of the main applications involving these metamaterials was related to solar panel packaging for space missions. Although they have been considered technologically infeasible for more than twenty years, origami-based metamaterials are nowadays in manufacture and many research groups are working on them, trying to efficiently describe their mechanical properties.

Several different structures have been proposed in the literature based on the periodic repetition in a bi-dimensional array of a foldable unit cell. As far as mechanical properties are concerned, it is worth analyzing two different origami patterns: one is based on a Miura-ori cell and the other is the so-called egg-box tessellation.

Let us start with the Miura-ori scheme which was introduced by Miura [94] in order to find an efficient way for packaging and deploying sheets made up of solar panels for space missions. This kind of tessellation is also present in many natural systems like leaves, or embryonic intestine and in general they can be observed in bi-dimensional deformed surfaces subject to biaxial compressions. In Miura's pioneering work the aforementioned engineering problem (packaging of solar panels) was related to the geometrical problem of finding a transformation which is able to map a flat sheet into a folded one. The solution which was proposed amounts to considering a developable double corrugated surface, obtained via the repetition in a bi-dimensional array of a fundamental cell as represented in Fig. 2.12. Developability means that the surface can be rigidly mapped into a flat plane. Since the mechanical properties of this structure are a consequence of its geometry, this system is scale invariant, which means that its mechanical behaviour is not related to some characteristic length of the microstructure.

The fundamental cell is made up of four congruent parallelograms, each one characterized by the lengths of its two sides l_1, l_2 and one angle α (the other angle β is its supplemental), sharing one common vertex. The four parallelograms are disposed in such a way that the sum of the four angles which meet at one vertex is 2π, which is exactly the condition for having a developable surface. Furthermore, the edges of the parallelograms form a re-entrant lattice. The geometry of this tessellation pattern can be described in terms of four parameters: two lengths, l_1 and l_2, and two angles, α and δ,

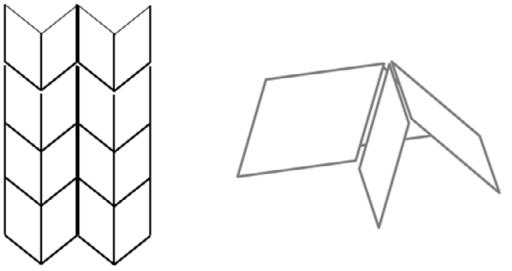

Figure 2.12 The fundamental cell of a Miura-ori tessellation. There are four parallelograms which are folded as shown in the picture on the right.

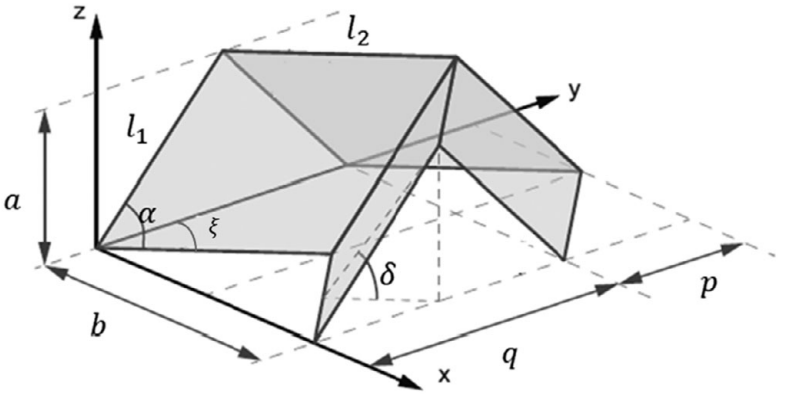

Figure 2.13 The parameters characterizing the fundamental cell of a Miura-ori tessellation.

where δ is the angle between the flat plane and one of the parallelograms in the folded configuration (see Fig. 2.13). Therefore, one can write the following relations:

$$\begin{aligned} a &= l_1 \sin\delta \sin\alpha, \\ b &= l_2 \frac{\cos\delta \tan\alpha}{\sqrt{1+\cos^2\delta \tan^2\alpha}}, \\ p &= l_1 \sqrt{1+\cos^2\delta \tan^2\alpha}, \\ q &= l_2 \frac{1}{\sqrt{1+\cos^2\delta \tan^2\alpha}}. \end{aligned} \tag{2.4}$$

Let us now analyze the possible deformations of the fundamental structure. In particular, we have to distinguish between in-plane and out-of-plane deformations (we consider in-plane and out-of-plane deformations with respect to a flat sheet passing through the valley and mountains, i.e. a plane surface resulting from the average of the mountain and valley array). As far as in-plane deformations are concerned, the behaviour of the system is described by the in-plane (referred to as the xy plane) Poisson's ratio:

$$\nu_{\text{in}} = -\frac{\epsilon_p}{\epsilon_b} = -\frac{b}{p}\frac{dp}{db} = -\tan^2\xi = -\frac{S^2}{V^2}\,.$$

From this expression one immediately notices that the in-plane Poisson's ratio is always negative and depends only on the in-plane angle ξ. The auxetic behaviour of this tessellation makes possible an efficient packaging and deployment of the system. Indeed, a Miura-ori textured sheet can be packaged just by pushing two opposite end points and unfolded by pulling them back in the reverse direction.

When one considers out of plane deformations, a different behaviour can be noticed. Firstly, these deformations can occur only if the facets of any cell start bending. Then, experimental evidence has proved the existence of two low-energy deformation modes: twisting and saddle modes. The latter is a typical behaviour associated with positive Poisson's ratio, with respect to out-of-plane deformations. Therefore Miura-ori tessellations are characterized by a negative in-plane and a positive out-of-plane Poisson's ratio.

In order to describe the behaviour of these metamaterials, we will consider the simplified mechanical system introduced by Schenk and Guest in [98, 99], which replaces the sheet with a system of bars interconnected via spherical pin-joints. Of course, other descriptions are possible: for instance one could model the whole sheet as a thin shell and use finite element methods to find the possible deformed configurations, or only consider facets moving rigidly. However, the model which we will consider is a good compromise between the limitation of rigid motions and a detailed microscopic analysis based on finite elements. The pin-joints are located at the vertices of each parallelogram while the bars are along the edges. Additional bars are inserted along the shorter diagonal of the parallelogram, in order to approximate the bending of the facets.

Therefore, the original problem has been replaced with a simplified one which is well known in structural mechanics. There are three governing equations in the linear regime:

$$N\boldsymbol{\tau} = \mathbf{f}, \tag{2.5}$$

$$V\mathbf{u} = \boldsymbol{\epsilon}, \tag{2.6}$$

$$R\boldsymbol{\epsilon} = \boldsymbol{\tau}, \tag{2.7}$$

where N is the so-called equilibrium matrix, which express the relations between the internal tension of the bar, $\boldsymbol{\tau}$, and the forces applied at the vertices, $\mathbf{f}$. $V = N^T$ is the compatibility matrix which connects the displacements of the nodes, $\mathbf{u}$, to the elongation of each bar, $\boldsymbol{\epsilon}$. Eventually, the third equation represents the constitutive relation containing the material stiffnesses of the bars along the diagonal. The bending of the facets is described by means of the folding angle β between two adjacent tiles, which can be expressed in terms of the positions of the vertices composing a cell. Referring to Fig. 2.14, one can write

$$\sin\beta = \frac{1}{\sin(\gamma)\sin(\theta)} \frac{1}{|e_3|^3 \cdot |e_1| \cdot |e_2|} (\mathbf{e}_3 \times (\mathbf{e}_2 \times \mathbf{e}_2)) \cdot (\mathbf{e}_3 \times \mathbf{e}_1).$$

The differential of this constraint makes it possible to linearly relate the angle $d\beta$ to the displacements of the vertices and therefore one obtains a second compatibility condition which can be written as follows:

$$C\mathbf{u} = \boldsymbol{d\beta},$$

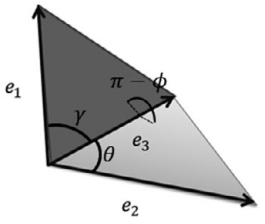

Figure 2.14 Showing the additional beam which is introduced to describe the folding of each parallelogram.

where $\boldsymbol{d\beta}$ is the vector collecting all the folding angles among adjacent facets.

From Eqs. (2.5)–(2.7) the following expression is easily derived for the stiffness matrix:

$$K\mathbf{u} = V^T R V \mathbf{u} = \mathbf{f}\,. \tag{2.8}$$

One can extend this relation in order to include also the other compatibility condition in such a way that an extended stiffness matrix can be written as:

$$K = V^T R V + C^T R_C C\,,$$

where R_C includes the stiffnesses of the edges (K_{edge}) and the facets (K_{facet}).

Eigenvalues and eigenvectors of this matrix describe the eigenmodes of the systems. Furthermore, the kernel of the compatibility matrix V represents the space of displacements which provide zero bar elongation. These modes are called *mechanisms*. By considering suitable boundary conditions it is possible to show that the space of mechanisms is three-dimensional and contains exactly the deformation modes which were previously described: planar, saddle and twisting modes. For these configurations, it is possible to compute also the ratio of the unit cell curvatures, which is the out-of-plane coupling coefficient ν_{out}. In [98] the analysis is performed in detail for the saddle mode and the final result is that the out-of-plane coupling coefficient is equal and opposite to the in-plane Poisson's ratio.

This simplified model has some limitations as, for instance, shear deformations cannot be described according to it. More detailed models have to be applied, which, for instance, contain a larger class of possible deformations of any constituent, or it may be necessary to adopt a shell model, as already discussed.

Three-dimensional metamaterials obtained by stacking several layers of origami sheets have been proposed and analyzed in many recent works [100]. Several applications have been put forward for origami-based metamaterials, for instance they could be employed for building medical stents or programmable materials [22, 101].

A different origami-based material can be obtained by means of the so-called egg-box tessellation pattern (see Fig. 2.15). The pattern is obtained by alternating pyramids with a quadrilateral base which have two opposite orientations. This structure cannot be obtained by suitably folding a flat sheet, since the sum of the angles at each vertex is less than 2π and consequently the Gaussian curvature of the surface is different from

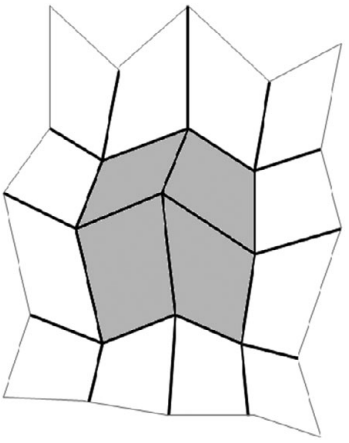

Figure 2.15 A sheet folded according to an egg-box pattern.

zero. From the point of view of mechanical properties, this pattern presents a positive in-plane Poisson's ratio, whereas the out-of-plane coupling coefficient has the opposite sign. In other words, the egg-box pattern has an opposite behaviour with respect to Miura-ori tessellation. However, the previous model can be applied also in this case and the results of the analysis are shown in [99].

Homogenization Techniques Applied to Origami-based Microstructures

In this sub-section we will illustrate the approach proposed by Nassar *et al.* [102] in order to deal with the problem of finding the surfaces which can be tesselated via an egg-box pattern, in the limit for the characteristic length of every pyramid going to zero. The proposed solution involves techniques similar to those used in two-scale asymptotic homogenization processes, where the result of the limiting procedure is a continuous model.

Let us start with the deformation of a single pyramid forming the egg-box pattern, as shown in Fig. 2.16, whose characteristic length (the dimension of the edge of the pyramid) is r. Each pyramid can undergo one deformation mode which is described by α, one of the angles of its quadrilateral base. The other angle which characterizes the mode is α^* and it is related to α by the following relation:

$$2\cos\left(\frac{\alpha}{2}\right)\cos\left(\frac{\alpha^*}{2}\right) = 1\,.$$

Let us now consider a periodic array made up of alternating pyramids, oriented in two opposite directions. If one knows the positions of all the vertices disposed along two consecutive diagonals of the structure it is possible to construct the whole set of vertices of the periodic structure. Therefore a configuration of the egg-box tessellation is parameterised by two families of vectors, $A = \{a_n\}$ and $B = \{b_n\}$, connecting the vertices on the two chosen diagonals. On the other hand, because of the periodicity of

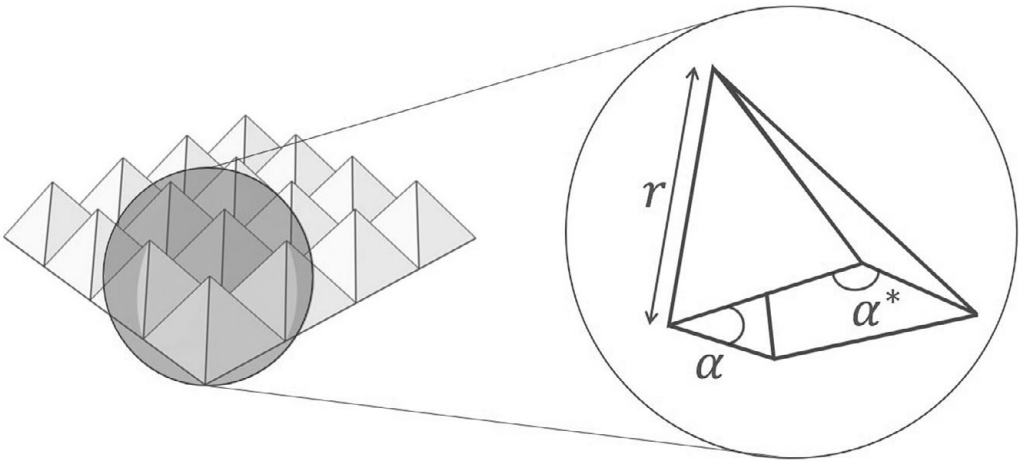

Figure 2.16 A basic pyramid of an egg-box tessellation. The parameters which characterize the structure are the length of the edges, r, and the folding angles α and α^*, which, however, are not independent.

the array, one can represent the pattern by means of a set of equivalent vertices, denoted by $V_{i,j}$, all disposed on the same plane.

The problem which has been described in [102] is the fit of a surface Σ by means of a suitable egg-box tessellation. The fit is built as follows. First of all, one point $M \in \Sigma$ is chosen: it coincides with one vertex of the egg-box. A portion $S(M) = \{V_{i,j}, A(M), B(M)\}$ of this egg-box is deformed in order to fit a small neighbourhood of M on the surface Σ. The same procedure is extended to the other points of the surface and the local egg-boxes are all glued together in order to obtain a single tessellation. Then, we consider the rescaled egg-box $rS^r(M) = \{rV_{i,j}(A^r(M), B^r(M))\}$, and it will once more fit a small neighbourhood of the point $M \in \Sigma$. This procedure, repeated for all the points of the surface, will produce a rescaled fit. Eventually, one takes the limit for $r \to 0$. As we have already anticipated, this procedure is analogous to the two-scale asymptotic expansions typical of homogenization procedures (see for instance [103]), where there is a slow-varying variable, the point M in this case, and one fast variable, the one characterizing the egg-box.

Let us now consider the fitted neighbourhood $rS^r(M)$ of a point M. As $r \to 0$, the egg-box converges to a single point and we require that the finite differences between two subsequent vertices tend to a basis for the tangent space to Σ at the point M, independently of the pair (i, j). We can write this condition as follows:

$$\frac{rV_{i+1,j} - rV_{i,j}}{r} \to_{r\to 0} \partial_x \theta(x, y) \equiv \theta_x(x, y), \tag{2.9}$$

$$\frac{rV_{i,j+1} - rV_{i,j}}{r} \to_{r\to 0} \partial_y \theta(x, y) \equiv \theta_y(x, y), \tag{2.10}$$

where we have supposed the existence of a smooth parameterisation $\theta(x, y)$ of the surface Σ and the pair (x, y) labels the point M (see Fig. 2.17). In order to find some conditions according to which a surface can be tessellated via the previous procedure,

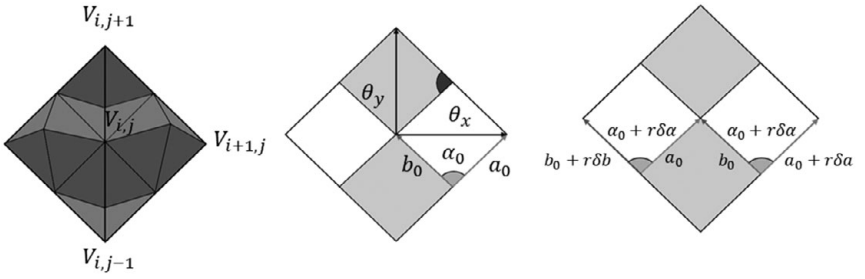

Figure 2.17 A series showing the kinematical characteristics of the homogenization procedure for an egg-box tessellation. On the left a set of equivalent vertices in the neighbourhood of $V_{i,j}$. The figure in the centre represents the homogenized limit with the tangent vector θ_x and θ_y, and the unit vectors a_0 and b_0. On the right the effect of the rescaling in r.

we go on to consider the metric and the second fundamental form. The components of the metric tensor can be written in terms of the tangent vectors as follows:

$$G(x,y) = \begin{pmatrix} \langle \theta_x(x,y), \theta_x(x,y) \rangle & \langle \theta_x(x,y), \theta_y(x,y) \rangle \\ \langle \theta_y(x,y), \theta_x(x,y) \rangle & \langle \theta_y(x,y), \theta_y(x,y) \rangle \end{pmatrix}, \tag{2.11}$$

where the brackets denote the Euclidean scalar product in $\mathbb{R}^3$. Because of the periodicity of the structure, the limiting families of vectors $A^0(M)$ and $B^0(M)$ will be described in terms of a single degree of freedom, i.e. the angle $\alpha(x,y)$ which is one of the internal angles of the deformed pyramid. In terms of this angle, the metric tensor can be expressed as follows:

$$I(\alpha) = \begin{pmatrix} 4\sin^2\left(\frac{\alpha}{2}\right) & 0 \\ 0 & 4\sin^2\left(\frac{\alpha^*}{2}\right) \end{pmatrix}. \tag{2.12}$$

From this expression the in-plane Poisson's ratio is very easily computed, which can be written in terms of the following relation:

$$\nu_{\text{in}} = -\frac{\sin\left(\frac{\alpha}{2}\right)}{\sin\left(\frac{\alpha^*}{2}\right)} \frac{d\sin\left(\frac{\alpha}{2}\right)}{d\sin\left(\frac{\alpha^*}{2}\right)} = \frac{\tan^2\left(\frac{\alpha^*}{2}\right)}{\tan^2\left(\frac{\alpha}{2}\right)}. \tag{2.13}$$

We remark that it is a positive quantity, in contrast to the auxetic in-plane behaviour of the Miura-ori tessellation.

Let us now consider the second fundamental form of the surface Σ. It involves the second derivative of the parameterisation θ and, therefore, it can be approximated by using second-rank finite differences. In particular as $r \to 0$ one requires that these quantities approach the second-order partial derivatives of the parameterisation, i.e.

$$\frac{\Delta_{xx} r V_{i,j}}{r^2} \to_{r\to 0} \phi_{xx}(x,y), \tag{2.14}$$

$$\frac{\Delta_{yy} r V_{i,j}}{r^2} \to_{r\to 0} \phi_{yy}(x,y), \tag{2.15}$$

$$\frac{\Delta_{xy} r V_{i,j}}{r^2} \to_{r\to 0} \phi_{xy}(x,y), \tag{2.16}$$

where Δ_{ij} is the second-rank finite difference operator. To the first order in the scaling parameter r, this set of equations can be written as a linear system in the first-order corrections to the set of vertices of the limiting egg-box pattern. In particular, the independent corrections form a set of five degrees of freedom, which are illustrated in Fig. 2.17:

- $\delta\alpha$ is the variation of the angle $\alpha(x, y)$ between the vectors $A^0(M)$ and $B^0(M)$;
- the vector δa, which is orthogonal to the vectors $a_n^0(M) \in A^0(M)$ and corrects them;
- the vector δb, which is orthogonal to the vectors $b_n^0(M) \in B^0(M)$ and corrects them.

As far as curvatures are concerned, there is no dependence on the correction $\delta\alpha$ and one can actually write:

$$\boldsymbol{\theta^{(2)}} = Q\boldsymbol{\delta V}, \tag{2.17}$$

where $\boldsymbol{\theta^{(2)}}$ is the vector containing all the second derivatives of the parameterisation and $\boldsymbol{\delta V}$ is the vector containing the corrections δa and δb.

In addition to this set of equations, there are five compatibility conditions which the second order derivatives have to satisfy: four of these conditions involve the Christoffel symbols of the Levi-Civita connection of the metric tensor $I(\alpha)$, whereas the last condition involves the out-of-plane Poisson's ratio. Indeed, one has that

$$\nu_{\text{out}} = -\frac{k_x}{k_y}\,.$$

If one considers the second fundamental form of the surface:

$$R = \begin{pmatrix} L & M \\ M & N \end{pmatrix} = \begin{pmatrix} \langle \theta_{xx}, \hat{n} \rangle & \langle \theta_{xy}, \hat{n} \rangle \\ \langle \theta_{xy}, \hat{n} \rangle & \langle \theta_{yy}, \hat{n} \rangle \end{pmatrix}, \tag{2.18}$$

where $\hat{n}$ is the positive normal to the surface, one can write the two curvatures k_x and k_y according to the following formulas:

$$k_x = \frac{L}{||\theta_x||^2}, \qquad k_y = \frac{N}{||\theta_y||^2}\,. \tag{2.19}$$

Therefore, one has that the second derivatives have to satisfy the constraint:

$$\nu_{\text{out}} = -\frac{\tan^2\left(\frac{\alpha^*}{2}\right)}{\tan^2\left(\frac{\alpha}{2}\right)} = -\nu_{\text{in}}\,.$$

Note that, again, the tessellated surfaces have an out-of-plane Poisson's ratio which is opposite to the in-plane Poisson's ratio.

Since the second order derivatives satisfy these five additional linear compatibility relations, they belong to the rank of the matrix Q.

In short, one can state that if a surface Σ can be fitted asymptotically via an egg-box pattern, then there exists a parameterisation θ of Σ and two functions α and α^*

satisfying $2\cos\left(\frac{\alpha}{2}\right)\cos\left(\frac{\alpha^*}{2}\right)=1$ such that metric tensor and second fundamental form assume the form written in Eqs. (2.12) and (2.18), with the compatibility condition

$$L = N\frac{\cos^2\left(\frac{\alpha}{2}\right)}{\cos^2\left(\frac{\alpha^*}{2}\right)}\,. \tag{2.20}$$

An equivalent solution can be given if one replaces the parameterisation θ with a set of three functions (L, M, N) satisfying the Gauss–Mainardi–Codazzi equations. This set of PDE has the following form:

$$\frac{LN-M^2}{16\sin^2(\alpha/2)\sin^2(\alpha^*/2)} = -\frac{1}{8\sin(\alpha/2)\sin(\alpha^*/2)}\left[\left(\frac{(\sin^2(\alpha^*/2))_x}{\sin(\alpha/2)\sin(\alpha^*/2)}\right)_x + \left(\frac{(\sin^2(\alpha/2))_y}{\sin(\alpha/2)\sin(\alpha^*/2)}\right)_y\right]$$

$$L_y - M_x = \frac{\left(\sin^2(\alpha/2)\right)_y}{2\sin^2(\alpha/2)}L + \left(\frac{(\sin^2(\alpha^*/2))_x}{2\sin^2(\alpha^*/2)} - \frac{(\sin^2(\alpha/2))_x}{2\sin^2(\alpha/2)}\right)M + \frac{\left(\sin^2(\alpha/2)\right)_y}{2\sin^2(\alpha^*/2)}N$$

$$M_y - N_x = -\frac{\left(\sin^2(\alpha^*/2)\right)_x}{2\sin^2(\alpha/2)}L + \left(\frac{(\sin^2(\alpha^*/2))_y}{2\sin^2(\alpha^*/2)} - \frac{(\sin^2(\alpha/2))_y}{2\sin^2(\alpha/2)}\right)M - \frac{\left(\sin^2(\alpha^*/2)\right)_x}{2\sin^2(\alpha^*/2)}N$$

subject to the constraint (2.20).

Therefore, by means of the procedure outlined in this sub-section, we have shown how to convert the problem of finding a suitable tessellation of a given surface into a homogenized problem consisting of the search for continuous fields satisfying a specific set of PDEs. Finding solutions of these equations is not an easy task. A series of solutions, obtained starting with some symmetry requirements, can be found in [102].

Theory Driven Design: Cauchy Modelling

In this sub-section we will particularly focus on the work by Milton and Cherkaev, dating back to 1992 [21], aimed at addressing some key questions regarding the synthesis problem of (extremal) metamaterials. Before entering into the details, however, let us make some general observations on the characteristics which a continuum model should possess in order to properly describe the properties of extremal metamaterials.

Let $\chi : \mathcal{B} \subset \mathcal{E} \to \mathcal{E}$ be a placement field, and let the pair $(\mathcal{E}, \mathbb{R}^3)$ be the Euclidean three-dimensional affine space into which the continuum $\mathcal{B}$ is embedded. If $F = \frac{\partial \chi^i}{\partial X^A} e_i \otimes e^A$ is the gradient of the displacement field (lower case index refers to the current configuration and uppercase index refers to the reference one; this being a standard notation we omit further explanation), a measure of the deformation of the body is represented by the second-rank tensor $G = \frac{1}{2}\left(F^T F - I\right)$. Let $\mathbf{p}$ and $\mathbf{q}$ be

two orthogonal material vectors applied to a given point $X \equiv (X^A)$ in the reference configuration of the continuum. In the current configuration they are deformed into the new vectors $F\mathbf{p}, F\mathbf{q}$ which, in general, are no longer orthogonal: the angle between them is $\frac{\pi}{2} - \gamma$. The shear strain with respect to $\mathbf{p}$ and $\mathbf{q}$ is represented by the angle γ, which satisfies the following relation:

$$\sin(\gamma) = \cos\left(\frac{\pi}{2} - \gamma\right) = \frac{F\mathbf{p} \cdot F\mathbf{q}}{||F\mathbf{p}||||F\mathbf{q}||} = \frac{\mathbf{q}^T(2G + I)\mathbf{p}}{||F\mathbf{p}||||F\mathbf{q}||}. \tag{2.21}$$

A Cauchy model describing an extremal metamaterial has to satisfy prescribed relations. For instance, in the case of dilational metamaterials, where the only possible deformation is a volume modification which preserves the shape of the system, they need to have zero shear strain for all pairs of orthogonal material directions. Therefore, the strain tensor G has to be equal to the identity tensor times a constant number.

Let us now outline the approach advanced by Milton and Cherkaev, which has led to introducing extremal metamaterials. They have developed their theory in the context of Cauchy linear elasticity: 'it is well known that elasticity tensors are positive definite, but what about the converse question: given an arbitrary positive definite fourth order tensor C satisfying the usual symmetries of elasticity tensors, is it possible to manufacture a material with C as its elasticity tensor?' The answer is affirmative: laminates made made up of suitably designed layers of two different materials, one very compliant and the other very stiff, have effective elasticity tensors which can generate all the thermodynamically admissible elasticity tensors. An alternative solution to the problem, developed contemporarily but independently, was advanced by Sigmund [104], but his approach was based on numerical techniques. It is worth remarking that, since the whole description is confined to the linear regime, some of the presented microstructures can undergo instability phenomena after some critical loads (whose description is therefore beyond the scope of the present analysis). For, we will consider only bi-dimensional elastic continua: the three dimensional case is an almost straightforward generalization. Following [37], we represent strain and stress tensors in Voigt notation, that is by means of a three-dimensional vector containing the three independent coordinates of a symmetric second order tensor in a bi-dimensional space. Consequently, the elastic tensor in Voigt notation, is represented via a 3×3 matrix which relates the vector $\boldsymbol{\sigma}$ (stress) to the vector $\boldsymbol{\epsilon}$ (strain), via the following formula:

$$\boldsymbol{\sigma} = C\boldsymbol{\epsilon}\,.$$

From the positivity and symmetry of the matrix C, one derives that it can be diagonalized via an orthogonal matrix Q and its eigenvalues will be all positive, i.e.

$$C = Q^T \begin{pmatrix} \lambda_1 & 0 & 0 \\ 0 & \lambda_2 & 0 \\ 0 & 0 & \lambda_3 \end{pmatrix} Q\,.$$

Eigenmodes of C corresponding to very small (with respect to others) eigenvalues are called easy modes or strains; if the eigenvalue is actually zero they are usually called floppy modes. Corresponding to the number of easy modes, extremal metamaterials are divided into null-mode, uni-mode, bi-mode and tri-mode materials, as discussed

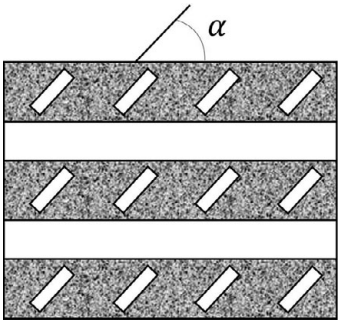

Figure 2.18 Oblique box metamaterial made up of alternating layers: white parts are a stiff component, whereas dotted areas are a compliant one. The angle α parameterises the structure by specifying the inclination of the small stiff plates immersed in the compliant matrix.

previously. If one considers three-dimensional elasticity, one can have up to six easy modes. As already stated, we will limit our analysis to plane strain elasticity. In particular, we will provide a detailed description of how to design uni-mode metamaterials with Poisson's ratio close to $\nu = -1$. Analogous ways of reasoning, indeed, lead to bi-mode metamaterials, as shown in [37]. Before concluding the current sub-section, however, we discuss how these metamaterials allow for the generation of the whole set of admissible, i.e. positive definite, elasticity tensors.

Let us consider the microstructure shown in Fig. 2.18, also called an 'oblique box' microstructure. It is a laminated composite made up of several horizontal layers: the white stripes are a stiff material, whereas the dotted regions are a compliant material. There are two types of alternating layers: one is made up only of stiff material, the other one contains an array of stiff plates embedded in the compliant phase and arranged so as to form an angle α with respect to the horizontal axis. This is an example of a uni-mode material with the easy mode represented by the following strain tensor:

$$a \begin{pmatrix} 0 & -\sin\alpha \\ -\sin\alpha & 2\cos\alpha \end{pmatrix}, \tag{2.22}$$

where a is an arbitrary constant. The limiting cases – α varies between 0 and $\frac{\pi}{2}$ – are represented by the following strains:

$$\begin{pmatrix} 0 & 0 \\ 0 & -2a \end{pmatrix} \qquad \begin{pmatrix} 0 & -a \\ -a & 0 \end{pmatrix}. \tag{2.23}$$

Applying a rotation to (2.22) one can obtain all the uni-mode materials with an easy strain represented by the matrix

$$\begin{pmatrix} \epsilon_{xx} & \epsilon_{xy} \\ \epsilon_{xy} & \epsilon_{yy} \end{pmatrix} \tag{2.24}$$

with non-positive determinant. In particular, by starting with a given matrix ϵ of the form:

$$\begin{pmatrix} \epsilon_{\xi\xi} & \epsilon_{\xi\eta} \\ \epsilon_{\eta\xi} & \epsilon_{\eta\eta} \end{pmatrix}, \tag{2.25}$$

the rotated one can be obtained by means of the following transformation rule:

$$\begin{pmatrix} \epsilon_{xx} & \epsilon_{xy} \\ \epsilon_{xy} & \epsilon_{yy} \end{pmatrix} = R^T \begin{pmatrix} 0 & \epsilon_{\xi\eta} \\ \epsilon_{\eta\xi} & \epsilon_{\eta\eta} \end{pmatrix} R\,, \tag{2.26}$$

where R is a given rotation matrix depending on an angle ϑ. Therefore, the resulting equation can be written as follows:

$$\begin{pmatrix} \epsilon_{xx} & \epsilon_{xy} \\ \epsilon_{xy} & \epsilon_{yy} \end{pmatrix} = \begin{pmatrix} -\epsilon_{\xi\eta}\sin(2\vartheta) + \epsilon_{\eta\eta}\sin^2(\vartheta) & \frac{1}{2}\left(2\epsilon_{\xi\eta}\cos(2\vartheta) - \epsilon_{\eta\eta}\sin(2\vartheta)\right) \\ \frac{1}{2}\left(2\epsilon_{\xi\eta}\cos(2\vartheta) - \epsilon_{\eta\eta}\sin(2\vartheta)\right) & \epsilon_{\eta\eta}\cos^2(\vartheta) + \epsilon_{\xi\eta}\sin(2\vartheta) \end{pmatrix}.$$

However, there are still some missing uni-mode materials. Indeed, all the materials with easy strain possessing a positive determinant are not described by this scheme. Among these uni-mode materials there are also dilational metamaterials, where the easy strain is proportional to the identity. In order to obtain such a family, let us consider again the "oblique box" in Fig. 2.18 and let us mirror it with respect to a plane orthogonal to the horizontal lattices. The new strain, therefore, will be written as follows:

$$\epsilon^{(I)} = \begin{pmatrix} \epsilon_{xx} & -\epsilon_{xy} \\ -\epsilon_{xy} & \epsilon_{yy} \end{pmatrix}. \tag{2.27}$$

If we now slice both the original and the mirrored material, we can form a new composite by rotating the slices and arranging them in such a way that the stiff layers create a herringbone pattern, with the re-entrant ribs typical of an auxetic behaviour. An illustration of the resulting microstructure is shown in Fig. 2.19.

The easy strain of the resulting composite can be expressed as the sum of the average of strain ϵ and the strain $\epsilon^{(I)}$, i.e. one gets the following expression:

$$\epsilon' = \frac{\left(\epsilon + \epsilon^{(I)}\right)}{2} = \begin{pmatrix} \epsilon_{xx} & 0 \\ 0 & \epsilon_{yy} \end{pmatrix}. \tag{2.28}$$

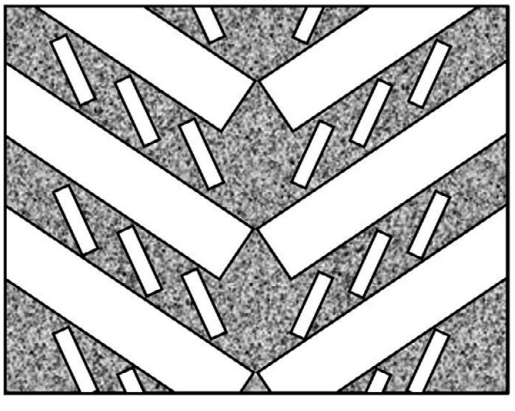

Figure 2.19 A uni-mode metamaterial whose easy mode has negative determinant: slices of an "oblique box," suitably arranged, produced this laminate with a herringbone pattern.

Consequently, a suitable choice of the parameters α, ϑ, c, makes it possible to obtain easy strain proportional to the identity. Eventually, the condition $\epsilon_{xx} = \epsilon_{yy}$ can be written as follows:

$$-2\epsilon_{\xi\eta}\sin(2\vartheta) = \epsilon_{\eta\eta}\cos(2\vartheta)\,.$$

Second Gradient Models for the Macroscopic Description of Microstructured Materials

Second gradient continua, i.e. continua whose deformation energy depends on the second gradient of displacement (or, equivalently, of placement), may arise in the homogenization process of microstructured materials, thus describing the emerging behaviour of such systems at macro-scale. There are many examples of second gradient materials which can be obtained as homogenized limits of suitable microstructured metamaterials [115–122]. A paradigmatic example is given by pantographic lattices. Here we will review an approach firstly introduced for such structures in [123] and subsequently investigated in [133, 200] (in such works modelling at micro-scale – i.e. the Hencky-type spring model presented here and a more refined Cauchy one – and at macro-scale as derived by homogenization have been compared, see also Fig. 2.22). Starting from a discrete Hencky-type micro model, a 2D continuum macro-model is derived in this appproach via suitable heuristic micro–macro identification procedures. Trying to comply with the experimental evidence reported in [123] and in [51], extension of fibres is taken into account by connecting adjacent material particles belonging to the same fibre-direction with extensional springs at micro-scale.

Micro Model

To account for the fact that such materials show two favoured material directions we introduce a Lagrangian Cartesian orthonormal coordinate system whose associated basis of unit vectors is $(\mathbf{D}_1, \mathbf{D}_2)$, constituted by two orthonormal vectors which represent the directions of the families of fibres constituting the pantographic structure in the reference configuration.

In such a configuration the lattice body points are located at the positions

$$P_{i,j} = (i\varepsilon, j\varepsilon), \quad i = 0, 1, \ldots, N \text{ and } j = 0, 1, \ldots, M, \tag{2.29}$$

and $p_{i,j}$ denotes the current configuration position of the body point placed at $P_{i,j}$ in the reference configuration. The body points at the nodes $P_{i,j}$ are connected by extensional springs along each of the coordinate lines (see Figs. 2.20 and 2.21) and their deformation energies depend on the distances between adjacent contiguous points in the current configuration, i.e. on the distance between $p_{i,j}$ and $p_{i,j+1}$ for those fibres parallel to $\mathbf{D}_1$ in the reference configuration and on the distance between $p_{i,j}$ and $p_{i+1,j}$ for those fibres parallel to $\mathbf{D}_2$ in the reference configuration. The first kind of extensional spring is characterized by the stiffness $K^1_{i,j}$ and the second kind by the stiffness $K^2_{i,j}$. Such extensional stiffnesses are related to the extensional behaviour of the two families of fibres. As mentioned before, at each node there are also three rotational springs whose deformation energies depend respectively on the angles.

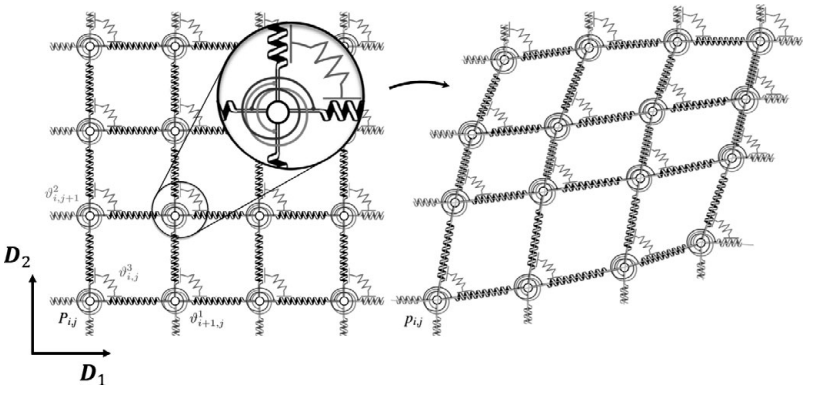

Figure 2.20 Reference and deformed configurations for micro-model of a pantographic sheet with a detail of the three rotational springs employed [123].

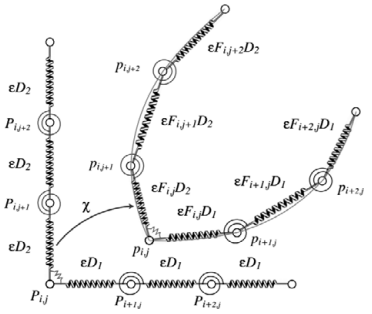

Figure 2.21 Hencky-type discrete micro-model of a pantographic sheet: kinematics [123].

1. $\vartheta^1_{i,j}$ formed by the vectors $p_{i-1,j} - p_{i,j}$ and $p_{i+1,j} - p_{i,j}$,
2. $\vartheta^2_{i,j}$ formed by the vectors $p_{i,j-1} - p_{i,j}$ and $p_{i,j+1} - p_{i,j}$,
3. $\vartheta^3_{i,j}$ formed by the vectors $p_{i,j+1} - p_{i,j}$ and $p_{i+1,j} - p_{i,j}$.

Thus, such a discrete model can be regarded as obtained by hinging at their intersection points two orthogonal families of straight discrete Elasticae. The postulated deformation energy for the micro Lagrangian discrete system having its configuration specified by the set of Lagrangian parameters $\{p_{i,j}\}$ is

$$
\begin{aligned}
U(\{p_{i,j}\}) = &\sum_j \sum_i \frac{k^1_{i,j}}{2}(\|p_{i+1,j} - p_{i,j}\| - \varepsilon)^2 + \sum_j \sum_i b^1_{i,j}(\cos\vartheta^1_{i,j} + 1) \\
&+ \sum_j \sum_i \frac{k^2_{i,j}}{2}(\|p_{i,j+1} - p_{i,j}\| - \varepsilon)^2 + \sum_j \sum_i b^2_{i,j}(\cos\vartheta^2_{i,j} + 1) \\
&+ \sum_j \sum_i \frac{b^3_{i,j}}{2}\left|\vartheta^3_{i,j} - \frac{\pi}{2}\right|^{\xi}. \qquad (2.30)
\end{aligned}
$$

It is clear that, on the one hand, the stiffnesses $b^1_{i,j}$s and $b^2_{i,j}$s are related, respectively, to the bending behaviour of the two families of fibres and that the stiffnesses $b^3_{i,j}$s, on the other hand, are related to the torsional stiffness of the pivots connecting the two families of fibers, ξ being a parameter which is equal to 2 in the simplest (materially linear) case.

Macro Model

According to the nomenclature introduced previously, let us now consider a 2D continuum whose reference shape is given by a rectangular domain $\Omega = [0, N\varepsilon] \times [0, M\varepsilon] \subset \mathbb{R}^2$. By assuming planar motions, the current shape of Ω is described by the suitably regular macro placement $\boldsymbol{\chi} : \Omega \to \mathbb{R}^2$. As before, we now have to specify a kinematical map and we choose $p_{i,j} = \boldsymbol{\chi}(P_{i,j}) \quad \forall i = 1, \ldots, N, \ \forall j = 1, \ldots, M$.

Assuming that $\boldsymbol{\chi}(\cdot)$ is at least twice differentiable at $P_{i,j}$s we can perform the following second order order approximations:

$$\begin{aligned}
\|p_{i+1,j} - p_{i,j}\| &= \|\boldsymbol{\chi}(P_{i+1,j}) - \boldsymbol{\chi}(P_{i,j})\| \backsimeq \varepsilon \|\mathbf{F}(P_{i,j})\mathbf{D}_1 + \frac{\varepsilon}{2}\nabla\mathbf{F}(P_{i,j})|\mathbf{D}_1 \otimes \mathbf{D}_1\|, \\
\|p_{i,j+1} - p_{i,j}\| &= \|\boldsymbol{\chi}(P_{i,j+1}) - \boldsymbol{\chi}(P_{i,j})\| \backsimeq \varepsilon \|\mathbf{F}(P_{i,j})\mathbf{D}_2 + \frac{\varepsilon}{2}\nabla\mathbf{F}(P_{i,j})|\mathbf{D}_2 \otimes \mathbf{D}_2\|,
\end{aligned} \tag{2.31}$$

where $\mathbf{F}$ is the deformation gradient $\nabla\boldsymbol{\chi}$ and the reader is referred to the original papers [123, 133, 200] for further details.

Equations (2.31) have been used for the homogenization procedure of two addends of (2.30). In order to address the homogenization of the remaining terms we consider expressing the cosines of the angles $\vartheta^\alpha_{i,j}$ ($\alpha = 1, 2$) and $\vartheta^3_{i,j}$ as functions of the macro placement $\boldsymbol{\chi}$. Using analogous Taylor's approximations to those in (2.31) and neglecting $o(\varepsilon^2)$-terms, we get

$$\begin{aligned}
&\cos\vartheta^\alpha_{i,j} \\
&\quad = \frac{\left[-\mathbf{F}(P_{i,j})\mathbf{D}_\alpha + \frac{\varepsilon}{2}\nabla\mathbf{F}(P_{i,j})|\mathbf{D}_\alpha \otimes \mathbf{D}_\alpha\right] \cdot \left[\mathbf{F}(P_{i,j})\mathbf{D}_\alpha + \frac{\varepsilon}{2}\nabla\mathbf{F}(P_{i,j})|\mathbf{D}_\alpha \otimes \mathbf{D}_\alpha\right]}{\| - \mathbf{F}(P_{i,j})\mathbf{D}_\alpha + \frac{\varepsilon}{2}\nabla\mathbf{F}(P_{i,j})|\mathbf{D}_\alpha \otimes \mathbf{D}_\alpha\| \|\mathbf{F}(P_{i,j})\mathbf{D}_\alpha + \frac{\varepsilon}{2}\nabla\mathbf{F}(P_{i,j})|\mathbf{D}_\alpha \otimes \mathbf{D}_\alpha\|} \\
&\quad \approx \mathbf{c}_{ij|\alpha} \cdot \mathbf{c}_{ij|\alpha} - (\mathbf{e}_{ij|\alpha} \cdot \mathbf{c}_{ij|\alpha})^2 \frac{\varepsilon^2}{2} - 1 \ \alpha = 1, 2,
\end{aligned} \tag{2.32}$$

where we defined the vectors

$$\mathbf{e}_{ij|\alpha} = \frac{\mathbf{F}(P_{i,j})\mathbf{D}_\alpha}{\|\mathbf{F}(P_{i,j})\mathbf{D}_\alpha\|}, \qquad \mathbf{c}_{ij|\alpha} = \frac{\nabla\mathbf{F}(P_{i,j})|\mathbf{D}_\alpha \otimes \mathbf{D}_\alpha}{\|\mathbf{F}(P_{i,j})\mathbf{D}_\alpha\|} \qquad \alpha = 1, 2.$$

We have that

$$\begin{aligned}
\mathbf{c}_{ij|\alpha} \cdot \mathbf{c}_{ij|\alpha} - (\mathbf{e}_{ij|\alpha} \cdot \mathbf{c}_{ij|\alpha})^2 &= \mathbf{c}_{ij|\alpha} \cdot \mathbf{c}_{ij|\alpha} - (\mathbf{e}_{ij|\alpha} \cdot \mathbf{c}_{ij|\alpha})(\mathbf{e}_{ij|\alpha} \cdot \mathbf{c}_{ij|\alpha}) \\
&= [\mathbf{c}_{ij|\alpha} - (\mathbf{e}_{ij|\alpha} \cdot \mathbf{c}_{ij|\alpha})\mathbf{e}_{ij|\alpha}] \cdot \mathbf{c}_{ij|\alpha} \\
&= \mathbf{c}_{ij|\perp} \cdot \mathbf{c}_{ij|\alpha} = \mathbf{c}_{ij|\alpha\perp} \cdot \mathbf{c}_{ij|\alpha\perp},
\end{aligned} \tag{2.33}$$

where $\mathbf{c}_{ij|\alpha\perp}$ is the orthogonal projection of $\mathbf{c}_{ij|\alpha}$ onto the direction given by $\mathbf{e}_{ij|\alpha}$ i.e. $\mathbf{c}_{ij|\alpha\perp} = \mathbf{c}_{ij|\alpha} - (\mathbf{e}_{ij|\alpha} \cdot \mathbf{c}_{ij|\alpha})\mathbf{e}_{ij|\alpha}$. Substituting (2.33) in (2.32) we finally get

$$\cos\vartheta^{\alpha}_{i,j}+1\approx(\mathbf{c}_{ij|\alpha\perp}\cdot\mathbf{c}_{ij|\alpha\perp})\frac{\varepsilon^2}{2}. \tag{2.34}$$

We now aim to express the product $\mathbf{c}_{ij|\alpha\perp}\cdot\mathbf{c}_{ij|\alpha\perp}$ appearing in (2.34) in terms of the kinematical descriptors of the macro model, i.e. the placement $\boldsymbol{\chi}$:

$$\begin{aligned}\mathbf{c}_{ij|\alpha\perp}\cdot\mathbf{c}_{ij|\alpha\perp}&=\mathbf{c}_{ij|\alpha}\cdot\mathbf{c}_{ij|\alpha}-(\mathbf{e}_{ij|\alpha}\cdot\mathbf{c}_{ij|\alpha})^2\\&=\frac{\|\nabla\mathbf{F}(P_{i,j})|\mathbf{D}_\alpha\otimes\mathbf{D}_\alpha\|^2}{\|\mathbf{F}_{i,j}\mathbf{D}_\alpha\|^2}-\left(\frac{\mathbf{F}(P_{i,j})\mathbf{D}_\alpha\cdot\nabla\mathbf{F}(P_{i,j})|\mathbf{D}_\alpha\otimes\mathbf{D}_\alpha}{\|\mathbf{F}_{i,j}\mathbf{D}_\alpha\|^2}\right)^2.\end{aligned} \tag{2.35}$$

We are therefore left with the following expression for $\cos\vartheta^{\alpha}_{ij}+1$:

$$\begin{aligned}&\cos\vartheta^{\alpha}_{i,j}+1\\&\quad\approx\left[\frac{\|\nabla\mathbf{F}(P_{i,j})|\mathbf{D}_\alpha\otimes\mathbf{D}_\alpha\|^2}{\|\mathbf{F}_{i,j}\mathbf{D}_\alpha\|^2}-\left(\frac{\mathbf{F}(P_{i,j})\mathbf{D}_\alpha\cdot\nabla\mathbf{F}(P_{i,j})|\mathbf{D}_\alpha\otimes\mathbf{D}_\alpha}{\|\mathbf{F}_{i,j}\mathbf{D}_\alpha\|^2}\right)^2\right]\frac{\varepsilon^2}{2}.\end{aligned} \tag{2.36}$$

In order to recast the micro energy in (2.30) as a function of the kinematical descriptors of the macro model we now try to express $\vartheta^3_{i,j}$ as a function of $\boldsymbol{\chi}$. We first compute $\cos\vartheta^3_{i,j}$:

$$\begin{aligned}\cos\vartheta^3_{i,j}&=\frac{\big[\boldsymbol{\chi}(P_{i+1,j})-\boldsymbol{\chi}(P_{i,j})\big]\cdot\big[\boldsymbol{\chi}(P_{i,j+1})-\boldsymbol{\chi}(P_{i,j})\big]}{\|\boldsymbol{\chi}(P_{i+1,j})-\boldsymbol{\chi}(P_{i,j})\|\cdot\|\boldsymbol{\chi}(P_{i,j+1})-\boldsymbol{\chi}(P_{i,j})\|}\\&\approx\frac{\mathbf{F}(P_{i,j})\mathbf{D}_1\cdot\mathbf{F}(P_{i,j})\mathbf{D}_2}{\|\mathbf{F}(P_{i,j})\mathbf{D}_1\|\cdot\|\mathbf{F}(P_{i,j})\mathbf{D}_2\|}.\end{aligned} \tag{2.37}$$

By substituting (2.37) and (2.36) in (2.30) we get for the deformation energy of the micro model

$$\begin{aligned}U(\{p_{i,j}\})=&\sum_j\sum_i\sum_\alpha\frac{k^\alpha_{i,j}}{2}\varepsilon^2(\|\mathbf{F}(P_{i,j})\mathbf{D}_\alpha+\frac{\varepsilon}{2}\nabla\mathbf{F}(P_{i,j})|\mathbf{D}_\alpha\otimes\mathbf{D}_\alpha\|-1)^2\\&+\sum_j\sum_i\sum_\alpha b^\alpha_{i,j}\left[\frac{\|\nabla\mathbf{F}(P_{i,j})|\mathbf{D}_\alpha\otimes\mathbf{D}_\alpha\|^2}{\|\mathbf{F}_{i,j}\mathbf{D}_\alpha\|^2}\right.\\&\qquad\left.-\left(\frac{\mathbf{F}(P_{i,j})\mathbf{D}_\alpha\cdot\nabla\mathbf{F}(P_{i,j})|\mathbf{D}_\alpha\otimes\mathbf{D}_\alpha}{\|\mathbf{F}_{i,j}\mathbf{D}_\alpha\|^2}\right)^2\right]\frac{\varepsilon^2}{2}\\&+\sum_j\sum_i\frac{b^3_{i,j}}{2}\left|\arccos\left(\frac{\mathbf{F}(P_{i,j})\mathbf{D}_1\cdot\mathbf{F}(P_{i,j})\mathbf{D}_2}{\|\mathbf{F}(P_{i,j})\mathbf{D}_1\|\cdot\|\mathbf{F}(P_{i,j})\mathbf{D}_2\|}\right)-\frac{\pi}{2}\right|^\xi,\end{aligned} \tag{2.38}$$

where $o(\varepsilon^2)$-terms have been neglected.

Rescaling the stiffnesses, i.e. specifying their dependence upon ε, as

$$k^\alpha_{i,j}=\mathbb{K}^\alpha_e;\ b^\alpha_{i,j}=\mathbb{K}^\alpha_b;\ b^3_{i,j}=\mathbb{K}_p\varepsilon^2,$$

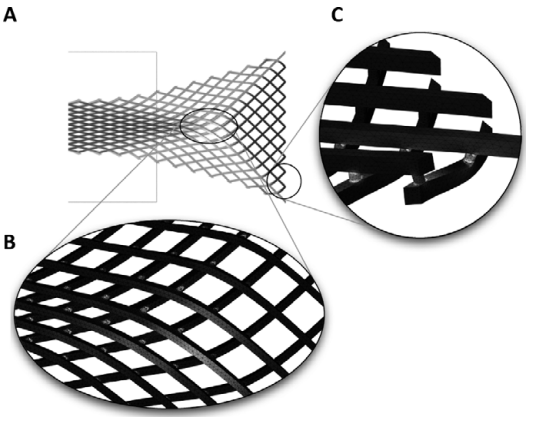

Figure 2.22 Rectangle bias pantographic sheet specimen subject to an extension test. Comparison between the deformed shapes of the homogenized 2D in-plane continuum (macro-model derived from Hencky meso-model) and 3D Cauchy modelling (micro-model) using isotropic hyperelastic material (top-left) [133]. Macroscopic continuum modelling is evaluated at material lines corresponding to fibres in the 3D model, and colours represent strain energy density for the macroscopic continuum model. Results for the two kinds of modelling overlap. Remaining plots show zoomed deformed configurations for Cauchy modelling. Colours represent strain energy density.

$\mathbb{K}_e^\alpha$, $\mathbb{K}_b^\alpha$ and $\mathbb{K}_p$ being independent of ε, and homogenizing, i.e. letting $\varepsilon \to 0$, we are finally left with the macro deformation energy

$$\begin{aligned} U(\boldsymbol{\chi}(\cdot)) = &\int_\Omega \sum_\alpha \frac{\mathbb{K}_e^\alpha}{2} \|\mathbf{F}\mathbf{D}_\alpha - 1\|^2 \mathrm{d}S \\ &+ \int_\Omega \sum_\alpha \frac{\mathbb{K}_b^\alpha}{2} \left[\frac{\|\nabla\mathbf{F}|\mathbf{D}_\alpha \otimes \mathbf{D}_\alpha\|^2}{\|\mathbf{F}\mathbf{D}_\alpha\|^2} - \left(\frac{\mathbf{F}\mathbf{D}_\alpha \cdot \nabla\mathbf{F}|\mathbf{D}_\alpha \otimes \mathbf{D}_\alpha}{\|\mathbf{F}\mathbf{D}_\alpha\|^2} \right)^2 \right] \mathrm{d}S \\ &+ \int_\Omega \frac{\mathbb{K}_p}{2} \left| \arccos\left(\frac{\mathbf{F}\mathbf{D}_1 \cdot \mathbf{F}\mathbf{D}_2}{\|\mathbf{F}\mathbf{D}_1\| \cdot \|\mathbf{F}\mathbf{D}_2\|} \right) - \frac{\pi}{2} \right|^\xi \mathrm{d}S. \end{aligned} \tag{2.39}$$

We note that $\|\mathbf{F}\mathbf{D}_\alpha - 1\|^2$ in the above formula is the stretch of material lines directed in the reference configuration along the fibres family α, while

$$\|\nabla\mathbf{F}|\mathbf{D}_\alpha \otimes \mathbf{D}_\alpha\|/\|\mathbf{F}\mathbf{D}_\alpha\| - \mathbf{F}\mathbf{D}_\alpha \cdot \nabla\mathbf{F}|\mathbf{D}_\alpha \otimes \mathbf{D}_\alpha/\|\mathbf{F}\mathbf{D}_\alpha\|^2 \tag{2.40}$$

depends upon the second gradient of the placement function and is the curvature of such material lines. We further note that a different elastic constitutive law could have been chosen in Eq. (2.30) for springs in the Hencky model. For example, instead of considering $(\cos\vartheta_{i,j}^\alpha + 1)$, we could have considered $(\vartheta_{i,j}^\alpha - \pi)^2$. Clearly, by Taylor expanding $(\cos\vartheta_{i,j}^\alpha$ in the neighbourhood of $\vartheta_{i,j}^\alpha = \pi$ up to $o(\vartheta_{i,j}^3)$, it is seen that up to $o(\vartheta_{i,j}^3)$ the two choices are equivalent. In order to homogenize $(\vartheta_{i,j}^\alpha - \pi)$ it is possible to exploit computations shown in Chapter 4, even if a different notation has been employed (cf. $\vartheta_{(i,j),\alpha}$).

2.2 Acoustic Metamaterials

2.2.1 Introduction

The definition of acoustic metamaterial was introduced for the first time by Walser [128] and can be efficaciously stated as *artificial materials synthesized with the aim of manipulating and controlling wave propagation*. Usually, according to the philosophy underlying the metamaterials' framework, non-standard behaviour at macro-scale is obtained by conceiving a microstructure constituted by an elementary cell that is periodically repeated.

The interest in acoustic metamaterials originates from results obtained studying the propagation of electromagnetic waves in optical metamaterials. Indeed, non-standard electromagnetic phenomena such as transformation optics, time reversal techniques, negative refraction index, sub-wavelength imaging, with their remarkable applications like cloaking, have acoustic and mechanical counterparts which could be of great interest.

The need to overcome issues in acoustic metamaterials exploiting Bragg scattering (i.e. diffraction) has driven the development of so-called locally resonant materials. This section will be mainly devoted to the description of this kind of metamaterials. The microstructure of locally resonant materials is usually conceived as a matrix of local resonators embedded in a host medium (theoretical and experimental interesting attempts can be found in [136–139, 139, 140]). By varying the parameters of the resonators and/or of the medium it is possible to tune the frequency band-gap(s) and/or other relevant macroscopic properties in a very precise way.

This section is organized in the following way. In Sub-section 2.2.2 a brief historical overview of developments in acoustic metamaterial research will be given. In Sub–section 2.2.3, we will discuss by means of simple arguments the modelling of single metamaterials cells, which is usually a key aspect in the understanding of the global material behaviour.

2.2.2 A Short Historical Overview

The field of acoustic metamaterials has been strongly inspired by phenomena observed in the propagation of electromagnetic waves.

The origin of the optical metamaterials field is usually traced back to the seminal paper (1967) by Victor Veselago, a Russian physicist who theoretically conjectured the existence of a material characterized by both negative magnetic permeability and electric permittivity. In particular, he proved that such an electromagnetic medium is characterized by a negative index of refraction [141]. This feature has several consequences, such as the possibility to build a flat convergent lens and to observe inverse Cerenkov radiation and inverse Doppler effect [142, 143]. However, the first steps toward the actual realization of Veselago's vision had to wait until the 1990s, thanks to the work of John Pendry (one of the pioneers of the metamaterials field) [144, 145] and only since 2000 have actual prototypes have been produced (see for instance [146, 147]).

Research aimed at replicating the fundamental principle of optical metamaterials for acoustic phenomena began in 2000 with the seminal paper by Liu *et al.* [148]. This work was probably the first attempt to exploit the analogies between acoustic and electromagnetic wave propagation phenomena. In particular, they provided the first experimental and numerical analyses of elastic wave propagation in a three-dimensional resonant structure made of an array of thin coated spheres. One of the first attempts at studying an acoustic medium analogous to Veselago's double negative optical material was reported in [149, 150], where a material with negative bulk modulus and negative density was studied. More recently, another example of such a material was proposed in [151] by Fang *et al.*, who studied experimentally the behaviour of a chain of split ring resonators filled with water, characterized by an effective negative stiffness, in an ultrasonic regime. On the theoretical side, Milton and collaborators did some remarkable work aimed at the modelling of acoustic metamaterials [152–154].

2.2.3 Locally Resonant Microstructures

Phenomena which occur in wave propagation through acoustic metamaterials strongly depend on the characteristic dimension of the internal microstructure and on the wavelength. The ratio between these two characteristic lengths makes it possible to divide acoustic metamaterials into two classes. If the characteristic length of the internal system is of the same order of magnitude as the wavelength, the material will behave like a so-called *diffraction* metamaterial (phononic crystals are an example of acoustic metamaterial intended to show its effects for wavelengths comparable with the characteristic length). On the other hand, if the microstructure characteristic length is much smaller than the relevant wavelengths (i.e. those for which interesting phenomena are to be exhibited), we refer to metamaterials based on *locally resonant* microstructures. A typical example is the microstructure realized by Liu *et al.* [148], which consists of an array of lead spheres coated with soft rubber and embedded in an epoxy matrix. From the technological point of view, this class of metamaterials can be exploited for several applications. Indeed, the particular arrangement of the microstructure can give rise to interesting features, like negative shear modulus, negative bulk modulus, negative effective mass, etc. In this section we will focus on this last class and we will sketch the main features of the mathematical modelling of their microstructure. The standard approach to describe the macroscopic behaviour of a metamaterial is to understand the basic working principle of a unit cell of the microstructure, and then to pass to a macroscopic description by means of a homogenization procedure. In the following subsections, we will describe how the features of locally resonant metamaterials are related to the microstructure. Then we will analyse some relevant homogenization procedures.

Negative Effective Mass

The first peculiar effect of locally resonant metamaterial that we want to investigate (we will partially follow the seminal book [155]) is the so-called effective negative mass

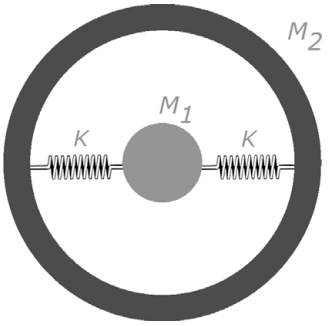

Figure 2.23 An elementary cell which exhibits negative effective mass in a particular frequency range.

(see for instance [149, 156]). The basic working principle of such structures can be exemplified by considering the microstructure in Fig. 2.23.

It is a mass–spring system, consisting of a small mass M_1 (spherical and modelled as a material particle), encapsulated into a hollow sphere of mass M_2 and connected to it by means of two springs with elastic constant K. The equations of motion of this system are:

$$\begin{aligned} M_1\ddot{x} &= 2K(X-x), \\ M_2\ddot{X} &= 2K(x-X), \end{aligned} \tag{2.41}$$

where we indicate with x and X the horizontal displacement of barycentres of masses M_1 and M_2, respectively. Since the resulting net force vanishes, the total linear momentum

$$P = M_1\dot{x} + M_2\dot{X} \tag{2.42}$$

is a constant of the motion. We consider harmonic solutions of Eq. (2.41), i.e.:

$$\begin{aligned} x(t) &= \bar{x}e^{i\omega t}, \\ X(t) &= \bar{X}e^{i\omega t}. \end{aligned} \tag{2.43}$$

By substituting them in the equations of motion (2.41) we obtain

$$M_1\omega^2\bar{x} = 2K(\bar{x}-\bar{X}), \tag{2.44}$$

from which we get

$$\frac{\bar{x}}{\bar{X}} = \frac{\omega_1^2}{\omega_1^2-\omega^2}, \tag{2.45}$$

where

$$\omega_1 = \sqrt{2\frac{K}{M_1}} \tag{2.46}$$

is called *resonance frequency*. The ratio of the total momentum P and the velocity $\dot{X}$ is called effective mass M_{eff} of the system. In this case it reads:

$$M_{\text{eff}} = M_1 \frac{\bar{x}}{\bar{X}} + M_2 \,. \tag{2.47}$$

By considering Eqs. (2.45) and (2.46), the previous expression becomes:

$$M_{\text{eff}} = M_1 \frac{\omega_1^2}{\omega_1^2 - \omega^2} + M_2 \,. \tag{2.48}$$

Looking at this expression we can note that the effective mass M_{eff} can be negative. In particular, it happens when

$$\omega_1 < \omega < \omega_1 \sqrt{\frac{M_1 + M_2}{M_2}}, \tag{2.49}$$

or equivalently when

$$K > \frac{1}{2}\mu\omega^2, \qquad \frac{K}{M_1} < \frac{\omega^2}{2}\,, \tag{2.50}$$

where μ indicates the reduced mass of the system:

$$\mu = \frac{M_1 M_2}{M_1 + M_2}. \tag{2.51}$$

By means of equations (2.50) it is possible to tune the system parameters to obtain an effective negative mass behaviour.

Now, let us consider a one-dimensional infinite array made by the periodic repetition of the cell in Fig. 2.23. The cells are connected by means of springs with stiffness k, and two hollow spheres are separated by a distance d, which is the length of undeformed springs (see Fig. 2.24).

If we indicate with r_i and $M_{\text{eff},i}$ the position and the effective mass of the ith cell, respectively, the system is governed by the following tri-diagonal autonomous linear system:

$$M_{\text{eff},i}\ddot{r} = k(r_{i-1} - 2r_i + r_{i+1}). \tag{2.52}$$

We want to compute the effective mass for this discrete system under the hypothesis $M_{\text{eff},i} = M_{\text{eff}}$, $\forall i$. From now on, we indicate the initial position of the ith cell with

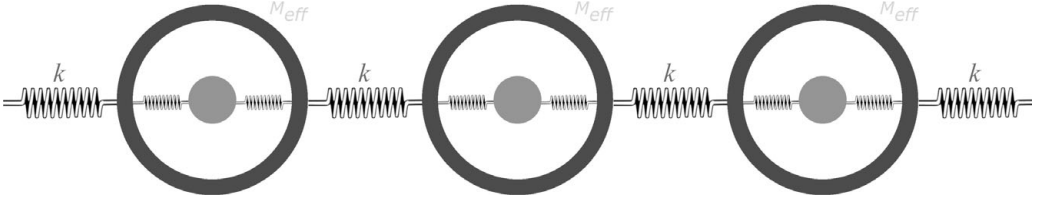

Figure 2.24 A periodic one-dimensional array of cells which exhibit negative effective mass.

x_i. By embedding the array in a continuous line $\mathcal{S}$, we are able to define the following Lagrangian field

$$u : \mathcal{S} \times [0, T] \longrightarrow \mathbb{R}, \tag{2.53}$$

with the (Piola's) ansatz $u(x_i, t) = r_i(t)$. It is possible to decompose the field u in Fourier series:

$$u(x, t) = \frac{1}{\sqrt{2\pi}} \int_{-\infty}^{+\infty} e^{iqx} \tilde{u}(q, t)\, dq, \tag{2.54}$$

where we have indicated with q the wave number of the corresponding Fourier mode and with $\tilde{u}(q, t)$ the Fourier transform of the function $u(x, t)$. According to the Piola's ansatz, we have that

$$\ddot{r}(x, t) = \frac{1}{\sqrt{2\pi}} \int_{-\infty}^{+\infty} e^{iqx} \ddot{u}(q, t)\, dq, \tag{2.55}$$

and by plugging it into Eq. (2.52) we obtain:

$$M_{\text{eff}} \int_{-\infty}^{+\infty} e^{iqx} \ddot{u}(q, t)\, dq = \int_{-\infty}^{+\infty} k e^{iqx} (2\cos(qd) - 2) u(q, t)\, dq, \tag{2.56}$$

and since the effective mass is uniform:

$$M_{\text{eff}} \ddot{u}(q, t) = 2k(\cos(qd) - 1) u(q, t). \tag{2.57}$$

Let us consider again a harmonic solution of (2.57), i.e.

$$u(q, t) = A(q) e^{i\omega t}. \tag{2.58}$$

By substituting it into Eq. (2.57) we obtain the dispersion relation of this discrete system:

$$M_{\text{eff}} \omega^2 = 2k(1 - \cos(qd)) = 4k \sin^2\left(\frac{qd}{2}\right). \tag{2.59}$$

If the frequency ω lies in the range of values that yields a negative effective mass, then q in the expression above has to be imaginary, so that $\sin\left(\frac{qd}{2}\right)$ is an imaginary number. An imaginary wave number implies that the superposition of harmonic waves gives rise to an evanescent wave, which means that the wave cannot propagate. This feature can be exploited for engineering applications. Indeed, by tuning the characteristic parameters of a single cell we can fix an interval of frequencies which yields negative effective mass. Equation (2.59) is telling us that this interval of frequencies corresponds to a band gap in the dispersion relation, meaning that waves with these frequencies cannot propagate in the medium. This result, which has been observed also experimentally (see for instance [157]), has led to several technological applications, like acoustic insulators [158].

Negative Bulk Modulus

Another peculiar feature of locally resonant acoustic metamaterials is the so-called negative effective bulk modulus. To show the basic working principle leading to negative effective bulk modulus, let us consider the microstructural unit cell depicted in Fig. 2.25.

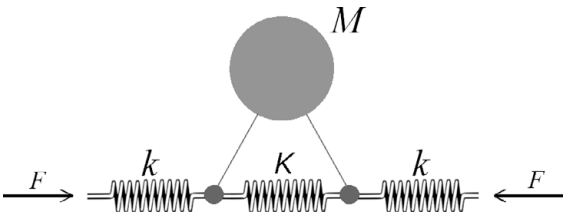

Figure 2.25 System which exhibits negative effective bulk modulus in a particular frequency range.

This system is made of a series of three massless springs, where the two extremal springs have stiffness k, while the central one has stiffness K. A key datum is that these springs are constrained to have only horizontal displacements. Two rigid bars are connected to the ends of the central spring by means of frictionless hinges. The two bars are in turn connected together at their top end by means of a mass M. We have denoted by $\bar{x}$ and x the horizontal displacement of the central and left springs, respectively. Two external forces $F(t)$ are horizontally applied to the two ends of the system, as shown in Fig. 2.25. The geometric constraint which obliges the springs to move only horizontally induces two vertical reaction forces to the hinges, which make the mass M move vertically. We will denote this vertical displacement as y, and the associated equation of motion is:

$$M\ddot{y} = f(t), \tag{2.60}$$

where we have expressed the vertical net force on M as $f(t)$. At both ends of the springs, we have:

$$F(t) = k(x(t) - \bar{x}(t)). \tag{2.61}$$

If we now consider only small displacements $\bar{x}$, the angle between the springs and the bars, say α, can be approximated as a constant and we have that

$$y(t) = \bar{x}\tan\alpha, \tag{2.62}$$

which implies:

$$f(t) = 2(F(t) - 2K\bar{x}(t))\tan\alpha. \tag{2.63}$$

By replacing this expression in (2.60) we obtain the following expression:

$$M\ddot{y} = 2(kx - y(t)(k + 2K))\tan^2\alpha. \tag{2.64}$$

Let us consider a harmonic force of the form

$$F(t) = F_0 e^{i\omega t}, \tag{2.65}$$

which will induce harmonic solutions

$$\begin{aligned} x(t) &= x_0 e^{i\omega t}, \\ \bar{x}(t) &= \bar{x}_0 e^{i\omega t}, \\ y(t) &= y_0(t) e^{i\omega t}. \end{aligned} \tag{2.66}$$

We now define the effective bulk modulus K_{eff} of this system as

$$K_{\text{eff}} = \frac{F_0}{2x_0}, \tag{2.67}$$

which, by replacing Eqs. (2.65) and (2.66) in Eq. (2.64), reads as:

$$K_{\text{eff}} = \frac{k}{2}\left[\frac{M\omega^2 - 4K\tan^2\alpha}{M\omega^2 - 2(K+k)\tan^2\alpha}\right]. \tag{2.68}$$

From this expression we can deduce that the effective bulk modulus of this system can assume negative values when the frequency ω lies in the range:

$$\sqrt{\frac{4K}{M}}\tan\alpha < \omega < \sqrt{2\frac{2K+k}{M}}\tan\alpha. \tag{2.69}$$

The physical interpretation of this phenomenon is that the oscillating external forces induce the oscillatory vertical motion of the mass M which is in turn transmitted to the horizontal springs by means of the rigid bars. In this way a vertical motion is converted into a horizontal one. This resonant behaviour causes a global horizontal dilation which gives rise to a negative effective bulk modulus, even for compressive forces.

Doubly Negative Materials

Following the analogy with the electromagnetic case, we shall now consider the possibility of obtaining double negative mechanical metamaterials, i.e. materials which exhibit both negative effective stiffness and effective mass. The seminal work [143] by Veselago was the first to raise the problem of studying effects of materials with both negative magnetic permeability and electric permittivity on electromagnetic wave propagation. The main point of interest is that double negative materials exhibit a negative refraction index. The study of this phenomenon has prompted major efforts in a new research direction called *lensing* [159], which has led to significant improvements in the factory production of flat lenses.

The acoustic counterpart of this phenomenon is clearly interesting for many technological applications and the challenge consists in designing a microstructure able to give at macro-scale both negative effective mass and stiffness [27, 160–162]. This kind of microstructure would then be characterized by an exotic wave propagation behaviour due to the negative refraction index.

Of course, in a first attempt one might contemplate assembling the two microstructures which we have discussed in the previous two sections, arranged as in Fig. 2.26. However, this microstructure shows a very narrow range of frequencies for which both effective mass and stiffness are negative, and this fact seriously limits the suitability of

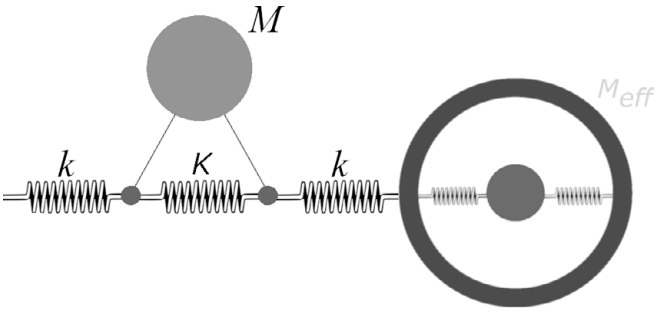

Figure 2.26 A possible system giving double negative properties.

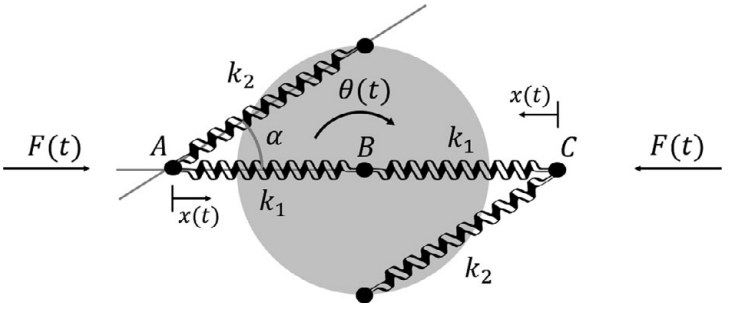

Figure 2.27 Model of basic unit cell for chiral elastic metamaterial.

such a system to resolve practical problems. Liu *et al.* [27] have recently designed a new microstructure called chiral elastic metamaterial (see Fig. 2.27).

Referring to Fig. 2.27 for the notation, we have that the force exerted by the spring with stiffness k_2 on the disk, say f_2, is:

$$f_2 = k_2(r\Theta - x\cos\alpha). \tag{2.70}$$

The disk is treated as a rigid body, whose equation of motion is

$$I\ddot{\Theta} = -2f_2 r, \tag{2.71}$$

while external forces F obey:

$$F = k_1 x - f_2 \cos\alpha. \tag{2.72}$$

Following the methods discussed in the previous sections, the expression for the effective bulk modulus of the system reads

$$K_{\text{eff}} = \frac{k_1}{2} + \frac{k_2}{2}\cos^2\alpha\left(1 - \frac{\omega_0^2}{\omega_0^2 - \omega^2}\right), \tag{2.73}$$

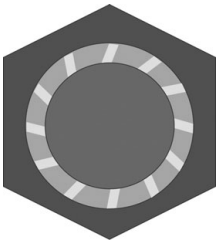

Figure 2.28 A possible unit cell physical realization for chiral elastic metamaterials.

where $\omega_0 = \sqrt{2\frac{k_2 r}{I}}$ is the resonance frequency. Again, this system admits a range of frequencies ω leading to negative bulk modulus, i.e.:

$$\omega_0\sqrt{k_1}k_1 + k_2\cos^2\alpha < \omega < \omega_0\,. \tag{2.74}$$

Showing that this system also admits negative effective mass can be easily done by following the same computations as used in Sub-section 2.2.3, while also considering horizontal translation for point B. Therefore, in the proper range of frequencies, namely the one in which both effective bulk modulus and effective mass are negative, this metamaterial is characterized by a negative refractive index. Among the many possible practical realizations of this system are soft-coated heavy cylinder cores embedded in a matrix (see Fig. 2.28), but several other interesting proposals, see for instance [163, 164], have been reported in the literature.

Bibliography

[1] J.H. Lee, J.P. Singer, and E.L. Thomas. Micro-/nanostructured mechanical metamaterials. *Advanced Materials*, 24(36):4782–4810, 2012.

[2] K. Wang, Y.H. Chang, Y. Chen, C. Zhang, and B. Wang. Designable dual-material auxetic metamaterials using three-dimensional printing. *Materials & Design*, 67:159–164, 2015.

[3] R.C. Rumpf, J. Pazos, C.R. Garcia, L. Ochoa, and R. Wicker. 3D printed lattices with spatially variant self-collimation. *Progress in Electromagnetics Research*, 139:1–14, 2013.

[4] J.F. Xing, M.L. Zheng, and X.M. Duan. Two-photon polymerization microfabrication of hydrogels: an advanced 3D printing technology for tissue engineering and drug delivery. *Chemical Society Reviews*, 44(15):5031–5039, 2015.

[5] S. Morville, M. Carin, P. Peyre, *et al.* 2D longitudinal modeling of heat transfer and fluid flow during multilayered direct laser metal deposition process. *Journal of Laser Applications*, 24(3):032008, 2012.

[6] P. Peyre, Y. Rouchausse, D. Defauchy, G. Régnier. Experimental and numerical analysis of the selective laser sintering (SLS) of PA12 and PEKK semi-crystalline polymers. *Journal of Materials Processing Technology*, 225:326–336, 2015.

[7] J.G. Ok, H.S. Youn, M.K. Kwak, *et al.* Continuous and scalable fabrication of flexible metamaterial films via roll-to-roll nanoimprint process for broadband plasmonic infrared filters. *Applied Physics Letters*, 101(22):223102, 2012.

[8] J.D. Morse. Nanofabrication technologies for roll-to-roll processing. Report from the NIST-NNN Workshop September 27-28, 2011. (http://www.internano.org/r2rworkshop/wp-content/blogs.dir/4/2012/10/Workshop-Report_Nanofabrication-Technologies-for-R2R_Final.pdf).

[9] M.J. Madou. *Manufacturing Techniques for Microfabrication and Nanotechnology*, Volume 2. CRC Press, 2011.

[10] Y. Lin. *Electrospinning Polymer Fibers for Design and Fabrication of New Materials*. PhD thesis, University of Akron, 2011.

[11] T.P. Lei, X.Z. Lu, and F. Yang. Fabrication of various micro/nano structures by modified near-field electrospinning. *AIP Advances*, 5(4):041301, 2015.

[12] P. Seppecher, J.-J. Alibert, and F. dell'Isola. Linear elastic trusses leading to continua with exotic mechanical interactions. *Journal of Physics: Conference Series*, 319(1):012018, 2011.

[13] J-J. Alibert, P. Seppecher, and F. dell'Isola. Truss modular beams with deformation energy depending on higher displacement gradients. *Mathematics and Mechanics of Solids*, 8(1):51–73, 2003.

[14] J. Alibert and A. Della Corte. Second-gradient continua as homogenized limit of pantographic microstructured plates: A rigorous proof. *Zeitschrift für angewandte Mathematik und Physik*, 66(5):2855–2870, 2015.

[15] F. dell'Isola, A. Della Corte, and I. Giorgio. Higher-gradient continua: The legacy of Piola, Mindlin, Sedov and Toupin and some future research perspectives. *Mathematics and Mechanics of Solids*, page 1081286515616034, 2016.

[16] F. dell Isola, P. Seppecher, and A. Della Corte. The postulations á la d'Alembert and á la Cauchy for higher gradient continuum theories are equivalent: A review of existing results. *Proc. R. Soc. A*, 471(2183):20150415, 2015.

[17] M. Kadic, T. Bückmann, N. Stenger, M. Thiel, and M. Wegener. On the practicability of pentamode mechanical metamaterials. *Applied Physics Letters*, 100(19):191901, 2012.

[18] R. Lakes. Foam structures with a negative Poisson's ratio. *Science*, 235:1038–1041, 1987.

[19] K. Bertoldi, P.M. Reis, S. Willshaw, and T. Mullin. Negative Poisson's ratio behavior induced by an elastic instability. *Advanced Materials*, 22(3):361–366, 2010.

[20] S. Babaee, J. Shim, J.C. Weaver, *et al.* 3D soft metamaterials with negative Poisson's ratio. *Advanced Materials*, 25(36):5044–5049, 2013.

[21] G.W. Milton. Composite materials with Poisson's ratios close to –1. *Journal of the Mechanics and Physics of Solids*, 40(5):1105–1137, 1992.

[22] J.L. Silverberg, A.A. Evans, L. McLeod, *et al.* Using origami design principles to fold reprogrammable mechanical metamaterials. *Science*, 345(6197):647–650, 2014.

[23] Q. Liu. Literature review: Materials with negative Poisson's ratios and potential applications to aerospace and defence. Technical report, DTIC Document, 2006.

[24] T. Bückmann, R. Schittny, M. Thiel, *et al.* On three-dimensional dilational elastic metamaterials. *New Journal of Physics*, 16(3):033032, 2014.

[25] G.W. Milton. Complete characterization of the macroscopic deformations of periodic unimode metamaterials of rigid bars and pivots. *Journal of the Mechanics and Physics of Solids*, 61(7):1543–1560, 2013.

[26] Z.G. Nicolaou and A.E. Motter. Mechanical metamaterials with negative compressibility transitions. *Nature Materials*, 11(7):608–613, 2012.

[27] X.N. Liu, G.K. Hu, G.L. Huang, and C.T. Sun. An elastic metamaterial with simultaneously negative mass density and bulk modulus. *Applied Physics Letters*, 98(25):251907, 2011.

[28] A. Rafsanjani, A. Akbarzadeh, and D. Pasini. Snapping mechanical metamaterials under tension. *Advanced Materials*, 27(39):5931–5935, 2015.

[29] F. dell'Isola, D. Steigmann, and A. Della Corte. Synthesis of fibrous complex structures: Designing microstructure to deliver targeted macroscale response. *Applied Mechanics Reviews*, 67(6):060804, 2015.

[30] F. dell'Isola, M. Cuomo, L. Greco, and A. Della Corte. Bias extension test for pantographic sheets: numerical simulations based on second gradient shear energies. *Journal of Engineering Mathematics*, pages 1–31, 2016.

[31] M. Cuomo, F. dell'Isola, L. Greco, and N.L. Rizzi. First versus second gradient energies for planar sheets with two families of inextensible fibres: Investigation on deformation boundary layers, discontinuities and geometrical instabilities. *Composites Part B: Engineering*, 2016.

[32] M. Spagnuolo, K. Barcz, A. Pfaff, F. dell'Isola, and P. Franciosi. Qualitative pivot damage analysis in aluminum printed pantographic sheets: Numerics and experiments. *Mechanics Research Communications*, 83:47–52, 2017.

[33] U. Andreaus, M. Spagnuolo, T. Lekszycki, and S. R. Eugster. A Ritz approach for the static analysis of planar pantographic structures modeled with nonlinear Euler–Bernoulli beams. *Continuum Mechanics and Thermodynamics*, 1–21, 2018.

[34] F. dell'Isola, P. Seppecher, J. J. Alibert, *et al.* Pantographic metamaterials: An example of mathematically driven design and of its technological challenges. *Continuum Mechanics and Thermodynamics*, 1–34, 2018.

[35] C. Lv, D. Krishnaraju, G. Konjevod, H. Yu, and H. Jiang. Origami based mechanical metamaterials. *Scientific Reports*, 4:5979, 2014.

[36] H. Yasuda and J. Yang. Reentrant origami-based metamaterials with negative Poisson's ratio and bistability. *Physical Review Letters*, 114(18):185502, 2015.

[37] G.W. Milton and A.V. Cherkaev. Which elasticity tensors are realizable? *Journal of Engineering Materials and Technology*, 117(4):483–493, 1995.

[38] G.W. Milton, D. Harutyunyan, and M. Briane. Towards a complete characterization of the effective elasticity tensors of mixtures of an elastic phase and an almost rigid phase. *Mathematics and Mechanics of Complex Systems*, 5(1):95–113, 2017.

[39] B. Nadler, P. Papadopoulos, and D.J. Steigmann. Multiscale constitutive modeling and numerical simulation of fabric material. *International Journal of Solids and Structures*, 43(2):206–221, 2006.

[40] D.J. Steigmann. Two-dimensional models for the combined bending and stretching of plates and shells based on three-dimensional linear elasticity. *International Journal of Engineering Science*, 46(7):654–676, 2008.

[41] M. Kadic, T. Bückmann, R. Schittny, and M. Wegener. On anisotropic versions of three-dimensional pentamode metamaterials. *New Journal of Physics*, 15(2):023029, 2013.

[42] G.F. Méjica and A.D. Lantada. Comparative study of potential pentamodal metamaterials inspired by Bravais lattices. *Smart Materials and Structures*, 22(11):115013, 2013.

[43] K.E. Evans, M.A. Nkansah, I.J. Hutchinson, and S.C. Rogers. Molecular network design. *Nature* 353(6340): 124, 1991.

[44] W. Yang, Z.M. Li, W. Shi, B.H. Xie, and M.B. Yang. Review on auxetic materials. *Journal of Materials Science*, 39(10):3269–3279, 2004.

[45] A. Alderson and K.L. Alderson. Auxetic materials. *Proceedings of the Institution of Mechanical Engineers, Part G: Journal of Aerospace Engineering*, 221(4):565–575, 2007.

[46] G.N. Greaves, A.L. Greer, R.S. Lakes, and T. Rouxel. Poisson's ratio and modern materials. *Nature Materials*, 10(11):823–837, 2011.

[47] V. H. Carneiro, J. Meireles, and H. Puga. Auxetic materials—a review. *Materials Science-Poland*, 31(4):561–571, 2013.

[48] M. Mir, M.N. Ali, J. Sami, and U. Ansari. Review of mechanics and applications of auxetic structures. *Advances in Materials Science and Engineering*, 2014:Article ID 753496, 2014. https://doi.org/10.1155/2014/753496.

[49] T.C. Lim. *Auxetic Materials and Structures*. Springer, 2014.

[50] R.F. Almgren. An isotropic three-dimensional structure with Poisson's ratio-1. *Journal of Elasticity*, 15:427–430, 1985.

[51] H.M.A. Kolken and A.A. Zadpoor. Auxetic mechanical metamaterials. *RSC Advances*, 7(9):5111–5129, 2017.

[52] Y. Liu and H. Hu. A review on auxetic structures and polymeric materials. *Scientific Research and Essays*, 5(10):1052–1063, 2010.

[53] L.J. Gibson and M.F. Ashby. The mechanics of three-dimensional cellular materials. *Proc. Roy. Soc. A*, 382(1782):43–59, 1982.

[54] L.J. Gibson. Biomechanics of cellular solids. *Journal of Biomechanics*, 38(3):377–399, 2005.

[55] A. Lorato, P. Innocenti, F. Scarpa, *et al.* The transverse elastic properties of chiral honeycombs. *Composites Science and Technology*, 70(7):1057–1063, 2010.

[56] K.W. Wojciechowski. Non-chiral, molecular model of negative Poisson ratio in two dimensions. *Journal of Physics A: Mathematical and General*, 36(47):11765, 2003.

[57] J.N. Grima, R. Gatt, N. Ravirala, A. Alderson, and K.E. Evans. Negative Poisson's ratios in cellular foam materials. *Materials Science and Engineering: A*, 423(1):214–218, 2006.

[58] G.W. Milton. New examples of three-dimensional dilational materials. *Physica Status Solidi (b)*, 252(7):1426–1430, 2015.

[59] J.N. Grima, A. Alderson, and K.E. Evans. Auxetic behaviour from rotating rigid units. *Physica Status Solidi (b)*, 242(3):561–575, 2005.

[60] J.N. Grima and K.E. Evans. Auxetic behavior from rotating squares. *Journal of Materials Science Letters*, 19(17):1563–1565, 2000.

[61] J.N. Grima, A. Alderson, and K.E. Evans. Negative Poisson's ratios from rotating rectangles. *Comput. Methods Sci. Technol.*, 10:137–145, 2004.

[62] J.N. Grima and K.E. Evans. Auxetic behavior from rotating triangles. *Journal of Materials Science*, 41(10):3193–3196, 2006.

[63] D. Attard and J.N. Grima. Auxetic behaviour from rotating rhombi. *Physica Status Solidi (b)*, 245(11):2395–2404, 2008.

[64] J.N. Grima, V. Zammit, R. Gatt, A. Alderson, and K.E. Evans. Auxetic behaviour from rotating semi-rigid units. *Physica Status Solidi (b)*, 244(3):866–882, 2007.

[65] E. Chetcuti, B. Ellul, E. Manicaro, *et al.* Modeling auxetic foams through semi-rigid rotating triangles. *Physica Status Solidi (b)*, 251(2):297–306, 2014.

[66] A. Alderson and K.E. Evans. Rotation and dilation deformation mechanisms for auxetic behaviour in the α-cristobalite tetrahedral framework structure. *Physics and Chemistry of Minerals*, 28(10):711–718, 2001.

[67] A. Alderson, K. L Alderson, D. Attard, *et al.* Elastic constants of 3-, 4-and 6-connected chiral and anti-chiral honeycombs subject to uniaxial in-plane loading. *Composites Science and Technology*, 70(7):1042–1048, 2010.

[68] D. Prall and R.S. Lakes. Properties of a chiral honeycomb with a Poisson's ratio of −1. *International Journal of Mechanical Sciences*, 39(3):305–314, 1997.

[69] R. Gatt, J.P. Brincat, K.M. Azzopardi, L. Mizzi, and J.N. Grima. On the effect of the mode of connection between the node and the ligaments in anti-tetrachiral systems. *Advanced Engineering Materials*, 17(2):189–198, 2015.

[70] C. S. Ha, M.E. Plesha, and R.S. Lakes. Chiral three-dimensional lattices with tunable Poisson's ratio. *Smart Materials and Structures*, 25(5):054005, 2016.

[71] R. Lakes and K.W. Wojciechowski. Negative compressibility, negative Poisson's ratio, and stability. *Physica Status Solidi (b)*, 245(3):545–551, 2008.

[72] Y. Panovko, I.I. Gubanova, and C.V. Larrick. Stability and oscillations of elastic systems. *Journal of Applied Mechanics*, 33:479, 1966.

[73] V.A. Eremeyev and L.P. Lebedev. On the loss of stability of von Mises truss with the effect of pseudo-elasticity. *Matemáticas: Enseñanza Universitaria*, XIV, 2006.

[74] Y.C. Wang and R.S. Lakes. Extreme stiffness systems due to negative stiffness elements. *American Journal of Physics*, 72(1):40–50, 2004.

[75] R.S. Lakes, T. Lee, A. Bersie, and Y.C. Wang. Extreme damping in composite materials with negative-stiffness inclusions. *Nature*, 410(6828):565–567, 2001.

[76] D.M. Correa, T. Klatt, S. Cortes, *et al.* Negative stiffness honeycombs for recoverable shock isolation. *Rapid Prototyping Journal*, 21(2):193–200, 2015.

[77] R.S. Lakes. Extreme damping in composite materials with a negative stiffness phase. *Physical Review Letters*, 86(13):2897, 2001.

[78] Y.C. Wang and R.S. Lakes. Composites with inclusions of negative bulk modulus: Extreme damping and negative Poisson's ratio. *Journal of Composite Materials*, 39(18):1645–1657, 2005.

[79] W.J. Drugan. Elastic composite materials having a negative stiffness phase can be stable. *Physical Review Letters*, 98(5):055502, 2007.

[80] I. Antoniadis, D. Chronopoulos, V. Spitas, and D. Koulocheris. Hyper-damping properties of a stiff and stable linear oscillator with a negative stiffness element. *Journal of Sound and Vibration*, 346:37–52, 2015.

[81] C.M. Lee, V.N. Goverdovskiy, and A.I. Temnikov. Design of springs with "negative" stiffness to improve vehicle driver vibration isolation. *Journal of Sound and Vibration*, 302(4):865–874, 2007.

[82] A.A. Sarlis, D.T.R. Pasala, M.C. Constantinou, *et al.* Negative stiffness device for seismic protection of structures. *Journal of Structural Engineering*, 139(7):1124–1133, 2012.

[83] R.H. Baughman, S. Stafström, C. Cui, and S.O. Dantas. Materials with negative compressibilities in one or more dimensions. *Science*, 279(5356):1522–1524, 1998.

[84] J.N. Grima and R. Caruana-Gauci. Mechanical metamaterials: Materials that push back. *Nature Materials*, 11(7):565–566, 2012.

[85] A.D. Fortes, E. Suard, and K.S. Knight. Negative linear compressibility and massive anisotropic thermal expansion in methanol monohydrate. *Science*, 331(6018):742–746, 2011.

[86] J.N. Grima, D. Attard, R. Caruana-Gauci, and R. Gatt. Negative linear compressibility of hexagonal honeycombs and related systems. *Scripta Materialia*, 65(7):565–568, 2011.

[87] J.N. Grima, R. Caruana-Gauci, D. Attard, and R. Gatt. Three-dimensional cellular structures with negative Poisson's ratio and negative compressibility properties. *Proc. Roy. Soc. A*, 468(2146):3121–3138, 2012.

[88] D.L. Barnes, W. Miller, K.E. Evans, and A. Marmier. Modelling negative linear compressibility in tetragonal beam structures. *Mechanics of Materials*, 46:123–128, 2012.

[89] R. Gatt and J.N. Grima. Negative compressibility. *Physica Status Solidi (RRL)*, 2(5):236–238, 2008.

[90] E. Turco, F. dell'Isola, N.L. Rizzi, *et al.* Fiber rupture in sheared planar pantographic sheets: Numerical and experimental evidence. *Mechanics Research Communications*, 76:86–90, 2016.

[91] F. dell'Isola, I. Giorgio, and U. Andreaus. Elastic pantographic 2D lattices: A numerical analysis on static response and wave propagation. In *Proceedings of the Estonian Academy of Sciences*, Volume 64, pages 219–225, 2015.

[92] F. dell'Isola, A. Della Corte, I. Giorgio, and D. Scerrato. Pantographic 2D sheets: Discussion of some numerical investigations and potential applications. *International Journal of Non-Linear Mechanics*, 80:200–208, 2016.

[93] A. Madeo, A. Della Corte, L. Greco, and P. Neff. Wave propagation in pantographic 2D lattices with internal discontinuities. *arXiv preprint arXiv:1412.3926*, 2014.

[94] K. Miura. Method of packaging and deployment of large membranes in space. *The Institute of Space and Astronautical Science Report*, 618:1, 1985.

[95] K. Miura. Map fold a la Miura style, its physical characteristics and application to the space science. *Research of Pattern Formation*, pages 77–90, 1994.

[96] Koryo Miura. A note on intrinsic geometry of origami. *Research of Pattern Formation*, pages 91–102, 1989.

[97] T. Kawasaki. On the relation between mountain-creases and valley-creases of a flat origami. In *Proceedings of the First International Meeting of Origami Science and Technology, 1991*, pages 229–237, 1991.

[98] M. Schenk and S.D. Guest. Geometry of Miura-folded Metamaterials. *Proceedings of the National Academy of Sciences*, 110(9):3276–3281, 2013.

[99] M. Schenk and S.D. Guest. Origami folding: A structural engineering approach. In *Origami 5: Fifth International Meeting of Origami Science, Mathematics, and Education*, pages 291–304. CRC Press, Boca Raton, FL, 2011.

[100] X. Zhou, S. Zang, and Z. You. Origami mechanical metamaterials based on the Miura-derivative fold patterns. *Proc. R. Soc. A*, 472:20160361, 2016.

[101] L.H. Dudte, E. Vouga, T. Tachi, and L. Mahadevan. Programming curvature using origami tessellations. *Nature Materials*, 15(5): 583, 2016.

[102] H. Nassar, A. Lebée, and L. Monasse. Curvature, metric and parameterisation of origami tessellations: theory and application to the eggbox pattern. *Proc. R. Soc. A*, 473:20160705, 2017.

[103] G. Allaire. Homogenization and two-scale convergence. *SIAM Journal on Mathematical Analysis*, 23(6):1482–1518, 1992.

[104] O. Sigmund. *Design of Materials Structures Using Topology Optimization*. Department of Solid Mechanics, Technical University of Denmark, 1994.

[105] Eugene Cosserat, François Cosserat, *et al.* Théorie des corps déformables. Hermann, Paris, 1909.

[106] R.A. Toupin. Elastic materials with couple-stresses. *Archive for Rational Mechanics and Analysis*, 11(1):385–414, 1962.

[107] R. D. Mindlin. Micro-structure in linear elasticity. *Archive for Rational Mechanics and Analysis*, 16(1):51–78, 1964.

[108] P. Germain. The method of virtual power in continuum mechanics. Part 2: Microstructure. *SIAM Journal on Applied Mathematics*, 25(3):556–575, 1973.

[109] F. dell'Isola, G. Maier, U. Perego, *et al. The Complete Works of Gabrio Piola:* Volume I. Cham, Switzerland: Springer, 2014.

[110] N. Auffray, F. dell'Isola, V. Eremeyev, A. Madeo, and G. Rosi. Analytical continuum mechanics à la Hamilton–Piola least action principle for second gradient continua and capillary fluids. *Mathematics and Mechanics of Solids*, 20(4):375–417, 2015.

[111] F. dell'Isola, U. Andreaus, and L. Placidi. At the origins and in the vanguard of peridynamics, non-local and higher-gradient continuum mechanics: An underestimated and still topical contribution of Gabrio Piola. *Mathematics and Mechanics of Solids*, 20(8):887–928, 2015.

[112] B. E. Abali, W. H. Müller, and F. dell'Isola. Theory and computation of higher gradient elasticity theories based on action principles. *Archive of Applied Mechanics*, 87(9): 1495–1510, 2017.

[113] B. E. Abali, W. H. Müller, V. A. Eremeyev. Strain gradient elasticity with geometric nonlinearities and its computational evaluation. *Mechanics of Advanced Materials and Modern Processes*, 1(1):4, 2015.

[114] P. Seppecher. Second-gradient theory: Application to Cahn-Hilliard fluids. In *Continuum Thermomechanics*, pages 379–388. Springer, 2000.

[115] R.S. Rivlin. Plane strain of a net formed by inextensible cords. In *Collected Papers of RS Rivlin*, pages 511–534. Springer, 1997.

[116] M.G. Hilgers and A.C. Pipkin. Energy-minimizing deformations of elastic sheets with bending stiffness. *Journal of Elasticity*, 31(2):125–139, 1993.

[117] W.-B. Wang and A.C. Pipkin. Plane deformations of nets with bending stiffness. *Acta Mechanica*, 65(1-4):263–279, 1987.

[118] D.J. Steigmann and A.C. Pipkin. Equilibrium of elastic nets. *Philosophical Transactions of the Royal Society of London A: Mathematical, Physical and Engineering Sciences*, 335(1639):419–454, 1991.

[119] Y. Rahali, I. Giorgio, J.F. Ganghoffer, and Francesco dell'Isola. Homogenization à la Piola produces second gradient continuum models for linear pantographic lattices. *International Journal of Engineering Science*, 97:148–172, 2015.

[120] C. Pideri and P. Seppecher. A second gradient material resulting from the homogenization of an heterogeneous linear elastic medium. *Continuum Mechanics and Thermodynamics*, 9(5):241–257, 1997.

[121] C. Pideri and P. Seppecher. A homogenization result for elastic material reinforced periodically with high rigidity elastic fibres. *Comptes Rendus de l'Academie des Sciences Series IIB Mechanics Physics Chemistry Astronomy*, 8(324):475–481, 1997.

[122] H. Abdoul-Anziz and P. Seppecher. Strain gradient and generalized continua obtained by homogenizing frame lattices. *Mathematics and Mechanics of Complex Systems*, 6(3): 213–250, 2018.

[123] F. dell'Isola, I. Giorgio, M. Pawlikowski, and N. Rizzi. Large deformations of planar extensible beams and pantographic lattices: Heuristic homogenization, experimental and numerical examples of equilibrium. *Proc. R. Soc. A*, 472(2185):20150790, 2016.

[124] L. Greco and M. Cuomo. B-Spline interpolation of Kirchhoff–Love space rods. *Computer Methods in Applied Mechanics and Engineering*, 256:251–269, 2013.

[125] L. Greco, I. Giorgio, and A.Battista. In plane shear and bending for first gradient inextensible pantographic sheets: Numerical study of deformed shapes and global constraint reactions. *Mathematics and Mechanics of Solids*, 22(10): 1950–1975, 2017.

[126] A. Cazzani, M. Malagù, and E. Turco. Isogeometric analysis of plane-curved beams. *Mathematics and Mechanics of Solids*, 21(5):562–577, 2016.

[127] A. Cazzani, M. Malagù, E. Turco, and F. Stochino. Constitutive models for strongly curved beams in the frame of isogeometric analysis. *Mathematics and Mechanics of Solids*, 21(2):182–209, 2016.

[128] R.M. Walser. Metamaterials: What are they? what are they good for? In *APS March Meeting Abstracts*, 2000.

[129] Arkadi Berezovski, Jüri Engelbrecht, and Tanel Peets. Multiscale modeling of microstructured solids. *Mechanics Research Communications*, 37(6):531–534, 2010.

[130] C. Boutin, I. Giorgio, L. Placidi, *et al.* Linear pantographic sheets: Asymptotic micro–macro models identification. *Mathematics and Mechanics of Complex Systems*, 5(2): 127–162, 2017.

[131] G. de Felice and N. Rizzi. Macroscopic modelling of Cosserat media. *Trends and Applications of Mathematics to Mechanics, Monographs and Surveys in Pure and Applied Mathematics*, 106:58–65, 1999.

[132] A. Di Carlo, N. Rizzi, and A. Tatone. Continuum modelling of a beam-like latticed truss: Identification of the constitutive functions for the contact and inertial actions. *Meccanica*, 25(3):168–174, 1990.

[133] I. Giorgio. Numerical identification procedure between a micro-Cauchy model and a macro-second gradient model for planar pantographic structures. *Zeitschrift für angewandte Mathematik und Physik*, 67(4)(95), 2016.

[134] L. Placidi, U. Andreaus, and I. Giorgio. Identification of two-dimensional pantographic structure via a linear d4 orthotropic second gradient elastic model. *Journal of Engineering Mathematics*, pages 1–21, 2016.

[135] F. dell'Isola, S. Bucci, and A. Battista. Against the fragmentation of knowledge: The power of multidisciplinary research for the design of metamaterials. In *Advanced Methods of Continuum Mechanics for Materials and Structures*, pages 523–545. Springer, 2016.

[136] F. Casadei, T. Delpero, A. Bergamini, P. Ermanni, and M. Ruzzene. Piezoelectric resonator arrays for tunable acoustic waveguides and metamaterials. *Journal of Applied Physics*, 112(6):064902, 2012.

[137] V.A. Eremeyev and H. Altenbach. On the eigenfrequencies of an ordered system of nanoobjects. In *IUTAM Symposium on Modelling Nanomaterials and Nanosystems*, pages 123–132. Springer, 2009.

[138] V.S. Fedotovskii. Transverse waves in a dispersive metamaterial with spherical inclusions. *Acoustical Physics*, 61(3):281–286, 2015.

[139] R.L. Weaver. Multiple-scattering theory for mean responses in a plate with sprung masses. *The Journal of the Acoustical Society of America*, 101(6):3466–3474, 1997.

[140] M. Oudich, M. Senesi, M.B. Assouar, *et al.* Experimental evidence of locally resonant sonic band gap in two-dimensional phononic stubbed plates. *Physical Review B*, 84(16):165136, 2011.

[141] V.G. Veselago. Properties of materials having simultaneously negative values of the dielectric and magnetic susceptibilities. *Soviet Physics Solid State USSR*, 8:2854–2856, 1967.

[142] V.G. Veselago. The electrodynamics of substances with simultaneously negative values of ϵ and μ. *Soviet physics uspekhi*, 10(4):509, 1968.

[143] V.G. Veselago. Electrodynamics of media with simultaneously negative electric permittivity and magnetic permeability. In *Advances in Electromagnetics of Complex Media and Metamaterials*, pages 83–97. Springer, 2002.

[144] J.B. Pendry, A.J. Holden, W.J. Stewart, and I. Youngs. Extremely low frequency plasmons in metallic mesostructures. *Physical Review Letters*, 76(25):4773, 1996.

[145] J.B. Pendry, A.J. Holden, D.J. Robbins, and W.J. Stewart. Magnetism from conductors and enhanced nonlinear phenomena. *IEEE Transactions on Microwave Theory and Techniques*, 47(11):2075–2084, 1999.

[146] R.A. Shelby, D.R. Smith, and S. Schultz. Experimental verification of a negative index of refraction. *Science*, 292(5514):77–79, 2001.

[147] D.R. Smith and N. Kroll. Negative refractive index in left-handed materials. *Physical Review Letters*, 85(14):2933, 2000.

[148] Z. Liu, X. Zhang, Y. Mao, *et al.* Locally resonant sonic materials. *Science*, 289(5485):1734–1736, 2000.

[149] J. Li and C.T. Chan. Double-negative acoustic metamaterial. *Physical Review E*, 70(5):055602, 2004.

[150] A.B. Movchan and S. Guenneau. Split-ring resonators and localized modes. *Physical Review B*, 70(12):125116, 2004.

[151] N. Fang, D. Xi, J. Xu, *et al.* Ultrasonic metamaterials with negative modulus. *Nature Materials*, 5(6):452–456, 2006.

[152] Graeme Milton, Marc Briane, and Davit Harutyunyan. On the possible effective elasticity tensors of 2-dimensional and 3-dimensional printed materials. *Mathematics and Mechanics of Complex Systems*, 5(1):41–94, 2017.

[153] G.W. Milton, M. Briane, and J.R. Willis. On cloaking for elasticity and physical equations with a transformation invariant form. *New Journal of Physics*, 8(10):248, 2006.

[154] G.W. Milton and N.A.P. Nicorovici. On the cloaking effects associated with anomalous localized resonance. In *Proceedings of the Royal Society of London A: Mathematical, Physical and Engineering Sciences*, 462: 3027–3059, 2006.

[155] P.M.C. Morse and K.U. Ingard. *Theoretical Acoustics*. International series in pure and applied physics. Princeton University Press, 1968.

[156] G.W. Milton and J.R. Willis. On modifications of Newton's second law and linear continuum elastodynamics. In *Proceedings of the Royal Society of London A: Mathematical, Physical and Engineering Sciences*, 463: 855–880, 2007.

[157] S. Yao, X. Zhou, and G. Hu. Experimental study on negative effective mass in a 1D mass-spring system. *New Journal of Physics*, 10(4):043020, 2008.

[158] H.H. Huang and C.T. Sun. Wave attenuation mechanism in an acoustic metamaterial with negative effective mass density. *New Journal of Physics*, 11(1):013003, 2009.

[159] J.B. Pendry. Negative refraction makes a perfect lens. *Physical Review Letters*, 85(18):3966, 2000.

[160] C.T. Chan, J. Li, and K.H. Fung. On extending the concept of double negativity to acoustic waves. *Journal of Zhejiang University-SCIENCE A*, 7(1):24–28, 2006.

[161] Y. Ding, Z. Liu, C. Qiu, and J. Shi. Metamaterial with simultaneously negative bulk modulus and mass density. *Physical Review Letters*, 99(9):093904, 2007.

[162] S. Nemat-Nasser and A. Srivastava. Negative effective dynamic mass-density and stiffness: Micro-architecture and phononic transport in periodic composites. *AIP Advances*, 1(4):041502, 2011.

[163] X. Liu, G. Hu, C. Sun, and G. Huang. Wave propagation characterization and design of two-dimensional elastic chiral metacomposite. *Journal of Sound and Vibration*, 330(11):2536–2553, 2011.

[164] R. Zhu, X. Liu, G. Hu, C. Sun, and G. Huang. Negative refraction of elastic waves at the deep-subwavelength scale in a single-phase metamaterial. *Nature Communications*, 5:5510, 2014.

[165] A. Javili, A. McBride, J. Mergheim, P. Steinmann, and U. Schmidt. Micro-to-macro transitions for continua with surface structure at the microscale. *International Journal of Solids and Structures*, 50(16):2561–2572, 2013.

[166] A. Misra and P. Poorsolhjouy. Identification of higher-order elastic constants for grain assemblies based upon granular micromechanics. *Mathematics and Mechanics of Complex Systems*, 3(3):285–308, 2015.

[167] D.J. Steigmann and F. dell'Isola. Mechanical response of fabric sheets to three-dimensional bending, twisting, and stretching. *Acta Mechanica Sinica*, 31(3):372–382, 2015.

[168] A. Bertram and G. Rainer. Gradient materials with internal constraints. *Mathematics and Mechanics of Complex Systems*, 4(1):1–15, 2016.

[169] G. Bevill, S. K. Eswaran, A. Gupta, P. Papadopoulos, and T. M. Keaveny. Influence of bone volume fraction and architecture on computed large-deformation failure mechanisms in human trabecular bone. *Bone*, 39(6):1218–1225, 2006.

[170] A.C. Eringen. *Continuum Physics. Volume 4-Polar and Nonlocal Field Theories*. Academic Press, Inc., New York, 1976.

[171] J.F. Ganghoffer. Spatial and material stress tensors in continuum mechanics of growing solid bodies. *Mathematics and Mechanics of Complex Systems*, 3(4):341–363, 2016.

[172] S. Saeb, P. Steinmann, and A. Javili. Aspects of computational homogenization at finite deformations: A unifying review from Reuss' to Voigt's bound. *Applied Mechanics Reviews*, 68(5):050801, 2016.

[173] R. Esposito and M. Pulvirenti. From particles to fluids. In *Handbook of Mathematical Fluid Dynamics*, ed. S. Friedlander and D. Serre, Vol. 3:1–82, NorthHolland, Amsterdam, 2004.

[174] M. Pulvirenti. Kinetic Limits for Stochastic Particle Systems. *Lecture Notes in Mathematics*, Springer-Verlag, 1996.

[175] S. Caprino, R. Esposito, R. Marra, and M. Pulvirenti. Hydrodynamic limits of the Vlasov equation. *Communications in Partial Differential Equations*, 18(5):805–820, 1993.

[176] A. De Masi and S. Olla. Quasi-static hydrodynamic limits. *Journal of Statistical Physics*, 161(5):1037–1058, Dec 2015.

[177] G. Carinci, A. De Masi, C. Giardinà, and Errico Presutti. Hydrodynamic limit in a particle system with topological interactions. *Arabian Journal of Mathematics*, 3(4):381–417, Dec 2014.

[178] A. De Masi, S. Luckhaus, and E. Presutti. Two scales hydrodynamic limit for a model of malignant tumor cells. *Annales de l'Institut Henri Poincare (B) Probability and Statistics*, 43(3), 2007.

[179] A. De Masi, I. Merola, E. Presutti, and Y. Vignaud. Coexistence of ordered and disordered phases in Potts models in the continuum. *Journal of Statistical Physics*, 134(2):243–306, 2009.

[180] J.D. Smith. Application of the method of asymptotic homogenization to an acoustic metafluid. *Proc. R. Soc. London A: Mathematical, Physical and Engineering Sciences*, 467(2135):3318–3331, 2011.

[181] I.V. Andrianov, V.I. Bolshakov, V.V. Danishevs'kyy, and D. Weichert. Higher order asymptotic homogenization and wave propagation in periodic composite materials. *Proc. R. Soc. London A: Mathematical, Physical and Engineering Sciences*, 464(2093): 1181–1201, 2008.

[182] J.A. Otero, R. Rodriguez-Ramos, G. Monsivais, and R. Perez-Alvarez. Dynamical behavior of a layered piezocomposite using the asymptotic homogenization method. *Mechanics of Materials*, 37(1):33–44, 2005.

[183] R.V. Craster, J. Kaplunov, and A.V. Pichugin. High-frequency homogenization for periodic media. *Proc.R.Soc.London A: Mathematical, Physical and Engineering Sciences*, 466(2120): 2341–2362, 2010.

[184] H. Chen and C.T. Chan. Acoustic cloaking and transformation acoustics. *Journal of Physics D: Applied Physics*, 43(11):113001, 2010.

[185] Zvi Hashin. Theory of mechanical behavior of heterogeneous media. Technical report, Pennsylvania Univ Philadelphia Towne School of Civil and Mechanical Engineering, 1963.

[186] J.R. Willis. Effective constitutive relations for waves in composites and metamaterials. *Proceedings of the Royal Society of London A: Mathematical, Physical and Engineering Sciences*, 467(2131):1865–1879, 2011.

[187] A.N. Norris, A.L. Shuvalov, and A.A. Kutsenko. Analytical formulation of three-dimensional dynamic homogenization for periodic elastic systems. *Proc. R. Soc. A*, 468(2142):1629–1651, 2012.

[188] A. Srivastava. Elastic metamaterials and dynamic homogenization: A review. *International Journal of Smart and Nano Materials*, 6(1):41–60, 2015.

[189] S.A. Cummer, B.I. Popa, D. Schurig, *et al.* Scattering theory derivation of a 3D acoustic cloaking shell. *Physical Review Letters*, 100(2):024301, 2008.

[190] S.A. Cummer and D. Schurig. One path to acoustic cloaking. *New Journal of Physics*, 9(3):45, 2007.

[191] A. Alù and N. Engheta. Achieving transparency with plasmonic and metamaterial coatings. *Physical Review E*, 72(1):016623, 2005.

[192] X. Zhou and G. Hu. Design for electromagnetic wave transparency with metamaterials. *Physical Review E*, 74(2):026607, 2006.

[193] M.D. Guild, A. Alu, and M.R. Haberman. Cancellation of acoustic scattering from an elastic sphere. *The Journal of the Acoustical Society of America*, 129(3):1355–1365, 2011.

[194] P.C. Waterman. New formulation of acoustic scattering. *The Journal of the Acoustical Society of America*, 45(6):1417–1429, 1969.

[195] D. Torrent, Y. Pennec, and B. Djafari-Rouhani. Effective medium theory for elastic metamaterials in thin elastic plates. *Physical Review B*, 90(10):104–110, 2014.

[196] U. Andreaus, F. dell'Isola, I. Giorgio, *et al.* Numerical simulations of classical problems in two-dimensional (non) linear second gradient elasticity. *International Journal of Engineering Science*, 108:34–50, 2016.

[197] E. Barchiesi and L. Placidi. A review on models for the 3D statics and 2D dynamics of pantographic fabrics. In *Wave Dynamics and Composite Mechanics for Microstructured Materials and Metamaterials*, pages 239–258. Springer, 2017.

[198] A. Battista, L. Rosa, R. dell'Erba, and L. Greco. Numerical investigation of a particle system compared with first and second gradient continua: Deformation and fracture phenomena. *Mathematics and Mechanics of Solids*, page 1081286516657889, 2016.

[199] L. Placidi, L. Greco, S. Bucci, E. Turco, and N.L. Rizzi. A second gradient formulation for a 2D fabric sheet with inextensible fibres. *Zeitschrift für angewandte Mathematik und Physik*, 67(5)(114), 2016.

[200] E. Turco, F. dell'Isola, A. Cazzani, and N.L. Rizzi. Hencky-type discrete model for pantographic structures: Numerical comparison with second gradient continuum models. *Zeitschrift für angewandte Mathematik und Physik*, 67, 2016.

[201] J.J. Faran Jr. Sound scattering by solid cylinders and spheres. *The Journal of the Acoustical Society of America*, 23(4):405–418, 1951.

[202] R. Hickling. Analysis of echoes from a solid elastic sphere in water. *The Journal of the Acoustical Society of America*, 34(10):1582–1592, 1962.

[203] R. Hickling. Analysis of echoes from a hollow metallic sphere in water. *The Journal of the Acoustical Society of America*, 36(6):1124–1137, 1964.

[204] G.W. Milton. *The Theory of Composites, Materials and Technology*, 117:483–493, 1995.

[205] R.V. Craster and S. Guenneau. *Acoustic Metamaterials: Negative Refraction, Imaging, Lensing and Cloaking*, Volume 166. Springer Science & Business Media, 2012.

[206] S.H. Lee, C.M. Park, Y.M. Seo, Z.G. Wang, and C.K. Kim. Acoustic metamaterial with negative density. *Physics Letters A*, 373(48):4464–4469, 2009.

[207] X. Zhou and G. Hu. Analytic model of elastic metamaterials with local resonances. *Physical Review B*, 79(19):195109, 2009.

[208] T.W. McDevitt, G.M. Hulbert, and N. Kikuchi. An assumed strain method for the dispersive global–local modeling of periodic structures. *Computer Methods in Applied Mechanics and Engineering*, 190(48):6425–6440, 2001.

[209] D.J. Mead. Free wave propagation in periodically supported, infinite beams. *Journal of Sound and Vibration*, 11(2):181–197, 1970.

[210] D.J. Mead. Wave propagation and natural modes in periodic systems: I. Mono-coupled systems. *Journal of Sound and Vibration*, 40(1):1–18, 1975.

[211] D.J. Mead. Wave propagation and natural modes in periodic systems: II. Multi-coupled systems, with and without damping. *Journal of Sound and Vibration*, 40(1):19–39, 1975.

[212] D.J. Mead. A new method of analyzing wave propagation in periodic structures: Applications to periodic Timoshenko beams and stiffened plates. *Journal of Sound and Vibration*, 104(1):9–27, 1986.

[213] F. Romeo and A. Luongo. Invariant representation of propagation properties for bi-coupled periodic structures. *Journal of Sound and Vibration*, 257(5):869–886, 2002.

[214] Y. Yong and Y.K. Lin. Propagation of decaying waves in periodic and piecewise periodic structures of finite length. *Journal of Sound and Vibration*, 129(1):99–118, 1989.

[215] F. dell'Isola, N. Ianiro, and L. Placidi. Instability of a pre-stressed solid-fluid mixture. In *'WASCOM 2005'13th Conference on Waves and Stability in Continuous Media*, page 6, 2006.

[216] L. Placidi, F. dell'Isola, N. Ianiro, and G. Sciarra. Variational formulation of pre-stressed solid–fluid mixture theory, with an application to wave phenomena. *European Journal of Mechanics-A/Solids*, 27(4):582–606, 2008.

[217] X. Zhou and G. Hu. Acoustic wave transparency for a multilayered sphere with acoustic metamaterials. *Physical Review E*, 75(4):046606, 2007.

[218] X. Zhou, G. Hu, and T. Lu. Elastic wave transparency of a solid sphere coated with metamaterials. *Physical Review B*, 77(2):024101, 2008.

[219] M. Brun, S. Guenneau, and A.B. Movchan. Achieving control of in-plane elastic waves. *Applied Physics Letters*, 94(6):061903, 2009.

[220] Z. Chang, J. Hu, and G. Hu. Transformation method and wave control. *Acta Mechanica Sinica*, 26(6):889–898, 2010.

[221] Z. Chang, J. Hu, G. Hu, R. Tao, and Y. Wang. Controlling elastic waves with isotropic materials. *Applied Physics Letters*, 98(12):121904, 2011.

[222] H. Chen and C.T. Chan. Acoustic cloaking in three dimensions using acoustic metamaterials. *Applied physics letters*, 91(18):183518, 2007.

[223] N.H. Gokhale, J.L. Cipolla, and A.N. Norris. Special transformations for pentamode acoustic cloaking. *The Journal of the Acoustical Society of America*, 132(4):2932–2941, 2012.

[224] J. Hu, Z. Chang, and G. Hu. Approximate method for controlling solid elastic waves by transformation media. *Physical Review B*, 84(20):201101, 2011.

[225] J. Hu, X. Zhou, and G. Hu. Design method for electromagnetic cloak with arbitrary shapes based on Laplace's equation. *Optics Express*, 17(3):1308–1320, 2009.

[226] A.N. Norris and W.J. Parnell. Hyperelastic cloaking theory: Transformation elasticity with pre-stressed solids. In *Proc. R. Soc. A*, 468: 2881–2903, 2012.

[227] D. Torrent and J. Sánchez-Dehesa. Acoustic cloaking in two dimensions: A feasible approach. *New Journal of Physics*, 10(6):063015, 2008.

[228] S. Zhang, C. Xia, and N. Fang. Broadband acoustic cloak for ultrasound waves. *Physical Review Letters*, 106(2):024301, 2011.

[229] F. Guevara Vasquez, G.W. Milton, and D. Onofrei. Mathematical analysis of the two dimensional active exterior cloaking in the quasistatic regime. *Analysis and Mathematical Physics*, 2(3):231–246, 2012.

[230] G.W. Milton and P. Seppecher. Realizable response matrices of multi-terminal electrical, acoustic and elastodynamic networks at a given frequency. In *Proceedings of the Royal Society of London A: Mathematical, Physical and Engineering Sciences*, 464: 967–986, 2008.

[231] A.N. Norris. Acoustic metafluids. *The Journal of the Acoustical Society of America*, 125(2):839–849, 2009.

[232] C.N. Layman, C.J. Naify, T.P. Martin, D.C. Calvo, and G.J. Orris. Highly anisotropic elements for acoustic pentamode applications. *Physical Review Letters*, 111(2):024302, 2013.

[233] A.N. Norris and A.J. Nagy. Acoustic metafluids made from three acoustic fluids. *The Journal of the Acoustical Society of America*, 128(4):1606–1616, 2010.

[234] J.B. Pendry and J. Li. An acoustic metafluid: realizing a broadband acoustic cloak. *New Journal of Physics*, 10(11):115032, 2008.

[235] B.I. Popa and S.A. Cummer. Homogeneous and compact acoustic ground cloaks. *Physical Review B*, 83(22):224304, 2011.

[236] B.I. Popa, L. Zigoneanu, and S.A. Cummer. Experimental acoustic ground cloak in air. *Physical Review Letters*, 106(25):253901, 2011.

[237] M. Ambati, N. Fang, C. Sun, and X. Zhang. Surface resonant states and superlensing in acoustic metamaterials. *Physical Review B*, 75(19):195447, 2007.

[238] X. Ao and C.T. Chan. Far-field image magnification for acoustic waves using anisotropic acoustic metamaterials. *Physical Review E*, 77(2):025601, 2008.

[239] K. Deng, Y. Ding, Z. He, *et al.* Theoretical study of subwavelength imaging by acoustic metamaterial slabs. *Journal of Applied Physics*, 105(12):124909, 2009.

[240] H. Jia, M. Ke, R. Hao, *et al.* Subwavelength imaging by a simple planar acoustic superlens. *Applied Physics Letters*, 97(17):173507, 2010.

[241] F. Liu, F. Cai, S. Peng, *et al.* Parallel acoustic near-field microscope: A steel slab with a periodic array of slits. *Physical Review E*, 80(2):026603, 2009.

[242] S. Zhang, L. Yin, and N. Fang. Focusing ultrasound with an acoustic metamaterial network. *Physical Review Letters*, 102(19):194301, 2009.

[243] J. de Rosny, G. Lerosey, and M. Fink. Theory of electromagnetic time-reversal mirrors. *IEEE Transactions on Antennas and Propagation*, 58(10):3139–3149, 2010.

[244] M. Fink. Time reversal of ultrasonic fields. I. Basic principles. *IEEE Transactions on Ultrasonics, Ferroelectrics, and Frequency Control*, 39(5):555–566, 1992.

[245] A. Derode, P. Roux, and M. Fink. Robust acoustic time reversal with high-order multiple scattering. *Physical Review Letters*, 75(23):4206, 1995.

[246] A. Derode, A. Tourin, J. de Rosny, *et al.* Taking advantage of multiple scattering to communicate with time-reversal antennas. *Physical Review Letters*, 90(1):14301, 2003.

[247] M. Fink, J. de Rosny, G. Lerosey, and A. Tourin. Time-reversed waves and super-resolution. *CR Phys*, 10:447–463, 2009.

[248] J. de Rosny and M. Fink. Overcoming the diffraction limit in wave physics using a time-reversal mirror and a novel acoustic sink. *Physical Review Letters*, 89(12):124301, 2002.

[249] Martin Hirsekorn. Small-size sonic crystals with strong attenuation bands in the audible frequency range. *Applied Physics Letters*, 84(17):3364–3366, 2004.

[250] Martin Philip Bendsøe and Noboru Kikuchi. Generating optimal topologies in structural design using a homogenization method. *Computer Methods in Applied Mechanics and Engineering*, 71(2):197–224, 1988.

[251] Martin P Bendsøe and Ole Sigmund. Topology optimization by distribution of isotropic material. In *Topology Optimization*, pages 1–69. Springer, 2004.

[252] Martin Hirsekorn, Pier Paolo Delsanto, Alan C Leung, and Peter Matic. Elastic wave propagation in locally resonant sonic material: Comparison between local interaction simulation approach and modal analysis. *Journal of Applied Physics*, 99(12):124912, 2006.

[253] Y W Gu, X D Luo, and H R Ma. Optimization of the local resonant sonic material by tuning the shape of the resonator. *Journal of Physics D: Applied Physics*, 41(20):205402, 2008.

[254] T Matsuki, T Yamada, K Izui, and S Nishiwaki. Topology optimization for locally resonant sonic materials. *Applied Physics Letters*, 104(19):191905, 2014.

[255] Grégoire Allaire, François Jouve, and Anca-Maria Toader. Structural optimization using sensitivity analysis and a level-set method. *Journal of Computational Physics*, 194(1):363–393, 2004.

[256] Michael Yu Wang, Xiaoming Wang, and Dongming Guo. A level set method for structural topology optimization. *Computer Methods in Applied Mechanics and Engineering*, 192(1):227–246, 2003.

[257] Takayuki Yamada, Kazuhiro Izui, Shinji Nishiwaki, and Akihiro Takezawa. A topology optimization method based on the level set method incorporating a fictitious interface energy. *Computer Methods in Applied Mechanics and Engineering*, 199(45):2876–2891, 2010.

[258] Alessandro Salandrino and Nader Engheta. Far-field subdiffraction optical microscopy using metamaterial crystals: Theory and simulations. *Physical Review B*, 74(7):075103, 2006.

[259] Zubin Jacob, Leonid V Alekseyev, and Evgenii Narimanov. Optical hyperlens: Far-field imaging beyond the diffraction limit. *Optics Express*, 14(18):8247–8256, 2006.

[260] Zhaowei Liu, Hyesog Lee, Yi Xiong, Cheng Sun, and Xiang Zhang. Far-field optical hyperlens magnifying sub-diffraction-limited objects. *Science*, 315(5819):1686–1686, 2007.

[261] Hyesog Lee, Zhaowei Liu, Yi Xiong, Cheng Sun, and Xiang Zhang. Development of optical hyperlens for imaging below the diffraction limit. *Optics Express*, 15(24):15886–15891, 2007.

[262] Yi Xiong, Zhaowei Liu, and Xiang Zhang. A simple design of flat hyperlens for lithography and imaging with half-pitch resolution down to 20 nm. *Applied Physics Letters*, 94(20):203108, 2009.

[263] Alexander V. Kildishev and Evgenii E. Narimanov. Impedance-matched hyperlens. *Optics Letters*, 32(23):3432–3434, 2007.

[264] Joo Hwan Oh, Young Kwan Ahn, and Yoon Young Kim. Maximization of operating frequency ranges of hyperbolic elastic metamaterials by topology optimization. *Structural and Multidisciplinary Optimization*, 52(6):1023–1040, 2015.

[265] Yong-Lae Park, Carmel Majidi, Rebecca Kramer, Phillipe Bérard, and Robert J. Wood. Hyperelastic pressure sensing with a liquid-embedded elastomer. *Journal of Micromechanics and Microengineering*, 20(12):125029, 2010.

[266] Balazs Czech, Rick van Kessel, Pavol Bauer, Jan Abraham Ferreira, and Ambroise Wattez. Energy harvesting using dielectric elastomers. *Power Electronics and Motion Control Conference (EPE/PEMC), 2010 14th International*, pages S4–18, 2010.

[267] William S. Oates and Fei Liu. Piezohydraulic actuator development for microjet flow control. *Journal of Mechanical Design*, 131(9):091001, 2009.

[268] Muthukrishnan Sathyamoorthy. *Nonlinear Analysis of Structures*, Volume 8. CRC Press, 1997.

[269] W. Lacarbonara. *Nonlinear Structural Mechanics: Theory, Dynamical Phenomena and Modeling*. Springer US, 2013.

[270] Astitva Tripathi and Anil K. Bajaj. Topology optimization and internal resonances in transverse vibrations of hyperelastic plates. *International Journal of Solids and Structures*, 81:311–328, 2016.

[271] Krister Svanberg. The method of moving asymptotes—a new method for structural optimization. *International Journal for Numerical Methods in Engineering*, 24(2): 359–373, 1987.

[272] P.A. Deymier. *Acoustic Metamaterials and Phononic Crystals*. Springer Series in Solid-State Sciences. Springer Berlin Heidelberg, 2013.

3 Pantographic Metamaterial: A (Not So) Particular Case

F. dell'Isola, M. Spagnuolo, E. Barchiesi, I. Giorgio, P. Seppecher

3.1 Introduction

This chapter is devoted to discussion of a particular class of metamaterial, termed as pantographic metamaterial. The research work on this type of metamaterial began in 2003. However, recently, owing to the very rapid development of 3D printing technologies, this work has been enriched through experimental evidence. The current chapter focuses upon the theoretical developments alone, since the fast emerging experimental aspects, which include design, characterization and evaluation of pantographic metamaterials, deserve their own dedicated discussion in a separate chapter.

Materials on Demand

In the last few years, the field of so-called metamaterials has been vigorously explored and exploited in many different ways. In the first (mechanical metamaterials) and second (acoustic metamaterials) chapters of this book, we have largely written about existing metamaterials. In the literature, metamaterials are generally treated as material systems endowed with particular microstructures, and, typically, the global properties of these material systems are analysed using methods devised within the framework of classical or generalized mechanical theories. In contrast, it is more interesting to regard metamaterials as material systems 'on demand', which are expected to fulfil certain functional requirements. In this sense, we must first conceive the theoretical governing equations that describe the requirements and, subsequently, search for a material system whose physics (or mechanical properties if the interest so demands) is specified, in some way, perhaps not exactly, by the conceived equations. Clearly, this point of view opens the horizon to innumerable possibilities of applications. Moreover, current capabilities to produce in a relatively simple way the designed microstructures make it possible to establish experimental foundations for certain mathematical theories which have been an object of varying controversy up to recent times. Thus, the general problem to be solved for designing a new metamaterial is the following: given a desired behaviour, to first find the evolution equations that mathematically describe such a behaviour, and then to specify the material (micro)structure governed by the chosen equations.

With the advancements in manufacturing techniques (e.g., 3D-printing technology and, more generally, of rapid prototyping techniques), the small scale production of materials with complex geometries has become more affordable than ever [1–4, 69–72]. The exploitation of these new technologies in recent years has driven development

of material systems with many different sub-structures. Consequently, there has been an acceleration in the determination and study of new microstructures that, at a well-specified macroscopic scale, exhibit behaviours that are best described by non-standard mathematical models like generalized continuum theories. For instance, the motivations that led to the consideration of pantographic microstructures, i.e. to be well-described at a certain macroscopic spatial scale by second gradient continuum theories, have been extensively discussed in the literature [5–7, 64–68]. As a significant consequence, these considerations have supported the development of a flourishing literature on the history of such higher gradient and generalized continuum theories, some of which have shown [8, 9] that many 'generalized' theories were formulated before or together with the so-called 'classical' theories and then lost, suggesting [10, 11] that some generalized theories were already known at least two centuries ago.

Pantographic Metamaterial

The mathematically driven design of pantographic metamaterial has clearly established that the pioneering efforts to give practical foundations to generalized continuum theories have shown the way to manufacture constructs (microstructures and mechanisms) using existing materials and emerging technology of additive manufacturing that have non-trivial, appealing and tailorable mechanical properties. A pantographic metamaterial (or fabric) conceived through this approach consists of a planar grid obtained by the superposition of two families of fibres (see Fig. 3.1) that are connected by means of small cylinders, called pivots. In the design of these pantographic structures, the aim was to find a material system exhibiting mechanical properties described by a second gradient theory. This theory, which has been studied by Germain [12], Toupin [13],

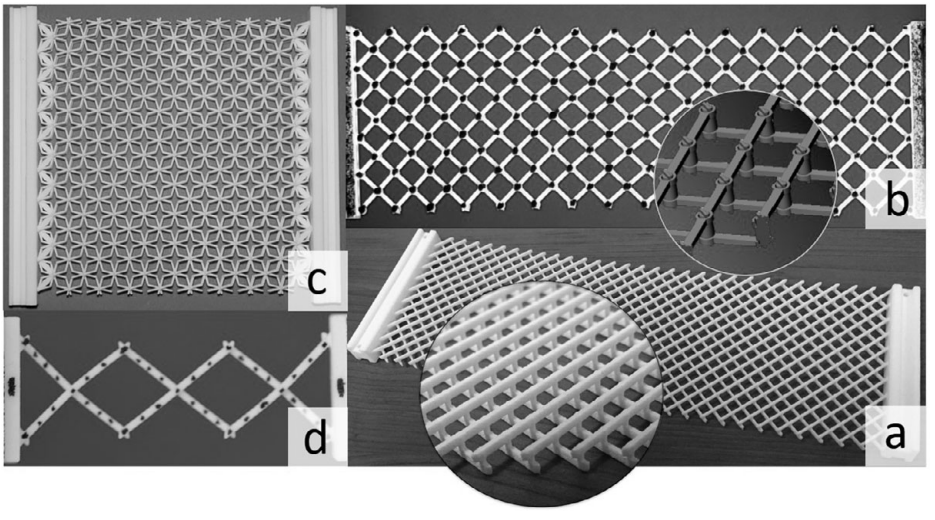

Figure 3.1 Example of polyamide 3D printed pantographic structures: (a) a 'standard' pantographic fabric; (b) a pantographic structure with perfectly compliant pivots; (c) a 'doubly' pantographic plate; (d) a 'millimetric' pantographic structure.

Mindlin [14] and Hellinger [15, 16], is based upon the consideration that the strain energy depends not only on the displacement gradient but also on its second gradient. In what follows, we will first introduce the result of the theory-driven design since this is the main concern of this chapter. We note, therefore, that we will refrain here from further exposition of the deductionist-falsificationist approach presented in the chapter dealing with model theory, which is the approach followed by the contributors to this subject and, as discussed in that chapter, is the preferred and the more powerful approach.

At the first stage of the research effort, the problem was approached from a theoretical point of view. The mathematical models, which were initially introduced, belong to the class of generalized continua, as we have mentioned before. The introduced independent kinematic fields include not only the displacement field but also, eventually, microstretch and microrotation fields. In the second stage it was necessary to develop numerical integration schemes and the corresponding codes for solving, in physically relevant cases, the equations chosen to describe the desired behaviour. Finally, it was necessary to physically realize the microstructures. We can set out a scheme for the whole research process in the following way (for a pictorial representation see Fig. 3.2):

i. design: modelling novel and exotic architectured metamaterials based on a mathematical understanding of the related mechanical problems and on suitably designed numerical simulations;
ii. production: building the designed prototypes by using 3D printing technology;
iii. testing: testing prototypes with experimental apparatuses;
iv. model calibration: producing a careful model fitting of the experimental data by systematic use of numerical simulations;
v. validation: elaborating the obtained data with image correlation techniques for comparing the proposed models with experimental evidence.

The Pantographic Paradigm: An Example of Theory Driven Design

Note a further peculiarity: the case of pantographic metamaterials constitutes a scientific paradigm, which can be translated to very different fields. Every scientific theory can be developed from two different starting points: conjecture, if there are not initial experimental observations, or hypothesis, if everything begins by an effort to interpret some experimental phenomena. The subsequent development of a scientific theory is then always based on validation of the proposed model by experiments. In this sense, the same word *theory* derives its meaning from the Greek θεωρός (*observer*, more precisely a θεωρός was an envoy sent to consult the oracle: similarly, the word theory catches the sense of looking to obtain some information), which is a word composed by θέα (*view*, sight) and the verb ὁράω (*to see*): we have to look at experimental observations to validate a scientific theory. From this point of view, it is interesting to consider the definition of theory as given by Russo in his book [8], because it is possible there to find the same logic employed in the development of the theory of pantographic structures. The rationale is a very old one: it is the basis of science. In his book, Russo states that (literal citation):

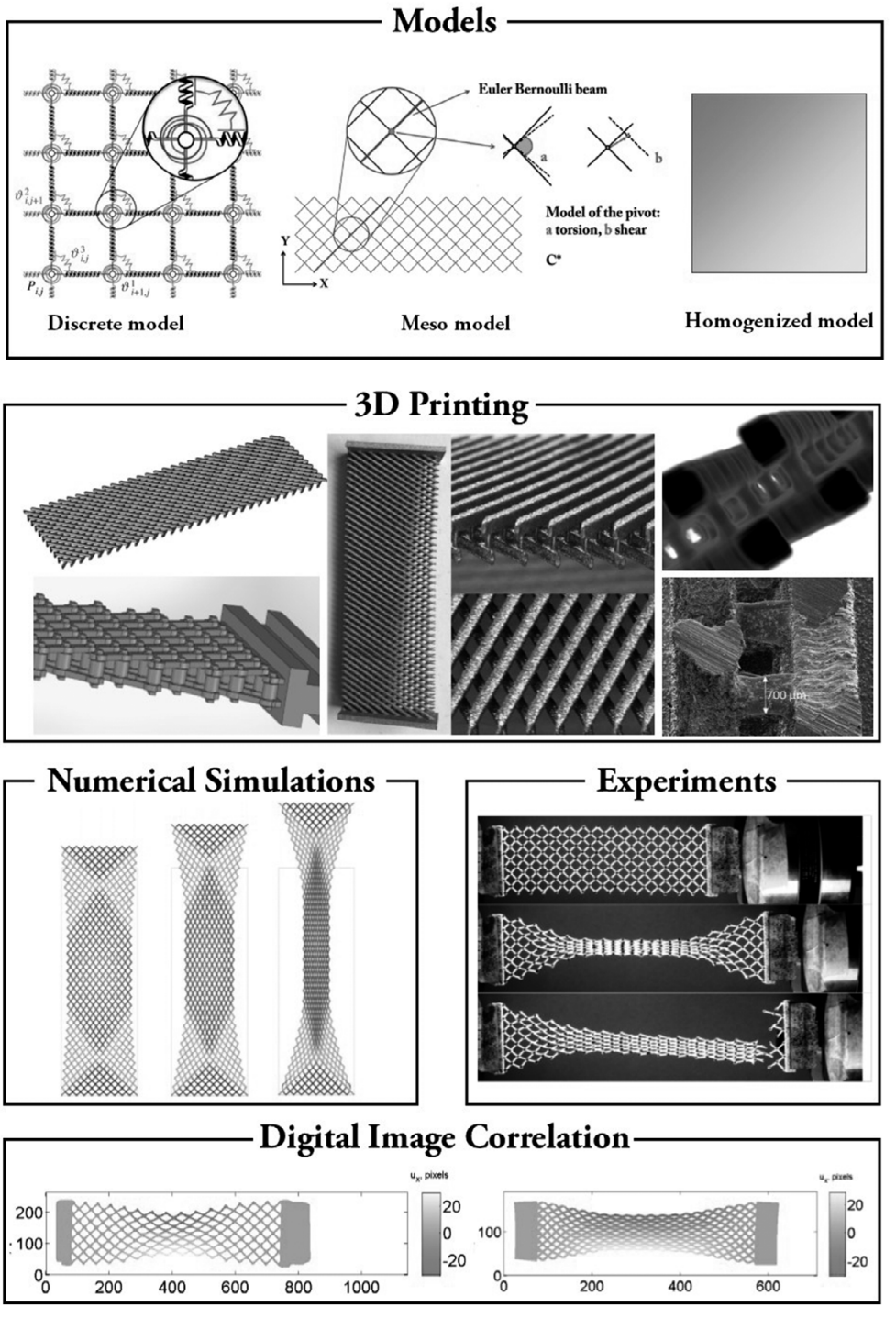

Figure 3.2 Stages of the research process.

A theory has to be such that:

1. Its statements are not about concrete objects, but about specific theoretical entities. [. . .]
2. The theory has a rigorously deductive structure; it consists of a few fundamental statements (called axioms, postulates, or principles) about its own theoretical entities, and it gives a unified and universally accepted means for deducing from them an infinite number of consequences. [. . .]
3. Applications to the real world are based on correspondence rules between the entities of the theory and concrete objects. [. . .]

Any theory with these three characteristics will be called a *scientific* theory. The same term will be used for some other theories, which we may call 'of a higher order'. They differ from the theories we have been considering so far in that they possess no correspondence rules for application to the real world – they are applicable only to other scientific theories.

For a long time, second gradient materials have been treated as the objects of a theory whose set of described phenomena was empty, as experimental evidence able to demonstrate the necessity of reverting to a theory different from classical Cauchy elasticity was missing. Pantographic fabrics provide not only an example of real materials whose description needs the introduction of a second gradient theory, but also an easy-to-handle example of a powerful methodological approach, which can be used to analyse more complex and exotic structures.

3.2 Modeling Pantographic Structures: A Rèsumè of Results Obtained

Pantographic structures have been studied from different points of view during the last decade. Here we give an overview of the models developed to describe the different aspects of this particular metamaterial. Specifically, the fundamental nucleus of the chapter is a presentation of the three main 2D models: the basic Hencky-type discrete model; an intermediate 'meso-model' in which the pantographic structure is considered as composed of Euler–Bernoulli beams; and a continuum second gradient model, which is derived by a heuristic homogenization of the discrete one. This last model represents one of the main reasons for the development of research on pantographic structures. In fact, the theoretical interest in pantographic structures is due to the fact that, for a correct description of their peculiar phenomenology, it is necessary to use higher gradient continuum theories [17, 18] with the relative problem of homogenization [19] and of different possibilities of numerical integration [20, 21]. The presentation of the three 2D models is preceded by an overview of some existing works which inspired the further formulation. Finally, we give some details on two elastic surface models representing a generalization of the 2D model, formulated in order to take into account the possibility that the structures undergo some out-of-plane deformations (e.g. buckling or wrinkling modes).

3.2.1 Pantographic (Micro-)Structures: The Original Path

The very first theory of a pantographic structure as a micro-model associated with a macroscopic second gradient continuum model can be found in [6]. The fundamental

idea was the following: to find the micro-model leading to, in the sense of some homogenization procedure, the simplest second gradient continuum model. The described development can be classified as a multiscale procedure. The history of mechanics offers many examples of multiscale procedures, developed principally to set the relations between macro-models and micro-models. Among the first examples, as reported by Benvenuto in his book about the history of structural mechanics [22], are those due to Maxwell and Saint-Venant [23].

In the field of multiscale procedures, a very efficient approach consists in *asymptotic identification*. Once the micro and macro models have been postulated a priori, a kinematic correspondence is found between them and, subsequently, the equality of the power expended in the corresponding (micro- and macro-) motions is enforced. Through this approach it is possible to evaluate the parameters of constitutive equations of the macro-model in terms of the parameters of the basic cells which form the micro-model. Before proceeding with the description of the model employed in [6], the reader should note a peculiar fundamental aspect of this approach. In this approach, we first postulate the macro-model as a second gradient continuum, and only after that do we look for a possible micro-model which produces the macro-model via homogenization. This theory-driven approach (see again the chapter on model theory) is, in our opinion, very powerful: we don't look at random microstructures hoping to find one which is suitable for our purposes, but rather, having in mind the theory, we want to build the microstructure needed to conform to the theoretical predictions.

At the time that pantographic structures were proposed as metamaterials, second gradient models were already present in the literature. As we have already remarked in the chapter about mechanical metamaterials, we can refer to the *elastica* studied by Euler, Bernoulli and Navier as the very first example of a second gradient model: so, it is necessary to go (at least) back to the beginning of the eighteenth century to find the roots of second gradient theories. The model proposed by Euler is a 1D model. It was after almost a century that the first (incomplete) second gradient 2D and 3D model attributed to the Cosserat brothers [24] was proposed, although it is notable that the origins of 3D higher gradient – and even peridynamic – models can be traced back at least to Piola [10]. We call a material an *incomplete second gradient material* if its deformation energy depends only on $\nabla\mathbf{u}$ and $\nabla\omega(\mathbf{u})$, where $\omega(\mathbf{u})$ is the skew-symmetric part of the gradient $\nabla\mathbf{u}$ of the displacement, $\omega(\mathbf{u}) = \nabla\mathbf{u} - \varepsilon(\mathbf{u})$ with $\varepsilon(\mathbf{u})$ the symmetric part of $\nabla\mathbf{u}$. It is possible to find complete 2D and 3D second gradient models in the description of capillarity or also in the theory of damage and plasticity (because of the well-posedness of mathematical problems related to second gradient models).

The simplest second gradient continuum model is the 1D planar beam studied by Casal in [26, 27] and quoted by Germain in [12]. We can write its (quadratic) deformation energy as

$$\mathcal{E}(u,v) = \frac{\alpha}{2}\int_0^L \left(\left(u''\right)^2 - 2\beta u''v'' + \left(v''\right)^2\right) dx, \tag{3.1}$$

where u and v are, respectively, the axial and transverse components of the displacement and α and β some parameters with $\alpha > 0$ and $|\beta| < 1$. The usual energetic

term due to elongation, proportional to the square of the first derivative of the axial displacement $(u')^2$, is not present in this formulation. From a phenomenological point of view this means that we have a material with a very particular behaviour, that is, it can be stretched without expending any energy. This is one of the most remarkable ways to characterize the pantographic microstructure. Indeed, during the research involved in the development of pantographic fabrics, the objective was to find a microstructure which could be stretched at zero energy (a so-called *floppy mode*).

As a generalization of the simple example proposed by Casal, we can consider a material with the following elastic energy:

$$\mathcal{E}(u) = \int_\Omega A\nabla\nabla u \cdot \nabla\nabla u, \tag{3.2}$$

which is a pure second gradient energy, i.e. it does not at all involve the first gradient of the displacement field. This material is in general subject to a volumic force f and to a generalized boundary force (traction, double forces...) F. We note that, indeed, when considering a similar material, the mechanical interactions with the external world which are involved are not only traction forces but also generalized ones (such as, for example, double forces). If we set $\sigma = 2A\nabla\nabla u$ for simplicity (σ is a third order tensor) then we can write the variational formulation as

$$\forall v,\ \int_\Omega \sigma \cdot \nabla\nabla v - \int_\Omega f \cdot v - \int_{\partial\Omega} F \cdot v = 0. \tag{3.3}$$

Through successive integrations by parts we get the boundary conditions in second gradient theories:

$$div\,(div(\sigma)) - f = 0 \quad \text{on } \Omega \tag{3.4}$$

$$-div^s(\sigma \cdot n)_{/\!/} - div(\sigma) \cdot n = F \quad \text{on } \partial\Omega \tag{3.5}$$

$$(\sigma \cdot n) \cdot n = 0 \quad \text{on } \partial\Omega. \tag{3.6}$$

These boundary conditions are not interpretable on the basis of the standard Cauchy continuum mechanics, and clearly new mechanical interactions arise in higher order theories (we refer to [18] and to Chapter 1 for more details).

The pantographic structure, see a basic module in Fig. 3.3 and a 1D planar array in Fig. 3.4, was first introduced in the field of homogenized generalized media in [6, 28].

To obtain the corresponding homogenised macro-model it is necessary to consider a structure composed of n pantographic modules and to study its behaviour when n tends to infinity.

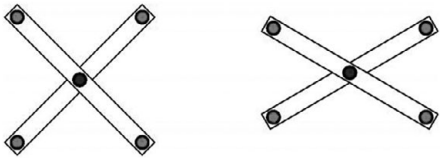

Figure 3.3 Basic module of a pantographic structure and its stretched configuration.

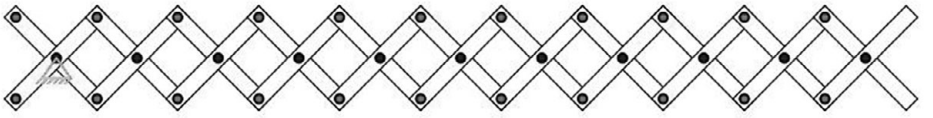

Figure 3.4 Pantographic microstructure of a 1D planar beam.

Some formal asymptotic expansion procedures, already used in [6, 28], are systematically considered in [29] for determining the effective properties of periodic structures consisting of welded linear elastic bars. Remarkably, for the case when the bending and torsion stiffnesses of isotropic homogeneous elastic bars are lower than the extension stiffness, interesting macro-models are obtained. In finding macro-models for micro-architectured metamaterials there is usually a complex estimate that needs to be made, namely, is the energy associated with second gradient displacements negligible with respect to first gradient energy? For a long time it was believed that second gradient energies were *always* negligible [11]. This belief was proven to be ungrounded at the dawn of modern continuum mechanics by Gabrio Piola [10, 30]. However the results of Piola have been ignored for a long time in the orthodox Cauchy–Truesdell school.

In order to show that synthesizing second gradient metamaterials with non-negligible second gradient energy is not only possible, but can be addressed mathematically, it has been proven that [6, 31]:

i. pantographic microstructures allow for the synthesis of Casal-type beams (see deformation energy in Eq. (3.1));
ii. using two families of pantographic substructures it is possible to synthesize second gradient plates: i.e. plates whose deformation energy depends on second gradients of in-plane displacements;[1]
iii. in the presence of perfect pivots[2] the macro deformation energy of short beam pantographic structures does not include any first gradient terms *at all*, and in pantographic fabrics one can observe so-called floppy-modes: i.e. homogeneous local deformations corresponding to vanishing deformation energy (see also the remark below);
iv. the mathematical treatment of second gradient linearized elastic continua (synthesized as described in this chapter) requires the introduction of anisotropic Sobolev spaces [32, 33].

REMARK *In so-called long-fibre pantographic metamaterials (see Fig. 3.5) there is only a* 1*-parameter family of floppy modes while in short-fibre pantographic metamaterials (see Fig. 3.6) there are* ∞^3 *floppy modes.*

[1] In classical plate theory the second gradients of transverse displacements only appear in the deformation energy.

[2] The reader will see in Chapter 6 that 3D printing allows for the construction of microstructures with so-called perfect pivots, i.e. hinges or pivots which can be twisted without expending any energy.

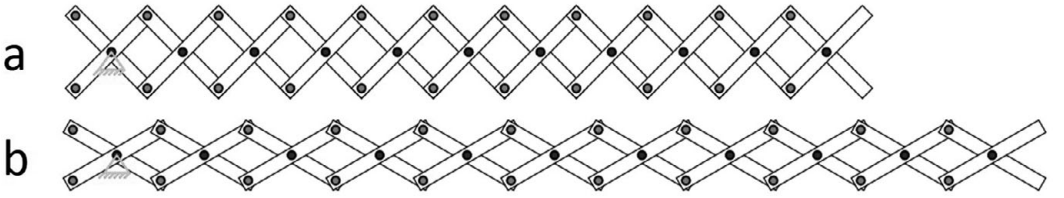

Figure 3.5 Reference configuration (a) and deformed configuration (b) of a pantographic beam. The deformed configuration (b) represents a so-called *floppy mode*.

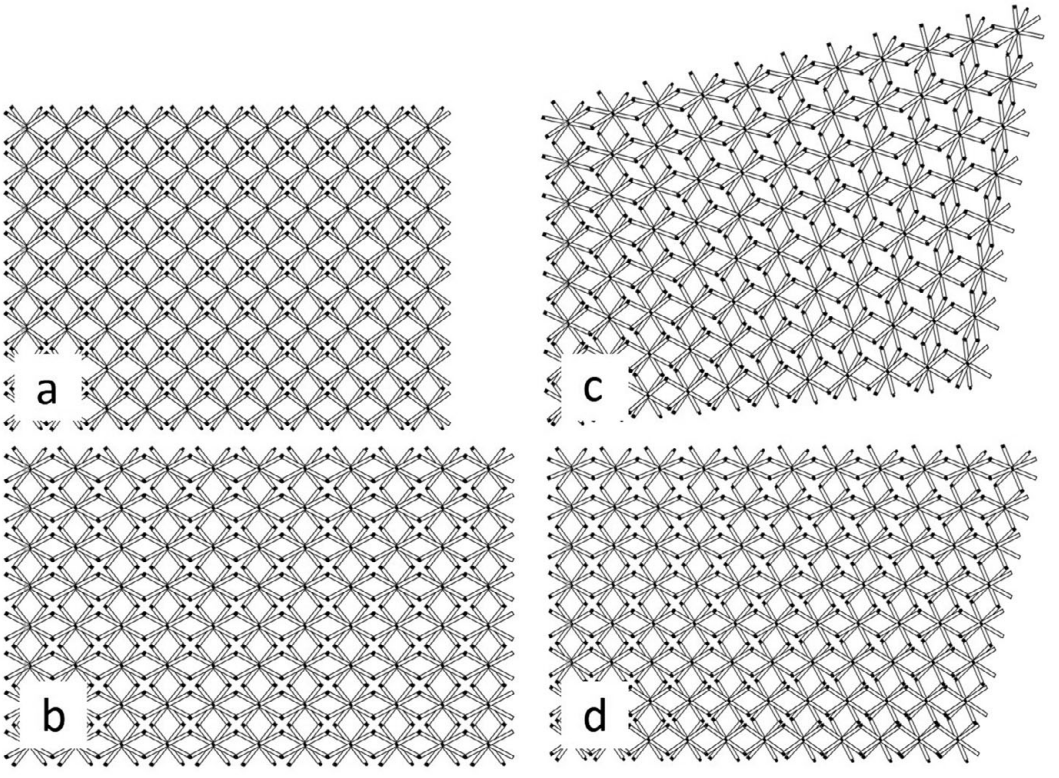

Figure 3.6 Reference configuration (a) and deformed configurations (b) of a pantographic 2D structure. The deformed configurations (b) represent some of the *floppy modes*.

We underline here, in particular reference to Chapter 4 on naive model theory, that we did not find the pantographic microstructures via a data-driven procedure, nor by trial and error. Instead, being guided by classical mechanics, we built some mechanisms whose degrees of freedom would produce 'floppy modes' at micro-level in the designed and desired metamaterials. Adding some extra constraints (i.e. considering the boundary conditions needed for second gradient continua, see [6, 31, 43], one 'blocks' macro

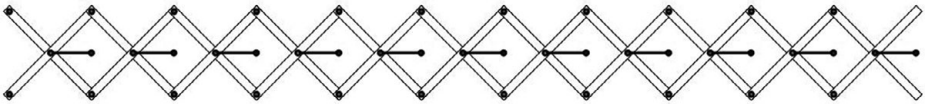

Figure 3.7 Warren-type pantographic microstructure, producing as a homogenized model a third gradient planar beam model.

floppy modes but leaves them active at the local (micro) level. We therefore achieve theory-driven synthesis of second gradient materials.

As a second example of synthesis of higher gradient materials, in [6] it is shown how, by considering a modified (Warren-type) pantographic structure as micro-model, it is possible to obtain a third gradient planar beam model (Fig. 3.7) as a homogenized macro-model. An interesting difference between the two models is that the pantographic beam does not store any energy when undergoing uniform extension, while the Warren-type pantographic beam undergoes a floppy-mode under uniform flexure.

3.2.2 Pipkin's Higher Gradient Plate Modelling Systems with Inextensible Fibres

The model we have previously presented is a linear model (see the energy reported in Eq. 3.1). We now describe the generalization to the non-linear case. The efforts in that direction are based upon work by Pipkin and co-workers [34–41] on inextensible fibres. Taking inspiration from this work, 2D continua composed by two orthogonal families of inextensible fibres have been studied in [42], and this work was further extended and applied to pantographic lattices in [5, 43]. The concept of a continuum model regarded as composed of fibres needs further explanation. Let us consider a $2D$ continuum with a rectangular domain $\Omega \subset \mathbb{R}^2$ as reference shape. The sides of the rectangle are in a ratio of 1:3 (so chosen since some remarkable features arise if we consider structures whose sides ratio is at least 1:3, as we will describe in the chapter dedicated to experimental methods). To invesigate the planar motions of this continuum, we introduce a suitably regular function $\boldsymbol{\chi} : \Omega \to \mathbb{R}^2$ (we call it 'macro-placement') which relates the reference positions to the current ones $(X_1, X_2) \overset{\boldsymbol{\chi}}{\mapsto} (x_1, x_2)$.

An orthogonal frame of reference (O, ξ_1, ξ_2), whose axes ξ_1 and ξ_2 are oriented along the inextensible fibres in the reference configuration, is introduced. Accordingly, we have the following non-dimensional coordinates:

$$\xi_1 \coloneqq \frac{1}{l}(X_1 - X_2) + \frac{1}{2} \ , \ \ \xi_2 \coloneqq \frac{1}{l}(X_1 + X_2) + \frac{1}{2}. \tag{3.7}$$

A graphical explanation of the introduced quantities is given in Fig. 3.8. The Cartesian frame (O, ξ_1, ξ_2) is chosen so that the members of its associated basis, namely the ordered couple of vectors (D_1, D_2), are oriented, in the reference configuration, as the two families of fibres. The inextensibility constraint can be introduced by considering that a curve γ is inextensible for a placement $\boldsymbol{\chi}$ if, for every part γ_1 of γ, $\boldsymbol{\chi}(\gamma_1)$ has the same length as γ_1. The presence of this 'inextensibility constraint' allows us to discuss *inextensible* fibres.

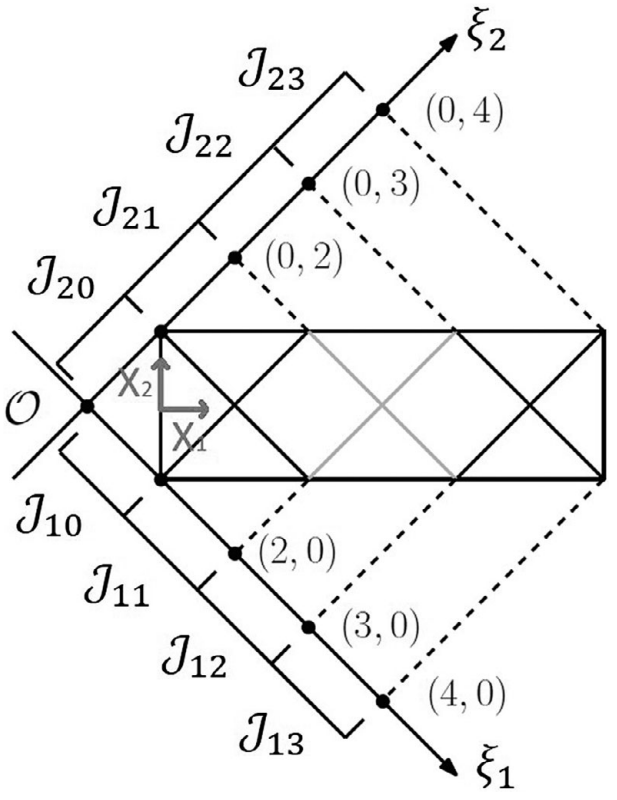

Figure 3.8 The inextensible fibre configuration and relative Lagrangian coordinates.

By definition, d_1 and d_2 are considered to be the transformed vectors in the current configuration, of the vectors D_1 and D_2, respectively, i.e. $d_\alpha = FD_\alpha,\ \alpha = 1, 2$, where $F = \nabla\boldsymbol{\chi}$. From their definition, which requires that $\boldsymbol{\chi}$ is at least locally continuously differentiable, it follows that the vectors d_α are tangent to the fibres in the current frame. Moreover, the inextensibility constraint implies that $\|d_1(\xi_1, \xi_2)\| = \|d_2(\xi_1, \xi_2)\| = 1$ for all (ξ_1, ξ_2). It can be shown (see Rivlin [44] for a formal demonstration) that, if we restrict our analysis to an open simply linearly connected set Δ of Ω, where $\boldsymbol{\chi}$ is twice continuously differentiable, the inextensibility of fibres allows the following representation formula:

$$\boldsymbol{\chi}^\Delta(\xi_1, \xi_2) = \boldsymbol{\chi}_1^\Delta(\xi_1) + \boldsymbol{\chi}_2^\Delta(\xi_2). \tag{3.8}$$

Moreover, if we denote with $\mu_1^\Delta(\xi_1)$ and $\nu_1^\Delta(\xi_1)$ the projections of $\boldsymbol{\chi}_1^\Delta(\xi_1)$ on D_1 and D_2, respectively, and $\nu_2^\Delta(\xi_2)$ and $\mu_2^\Delta(\xi_2)$ the projections of $\boldsymbol{\chi}_2^\Delta(\xi_1)$ on D_1 and D_2, respectively, then

$$\boldsymbol{\chi}_1^\Delta(\xi_1) = \mu_1^\Delta(\xi_1)D_1 + \nu_1^\Delta(\xi_1)D_2 \text{ and } \boldsymbol{\chi}_2^\Delta(\xi_2) = \nu_2^\Delta(\xi_2)D_1 + \mu_2^\Delta(\xi_2)D_2. \tag{3.9}$$

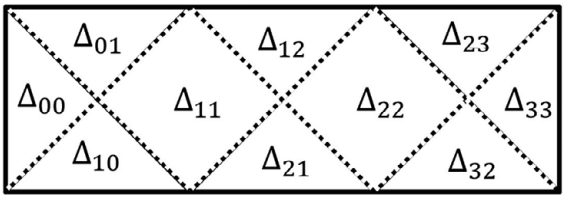

Figure 3.9 Domain pattern induced by the boundary conditions.

As we have already noted, the constraint of inextensibility can be expressed by imposing that the norm of d_1 and d_2 is equal to one. Therefore, we can introduce two quantities $\vartheta_1^\Delta(\xi_1)$ and $\vartheta_2^\Delta(\xi_2)$ such that

$$d_1^\Delta = \cos\vartheta_1(\xi_1)D_1 + \sin\vartheta_1(\xi_1)D_2 \text{ and } d_2^\Delta = \sin\vartheta_2(\xi_2)D_1 + \cos\vartheta_2(\xi_2)D_2. \quad (3.10)$$

We can now study the Pipkin continuum by considering some boundary conditions. In a standard bias extension test[3] we fix the left short side of the rectangle (denoted by Σ_1) and we impose a non-vanishing displacement u_0 on the right short side (denoted by Σ_2). Because of fibre inextensibility, the boundary conditions on Σ_1 and Σ_2 can be used to determine directly the placement field in the interior of Ω [42], i.e. on the regions Δ_{00} and Δ_{33} of Fig. 3.9. The determination of the function χ in the other regions then follows in a straightforward manner.

Due to the fibre inextensibility we can also establish a relation between the functions μ_i^Δ and ν_i^Δ

$$\|F\cdot D_1\|^2 = 1 \Rightarrow \left(\mu_{1,1}^\Delta\right)^2 + \left(\nu_{1,1}^\Delta\right)^2 = 1 \Rightarrow \nu_{1,1}^\Delta = \pm\sqrt{1-\left(\mu_{1,1}^\Delta\right)^2}, \quad (3.11)$$

$$\|F\cdot D_2\|^2 = 1 \Rightarrow \left(\mu_{2,2}^\Delta\right)^2 + \left(\nu_{2,2}^\Delta\right)^2 = 1 \Rightarrow \nu_{2,2}^\Delta = \pm\sqrt{1-\left(\mu_{2,2}^\Delta\right)^2}. \quad (3.12)$$

Hence, the admissible placements in the Pipkin's plate are only determined by the globally continuous and piecewise, twice continuously differentiable, fields $\mu_1(\xi_1)$ and $\mu_2(\xi_2)$. Equations (3.10)–(3.12) allow us to restrict our study to the ordinary differential equations

$$\frac{\mathrm{d}\mu_\alpha(\xi_\alpha)}{\mathrm{d}\xi_\alpha} = \cos\vartheta_\alpha(\xi),\ \alpha = 1,2. \quad (3.13)$$

In fibre-inextensible 2D Pipkin continua it is customary to introduce the *shear deformation* γ as a strain measure, defined as the scalar product of the fibre directions in the deformed configuration. Recalling the inextensibility assumption and Eq. (3.10), the *shear deformation* γ reads as

$$\gamma(\xi_1,\xi_2) \coloneqq d_1\cdot d_2 = \cos\left(\frac{\pi}{2} - \vartheta_1(\xi_1) - \vartheta_2(\xi_2)\right) = \sin\left(\vartheta_1(\xi_1) + \vartheta_2(\xi_2)\right). \quad (3.14)$$

[3] It should be clear now that the bias extension test plays a central role in the study of deformable fabrics.

Further, the following kinematic constraint should be enforced:

$$-\frac{\pi}{2} < \vartheta_1 + \vartheta_2 < \frac{\pi}{2} \ (\Longrightarrow \ -1 < \gamma < 1)\,, \tag{3.15}$$

if the case $\vartheta_1 + \vartheta_2 = \pm\frac{\pi}{2}$, which represents overlapping fibres, is to be avoided. Now that the fields $\vartheta_1(\xi_1)$ and $\vartheta_2(\xi_2)$ uniquely describe admissible placements, the strain energy density $W\left(\vartheta_1, \vartheta_2, \frac{\mathrm{d}\vartheta_1}{\xi_1}, \frac{\mathrm{d}\vartheta_2}{\xi_2}\right)$ may be introduced. We postulate that W has the following form:

$$W\left(\vartheta_1, \vartheta_2, \frac{\mathrm{d}\vartheta_1}{\xi_1}, \frac{\mathrm{d}\vartheta_2}{\xi_2}\right) = \alpha g(f(\gamma)) + \beta g(\|\nabla f(\gamma)\|), \tag{3.16}$$

with $g(x) = \frac{1}{2}x^2$. Different functions f have been studied [5, 43], among which:

S $f(\gamma) = \gamma$,
Q $f(\gamma) = \arcsin\gamma$,
T $f(\gamma) = \tan(\arcsin\gamma)$.

The two cases ($\alpha = 1, \beta = 0$) and ($\alpha = 0, \beta = 1$) are referred to as pure *first gradient energy* (1g) and pure *second gradient energy* (2g), respectively. Numerical results [45–49] show that the equilibrium configurations obtained by considering second gradient energies are substantially different if compared to the ones obtained with the first gradient approach (see Fig. 3.10). An experimental validation is needed to decide which model produces the best representation of reality. We will discuss this issue in detail in Chapter 6 concerning experimental methods.

3.2.3 Three Scales, Three Models: Micro, Meso and Macro Models for Non-linear 2D Pantographic Sheets

Using the theoretical framework we have discussed as our basis, we can now consider the non-linear 2D second gradient continuum model of a pantographic lattice with extensible fibres. Clearly we can approach the problem from different points of view. We note that we have introduced the necessary concepts needed to develop a micro model and its homogenized second gradient macro model. We are also able to find a homogenization procedure to connect the two different scales. Finally, a third approach has been proposed to model a particular class of pantographic structures (when the fibres of the same family are not too close to one another).

It is therefore important at this juncture to review how the modelling process relates to reality. Via a process of design and subsequent manufacturing (we will address this in the chapter about experimental methods), it is possible to obtain real samples which are ultimately 3D objects composed of fibres with a non-zero cross-sectional area and which are disposed in two parallel planes. Remember that in the models we refer to all the fibres of one plane as a 'family' of fibres. The fibres of any plane are all parallel one to the other and the two planes are separated by cylinders (or the pivots) which connect the fibres of one family to those of the second family. Reality plays a fundamental role in the definition of the representative elementary volume (REV). As can be observed

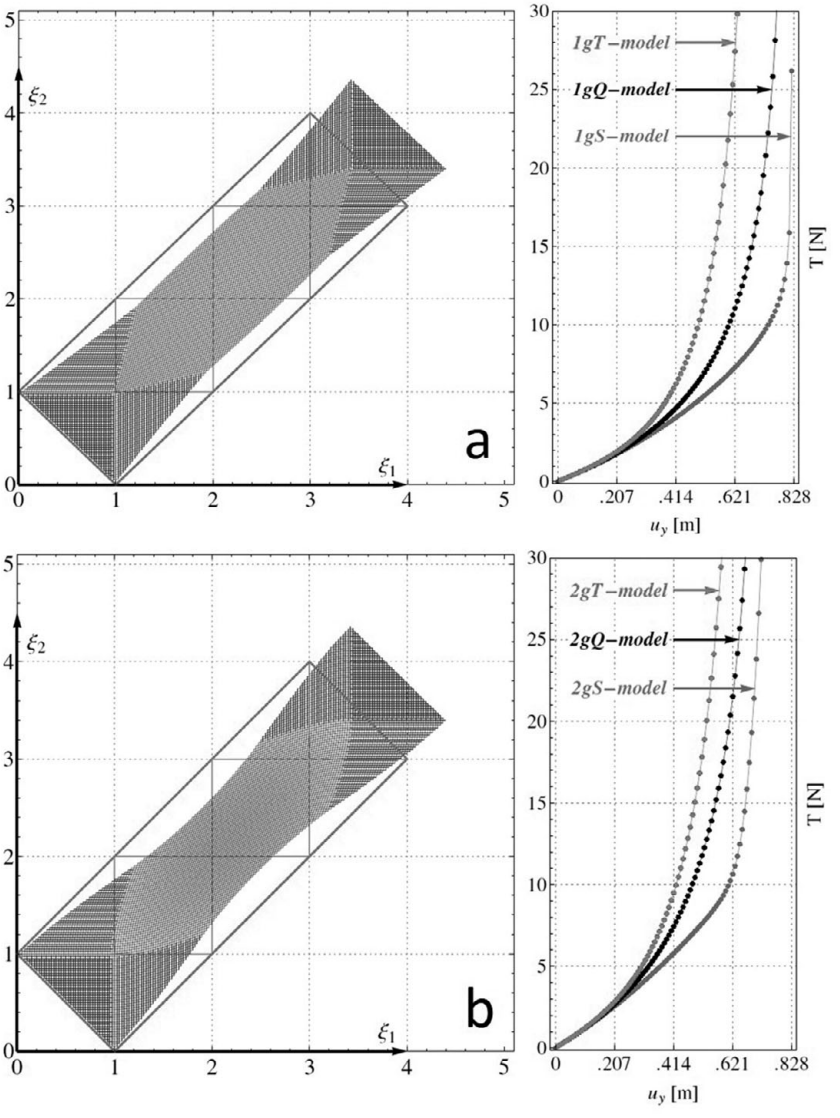

Figure 3.10 Deformed equilibrium configurations and resultant (normal) forces on the short side for a BIAS extension test for the first gradient 1gT (a) and second gradient 2gT (b) models.

in Fig. 3.11, at different scales we need different models for properly describing the phenomena. So, for example, we can use a homogenized continuum model if we regard the structure as a plate (Fig. 3.11a), but we will have to introduce a beam model to describe it if the chosen REV is the one depicted in Fig. 3.11b, or we will clearly need to use the standard Cauchy continuum model in the description of a small part of a fibre (Fig. 3.11c), and it is likely that we shall have to use some atomistic method if our REV contains only a few atoms.

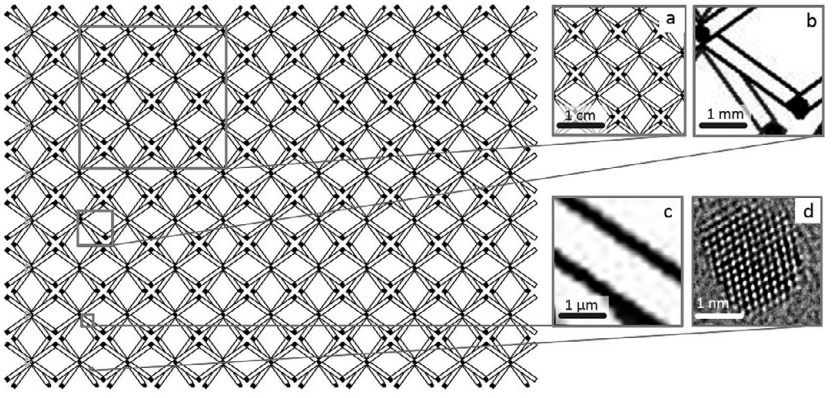

Figure 3.11 Different REVs for different scales imply different models: (a) Second gradient continuum model; (b) Beam theory; (c) Standard Cauchy continuum mechanics; (d) Quantum mechanics.

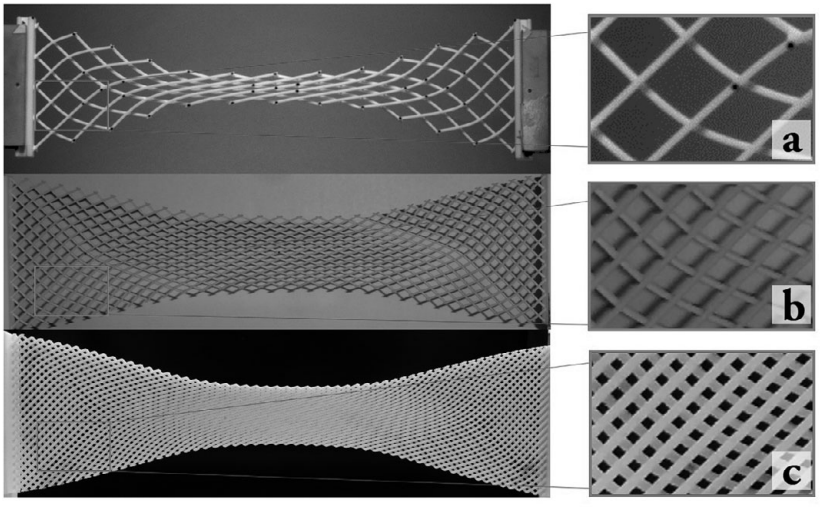

Figure 3.12 Three pantographic structures which differ in the density of fibres.

Clearly, the real sample *is* not a 2D continuum, but it will be *modelled* in the following discussion as if it were. Obviously, when the fibres are too far apart (see Fig. 3.12.a) we shall find that the continuum model is no longer applicable and for this specific case a 'meso' model which describes the structure as being composed of continuous fibres (so it is not continuous in the sense of a 2D plate, but only in the description of the fibres) has been developed.

Current research is directed toward investigation of the validity limits of the second gradient continuum model. First results show that it is in good agreement with experimental measurements also for structures not at all dense (in the sense of distribution

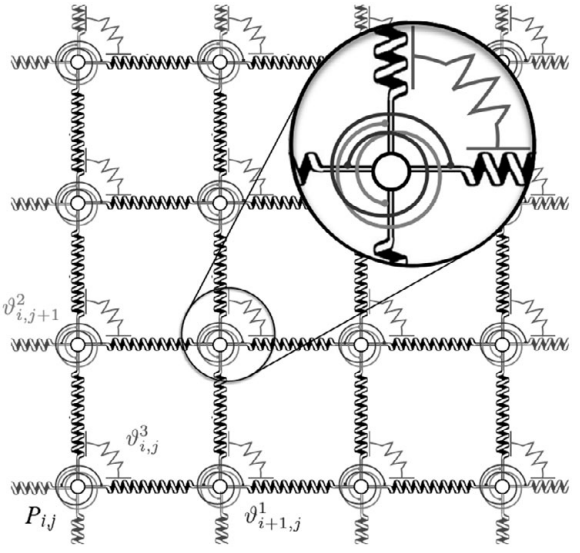

Figure 3.13 Representation of the discrete Hencky-type model of a pantographic sheet (in the detail the three rotational springs are shown).

of fibres) such as the one in Fig. 3.12.a. We will describe in the following, after the presentation of the three models, some very preliminary results of this research.

3.2.4 Discrete Hencky-type Model

In conformance with multiscale procedures, a discrete approach can be considered for modelling pantographic structures [28, 50, 51]. In the models previously presented we had an inextensibility constraint on the fibres composing the structure. Here, to obtain a better agreement with experimental evidence [5, 28] extension of fibres is accounted for by modelling the fibres as being composed by material particles connected by extensional springs. Moreover, for describing the bending of fibers at the micro level, we introduce rotational springs at each node of the lattice.

Let us consider a Lagrangian Cartesian orthonormal coordinate system with its associated basis of unit vectors (D_1, D_2) representing the fibre directions in the reference configuration. In this configuration the lattice points have the following positions:

$$P_{i,j} = (i\epsilon, j\epsilon), \quad i = 0, 1, \ldots, N \text{ and } j = 0, 1, \ldots, M, \tag{3.17}$$

where ϵ is the distance between two adjacent lattice points, and N and M are the numbers of points along the fibre directions (see Fig. 3.13). In the current configuration, we denote the positions of the lattice points (whose position in the reference configuration is labeled $P_{i,j}$) with $p_{i,j}$. The lattice points at the nodes $P_{i,j}$ are connected by extensional springs along two directions (Fig. 3.13). These extensional springs, characterized by the rigidities $k^1_{i,j}$ and $k^2_{i,j}$ for the two directions, provide energetic terms depending on the distances between adjacent contiguous points in the current configuration, i.e. the

distance $\|p_{i,j+1} - p_{i,j}\|$ for the fibres which are oriented along D_1 in the reference configuration, and on the distance $\|p_{i+1,j} - p_{i,j}\|$ for the fibres oriented D_2 in the reference configuration. Further energetic terms are provided by rotational springs which are positioned at each node. For a good representation of bending and shear of the structure, we have to consider three rotational springs, characterized by the rigidities $b^1_{i,j}$ and $b^2_{i,j}$ (bending of fibres) and $b^3_{i,j}$ (torsion of pivots), at each node. Their deformation energies depend, respectively, on the angles:

1. $\vartheta^1_{i,j}$ between the vectors $p_{i-1,j} - p_{i,j}$ and $p_{i+1,j} - p_{i,j}$,
2. $\vartheta^2_{i,j}$ between the vectors $p_{i,j-1} - p_{i,j}$ and $p_{i,j+1} - p_{i,j}$,
3. $\vartheta^3_{i,j}$ between the vectors $p_{i,j+1} - p_{i,j}$ and $p_{i+1,j} - p_{i,j}$.

We then postulate the following strain energy for the microscopic Lagrangian discrete system:

$$\begin{aligned} U(\{p_{i,j}\}) = &\sum_j \sum_i \frac{k^1_{i,j}}{2}(\|p_{i+1,j} - p_{i,j}\| - \epsilon)^2 + \sum_j \sum_i b^1_{i,j}(\cos\vartheta^1_{i,j} + 1) \\ &+ \sum_j \sum_i \frac{k^2_{i,j}}{2}(\|p_{i,j+1} - p_{i,j}\| - \epsilon)^2 + \sum_j \sum_i b^2_{i,j}(\cos\vartheta^2_{i,j} + 1) \\ &+ \sum_j \sum_i \frac{b^3_{i,j}}{2}\left|\vartheta^3_{i,j} - \frac{\pi}{2}\right|^{\xi}, \end{aligned} \tag{3.18}$$

where ξ is a parameter that is equal to 2 for a generic linear case. In [50, 51], the above described discrete model made of extensional and rotational (i.e. torsional) springs is solved at each iteration by energy minimisation.

As a numerical application of the model described, see Figs. 3.14 and 3.15. In Fig. 3.14 the deformed shape of a pantographic structure is shown resulting from a BIAS extension test simulation using the discrete energy in Eq. (3.18). In the same manner, in Fig. 3.15 we show the deformed shape of a pantographic structure resulting from a shear test simulation.

3.2.5 Euler–Bernoulli Non-linear Beam Theory Meso-model

As noted, a homogenized model cannot be properly (exactly) used to describe all the details of structures such as the one in Fig. 3.16 (even if we have already suggested that the error in some sense is rather small). To reveal certain additional details for this kind of structure one can consider so-called 'meso-models', which are intermediate between the discrete and the homogenized. This model, along with an example of its numerical application, was first presented in [52]. In this case, the fibres of the pantographic structure are modelled as non-linear Euler–Bernoulli beams.

This model, which we discuss briefly here, makes it possible to describe structures composed of two families of fibres (which are not very close to each other, see

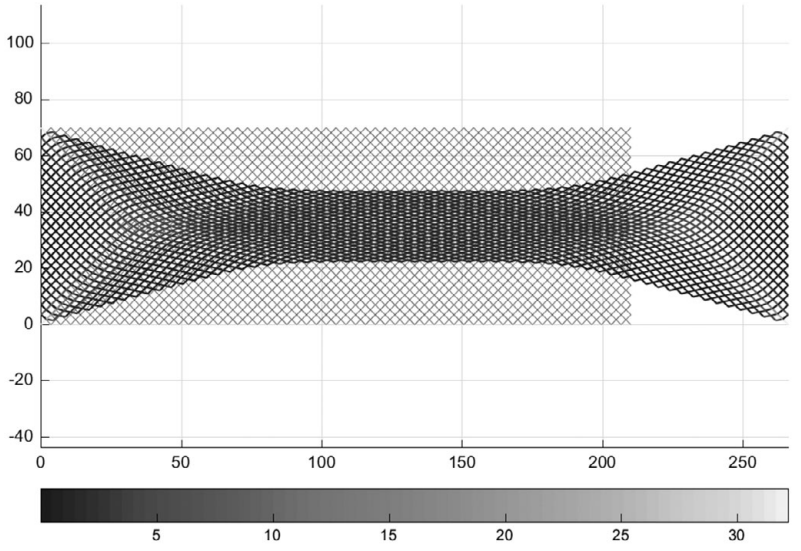

Figure 3.14 BIAS extension test numerical simulation of a pantographic structure described by the discrete Hencky-type model: reference configuration (in *grey*) and current shape.

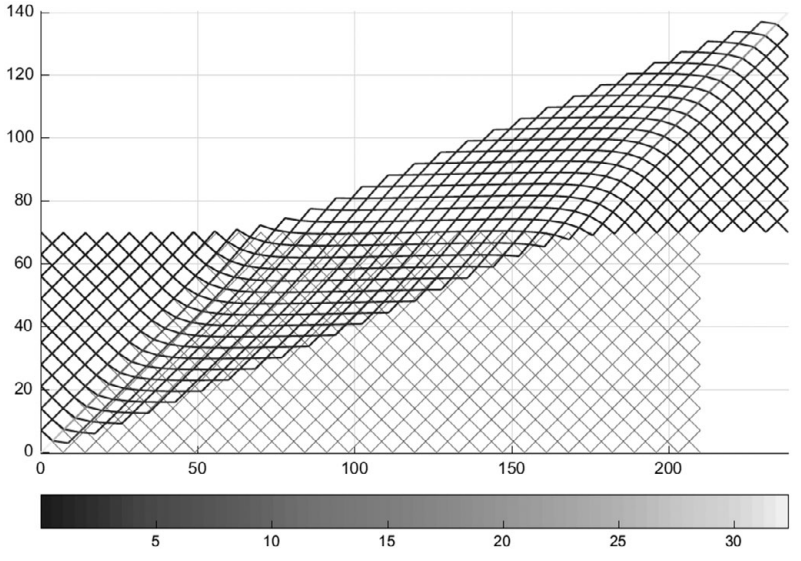

Figure 3.15 Shear-extension test numerical simulation of a pantographic structure described by the discrete Hencky-type model: reference configuration (in *grey*)and current shape.

Fig. 3.16) interconnected by some cylinders (the real pivots) whose torsion and flexion are a priori non-negligible. Pivots are modelled by adding in every interconnection a torsional spring (accounting for the shear of the pantographic structure at a macro level) and, possibly, an extensional spring (allowing for the sliding of a fibre with respect to

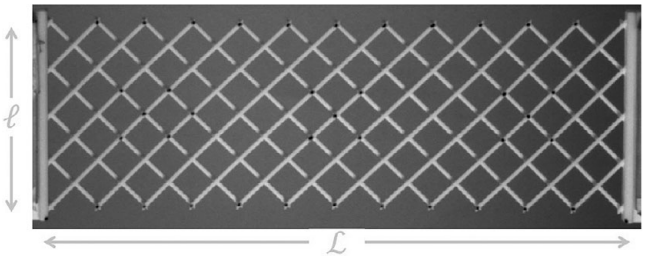

Figure 3.16 Specimen in the reference configuration.

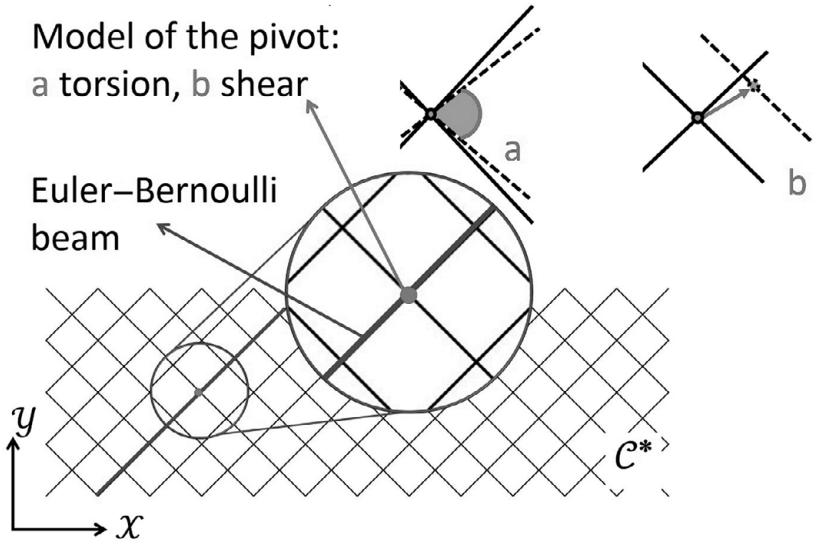

Figure 3.17 Reference configuration of the pantographic structure and representation of the pivot mechanisms.

the corresponding one in the other family, i.e. the fibre in the other family connected to it by the pivot, see Fig. 3.17). Each fibre element of length L_i (L_i is the distance between two adjacent pivots in the current configuration) is then modelled as an Euler–Bernoulli beam, endowed with a stretching energy W_s^i and a bending energy W_b^i. The total number of fibre elements is denoted by M.

The deformation energy, which by a numerical minimisation makes it possible to determine equilibrium configurations, is defined as follows: for a single fibre element i of length L_i we have an elastic energy depending quadratically on axial strain (stretching energy):

$$W_s = \sum_{i=1}^{M} \frac{1}{2} \int_0^{L_i} EA\epsilon^2 \, dx, \tag{3.19}$$

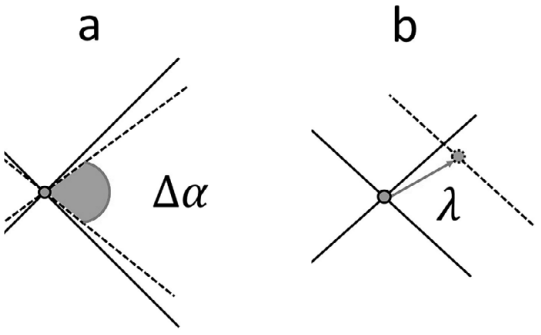

Figure 3.18 Representation of pivot energetic terms.

and curvature (bending energy)

$$W_b = \sum_{i=1}^{M} \frac{1}{2} \int_0^{L_i} EI\kappa^2 \, dx. \tag{3.20}$$

Referring to Fig. 3.18.a, a pivot torsion energy term can be written as follows:

$$W_p = \sum_{i=1}^{N_p} \frac{1}{2} k_p \left(\frac{\pi}{2} - \Delta\alpha_i \right)^2, \tag{3.21}$$

where $\Delta\alpha_i$ represents the change of the angle between two intersecting fibres in the deformed configuration with respect to the reference configuration. In [52] an additional energetic term is considered that allows us to describe the (possible) sliding of fibres in at the interconnecting pivots. We will consider this possibility in Chapter 6 about experimental methods.

The total potential energy is thus given as

$$W = W_s + W_b + W_p. \tag{3.22}$$

Now by considering the minimum of potential energy,

$$\delta W = 0, \tag{3.23}$$

we can obtain the equilibrium configurations. It is evident that the problem presented cannot be solved analytically. The Ritz approach is employed in [52] to solve this problem, and consists in discretising the energy (3.22) and minimising it, after having introduced some shape functions for the displacement. For all the details we refer the reader directly to the article. In Fig. 3.19, a comparison between the calculated deformed shapes and the measured is shown.

3.2.6 Second Gradient Homogenized Model

In order to make this chapter self-contained we now present again the central feature in the field of pantographic metamaterials which is the $2D$ continuum macro-

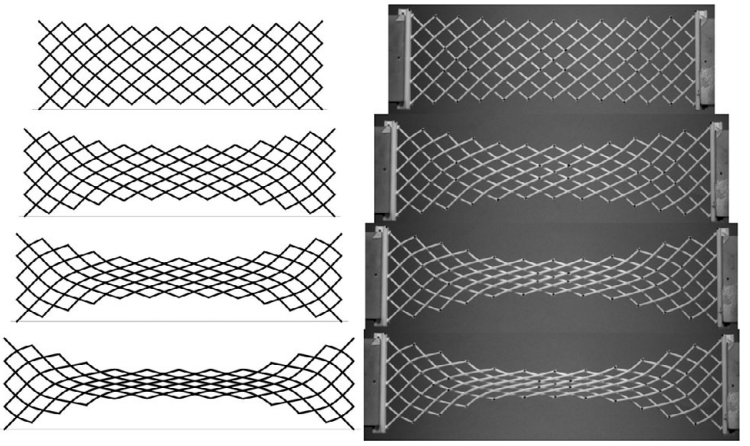

Figure 3.19 Comparison between experimental (right) and numerical (left) shapes of the pantographic structure. They differ in the imposed displacement: (a) 0.014 m, (b) 0.037 m, (c) 0.048 m, (d) 0.054 m.

model obtained via homogenization of the discrete Hencky-type micro-model presented previously. Expanding in truncated Taylor series the kinematic map as explained in [28], we can compute the micro-placement field of material particles at the nodes of the reference lattice by using the values, in such nodes, of a regular macro-placement and its first gradient. Such a map determines a unique micro-motion once a macro-motion is given. The micro–macro transition is obtained by equating the micro-strain energy with the macroscopic counterpart, thus obtaining a macroscopic Lagrangian surface density of strain energy in terms of the constitutive coefficients appearing in the postulated expression of the micro-strain energy. Numerical simulations with both discrete and homogenized models show that the homogenized model is representative of the microscopic response [50, 51]. Following the notation introduced above, we now consider a $2D$ continuum whose reference shape is given by a rectangular domain $\Omega = [0, N\epsilon] \times [0, M\epsilon] \subset \mathbb{R}^2$. Very often, it is assumed that $N = 3M$, which, as we have already remarked, is the standard relation between the width and height of a fabric specimen for experimental and numerical tests. If we want to study only planar motions, then the current shape of the rectangle Ω is mathematically described by regular macro-placement $\boldsymbol{\chi} : \Omega \to \mathbb{R}^2$. Following the so-called Piola's Ansatz, it is chosen that $p_{i,j} = \boldsymbol{\chi}(P_{i,j}) \quad \forall i = 1, \ldots, N, \forall j = 1, \ldots, M$. Assuming that $\boldsymbol{\chi}(\cdot)$ is at least twice differentiable at $P_{i,j}$, the following second order approximations are obtained

$$\|p_{i+1,j} - p_{i,j}\| = \|\boldsymbol{\chi}(P_{i+1,j}) - \boldsymbol{\chi}(P_{i,j})\| \backsimeq \epsilon \|F(P_{i,j})D_1 + \frac{\epsilon}{2}\nabla F(P_{i,j})|D_1 \otimes D_1\|, \tag{3.24}$$

$$\|p_{i,j+1} - p_{i,j}\| = \|\boldsymbol{\chi}(P_{i,j+1}) - \boldsymbol{\chi}(P_{i,j})\| \backsimeq \epsilon \|F(P_{i,j})D_2 + \frac{\epsilon}{2}\nabla F(P_{i,j})|D_2 \otimes D_2\|, \tag{3.25}$$

where F denotes the deformation gradient $\nabla\boldsymbol{\chi}$. Further details can be found in [28, 50, 51]. Equations (3.24) and (3.25) present the ϵ-truncated Taylor expansion of the first and the third addends in Eq. (3.18) (extensional terms). Letting $\epsilon \to 0$ one finally recovers the homogenized terms. To homogenize the bending and torsional energetic terms, it is necessary to rewrite the three angles $\vartheta^{\alpha}_{i,j}$ ($\alpha = 1, 2$) and $\vartheta^{3}_{i,j}$ as functions of the macro-placement $\boldsymbol{\chi}$. Specifically, we express the cosines of these angles in terms of $\boldsymbol{\chi}$. Using analogous Taylor expansions to those in Eq. (3.25), neglecting $o(\epsilon^2)$ terms, and writing all quantities in terms of the displacement $\boldsymbol{\chi}$, the strain energy of the micro-model becomes

$$\begin{aligned} U(\{p_{i,j}\}) = &\sum_j \sum_i \sum_\alpha \frac{k^{\alpha}_{i,j}}{2}\epsilon^2 \left(\|F(P_{i,j})D_\alpha + \frac{\epsilon}{2}\nabla F(P_{i,j})|D_\alpha \otimes D_\alpha\| - 1 \right)^2 \\ &+ \sum_j \sum_i \sum_\alpha b^{\alpha}_{i,j} \left[\frac{\|\nabla F(P_{i,j})|D_\alpha \otimes D_\alpha\|^2}{\|F_{i,j}D_\alpha\|^2} \right. \\ &\left. - \left(\frac{F(P_{i,j})D_\alpha \cdot \nabla F(P_{i,j})|D_\alpha \otimes D_\alpha}{\|F_{i,j}D_\alpha\|^2} \right)^2 \right] \frac{\epsilon^2}{2} \\ &+ \sum_j \sum_i \frac{b^{3}_{i,j}}{2} \left| \arccos\left(\frac{F(P_{i,j})D_1 \cdot F(P_{i,j})D_2}{\|F(P_{i,j})D_1\| \cdot \|F(P_{i,j})D_2\|} \right) - \frac{\pi}{2} \right|^{\xi}. \end{aligned} \tag{3.26}$$

Rescaling the rigidities as

$$k^{\alpha}_{i,j} = \mathbb{K}^{\alpha}_{e};\ b^{\alpha}_{i,j} = \mathbb{K}^{\alpha}_{b};\ b^{3}_{i,j} = \mathbb{K}_{p}\epsilon^2, \tag{3.27}$$

and letting $\epsilon \to 0$, the strain energy of the macroscopic system reduces to

$$\begin{aligned} U(\boldsymbol{\chi}(\cdot)) = &\int_\Omega \sum_\alpha \frac{\mathbb{K}^{\alpha}_{e}}{2} \|FD_\alpha - 1\|^2 \mathrm{d}S \\ &+ \int_\Omega \sum_\alpha \frac{\mathbb{K}^{\alpha}_{b}}{2} \left[\frac{\|\nabla F|D_\alpha \otimes D_\alpha\|^2}{\|FD_\alpha\|^2} - \left(\frac{FD_\alpha \cdot \nabla F|D_\alpha \otimes D_\alpha}{\|FD_\alpha\|^2} \right)^2 \right] \mathrm{d}S \\ &+ \int_\Omega \frac{\mathbb{K}_{p}}{2} \left| \arccos\left(\frac{FD_1 \cdot FD_2}{\|FD_1\| \cdot \|FD_2\|} \right) - \frac{\pi}{2} \right|^{\xi} \mathrm{d}S. \end{aligned} \tag{3.28}$$

The homogenized energy in Eq. (3.28) can be used to perform numerical simulations: in Fig. 3.20, numerical simulations of the BIAS extension test and shear test are shown. Such a homogenization process can be used to support the argument that the description of pantographic fabric at a certain macro-level requires the use of second gradient continua.

Numerical Identification of Homogenized Model

A general problem in building scientific theories consists in identification of the constitutive parameters of a model. Typically, the identification of constitutive parameters is based upon a comparison between the model and reality by performing experiments.

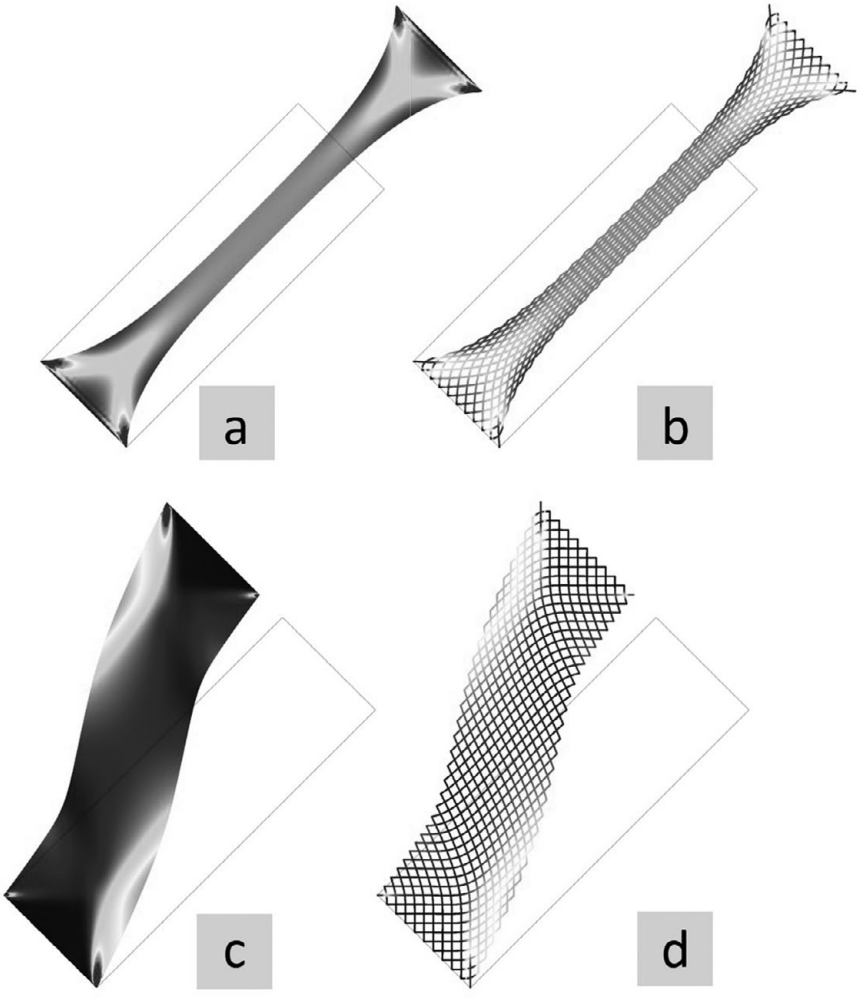

Figure 3.20 BIAS extension test (a) and shear test (c) of a pantographic lattice. In the right images the 'fibre' directions are shown.

In cases where more than a single model can be used to describe the phenomena, there is an opportunity for mutual identification of parameters of two selected models. In the case of pantographic structures we have the three models introduced above (i.e. micro, meso and macro). Furthermore, these structures could be modelled in a rather crude manner using the standard Cauchy continuum theory. Here we describe an identification between the homogenized second gradient model, whose energy is (3.28), and a discrete model based upon standard Cauchy theory.

To this end, in [50], the parameters $\mathbb{K}_a^\alpha$, $\mathbb{K}_b^\alpha$ and $\mathbb{K}_p$ appearing in the strain energy (3.28) (assumed to be independent of the position and family of beams) are identified numerically, i.e. they are calibrated by means of some numerical computations performed with the 3D Cauchy model for isotropic and homogeneous elastic materials

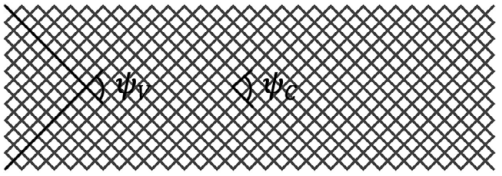

Figure 3.21 The two control angles employed in the identification procedure.

undergoing arbitrarily large strains. BIAS extension test simulations [53] have been performed using both the standard Cauchy model and the second gradient one. For identifying the constitutive parameters it has been decided to compare the computed energy and two independent deformations at specific points of the lattice, the angles ψ_C and ψ_V shown in Fig. 3.21, i.e. the angles at the center *C* of the specimen and at the corner *V* of the 'quasi-rigid' triangle near the short side of the pantographic fabric.

The material parameters of the macro-model $\mathbb{K}_e$, $\mathbb{K}_b$ and $\mathbb{K}_p$ are estimated by minimisation of the squared errors for the energy and the two angles ψ_C, ψ_V, computed both with the homogenized and the discrete Cauchy models . The choice of the two angles ψ_C, ψ_V, instead of other possible quantities, is justified by the fact that it is possible to relate their change to one of the last two energy terms Eq. (3.28), each one depending only on one parameter: the energetic term involved in the variation of ψ_C is mostly governed by the parameter $\mathbb{K}_p$, while the variation of ψ_V depends especially on the bending energetic term related to $\mathbb{K}_b$. This fact allows us to find the minimum of the squared error by separately tuning $\mathbb{K}_e$ and $\mathbb{K}_b$. The last parameter $\mathbb{K}_e$ is obtained by considering the whole stored energy.

Astounding Power of the Second Gradient Homogenized Model

As a preliminary conclusion of this chapter we show the astounding simulations in Fig. 3.22. In this figure, which inspired the analysis in [54], two comparisons between numerical simulations performed with two different models in the same BIAS extension test are shown. We have already described the results in Fig. 3.22a obtained by using a model which consider the fibres composing the pantographic fabrics modelled as nonlinear Euler–Bernoulli beams. We have remarked that this particular 'meso' model has been used in the case of pantographic structures which are composed of very few fibres. In that case, in fact, the hypothesis of a continuum (an effective 2D continuum) is not well-suited and we are obliged, at least in principle, to use a model which is intermediate between the discrete and the continuum ones.

Let us consider Fig. 3.22b. The simulation presented in this figure has been performed by minimising the second gradient energy reported in Eq. (3.28), modified by an additional term which takes into account the possibility that the fibres of the two families slide one with respect to the other at their interconnecting pivots. This additional term was considered for the first time in [55]. The consequence of including this additional term will be further discussed in the chapter about experimental methods in pantographic structures and their damage/fracture behaviour based upon

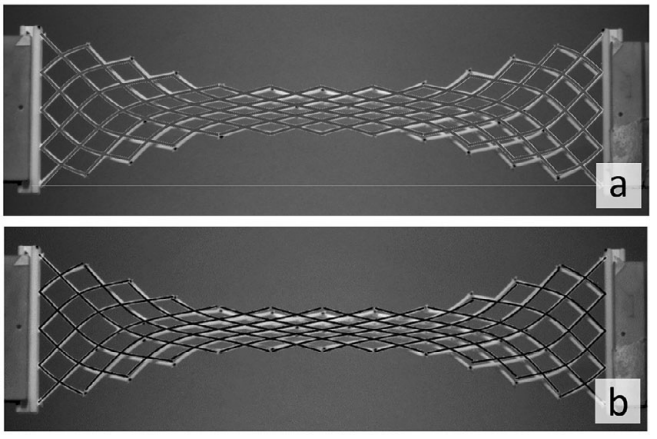

Figure 3.22 Comparison between simulation performed by using the 'meso' non-linear Euler–Bernoulli beam theory-based model (a) and the homogenized second gradient model (b).

the results obtained in [55]. We note that in [52], which has been presented above, an analogous additional term can be recognized. However, it is remarkable and surprising that a continuum homogenized model is capable of replicating results in the case of a specimen with so few fibres. Clearly, the inclusion of second gradient terms enriches the model sufficiently to capture phenomena that are otherwise not modelled based upon the standard Cauchy theory.

3.2.7 Higher Gradient Elastic Surfaces

In the preceding discussions, we have focused upon the pantographic lattice represented as a 2D object undergoing planar deformations, as in the case of the BIAS extension and the shear tests. However, it is possible for a 2D surface, planar in the reference configuration, to undergo out-of-plane deformations. Needless to say, we can envision a torsion experiment of the considered surface – which has now to be considered as embedded in 3D space – but we can also have cases in which in response to a planarly imposed deformation (as in the BIAS or in the shear tests) the 2D surface suffers some out-of-plane buckling or wrinkling deformation. To describe the topology of this out-of-plane deformation we are then obliged to generalize the presented model of a pantographic lattice to consider the embedding of the pantographic surface in a 3D space. The possibility of modelling out-of-plane deformations has been widely explored in work by dell'Isola, Steigmann *et al.* [1, 56–58] and recently by Giorgio, Rizzi *et al.* [59]. Here we consider the fundamental points of the two approaches.

In [60] the pantographic lattice is considered as an elastic surface embedded in a three-dimensional Euclidean space. To account for the geodesic and out-of-plane bending of fibres, the deformation gradient is defined in the following way, wherein the fibres are considered to be oriented along the two material directions of a Lagrangian Cartesian

orthonormal coordinate system, whose associated basis of unit vectors is (D_1, D_2), denoted in the same manner as used previously:

$$F = d_1 \otimes D_1 + d_2 \otimes D_2, \tag{3.29}$$

where d_1 and d_2 are defined as the push-forward vectors in the current configuration of the vectors D_1 and D_2 respectively, i.e. $d_\alpha = F D_\alpha,\ \alpha = 1, 2$. If we denote the fibre stretches $\|D_\alpha\|$ as λ and μ, then Eq. (3.29) can be rewritten as

$$F = \lambda \tilde{d}_1 \otimes D_1 + \mu \tilde{d}_2 \otimes D_2, \tag{3.30}$$

where $\tilde{d}_\alpha = \frac{d_\alpha}{\|d_\alpha\|}$ are the unit vectors associated with d_α.

These vectors are used to define the fibre shear strain γ as $\sin\gamma = \tilde{d}_1 \cdot \tilde{d}_2$ [28, 60]. From Eqs. (3.29) and (3.30) the right Cauchy–Green tensor reads

$$C = F^{\mathsf{T}} F = \lambda^2 D_1 \otimes D_1 + \mu^2 D_2 \otimes D_2 + \lambda\mu \sin\gamma \left(D_1 \otimes D_2 + D_2 \otimes D_1\right), \tag{3.31}$$

and

$$Jn = F D_1 \times F D_2 = d_1 \times d_2, \tag{3.32}$$

where n is the unit normal vector to the deformed surface field, and $J = \lambda\mu|\cos\gamma|$. The second gradient of the displacement is proven to have the following expression

$$\begin{aligned} \nabla\nabla\boldsymbol{\chi} = {} & (g_1 + K_1 n) \otimes D_1 \otimes D_1 + (g_2 + K_2 n) \otimes D_2 \otimes D_2 \\ & + (\boldsymbol{\Gamma} + T n) \otimes (D_1 \otimes D_2 + D_2 \otimes D_1), \end{aligned} \tag{3.33}$$

with

$$g_1 = \lambda\eta_1 p + (D_1 \cdot \nabla\lambda)\, \tilde{D}_1;\ g_2 = \mu\eta_2 q + (D_2 \cdot \nabla\mu)\, \tilde{D}_2, \tag{3.34}$$

$$\boldsymbol{\Gamma} = (D_1 \cdot \nabla\mu)\, \tilde{D}_2 + \lambda\mu\phi_1 q = (D_2 \cdot \nabla\lambda)\, \tilde{D}_1 + \lambda\mu\phi_2 p, \tag{3.35}$$

$$q = n \times \tilde{D}_2;\ p = n \times \tilde{D}_1, \tag{3.36}$$

$$K_1 = \lambda^2\kappa_1;\ K_2 = \mu^2\kappa_2;\ T = \lambda\mu\tau, \tag{3.37}$$

where η_1 and η_2 are the geodesic curvatures of the deformed fibres, ϕ_1 and ϕ_2 the so-called Tchebychev curvatures, κ_1 and κ_2 the normal curvatures of the deformed fibres, and τ the twist of the deformed surface. For the technical details about geodesic and Tchebychev curvatures we refer directly to [1, 56–58]. We can lastly write a strain energy density function depending on the first and second gradients of the deformation [58]:

$$W = w(\lambda, \mu, J) + \frac{1}{2}\left(A_1|g_1|^2 + A_2|g_2|^2 + A_\Gamma|\boldsymbol{\Gamma}|^2 + k_1 K_1^2 + k_2 K_2^2 + k_T K_T^2\right), \tag{3.38}$$

where $A_1,\ A_2,\ A_\Gamma,\ k_1,\ k_2,\ k_T$ are constitutive constants.

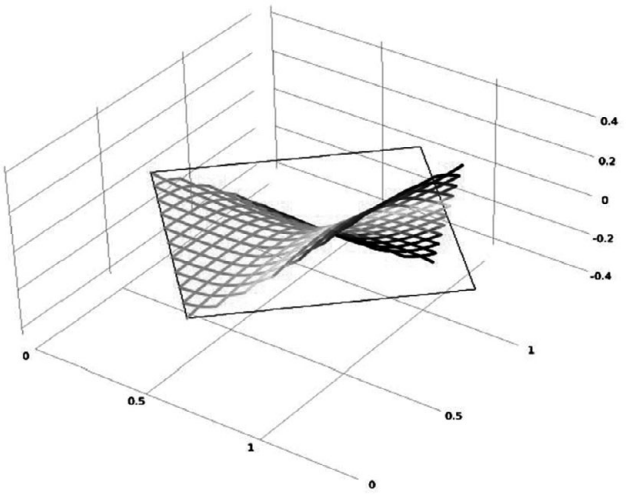

Figure 3.23 Numerical simulation of torsion of a square pantographic sheet (the angle of torsion is $\theta = 60°$) performed by using the elastic surface model.

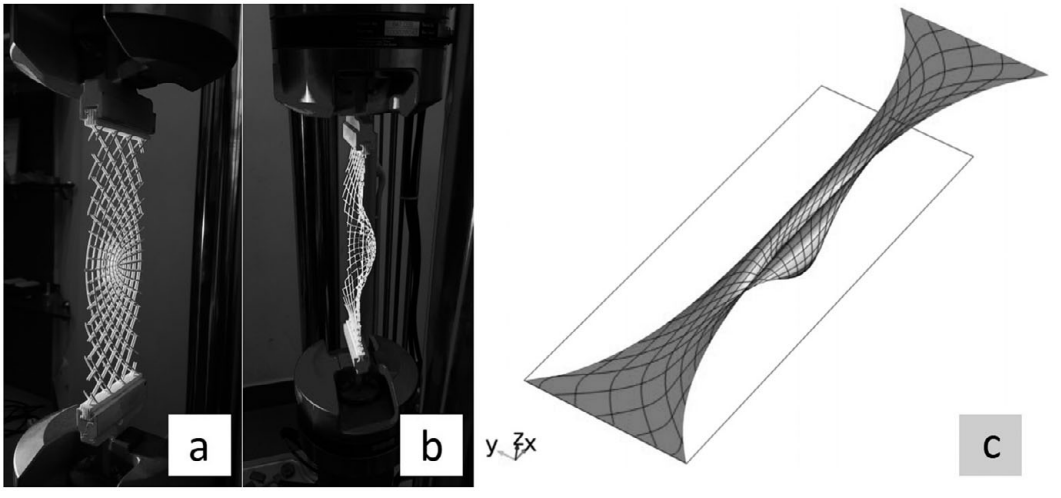

Figure 3.24 Bias extension test on parabolic pantographic fabric (a). Out-of-plane buckling is observed after critical loading (b). Simulation of bias extension test on parabolic pantographic fabrics (c).

In Fig. 3.23 numerical simulations of the torsion of a square sheet using this model are shown. Many fibre reference curvatures have been considered (e.g., sinusoidal, spiral, parabolic fibres) and, for parabolic fibres, experiments (Figs. 3.24a and 3.24b) and the model (Fig. 3.24c) both show that, after a critical load, out-of-plane buckling occurs during bias extension, because the transverse (curved) beams in the middle of the specimen undergo buckling induced by the shortening of the middle width of the specimen.

A 2D continuum model embedded in a 3D space has also been proposed [59] where, relying on a variational framework, the following strain energy density is proposed:

$$\pi = \frac{1}{2}\left\{ \mathrm{K}_e \left[\left(\epsilon^1\right)^2 + \left(\epsilon^2\right)^2 \right] + \mathrm{K}_s \gamma^2 \right. \\ \left. + \mathrm{K}_t \left[\left(\kappa_1^1\right)^2 + \left(\kappa_1^2\right)^2 \right] + \mathrm{K}_n \left[\left(\kappa_2^1\right)^2 + \left(\kappa_2^2\right)^2 \right] + \mathrm{K}_g \left[\left(\kappa_3^1\right)^2 + \left(\kappa_3^2\right)^2 \right] \right\}. \tag{3.39}$$

It corresponds to a system of two orthogonal continuous families '1' and '2' of straight shear-undeformable beams arranged along the coordinate axes in the reference configuration and resembling the pantographic microstructure. The fibres of family α are parallel to the direction $\hat{e}_\alpha$. The contributions $\frac{1}{2}\mathrm{K}_e \left(\epsilon^1\right)^2$ and $\frac{1}{2}\mathrm{K}_e \left(\epsilon^2\right)^2$ stand for the elongation of fibres belonging to, respectively, the families 1 and 2. The strain measure $\boldsymbol{\epsilon}^\alpha$, with $\alpha = 1, 2$, is defined as

$$\epsilon^\alpha = \left\| \frac{\partial \chi}{\partial X_\alpha} \right\| - 1, \tag{3.40}$$

and $\mathrm{K}_e \in [0, \infty)$ is the corresponding stiffness, which is assumed to be the same for both families of fibres. The contribution $\mathrm{K}_s \gamma^2$ is accounting for the shear deformation of the sheet, i.e. it is due to the relative rotation of two orthogonal intersecting fibres. It represents the strain energy stored in the pivot because of its torsion, of angle γ. The strain measure $\gamma \in [-\frac{\pi}{2}, \frac{\pi}{2}]$, also referred to as the shear angle, is expressed as

$$\gamma = \arcsin \frac{\frac{\partial \chi}{\partial X_1} \cdot \frac{\partial \chi}{\partial X_2}}{\left\| \frac{\partial \chi}{\partial X_1} \right\| \left\| \frac{\partial \chi}{\partial X_2} \right\|} \tag{3.41}$$

and K_s is a positive constitutive parameter.

The terms $\frac{1}{2}\left[\mathrm{K}_t \left(\kappa_1^1\right)^2 + \mathrm{K}_n \left(\kappa_2^1\right)^2 + \mathrm{K}_g \left(\kappa_3^1\right)^2 \right]$ and $\frac{1}{2}\left[\mathrm{K}_t \left(\kappa_1^2\right)^2 + \mathrm{K}_n \left(\kappa_2^2\right)^2 + \mathrm{K}_g \left(\kappa_3^2\right)^2 \right]$ are due to twist, normal bending and geodesic bending of beams belonging, respectively, to families 1 and 2 of the fibres. The strain measures κ_1^α, κ_2^α, κ_3^α are the coordinates, in the augmented levorotatory reference Cartesian frame, of the axial vector corresponding to the skew tensor $W^\alpha = (R^\alpha)^{\mathrm{T}} \frac{\partial R^\alpha}{\partial X_\alpha}$, which is the so-called current curvature tensor. The orthogonal tensor R^α transforms the augmented levorotatory reference Cartesian frame vectors into the following ordered triplet: i) the unitary vector tangent to the deformed coordinate line α; ii) the unitary vector normal to the previous one and lying in the plane tangent to the deformed surface; iii) the unitary vector normal to the plane tangent to the deformed surface. Explicit (lengthy) derivations can be found in Ref. [59]. Using the above model, shear test simulations have been performed reporting the occurrence of out-of-plane buckling (Fig. 3.25).

3.2.8 Dynamics

The final theoretical aspect in the framework of pantographic metamaterial we want to discuss here consists in the study of the dynamics of pantographic structures. One

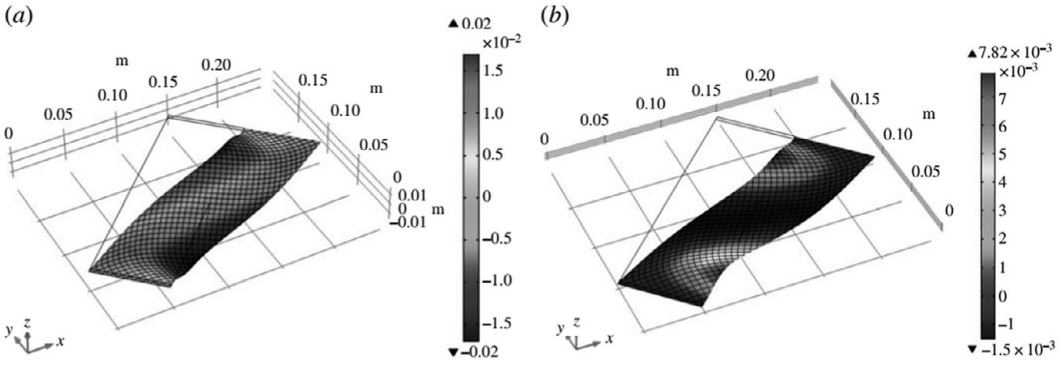

Figure 3.25 Shear test. Qualitative buckled shapes of the first two bifurcation modes. Colours indicate values of the out-of-plane displacement. (a) First and (b) second buckling modes.

can imagine several (completely different) dynamical problems involving pantographic fabrics, but, clearly, the one that emerges naturally is the phenomenon of wave propagation in pantographic wave-guides. This application of pantographic structures has only recently been investigated and its research horizons are yet unexplored.

In [61], a first model for studying dynamics in pantographic fabrics, regarded as 'long' wave-guides, has been introduced and, subsequently, has been employed in [62, 63]. The main idea is to set time-dependent boundary displacements inducing the onset of travelling waves. The impulse function $\mathfrak{I} = u_0 * \text{sech}\,[\tau(t - t_0)]$, where the parameter τ controls the pulse duration is used as the prescribed displacement. Figure 3.26 shows the reference configuration of the pantographic sheet (on the left), where the frictionless hinges, representing perfect pivots, do not interrupt the continuity of the fibres, and (on the right) the impulse function representing the prescribed displacement.

Numerical simulations based upon the homogenized second gradient macromodel previously presented were performed to obtain deformed shapes of the pantographic wave-guide. Figure 3.27(left), gives the results for the case of a propagating wave that originates due to a vertical impulse applied on the upper short side, while the opposite short side is clamped. The deformed shapes in Fig. 3.27(right) are obtained by imposing a double impulse (i.e. a couple of equal opposite displacements) applied at the middle height of the specimen. These displacements are applied at two points at the opposite ends of two adjacent beams, i.e consecutive beams belonging to the same orthogonal family of $1D$ continua, and their amplitude over time is shown in Fig. 3.26.

First experimental observations of the dynamical behaviour of pantographic metamaterial have recently been performed and are reported in [77]. Other studies on dynamics relevant to the analyses here presented can be found in [78–86].

3.3 Conclusion

The pantographic metamaterial represents a class of metamaterials precisely defined by its microstructure. In this chapter we have limited our attention to 1D and 2D

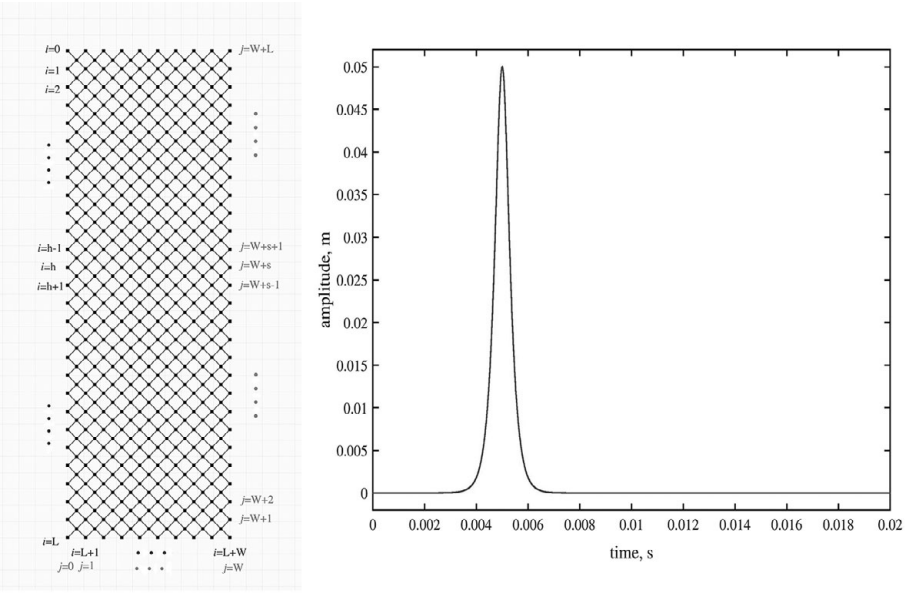

Figure 3.26 Reference configuration(left) and time history of the impulse (right).

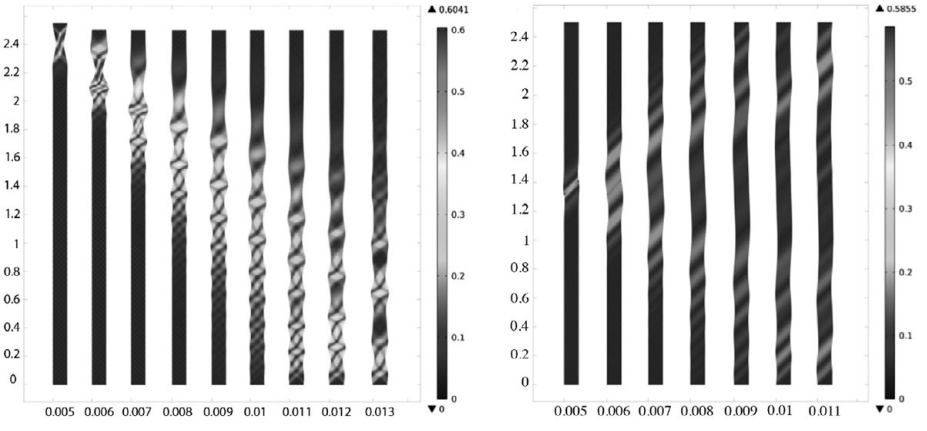

Figure 3.27 Qualitative displacement plot of a wave propagating after a prescribed vertical displacement on the upper side (left). Wave propagating after double impulse (right).

pantographic metamaterials. The extension to the synthesis of such 3D constructs is quite feasible regardless of the theoretical and technological challenges.

A fundamental characteristic of pantographic metamaterial, which is also a motivation for dedicating a whole chapter to this metamaterial, is the fact that it represents an archetype of theory-driven design. We have widely remarked that the genesis of pantographic structures was in response to a very simple question. Can we conceive and

realize a material system whose energy consists of a purely second gradient type? At the level of the micro-structure, as we have shown, it is necessary to consider a structure which exhibits, locally, a wider class of floppy modes than just rigid motions. This is the rationale that first stimulated us to conceive an ideal pantograph. In strict adherence to the spirit of the theory-driven research approach nothing has been randomly explored. We have shown here how the answer to a basic question originating in the theory was developed and, further, how this development led to the many theoretical predictions found through numerical computations. To validate the followed approach, an essential aspect is to devise methods for experimentally demonstrating the predictions. In the chapter about experiments in pantographic structures, experimental observations and their relation with modelling will be treated in detail. In particular, a novel approach, based on digital image correlation [73–76], will be presented and exploited to perform very precise analyses of displacement and deformation in pantographic structures.

Acknowledgements

Mario Spagnuolo has received funding from the European Union's Horizon 2020 research and innovation programme under the Marie Skłodowska-Curie grant agreement No 665850.

Bibliography

[1] F. dell'Isola, D. Steigmann, and A. Della Corte. Synthesis of fibrous complex structures: Designing microstructure to deliver targeted macroscale response. *Applied Mechanics Reviews*, 67(6):060804, 2015.

[2] Graeme Milton, Marc Briane, and Davit Harutyunyan. On the possible effective elasticity tensors of 2-dimensional and 3-dimensional printed materials. *Mathematics and Mechanics of Complex Systems*, 5(1):41–94, 2017.

[3] Victor A. Eremeyev and Wojciech Pietraszkiewicz. Material symmetry group and constitutive equations of micropolar anisotropic elastic solids. *Mathematics and Mechanics of Solids*, 21(2):210–221, 2016.

[4] Albrecht Bertram and Rainer Glüge. Gradient materials with internal constraints. *Mathematics and Mechanics of Complex Systems*, 4(1):1–15, 2016.

[5] F. dell'Isola, T. Lekszycki, M. Pawlikowski, R. Grygoruk, and L. Greco. Designing a light fabric metamaterial being highly macroscopically tough under directional extension: First experimental evidence. *Zeitschrift für angewandte Mathematik und Physik*, 66:3473–3498, 2015.

[6] J-J. Alibert, P. Seppecher, and F. dell'Isola. Truss modular beams with deformation energy depending on higher displacement gradients. *Mathematics and Mechanics of Solids*, 8(1):51–73, 2003.

[7] Catherine Pideri and Pierre Seppecher. A second gradient material resulting from the homogenization of an heterogeneous linear elastic medium. *Continuum Mechanics and Thermodynamics*, 9(5):241–257, 1997.

[8] Lucio Russo. *The Forgotten Revolution: How Science Was Born in 300 BC and Why It Had to Be Reborn*. Springer Science & Business Media, 2013.

[9] Stephen M. Stigler. Stigler's law of eponymy. *Transactions of the New York Academy of Sciences*, 39(1 Series II):147–157, 1980.

[10] F. dell'Isola, U. Andreaus, and L. Placidi. At the origins and in the vanguard of peridynamics, non-local and higher-gradient continuum mechanics: An underestimated and still topical contribution of Gabrio Piola. *Mathematics and Mechanics of Solids*, 20(8): 887–928, 2015.

[11] F. dell'Isola, A. Della Corte, and I. Giorgio. Higher-gradient continua: The legacy of Piola, Mindlin, Sedov and Toupin and some future research perspectives. *Mathematics and Mechanics of Solids*, 22(4):852–872, 2017.

[12] Paul Germain. The method of virtual power in continuum mechanics. Part 2: Microstructure. *SIAM Journal on Applied Mathematics*, 25(3):556–575, 1973.

[13] Richard A. Toupin. Elastic materials with couple-stresses. *Archive for Rational Mechanics and Analysis*, 11(1):385–414, 1962.

[14] Raymond David Mindlin. Micro-structure in linear elasticity. *Archive for Rational Mechanics and Analysis*, 16(1):51–78, 1964.

[15] Simon R. Eugster and Francesco dell'Isola. Exegesis of the Introduction and Sect. I from "Fundamentals of the Mechanics of Continua" by E. Hellinger. *ZAMM-Journal of Applied Mathematics and Mechanics/Zeitschrift für Angewandte Mathematik und Mechanik*, 97(4):477–506, 2017.

[16] Simon R. Eugster and Francesco dell'Isola. Exegesis of Sect. II and III. A from "Fundamentals of the mechanics of continua" by E. Hellinger. *ZAMM-Journal of Applied Mathematics and Mechanics/Zeitschrift für Angewandte Mathematik und Mechanik*, 98(1):31–68, 2018.

[17] F. dell Isola, P. Seppecher, and A. Della Corte. The postulations á la d' Alembert and á la Cauchy for higher gradient continuum theories are equivalent: a review of existing results. In *Proc. R. Soc. A*, 471, 20150415. 2015.

[18] N. Auffray, F. dell'Isola, V. Eremeyev, A. Madeo, and G. Rosi. Analytical continuum mechanics à la Hamilton–Piola least action principle for second gradient continua and capillary fluids. *Mathematics and Mechanics of Solids*, 20(4):375–417, 2015.

[19] Y. Rahali, I. Giorgio, J.F. Ganghoffer, and F. dell'Isola. Homogenization à la Piola produces second gradient continuum models for linear pantographic lattices. *International Journal of Engineering Science*, 97:148–172, 2015.

[20] A. Bilotta, G. Formica, and E. Turco. Performance of a high-continuity finite element in three-dimensional elasticity. *International Journal for Numerical Methods in Biomedical Engineering*, 26(9):1155–1175, 2010.

[21] A. Cazzani, M. Malagù, and E. Turco. Isogeometric analysis: A powerful numerical tool for the elastic analysis of historical masonry arches. *Continuum Mechanics and Thermodynamics*, 28(1-2):139–156, 2016.

[22] Edoardo Benvenuto. *An Introduction to the History of Structural Mechanics. Part i: Statics and Resistance of solids. Part ii: Vaulted Structures and Elastic Systems*. Springer-Verlag, New York, 1991.

[23] M de Saint-Venant. *Mémoire sur la torsion des prismes: avec des considérations sur leur flexion ainsi que sur l'équilibre intérieur des solides élastiques en général: et des formules pratiques pour le calcul de leur résistance à divers efforts s' exerçant simultanément*. Imprimerie nationale, 1856.

[24] Eugene Cosserat, François Cosserat, *et al. Théorie des corps déformables*. Hermann, Paris, 1909.

[25] Francesco dell'Isola, Giulio Maier, Umberto Perego, *et al. The Complete Works of Gabrio Piola:* Volume i. Cham, Switzerland: Springer, 2014.

[26] P. Casal. La capillarité interne. *Cahier du groupe Français de rhéologie, CNRS VI*, 3:31–37, 1961.

[27] P. Casal. Theory of second gradient and capillarity. *Comptes Rendus Hebdomadaires des Seances de l'Academie des Sciences Serie A*, 274(22):1571, 1972.

[28] F. dell'Isola, I. Giorgio, M. Pawlikowski, and N. Rizzi. Large deformations of planar extensible beams and pantographic lattices: Heuristic homogenization, experimental and numerical examples of equilibrium. *Proc. R. Soc. A*, 472(2185):23 pages, 2016.

[29] H Abdoul-Anziz and Pierre Seppecher. Strain gradient and generalized continua obtained by homogenizing frame lattices. *Mathematics and Mechanics of Complex Systems*, 6(3): 213–250, 2018.

[30] Francesco dell'Isola, Alessandro Della Corte, Raffaele Esposito, and Lucio Russo. Some cases of unrecognized transmission of scientific knowledge: from antiquity to Gabrio Piola's peridynamics and generalized continuum theories. In *Generalized Continua as Models for Classical and Advanced Materials*, pages 77–128. Springer, 2016.

[31] P. Seppecher, J.-J. Alibert, and F. dell'Isola. Linear elastic trusses leading to continua with exotic mechanical interactions. In *Journal of Physics: Conference Series*, volume 319, page 012018. IOP Publishing, 2011.

[32] Victor A. Eremeyev, Francesco dell'Isola, Claude Boutin, and David Steigmann. Linear pantographic sheets: existence and uniqueness of weak solutions. 10.1007/s10659-017-9660-3, 2017.

[33] Victor A. Eremeyev and Francesco dell'Isola. A note on reduced strain gradient elasticity. In *Generalized Models and Non-classical Approaches in Complex Materials 1*, pages 301–310. Springer, 2018.

[34] G.C. Everstine and A.C. Pipkin. Boundary layers in fiber-reinforced materials. *J. Appl. Mech.*, 40:518–522, 1973.

[35] M.G. Hilgers and A.C. Pipkin. Elastic sheets with bending stiffness. *Q. J. Mech. Appl. Math.*, 45:57–75, 1992.

[36] M.G. Hilgers and A.C. Pipkin. Energy-minimizing deformations of elastic sheets with bending stiffness. *J. Elast.*, 31:125–139, 1993.

[37] M.G. Hilgers and A.C. Pipkin. Bending energy of highly elastic membranes II. *Q. Appl. Math*, 54:307–316, 1996.

[38] M.Z. Hu, H. Kolsky, and A.C. Pipkin. Bending theory for fiber-reinforced beams. *J. Compos. Mater*, pages 235–249, 1985.

[39] A.C. Pipkin. Generalized plane deformations of ideal fiber-reinforced materials. *Q. Appl. Math*, 32:253–263, 1974.

[40] A.C. Pipkin. Energy changes in ideal fiber-reinforced composites. *Q. Appl. Math*, 35:455–463, 1978.

[41] A.C. Pipkin. Some developments in the theory of inextensible networks. *Q. Appl. Math*, 38:343–355, 1980.

[42] F. dell'Isola, M.V. d'Agostino, A. Madeo, P. Boisse, and D. Steigmann. Minimization of shear energy in two dimensional continua with two orthogonal families of inextensible fibers: the case of standard bias extension test. *Journal of Elasticity*, 122(2):131–155, 2016.

[43] L. Placidi, L. Greco, S. Bucci, E. Turco, and N.L. Rizzi. A second gradient formulation for a 2D fabric sheet with inextensible fibres. *Zeitschrift für angewandte Mathematik und Physik*, 67(5)(114), 2016.

[44] R.S. Rivlin. Plane strain of a net formed by inextensible cords. In *Collected Papers of R.S. Rivlin*, pages 511–534. Springer, 1997.

[45] L. Greco, I. Giorgio, and A. Battista. In plane shear and bending for first gradient inextensible pantographic sheets: numerical study of deformed shapes and global constraint reactions. *Mathematics and Mechanics of Solids*, page 1081286516651324, 2016.

[46] M. Cuomo, F. dell'Isola, L. Greco, and N.L. Rizzi. First versus second gradient energies for planar sheets with two families of inextensible fibres: Investigation on deformation boundary layers, discontinuities and geometrical instabilities. *Composites Part B: Engineering*, 115:423–448, 2017.

[47] M. Cuomo, F. dell'Isola, and L. Greco. Simplified analysis of a generalized bias test for fabrics with two families of inextensible fibres. *Zeitschrift für angewandte Mathematik und Physik*, 67(3):1–23, 2016.

[48] F. dell'Isola, M. Cuomo, L. Greco, and A. Della Corte. Bias extension test for pantographic sheets: numerical simulations based on second gradient shear energies. *Journal of Engineering Mathematics*, 103(1):127–157, 2017.

[49] L. Greco, I. Giorgio, and A. Battista. In plane shear and bending for first gradient inextensible pantographic sheets: Numerical study of deformed shapes and global constraint reactions. *Mathematics and Mechanics of Solids*, 22(10):1950–1975, 2017.

[50] I. Giorgio. Numerical identification procedure between a micro-Cauchy model and a macro-second gradient model for planar pantographic structures. *Zeitschrift für angewandte Mathematik und Physik*, 67(4)(95), 2016.

[51] E. Turco, F. dell'Isola, A. Cazzani, and N.L. Rizzi. Hencky-type discrete model for pantographic structures: Numerical comparison with second gradient continuum models. *Zeitschrift für angewandte Mathematik und Physik*, 67:28 pages, 2016.

[52] Ugo Andreaus, Mario Spagnuolo, Tomasz Lekszycki, and Simon R. Eugster. A Ritz approach for the static analysis of planar pantographic structures modeled with nonlinear Euler–Bernoulli beams. *Continuum Mechanics and Thermodynamics*, 2018.

[53] L. Placidi, E. Barchiesi, E. Turco, and N.L. Rizzi. A review on 2D models for the description of pantographic fabrics. *Zeitschrift für angewandte Mathematik und Physik*, 67(5)(121), 2016.

[54] Mario Spagnuolo, Francesco dell'Isola, and Ivan Giorgio. Astounding evidences of applicability of higher gradient models: if a continuum model is capable to predict the good results also in case of a discrete reality. *to appear*, 2019.

[55] M. Spagnuolo, K. Barcz, A. Pfaff, F. dell'Isola, and P. Franciosi. Qualitative pivot damage analysis in aluminum printed pantographic sheets: numerics and experiments. *Mechanics Research Communications*, 83:47–52, 2017.

[56] D.J. Steigmann and F. dell'Isola. Mechanical response of fabric sheets to three-dimensional bending, twisting, and stretching. *Acta Mechanica Sinica*, 31(3):373–382, 2015.

[57] I. Giorgio, A. Della Corte, F. dell'Isola, and D. Steigmann. Buckling modes in pantographic lattices. *Comptes rendus Mecanique*, 344:487–501, 2016.

[58] I. Giorgio, R. Grygoruk, F. dell'Isola, and D.J. Steigmann. Pattern formation in the three-dimensional deformations of fibered sheets. *Mechanics Research Communications*, 69:164–171, 2015.

[59] I. Giorgio, N.L. Rizzi, and E. Turco. Continuum modelling of pantographic sheets for out-of-plane bifurcation and vibrational analysis. *Proc. R. Soc. A*, 21 pages, 2017 (http://dx.doi.org/10.1098/rspa.2017.0636).

[60] F. dell'Isola and D.J. Steigmann. A two-dimensional gradient-elasticity theory for woven fabrics. *J. Elasticity*, 18:113–125, 2015.

[61] F. dell'Isola, I. Giorgio, and U. Andreaus. Elastic pantographic 2D lattices: A numerical analysis on static response and wave propagation. In *Proceedings of the Estonian Academy of Sciences*, 64:219–225, 2015.

[62] F. dell'Isola, A. Della Corte, I. Giorgio, and D. Scerrato. Pantographic 2D sheets: Discussion of some numerical investigations and potential applications. *International Journal of Non-Linear Mechanics*, 80:200–208, 2016.

[63] A. Madeo, A. Della Corte, L. Greco, and P. Neff. Wave propagation in pantographic 2D lattices with internal discontinuities. *arXiv preprint arXiv:1412.3926*, 2014.

[64] B. Emek Abali, Wolfgang H. Müller, and Francesco dell'Isola. Theory and computation of higher gradient elasticity theories based on action principles. *Archive of Applied Mechanics*, 87(9):1495–1510, 2017.

[65] B. Emek Abali, Wolfgang H. Müller, and Victor A. Eremeyev. Strain gradient elasticity with geometric nonlinearities and its computational evaluation. *Mechanics of Advanced Materials and Modern Processes*, 1(1):4, 2015.

[66] Houssam Abdoul-Anziz and Pierre Seppecher. Strain gradient and generalized continua obtained by homogenizing frame lattices. *Mathematics and Mechanics of Complex Systems*, 6(3):213–250, 2018.

[67] Nicolas Auffray. On the isotropic moduli of 2D strain-gradient elasticity. *Continuum Mechanics and Thermodynamics*, 27(1-2):5–19, 2015.

[68] Samuel Forest. Mechanics of generalized continua: Construction by homogenizaton. *Le Journal de Physique IV*, 8(PR4):Pr4–39, 1998.

[69] Maciej Golaszewski, Roman Grygoruk, Ivan Giorgio, Marco Laudato, and Fabio Di Cosmo. Metamaterials with relative displacements in their microstructure: Technological challenges in 3D printing, experiments and numerical predictions. *Continuum Mechanics and Thermodynamics*, pages 1–20, 2018.

[70] P Harrison, F Abdiwi, Z Guo, P Potluri, and WR Yu. Characterising the shear–tension coupling and wrinkling behaviour of woven engineering fabrics. *Composites Part A: Applied Science and Manufacturing*, 43(6):903–914, 2012.

[71] Philip Harrison, Michael J. Clifford, and A.C. Long. Shear characterisation of viscous woven textile composites: A comparison between picture frame and bias extension experiments. *Composites Science and Technology*, 64(10-11):1453–1465, 2004.

[72] Philip Harrison, Joram Wiggers, and Andrew C. Long. Normalization of shear test data for rate-independent compressible fabrics. *Journal of Composite Materials*, 42(22):2315–2344, 2008.

[73] François Hild, Bumedijen Raka, Maud Baudequin, Stéphane Roux, and Florence Cantelaube. Multiscale displacement field measurements of compressed mineral-wool samples by Digital Image Correlation. *Applied Optics*, 41(32):6815–6828, 2002.

[74] François Hild and Stéphane Roux. Digital image correlation: From displacement measurement to identification of elastic properties–a review. *Strain*, 42(2):69–80, 2006.

[75] François Hild and Stéphane Roux. Comparison of local and global approaches to digital image correlation. *Experimental Mechanics*, 52(9):1503–1519, 2012.

[76] Stéphane Roux and François Hild. Stress intensity factor measurements from digital image correlation: Post-processing and integrated approaches. *International Journal of Fracture*, 140(1-4):141–157, 2006.

[77] M. Laudato, L. Manzari, E. Barchiesi, F. Di Cosmo, and P. Göransson. First experimental observation of the dynamical behavior of a pantographic metamaterial. *Mechanics Research Communications*, 94:125–127, 2018.

[78] Stephane Hans and Claude Boutin. Dynamics of discrete framed structures: A unified homogenized description. *Journal of Mechanics of Materials and Structures*, 3(9):1709–1739, 2008.

[79] Jacek Chróścielewski, Rüdiger Schmidt, and Victor A. Eremeyev. Nonlinear finite element modeling of vibration control of plane rod-type structural members with integrated piezoelectric patches. *Continuum Mechanics and Thermodynamics*, pages 1–42, 2018.

[80] Angelo Luongo and Francesco D'Annibale. Double zero bifurcation of non-linear viscoelastic beams under conservative and non-conservative loads. *International Journal of Non-Linear Mechanics*, 55:128–139, 2013.

[81] Angelo Luongo and Giuseppe Piccardo. Linear instability mechanisms for coupled translational galloping. *Journal of Sound and Vibration*, 288(4-5):1027–1047, 2005.

[82] Angelo Luongo, Daniele Zulli, and Giuseppe Piccardo. Analytical and numerical approaches to nonlinear galloping of internally resonant suspended cables. *Journal of Sound and Vibration*, 315(3):375–393, 2008.

[83] Giuseppe Rosi and Nicolas Auffray. Anisotropic and dispersive wave propagation within strain-gradient framework. *Wave Motion*, 63:120–134, 2016.

[84] Giuseppe Rosi, Ivan Giorgio, and Victor A. Eremeyev. Propagation of linear compression waves through plane interfacial layers and mass adsorption in second gradient fluids. *ZAMM-Journal of Applied Mathematics and Mechanics/Zeitschrift für Angewandte Mathematik und Mechanik*, 93(12):914–927, 2013.

[85] Angelo Di Egidio, Angelo Luongo, and Achille Paolone. Linear and non-linear interactions between static and dynamic bifurcations of damped planar beams. *International Journal of Non-Linear Mechanics*, 42(1):88–98, 2007.

[86] Francesco D'Annibale, Giuseppe Rosi, and Angelo Luongo. Linear stability of piezoelectric-controlled discrete mechanical systems under nonconservative positional forces. *Meccanica*, 50(3):825–839, 2015.

Part II

Mathematical and Numerical Methods

4 Naive Model Theory: Its Applications to the Theory of Metamaterials Design

F. dell'Isola, E. Barchiesi, A. Misra

4.1 Introduction

In the online *Stanford Encyclopedia of Philosophy*[1] one finds an accurate account of formal modern model theory, with a careful description of the underlying philosophical and mathematical arguments. Model theory was developed, in a more recent époque, by Alfred Tarski. It appears though that (see the *Forgotten Revolution* by Lucio Russo [1]) Hellenistic scientists had already found and systematically used many of its deepest concepts, as also the developments in pre-classical Indian science (e.g. *Aṣṭādhyāyī* of Panini and *Caraka-saṃhitā*) were underpinned by logic and epistemological considerations.[2]

4.1.1 Why *Naive* Model Theory?

In the aforementioned entry[3] one finds the statement:

To model a phenomenon is to construct a formal theory that describes and explains it.

Indeed, it is well accepted that a (mathematical) model is a theory which describes existing objects and/or already observed phenomena. In other words, a physicist is assumed to observe the phenomena occurring within existing systems and, subsequently, to find models which allow their descriptions as well as the possibility of forecasting what has not yet been observed.

However, very often, physicists and engineers model objects which do not already exist, but whose existence may be desired. Indeed, in the same entry, one finds the following sentence immediately after the previous one:

This chapter is dedicated by FdI to the memory of Professor Luigi De Luca, his beloved uncle. Professor De Luca mentored generations of students, educating them in the use of rationality by teaching ancient Greek, Latin, Grammar, Syntax and Epicurean Philosophy of Science. The scientific studies of FdI were inspired by his guidance and tutorship. The material presented herein reflects and has been inspired by his deep understanding of Science.

[1] See the entry Model Theory at https://plato.stanford.edu/entries/model-theory.

[2] See the entries Epistemology in Classical Indian Philosophy at https://plato.stanford.edu/entries/epistemology-india/ and Logic in Classical Indian Philosophy at https://plato.stanford.edu/entries/logic-india. Also The Encyclopedia of Indian Philosophies: Indian metaphysics and epistemology edited by Karl H. Potter, 1977, Motilal Banarsidass, New Delhi.

[3] See Footnote 1.

In a closely related sense, you model a system or structure that you plan to build, by writing a description of it.

The formal study of the (meta-) theory needed to describe the structure of a theory (and also the possible ways of finding its meaning) remains an attractive challenge in modern mathematics just as it was in the ancient times. Needless to say, such a study is well beyond the intended scope of this chapter. The reduced ambitions of our presentation, therefore, follow what is done when mathematicians decide to present *Naive* Set Theory. In the Introduction of his celebrated mathematical textbook Paul Halmos writes:

Every mathematician agrees that every mathematician must know some set theory; the disagreement begins in trying to decide how much is some. This book contains my answer to that question. The purpose of the book is to tell the beginning student of advanced mathematics the basic set-theoretic facts of life, and to do so with the minimum of philosophical discourse and logical formalism. [. . .]. From this point of view the concepts and methods of this book are merely some of the standard mathematical tools; the expert specialist will find nothing new here. Scholarly bibliographical credits and references are out of place in a purely expository book such as this one. The student who gets interested in set theory for its own sake should know, however, that there is much more to the subject than there is in this book. One of the most beautiful sources of set-theoretic wisdom is still Hausdorff's Set Theory. *A recent and highly readable addition to the literature, with an extensive and up-to-date bibliography, is* Axiomatic Set Theory *by Suppes.*

Halmos' preface is so elegant and communicative that we do not dare to rephrase it in accordance with the subject of the current chapter. *Si parva licet componere magnis* (Virgil, Georgics, IV, 176, i.e. in Dryden's translation [2]: *If little things with great we may compare*) we believe that the reader will understand the spirit of the present chapter by replacing in the previous citation:

i) the words *mathematics* and *mathematician* with, respectively, the words *mechanics* and *mechanician* or the word *engineering sciences* and *engineer;*
ii) the word *set* with the word *model;*
iii) the references about set theory cited by Paul Halmos with those about model theory cited several times in the above mentioned entry.

4.1.2 Do Mechanicians, Engineers or Applied Scientists Need Model Theory?

The first part of this book is intended to cover those topics from the theory of metamaterials design which we believe to be interesting and topical. One might legitimately ask why we have decided to insert here a chapter which deals with a topic that appears to be more pertinent to the philosophy of science, and is not generally regarded as relevant to engineering sciences or mechanics.

An initial answer could be found by invoking the principle of authority. The subject of mechanics, as a part of physics and engineering sciences, in its contents and setting, has been elaborated by many generations of scientists and natural philosophers. In all presentations – even those that may be considered at the bottom of the heap both

from the scientific and technological (when considering the selection of topics) and the pedagogic (when considering the way in which the selected topics are explained) points of view – there is an attempt to base the discipline starting from a sound analysis of its scientific principles. Although at times this attempt is pursued only by means of subterfuge: namely, by use of esoteric language.[4]

Further, during the Renaissance, the foundations of mechanics due to Hellenistic Science were rediscovered, among others, by Galileo, Euler, at least two members of the Bernoulli family, Lagrange, Navier, Cauchy, Saint-Venant, Maxwell, and Beltrami. And since the establishment of the École Polytechnique in Paris, theoretical mechanics has become a part of the fundamental cultural background of any engineer. Indeed, mechanics is not a professionalizing discipline, as it does not directly deal with the technical rules for the safe and efficient design of engineering artifacts.[5] Instead, the ultimate goal of teaching mechanics is to bring to the knowledge of engineering scholars, and future professionals, those mathematical models that describe, in a unified and synthetic treatment, the many phenomena whose description is necessary for the design, control and prediction of the behavior of a great number of devices which are relevant for topical technology.

However, mechanics is not a basic discipline for engineering as are mathematics, physics, or chemistry. Indeed, when modeling the mechanical phenomena involved in the behavior of complex structures, one has to keep in mind the simplifying assumptions necessary to obtain mathematically tractable models which, still, have to be capable of describing the non-trivial phenomena of interest in the engineering applications. Hence, its treatment cannot and must not be purely deductive because, otherwise, we would confuse mechanics with a part of the mathematics it uses. Moreover, the study of mechanics for engineers should not be as general and *fundamental* as the study of physics or chemistry tends to be. Indeed, in mechanics, the scope of modeling is usually confined to a special class of phenomena, always keeping in mind the potential uses of the introduced models in the engineering practice. This explicitly stated self-limitation to the scope of its interests should not be misunderstood: recently, models traditionally developed in classical mechanics have proven to be topical and modern, playing a crucial role in the development of new and important technologies. Models developed in the framework of classical mechanics make it possible to deal, for instance, with those mechanical phenomena involved in biomechanics, piezoelectricity, magnetostriction and ferromagnetism, which are proving to be very important in many fields of environmental, biomedical, aerospace, electronic and telecommunications engineering.

The vision presented above is widely shared by those who, in the past, faced the problem of selecting topics for monographs in mechanical sciences targeting an audience of scholars and students. Even if conceived many decades ago, in our opinion, the

[4] Of course, the esoteric language which is more likely to impress the layman is the one provided by mathematics. The desired effect is more easily pursued the more recent is the formalism employed and, hence, the more restricted is the group of readers sufficiently familiar with it. Nevertheless, let us note that languages for initiates, specific to people working in any specific part of mechanics, have been developed. These languages are sometimes used only to claim their special status of *abstract* technologists.

[5] Actually these rules are very important and their scientific, cultural and formative value must not, and will not, be questioned here.

textbooks dealing with structural mechanics by Colonnetti [3] and Baldacci [4] are very inspiring. We found to be particularly illuminating the preface written by Colonnetti to his oeuvre:

These pages –in which I have gathered the lectures I have given this year to my students of Politecnico di Torino– reflect faithfully the pedagogical conception to which I inspire my teaching; which is aimed, deliberately, to privilege the purpose of transmitting high culture and in considering as secondary the purpose of transmitting knowledge to be used immediately in the professional practice. The choice of the topics of my lectures has been based only on this preoccupation: to offer to the scholar the fundamental principles, to deepen the study of their meaning and scope of applicability, to see how it is possible to base on them a rational body of doctrines, and to see how this body can be then, when it is necessary, used to solve concrete problems. The topics which are more suitable to this aim have been completely developed. Other topics, which by themselves are not less important, but which are less thought-provoking from this point of view, have been totally or partially neglected. [Boldface is by the authors] ***The reader will not find here the usual gathering of already given solutions, which he can apply -sometimes appropriately and sometimes not appropriately- to all problems which the technical practice will present to him. On the contrary, he will learn how to analyze and how to solve each among those problems, clearly understanding the value of the hypotheses on which the solution is based and clearly evaluating the degree of approximation that is accepted in finding such a solution.***

In the same vein, we also found instructive discussions in the more modern texts used at Ecole Polytechnique by Germain [5] or by Salençon [6].

For those who are content to conform to the most recognized authorities in the field of theoretical mechanics, the above arguments for the necessity of the ensuing presentation may suffice. The principle of authority alone, however, is not enough to motivate the choice of presenting ideas of model theory in the present context. To support our arguments for this class of readers, we shall pursue an alternative line of reasoning.

In every textbook of structural mechanics, the fundamentals of beam theory and of the theory of deformable bodies are addressed, and these theories are regarded as a fundamental part of the education of an engineer. These theories study the mechanical behavior of some particular constrained structures when subject to external loads. In these theories, the same (slender) body, subject to a given system of loads, is modeled in ways which can be very different one from another, such as:

1. using the *Euler–Bernoulli planar beam model*, the kinematics of the body is described by means of its axial line and its resistance by means of one or, at most, two rigidities (flexural and extensional); or
2. using the *Timoshenko model*, such a kinematics is further specified by introducing the field of rotations of its cross-sections (i.e. transversal to the axial line) so that, at least, a shear rigidity has to be added; or
3. using the *Cauchy approach* (even considering only small deformations), the kinematics of the same body is very involved, being characterized by a field of displacements defined over a three-dimensional shape of the body, customarily referred to as the reference shape, while in general, in order to describe deformability, 21 rigidities are needed;

4. using an *atomistic theory* (this was the approach initially employed, for instance, by Navier) the kinematics is the one of many moles (in the sense of Avogadro) of material particles linked between each other;
5. from here a very detailed description of the deformation undergone by the considered body) by central elastic forces.

Note that a (naive) empiricist's analysis of the above list of descriptions of the same physical object could conclude that each of those descriptions is more *realistic* than the preceding one. At the outset one has to admit, however, that such an analysis would lack plausibility given the fact that the chosen order is not chronological. Even more tough would be finding the reasons why the use of some quantum-relativistic theory, employing quarks or some other even more elementary constituents of matter, is not being proposed and considered. Clearly, this regression toward the infinitely detailed, attempting to identify the *real nature* of the mechanical systems under study, is hopeless, because at this level of detail it is not even feasible to study the behavior of very simple structures used in many applications.

A more appropriate approach is the one proposed in the context of model theory (an elegant but elementary presentation can be found, for instance, in the beautiful essay by Aris [7]): we abandon the effort to uncover the true nature of the considered physical entity, and instead we limit ourselves to modeling some of its relevant aspects in a specific class of situations and phenomena.

We note that a Cauchy model is appropriate when studying in detail the deformation of cross-sections of the slender body; that the Euler model is appropriate when such deformation is negligible, leaving the cross-sections orthogonal to the axial line; and that the Timoshenko theory is useful when shear deformations, namely orthogonality defects of the cross-sections, actually occur and are relevant.

As far as is known, study of the structure of an airplane's wing at the atomic level, or at speeds close to the speed of light, has not been of immediate use, even if it may not be wise to exclude the possibility that such needs might occur in future. Note (the reader is again referred to Aris [7] and to the handbook *The Man-made World. Technology Foundation Course* of the Open University [8, 9]) that the various models of deformable bodies and framed structures proposed above can be systematically referred to as successful case studies. In the context of the general statements of model theory, it is seen that these combine the rare characteristics of being easy to handle and of being able to provide a description of reality which is satisfactory for many engineering applications. These peculiar characteristics are the most desirable ones in every mathematical model of a physical phenomenon.

It is very likely that the approach frequently (and positively) adopted by scholars in mechanical sciences and structural mechanics towards epistemology can be explained without invoking unnecessary psychological theories (as sometimes the most reluctant among their students may try to do). Indeed, a familiarity with the many models of deformable body which were developed in the various periods of the history of mechanics – together with the required ability to pass from one description to another, while the physical entity to be described remains the same – and the need to establish the possible

relations between such different descriptions do have an important effect on their way of reasoning. They develop a great sensitivity to the most delicate issues of the philosophy of science. Indeed, they are quite often simultaneously inclined to the study of applications, to the related mathematical abstractions and to metaphysical discussions. The tendency to be extremely precise in their conversations, together with an almost obsessive carefulness in choosing words, are also among their peculiar characteristics.

These characteristics are obviously motivated if one considers that, when dealing with many models (as in their studies), it is very important to distinguish, by assigning to them different names, the entities involved: physical entities, which belong to the world of phenomena they are aimed at describing (e.g. *deformable bodies*), and abstract ones, which are employed as mathematical models of the physical entities (e.g. *Euler beam*, *Timoshenko beam*, *Cauchy continuum*). We note that the same physical object, in different physical situations, is modeled with different, and seemingly contradictory, mathematical models.

The classical case of such a multiplicity of models was already known, most likely, by Archimedes (see also [1]). Indeed, when studying the theory of floating bodies, Archimedes assumed the surface of the sea to be planar, even if it was known to him that the Earth is spherical, as had been definitively proven by his contemporary Eratosthenes. Archimedes knew well, indeed, that the laws governing the floating of a ship can be formulated by assuming that the involved part of sea is planar, to the extent that the dimensions of the ship are small compared with the radius of the Earth. Archimedes also knew, from Aristarchus, that the structure of the Universe was more complex than had been believed initially. Aristarchus' original text has been lost, but a quote in Archimedes' work *The Sand Reckoner* describes it. We know that Aristarchus proposed the heliocentric model, as an alternative model to geocentrism. Thomas Heath gives the following English translation of Archimedes' text:

> *You are now aware* [*"you" being King Gelon*] *that the* "*universe*" *is the name given by most astronomers to the sphere the centre of which is the centre of the earth, while its radius is equal to the straight line between the centre of the sun and the centre of the earth. This is the common account (τά γραφόμενα) as you have heard from astronomers. But Aristarchus has brought out a book consisting of certain hypotheses, wherein it appears, as a consequence of the assumptions made, that the universe is many times greater than the* "*universe*" *just mentioned. His hypotheses are that the fixed stars and the sun remain unmoved, that the earth revolves about the sun on the circumference of a circle, the sun lying in the middle of the orbit, and that the sphere of the fixed stars, situated about the same centre as the sun, is so great that the circle in which he supposes the earth to revolve bears such a proportion to the distance of the fixed stars as the centre of the sphere bears to its surface.*

The reader will remark that Archimedes seems to use a sophisticated version of Popper's falsificationism. Indeed, Popper's ideas can be condensed in a nutshell by stating that he envisions science as a process of, sequentially, formulating theories and, successively, rejecting them, as they are shown to be false by experimental evidence. Rejected theories must be replaced by other theories, wherein the latter address and fulfil anomalies not contemplated in the prior theory. In other words, a theory which replaces a theory shown to be false must have a greater explanatory power.

The preceding observations suggest that Archimedes may be seen as an ancient (a precursor of) Popper.[6] We note that he writes "This is the common account as you have heard from astronomers," "But Aristarchus has brought out a book consisting of certain hypotheses, wherein it appears, as a consequence of the assumptions made, that the universe is many times greater than the 'universe' just mentioned." "His hypotheses are that." Clearly, Archimedes knew about the conjectural value of scientific hypotheses.

Attempting to avoid the distinction between physical objects and their models almost always results in an inextricable confusion of concepts and meanings. In the Archimedean example, one could seek clarification by asking if the external surface of the Earth, for Archimedes, was spherical or flat. Many historians, after reading only his works on floating bodies, claimed that Archimedes had a limited understanding of cosmological theories. Archimedes seems to master perfectly the distinction between a physical object and its different models, as a reader of his *On the Method* can readily conclude.

Finally, the needful comparison between the performances of different models can explain the dichotomous tendencies shown by mechanicians: one towards metaphysics and the other to the necessity to choose different names for the different mathematical entities which are, in different situations, used to describe the same physical entity. Since a reasonable mastery of mechanics requires the use of different abstract and specialized languages, very often the students of engineering do not accept its usefulness, thinking it is puzzling and far from the *practise*.

To readers who, at this juncture, are still unconvinced of the value of the following sections we suggest, *tout simplement*, to skip them. Their position is as respectable as the one represented by the partisan literature cited to support the choices made in this chapter. The oldest known advocate of the uselessness of model theory and of its underlying vision was Sextus Empiricus, as clearly appears from the first lines of his *Adversus Mathematicos*. Together with a large number of his epigones, Sextus Empiricus resolutely denies the usefulness of mathematical models in describing the physical world. Sextus Empiricus writes (this citation is taken directly from Russo [1]):

If there is such a thing as mathema and it is attainable by humankind, it presupposes agreement on four things: the thing which is taught, the teacher, the learner, and the method of learning. However, the thing which is taught does not exist, nor does the teacher, the learner, nor the method of learning, as we shall demonstrate. Therefore, there is no mathema. (see also *Adv. mathematicos I, §9,* D.L. Blank's translation: *Against the Grammarians,* Clarendon, Oxford, 1998). We agree with Russo in leaving the word *mathema* untranslated (in contrast with Blank's translation); its meaning is learning, study, or an object thereof.

[6] It is more appropriate to state this in the reversed manner: that Popper is the modern Archimedes. It is curious that a book could have the following title: *Aristarchus of Samos, the ancient Copernicus; a history of Greek astronomy to Aristarchus, together with Aristarchus's Treatise on the sizes and distances of the sun and moon* (1913). If even Sir Thomas Little Heath, one of the most skilled historians of English literature, the same who translated so brilliantly Archimedes, produced such a title, then one must conclude that the superiority of modern intellectuals with respect to ancient ones will persist forever. After having read the ancient text one should state, as well, and as admitted by himself, that Copernicus is the modern Aristarchus.

For those who go on to read the succeeding sections we have the following cautionary message. It is possible to not fully appreciate the forthcoming examples before having mastered (or at least become familiar with) the concepts explained in the other chapters. This chapter is intended to reorganize the topics treated in the remaining part of the text. Therefore, one could read the forthcoming sections as an epilogue, i.e. at the end of the chapter, while many others could find them more useful as a prologue.

4.2 Morphisms

The most delicate aspect of our attempt to provide a logical representation of the physical world lies in the concept of the mathematical model. We want to explain this concept in a precise and modern way, notwithstanding that the most basic concepts among those which we discuss here are clearly present in the Archimedean *On the Method.* We believe the formalism of modern abstract algebra to be one of the best suited ways to provide the reader with the concept of mathematical model in a simple and concise manner. We aim at giving a precise description of such a concept because the formidable design challenges which we are required to face deserve such a treatment.

Metamaterials are complex systems whose (complex) behavior is what we want to exploit in order to find novel, designed artificial materials of exceptional performance. Therefore, when we consider metamaterials, (over)simplification is not a possibility. We are not pursuing a simplified model to be applied to a specific and limited range of situations. In other words, we are not ready to sacrifice complexity for getting predictiveness. We seek predictiveness without losing complexity.

Modeling complexity is a challenging task. Describing a complex system in relatively minute detail is usually untenable even when employing powerful computational tools in combination with advanced numerical codes. Therefore, to find a reasonable compromise between the computational burden and the prediction capacity, a possible option is trying to describe the same physical system by means of different mathematical models, each one having a different range of applicability. In particular, we may decide to use different models at different length scales. Then, we may try to use results obtained by considering some prototype problems at a smaller length (micro) scale as a tool for simplifying the study of a model valid at a larger (macro) length scale: for instance, we may produce macroscopic constitutive equations, as is done in many works dealing with the so-called homogenization procedures. Any confusion between the different mathematical models which may be used must therefore be carefully avoided.

In order to give a precise definition of the concept of mathematical model (we present here an elaboration of what is explained in the *Algebra* handbook of the Open University [10]) we have to resort to the algebraic notion of **morphism**, which follows below.

Let (X_1, X_2, X_3) and (Y_1, Y_2, Y_3) be two triples of sets. Let us define, for each of these triples, a binary operation. Such an operation associates to each pair of elements in $X_1 \times X_2$ (respectively $Y_1 \times Y_2$) an element of X_3 (respectively Y_3). If we denote with the symbols $\odot$ and $\boxdot$ these two operations, respectively, we have:

$$\begin{aligned} \odot &: X_1 \times X_2 \to X_3, \\ \boxdot &: Y_1 \times Y_2 \to Y_3, \end{aligned} \tag{4.1}$$

$$\begin{aligned} \odot &: (x_1, x_2) \in X_1 \times X_2 \mapsto (x_1 \odot x_2) \in X_3, \\ \boxdot &: (y_1, y_2) \in Y_1 \times Y_2 \mapsto (y_1 \boxdot y_2) \in Y_3. \end{aligned} \tag{4.2}$$

Moreover, let f_i $(i = 1, 2, 3)$ be a triple of injective maps from X_i to Y_i:

$$f_i : X_i \to Y_i, \qquad f_i : x_i \in X_i \mapsto f_i(x_i) \in Y_i. \tag{4.3}$$

We draw the following (commutation) diagram and consider the possibility that the equality sign after the question mark could hold:

$$\begin{array}{ccccc} (x_1, x_2) \in X_1 \times X_2 & & \overrightarrow{\odot} & & x_1 \odot x_2 \in X_3 \\ (f_1, f_2) \downarrow & & & \searrow & f_3 \\ (f_1(x_1), f_2(x_2)) \in Y_1 \times Y_2 & \underset{\rightarrow}{\boxdot} & f_1(x_1) \boxdot f_2(x_2) \in Y_3 & ?= & f_3(x_1 \odot x_2) \end{array}$$

Indeed, the two possible "ways" starting from the pair (x_1, x_2), a priori, do not lead to the same result.[7] Namely, in general, the equality symbol at the right-bottom of the diagram might not hold true. In the special case in which the two results always (namely, for every pair (x_1, x_2)) coincide, the triple (f_i) of applications is called **morphism** of the algebraic structure $(X_1 \times X_2 \times X_3, \odot)$ into the algebraic structure $(Y_1 \times Y_2 \times Y_3, \boxdot)$.

This formal definition may be off-putting to the reader. However, this abstraction is necessary, and the forthcoming examples will help to clarify the concept of morphism introduced above.

Example 4.1 The logarithm of a real positive number is a morphism of $\mathbb{R}$, endowed with the multiplication operation, into $\mathbb{R}$, endowed with the addition operation, since

$$\log(xy) = \log(x) + \log(y).$$

Note that, in this case, the three sets X_i and the three sets Y_i all coincide with $\mathbb{R}$, and all the three functions f_is coincide with log. As already proved by Archimedes in his Arenarius (the reader is referred to Boyer [11] and Russo [12]), such a morphism is very useful when computing products of relatively large numbers. In fact, there appears to be unanimity amongst historians of science that modern computing techniques started with the publication of Napier's tables of logarithms. These tables are the theoretical basis on which Napier's bones were constructed: Napier's bones was a manually-operated

[7] It is interesting that the validity of logical inference departing from a set of observations, i.e. the closure of the above morphism diagram, was questioned by the ancient school of Indian materialism. Indeed, Charvaka philosophy rejected inference as a means to establish universal knowledge, stating that, whenever one infers a conclusion from a set of observations, he/she has to take into account doubt, thereby considering inferred knowledge as conditional [Chandradhar Sharma. *A Critical Survey of Indian Philosophy*. Publisher: Motilal Banarsidass; 13th edition (September 1, 2016) ISBN-10: 8120803655, ISBN-13: 978-8120803657].

calculating device created by Napier which some historians of science consider, metaphorically, as one of the main flywheels of the first industrial revolution.

The senior authors of this chapter are old enough to have spent hours, in their middle and high school days, in learning how to use Napier's tables for computing the product of large real numbers. The fact that, for a scientist, the relevance of this competence has dramatically decreased in such a small time interval, combined with the fact that even the memory of its importance has faded in one generation, should suggest some considerations to the reader, particulary when contrasted to the fact that the content of the Archimedean *On the Method* is still considered very topical even after more than 23 centuries.

Example 4.2 Let us now consider: a) an RLC circuit connected in series with a voltage source $V(t)$; and b) a material particle having mass m, moving on a given straight line, subject to an assigned external force $F(t)$, to a linear elastic restoring force with constant k and a friction force proportional to the velocity, with viscosity coefficient μ. In addition, let us consider: i) the operation which associates to the RLC circuit and voltage source pair the capacitor charge signal $Q(t)$ corresponding to a certain initial state of the RLC circuit; ii) the operation which associates to the material particle and external force pair the motion $x(t)$ corresponding to a certain initial state of the particle; and iii) the functions associating the RLC constants to the constants μ, m, k, $V(t)$ to $F(t)$ and $Q(t)$ to $x(t)$ respectively (where all the considered quantities have been suitably non-dimensionalized). Experimental evidence allows us to state that, in a wide range of situations, the triplet of the above introduced functions, with respect to the operations, is a morphism. When such a morphism between physical phenomena occurs it is customary to say that a **physical analogy** has been established.

The concept of physical analogy has been employed very often in the teaching of technical and scientific subjects and in professional practise. Indeed, it is widely accepted that through its use one can obtain interesting hints regrading the behavior of the two phenomena so compared. In the past, as an instance, electrical circuits analogous to some structures of interest for applications in civil engineering have been found. Such circuits are to be considered as **analog computers**, instrumental for the design of the cited structures. Moreover, in the study of Saint-Venant beams it has been noticed that, using a startling physical analogy with deformation phenomena of a pressurized membrane with the same section, one can obtain interesting information about their torsional deformation. Nevertheless, the physical analogy between two phenomena is often supported only by relying on strong *experimental evidence*. In fact physical analogies are almost always obtained by means of the mediation of two mathematical modeling processes (here the reader is referred to the beautiful discussion developed by Feynman *et al.* [13] Vol.II, Chapter 12): i) two physical phenomena are modeled by means of suitable mathematical entities and differential equations; ii) a bijective correspondence between such entities and equations is established; iii) one proves that, if solutions to equations describing the first phenomenon are known, then those relative to the

second are known (and vice versa); iv) finally, one links together those features of the two phenomena which are deemed most important in the previously introduced mathematical models. Oftentimes unfortunately, the treatment of this complex procedure is simplified, without giving due considerations to the steps from i) to iii) and, simply, citing the result obtained in iv).

The construction of morphisms between mathematical objects and real phenomena is the ultimate scope of the activity of scientists. Many experts in mechanics of structures will agree that the subject of the Bernoulli–Navier beam theory (a formalization of ideas dating back to Euler) and of a good part of strength of materials courses is the construction and analysis of such morphisms.

Example 4.3 Let us now consider: a) the set Γ of piecewise C^1 curves in three-dimensional Euclidean space and the set of distributions (in the sense of Schwartz) of forces and moments defined on a generic curve $\gamma \in \Gamma$; b) the set of shapes of a deformable body $\mathfrak{B}$ and the set of possible mechanical interactions of such a body with the external world; let us further assume $\mathfrak{B}$ to be slender, namely that, as a consequence of the cited interactions, its shape is maintained such that one of its dimensions is much larger than the other two. We then consider: i) the operation that, through the solution of the differential equation of the elastica, associates to the curve γ_0, and to a given distribution of forces and moments, the curve γ; ii) the operation which associates to an interaction and to the undeformed shape of the body its final shape; iii) the functions which associate to a curve γ the shape of the body obtained translating a plane figure (called cross-section) along γ itself, and to a distribution of forces and moments the corresponding mechanical interaction. We notice that, in the example herein considered, the sets X_1 and X_3, Y_1 and Y_3 and the functions f_1 and f_3 coincide. Experimental evidence shows that, in a wide range of situations, the triplet of the above defined functions, with respect to the operations, is a morphism.

4.3 Mathematical Models of Physical Phenomena

Referring to Example 4.3, and according to the nomenclature employed by Aris [7], we can state that entities described at point b) are the *prototype* of the set of entities described at point a) which, in turn, due to the existence of the introduced morphism, are a *mathematical model* of those described at point b).

Given a class of entities and physical phenomena, a mathematical model for them is obtained by:

1. Choosing, a priori, a set of mathematical entities and a set of identification laws between the chosen mathematical entities, and the physical objects and phenomena which need to be investigated;
2. Determining the circumstances in which the above identification laws are actually a morphism, making use both of logical inference (to investigate relations between the introduced mathematical entities) and of the experimental method (to investigate relations between the considered physical entities).

The structure of the scientific theories which is implicit in the above proposed order, which presupposes the formulation of the mathematical concepts for the comparison of the abstract concepts with experimental evidence, has been long debated in the process leading to the rediscovery of the ancient Archimedean philosophy of science after the Renaissance. Inductivism, on the other hand, rejects the structure which is implicit in the said order, and actually reverses the order. Therefore, we discuss below the different points of view before formulating precisely the vision which appears to us the most appropriate.

4.3.1 An Inductivist Vision of the Concept of Mathematical Model

From the viewpoint of model formulation, one can have either an inductivist or a deductivist vision of the scientific method depending upon the choice of the domain of the functions f_is, appearing in the definition of morphism given in the previous section. Let us consider the following diagram representing a morphism:

$$\begin{array}{lll} \text{Set of physical objects} & \textit{physical operations} \longrightarrow & \text{physical results} \\ \textit{model} \downarrow & & \downarrow \textit{model} \\ \text{Set of mathematical objects} & \textit{mathematical operations} \longrightarrow & \text{mathematical results} \end{array} \tag{4.4}$$

The above morphism reflects an inductivist (and to our understanding also the Platonic and Newtonian) vision which is founded upon the hope of finding, possibly after a series of trials and errors, *the model*: namely, *the morphism* between the physical world and the set of mathematical objects employed in its description. The hope consists in believing that the whole reality can be represented in the mathematical universe and, hence, at least in principle, is completely foreseeable. This underlies the belief that the two worlds have substantially the same shape (Galilei states that *the great book of nature is written with the characters of mathematics and geometry*). In this vision, the progress of science consists simply in adding more and more details (namely, mathematical objects) in our description of the world. The universal validity of the model can be experimentally corroborated in an indisputable manner verifying the *closure of the diagram*, namely the perfect correspondence between mathematical and physical results.

In defense of the inductivist vision it is customary to recall (in our opinion, inappropriately) the accomplishments of Newtonian mechanics. As an instance, using the Newtonian model of the solar system, Gauss computed the effect of the presence of a planet on the orbit around the Sun of another moving inside its orbit. By analyzing the orbit of Uranus, Le Verrier, in 1846, confirmed the existence of Neptune. The trajectory of the presented argument was rather easily disproved by Bertrand Russell by means of

his anecdote about the inductivist turkey[8] (for further details see p. 24 of Chalmers [14]). The morphism scheme presented in 4.4 has also received criticism, in modern times, for instance by Duhem and Quine. The reader is referred to the entry *Underdetermination of Scientific Theory* in the Stanford Encyclopedia of Philosophy (see [15]).

It appears quite convincing that no definitely "true" scientific knowledge can be attained by the human mind. These thoughts were already manifest in the mind of Hellenistic scientists. As theologists in the Middle Ages could not accept such a line of thinking, the need for a revealed truth became unavoidable. In that moment of human history the split between scientific knowledge and theology occurred. Science, since Archimedes, has limited its interests to the formulation of models which conjecturally and tentatively explain only a specific set of phenomena. In this regard, we have found the essay [16] particularly illuminating.

4.3.2 A Deductivist and Falsificationist Vision of the Concept of Mathematical Model

The Newtonian (but also Platonistic) natural philosophy is considered too ambitious to be viable. More modestly, following the vision of Popper and Kuhn,[9] we have to reconcile ourselves to accepting that a scientific model is well-formulated when the following diagram is commutative, in place of (4.4):

$$\begin{array}{lll} \text{Set of mathematical objects} & \textit{mathematical operations} \longrightarrow & \text{mathematical results} \\ \textit{model} \downarrow & & \downarrow \textit{model} \\ \text{Set of physical objects} & \textit{physical operations} \longrightarrow & \text{physical results} \end{array} \tag{4.5}$$

In the deductivist and falsificationist vision one recognizes that theory precedes and guides observation. In this case, one ceases to consider theories as being formulated (even only probably) as true by virtue of experimental evidence and systematic observation. Instead, we must consider theories as purely speculative and only tentatively formulated conjectures. The most fundamental hypotheses of a theory (which we may

[8] In an American farmstead, a turkey decides to shape his vision of the world in a scientifically well founded manner. Unfortunately, the turkey was an inductivist. He found that, on his first morning at the turkey farm, he was fed at 9 a.m. Being a good and serious inductivist turkey, he did not jump to conclusions too quickly. He waited until he collected a large number of observations that he was fed at 9 a.m., and made these observations under a wide range of circumstances: on Wednesdays, on Thursdays, on cold days, on warm days, etc. Each day he added another observation statement to his list. Finally, he was satisfied that he had collected a number of observation statements to inductively infer that *I am always fed at 9 a.m.* However, on the morning of Thanksgiving Day, he was not fed but, instead, had his throat cut. Retrieved at https://mashimo.wordpress.com/2013/03/12/bertrand-russells-inductivist-turkey/ on April 16, 2018.

[9] We believe that already Archimedes shared such a vision: nevertheless, we will not insist on trying to defend this point of view, as in the present context such a priority attribution to Hellenistic science is not relevant.

call postulates) are created in the attempt to describe the appearances[10] of some aspects of reality or improved in order to solve the inconsistencies which have already occurred in the previously formulated theories.

Only after the formalization of the basic conjectural postulates and the logical deduction of a sufficiently large set of consequences from them, these basic conjectures can, and must, be compared with experimental evidence: in this way, the most effective theories are selected, while those being disproved are dismissed. Even if we abandon the claim that a theory can be true, we can still state that, in a given moment, it is the best available and more suitable than the previous ones. The steps to be followed then for formulating models may be enumerated as (the order is temporal):

1) to develop theories (in Greek theory means *vision, observation*),[11] namely to create systems of postulates and deduce from them a number of consistent theorems;
2) to establish correspondences between the objects of a given theory and some parts of reality (note once more that the functions f_is in the definition of morphism are injective but not surjective! In other words there are real objects which do not correspond to any mathematical entities[12]);
3) to check that all predictions given by the theory in its domain of application are not experimentally disproved (this is equivalent to saying that the functions f_is are a morphism, when restricted to some subset of phenomena and physical situations).

The reader will note that we are not stating that a theory is experimentally proven: we simply say that it is not disproved (or, following the nomenclature introduced by Popper, not falsified). We believe (see again Russo [1]) that Hellenistic science managed to supply to humankind a very powerful tool: the scientifically formulated mathematical models of reality, based on not-yet-falsified postulates.[13]

[10] The concept σώζειν τὰ φαινόμενα, which in Romanized Greek reads as *Sozein ta phainomena* and in English reads as *save the appearances* was already known by ancient Hellenistic scientists: for a more modern treatment of this concept, as inspired by ancient Hellenistic scientists, see e.g. [17].

[11] A thorough etymological study of the word "theory" would lead the reader to discover that it has the same root as the word theatre. We suggest that, in the opinion of the Greek and Hellenistic inventors of the word theory, a scientist formulating a theory is a spectator of the theater of phenomena; he/she observes their sequence and synthesizes them with mathematical methods.

[12] This situation is rather puzzling for many students and also for many scholars: for instance, in the theory of Euler–Bernoulli beams there is no mathematical object modeling the state of the whole set of material particles constituting the section of a beam. The orientation and the deformation of such sections are accounted for in an indirect way by the theory. It could be difficult to understand in what sense the Euler–Bernoulli model is "true." Actually, under certain circumstances, it is the curvature of the line representing the shape of the beam which is accounting for those phenomena occurring in the said sections, and which are those predominantly causing the material to store some deformation energy.

[13] Actually the Aristotelian school, i.e. the authors of *Posterior Analytics* I.3 72b1–15, made the first step in this mental construction. They introduced a rigorous mathematical language and thinking, allowing western civilization to go beyond the Platonistic idealistic vision of mathematics. The formulation of precise mathematical theories based on the distinction between primitive notions and defined notions was possible since then, as in *Posterior Analytics* the "notions" are concepts invented by the human mind, and which are organized in well-formulated sentences, respecting the rules of syntax and having a precise meaning given by their semantics. Following Aristotelians, roughly speaking, defined notions have a meaning which can be reduced, via a definition, to the meaning of primitive notions, while primitive

Note that, often, it is not even possible to falsify a postulate or one of its consequences directly. There are many primitive and defined concepts whose correspondence with physical objects is difficult, if not impossible, to define. Following D'Alembert, an example of an abstract concept which cannot correspond to a physical entity is the concept of "force." Indeed, in D'Alembert's *Traité de Dynamique* one finds the following, rather meaningful, statements:

I have proscribed completely the forces relative to the bodies in motion, entities obscure and metaphysical, which are capable only to throw darkness on a Science which is clear by itself.

I must warn [the reader] that in order to avoid circumlocutions, I have used often the obscure term 'force', & some other terms which are used commonly when treating the motion of bodies; but I never wanted to attach to this term any other idea different from those which are resulting from the Principles which I have established both in the Preface and in the first part of this treatise.

Indeed, forces have never been measured directly. Forces are usually measured indirectly via some measurements concerning other quantities, e.g. elongations, changes of angles, etc. The relationship between measured quantities and the abstract concept of force depends on the theory considered. Falsification of a prediction in the framework of a theory may be caused by many independent wrong conjectures. For instance: the observed deviation in the motion of a planet may be caused by the existence of a not yet observed planet, by a wrong assumption about the dependence of gravitational potential energy on the distance between interacting masses or by a wrong assumption about the invariance of laws of physics on the change of observer.

The reader is thus invited to ponder carefully statements like: the principle of inertia is true because of experimental evidence. Let us agree that such a principle (or postulate) states: there exists at least one observer (called inertial observer) for which all free bodies (i.e. bodies which are not interacting with anything else in the universe) move with a constant velocity. Now, even if we admit that we are lucky and that we have found such an observer (even though we cannot understand how this has been possible), how

notions are concepts whose meaning is made precise by the axioms they must verify, by an arbitrary choice (the word *axiom* derives from a Greek word meaning exactly *choice*!). One assumes that axioms are true for primitive concepts: the only possible problem arising in such an axiomatic process could consist in a choice of axioms which is not consistent, i.e. contradictory.

Using the words of a modern mathematician (who could be suspected, however, of being Platonistic when he states that the primitive concepts "seem to us as immediately understandable"), one can say that (see Tarski and Tarski, *Introduction to Logic and the Methodology of the Deductive Sciences*, page 118, Oxford University Press, 1946 [18]):

When we set out to construct a given discipline, we distinguish, first of all, a certain small group of expressions of this discipline that seem to us to be immediately understandable; the expressions in this group we call PRIMITIVE TERMS or UNDEFINED TERMS, and we employ them without explaining their meanings. At the same time we adopt the principle: not to employ any of the other expressions of the discipline under consideration, unless its meaning has first been determined with the help of primitive terms and of such expressions of the discipline whose meanings have been explained previously. The sentence which determines the meaning of a term in this way is called a DEFINITION . . .

Axioms are chosen to be true in order to give a meaning to the primitive concepts. Postulates are statements whose truth is a conjecture aimed to describe physical phenomena. Axioms are true by definition, Postulates could be true or false. One assumes as a starting point of a scientific theory that a postulate is true, even if, in principle, it might be false. Postulates must be falsifiable.

can we check that *all* the *free* bodies (which are many and, maybe, even infinite) are observed to move with constant velocity, in every time instant? Clearly, it is possible to falsify the statement: the observer O is inertial. Indeed, if one finds a free body which is not moving with constant velocity in a certain time interval then O is not inertial. However, there are infinite observers and one cannot check what happens to infinite free bodies as observed by infinite observers.

In conclusion:

1. To state that a postulate is based on experimental evidence is naive (one could potentially talk about naive inductivism, in this context).
2. A fundamental characteristic of models must be the (potential) falsifiability of its postulates and of all the logical consequences of its postulates. In the context of a given model, it is essential to be able to predict whether a phenomenon will happen or not, so that experimental evidence can either confirm or disprove (falsify) the proposed model.
3. It is very difficult to falsify some statements, and in particular those concerning abstract concepts which do not correspond to any physical entity via the functions which are conjectured to establish the morphism under discussion.

This conception of the scientific method, even if seemingly restrictive, is likely to yield a unitary and comprehensible framework to the methods of investigation in science. Certainly, it accounts for the bulk of scientific activity of scholars since Hellenistic times to the present. It is interesting to notice that, in formulating his famous abjuration, Galileo embraced an epistemological doctrine very similar to the falsificationist one, and that, successively, in the prison of Arcetri, he had permission to study *only* the new science of the deformation of Bodies. Those who still want to maintain their inductivist position should also ponder that Newtonian mechanics cannot be considered proved by Le Verrier experiences. Indeed, more recently, it has been possible to describe experimental evidence regarding the motion of Mercury only by employing relativistic mechanics.

4.4 Relation between Mathematics, Science, and Technology

The theses outlined in this section are substantially borrowed from the essay of Russo [1], to which the reader is referred for a more in-depth study, this being in our opinion an enlightening monograph.

Paradoxically, the deductionist hypothetico-deductive conception presented in the previous section is probably older than the inductivist one, dating back, at least, to the scientific and technological Hellenistic School of the third century BC. It seems permissible to infer this when reading, in addition to the other works of the same school that have reached us from the annals of time, The *Method of Mechanical Theorems*, also referred to as The *Method*, of Archimedes of Syracuse.[14] The following extract is taken from [19]:

[14] The only copy of The *Method* has come to us in a very fortuitous way: the work was originally thought to be lost, but in 1906 was rediscovered by Heiberg, in carefully looking at the not-completely-scratched Archimedean text which had been used to constitute a palimpsest of prayers of the Orthodox Church,

Archimedes to Eratosthenes greeting . . . Seeing moreover in you, as I say, an earnest student, a man of considerable eminence in philosophy, and an admirer [of mathematical inquiry], *I thought fit to write out for you and explain in detail in the same book the peculiarity of a certain method, by which it will be possible for you to get a start to enable you to investigate some of the problems in mathematics by means of mechanics. This procedure is, I am persuaded, no less useful even for the proof of the theorems themselves; for certain things first became clear to me by a mechanical method, although they had to be demonstrated by geometry afterwards because their investigation by the said method did not furnish an actual* [mathematical] *demonstration. But it is of course easier, when we have previously acquired, by the method, some knowledge of the questions, to supply the proof than it is to find it without any previous knowledge.* [. . . the computation of the area subtended by an arc of parabola, using results on the equilibrium of forces obtained by Archimedes in the work *On the Equilibrium of Planes*, follows the previous statements . . .]. *Now the fact here stated is not actually demonstrated by the argument used; but that argument has given a sort of indication that the conclusion is true. Seeing then that the theorem is not demonstrated, but at the same time suspecting that the conclusion is true, we shall have recourse to the geometrical demonstration which I myself discovered and have already published.*

As Gustavo Colonnetti does, we recognize Archimedes as a father of mathematical-physics[15] and, for this reason, as does Boyer [11], we support the thesis that Archimedes could well have given a theoretical course in naval architecture (or statics or mechanics of structures or hydraulics or hydraulic constructions), although probably he would have preferred, a course in pure mathematics. He was not a purely theoretical scientist (by the way, one could even argue about their existence): when needed, he was able to exploit his ability in mechanics. The most suitable role in the modern university system for a scientist and technologist, as Archimedes was, is explained by Heron of Alexandria in his works where he describes as a whole body of knowledge, the theories and their practical applications.

All Archimedean texts (the reader is referred, e.g., to the books *On the Equilibrium of Planes* or *Hydrostatics*) begin with a listing of the objects and theorems constituting the first line of the scheme set out in (4.5) above and, only afterwards do they address the issue of establishing the morphism relations f_is necessary to give a physical meaning to the model. We can hence conclude that Archimedes: 1) could very well distinguish the physical object from its mathematical model; 2) was aware that a mathematical proof of a certain property in the context of the model is totally independent of the fact that the same property seems to hold in a particular physical instance; and 3) was accepting the hypothetico-deductive method. To understand the extent to which Archimedes (and all the Hellenistic school) was keeping this method in consideration for the study of technical issues, we again refer the reader to Heron.

We believe that, in the succeeding literature, the accent on the priority of mathematical formulation, with respect to the other steps of the development of the model, has been misunderstood. To state that formulation of the mathematical model is the first step in scientific investigations does not mean that one is a Platonistic scientist

written in the thirteenth century AD. Palimpsests were created by scraping the ink from existing works and reusing their parchment. It was a common practice in the Middle Ages, as vellum was expensive.

15 Even if not unanimously accepted, by the term mathematical-physics we mean that part of science dealing with the formulation of logical and deductive falsifiable models for the description of physical phenomena.

and it does not mean that one despises applications. Because of this misunderstanding due to empiricists, along the lines of Sestus Empiricus, the belief that Archimedes and all the Hellenistic scientists despised applications spreads. On the contrary, it is clear that Hellenistic science places empiricism in the right place. The correspondence with experience is only a way (perhaps the only way) for selecting valid conjectures and rejecting bad ones. Hellenistic science was probably the first to state that the falsificationist-deductionist approach described above is the only one producing reliable predictions in applications. We believe Lucio Russo to be right when claiming that the following assertions, some of which are now accepted by a good part of modern scientists and that we support *in toto*, could have been stated by Archimedes in one of his lectures:

1. The great utility of *exact* science consists in providing models of the real world, guaranteeing that "true" statements can be distinguished from "false" ones.
2. Science can guarantee the *truth* of its statements, only when they are restricted to a precise range of applicability of the models.
3. Such models make it possible to describe and predict natural phenomena and can auto-extend themselves with the deduction method, hence becoming models in technological fields. Their predictivity is employed to design new technological devices.
4. *Scientific technology*, that makes use of design in the context of *scientific theories*, seems intrinsically related to the methodological structure of the exact science and can only arise from this last.
5. No society is known to have developed a technology able to produce truly new devices without being supported by a set of scientific theories. Quite likely, the Hellenistic world (third to second century BC) was among the earliest cultures able to develop a scientific technology. Technological knowledge, without its scientific bases, was conserved, at most, up to the Roman era. Besides, it was only with the advent of the second-Renaissance-scientific-revolution that new scientific theories, and hence new technological advancements were developed.

It is easy to frame statements 3 and 4 in the specific context of the study and developments of metamaterials. This is the objective of the last sections of the present chapter.

4.5 A Digression on Mathematics and Mechanics

The meanings of words in a given language often shift with time. When knowledge is transmitted from one language to another, then the process of "shift in meaning" becomes even more frequent and keenly experienced. This process has also affected the two words playing the most relevant role in the subject of the present monograph: mathematics and mechanics. We begin by recalling some important changes that have occurred in the standard choice of the language to be used in scientific communication, and we then progress to suggesting explanations for some shifts in meaning.

4.5.1 Recurring Changes of the *Lingua Franca* in Science and Their Effects

We are persuaded that, although its fundamental causes are yet to be understood, a well-described phenomenon of degeneration of scientific knowledge occurs in a recursive way within every, *corpus* of knowledge, even after it has become well established. This phenomenon most likely determined the decadence of Hellenistic civilization and science, at the end of the long process that commenced with the fall of Carthaginian civilization due to the development of the military power of Rome. We claim that (see [20], and [21]) such a phenomenon can be observed also in some more recent, and even contemporary, scientific milieux, having very similar forms as those described in [1].

One of the main concurrent causes of the erasure of important segments of scientific knowledge, and of the consequent shift of the meaning of scientific words, during their transmission from one generation of scientists to the following one, can be related to the change of the universal communication language used (and understood by) all active scientists all over the world. It is possible to state that if, for one reason or another, the *lingua franca* of science is changed, then one can observe nearly systematic relevant losses of great parts of previously well-established knowledge. In [1] one finds a description of the process which caused the decline of Greek as universal scientific language, and of some of the events that occurred when Arabic, Persian, and Latin, among others, tried to replace it.

Undoubtedly, Greek was the first dominant language used to pioneer scientific knowledge in the western world (west of Persia). This can be supported by many arguments, but one of them seems to us the most convincing, namely that: in every modern language, the great majority of scientific terms have, without any doubt, a Greek root and origin. Scientific advances in the Indian subcontinent, such as the *Vaiśeṣika Sūtra* (dating prior to the eastward Hellenic spread), in Sanskrit and other pre-classical languages of the subcontinent, though substantial and influential (e.g. the contribution to mathematics including that of numerals and place value of zero that came to the medieval western world through Arabic), never achieved universal acclaim. Further developments thereof appear to be either place bound or non-technological (information regarding Indian science remains sketchy and largely undiscovered with wide variations and contradictions in the literature regarding definitive dates and contributions). Eventually, Greek science came to dominate the technological developments and become the basis for further scientific advances.

With the rise of the Roman Empire, Latin became the new *lingua franca,* in Western Civilization. When it was abandoned, a long struggle involving many national languages started, among which we list French and Russian, until English managed to be accepted universally in this role. In the period between the Renaissance and the beginning of the French Revolution, Latin was spoken and understood by every scholar. After the Revolution, a well-educated scientist had to master many languages, including at least German, French, and sometimes even Italian,[16] depending upon their particular fields of interests. For instance, German competed with English, at least in philology and chemistry, for a very long time.

[16] The masterpieces of Galileo Galilei are not, even now, completely translated into English.

Until the collapse of the Soviet Union, there was an attempt to impose Russian in parts of the globe under Soviet influence. Many scholars educated in Russian schools, those established by the Communist International (Comintern, known also as the Third International in many countries) can, even nowadays, read the beautiful textbooks published by MIR publishers directly in Russian. Many of these books were translated into many languages, to make Soviet science universally available. But even the Soviet efforts to perpetuate the babel of languages, or at least a duopoly in the market of languages, eventually failed.

When English became dominant, many important theories expressed in *lost* languages were either misunderstood or simply rediscovered: in other words, these theories were published in English by English speaking authors as if such theories were novel. Often (see [20, 22]), the "novel" English theories were even less general and complete than the original ones.

This process of complete or partial rediscovery, with misattribution of originality, is one of the reasons why we must conclude that science and technological capacity (and, in general, human knowledge) cannot be regarded as being systematically accumulated and stored in an orderly manner, so as to produce an increasing capacity and understanding.

Science is not advancing by simple additions, improvements and progress. One cannot state categorically that more-modern textbooks, theories and civilizations are necessarily more advanced than those which preceded them. Indeed it is clear that:

i) science may move *some steps forward and some steps backward* (see [1]);
ii) it can happen that some époques with higher scientific culture may be followed by more decadent or regressive ones;
iii) some ideas may be *lost in translation* because of the intrinsic difficulties of some theoretical concepts; a very meaningful example is given, in this context, by the elaboration, formulated in English by Noll, of the classical field theories described, in German, in an exceptional article by Hellinger (see [20, 22]): as Noll did not appreciate variational principles, which were at the basis of Hellinger's presentation, he tried to reformulate classical theories on a different postulation scheme, which, most likely (see [21]), is not as general and effective as the original variational scheme preferred by Hellinger;[17]
iv) in one époque (for example during the Roman Empire) it may happen that, at the same time, theoretical scientific knowledge declines while technology flourishes, as the technological knowledge previously acquired in a more mature scientific époque may cause a delayed development of economical capacity and, consequently, a better life-style.

This last circumstance may be greatly misleading, as it blurs the otherwise evident correlation of cause and effect between science and technology. Some are confused by these delayed effects, and are led to believe that technology may arise without

[17] This is a crucial consideration in the context of the topic dealt with in the present monograph: the conciseness, power, and effectiveness of variational principles are needed when, as in the case of the design of metamaterials, novel ideas are to be discovered and developed.

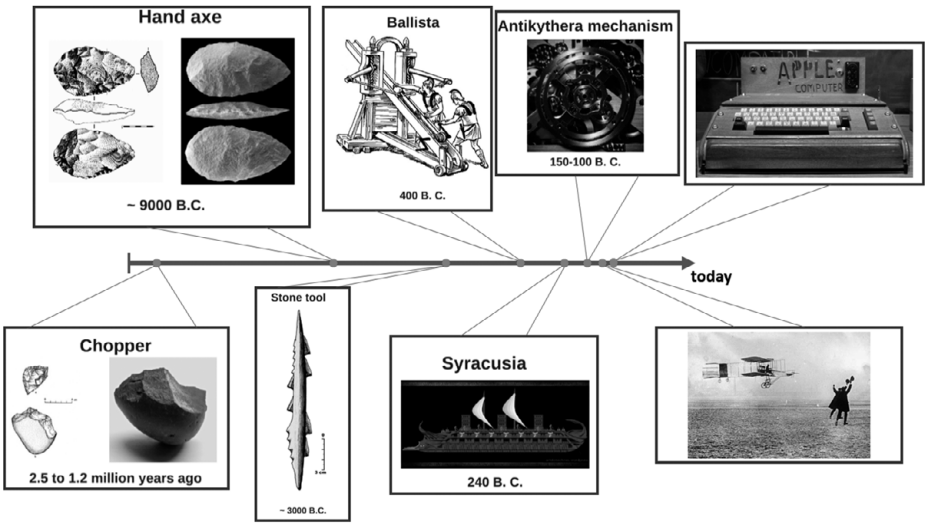

Figure 4.1 Timeline of some technological discoveries.

the solid foundation given by theoretical sciences. Instead, our belief is that without scientific knowledge technological development is not possible. Therefore, paramount in the discussion concerning the best methods to be used in designing metamaterials, is the problem of determining the true nature of the processes of scientific discovery and technological development, as well as the logical connections between them.

If one loses the historical knowledge that theoretical Hellenistic science was very deep, and unequivocally comparable to the science flourishing in Paris during the French Revolution (see [1]), then one can also believe that Roman technology was simply born by means of a "practical" process of subsequent tests and trials of technological solutions. Such a persuasion may induce the modern technologist to believe that theoretical knowledge is useless in the advancement of technology. A mere inspection of the subsequent technological discoveries of *homo sapiens* proves that via "practise" or "mimesis" the capacity of producing technological innovation is meagre and slow.

Instead we can say, for instance, with only an apparent oxymoron, that the rise of the Roman Empire coincided with the beginning of its decadence, because with the fall of Carthage and of the Hellenistic States, the Hellenistic science was soon forgotten, while Hellenistic technology could still be used and even, sometimes, improved. Indeed, preserving and transmitting mathematical and scientific knowledge is much more difficult than transmitting *knowhow* i.e. a series of *recipes* or of instructions for building things. The treatise *De architectura* (On architecture, published as *Ten Books on Architecture*) written by Marcus Vitruvius Pollio is an example (see [1]) of list of rules for constructing buildings which hides, more or less carefully, how these rules were conceived: i.e. by using a sophisticated mechanical theory. While Russo uses Vitruvius to discover the scientific roots of Roman technology, many, more naive scholars, use Vitruvius to prove the following inconsistent statement. The only way to learn how to build things is by

building things. Now, the reader could ponder the time-line in Fig. 4.1.: why learning how to make a simple stone axe required an enormous amount of time, while learning how to build an aqueduct took less trial and error?

The success of English as *lingua franca* is obviously connected with the rise of the British Empire and the predominance of the United States. However, it was favored also by two specific features:

i) its grammatical and syntactical structure, while being formalized by scholars influenced by Hellenistic culture via the intermediation of Latin and, later, of French, was, however, conceived to be simpler than all other spoken languages;
ii) it incorporated a larger number of words, taking them from Latin, Anglo-Saxon, or Greek roots as well as many other languages.

The establishment of a new *lingua franca* may cause, naturally, a specific attitude in the scientists having it as their mother tongue. Indeed, they may decide to ignore everything which is not written in their own language and to "rediscover" the theories not written in it, instead of trying to understand and translate the original sources. This tendency continues to persist as exemplified by the modern rediscovery of peridynamics (see [23]). Piola's formulation has been rediscovered (after 150 years) by English-speaking scientists, who did not manage to read the many copies of Piola's works stored in the libraries of United States, since Italian, as a scientific language, is forgotten.

4.5.2 The Necessary Mathematical Abstraction is Another Cause of Knowledge Loss

Linguistic barriers are not the only cause of loss of scientific knowledge. The intrinsic mathematical difficulties presented by some powerful and sophisticated theories are challenging barriers. Indeed, the technical knowledge of many parts of mathematics is needed to understand mechanical theories and, in particular, to conceive advanced technological solutions. Mathematical physics, as the union of mathematical modeling, experimental practice and development of novel technological solutions, is the scientific tradition to which we shall refer. It was established by many of its Hellenistic founders, among whom Archimedes of Syracuse seemed to his contemporaries the most prominent.[18]

The process of building the morphism which has been described in the previous sections presents, undoubtedly, some technical difficulties. This is proven, for instance, by the fact that some of the most profound among Archimedes' works are being completely rediscovered and fully understood only recently (see the edition by Heiberg 1889–1906 of the works by Archimedes). Archimedes was the main character of the scientific and technological revolution which occurred during Hellenistic times. No ancient author has disputed his standing, both as a scientist and as an engineer. Notwithstanding this reputation, many of his books were not reproduced in enough numbers to survive the Middle Ages. Some of his most important contributions reached us via a sequence of unbelievably fortuitous circumstances (see again [1]). This suggests that when a body

[18] Note that the name Archimedes, as referring to the greatest ancient scientist, exists in at least 150 ancient and modern languages.

of knowledge is based on a particularly abstract mathematical technique, it is likely that its rather complex content can be lost.

It appears that the more a theory is based on abstract mathematics the more difficult its preservation and transmission can be. The reputation of the author also plays a strange role. Archimedes has been placed in an Empyrean Heaven of great geniuses who cannot be understood because of their exceptionality. This sanctification has as a final result that the ideas of these presumed semi-gods are lost because only rare attempts are made to understand their exalted works. In [1] it is, in our opinion, proven without doubt that the concept of "genius out of his times" or "outstanding exceptional mind" who "cannot be understood by his contemporaries" is false. Archimedes was maybe *primus* (first) but for sure he was *inter pares* (among peers). There was at least a beta (i.e. a second, in the person of Eratosthenes of Cyrene) after Archimedes and a beloved friend whom he treated as a peer, i.e. Conon of Samos. The true situation is that every great advancement of science is a collaborative challenge overcome by a group of scientists, creating a "cultural paradigm" in the sense of Kuhn. Using the tools developed by this group, finally, remarkable results are obtained, maybe thanks to the last effort of one of its most talented representatives. Archimedes was without any doubt an outstanding genius: however, he was surrounded by peers who understood and appreciated his work. He had been a pupil belonging to a strong school (most likely he studied in Alexandria), and he contributed to the formation of successors. In his *On the Method* he explicitly states that he writes to show to his successors the proof strategy he had used to get his results. In several aspects Archimedes has been believed to be a solitary genius who was predestined not to be understood. However, he was a member of a community where mathematical knowledge was highly regarded and cultivated.

We cannot understand why Lagrange, the more recent and inventive follower of Archimedes, is not as highly and universally appreciated by modern mechanicians. Possibly, the reason for his undervaluation can be found in the works by Truesdell, where one can find the following, rather surprising, statements:

Granted his more modest scope, estimates of Lagrange's performance must remain a matter of taste. In music, in painting, in literature, tastes have changed in the past century. Why should they not also change in mechanics? The historians delight in repeating Hamilton's praise of the Mechanique Analitique as "a kind of scientific poem", but it is unlikely that many persons today would find Hamilton's recommendations in non-scientific poetry congenial.

Lagrange's best ideas in mechanics derive from his earliest period, when he was studying Euler's papers and had not yet fallen under the personal influence of D'Alembert.[19]

and finally:

While the knowledge he thus acquires does not of itself put applications into his hands, it gives him the tools to fashion them efficiently, or at least to classify, describe, and teach the applications already known. By consistently leaving applications to the appliers, Lagrange set them on common ground with the theorists who sought to pursue the mathematics further: Both had been trained in the same workshop and spoke the same jargon. Even today this comradeship

[19] Therefore, if one must believe Truesdell, Lagrange was like Pinocchio under the influence of the bad boy D'Alembert!

of infancy lingers on, provided discrete systems and rigid bodies exhaust the universe of mechanical discourse, In 1788 the mechanics of deformable bodies, which is inherently not only subtler, more beautiful, and grander but also far closer to nature than is the rather arid special case called "analytical mechanics", had been explored only in terms of isolated examples, brilliant but untypical. Unfortunately most of these fitted into Lagrange's Scheme; those that did not, he passed over in silence.

This last Truesdellism is a flagrant fake. Both Lagrange, and later Gabrio Piola, systematically developed continuum mechanics (see [21, 23, 24]). Truesdell apparently did not master the mathematical tools needed for understanding the calculus of variations and the theory of distributions, which are the most fundamental mathematical theories in formulating continuum models and which are indispensable for basing physics on variational postulates. Indeed, in order to base continuum mechanics on precise mathematical concepts, it is necessary to use the powerful tools developed by Laurent Schwartz in his theory of distributions. The principle of virtual velocities (or, as known in more recent times, the principle of virtual work) is probably the most ancient conceptual tool using which (eventually all) physical theories can be formulated (see also [25]). This principle is formulated by borrowing the structure of the extremality (or stationarity) condition for a functional, and to be formulated needs the concepts of Fréchet spaces and derivatives and the knowledge of their application to the construction of the topological space of Schwartz distributions. Even if Lagrange seems to have understood the main ideas of such a sophisticated mathematical theory, it is clear that, only when it was fully developed, its pivotal role in formulating so-called analytical continuum mechanics (see e.g. [26]) could be recognized. Those who refuse the Archimedean spirit in formulating scientific models may refuse the effort needed to master such abstract concepts. As a consequence, their efforts to simplify the postulation scheme of the available models may produce a relevant loss of scientific knowledge.

4.5.3 The Shift in the Meaning of the Word "Mathematics"

Let us start by citing an ancient source (i.e. the most ancient among those found by the authors): Anatolius, Bishop of Laodicea, sometimes known as Anatolius of Alexandria, flourished around 280 AD, as cited by Heron (Heron, *Definitions*, ed. Heiberg 160, 8-162, 2). The translation from Greek is due to Ivor Thomas, as published in the Loeb Classical Library [27]:

Why is mathematics so named? The Peripatetics say that rhetoric and poetry and the whole of popular music[20] *can be understood without any course of instruction, but no one can acquire knowledge of the subjects called by the special name mathematics unless he has first gone through a course of instruction in them ; and for this reason the study of these subjects was called mathematics. The Pythagoreans are said to have given the special name mathematics only to geometry and arithmetics; previously each had been called by its separate name, and there was no name common to both.*

[20] Note by Ivor Thomas: i.e. singing or playing as opposed to the mathematical study of musical intervals.

Ivor Thomas then adds the following comment, whose final part, however, could be questioned:

The Greek word máthema derives from the verb form matheîn which means in the first "that which is learnt." In Plato it is used in the general sense for any subject of study or instruction, but with a tendency to restrict it to the studies now called mathematics. By the time of Aristotle this restriction had become established.

Actually, in our opinion, the study presented in [1] proves that in the Hellenistic scientific tradition the word mathematics was used with the meaning of "knowledge which, to be understood, needs a course of instruction." It is universally accepted that the Pythagorean school used the word "mathematician" as equivalent to the expression "scientist" or "scholar who has been inducted to knowledge." Indeed, as stated again by Ivor Thomas:

The esoteric members of the Pythagorean school, who had learnt the Pythagorean theory of knowledge in its entirety, are said to have been called mathematicians (mathēmatikoi) whereas the exoteric members, who merely knew the Pythagorean rules of conduct, were called hearers (akousmatikoi). See Lamblichus, De Vita Pythag. *18. 81, ed. Deubner 46. 24 ff.*

Also in an authoritative source[21] one finds the following statements which agree with the point of view presented here:

Little is known about Pythagorean activity during the latter part of the fifth century. The differentiation of the school into two main sects, later called akousmatikoi (from akousma, viz., the esoteric teachings) and mathēmatikoi (from mathēmatikos, "scientific"), may have occurred at that time. The acousmatics devoted themselves to the observance of rituals and rules and to the interpretation of the sayings of the master; the "mathematics" were concerned with the scientific aspects of Pythagoreanism. Philolaus, who was rather a mathematic, probably published a summary of Pythagorean philosophy and science in the late fifth century.

The reader will remark that, in the Pythagorean school, the organization of studies was already considering two kinds of disciples. The question now arises: do we consider all engineering students as *akousmatikoi* or do we believe that some of them must be regarded as *mathēmatikoi*? Those who founded the école Polytechnique in Paris believed that the élite among the engineers had to be considered as a particular class of mathēmatikoi. Unfortunately, there is now an inclination to consider engineering studies as part of exoteric knowledge. And, as a consequence, engineers are considered as a kind of second-rank intellectuals who merely must know the rules of conduct as formulated following the complete scientific (mathematical) knowledge. This tendency will reduce engineers to the rank of hearers (akousmatikoi). We deplore and actively oppose such a tendency. There are also some epigones of Sextus Empiricus who declare that mathematics is not existing and that only exoteric knowledge really exists. This chapter is intended to prove that these epigones are wrong.

We believe that it is really interesting to remark (see the entry *manthánō* in Chantraine *et al.* [28]) that:

[21] https://www.britannica.com/science/Pythagoreanism#ref560026

1) the verb form *matheîn* seems to originate the word "mathematics" in all the Indo-European languages, but it is only in Greek that the derived forms of this verb form have taken some meanings close to the verbs "to learn" or "to understand";
2) the evolution of the use of the verb forms linked to *manthánō* (also cognate manthan: Sanskrit) is really thought-provoking: in the most ancient sources this verb means "to learn by practice, learn by experience, learn how to do"; then the meaning becomes simply "understand," subsequently it produces the words *máthos* = knowledge, *philomathēs* = lover of the study or scientist, *amathēs* = ignorant, *máthēma* = that which is taught, *mathētikos* = scholar, *mathēteía* = teaching and, finally, one arrives at the expression *tà mathēmata* = mathematics which is believed to have been invented by the mathematician, mechanician and statesman Archytas of Tarentum (i.e. Taras in Magna Graecia) who lived in the fourth century BC.

An ancient source is attributed to Archytas, whose arguments, we consider, remain topical and truly valid even after more than 2400 years.[22] Indeed, Ivor Thomas (see page 5 in [27]) translates a citation of Archytas reported by Porphyry in his *Commentary on Ptolemy's Harmonics*, ed. Wallis, Opera Mathematica iii. 236. 40– 237. 1 ; Diels, Vors. i[5]. 431. 26–432. 8. This citation says that in the book *On Mathematics,* right at the beginning of the argument, Archytas writes the following statements:

The mathematicians seem to me to have arrived at true knowledge, and it is not surprising that they rightly conceive the nature of each individual thing; for, having reached true knowledge about the nature of the universe as a whole, they were bound to see in its true light the nature of the parts as well. Thus they have handed down to us clear knowledge about the speed of the stars, and their risings and settings, and about geometry, arithmetic, and sphaerics,[23] and, not least, about music; for these studies appear to be sisters.

We believe that, as they must describe and predict several phenomena occurring in the physical world, engineers must master mathematics, as it is the only tool which allows humankind to "reach the true knowledge about the nature of the universe." Therefore, in their studies and in their education, mathematics must play a fundamental role. Indeed, in their speculations about the most suitable methods for educating young minds, our Greek ancestors arrived at the conclusion that mathematics has to be part of the education of every intellectual, independently of the future specialization which they may choose later in their studies. This thesis is shared by another giant of the Greek culture of the fourth century BC, who also can be considered an intellectual of Magna Graecia, as he spent many years in the most important cultural institutions of Magna Graecia. We cite here some excerpts from *The Republic* (*Πολιτεία, Politeia; Res Publica*) by Plato. The translation is ours, obtained by consulting and elaborating page 256 of [30].

[22] The reader will be astonished to discover that the very ancient words of an eminent intellectual of Magna Graecia needed to be repeated by some modern epigones. Indeed, he/she will find a pure rephrasing of what was said by Archytas in the beautiful divulgation essays by Barrow (see e.g. [29]).

[23] We prefer to use here the word "sphaerics" instead of "sphaeric," as in the Greek text there is an accusative plural. Heath in [Heath, Thomas. *A History of Greek Mathematics* 2 vols. (1921)] made it clear that in this context sphaerics has to be understood as "the geometry of the sphere considered solely with reference to the problem of accounting for the motions of the heavenly bodies."

There are things which excite the intelligence, while there are things which do not manage to do so . . . However, the logistikē and the arithmetics deal with numbers . . . and these things lead to the truth . . . and they will be, therefore, some disciplines which we desire [to educate the young minds]. Indeed, to the warriors it is needed to teach these things to allow them to become suitable to the military activities, while it is needed to teach them to the philosopher as he must understand the ontology of the reality, becoming able to distinguish the true essence of things from the contingent circumstances . . . Therefore, it will be convenient to impose the study of this discipline by establishing a law, and it is necessary to persuade those who will become in future the highest officers of the State [the Polis] to direct their studies towards the logistikē and to continue their studies . . . until they will arrive, by using the pure intellect, to the contemplation of the nature of the numbers, and they should not study it as it is done by the merchants . . . who are interested only in buying and selling . . . instead, they should study it to induce their mind to arrive from the contingent appearances to the truth and to the nature of the existence . . . And I want to talk about the discipline which is cultivated by the mathematicians and to argue that it is elevated and, in many aspects, useful for that which we want, under the condition that one is cultivating it to the aim of understanding and not for trafficking . . . Can you see, therefore, that such a discipline is for us most likely really necessary, as it appears the right tool for obliging the mind to make use of the pure intelligence to reach the pure truth? Moreover, have you already noticed that the persons who are by nature skilled for the logical calculations are born . . . to be capable in all intellectual disciplines and that also those persons whose mind is slower, when they are seriously educated and are exercising themselves in this discipline, all really do manage to progress to become more clever than they were before their education?

In our opinion the Greek word *logistikē* must be translated with the expression "mathematical logics" or simply with "mathematics."

4.5.4 The Shift in the Meaning of the Word "Mechanics"

We use in this subsection the corresponding entries from the Liddel-Scott *Lexicon* or the Chantraine *Dictionnaire*, which both represent invaluable sources of linguistic knowledge. We start from the Greek verb *Mechanàomai*, which has to be translated as "to realize by means of ingenuity." Then we have found, among many others, the entries:

- *Mechanè* which is any means or artificial tool or instrument which is used for doing something. In particular: an elevator, a crane, a system for mounting a bridge made of floating elements, pumps or any system for irrigating, hydraulic presses, war machines such as siege towers and ramrods, tools for theater representations, or any tool for personal or city protection;
- *Mechan'arios* = Engineer;
- *Ta mechanicà* = science of machines;
- *Mechanikòs* = that which uses or the person which uses ingenuity for solving problems;
- *Mechanourghìa* = the techniques for machine construction;
- *Mechànoma* = self-propelling crane.

A certain Anglo Saxon historiography (mainly, but not exclusively) managed to propagate the fable about a Greek culture inclined towards the theory, carefully avoiding practical applications. This historiography then claims that it was the Roman culture (as distinguished from the Greek culture) which, instead, cultivated the technological

practice. Such fables lead to the following questions immediately. Can the inventors of this legend explain why Greek culture, supposedly refraining from the practical applications of the theories which it formulated, invented such a wealth of technical words? Why did such a culture invent the Antikythera mechanism and so many other technological devices?

Probably, this legend was born because of a superficial understanding of the comedy *The Clouds* by Aristophanes. In it, by using an exuberant language and a witty satirization, this author describes the behavior of a leading contemporary figure: the natural philosopher or the mathematician. Such a figure is described as a permanently distracted person, completely dedicated to the development of his theories and completely incapable of organizing the minute details of their everyday life. In our hyper-technological lives, the stereotype corresponding to the mathematician is, very often, similar to the one described by Aristophanes. However, one should consider that, if Aristophanes needed to satirize mathematicians, it is likely due to the social importance which these intellectuals had managed to acquire in his society. In reality, practical capacity is always associated with theoretical knowledge. The theoretical vision of human knowledge, invented during (and peculiar to) the Hellenistic époque, allowed for the inventions of *ta mechanica*. This science, then, gave momentum to the *tèchne*, and allowed for the wonderful and surprising economical development of Hellenistic States. These states, once they were integrated into the Roman Empire, became its industrial driving force.

The Heron's Mechanics School[24] is described in the *Mechanics* by Pappus (see Papp. Coll. vui., Praef. 1-3, ed. Hultsch 1022. 3-1028. 3 as translated by Ivor Thomas) in a way which shows the modern relevance of the Hellenistic conception of applied sciences:

The science of mechanics, my dear Hermodorus, has many important uses in practical life, and is held by philosophers to be worthy of the highest esteem, and is zealously studied by mathematicians, because it takes almost first place in dealing with the nature of the material elements of the universe. For it deals generally with the stability and movement of bodies [about their centres of gravity], and their motions in space, inquiring not only into the causes of those that move in virtue of their nature, but forcibly transferring [others] from their own places in a motion contrary to their nature; and it contrives to do this by using theorems appropriate to the subject matter. The mechanicians of Heron's school say that mechanics can be divided into a theoretical and a manual part; the theoretical part is composed of geometry, arithmetic, astronomy and physics, the manual of work in metals, architecture, carpentering and painting and anything involving skill with the hands. The man who had been trained from his youth in the aforesaid sciences as well as practised in the aforesaid arts, and in addition has a versatile mind, would be, they say, the best architect and inventor of mechanical devices. But as it is impossible for the same person to familiarize himself with such mathematical studies and at the same time to learn the above-mentioned arts, they instruct a person wishing to undertake practical tasks in mechanics to use the resources given to him by actual experience in his special art. Of all the [mechanical] arts the most necessary for the purposes of practical life are: (1) that of the makers of mechanical powers they themselves being called mechanicians by the ancients –for they lift great weights by mechanical means to a height contrary to nature, moving them by a lesser force (2) that of the makers of engines of war, they also being called mechanicians– for they hurl to a great distance weapons made of stone and iron and such-like objects, by means of the instruments, known as catapults, constructed by them; (3) in addition, that of the men who are

[24] It is a late Hellenistic textbook listing, without many theoretical details, some technological solutions of use in engineering sciences.

properly called makers of engines –for by means of instruments for drawing water which they construct water is more easily raised from a great depth; (4) the ancients also describe as mechanicians the wonder-workers, of whom some work by means of pneumatics, as Heron in his Pneumatica, some by using strings and ropes, thinking to imitate the movements of living things, as Heron in his Automata and Balancings, some by means of floating bodies, as Archimedes in his book On Floating Bodies, or by using water to tell the time, as Heron in his Hydria, which appears to have affinities with the science of sun-dials; (5) they also describe as mechanicians the makers of spheres, who know how to make models of the heavens, using the uniform circular motion of water. Archimedes of Syracuse is acknowledged by some to have understood the cause and reason of all these arts; for he alone applied his versatile mind and inventive genius to all the purposes of ordinary life, as Geminus the mathematician says in his book On the Classification of Mathematics*. Carpus of Antioch says somewhere that Archimedes of Syracuse wrote only one book on mechanics, that on the construction of spheres, not regarding any other matters of this sort as worth describing.*[25] *Yet that remarkable man is universally honoured and held in esteem, so that his praises are still loudly sung by all men, but he himself on purpose took care to write as briefly as seemed possible on the most advanced parts of geometry and subjects connected with arithmetic; and he obviously had so much affection for these sciences that he allowed nothing extraneous to mingle with them. Carpus himself and certain others also applied geometry to some arts, and with reason; for geometry is in no way injured, but is capable of giving content to many arts by being associated with them, and, so far from being injured, it is obviously, while itself advancing those arts, appropriately honoured and adorned by them.*

We add here the comment added in footnote by Ivor Thomas, which shows how he would have agreed with the analysis presented in [1]:

With the great figure of Pappus, these selections illustrating the history of Greek mathematics may appropriately come to an end. Mathematical works continued to be written in Greek almost to the dawn of the Renaissance, and they serve to illustrate the continuity of Greek influence in the intellectual life of Europe. But, after Pappus, these works mainly take the form of comment on the classical treatises. Some, such as those of Proclus, Theon of Alexandria*, and Eutocius of Ascalon have often been cited already, and others have been mentioned in the notes.*

Leaving it to the reader to make appropriate comments on the words by Pappus, we state here that:

- The Hellenistic mechanics (in Greek ***Ta mechanicà*** is plural) in the mind of Pappus coincides with the modern engineering sciences.
- Mechanics, as the science of the motion of bodies, is the first physical theory which was shaped with a logical-deductive Euclidean form, and a rigorous presentation of mechanical theories is already present in the works of Archimedes.
- Because of the predictive use of mathematics, the mechanical theories have allowed for the design of many sophisticated devices since the Hellenistic époque, and have also served as the conceptual basis of a unifying description of the Universe.
- Hellenistic tradition arrived via Middle Ages comments to the Renaissance and later scientists, eventually leading to the Laplace Mechanicism. Leonardo da Vinci, a great admirer of Hellenistic science, writes in his comments that "Mechanics is the paradise of mathematical sciences."

[25] Note by the authors: also in the post Hellenistic science many scholars decided that only the books which they had in their hands could have existed!

Many new theories, technical innovations and machines have been invented since the Renaissance. To underline the originality with respect to what had been done by the ancients, and also for respecting the tradition which limited the range of applicability of the mechanical theories to specific fields, modern scientists have introduced new names for new parts of scientific knowledge. The name *mathematics* became dedicated to the study of logical structure of scientific theories, and the name *mechanics* was limited to a specific class of mathematical models. For instance, electromagnetism was born as a specific application of mechanics to the phenomena concerning light propagation but, after Maxwell, it became an independent discipline. New branches of engineering sciences were established: aeronautics, astronautics, informatics, telecommunication sciences, and so on. What was new, however, was only the object of their study, i.e. the phenomenology which they aimed at describing. The methods and the fundamental world-vision underlying their formulation remained Archimedean. The word "machine" has been limited to those technological apparatuses developed by using the "ancient" theories and their further developments. For Archimedes, a valve, a transistor, a telephone, or a television, would all be called a "machine," although the modern scientists may sometimes disagree with such a usage.

In the shift of meanings which has occurred more recently, a mechanician is a specialized worker capable of repairing cars or some complex devices whose mechanisms are "macroscopic," i.e. characterized by a length scale of some millimeters or tens of millimeters. However, when serious and highly novel ideas are introduced, the ancient noble meaning resurfaces: quantum mechanics is the conceptual theoretical basis for chemistry and electronics, structural mechanics is the theoretical basis of the technological solutions used, for instance, in civil and aeronautical engineering, fluid mechanics is the basis of hydraulics, relativistic mechanics produces a set of cosmological models, etc. Finally, in automation engineering, in computer science, or in the theory of computation, one finds concepts such as the Turing Machine or von Neumann Machine.

4.6 Materials or Metamaterials? A Dichotomy?

It is not true that mechanics is a discipline whose capacity to produce theoretical and technological innovation has been completely exhausted. Many new ideas, methods and technological applications are being discovered while still adhering to the original ancient Archimedean spirit.

Among many others, one can precisely locate a very topical frontier in contemporary research in mechanical sciences. Along this frontier many research groups fight their cultural battles and all together try to advance knowledge. The contemporary debate centers on which materials can be considered as "standard" and which as "exotic" and thus deserving of attention. The frontier, in this case, divides standard from exotic materials.[26] There is a general consensus about the existence of such a frontier. However

[26] In the title of this section the English word *dichotomy* is a so-called loan-translation of the Greek word διχοτομία (dichotomía), which means "dividing in two," from δίχα (dícha) "in two, asunder" and τομή (tomé) "a cutting, incision."

there are discordant opinions about where it has to be placed. It is indeed clear that to the words "standard" and "exotic" one can give several (and rather imprecise) meanings.

We remark explicitly here that a change of conceptual paradigm seems to be needed when confronting the problem of designing metamaterials. The difficulty seems to consist in understanding the difference between physical objects which already exist and those which can *logically* exist, but whose existence is, at the moment, purely *potential*. The philosophical implications of this difference are the subject of ancient doctrines, which are at the basis of the branch of philosophy called ontology.[27]

4.6.1 Models for Materials and Design of Metamaterials.

The endeavor needed to model the mechanical properties of ***an already existing material*** requires the capacity to invent the (somehow optimized) mathematical model which best describes its behavior. In this case the material (and its physical properties) may already be given, and the scientist must find a mathematical model which is both i) simple enough to produce solvable and computable[28] mathematical problems for predicting the behavior of the considered material and ii) complex enough to describe all phenomena of interest.

The interplay between the need to describe the widest possible set of phenomena and the need to have mathematical problems whose solution is computable is the essence of the optimization procedure to be solved in this modeling effort. It is essential to understand that the expression "already existing material" is sometimes replaced by the expression "a material which already exists 'in nature."' This second one is ambiguous: does stainless inoxidizable steel already exist in nature? Or is it, rather, the result of a technological process (and therefore artificial)? To be precise, stainless steel was invented, on the basis of the theory which we call chemistry (which at that time was clearly much different from our current understanding), to obtain a material which resists the oxidation processes. Therefore, it is the product of a theory and it is not "natural." i.e. existing independently of the action of humankind. On the other hand, stainless steel was not designed explicitly to show a precisely defined mechanical behavior and, therefore, the mechanical modeler must study it ***ex novo*** as a material which is existing and whose behavior is known, as it were a natural material.

On the contrary, the endeavor needed for ***designing a material whose mechanical properties are those desired for a specific application*** requires the invention of microstructures and compositions which, at a given macro-scale, show the demanded global behavior. The work of the scholar when confronting this second endeavor is rather different. Indeed, the role of mathematics is even more fundamental. One must start by specifying the desired mechanical behavior. This specification, because words in natural language have ambiguous meanings, is possible only by assigning ***the evolution equations which must govern the behavior of the material to be designed***. Then, one

[27] It can be defined as "the philosophical study of the nature of being, becoming, existence, or reality, as well as the basic categories of being and their relations." Parmenides is the Greek philosopher who is universally credited to be the founder of this study.

[28] Using the computation tools which are available when the modeling effort is performed.

must confront the problem of synthesis: that is the problem of designing a microstructure and composition which, at a well specified length scale, behaves in such a way that the equations chosen a priori are predictive. Finally, one has to establish the range of validity of the equations chosen a priori, i.e. the set of phenomenological conditions in which they are predictive.

Even if the change of paradigm is neither revolutionary nor completely new, as the challenge described has some precedents in engineering sciences, it requires remarkable changes in the both the theoretical and experimental methodologies. We simply remark here that, before the final prevalence of digital computer devices, analog circuits had to be synthesized to provide analog computers for calculating solutions of differential equations. The point of view to be used in the design of metamaterials is therefore the same as the one which was used in the design of analog computers. One of the most innovative designers of analog electric circuits has been Gabriel Kron (see [31, 32]), whose deep understanding of mathematical physics greatly contributed to many innovative technological advancements by General Electrics. Some novel multiphysics multiscale metamaterials have been designed and built directly using the results obtained by Kron, and the most modern piezoelectric transducers (see, e.g., [33–36]).

The nominalistic issues which we are facing here are perfectly analogous to those which were faced by Archytas when he decided to introduce the word "mechanics" for specifying a precise field of study. The reasons why we believe that all the previous considerations are important in the present context can be understood by examining the following questions. Is it meaningful and useful to introduce a new name (i.e. "metamaterial") for describing what we are studying? In what sense are the intellectual efforts needed to develop the theory which we present in this book different from the activity which produced all known innovations in mechanical and engineering sciences? The previous considerations may suggest that a novel name is needed. Indeed, a rather unusual logical procedure has to be followed in the present context. However, a truly perceptive reader may anticipate a need to specify at first the meaning of the word "material" and the difficulties involved in its definition. We believe that any responsible discussion of these fundamental questions would be remiss without a thorough discussion of the concept of "material" leaving it open to interpretation with a *vague* meaning. These considerations are present in all books of continuum mechanics, statistical mechanics and theory of materials. Their origin could be traced up to the ancient atomistic Epicurean theories formulated by Democritus. We leave the historical considerations to those who may be interested without further imposing upon the reader who has been patient with our many historical remarks.[29] Here we consider the following questions:

Can a complex mechanical system such as the one depicted in Fig. 4.2 (i.e. what we have called a pantograph microstructure with perfect pivots) be called a material? And if it can be called so, and therefore described by the mathematical models used for materials, when is such a description is appropriate?

[29] See https://plato.stanford.edu/entries/democritus/ ; https://plato.stanford.edu/entries/atomism-ancient/ https://plato.stanford.edu/entries/atomism-modern/ and https://plato.stanford.edu/entries/statphys-statmech/.

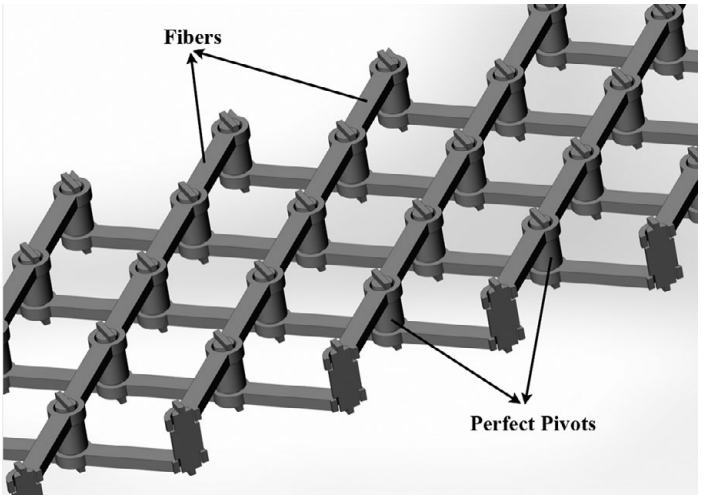

Figure 4.2 Pantographic fabric with perfect pivots.

The aforementioned system is characterized by at least two length scales. At the smallest scale it is constituted by matter spatially distributed in a precise and complex geometrical microstructure. This microstructure includes some gaps which divide different deformable microscopic parts to form nearly perfect pivots, with rotating parts. These pivots allow for (possibly!) very large and very localized relative rotations and displacements. This microstructure can be recognized to be (at least locally) what may be called, following an ancient nomenclature "a machine" or mechanisms. At the largest scale the whole system may appear as a "metamaterial" whose deformation energy may be independent of local displacement gradients and depend only on some second gradients of displacement. A further related question arises:

In what sense may "microscopic mechanisms" produce at macro-level a (meta)material?

A critical reader may maintain that, if, in the mechanical system which we are considering, one can find a material at all, one must find it only at a certain microscopic level. Such a point of view, in our opinion, is rather limiting.[30] The underlying idea supported by our critical reader would be that there is a preferred specific length-scale, and that the true nature of a material is evident only at that scale. This point is strictly linked with the atomistic vision of nature. The characteristic length scale at which a physical system behaves as a material is, in this vision, large enough to include many atoms but small enough to show homogeneous physical properties. Characteristic scales of more complex structures must be, as a consequence, larger than the scale at which we observe materials.

[30] It resembles somehow the Aristotelian assumption about the existence of a center of the Universe placed in the center of the Earth.

This vision, in our view, is rather crude and lacks imagination. It is also very close to the one accepted in the literature when introducing the concept of Cauchy continuum models for materials (see [20, 22, 23, 37]). Some materials may may be consistent with the just stated assumptions. However, a large class of materials and, in particular, the metamaterials which we have in mind are not. This is the reason why the models based on Cauchy continuum theory simply cannot supply the starting equations for designing truly exotic metamaterials. The designed metamaterials have to be modeled, at large scales, with more sophisticated continuum models. For example, a second gradient continuum can offer a suitable approach for the material system in our discussion given in Fig. 4.2.

In the case of this example such an assumption would imply that a material can be considered only at a length scale of a fraction of the dimensions of the depicted pivot. Note that this material system is obtained via laser sintering of polyamide powder during a 3D printing process. Therefore, an even more critical reader might argue that, simply by going down in scale (i.e. "zooming"), one can observe another microstructure. Such a microstructure would be constituted by the eventual partial fusion of the grains of polyamide used in the 3D printing process. These grains will be only partially melted and agglomerate into grain clusters. The process of production of the 3D printed specimens will, thus, lead to an overall material, which, although compositionally very similar (with some small variation in density), has mechanical properties which could be vastly different from those of the bulk form of the initial raw material that now exists at a lower scale. In different contexts and in different situations, these critical remarks have often been repeated to try to capture the ultimate nature of mechanical phenomena (see e.g. [23, 24] and Feynman's lecture notes in physics).

Therefore, we will abandon any attempt to define a specific length scale at which something can be called a "material." Instead, we will accept a "relativistic" point of view that emphasizes the "dual" nature of material-structure. We will conjecture that, at a given length scale, a mechanical system either is a material with some structure, or is a structure of elements constituted by some material. This is the reason why we have tried to be precise and decided, in the introduction, to specify the concept of locally "homogeneous material" by using a kind of "sampling window." By rephrasing the definition given there:

We say that a microscopically complex mechanical system can be modeled as a homogeneous material when one can find a length scale L such that, by moving a cubic volume whose sides are L, (i.e. a Representative Elementary Volume or, shortly, a REV) in the system, the overall (i.e. macro) mechanical properties of the part of the system included in the REV do not change, so that these properties can be described precisely enough in terms of overall (macro) kinematical descriptors, to be assumed as constant for every REV.

Going back to the 3D printed specimen described before we can remark that if one chooses a REV which includes a sufficiently large amount of grains, "printed polyamide" can be regarded as a homogeneous material of granular microstructure according to our previous characterization. Clearly, the printed polyamide is a different material if compared with the material constituting each polyamide grain used to form the powder placed in the chamber of 3D printers, before the printing process. Moreover,

if one were able to fully melt this powder, pour the obtained liquid in a mold, and use a specific cooling process to get a solid object, the obtained material would be yet a third one. Printed polyamide is constituted by bigger grains having larger size than the grains of polyamide powder. These larger grains incorporate smaller grains, partially melted, and fused together by fully melted polyamide powder. If, instead, one chooses the REV to have a size smaller than the size of the initial powder grain one may find a "fundamental polyamide," which has rather different mechanical properties when compared to "printed polyamide."

The characteristics of the pantographic sheet emerge at a larger length scale. In order to perceive its peculiar mechanical behavior one has to choose a REV including some pantographic cells (which in this case is composed of the primitive lattice square formed by the beams connected by pivots). The REV, so chosen, represents another macro material, although it is constituted, at a lower length scale, by a different material, i.e. printed polyamide, and, at an even smaller scale, by another one, i.e. "fundamental polyamide." One could indefinitely go to lower scales, considering molecules or atoms and so on to even smaller fundamental components of matter, or to larger scales, by considering materials constituted by variously interconnected pantographic sheets. We must, therefore, abandon any further analysis of the concept of material, invoking some of the fundamental philosophical ideas and investigations which guided the birth of Hellenistic science. We do not have the possibility to further investigate the ideas of Heraclitus and Democritus, or to see how Epicurus influenced modern scientists, or what was his influence on Boltzmann, and to finally analyze the influence of Truesdellism in the debate about the most fundamental nature of materials (however see for more details e.g. [20, 22]).

The discrete and continuum approaches offer two possible ways to describe the behavior of a physical entity. In some cases continuum models are to be preferred over the discrete ones in order to extract relevant information. In other circumstances discrete models, like Hencky type models for beams, are more suitable. Moreover, the first gradient Cauchy continuum model is not capable of describing the behavior of every material. For some phenomena and some materials generalized continuum models are needed. Consequently, in order to be able to design more general metamaterials, the conceptual straightjacket represented by Cauchy limiting assumptions must be removed. In fact, every conceptual straightjacket must be avoided by open-minded scientists. A wise mechanician must use the conceptual tools which, in a given moment and for a given class of problems, are more suitable.

4.6.2 A Tentative General Definition of Metamaterials

We shall now try to add further details to the considerations with which we started in the Introduction on the subject. In order to "go beyond" the concept of material, we have attempted, in the preceding section, to specify in as much detail as possible our understanding in this respect. Even if many weak points can be found in our arguments we believe that we have made our point clearly enough. On the other hand, it is unquestionable that in order to get a generalization of a concept one has to make it clear enough.

In this regard our hope is that we have managed to avoid those "Girandole di Parole"[31] harshly criticized by Galileo.

A definition of "metamaterial" can be obtained by reformulating the entry in Wikipedia (as read on Dec 6, 2017). Note that there is a tradition, in western science, to start every subject, may it be one of the exact or one of the human sciences, by some etymological notes about the origin of the words used in that subject and in particular about the name used for specifying the subject. We have paid our tribute to this tradition in Section 5, however, some other etymological notes are necessary.

To make the reading of these pages easier we repeat our definition here.

> Metamaterials – a combination of the Greek word μετά, meaning "beyond," and the late Latin word "materialis" (from Latin materia = "matter," from māter = "mother"), an adjective already used in Middle English in the sense of "relating to matter"– are materials engineered to have a property that is not found in nature. They are assemblies of multiple elements made up of materials such as metals or plastics. The constituting materials are *usually* [our italic] arranged in repeating patterns, at scales that are smaller than the wavelengths of the phenomena they influence. Metamaterials derive their properties not from the properties of the base materials, but from their newly designed structures.

We have repeated this definition because we believe that it manages to capture some important ideas and meanings. However, in order to critically review this definition we feel that some additional discussion is warranted.

First of all we do not agree with the use of the adverb "usually" (in italic in the text). It is a rhetorical artifice for hiding many concepts and situations. Metamaterials can be constituted by periodically repeated cells, or by microstructures which may vary in the passage from one cell to the closer ones. One can organize the microstructure of the mechanical system in several ways, by changing the geometry and the mechanical properties of the considered complex system more or less continuously from one microstructural cell to the others. One could even imagine some interactions between distant cells, without any specific periodicity. On the other hand the microstructure must, indeed, be present at a length scale lower than a chosen one and the microstructural patterns must be well-specified and very precisely determined.

Second we believe that the sentence "Metamaterials derive their properties not from the properties of the base materials, but from their newly designed structures." is misleading. The true concept of metamaterial cannot be limited to the systems in which the complexity at micro level concerns only the geometry of considered mechanical systems. There are metamaterials which exploit the use, at micro level, of many materials, having very high contrast in their mechanical properties. In other words one can get exotic materials by combining a clever geometry of mass distribution with another, equally clever, distribution of one of the several physical properties, as for instance, elastic stiffness.

Finally: the meaning of "…not found in nature" is vague and incomprehensible. Stainless steel, and even iron, cannot be unequivocally classified as natural materials.

[31] Girandole became an English word meaning: a rotating and radiating firework. In Italian Girandole is plural. Galileo says that some scholars use Girandole of words, i.e. marvelous constructions of meaningless statements, in order to astonish the reader and the audience.

Thousand of years of scientific and technological development preceded the invention and advent of such materials, which did NOT exist in nature in this form. Nobody finds a piece of steel or other similar materials in a mine, simply excavating some rocks. However we do not want to categorize these as "metamaterials." Our specific intention is to avoid calling materials "natural" simply because we have become familiar with their existence to the extent that it has been forgotten that they resulted from a series of serious theoretical and experimental efforts that led the scholars of previous generations to surprising results. We simply state that:

A "metamaterial" is a material which has been designed to meet a specific purpose governed by a desired specific behavior that is described by a given set of evolution equations.

A metamaterial is found by means of a synthesis process that can be divided into theoretical and technological parts. The synthesis proceeds by imagining a physical entity of complex geometrical structures formed of parts made from many fundamental materials (i.e. materials whose characteristic length scale is smaller than the length scale at which the metamaterial must be used). The introduced parts in this entity are joined using some suitable physical links in order to establish specific interactions between them.

In this context, the "microstructure" of the considered metamaterial is denoted by the set of shapes, geometric mass distribution, the distribution of physical properties and the conceived elementary interactions which we have thus established. The considered interactions may involve different physical phenomena. However, following a well-established tradition, we will call *mechanical metamaterials* those metamaterials where the interactions exploited at the length scale of the microstructure are purely mechanical. Of course if one considers length scales close to atomic dimension, all interactions are electromagnetic, or nuclear, or even more fundamental. We consider here as mechanical those interactions which can be described with classical kinetic and deformation energy at a given length scale.We explicitly remark here, as an example, that piezoelectromechanical beams, see [33–35], cannot be regarded as mechanical metamaterials according to our definition as, at the length scale of the designed microstructure, their behavior is determined by piezoelectric phenomena. Further it should be understood that we have systematically applied the term "micro" for the length scale where the exploited microstructure is designed to have all its physical inhomogeneity and where it shows in-full its complex behavior, and we have used the term "macro" for the length scale at which the designed system can be regarded as a homogeneous material.

It is remarkable that in the more interesting cases (see [38–41]), in which the macro metamaterial shows behaviors that are completely different when compared with the micro behavior of its constituent materials, the microstructure, typically, presents a marked contrast of mechanical and geometrical properties. In this regard, the "metamaterials" introduced in Fig. 4.2 are "extreme" in all aspects. These metamaterials consist of very thin (and soft) structural elements that are interconnected via (much) stiffer elements, and some other elements that have negligible stiffness (such as the perfect pivots that behave like hinges, i.e. do not resist the relative rotation of interconnected beams). Their geometry is also extremely inhomogeneous with empty spaces used to

partially separate the elastic response of interconnected elements (this is, for instance, the function of the perfect pivots).

We reassert that, in order to characterize the specific purpose of a new metamaterial to be invented, mathematics is needed. *Indeed, we can state that the only way to invent a metamaterial implies the choice of their governing evolution equations and the subsequent determination of the microstructure which, at macro level, is described by a given equation.* The problem just formulated is often called the ***problem of synthesis*** of a given set of evolution equations.

4.6.3 Some Basics of Ontology of Metamaterials: What Can Exist?

The problem which we want to discuss in this section has been so widely debated as to deserve a treatise (of several volumes) by itself. We will discuss here only the aspects of this debate which concern specifically the design of metamaterials. In particular, we will limit ourselves to a short discussion of some aspects of thermomechanical theories in which the ontological question, which we simply evoke here, has historically played a relevant role.

We consider first the controversy about the elastic constants for deformable bodies in small deformations. This controversy is based on the question: which kinds of homogeneous linear elastic body may exist? Or, once one has formulated a corresponding mathematical problem: how many independent elastic constants can be determined?

This is a typical ontological problem which Parmenides of Elea would have considered of major importance. Navier, Cauchy and Poisson[32] did formulate a discrete micro-theory[33] starting from the assumption that micro-particles were placed in the reference configuration in a regularly spaced lattice, and that their interactions occurred via a central force characterized by a unique elastic micro-constant. After a certain homogenization procedure they deduced, at macro-level, the constitutive equations of an isotropic material. Unfortunately, these equations did not manage to describe the mechanical behavior of all isotropic materials except those having Poisson ratio equal to 0.25.

It is somehow paradoxical that Poisson believed this elastic constant to attain a unique and well-defined value,[34] but this is not the case. Even more paradoxical is the circumstance that, recently, a lot of research, which increased the occurrence of the name "Poisson" in modern publications, has been dedicated to the synthesis of auxetic metamaterials, i.e. materials having negative Poisson ratio, whose existence was firmly denied by Poisson. In the theory and practice, auxetic metamaterials are of great importance. For this reason, we have chosen here to discuss the genesis of the related theoretical concepts.

[32] Our source here is the essay by Edoardo Benvenuto *et al.* [42].

[33] We refrain from describing here how Gabrio Piola (see [24]) underlined the weak points in their deductions. This will be the subject of future specific essays.

[34] A beautiful historical presentation of this subject is given in [43] where, however, both the contributions by Green and the role of the energetic principles is underestimated, while a definitely exaggerated role is attributed to "empirical knowledge."

When facing indisputable experimental evidence, Cauchy followers needed to try to adapt the theory to "preserve appearances" (see [17]). A controversy started about the way the theory could be adjusted. Indeed, many "epicycles" were added, until the Lagrangian School, using an evident "economy of thought" (see e.g. [44]), managed to find the solution. Green[35] solved the controversy by resorting to Lagrangian ideas and methods. He described the point of view expounded here in such a brilliant and effective way, that we prefer to cite him directly (see pp. 245–246 in [45]), as we expect that the reader will not be distracted by the accidental (and not relevant) reference to the theory of "luminiferous ether." Here are the exact words by Green:

M. Cauchy seems to have been the first who saw fully the utility of applying to the Theory of Light those formulae which represent the motions of a system of molecules acting on each other by mutually attractive and repulsive forces; sup- posing always that in the mutual action of any two particles, the particles may be regarded as points animated by forces directed along the right line which joins them. This last supposition, if applied to those compound particles, at least, which are separable by mechanical division, seems rather restrictive; as many phenomena, those of crystallization for instance, seem to indicate certain polarities in these particles. If, however, this were not the case, we are so perfectly ignorant of the mode of action of the elements of the luminiferous ether on each other, that it would seem a safer method to take some general physical principle as the basis of our reasoning, rather than assume certain modes of action, which, after all, may be widely different from the mechanism employed, by nature; more especially if this principle include in itself, as a particular case, those before used by M. Cauchy and others, and also lead to a much more simple process of calculation. The principle selected as the basis of the reasoning contained in the following paper is this: In whatever way the elements of any material system may act upon each other, if all the internal forces exerted be multiplied by the elements of their respective directions, the total sum for any assigned portion of the mass will always be the exact differential of some function. But, this function being known, we can immediately apply the general method given in the Mécanique Analytique, and which appears to be more especially applicable to problems that relate to the motions of systems composed of an immense number of particles mutually acting upon each other. One of the advantages of this method, of great importance, is, that we are necessarily led by the mere process of the calculation, and with little care on our part, to all the equations and conditions which are requisite and sufficient for the complete solution of any problem to which it may be applied.

One has to remark that Green was British, while Cauchy was French. It is therefore false that variational principles are preferred by the French School. Interestingly, perhaps in an ironical sense, Lagrange (Lagrangia) was Italian, born in Turin. Even if Green does not explicitly state that every Poisson ratio may actually be observed, by using the principle stated in the previous excerpt, i.e. by using the existence of a deformation energy function, and by assuming that it is definite positive, it is easy to prove that the Poisson ratio must vary between -1 and 0.5.

[35] Who is not afraid to declare to be a follower of Lagrange.

Many scientists did not believe that it was possible to observe a negative Poisson ratio, and they even tried to prove it. However, if the Poisson ratio is greater than -1, there is no "creation of energy" argument which is prohibiting it. And the modern theory of metamaterials and 3D printing technology has proved that, once more, something which is not prohibited by the conservation of energy can exist.

It has to be remarked that all the dispute about the Poisson ratio may seem to be a vain and purely abstract theoretical discussion, and that actually many "practical" scholars may have believed that it was a dispute very similar to the one concerning the "sex of the angels," which occupied many ancient theologians. We do not believe that this is the case as the theoretical controversy anticipated for many years the practical application of the corresponding technology. For instance, Goretex is a material having negative Poisson ratio, whose application in surgery has saved the lives of many children.[36] There is little doubt about the existence of a cause/effect relationship between the anticipation and the actual realization. Needless to say, the ontological problem asking:

What can exist?

and the related problem

What do we expect could be observed?

are too general to be studied using the scientific method. However, if we limit ourselves to a more particular problem:

What Poisson ratios can be observed?

then it is possible to build a robust theory (never falsified up to now) that can answer this question.

In thermodynamics and continuum mechanics, similar ontological problems have been formulated and discussed. A detailed historical presentation of the related ideas can be found in [20, 22] and an erudite, but greatly biased, collection of results in the field is given in [46] and [47]. While it is clear that in order to encompass heat transfer phenomena the principles of mechanics must be somehow enlarged, the effort by Coleman and Noll (see again [46]) to base mechanics on thermodynamical principles involving dissipation (or the absence of dissipation) may be criticized.[37]

Actually, the postulations of mechanics based on the choice of suitable balance laws require the introduction of suitable constitutive equations to formulate well-posed mathematical problems. The choice of such constitutive equations, as is usually done in incomplete mathematical theories, is assumed to be necessary after the observation of experimental evidence. From an epistemological point of view such a process too much resembles a form of inductivism to be completely acceptable. Moreover, clearly, not all the logically possible constitutive equations necessarily describe some observable phenomena. Therefore, following the ideas of Clausius and Duhem, the introduction of a criterion to determine whether this is the case or not, is required.

[36] see, e.g., https://www.goremedical.com/products/cardiovascularpatch.

[37] Gabrio Piola was among the earliest who maintained the point of view that a mechanical theory should be formulated without resorting to thermodynamics (see [24]).

Here the literature splits. On the one side there is the so-called continuum thermodynamics, whose biggest modern champion has been Truesdell. The mechanical balance laws are completed by a law of conservation of energy and the demand that entropy production is always positive. Only constitutive equations assuring this last condition are said to be physically admissible. The ontological implications of the entropy principle are therefore clear.

On the other side, it is possible to introduce, for purely mechanical phenomena, a Lagrangian postulation scheme which departs from the choices made by Truesdellians (see, e.g., the works of Toupin, Mindlin Sedov, Germain, Landau). The extended Hamilton–Rayleigh principle is assumed to be the basis of (possibly) dissipative mechanics, and a purely mechanical theory can be developed without explicit reference to any thermal phenomenon. In our opinion, the spirit of Green is closer to this last postulation choice and the one preferred in the present work. As a consequence in this book we have assumed that:

Given a certain set of Lagrangian kinematical descriptors (belonging to a finite or infinite dimensional space of configurations), a Lagrangian density function and a Rayleigh dissipation function, both positive definite in the velocity variables, it is possible to synthesize a (meta)material whose motion is governed by the corresponding extended Rayleigh–Hamilton principle.

The reader may wonder why such a conjecture is believed to be true. We remark that the stated conjecture is only a "working assumption," a "postulate," and represents a powerful tool of scientific investigation, even though one cannot exclude the possibility that it may be falsified in the future.

4.6.4 Same Name for Different Things or Different Names for the Same Thing?

Mathematics is the art of giving the same name to different things. Henry Poincaré in Science and Method.[38]

It has been claimed that the quote which starts this subsection was a response to this other quote: "Poetry is the art of giving different names to the same thing." Even if we cannot delve here into the investigations needed to distinguish between the different natures of the these activities of the human mind, that is mathematics and poetry, it is clear that the "economy of thought" evoked by Mach is a peculiar characteristic of any scientific intellectual activity. On the contrary, as formalized in his "*Satirical verses*" by Giambattista Marino:[39]

[38] The authors must thank Richard Toupin for having shared with the elder of them the considerations which are presented here.

[39] Giambattista Marino (sometimes called Giovan Battista Marini, 1569–1625) was a Neapolitan poet, most famous for his long epic L'Adone. For sure, Marino includes in his techniques "the art of giving different names to the same thing" for impressing the reader.
The Cambridge History of Italian Literature states the he is "one of the greatest Italian poets of all time." He founded the school of Marinism, also called "Secentismo" (i.e. the art of poetry of the seventeenth century) characterized by the "use of extravagant and excessive conceits." Marino's poetry, further magnifying the "artificiality of Mannerism," was based on a systematic construction of antitheses, on the use of a large range of complex wordplays, on exaggeratedly detailed and pompous descriptions and on a

È del poeta il fin la meraviglia…,

that is: "the aim of the poet is the marvel [of the reader]".[40] This belief is widespread in literary criticism. For instance, in [49] we find the statement:

> … given this freedom to manipulate the historical ***materia*** [in Italian in the text] the poet must fashion the imitation to delight the reader's intellect and to induce marvel, or ***meraviglia***. The features distinguishing poetry from history thus involve two basic criteria that seem mutually incompatible: verisimilitude and marvel.

In our opinion scientists should not pursue the search of marvel and should systematically call by the same name concepts which are coincident.

There are too many different "labels" used in modern theoretical and applied mechanics which are invented to characterize "novel" or "original" research fields or specialist disciplines[41] These labels are a kind of "flag" or a kind of "coat of arms"[42] used to distinguish one camp from another. Without the acceptance by the establishment (camp) owning the name, as if it were a trademark, one cannot claim to be an expert in a discipline. Many academic battles are fought to become the owners of such trademarks. In the introduction section whose title is *The importance of a universal terminology* we have listed some of the aforementioned coats of arms in the field of the theory of metamaterials and some related fields in experimental mechanics, having some relevance in technology. We could continue here by adding many other names and many other references. Clearly such an enlargement would be useless, as we believe that our point is already sufficiently clear.

The multiplication of labels is misleading, as the layman or the young scholar may believe that he is dealing with different research fields while they are in reality coincident. There are papers in which the only contribution consists in rephrasing some theories in a different language or in calling well-known objects by different names. Such social phenomena are omnipresent in the history of science and are likely to continue into the future. Often the only result which the aforementioned rephrasing process produces concerns the change of destination, from one research group to another, of some research grants. This is an unfortunate circumstance in the perspective of the advancement of science.

refined and elegant musicality of the verse, which seemed to be obtained after a long research work. His style enjoyed an immense success in the whole western culture.

[40] He continues by stating: "…parlo dell'eccellente e non del goffo, / chi non sa far stupir, vada alla striglia!" i.e. "…I am talking about the excellent [poet] and [I am not referring to the] vapid [one], / who knows not how to stupefy, let him go back to the stable and currycomb!" (the second part being taken from [48]).

[41] We claim that the theory of metamaterials is a part of theoretical and applied mechanics.

[42] The original meaning of the expression denoted the principal part of a system of hereditary symbols … used primarily to establish identity in battle. Subsequently the meaning of the word arms evolved and assumed the meaning of family descent, adoption, alliance, property ownership, and, eventually, profession. In modern science the name of a discipline professed is used to denote the group of allied researchers fighting, e.g. to get financial support from various financing entities.

4.6.5 Continuum Models versus Discrete Models for Metamaterial Design and Modeling

The ideas of continuum mechanics are used, in general, to model the deformation phenomena occurring in all types of physical entities. Naturally they are used frequently to describe the mechanical behavior of metamaterials. Following a tradition established in the first half of the nineteenth century (see [23, 24]), the macroscopic behaviour of metamaterials, consisting of mechanical systems at some microscopic length scale, are described with continuous models. However, we see no persuasive reason which may justify such an assumption, in the most general case.

Recently, the specific problem of the synthesis of (meta)materials having a deformation energy which depends only on second gradient of displacement has been, at first, attacked and theoretically shown to be resolvable by using homogenization methodologies. In [38] this has been done in the case where both at the micro and macro scales, the considered mechanical systems can be described by means of continuous models.

It should be noted explicitly that the problem of synthesizing a "second gradient" (meta)material, was not motivated initially by any technological demand. Instead the problem of determining if one can find a microstructure which is able to show at a certain macro level a second gradient behavior was purely a theoretical one. Although it is clear (see [50]) that strong motivations can be established from engineering applications for such intellectual efforts, the synthesis problem was initially formulated to face a theoretical challenge. The driving theoretical reason was that even the consistency of mathematical continuum models involving deformation energies depending on the second (and higher) gradient of displacements was continuously and everely questioned both from a physical and a mathematical point of view. Certain ambiguous statements in [51], suggested to some scholars that higher gradient models were not compatible with the second principle of thermodynamics. Many years later, Gurtin himself clearly dismissed such an interpretation of his results.[43]

In reality, the scientific controversy regarding the physical meaning and the logical status of higher gradient models is not at all modern. Gabrio Piola had already been criticized when he formulated his mathematical models for continuous materials by introducing deformation energies depending on higher gradients of displacement (it is further noteworthy that Piola had also formulated peridynamics in 1850, see [23]). Piola himself, in order to answer the attacks on the soundness of his continuum models and the true physical content of his theories, decided to resort to the study of a homogenization problem, exactly as done more recently for instance in [38] or [53]. Indeed, Piola could prove the existence of mechanical systems which had to be modeled with his more complex mathematical theories by using a micro–macro identification and homogenization process. This process was based on the following steps:

[43] In [52] one finds the words "In two monumental works, Toupin [a and b, see below] derived general balance equations and associated traction boundary conditions for an elastic body whose strain energy depends on first and second gradients of the deformation," where the references are a. Toupin R.A. (1962). Elastic materials with couple-stresses. *Arch. Ration. Mech. Anal.* 11:385–414 and b. Toupin R.A. (1964). Theory of elasticity with couple-stresses. *Arch. Ration. Mech. Anal.* 17:85–112.

i) the introduction of a discrete model for a microscopic mechanical system characterized by simply interacting particles distributed, in the reference configuration, on a geometric lattice;
ii) the description of the microscopic system of particles by means of a finite dimensional model, characterized by a finite set of Lagrange parameters and an action functional;
iii) the formulation of the principle of virtual work at micro-level;
iv) the introduction of a macro–micro kinematical correspondence (via what we can call Piola's Ansatz) and the subsequent formulation of the principle of virtual work at the macroscopic level in terms of macroscopic kinematical descriptors and microscopic constitutive equations;
v) the determination of macroscopic constitutive equations by assuming that the microscopic and macroscopic virtual works are quantitatively equal.

To our knowledge, Piola supplies one of the first homogenization procedures, and possibly the first formulation of macroscopic higher gradient continuum models, found by assuming that inter-particle interactions at the micro-level have a short range. The postulation of the theories of higher gradient continua, as formulated by Piola starting from the principle of virtual work, generalizes the postulation preferred by Cauchy and all of his epigones. The postulation based on the principle of virtual work is mathematically more sophisticated and complex, and this circumstance gained many opponents to the point of view championed by Piola. Such a circumstance is not completely surprising as one should expect to formulate more complicated models for more complicated mechanical systems. However, Cauchy continua became the preferred model in engineering sciences. Their application to a very large class of phenomena and materials allowed for surprisingly quick and really relevant advancements in many technological problems. Moreover they allowed for the clear understanding of many important mechanical phenomena. In a sense, engineering sciences have been hostage of the great success of Cauchy continua. Indeed too many scholars, notwithstanding the early warnings formulated by Piola, finally started to believe that they represent, for deformable systems, the most general model which one can possibly formulate.

In our opinion, instead, it is very important to try to solve the following class of problems (see [25, 40]:

Given a macroscopic length scale, a set of kinematical macroscopic descriptors, a deformation energy functional and a Rayleigh dissipation functional, to find one or more microscopic length scales, a set of microscopic materials and suitable microstructures such that the complex microscopic system behaves at macro-level as specified by the given macroscopic functionals.

Based upon the ontological considerations developed in the previous subsections, we deem that such a class of problems can be solved, and that indeed such complex mechanical systems truly exist.

The particular problem of the synthesis of second gradient materials has been solved by using architectured microstructures. The proposed synthesis problem was proven to have a solution by using a "double scale" or "two steps" homogenization process in [53, 54]. The strategy chosen in these papers is the following: at first,

"slender" continua are considered to give, after a first homogenization process, some beam elements; in a second step, the beams are interconnected by ideal pivots and, subsequently, a second homogenization process is performed, finally proving that at the chosen length scale the designed mechanical system really behaves as a second gradient material.

In the aforementioned papers, the synthesis process described is simply conceived at a conceptual level, while in, e.g., [50] it is proven that using 3D printing it is possible to practically realize such structures. When considering a lattice of beams as a basic microstructure, the ideal pivots appear to represent a preferred or, even, an essential class of constraints for the synthesis of second gradient macroscopic continua. In this context, it is remarkable that the homogenized macro equations obtained (see [39]) present some apparent mathematical pathologies. To be precise, certain well-posedness results cannot be immediately proven for the second gradient equilibrium equations obtained. Some nontrivial elaborations of available mathematical results are needed to extend even the existence and uniqueness results for equilibrium configurations in linearized regimes. These mathematical aspects of the formulated models reflect the behavior peculiarities of the metamaterials considered.[44]

In order to investigate experimentally the behavior of perfect pivots as constraints occurring in synthesized microstructures, one has to face the following technological problem [56]:

Is it possible to find innovative design strategies and some related production process which allow for the construction, with additive manufacturing, of the conceptually conceived pantographic sheets, whose pivots can be twisted without storing any relevant deformation energy and with negligible dissipation?

Fortunately, it was possible to find a design and realization strategy which allowed for the printing of such constructs as monolithic specimens. The realization procedure was such that no post-assembly is required to have a functioning specimen.

The driving motivations to construct and study pantographic sheets with perfect pivots were the purely theoretical problems and demands concerning continuum models (i.e. the relationships between microscopic and macroscopic models, their logical consistency and their predictive capacity). Quite unsurprisingly, however, useful byproducts of interesting microstructures which are very promising for engineering applications were obtained (see, e.g., [50, 57, 59, 60]).

In order to design engineering devices by applying the so found generalized continuum models, one has to predict and control the behavior of the novel metamaterials. To this aim, it is necessary to solve, in general, the complex nonlinear equilibrium or dynamical problems. This can be done by using suitable and sophisticated numerical methods. In this context, ***we have remarked the existence of a vicious circle*** when deducing and using continuum models. Indeed, we observe that:

[44] On the other hand, the mathematical (apparent pathologies) mentioned possibly may have great interest of their own. Indeed, the theoretical problems to be solved for overcoming them are a beautiful conceptual challenge, but also may disclose new phenomena of relevance in the applications.

- The mechanical behavior of metamaterial microstructures in many cases is more readily described by postulating finite dimensional Lagrangian models, and, if necessary, by considering a Rayleigh potential together with the Lagrangian, in order to account for dissipation phenomena. This was the point of view adopted by Piola (see [24]).
- The Euler–Lagrange equations obtained by imposing the stationarity of action, eventually modified by introducing a Rayleigh potential, may supply a system of ordinary differential equations. These equations are, in general, nonlinear and possibly involve as many unknown functions as Lagrangian parameters. This means that, without powerful numerical computation tools, discrete Lagrangian models do not supply a viable method for obtaining predictions.
- Piola (and his contemporaries), in order to get some predictions suitable for some well-specified engineering problems, introduced homogenization procedures leading to continuous models. These models could be studied by the methods of classical mathematical analysis. In other words, Piola transformed the Euler–Lagrange equations deriving from the stationarity of an action functional for a finite dimensional system into partial differential equations (see [25]). It is noteworthy that the homogenized continuum models have a range of applicability which is restricted by the finite size of the primitive cell constituting the microstructure.
- The theory of partial differential equations could, in many cases, present much greater mathematical difficulties than the theory of ordinary differential equations.[45] Therefore, the homogenization process is useful only in those cases of designed metamaterials in which the obtained reduction of the number of unknown functions compensates the increase of difficulty in the solution of the resulting partial differential equations. This last circumstance happens, for instance, when semi-inverse methods à la De Saint-Venant or the method of separation of variables are applicable.
- Finally, in order to get predictions by means of continuous models, discretization methods are necessarily introduced, using, for instance, finite differences or finite element methods.

The above points indicate the possibility that a vicious circle may appear in many of the investigations presented in the recent mechanical literature. Indeed, one could question the necessity of introducing the described intermediate step involving homogenization. As the intermediate continuum model is to be subsequently discretized in any case, one could decide to apply numerical methods directly to the initial discrete model. Moreover, this initial model is usually formulated on the basis of a mechanical understanding of the considered system, while in the discretization of the continuum model one is usually driven only by the considerations of computational nature. In

[45] There exists an existence and uniqueness theorem for Lipschitz continuous explicit systems of ordinary differential equations, while Hadamard has shown that such a general theorem is far from being formulated for partial differential equations. Therefore, in general, the second equations are "more difficult" to solve than the first.

the cases in which an initial discrete model has been inferred, it is unclear why it should be convenient to first homogenize (to find a continuum model) and then, again, to discretize the continuum model, losing in this last step all of the presumed phenomenological understanding of the first step. We suspect that Lagrange and Piola were aware of the central role of continuum models in mechanics. It is quite likely that they considered continuum models simply as a useful calculation tool, but there is a need for a detailed exegesis of their published works to confirm this suspicion. We believe that this Gordian Knot must eventually be cut. This can be done by simply refraining from the introduction of any continuum model to describe metamaterials. For this reason, we have described the general method of discrete Lagrangian modeling in a separate chapter and we have shown how pantographic sheets can be described by using such a method. Moreover, we have also shown how discrete models and the discretization of homogenized continua may produce exactly the same predictions.

4.6.6 Therefore: Why Discrete Models?

Continuous models were introduced at the beginning of the nineteenth century probably as a "computational tool." Indeed, discrete, atomistic models which, by the way, were believed then to be more physically meaningful, presented formidable mathematical problems. They required the solution of systems of ODEs having many (too many) unknown functions or the determination of equilibria attained in configurations characterized by the same amount of unknown parameters.

Homogenization and the solution of PDEs seemed, at the époque, the most powerful way for applying mathematical analysis. Modern engineering sciences started successfully, in this way, to produce valuable predictive tools for technological applications. However, soon, the closed form methods of solutions started to show some limits in their range of applicability. Even if the Soviet school (see, e.g., [61]) did manage to push beyond any imaginable limit the power of the analytical techniques and could find beautiful solutions to very interesting problems, continuum models, without the support of powerful numerical computing machines, were unable to continue supporting the technological innovations already developed at the beginning of the second half of the twentieth century. Discretization of continuum models then became necessary, especially for solving nonlinear problems.

This endeavor, and the related issue of finding the correct mathematical formulation for existence and (eventually) uniqueness problems, required the development of sophisticated mathematical theories. Again, the Soviet school contributed greatly. Sobolev spaces theory supplied the required strong foundation for both theoretical and numerical investigations. Functional analysis showed immediately that infinite dimensional configuration spaces hide very complex structures and, sometimes, very pathological mathematical phenomena.

Some scholars have therefore decided to avoid having to face the pathologies exhibited by continuous models, which do not seem to be always physically meaningful, or whose possible phenomenological relevance needs deeper investigation. Hence, they

have tried to bypass the formulation of continuum models: it was preferred to conceive discrete Lagrangian models directly, even for the most complex mechanical systems. In doing so, the discrete models directly reflect the most relevant mechanical properties to be modeled (see [62–68]).

Accepting this point of view, one can avoid considering all the mathematically difficult problems concerning the well-posedness of boundary value problems for nonlinear PDEs. The existence of functions like Cantor Devil's staircase (which is uniformly continuous but not absolutely continuous, and is strictly increasing but has almost everywhere zero derivative) introduces, in continuum models, some mathematical entities whose mechanical counterpart is not always evident, and in some cases impossible to find.

The theory of discrete Lagrangian systems, on the other hand, supplies problems whose well-posedness is assured by relatively simple existence and uniqueness theorems such as, for instance, the existence and uniqueness theorem valid for Lipschitzian ODEs (Picard–Lindelöf theorem), or the more general existence theorems due to Peano or Carathéodory. Therefore, the modeler, after having chosen the family of mechanical systems he/she wants to describe, can begin his/her analysis by introducing the finite set of Lagrangian parameters whose determination seems sufficient to specify, in a satisfactory way, the state of the considered system.

Describing, for example, the case of pantographic sheets with perfect pivots, this set of parameters must include (but in general may not be exhausted by) the positions of the pivots interconnecting the two families of fibers (see Fig. 4.2). Such a choice is sufficient to describe the deformation state of the sheet, if one can assume that the said pivots move in such a way that the pair of beams they are interconnecting always remain at a fixed distance. On the other hand, when the said pair of beams have a separation which varies in the deformation process, it may be necessary to introduce (see the treatment proposed in [59]) a richer set of Lagrange parameters. In the case of perfect pivots, only the beam segments interconnecting the pivots are storing deformation energy, and they will be modeled by introducing suitable expressions for elastic energies and stiffnesses. It can be observed that to describe the deformation energy of the said segments, further deformation mechanisms (not accounted for in [41]) and kinematical descriptors are needed.

Therefore, the discrete Piola–Hencky model previously considered can be improved by adding additional degrees of freedom, i.e. by considering the positions of points interconnecting two beam subsegments (between adjacent pivots). Once a mechanical understanding of this choice of Lagrangian parameters is attained, one can recognize that: i) the pivots are where the interactions between pairs of fibers can be localized; ii) the extra bending energy relative to each family of fibers can be localized in the points interconnecting two beam subsegments. In the most general Lagrangian discrete model, the complete set of kinematical parameters includes also the positions of these newly introduced intermediate points, those whose displacement describes the bending deformation of the fibers between two interconnecting pivots. Once the set of Lagrange parameters is found and the kinetic and potential energies of the systems are

conjectured by introducing suitable Lagrangian functions, then the problem of determining the motion (or the equilibrium configurations) reduces to the integration of a set of ODEs, for which a complete (and numerically implementable) theory exists (and is well established).

In this way, the problem of predicting the behavior of the considered mechanical system is reduced to the choice of an efficient step-wise procedure for the determination of stable equilibrium points. Very efficient methods, that are also applicable to the case of nonlinear problems, proceed by finding equilibrium configurations depending on a "load" parameter appearing in the Lagrangian, or constraining the Lagrange coordinates. For certain specific values of the load parameter, it is often possible to find the equilibrium configurations easily. Then, by slowly varying the load parameter and by using linearizations with respect to this parameter, one numerically constructs, in a reliable way, a whole family of equilibrium configurations for the corresponding family of nonlinear problems. The reason why the aforementioned modeling procedure is successful can be easily explained. Indeed, the numerical codes so conceived apply to a discrete model, which is directly inspired by the mechanical understanding of the deformation mechanism of the systems under study. In these cases, there is no need to develop complex constructions and to apply advanced mathematical theories aimed at developing efficient discretization procedures of (mathematically) very rich continuum models.

To summarize, we observe that when homogenized continuum models are introduced, the space of configurations is very rich, and includes some configurations which it is quite likely will not be observed. This not-always-useful richness and complexity encumbers the mathematical modeling and the search for the solutions to the corresponding problems. A non-necessarily-complex model must be simplified to exclude "non-physical" solutions with a similarly complex mathematical effort (i.e. the formulation of the right finite element code). Starting directly from a judicious discrete model leads us to bypass problems which are "useless" in a specific modeling context. In choosing discrete models, we can often use robust and efficient numerical algorithms. Such algorithms can be used for finding motion or equilibrium configurations of a system as subroutines in complicated structural optimization procedures, which are paramount in metamaterials design.

We have given here a tangible example of a "theory driven" study for complex phenomenologies, i.e. the phenomenologies of "to-be-invented" metamaterials, a field in which some (ancient) ontological problems have a relevant technological impact. We are aware that structural optimization procedures are relevant in the process of designing metamaterials. We believe that logically rigorous methods, based on a theoretically founded procedure, are the only ones which may lead to technologically important results.

Therefore, we deem that studies based on purely "data-driven" approaches will always require an untreatable and probably useless amount of computing. Indeed, in our opinion, when an effective artificial intelligence is conceived, it will have to use as its basis an extremely advanced version of "theory-driven" metamaterial design.

4.7 Data-Driven or Theory-Driven? Final Epistemological Reflections Motivated by the Desire to Design Novel Metamaterials

There are scholars who use an "extravagant" way for designing metamaterials. They use their artistic inspiration, similitude considerations and "physical" intuition[46] to "print" microstructures. This is nowadays very easy as, by using simple software to draw a geometrical figure, it is possible to have constructed, via a 3D printer, very complex specimens. The deep scientific understanding needed to design a 3D printer and the profound mastering of the logical structures of programming languages needed to drive it can be ignored by the final user of this technology. Thus, such a final user may believe that a 3D printer emerged as the final product of a test-and-trial process. Therefore, this user continues their researches on metamaterials following the same attitude.

It is not uncommon that a previous deep scientific knowledge is used in a naive and non-systematic way to try to advance knowledge. A paradigmatic example, in the history of science, is given by the Architecture School started by Vitruvius. His poor understanding of scientific theories is described carefully in [1]. Vitruvius simply transmitted to Roman culture some "rules" of practical use in engineering, without framing them into well-posed and complete theories.[47] However, his treatise managed to give momentum to the technological development of Rome.

Those scholars in metamaterial design, who follow the tenets of Vitruvius, write papers showing beautiful images of 3D printed specimens, and then discuss informally the properties of what has been printed. The need for introducing a mathematical model is understood only by a few. However, the belief that the only available theory is 3D Cauchy continuum mechanics, as the accepted text by Truesdell states, remains rather prevalent. Consequently, the mathematical models introduced by these scholars remain too inhibited to be predictive. As it is believed that the most general possible mathematical model has been used, very often, ambiguous conclusions and statements are made implying that the findings of these works are too advanced to be mathematically described.

In a sense, there are scholars who generate certain microstructures, more or less randomly, and then try to verify ***a posteriori*** if the built physical object has some interesting properties. Such scholars believe in the heroic vision of scientific progress. Their approach clearly clash with the methodology expounded by Archimedes in his *On the Method*. Techniques based upon the random generation of a huge amount of microstructures and their subsequent analysis via some "data-driven" theory are indeed a more modern evolution of the heroic vision of science. The saving role of the geniuses'

[46] We have often heard talk of physical intuition. However, what it is or what is its nature, we have been unable to understand.

[47] However, it is possible to state that Vitruvius was aware, by looking at the available sources, of the importance of a theory. Indeed, he writes that: "Wherefore the mere practical architect is not able to assign sufficient reasons for the forms he adopts; and the theoretic architect also fails, grasping the shadow instead of the substance. He who is theoretic as well as practical, is therefore doubly armed; able not only to prove the propriety of his design, but equally so to carry it into execution." (LacusCurtius, Vitruvius: On Architecture, Book I. Retrieved 25 March 2018 at http://penelope.uchicago.edu/Thayer/E/Roman/Texts/Vitruvius/home.html).

intuition, which is claimed to have allowed for the advancement of science in the past, is nowadays assigned to the calculation power of modern computers. Unfortunately, research in artificial intelligence, a serious and promising branch of Archimedean science, has not yet reached the level needed to replace human scientific elaboration of theories for modeling phenomena.[48]

On the other hand, some lessons from computer-aided manufacturing and the systematic study of the theory of elasticity must be accepted. The pioneering work by Milton and Cherkaev gave a theoretical frame in 1995 for the realizability of some metamaterials [70]. Only in 2012, being guided by the theoretical understanding gained by the previously obtained mathematical results, some very interesting physical objects were actually built by using 3D printing technology [71].

In the last few years a wide discussion has been opened on the possibility of deriving valuable knowledge by simply using "smart" algorithms capable of extracting the relevant correlations from large bases of raw data. The importance of a robust theoretical approach has therefore been questioned in those fields that are collected under the common label of "Big Data" research. However, when discussing in detail the methods used in this Big Data research one almost immediately discovers that data are always organized by means of some a priori assumptions, which are too often very simple and, sometimes, even naive. Indeed, some parameterized functional relationships are postulated a priori and the needed parameters are calculated with varying degrees of sophisticated interpolation techniques starting from raw data. Such an approach essentially coincides with naive inductivism and has been definitively rejected by modern epistemology (see again [17]).

Of course, computer-aided manufacturing techniques can easily furnish very large sets of raw data which one may consider treating with the aforementioned methods. However, in this book, we provide and discuss examples showing that such an approach is superficial and has a very limited, or even totally no, prediction power. In particular, in nonlinear elasticity there are interesting equilibrium configurations much more easily envisaged by means of geometrical reasoning and suitable methods of calculus of variations than by means of the blind analysis of enormous databases, either of a numerical or experimental kind (see [72]). With the examples discussed in this book we hope to contribute to the debate about the viability of "data-based" approaches, suggesting that their *in vogue* position which is privileging them leads to misjudgment of scientific results and, often, to application of improperly and ill-derived conclusions. In the theory of the synthesis of metamaterials, we look for physical systems whose phenomenology is described by the equations which we have chosen "a priori." We are certain that, once more, the ancient and powerful vision presented by Archimedes of Syracuse, and developed in more recent times by Popper and Kuhn, will be the lodestar in our scientific

[48] The oldest author of this chapter heard from one of his most prestigious professors the following statement in 1984: "It is impossible that a computer will manage to win a chess game against a human player, as the computer needed to perform this task should be bigger than the solar system." In 1996 Deep Blue won a chess match against Kasparov. This result has been questioned but in 2006 a match between Deep Fritz and the world chess champion Vladimir Kramnik dissipated every doubt. In less than 20 years, the prophecy of a wise and reputed scholar has been disproved. Therefore, we will not try to forecast when artificial intelligence will be able to replace the human mind in formulating mathematical models.

understanding of reality, and will propel us towards the bleeding-edge of technological progress.

Serious scientific or technological problems cannot be solved with purely "data-driven" methods. Therefore, we do not believe that by simply elaborating a great amount of data one can solve the problem of the synthesis of useful metamaterials. It is unlikely that useful metamaterial will be found by randomly choosing microstructures and then checking the behaviors of the so-chosen microstructures. Moreover, no blind elaboration of data will lead to reasonable results in a reasonable time span. Data must be elaborated by an intelligence. It is unimportant that the form is human or artificial, but a form of intelligence is needed.

In the design of metamaterials, "theory-driven" analysis may lead to an effective understanding and mastering of technological applications. In this specific context, the change of scientific paradigm needed to efficiently design metamaterials is clearly incompatible with a vision which regards science as an activity based upon the barbaric gathering, not driven by any rationale and not organized with logical tools, of data which have to be merely treated numerically. To describe the process of the birth of a star, the seismic response of a complex structure or the design process of a resilient structure ready to resist strong seismic actions, or to synthesize a novel metamaterial are all research activities which must be guided by an Archimedean epistemological vision.

One must start with a theory, i.e. a logically consistent series of conjectures (otherwise called postulates), and by using this theory one must get predictions to be verified by experimental evidence.

Data must be organized by means of a theory, but they can never produce a theory by mere induction. Naive inductivism must be replaced by a sophisticated form of falsificationism. In his *On the Method*, which we have cited several times, Archimedes had already suggested such a methodology to us in the third century BC, and we do not yet see any reason for changing it.

Bibliography

[1] L. Russo. *The Forgotten Revolution: How Science Was Born in 300 BC and Why It Had to Be Reborn*. Springer Science & Business Media, 2013.

[2] J. Dryden. *The Georgics*. Mid Northumberland Arts Group, 1981.

[3] G. Colonnetti. *Scienza delle costruzioni*. Manuali Einaudi. Ser. di ingegneria. Edizioni scientifiche Einaudi, 1941.

[4] R. Baldacci. *Scienza delle costruzioni*. Number v. 1 in Varia. Architettura. UTET, 1984.

[5] Paul Germain. Cours de mécanique des milieux continus. Tome i, Théorie Générale. Masson et Cie, Editeurs, Paris, 1973.

[6] J. Salençon. *Mécanique des continus. Tome I: Concepts généraux*. AUF, Ellipses, 1995.

[7] R. Aris. *Mathematical Modelling Techniques*. Dover Books on Computer Science Series. Dover Publications, 1978.

[8] Open University (Milton Keynes). *Pensare per modelli: schemi logici e strumenti di calcolo*. Tascabili delle edizioni scientifiche e tecniche. A. Mondadori, 1979.

[9] Open University. Faculty of Technology. *The Man-made World: Technology Foundation Course*. Open University Educational Enterprises, 1972.

[10] Open University. *Introduzione all'analisi e all'algebra*. Biblioteca della EST. Mondadori, 1979.

[11] C.B. Boyer. *Storia della matematica*. Studio. Mondadori, 1987.

[12] L. Russo. *La rivoluzione dimenticata: il pensiero scientifico greco e la scienza moderna*. Saggi universale economica Feltrinelli. Feltrinelli, 2001.

[13] R.P. Feynman, R.B. Leighton, M. Sands, and S. Franchetti. *La fisica di Feynman. Ediz. italiana e inglese*. Number v. 2 in La fisica di Feynman. Ediz. italiana e inglese. Zanichelli, 2007.

[14] A.F. Chalmers. *Che cos'é questa scienza: la natura e i suoi metodi*. Mondadori, 1979.

[15] Kyle Stanford. Underdetermination of scientific theory. In Edward N. Zalta, editor, *The Stanford Encyclopedia of Philosophy*. Metaphysics Research Lab, Stanford University, winter 2017 edition, 2017.

[16] Thomas Bonk. *Underdetermination: An essay on evidence and the limits of natural knowledge*, Volume 261. Springer, 2008.

[17] Pierre Maurice Marie Duhem. *Sauver les apparences: essai sur la notion de théorie physique, de Platon à Galilée*. Vrin, 2004.

[18] Alfred Tarski and Jan Tarski. *Introduction to Logic and to the Methodology of the Deductive Sciences*. Number 24. Oxford University Press on Demand, 1994.

[19] T.L. Heath. *The Works of Archimedes, in English, translated and annotated by T.L. Heath, 1897, with a supplement "The Method of Archimedes," discovered by Heiberg*. Cambridge University Press, 1912, reissued by Dover Publications, New York, 2002.

[20] S. R. Eugster and F. dell'Isola. Exegesis of the introduction and Sect. I from fundamentals of the mechanics of continua, by E. Hellinger. *Z Angew Math Mech (in press). doi*, 10.

[21] Francesco dell'Isola, Alessandro Della Corte, Raffaele Esposito, and Lucio Russo. Some cases of unrecognized transmission of scientific knowledge: From antiquity to Gabrio Piola's peridynamics and generalized continuum theories. In *Generalized Continua as Models for Classical and Advanced Materials*, pages 77–128. Springer, 2016.

[22] Simon R Eugster *et al.* Exegesis of Sect. ii and iii. a from "Fundamentals of the Mechanics of Continua" by E. Hellinger. *ZAMM-Journal of Applied Mathematics and Mechanics/Zeitschrift für Angewandte Mathematik und Mechanik*, 98(1):31–68, 2018.

[23] Francesco dell'Isola, Ugo Andreaus, and Luca Placidi. At the origins and in the vanguard of peridynamics, non-local and higher-gradient continuum mechanics: An underestimated and still topical contribution of Gabrio Piola. *Mathematics and Mechanics of Solids*, 20(8):887–928, 2015.

[24] Francesco dell'Isola, Giulio Maier, Umberto Perego, *et al. The Complete Works of Gabrio Piola*: Volume i. Cham, Switzerland: Springer, 2014.

[25] Francesco dell'Isola and Luca Placidi. Variational principles are a powerful tool also for formulating field theories. In *Variational Models and Methods in Solid and Fluid Mechanics*, pages 1–15. Springer, 2011.

[26] Paul Germain. Functional concepts in continuum mechanics. *Meccanica*, 33(5):433–444, 1998.

[27] Ivor Thomas. *Greek Mathematics*, Volume i, Loeb Classical Library, no. 362, 1991.

[28] Pierre Chantraine, Jean Taillardat, Olivier Masson, *et al.* Dictionnaire étymologique de la langue grecque: histoire des mots. 1968. Nouv. Ed., Klincksieck, Paris, 2009.

[29] John D Barrow. The mathematical universe. *World and I Magazine*, (May), 1989.

[30] La Repubblica/Platone., Trad. di Francesco Gabrieli. BUR, Milano, 1994.

[31] Gabriel Kron. Equivalent circuit of the field equations of Maxwell-I. *Proceedings of the IRE*, 32(5):289–299, 1944.

[32] Gabriel Kron. A set of principles to interconnect the solutions of physical systems. *Journal of Applied Physics*, 24(8):965–980, 1953.

[33] Hui Shen, Jinhao Qiu, Hongli Ji, *et al.* A low-power circuit for piezoelectric vibration control by synchronized switching on voltage sources. *Sensors and Actuators A: Physical*, 161(1-2):245–255, 2010.

[34] Ivan Giorgio, Antonio Culla, and Dionisio Del Vescovo. Multimode vibration control using several piezoelectric transducers shunted with a multiterminal network. *Archive of Applied Mechanics*, 79(9):859, 2009.

[35] Ivan Giorgio, Luca Galantucci, Alessandro Della Corte, and Dionisio Del Vescovo. Piezo-electromechanical smart materials with distributed arrays of piezoelectric transducers: Current and upcoming applications. *International Journal of Applied Electromagnetics and Mechanics*, 47(4):1051–1084, 2015.

[36] Maurizio Porfiri, E Santini, *et al.* Modeling and design of passive electric networks interconnecting piezoelectric transducers for distributed vibration control. *International Journal of Applied Electromagnetics and Mechanics*, 21(2):69–87, 2005.

[37] Francesco dell'Isola, Alessandro Della Corte, and Ivan Giorgio. Higher-gradient continua: The legacy of Piola, Mindlin, Sedov and Toupin and some future research perspectives. *Mathematics and Mechanics of Solids*, 22(4):852–872, 2017.

[38] Catherine Pideri and Pierre Seppecher. A second gradient material resulting from the homogenization of an heterogeneous linear elastic medium. *Continuum Mechanics and Thermodynamics*, 9(5):241–257, 1997.

[39] C. Boutin, F. dell'Isola, I. Giorgio, and L. Placidi. Linear pantographic sheets: Asymptotic micromacro models identification. *Math Mech Complex Systems*, 5(2):127–162.

[40] Jean-Jacques Alibert and Alessandro Della Corte. Second-gradient continua as homogenized limit of pantographic microstructured plates: A rigorous proof. *Zeitschrift für angewandte Mathematik und Physik*, 66(5):2855–2870, 2015.

[41] F. dell'Isola, I. Giorgio, Marek Pawlikowski, and N.L. Rizzi. Large deformations of planar extensible beams and pantographic lattices: Heuristic homogenization, experimental and numerical examples of equilibrium. *Proc. R. Soc. A*, 472(2185):20150790, 2016.

[42] Edoardo Benvenuto, Antonio Becchi, Massimo Corradi, and Federico Foce. *La scienza delle costruzioni e il suo sviluppo storico*. Edizioni di storia e letteratura, 2006.

[43] G. Neville Greaves. Poisson's ratio over two centuries: Challenging hypotheses. *Notes Rec. R. Soc.*, 67(1):37–58, 2013.

[44] Erik C. Banks. The philosophical roots of Ernst Mach's economy of thought. *Synthese*, 139(1):23–53, 2004.

[45] George Green. *Mathematical Papers of the Late George Green*. Cambridge University Press, 2014.

[46] Clifford Truesdell. *Rational Thermodynamics*. Springer Science & Business Media, 2012.

[47] Clifford Truesdell. *The Tragicomical History of Thermodynamics, 1822–1854*, Volume 4. Springer Science & Business Media, 2013.

[48] Harold Priest. Marino and Italian baroque. *Bulletin of the Rocky Mountain Modern Language Association*, 25(4):107–111, 1971.

[49] Jonathan Unglaub and Nicolas Poussin. *Poussin and the Poetics of Painting: Pictorial Narrative and the Legacy of Tasso*. Cambridge University Press, 2006.

[50] Francesco dell'Isola, Tomasz Lekszycki, Marek Pawlikowski, Roman Grygoruk, and Leopoldo Greco. Designing a light fabric metamaterial being highly macroscopically tough under directional extension: First experimental evidence. *Zeitschrift für angewandte Mathematik und Physik*, 66(6):3473–3498, 2015.

[51] Morton E. Gurtin. Thermodynamics and the possibility of spatial interaction in elastic materials. *Archive for Rational Mechanics and Analysis*, 19(5):339–352, 1965.

[52] Eliot Fried and Morton E. Gurtin. Tractions, balances, and boundary conditions for nonsimple materials with application to liquid flow at small-length scales. *Archive for Rational Mechanics and Analysis*, 182(3):513–554, 2006.

[53] Pierre Seppecher, Jean-Jacques Alibert, and Francesco dell'Isola. Linear elastic trusses leading to continua with exotic mechanical interactions. In *Journal of Physics: Conference Series*, Volume 319, page 012018. IOP Publishing, 2011.

[54] Jean-Jacques Alibert, Pierre Seppecher, and Francesco dell'Isola. Truss modular beams with deformation energy depending on higher displacement gradients. *Mathematics and Mechanics of Solids*, 8(1):51–73, 2003.

[55] Victor A. Eremeyev, Francesco dell'Isola, Claude Boutin, and David Steigmann. Linear pantographic sheets: existence and uniqueness of weak solutions. *Journal of Elasticity*, pages 1–22, 2017.

[56] M. Golaszewski, R. Grygoruk, I. Giorgio, M. Laudato, and F. Di Cosmo. Metamaterials with relative displacements in their microstructure: Technological challenges in 3D printing, experiments and numerical predictions. *Continuum Mechanics and Thermodynamics*, 31(4):1015–1034, 2019.

[57] Anil Misra, Tomasz Lekszycki, Ivan Giorgio, *et al.* Pantographic metamaterials show atypical Poynting effect reversal. *Mechanics Research Communications*, 89:6–10, 2018.

[58] Gregor Ganzosch, Francesco dell'Isola, Emilio Turco, Tomasz Lekszycki, and Wolfgang H. Müller. Shearing tests applied to pantographic structures. *Acta Polytechnica CTU Proceedings*, 7:1–6, 2016.

[59] M. Spagnuolo, K. Barcz, A. Pfaff, F. dell'Isola, and P. Franciosi. Qualitative pivot damage analysis in aluminum printed pantographic sheets: Numerics and experiments. *Mechanics Research Communications*, 83:47–52, 2017.

[60] Ivan Giorgio, Roman Grygoruk, Francesco dell'Isola, and David J. Steigmann. Pattern formation in the three-dimensional deformations of fibered sheets. *Mechanics Research Communications*, 69:164–171, 2015.

[61] Nikolaĭ Ivanovich Muskhelishvili. *Some Basic Problems of the Mathematical Theory of Elasticity*. Springer Science & Business Media, 2013.

[62] Emilio Turco, Maciej Golaszewski, Antonio Cazzani, and Nicola Luigi Rizzi. Large deformations induced in planar pantographic sheets by loads applied on fibers: Experimental validation of a discrete Lagrangian model. *Mechanics Research Communications*, 76:51–56, 2016.

[63] Emilio Turco, Francesco dell'Isola, Antonio Cazzani, and Nicola Luigi Rizzi. Hencky-type discrete model for pantographic structures: Numerical comparison with second gradient continuum models. *Zeitschrift für angewandte Mathematik und Physik*, 67(4):85, 2016.

[64] Emilio Turco and Nicola Luigi Rizzi. Pantographic structures presenting statistically distributed defects: Numerical investigations of the effects on deformation fields. *Mechanics Research Communications*, 77:65–69, 2016.

[65] Slaviša Šalinić. An improved variant of Hencky bar-chain model for buckling and bending vibration of beams with end masses and springs. *Mechanical Systems and Signal Processing*, 90:30–43, 2017.

[66] Satish Kumar and Ronald G. Larson. Brownian dynamics simulations of flexible polymers with spring–spring repulsions. *The Journal of Chemical Physics*, 114(15):6937–6941, 2001.

[67] C.M. Wang, Hui Zhang, R.P. Gao, W.H. Duan, and N. Challamel. Hencky bar-chain model for buckling and vibration of beams with elastic end restraints. *International Journal of Structural Stability and Dynamics*, 15(07):1540007, 2015.

[68] Hong Zhang, C.M. Wang, and Noël Challamel. Buckling and vibration of Hencky bar-chain with internal elastic springs. *International Journal of Mechanical Sciences*, 119:383–395, 2016.

[69] Emilio Barchiesi, Francesco dell'Isola, Marco Laudato, Luca Placidi, and Pierre Seppecher. A 1D continuum model for beams with pantographic microstructure: Asymptotic micro–macro identification and numerical results. In *Advances in Mechanics of Microstructured Media and Structures*, pages 43–74. Springer, 2018.

[70] Graeme W. Milton and Andrej V. Cherkaev. Which elasticity tensors are realizable? *Journal of Engineering Materials and Technology*, 117(4):483–493, 1995.

[71] Muamer Kadic, Tiemo Bückmann, Nicolas Stenger, Michael Thiel, and Martin Wegener. On the practicability of pentamode mechanical metamaterials. *Applied Physics Letters*, 100(19):191901, 2012.

[72] Alessandro Della Corte, Francesco dell'Isola, Raffaele Esposito, and Mario Pulvirenti. Equilibria of a clamped Euler beam (elastica) with distributed load: Large deformations. *Mathematical Models and Methods in Applied Sciences*, 27(08):1391–1421, 2017.

5 Lagrangian Discrete Models: Applications to Metamaterials

F. dell'Isola, E.Turco, E. Barchiesi

5.1 Introduction

In this chapter, we discuss the Lagrangian formulation of mechanics for discrete systems and its application to mathematical modeling in modern metamaterials science. In order to distinguish between the discrete or continuous nature of a mechanical system one has to assess the number of parameters needed to describe its state and evolution. For instance, the description of positions and velocities of a system made of a set of N particles moving in a box will require the introduction of $6N$ variables, since each particle can move in three independent spatial directions with three independent components of the velocity. Instead, a continuous system will require an infinite number of variables to describe its state, since one has to furnish the position and velocity of a dense set of "infinitely close particles." An example from the mechanical world is the description of the deformed shape of a beam subject to certain external loads. In this case, the state of the system is described in terms of a function, whose domain is the region of space occupied by the body itself. In both cases it is possible to give a Lagrangian description of the state and of the evolution of the mechanical system under analysis. However, while the fundamental tools for their study are the same (namely, both are founded on the calculus of variations), the technical and mathematical problems which could emerge are quite different, as will be explained below. Of course, it is not possible to state in general which approach would better suit the description of a mechanical system, as it depends on the kind of analysis which we are interested in. It could be useful to study the relations between discrete and continuous Lagrangian descriptions of the same mechanical system, in order to investigate when a certain modeling and forecasting technique is better than another [1–7]. This is true, in particular, in the framework of mechanical metamaterials, where the relations between the (discrete) complex microstructure and the related (continuous) homogenized field theory are required to motivate and understand the exotic macroscopic behavior. Indeed, it is quite common in today's metamaterial science to consider highly controlled microstructures consisting of (discrete) beam lattices [8, 9, 11–19, 91]. The problem of studying such types of structures is, however, not at all new. Indeed, in 1864, work by Maxwell [20] had already addressed the problem of systematically studying beam (not only truss!) lattices. Unfortunately, his contribution, still representing a cornerstone in the study of such systems, has been somewhat underestimated and overshadowed by his other great contributions, despite the fact that the topic was of primary importance at

the time. Indeed, not much later, with the advent of the Industrial Revolution brought about by the large-scale production of steel, the theory of structures quickly became an elective discipline in engineering sciences, leading to many engineering successes, like the construction of the Eiffel Tower. The same tool can be successfully applied also to meet the ever more demanding performances needed in today's engineering systems: optimization topology is playing a crucial role for designing structures and materials which can be produced by additive manufacturing, as well as for the development of material microstructures for designing multi-scale macro-structures, or for exploiting micro-scale properties to obtain optimal configurations [21–27].

Nowadays, numerical methods play a major role in mechanics, and especially in the description of metamaterials' behavior [28–34]. The use of numerical methods has indeed allowed the majority of the recent advancements in the field of metamaterials and, more generally, mechanics. Indeed, the high complexity characterizing the microstructure of modern metamaterials gives rise to a comparably complex homogenized continuous model (these are usually called *generalized continuum theories*, see [3, 35, 37–47] for interesting applications) which are, in general, not solvable by means of the usual calculus techniques. Numerical methods make it possible to discretize the problem, reducing it to a finite set of ordinary differential equations. Although numerical methods are a valuable tool in several applications, the discretization techniques behind them may conceal some disadvantages that could limit their predictive power. Indeed, such discretization techniques may not take account of the intrinsic microstructure of the metamaterial, and this could lead to misleading results. The main aim of this work is to discuss and review an idea proposed in [48] and subsequently developed in [49–51], in which an *ab initio* discrete model for a complex mechanical system has been introduced. This model is directly inspired by the metamaterial's microstructure and allows an efficient (as regarding computational efforts) and accurate description of the system behavior. In particular, we will focus on two systems: the pantographic lattice and the three-dimensional *Elastica*.

The chapter is divided in the following way: in Section 5.2 we will recall the Lagrangian formalism of mechanics. This will be the fundamental tool for the subsequent discussions. In Section 5.3, we will discuss in a more precise way the relation between discrete and continuous Lagrangian descriptions and its importance in modern mechanics. In Section 5.4, we will introduce the Hencky-type discrete model for a pantographic sheet. Comparisons between continuous and discrete models with experimental data will be presented and discussed. Finally, in Section 5.5, a Hencky-type discrete model for three-dimensional *Elastica* will be discussed.

5.2 Lagrangian Formulation of Mechanics

This section is devoted to recalling the main features of the Lagrangian formulation of mechanics. This elegant theory is the result of the efforts of many eminent physicists and mathematicians of the caliber of Euler, Laplace, Lagrange, Legendre, Gauss, Liouville, Poisson, Hamilton, and many others. Their motivation was to find a general

mathematical setting able to unify in a single theory all the physical knowledge of the observed world. In a sense, Lagrangian mechanics (and of course its complement, Hamiltonian mechanics) can be considered as one of the first "theory of everything" in the history of modern science.[1] The name of this theory is of course a tribute to one of the most influential and gifted mathematicians of the last centuries, the Italian–French Joseph-Louis Lagrange. In his famous treatise *Méchanique Analytique* (1788), he presented for the first time Analytical Mechanics, a general method aimed to analyze dynamical systems by means only of the techniques of infinitesimal analysis. Its generality and independence from any geometrical considerations is underlined in the introduction of his treatise by announcing: *On trouvera point de figures dans cet Ouvrage*.[2] Actually, the field of applications of Lagrangian mechanics in modern science is astonishingly vast: it is the mathematical framework of dynamical systems, solid mechanics, signal processing, classical and quantum field theories, network analysis, quantitative finance, quantum mechanics, biomechanics, etc. (see [54–68] for multi-physics applications). The reason behind its extensive use lies mainly in the fact that it is simple to produce, by means of a general procedure, a well-posed problem in terms of differential equations. In Lagrange's own words:[3]

There already exist several treatises on mechanics, but the purpose of this one is entirely new. I propose to condense the theory of this science and the method of solving the related problems to general formulas whose simple application produces all the necessary equations for the solution of each problem. In addition, this work will have another use. The various principles presently available will be assembled and presented from a single point of view in order to facilitate the solution of the problems of mechanics. Moreover, it will also show their interdependence and mutual dependence, and will permit the evaluation of their validity and scope. I have divided this work into two parts: Statics or the Theory of Equilibrium, and Dynamics or the Theory of Motion. In each part, I treat solid bodies and fluids separately. No figures will be found in this work. The methods I present require neither constructions nor geometrical or mechanical arguments, but solely algebraic operations subject to a regular and uniform procedure. Those who appreciate mathematical analysis will see with pleasure mechanics becoming a new branch of it and hence, will recognize that I have enlarged its domain.

The mathematical backbone of Lagrangian mechanics is the calculus of variations. In the following, we will discuss in details its application to finite-dimensional mechanical systems. We want to use some space here to point out that, although the original formulation of Lagrangian mechanics was limited to finite-dimensional systems, it is possible to extend it to infinite dimensional cases. Indeed, Lagrangian mechanics is a well-established tool in field theories (standard references are the Landau–Lifchitz textbook series [69] and Arnold's works on fluid dynamics [70], see also [71]) where the governing equations of such theories can be obtained by means of a least action principle, defined in terms of an action functional. Going from infinite to finite dimensional systems, a common application is the so-called *modal analysis*, performed by means of the Fourier series theory in Hilbert spaces. In particular, let us suppose that a

[1] Note that the founding ideas behind the variational formulation can be traced back to the ancient Greeks. See [52] Russo for an interesting analysis.
[2] "*No figures will be found in this work.*" [53].
[3] *Avertissement*, in [53].

given model describes the motion of a system in terms of a partial differential equation (including time derivatives). By expanding in Fourier series the unknown field (in terms of space variables with respect to a suitable basis of functions), the initial differential equation gives rise to many (countably) ordinary differential equations (in the time variable) whose unknown functions are, indeed, the previously introduced Fourier coefficients. By introducing suitable approximations, only a finite number of those coefficients will be relevant for the description of the phenomena under study. This approximation allows the infinite-dimensional model to be *projected* (in the sense of the geometry in Hilbert spaces) onto a finite-dimensional model. To clarify this point, let us introduce an example. A certain force per unit length is acting on an extensible homogeneous wire constrained on a plane, whose ends have fixed positions. In the D'Alembert model, the wire's motion is represented by a scalar field u, (whose domain is the segment $[0, l]$), which describes the wire's displacement along the direction orthogonal to $[0, l]$ with respect to a straight reference configuration. In other words, in the D'Alembert model, the state of the system is characterized in terms of a function which belongs to the (infinite dimensional) space of two times differentiable functions with respect to time and space variables. The following equation describes the time evolution of this field u:

$$\frac{\partial^2 u}{\partial t^2} - a^2 \frac{\partial^2 u}{\partial x^2} = g(x,t)\,, \quad \text{in } [0,l] \times [t_0, \infty]\,, \tag{5.1}$$

where the constant a is the mechanical waves' speed of propagation through the wire, and the function $g(x,t)$ represents the aforementioned forces per unit length acting on the wire. It is possible to expand the functions $u(x,t)$ and $g(x,t)$ in Fourier series as

$$u(x,t) = \sum_{n=1}^{\infty} u_n(t)\phi_n(x)\,, \qquad g(x,t) = \sum_{n=1}^{\infty} f_n(t)\phi_n(x)\,, \tag{5.2}$$

where the sequence of functions $\phi_n(x)$ satisfies:

$$\frac{d^2 \phi_n}{dx^2} = \lambda_n \phi_n, \quad \forall n\,. \tag{5.3}$$

In this hypothesis, the evolution equation (5.1) is verified if, for all n,

$$\frac{d^2 u_n}{dt^2} - a^2 \lambda_n u_n(t) = f_n(t)\,, \quad \text{in } [0,l] \times [t_0, \infty]\,. \tag{5.4}$$

By introducing some approximations (for instance, due to experimental limitations) all the Fourier coefficients after a certain order $n > N$ can be neglected. In this way, the original infinite dimensional model reduces to a finite dimensional one described in terms of the finite set of Fourier coefficients u_i such that $i = 1, \ldots, N$, whose evolution is given by Eq. (5.4).

Let us now introduce the main quantities which we need in order to describe a finite dimensional dynamical system in the Lagrangian formalism. In this case, the state of the dynamical system is characterized by a finite number of degrees of freedom, described by *n Lagrangian coordinates*

$$\mathbf{q} = (q_1, \ldots, q_n), \tag{5.5}$$

which define the so-called *configuration space*.

Let us introduce the following definitions:

- Let S be a dynamical system. Its *motion*, $\mathbf{q}(t)$, is represented by a function

$$\mathbf{q} : [t_0, t_1] \subset \mathbb{R} \longrightarrow \mathbb{R}^n, \quad t \mapsto \mathbf{q}(t) = \begin{pmatrix} q_1(t) \\ q_2(t) \\ \vdots \\ q_n(t) \end{pmatrix}, \tag{5.6}$$

  which, for each instant of time t, associates $\mathbf{q}(t)$ of its Lagrangian coordinates. The set of all the motions of S will be denoted by $M = C^2([t_0, t_1], \mathbb{R}^n)$.
- A curve $\mathbf{q}([t_0, t_1]) \subset \mathbb{R}^n$ is called a *trajectory* of the system.
- We call *Lagrangian velocity* (resp. *Lagrangian acceleration*) the vector obtained by computing the time derivative of $\mathbf{q}(\cdot) \in M$ (resp. $\dot{\mathbf{q}}(\cdot)$):

$$\dot{\mathbf{q}}(t) = \frac{d\mathbf{q}(t)}{dt} = \begin{pmatrix} \dot{q}_1(t) \\ \dot{q}_2(t) \\ \vdots \\ \dot{q}_n(t) \end{pmatrix}, \quad \ddot{\mathbf{q}}(t) = \frac{d^2\mathbf{q}(t)}{dt^2} = \begin{pmatrix} \ddot{q}_1(t) \\ \ddot{q}_2(t) \\ \vdots \\ \ddot{q}_n(t) \end{pmatrix}. \tag{5.7}$$

5.2.1 Optimum Problems and Fundamentals of Calculus of Variations

Once the suitable mathematical entities have been introduced, i.e. once the *kinematics* of the system has been fixed, the time evolution of the dynamical system is determined by a set of differential equations. Their role is to model the effects of the external world on the system, while their solutions will determine the admissible motions, among all the possible ones in M, determined by the particular boundary conditions under analysis. The choice of such *evolution equations* has to be done judiciously, taking care that, once the initial state of the system has been specified, as well as the interactions with the external world, the motion of the system has to be uniquely determined. In this regard, uniqueness theorems for the evolution equations' solutions have to be proved.

Example 5.1 A particular motion is the one of a finite-dimensional dynamical system at rest in an equilibrium position. Such equilibrium positions are stationary points of its potential energy, U, which is a function of the n Lagrangian coordinates $q_1, q_2, \ldots, q_n$. As is well known from physics courses and as we will see in the following, to determine the equilibrium positions of a given system, one needs to find the set of vectors $\mathbf{q}$ for which the gradient of U, and hence its first variation, is zero.[4]

---

[4] Let us consider the Taylor expansion of U:

$$U(\mathbf{q}) = U(\mathbf{q}_0) + \boxed{\nabla U|_{\mathbf{q}=\mathbf{q}_0} \cdot (\mathbf{q} - \mathbf{q}_0)} + o(\|\mathbf{q} - \mathbf{q}_0\|).$$

The term in the frame is stated to be the *first variation* of the function U in the neighbourhood of $\mathbf{q}_0$.

Determination of the evolution equations for a dynamical system is a crucial step. However, it may be far from being a trivial task. One of the most important merits of the Lagrange formulation of mechanics is that it furnishes an algorithmic way to deduce the differential equations governing a generic dynamical system following the least action principle expressed below.

Least action principle. Let (S, I), be the pair made up of the dynamical system S and the interactions I of the external world with the system. There exists a scalar quantity, called *action*, such that the motions of S determined by I make the action stationary.

It is not clear who, among the eminent mathematicians who worked on this problem, was the first to state this axiom. Without any doubt, D'Alembert proposed to generalize the Fermat principle for optical paths and Hamilton was able to prove a least action principle (and as we will see in the following sections, this is the so-called Hamilton's principle) starting from the cardinal law of dynamics. Moreover, there are hints that Lagrange and the Italian mathematician Gabrio Piola were already aware of these results. We shall not pursue, however, any polemical dispute about any originality claim. In the following, instead, we will discuss the procedure to derive the evolution equations of a finite-dimensional dynamical system in general by exploiting the aforementioned least action principle.

First, let us clarify the nature of the action. From the mathematical side, once the set of Lagrangian coordinates and the corresponding set of motions is established, it is a functional A which associates with any motion a real number, i.e.:

$$A \,:\, \mathbf{q}(\cdot) \in M \longmapsto A\big(\mathbf{q}(\cdot)\big) \in \mathbb{R}. \tag{5.8}$$

Let us now give some examples of functionals:

- A first simple example of a functional is represented by the length of a curve lying on a plane π. Let $\Gamma \,:\, t \in [t_0, t_1] \mapsto (x_1(t), x_2(t)) \in \pi$ be a one time differentiable function; the functional *length* associates with the pair of real variable functions $\{x_1(\cdot), x_2(\cdot)\}$ the real number l,

$$l = \int_{t_0}^{t_1} \sqrt{\dot{x}_1^2(t) + \dot{x}_2^2(t)}\, dt\,, \tag{5.9}$$

  where the symbol $\dot{x}$ indicates the time derivative of the function x.
- A second example of a functional is given by the area of a plane region whose boundary is a closed curve Γ. In this case, the functional *area* associates with the pair of functions $\{x_1(\cdot), x_2(\cdot)\}$ a real number $A(\Gamma)$:

$$A(\Gamma) = \int_{t_0}^{t_1} x_2(t)\dot{x}_1(t)\, dt = \oint_{\Gamma} x_2\, dx_1\,. \tag{5.10}$$

- Let us consider a material particle of mass m under the action of a conservative force with a potential U. We call *action* the functional which associates with the motion $\mathbf{x}(\cdot)$ of the material particle in the interval $[t_0, t_1]$ the real number

$$A\big(\mathbf{x}(\cdot)\big) = \int_{t_0}^{t_1} \Big(\frac{m}{2}\dot{\mathbf{x}}^2(t) - U(\mathbf{x}(t))\Big)\, dt. \tag{5.11}$$

- Let us consider a firm F which produces n goods. Let $\mathbf{q}(t) = (q_1(t), \ldots, q_n(t))$ be the production per unit time vector, at instant t, of the goods and let $\mathbf{p}(t) = (p_1(t), \ldots, p_n(t))$ be the market prices vector. Finally, let C be the function which associates with the produced quantity $\mathbf{q}(t)$ and the production rate $\dot{\mathbf{q}}(t)$ the production cost. If F is subject to an interest rate μ, then its profit in the interval $[t_0, t_1]$ is given by the functional:

$$G = \int_{t_0}^{t_1} \exp\big(-\mu(t - t_0)\big)\big(\mathbf{p} \cdot \mathbf{q} - C(\mathbf{q}, \dot{\mathbf{q}})\big)\, dt. \tag{5.12}$$

  Clearly, the firm F is interested in the production strategy $\mathbf{q}(t)$ which will maximise the profit functional G.

In order to give a more constructive formulation of the aforementioned axiom, let us consider a dynamical system S described in terms of a set of Lagrangian coordinates $\mathbf{q}$. Let $MI(t_0, \mathbf{q}_0, t_1, \mathbf{q}_1) \subset M$ be the subset of *isochronic motions*, i.e. all the motion $\mathbf{q}(\cdot) \in M$ such that:

$$\mathbf{q}(t_0) = \mathbf{q}_0\,, \quad \mathbf{q}(t_1) = \mathbf{q}_1\,. \tag{5.13}$$

In other words, the set MI contains all the motions characterized by the same initial and final configurations which take place in the same interval of time (t_0, t_1). Therefore, by considering a motion $\mathbf{q} \in MI(t_0, \mathbf{q}_0, t_1, \mathbf{q}_1)$, we can define a function $\delta\mathbf{q}(t)$ such that

$$\delta\mathbf{q}(t_0) = 0 \quad \text{and} \quad \delta\mathbf{q}(t_1) = 0\,, \tag{5.14}$$

an *admissible variation of the motion*. This requirement implies that any motion $\mathbf{q}(t) + \delta\mathbf{q}(t)$ is isochronic to $\mathbf{q}(t)$.

Let us now introduce a function

$$\mathscr{L} : \mathbb{R}^n \times \mathbb{R}^n \times \mathbb{R} \longrightarrow \mathbb{R}, \tag{5.15}$$

whose Hessian with respect to Lagrangian velocities is positive definite, namely:

$$\left|\left| \frac{\partial^2 \mathscr{L}}{\partial \dot{q}_i \partial \dot{q}_j} \right|\right| > 0\,. \tag{5.16}$$

We will call such a function $\mathscr{L}$ satisfying the condition (5.16) a *Lagrangian function*. The role of this function is crucial. Indeed, as we will show soon, it is the basic ingredient of the action functional and it has to contain information about the constitutive properties of the dynamical system as well as its interaction with the external world. Once a Lagrangian function is chosen, it is possible to define the following action functional, defined in terms of the set of motions $\mathbf{q}(\cdot) \in M$:

$$\mathfrak{A}\big(\mathbf{q}(\cdot)\big) = \int_{t_0}^{t_1} \mathscr{L}\big(\mathbf{q}(t), \dot{\mathbf{q}}(t), t\big)\, dt\,. \tag{5.17}$$

We are now ready to state, for the case of finite-dimensional systems, a more precise formulation of the least action principle by D'Alembert:

AXIOM 5.1 ***Lagrangian least action principle.*** *Once a Lagrangian $\mathscr{L}$ has been chosen, the interaction that is modeled by $\mathscr{L}$ determines an evolution of the system considered in terms of the motion $\boldsymbol{q}^*$ which yields the action functional (5.17) stationary, when such a functional is restricted to the set MI of isochronic motions to $\boldsymbol{q}^*$.*

The condition for a motion to yield the action functional stationary is that the functional's first variation vanishes when evaluated on that motion. In the next subsection, we explicitly show how this requirement provides us with the evolution equations of the dynamical system. By not making explicit the form of the Lagrangian function, we will keep the discussion general, obtaining in this way the general expression of the evolution equations of a generic finite-dimensional dynamical system in the Lagrangian formalism, namely the *Euler–Lagrange equations*.

5.2.2 Euler–Lagrange Equations

The first variation of the action functional on motions isochronic to $\mathbf{q}^*$ is defined as:

$$\begin{aligned}\delta\mathfrak{A}\big|_{\mathbf{q}^*} &:= \mathfrak{A}(\mathbf{q}^* + \delta\mathbf{q}) - \mathfrak{A}(\mathbf{q}^*) \\ &= \int_{t_0}^{t_1} \left[\mathscr{L}(\mathbf{q}^* + \delta\mathbf{q}, \dot{\mathbf{q}}^* + \delta\dot{\mathbf{q}}, t) - \mathscr{L}(\mathbf{q}^*, \dot{\mathbf{q}}^*, t)\right] dt\,.\end{aligned} \tag{5.18}$$

Assuming $\mathscr{L}$ differentiable and by expanding the difference in Eq. (5.18) in Taylor series, the previous expression becomes

$$\mathscr{L}(\mathbf{q}^* + \delta\mathbf{q}, \dot{\mathbf{q}}^* + \delta\dot{\mathbf{q}}, t) - \mathscr{L}(\mathbf{q}^*, \dot{\mathbf{q}}^*, t) = \left.\frac{\partial\mathscr{L}}{\partial q_i}\right|_{\mathbf{q}^*} \delta q_i + \left.\frac{\partial\mathscr{L}}{\partial\dot{q}_j}\right|_{\mathbf{q}^*} \delta\dot{q}_j + o(\delta q_i, \delta\dot{q}_j)\,, \tag{5.19}$$

where Einstein's notation for the sum is assumed. By replacing this expression in Eq. (5.18) we obtain the action functional's first variation as:

$$\delta\mathfrak{A}\big|_{\mathbf{q}^*} = \int_{t_0}^{t_1} \left(\left.\frac{\partial\mathscr{L}}{\partial\mathbf{q}}\right|_{\mathbf{q}^*} \cdot \delta\mathbf{q} + \left.\frac{\partial\mathscr{L}}{\partial\dot{\mathbf{q}}}\right|_{\mathbf{q}^*} \cdot \delta\dot{\mathbf{q}}\right) dt\,. \tag{5.20}$$

By using Leibniz's rule on the second addend

$$\frac{d}{dt}\left(\frac{\partial\mathscr{L}}{\partial\dot{\mathbf{q}}} \cdot \delta\mathbf{q}\right) = \frac{d}{dt}\left(\frac{\partial\mathscr{L}}{\partial\dot{\mathbf{q}}}\right) \cdot \delta\mathbf{q} + \frac{\partial\mathscr{L}}{\partial\dot{\mathbf{q}}} \cdot \delta\dot{\mathbf{q}}\,, \tag{5.21}$$

since

$$\delta\mathbf{q}(t_0) = \delta\mathbf{q}(t_1) = 0 \implies \left[\frac{\partial\mathscr{L}}{\partial\dot{\mathbf{q}}} \cdot \delta\mathbf{q}\right]_{t_0}^{t_1} = 0\,, \tag{5.22}$$

one obtains:

$$\delta\mathfrak{A}\big|_{\mathbf{q}^*} = \int_{t_0}^{t_1} \left[\left.\frac{\partial\mathscr{L}}{\partial\mathbf{q}}\right|_{\mathbf{q}^*} \cdot \delta\mathbf{q} - \frac{d}{dt}\left(\frac{\partial\mathscr{L}}{\partial\dot{\mathbf{q}}}\right) \cdot \delta\mathbf{q}\right] dt\,. \tag{5.23}$$

A motion $\mathbf{q}$ is said to be *stationary* (or *extremal*) for the action functional if the first variation of the action $\delta\mathfrak{A}|_{\mathbf{q}^*}$ is zero. In formulas, $\mathbf{q}^*$ is extremal if and only if:

$$\delta\mathfrak{A}|_{\mathbf{q}^*} = 0,\ \forall\delta\mathbf{q}:\ \delta\mathbf{q}(t_0) = \delta\mathbf{q}(t_1) = 0. \tag{5.24}$$

This can be seen as a generalization of the concept of gradient for real functions of several variables. The modern formalization of this idea was due to Gâteau and Fréchet (see for example [76]), but the first to propose it was probably Euler. To make this analogy clearer, let us discuss the following example: by computing the first order Taylor expansion of a function $f(x)$ one has that, up to infinitesimals of greater order:

$$f(x) - f(x_0) \cong \text{GRAD}\, f|_{x=x_0}\,(x - x_0). \tag{5.25}$$

We call a point x_0 a stationary point of $f(x)$ if and only if $\text{GRAD}\ f|_{x_0} = 0$. In other words, we require that, in correspondence of stationary points, the first variation of f vanishes. Therefore, we define Eq. (5.23) in an analogous way to (5.25) and we observe that the first variation of the function f and of the functional $\mathfrak{A}$ have been obtained by applying to the variations $(x - x_0)$ and $\delta\mathbf{q}$, linear maps whose images are given by $\text{GRAD}\ f|_{x=x_0}\,(x - x_0)$ and by $\delta\mathfrak{A}|_{\mathbf{q}^*}$, respectively.

We are ready to state the following theorem:

THEOREM 5.1 ***Euler–Lagrange theorem.*** *For an action $\mathfrak{A}$, a motion $\boldsymbol{q}^*$ is stationary if and only if*

$$\delta\mathfrak{A}\big|_{\boldsymbol{q}^*} = \int_{t_0}^{t_1} \left[\left(\frac{\partial \mathscr{L}}{\partial \boldsymbol{q}} - \frac{d}{dt}\left(\frac{\partial \mathscr{L}}{\partial \dot{\boldsymbol{q}}} \right) \right)_{\boldsymbol{q}^*} \cdot \delta\boldsymbol{q} \right] dt = 0\,, \quad \forall\delta\boldsymbol{q} : \delta\boldsymbol{q}(t_0) = \delta\boldsymbol{q}(t_1) = 0\,. \tag{5.26}$$

Let us now introduce the following theorem by Lagrange:

THEOREM 5.2 ***Lagrange theorem.*** *Let $I \subset \mathbb{R}$ and*

$$g_1 : I \longrightarrow \mathbb{R}, \quad g_2 : I \longrightarrow \mathbb{R} \tag{5.27}$$

be continuous in their domains. Then:

$$\int_I g_1(t) g_2(t) dt = 0\,,\ \forall g_2(t) \iff g_1(t) = 0\,,\ \forall t \in I\,. \tag{5.28}$$

Due to the previous theorem, we have the following proposition:

PROPOSITION 5.1 ***Euler–Lagrange equations.*** *A motion $\boldsymbol{q} = \boldsymbol{q}(t) \in M$ yields the action stationary for synchronous variations between fixed extremes if and only if it is a solution of the following differential problem:*

$$\left(\frac{\partial \mathscr{L}}{\partial \boldsymbol{q}} - \frac{d}{dt}\left(\frac{\partial \mathscr{L}}{\partial \dot{\boldsymbol{q}}} \right) \right)_{\boldsymbol{q}^*} = 0, \quad \begin{cases} q_k^*(t_0) = q_{k1} \\ q_k^*(t_1) = q_{k2} \end{cases}, \quad k = 1, \ldots n. \tag{5.29}$$

Equations (5.29) are known as the Euler–Lagrange equations associated with the variational problem (5.26).

Some observations are now in order:

- We remark firstly that the Euler–Lagrange equations are non-linear ordinary differential equations and therefore to find their solutions is, in general, not an easy task. Actually, only in a few cases is it possible to integrate in closed form non-linear differential equations, namely to determine the set of their solutions in terms of elementary functions or series of elementary functions. However, thanks to several results, obtained mainly by Arnold, Poincaré, Laplace and Gauss, it is possible to exploit geometrical methods to infer the main features of the solutions of different kinds of Lagrange equations. Moreover, in some cases, it is possible to perform qualitative analyses of these solutions, so as to be able to infer for example:
  - the so-called system's *attractors*, i.e. those regions of the configuration space of the system toward which its motion tends to "converge";
  - those regions of the configuration space in which the motion remains confined;
  - the effects on the trajectory of the motion due to different external actions or variations of initial data.

  We can also study Lagrange equations quantitatively, by using numerical methods. Indeed, the proof of the existence and uniqueness theorem for the solution to differential problems, which is due to Cauchy, is a constructive demonstration: it is based on the formulation of an algorithm which makes it possible to generate a sequence of functions converging to the solution. Moreover, and this is very important in applications, it provides an estimate of the error introduced when substituting an approximation to the exact solution. It is for this reason that with the coming of modern digital calculators, which entails an increasing computational capacity, the Lagrangian method is gaining even more importance for the description of the time evolution of physical systems: once a Lagrangian has been determined which is considered reliable for the description of a given class of phenomena, it is possible to forecast the behavior of the system with considerable accuracy and reliability. It is noteworthy that for non-dissipative dynamical systems, i.e. for those systems in which the energy is conserved, it is always possible to describe the dynamical evolution of the system in terms of Euler–Lagrange equations. Being aware of this result, Laplace hailed the Euler–Lagrange equations as "the equations of the Universe." Indeed, following Democritus, by considering the Universe as made up of a (huge but) finite number of particles, in the hypothesis for which the first principle of thermodynamics holds, it is possible to introduce an accurate enough model of the Universe by means of a Lagrangian function defined in terms of a finite number of Lagrangian coordinates. Laplace, driven by the necessity to furnish evidence for this conjecture, developed his celestial mechanics that is able to describe, in a very accurate way, the solar system's behavior. Nevertheless, it is possible to furnish a Lagrangian description also for non-conservative systems. To this end, the reader is encouraged to consider the following time-dependent Lagrangian function:

$$\mathscr{L} = \exp(\mu t)\left(\frac{1}{2}m\dot{x}^2 + \frac{1}{2}kx^2\right), \tag{5.30}$$

of a system with only one degree of freedom, x, and to compute the corresponding Euler–Lagrange equation. That equation will turn out to be one of a damped harmonic oscillator: thus, the reader may begin to doubt the fact that Lagrangian formalism can be used only when dealing with conservative systems.

- Let us compute explicitly the time derivative in Eq. (5.29):

$$\frac{\partial^2 \mathscr{L}}{\partial \dot{\mathbf{q}} \partial \dot{\mathbf{q}}}\ddot{\mathbf{q}}^* + \frac{\partial^2 \mathscr{L}}{\partial \mathbf{q} \partial \dot{\mathbf{q}}}\dot{\mathbf{q}}^* + \frac{\partial^2 \mathscr{L}}{\partial \dot{\mathbf{q}} \partial t} - \frac{\partial \mathscr{L}}{\partial \mathbf{q}} = 0. \tag{5.31}$$

Due to the condition (5.16) on the Hessian of the Lagrangian function, it is possible to multiply for its inverse on the left. In this way, Eq. (5.31) can be turned into normal form:

$$\ddot{\mathbf{q}}^* = \left(\frac{\partial^2 \mathscr{L}}{\partial \dot{\mathbf{q}} \partial \dot{\mathbf{q}}}\right)^{-1}\left(\frac{\partial \mathscr{L}}{\partial \mathbf{q}} - \frac{\partial^2 \mathscr{L}}{\partial \dot{\mathbf{q}} \partial \mathbf{q}}\dot{\mathbf{q}}^* - \frac{\partial^2 \mathscr{L}}{\partial \dot{\mathbf{q}} \partial t}\right). \tag{5.32}$$

By recasting Euler–Lagrange equations in normal form, we have ensured that the existence and uniqueness theorem holds, once some initial (Cauchy) data are fixed. Therefore, it is possible to conclude that the least action principle implies that the *mechanical determinism law* holds: its initial Lagrangian coordinates and velocities uniquely determine the evolution of the dynamical system.

5.2.3 Kinetic and Potential Energy in Constrained Multi-body Systems

In this section, an important result due to Hamilton (the so-called *Hamilton principle*) will be discussed: for every finite-dimensional multi-body dynamical system which is under the effects of conservative forces and which is subject to friction-free constraints, a least action principle is equivalent to the cardinal equations of dynamics. We observe that neglecting friction in engineering applications leads to underestimating the capability to endure external loads. Moreover, note that Hamilton's principle does not imply that an action for non-conservative systems cannot be found (an example has been provided in the previous subsection).

Let S be a dynamical system made of N constrained bodies with n degrees of freedom. Let us introduce the n-tuple of Lagrangian coordinates $\mathbf{q}$ so that the position of each material point P of such a multi-body system is given by a relation like:

$$\mathbf{r}_P = \mathbf{r}_P(\mathbf{q}, t). \tag{5.33}$$

This function $\mathbf{r}$, which associates with any triple $(P, \mathbf{q}, t)$ the corresponding position $\mathbf{r}_P(\mathbf{q}, t)$, is called the *configuration function* of the system S. By considering a motion $\mathbf{q}(t)$ of S, it is possible to express the velocity field $\mathbf{v}(P, \mathbf{q}, \dot{\mathbf{q}}, t)$ of the system in terms of $\mathbf{r}_P(\mathbf{q}, t)$ by:

$$\mathbf{v}(P, \mathbf{q}, \dot{\mathbf{q}}, t) := \frac{d}{dt}\mathbf{r}_P(\mathbf{q}(t), t) = \frac{\partial \mathbf{r}_P(\mathbf{q}(t), t)}{\partial t} + \frac{\partial \mathbf{r}_P(\mathbf{q}(t), t)}{\partial \mathbf{q}}\dot{\mathbf{q}}. \tag{5.34}$$

Analogously, it is possible to express the acceleration field $\mathbf{a}(P, \mathbf{q}, \dot{\mathbf{q}}, \ddot{\mathbf{q}}, t)$ by means of the configuration function $\mathbf{r}_P(\mathbf{q}, t)$ as:

$$\begin{aligned}\mathbf{a}(P, \mathbf{q}, \dot{\mathbf{q}}, \ddot{\mathbf{q}}, t) :&= \frac{d}{dt}\mathbf{v}(P, \mathbf{q}, \dot{\mathbf{q}}, t) \\ &= \frac{\partial \mathbf{r}_P(\mathbf{q}(t), t)}{\partial \mathbf{q}}\ddot{\mathbf{q}} + \dot{\mathbf{q}}^T \frac{\partial^2 \mathbf{r}_P(\mathbf{q}(t), t)}{\partial \mathbf{q}^2}\dot{\mathbf{q}} + \frac{\partial^2 \mathbf{r}_P(\mathbf{q}(t), t)}{\partial \mathbf{q}\partial t}\dot{\mathbf{q}} \\ &\quad + \frac{\partial^2 \mathbf{r}_P(\mathbf{q}(t), t)}{\partial t \partial \mathbf{q}}\dot{\mathbf{q}} + \frac{\partial \mathbf{r}_P(\mathbf{q}(t), t)}{\partial t^2}.\end{aligned} \tag{5.35}$$

A constraint for which a configuration $\bar{\mathbf{q}}$ such that

$$\frac{\partial \mathbf{r}_P(\bar{\mathbf{q}})}{\partial t} \neq 0 \tag{5.36}$$

exists, will be called a *time dependent constraint*. Let us now consider a configuration $\mathbf{q}^*$. We will define *virtual displacements* of S starting from $\mathbf{q}^*$, using the following functions:

$$\delta \mathbf{r}_P(\mathbf{q}^*, \delta \mathbf{q}, t) = \sum_{h=1}^{n} \frac{\partial \mathbf{r}_P(\mathbf{q}^*, t)}{\partial q_h}\delta q_h = \frac{\partial \mathbf{r}_P(\mathbf{q}^*, t)}{\partial \mathbf{q}}\delta \mathbf{q}\,. \tag{5.37}$$

Therefore, we will define the *set of virtual displacements* of S, around the configuration $\mathbf{q}^*$ as the set of displacement fields obtained by varying $\delta \mathbf{q}$ in (5.37). Note that these displacement fields are obtained by varying the Lagrangian and by keeping fixed the constraints at the instant t.

Let us consider a generic element C_i (i = 1,...,N) of the multi-body system S and the velocity field $\mathbf{v}(P, t)$. We define the *kinetic energy* of S as

$$T = \sum_{i=1}^{N} \frac{1}{2} \int_{C_i} \mathbf{v}(P, t) \cdot \mathbf{v}(P, t)\, dm_P\,, \tag{5.38}$$

where dm_P denotes the mass density of the point P. By replacing the velocity field in the previous equation with its explicit expression, we get:

$$T = \frac{1}{2} \sum_{i=1}^{N} \int_{C_i} \left[\frac{\partial \mathbf{r}_P}{\partial q_h}\dot{q}_h + \frac{\partial \mathbf{r}_P}{\partial t}\right] \cdot \left[\frac{\partial \mathbf{r}_P}{\partial q_k}\dot{q}_k + \frac{\partial \mathbf{r}_P}{\partial t}\right] dm_P\,. \tag{5.39}$$

Since the Lagrangian velocity $\dot{\mathbf{q}}$ is independent of P, it is possible to express the *kinetic energy in Lagrangian form* as

$$T = \frac{1}{2} a_{hk}(\mathbf{q}, t)\dot{q}_h\dot{q}_k + b_h(\mathbf{q}, t)\dot{q}_h + b_0(\mathbf{q}, t)\,, \tag{5.40}$$

where:

$$a_{hk}(\mathbf{q}, t) := \sum_{i=1}^{N} \int_{C_i} \left(\frac{\partial \mathbf{r}_P}{\partial q_h} \cdot \frac{\partial \mathbf{r}_P}{\partial q_k}\right) dm_P\,, \tag{5.41}$$

$$b_h(\mathbf{q},t) := \sum_{i=1}^{N} \int_{C_i} \left(\frac{\partial \mathbf{r}_P}{\partial q_h} \right) \cdot \frac{\partial \mathbf{r}_P}{\partial t}\, dm_P\,, \tag{5.42}$$

$$b_0(\mathbf{q},t) := \frac{1}{2} \sum_{i=1}^{N} \int_{C_i} \frac{\partial \mathbf{r}_P}{\partial t} \cdot \frac{\partial \mathbf{r}_P}{\partial t}\, dm_P\,. \tag{5.43}$$

If we assume that constraints are independent of time and by denoting with $A = a_{hk}$ the *kinetic energy matrix*, we can write Eq. (5.40) as

$$T = \frac{1}{2} \dot{\mathbf{q}}^T A \dot{\mathbf{q}} = \frac{1}{2} a_{hk}(\mathbf{q},t) \dot{q}_h \dot{q}_k, \tag{5.44}$$

where we notice that

- due to the scalar product symmetry, $A = A^T$;
- in general, A will depend on the system configuration;
- A is positive definite.

Moreover, from Eq. (5.44) we can deduce that, in order to determine the expression of the kinetic energy in Lagrangian form, one has to furnish:

- the kinematics and the geometrical structure of the system in terms of the configuration functions;
- the bodies' mass distribution of S.

Let us state the following theorem:

THEOREM 5.3 ***Kinetic energy theorem.*** *The kinetic energy's first variation, relative to an admissible variation of the motion $\delta\boldsymbol{q}(t)$ and valued for the motion $\boldsymbol{q}^*(t)$, is equal to the work done by inertial forces on the virtual displacement $\delta \boldsymbol{r}_P(\boldsymbol{q}^*, \delta\boldsymbol{q}(t), t)$. Namely:*

$$\begin{aligned} &\delta \left(\int_{t_0}^{t_1} T(\boldsymbol{q}(t), \dot{\boldsymbol{q}}(t), t)\, dt \right) \Bigg|_{\boldsymbol{q}^*} \\ &\quad = \int_{t_0}^{t_1} \left(\sum_{i=1}^{N} \int_{C_i} -\boldsymbol{a}(P, \boldsymbol{q}^*, \dot{\boldsymbol{q}}^*, t) \cdot \delta \boldsymbol{r}_P(\boldsymbol{q}^*, \delta\boldsymbol{q}(t), t)\, dm_P \right) dt\,. \end{aligned} \tag{5.45}$$

Proof Let us begin by applying the Euler–Lagrange theorem to compute the kinetic energy's first variation:

$$\delta \left(\int_{t_0}^{t_1} T(\mathbf{q}(t), \dot{\mathbf{q}}(t), t) \mathrm{d}t \right) \Bigg|_{\mathbf{q}^*} = \int_{t_0}^{t_1} \left[\left(\frac{\partial T}{\partial \mathbf{q}} - \frac{\mathrm{d}}{\mathrm{d}t} \left(\frac{\partial T}{\partial \dot{\mathbf{q}}} \right) \right)_{\mathbf{q}^*} \cdot \delta \mathbf{q}(t) \right] \mathrm{d}t. \tag{5.46}$$

Subsequently, let us consider the following equalities obtained by definitions (5.38) and (5.34)

$$\frac{\partial T}{\partial \mathbf{q}} = \sum_{i=1}^{N} \int_{C_i} \frac{\partial \mathbf{v}(P,t)}{\partial \mathbf{q}} \cdot \mathbf{v}(P,t) \mathrm{d}m_P, \tag{5.47}$$

$$\frac{\partial T}{\partial \dot{\mathbf{q}}} = \sum_{i=1}^{N} \int_{C_i} \frac{\partial \mathbf{v}(P,t)}{\partial \dot{\mathbf{q}}} \cdot \mathbf{v}(P,t) \mathrm{d}m_P = \sum_{i=1}^{N} \int_{C_i} \frac{\partial\, \mathbf{r}_P\, (\mathbf{q}(t),t)}{\partial\, \mathbf{q}} \cdot \mathbf{v}(P,t) \mathrm{d}m_P, \tag{5.48}$$

$$\frac{\mathrm{d}}{\mathrm{d}t}\left(\frac{\partial T}{\partial \dot{\mathbf{q}}}\right) = \sum_{i=1}^{N}\int_{C_i}\frac{\partial \mathbf{r}_P\left(\mathbf{q}(t),t\right)}{\partial \mathbf{q}}\cdot\mathbf{a}(P,t)\mathrm{d}m_P + \sum_{i=1}^{N}\int_{C_i}\frac{\partial \mathbf{v}_P\left(\mathbf{q}(t),t\right)}{\partial \mathbf{q}}\cdot\mathbf{v}(P,t)\mathrm{d}m_P, \tag{5.49}$$

$$\frac{\partial T}{\partial \mathbf{q}} - \frac{\mathrm{d}}{\mathrm{d}t}\left(\frac{\partial T}{\partial \dot{\mathbf{q}}}\right) = \sum_{i=1}^{N}\int_{C_i} -\mathbf{a}(P,t)\cdot\frac{\partial\, \mathbf{r}_P\left(\mathbf{q}(t),t\right)}{\partial\, \mathbf{q}}\mathrm{d}m_P. \tag{5.50}$$

To get (5.45) it is now sufficient to multiply both sides of (5.50) by $\delta\mathbf{q}(t)$, to integrate on the interval $[t_0, t_1]$ and to recall (5.37). □

Let us now introduce a system of forces Σ, whose density is $d\mathbf{f}_P(\mathbf{q}^*, \dot{\mathbf{q}}^*, t)$, which act, at instant t, on a generic point P of S. The system of forces Σ does work on the virtual displacement $\delta\mathbf{r}_P(\mathbf{q}^*, \delta\mathbf{q}, t)$ which is equal to

$$\mathscr{L}^{(\Sigma)} = \sum_{i=1}^{N}\int_{C_i} d\mathbf{f}_P(\mathbf{q}^*, \dot{\mathbf{q}}^*, t)\cdot\delta\mathbf{r}_P(\mathbf{q}^*, \delta\mathbf{q}, t)\, dV =: \mathbf{Q}(\mathbf{q}^*, \dot{\mathbf{q}}^*, t)\cdot\delta\mathbf{q}\,, \tag{5.51}$$

where we have indicated with $\mathbf{Q}(\mathbf{q}^*, \dot{\mathbf{q}}^*, t)$ the *vector of the Lagrangian components of* Σ. In components, it reads:

$$Q_h(\mathbf{q}^*, \dot{\mathbf{q}}^*, t) := \sum_{i=1}^{N}\int_{C_i} d\mathbf{f}_P(\mathbf{q}^*, \dot{\mathbf{q}}^*, t)\cdot\frac{\partial \mathbf{r}_P(\mathbf{q}^*, t)}{\partial q_h}\, dV\,. \tag{5.52}$$

If the Lagrangian components of a system of forces Σ do not depend on the Lagrangian velocities and if it is possible to find a *potential energy*, i.e. a scalar function $U(\mathbf{q}^*, t)$ such that

$$Q_h(\mathbf{q}^*, t) = -\frac{\partial U(\mathbf{q}^*, t)}{\partial q_h}\,, \tag{5.53}$$

then the system is said to be *conservative*. After having introduced all the preparatory definitions, we are ready to state *Hamilton's theorem*:

THEOREM 5.4 ***On the existence of an action for a multi-body finite-dimensional constrained system.*** *Given a multi-body finite-dimensional system, in the presence of ideal constraints and under the action of conservative forces, the principle of stationary action is equivalent to Kirchhoff's law and cardinal equations of dynamics, and the Lagrangian function is defined as the difference between kinetic energy and potential energy.*

Proof In the full general case, the proof of this theorem is quite cumbersome in the context of Noll's axiomatic framework,[5] which we have temporarily adopted. For the sake of clarity, we discuss the case of a dynamical system S, made up of N bodies C_i $(i = 1, \ldots, N)$ that undergo only rigid motions. Let us consider the function $\mathbf{q}^*(t)$ which describes the motion of S in a time interval $[t_0, t_1]$, once the initial configuration

[5] In this axiomatic framework, the force is considered as a primitive quantity, while the power is a derived concept.

and velocity of the system have been fixed. For each body C_i, the cardinal equations of dynamics hold:

$$\begin{cases} 0 = R_i^* = R_i^{(a)} + R_i^{(v)} + R_i^{(m)} \\ 0 = M_i^* = M_i^{(a)} + M_i^{(v)} + M_i^{(m)}, \end{cases} \tag{5.54}$$

where R_i^* and M_i^* represent the total force and the total moment applied to C_i during the motion $\mathbf{q}^*(t)$, respectively. In particular, the terms $R_i^{(m)}$ and $M_i^{(m)}$ describe the contributions given by inertial forces, $R_i^{(a)}$ and $M_i^{(a)}$ are the resultant force and moment due to the active forces, and $R_i^{(v)}$ and $M_i^{(v)}$ are related to constrained forces and can be determined by the Kirchhoff's postulate. At instant t, let us consider an admissible variation $\delta\mathbf{q}(t)$ of the Lagrangian coordinates, compatible with the constraints, around $\mathbf{q}^*$ and the associated virtual displacement field $\delta\mathbf{r}_P(\mathbf{q}^*(t), \delta\mathbf{q}(t), t)$. Since we are limiting the proof only to rigid motion, such a virtual displacement will result in an infinitesimal rotation $\delta\varphi_i(\mathbf{q}^*(t), \delta\mathbf{q}(t), t)$ for each body C_i. If we consider now a material point O_i of C_i and its displacement $\delta\mathbf{r}_{O_i}(\mathbf{q}^*(t), \delta\mathbf{q}(t), t)$, we can compute the following scalar product:

$$\begin{cases} 0 = (R_i^{(a)} + R_i^{(v)} + R_i^{(m)}) \cdot \delta\mathbf{r}_{O_i}(\mathbf{q}^*(t), \delta\mathbf{q}(t), t) \\ 0 = (M_i^{(a)} + M_i^{(v)} + M_i^{(m)}) \cdot \delta\varphi_i(\mathbf{q}^*(t), \delta\mathbf{q}(t), t). \end{cases} \tag{5.55}$$

By considering the sum over all the bodies and by recalling the expression for the work done on a rigid displacement, (5.51), Eq. (5.55) reads

$$\mathfrak{L}^{(a)} + \mathfrak{L}^{(v)} + \mathfrak{L}^{(m)} = 0\,, \tag{5.56}$$

where $\mathfrak{L}^{(a)}$, $\mathfrak{L}^{(v)}$, and $\mathfrak{L}^{(m)}$ are the work done by active forces on the virtual displacement field $\delta\mathbf{r}_P(\mathbf{q}^*, \delta\mathbf{q}(t), t)$ of S, by constraint reactions, and by inertial forces, respectively. Since we are in the presence of ideal constraints, we can set $\mathfrak{L}^{(v)} = 0$ and write the *symbolic D'Alembert's relation* as

$$\mathfrak{L}^{(a)} + \mathfrak{L}^{(m)} = 0\,, \tag{5.57}$$

which can be read as: *the work done by inertial forces is equal to the work done by active forces on virtual displacement, taken with opposite sign.* Moreover, if we assume that the system is at rest in a configuration $\mathbf{q}^*(t) = \bar{\mathbf{q}}$, inertial forces vanish and Eq. (5.57) reduces to:

$$\mathfrak{L}^{(a)} = 0\,. \tag{5.58}$$

This last relation can be rephrased as: *in the presence of ideal constraints, the work done by a system of active forces on a virtual displacement is zero when starting from an equilibrium condition.*[6] The theorem is proved if we consider the following Lagrangian function:

$$\mathscr{L}(\mathbf{q}, \dot{\mathbf{q}}, t) = T(\mathbf{q}, \dot{\mathbf{q}}, t) - U(\mathbf{q}, t)\,. \tag{5.59}$$

[6] In his *On the Equilibrium*, Archimedes repeatedly uses Eq. (5.58), in particular to deduce equilibrium laws for levers.

Indeed, by means of Eqs. (5.51) and (5.53), the first variation of the action associated with this Lagrangian function reads:

$$\delta\mathfrak{A}\big|_{\mathbf{q}^*} = \int_{t_0}^{t_1} \left(\mathfrak{L}^{(a)} + \mathfrak{L}^{(m)}\right) dt\,. \tag{5.60}$$

□

5.2.4 Motions about a Stable Equilibrium Configuration

In this subsection, we will analyze the useful subclass of motions which are constant functions with respect to the time variable. The system considered for these motions will remain in the same configuration for every instant of time. D'Alembert and Lagrange explicitly established that the laws of mechanics could be formulated to give a unified description of both static and dynamic phenomena, where the latter are those phenomena in which the relevant system changes its configuration in time. As already stressed in the introduction of this chapter, after the foundation of analytic mechanics the division of mechanics into statics and dynamics does not make sense any more, at least at the axiomatic formulation level.

Once an external action is assigned, some equilibrium configurations could exist. If the system has zero velocity in this configuration, it will remain in such a a configuration indefinitely in time. It is possible to distinguish equilibrium configurations as "stable" or "unstable": in particular, we will say that an equilibrium configuration is stable if *small* variations of the equilibrium configuration of the system correspond to a motion of the system confined within a *small* neighborhood of the equilibrium configuration. Dirichlet, in order to characterize stable equilibrium configurations, conjectured that the positions of stable equilibrium were minima for the potential energy and vice versa.

To sketch a satisfactory proof of this conjecture, we need to introduce sound definitions for equilibrium positions and their stability. For simplicity we will restrict the analysis to time independent Lagrangian functions:

$$\mathscr{L} : \mathbf{q} \longmapsto T(\mathbf{q}, \dot{\mathbf{q}}) - U(\mathbf{q})\,. \tag{5.61}$$

A configuration $\mathbf{q}_0$ such that the motion $\mathbf{q} : t \mapsto \mathbf{q}_0$ is a solution of the Euler–Lagrange equations is said to be an *equilibrium configuration*. More precisely, one can prove the following proposition:

PROPOSITION 5.2 *A configuration $\boldsymbol{q}_0$ is an equilibrium configuration if and only if*

$$\left.\frac{\partial U}{\partial \mathbf{q}}\right|_{\mathbf{q}_0} = 0\,. \tag{5.62}$$

Proof Proof of the direction $\Rightarrow$. Since

$$\frac{\partial U}{\partial \dot{\mathbf{q}}} = 0 \Rightarrow \frac{\mathrm{d}}{\mathrm{d}t}\left(\frac{\partial \mathscr{L}}{\partial \dot{\mathbf{q}}}\right) = \frac{\mathrm{d}}{\mathrm{d}t}\left(\frac{\partial T}{\partial \dot{\mathbf{q}}}\right), \quad \frac{\mathrm{d}}{\mathrm{d}t}\left(\frac{\partial \mathscr{L}}{\partial \dot{\mathbf{q}}}\right)\bigg|_{\mathbf{q}_0} - \left.\frac{\partial \mathscr{L}}{\partial \mathbf{q}}\right|_{\mathbf{q}_0} = 0, \tag{5.63}$$

we have:

$$\left[\frac{\mathrm{d}}{\mathrm{d}t}\left(\frac{\partial T}{\partial \dot{\mathbf{q}}}\right) - \frac{\partial T}{\partial \mathbf{q}} + \frac{\partial U}{\partial \mathbf{q}}\right]\Bigg|_{\mathbf{q}_0} = 0. \tag{5.64}$$

Recalling (5.44), we get:

$$\begin{aligned} &\frac{\mathrm{d}}{\mathrm{d}t}\left(\frac{\partial T}{\partial \dot{q}_h}\right)\Bigg|_{\mathbf{q}(t)=q_0} = \sum_{k=1}^{n}\sum_{l=1}^{n}\frac{\partial a_{hk}}{\partial q_l}\dot{q}_l\dot{q}_k + \sum_{k=1}^{n} a_{hk}\,(q)\,\ddot{q}_k\Bigg|_{\mathbf{q}(t)=\mathbf{q}_0} = 0 \\ &\frac{\partial T}{\partial q_r}\Bigg|_{\mathbf{q}(t)=\mathbf{q}_0} = \sum_{h=1}^{n}\sum_{k=1}^{n}\frac{\partial\, a_{hk}}{\partial\, q_r}\dot{q}_h\dot{q}\Bigg|_{\mathbf{q}(t)=\mathbf{q}_0} = 0. \end{aligned} \tag{5.65}$$

Hence, if $\mathbf{q}_0$ is an equilibrium position, (5.64) implies:

$$\frac{\partial U}{\partial \mathbf{q}}\Bigg|_{\mathbf{q}_0} = 0. \tag{5.66}$$

Proof of the direction $\Leftarrow$. If $\frac{\partial U}{\partial \mathbf{q}} = 0$, Euler–Lagrange equations are immediately fulfilled by $\mathbf{q}(t) = \mathbf{q}_0$ because, as was seen before, $\frac{\mathrm{d}}{\mathrm{d}t}\left(\frac{\partial T}{\partial \dot{\mathbf{q}}}\right)$ and $\frac{\partial T}{\partial \mathbf{q}}$ are equal to zero. □

PROPOSITION 5.3 *The configuration $\boldsymbol{q}^*$ is said to be a Lyapunov stable equilibrium configuration if:*

$$\begin{aligned} &\forall \epsilon > 0,\ \exists \delta_p(\epsilon, \boldsymbol{q}^*),\ \delta_v(\epsilon, \boldsymbol{q}^*) \in \mathbb{R}^+ : \| \boldsymbol{q}_0 - \boldsymbol{q}^* \| < \delta_p(\epsilon, \boldsymbol{q}^*),\ \| \dot{\boldsymbol{q}}_0 \| < \delta_v(\epsilon, \boldsymbol{q}^*) \\ &\qquad \Longrightarrow \quad \| \boldsymbol{q}(t, \boldsymbol{q}_0, \dot{\boldsymbol{q}}_0) - \boldsymbol{q}^* \| < \epsilon,\ \| \dot{\boldsymbol{q}}(t, \boldsymbol{q}_0, \dot{\boldsymbol{q}}_0) \| < d^*\epsilon,\ \forall t \in \mathbb{R}^+, \end{aligned} \tag{5.67}$$

where we have indicated with $\boldsymbol{q}(t, \boldsymbol{q}_0, \dot{\boldsymbol{q}}_0)$ the motion of S associated with the initial data $\boldsymbol{q}_0$ and $\dot{\boldsymbol{q}}_0$, while the dimensional factor d^* depends on the system S and on the configuration $\boldsymbol{q}^*$. We will denote stability coefficients for S by the coefficients $\delta_p(\epsilon, \boldsymbol{q}^*)$ and $\delta_v(\epsilon, \boldsymbol{q}^*)$.

Although this definition may seem too abstract, it is strongly motivated by applications and allows a precise formulation of important engineering problems. For instance, let us consider the equilibrium configuration e of a reticular structure S which is subject to an operating load. Let us denote with $\bar{\delta}_p$ and $\bar{\delta}_v$ the maximum expected displacements and impulses induced by a further load[7] applied to S. Moreover, let ϵ be a measure of the maximum tolerable displacement. In order for S to be safe, we require that e is a stable equilibrium configuration in the sense of the Lyapunov definition. Namely, it is required that, at least for the considered perturbation, S does not go "too far" from e. Furthermore, a safe design will require also a quantitative estimate of the values of stability coefficients $\delta_p(\epsilon, \mathbf{q}^*)$ and $\delta_v(\epsilon, \mathbf{q}^*)$, in such a way as to verify the supplementary condition

$$\bar{\delta}_p \leq \alpha\delta_p(\epsilon, \mathbf{q}^*), \quad \bar{\delta}_v \leq \alpha\delta_v(\epsilon, \mathbf{q}^*), \tag{5.68}$$

[7] We consider, for the time being, only stationary loads applied starting from a fixed instant t_0 or impulses applied at the instant t_0 as well.

where $\alpha < 1$ is a suitable safety coefficient. Finally, let us introduce another stability criterion formulated by Dirichlet:

PROPOSITION 5.4 ***Dirichlet's stability criterion.*** *$\boldsymbol{q}^*$ is a stable equilibrium configuration if $\boldsymbol{q}^*$ is a minimum point for U.*

The converse of this stability criterion is not easy to demonstrate. However, it is possible to prove that

PROPOSITION 5.5 *$\mathbf{q}^*$ is a minimum point for U if $\mathbf{q}^*$ is a stable equilibrium configuration and $U \in C^3$.*

5.2.5 Resonance Phenomena and Linearization

Ensuring that a given structure S is in a stable equilibrium configuration under operating conditions and that its stability coefficients verify (5.68) is not sufficient to exclude that a given periodic perturbation, even of small amplitude, could imperil its stability. Indeed, it has been experimentally verified that, if the perturbation frequency equals one of the natural oscillation frequencies of the system which it is applied to, then, independently of its amplitude, resonance phenomena occur. Such phenomena, which lead to an unbounded growth in time of the amplitude of oscillations induced by the perturbation, are often really dangerous: as an example, consider the unforeseen oscillations induced on the Tacoma bridge by the winds blowing in the throat below the bridge.

In order to address this problem, it is convenient to assume that the perturbations around the equilibrium position are *small*. More formally, there exists a neighborhood of a stable equilibrium configuration, characterized by a diameter ϵ, in which all the trajectories of such motions are contained. Moreover, we set a bound from above on the Lagrangian velocity by requiring:

$$\| \dot{\mathbf{q}}(t, \mathbf{q}_0, \dot{\mathbf{q}}_0) \| < \eta \,. \tag{5.69}$$

Mathematically, we are allowed to consider an approximation of the Euler–Lagrange equations' solutions by neglecting all the $O(\eta^2)$ terms. The introduction of the dimensionless parameter η, which ensures that the intensity of the perturbation can be controlled, is the first step of a linearization procedure which gives rise to the following form of the Euler–Lagrange equations, namely the Cauchy problem:

$$\begin{cases} \dfrac{d}{dt}\left(\dfrac{\partial \mathscr{L}}{\partial \dot{\mathbf{q}}}\right) - \dfrac{\partial \mathscr{L}}{\partial \mathbf{q}} = \eta \mathbf{Q}_0(t) + \mathbf{Q}_1(t)(\mathbf{q} - \mathbf{q}^*) + \mathbf{Q}_2(t)\dot{\mathbf{q}}\,, \\ \mathbf{q}(t_0) = \mathbf{q}^* + \eta \mathbf{p}_0, \quad \dot{\mathbf{q}}(t_0) = \eta \dot{\mathbf{p}}_0, \end{cases} \tag{5.70}$$

where in the r.h.s. of the first of Eqs. (5.70) $\mathbf{Q}_0$ is the vector of Lagrangian components of the perturbation applied to the system and $\mathbf{Q}_1(t)$ and $\mathbf{Q}_2(t)$ are linear maps having as arguments $(\mathbf{q} - \mathbf{q}^*)$ and $\dot{\mathbf{q}}$, respectively. We have enough ingredients to formalize the hypothesis of small motions of a Lagrangian system. In particular, we will assume that the following expressions hold for the solution $\mathbf{q}(\cdot)$ of the system (5.70):

$$\begin{aligned}\mathbf{q}(t) &= \mathbf{q}^* + \eta\mathbf{p}(t, \mathbf{p}_0, \dot{\mathbf{p}}_0, \mathbf{Q}_i(\cdot)) + O(\eta^2)\,,\\ \dot{\mathbf{q}}(t) &= \eta\dot{\mathbf{p}}(t, \mathbf{p}_0, \dot{\mathbf{p}}_0, \mathbf{Q}_i(\cdot)) + O(\eta^2)\,,\\ \ddot{\mathbf{q}}(t) &= \eta\ddot{\mathbf{p}}(t, \mathbf{p}_0, \dot{\mathbf{p}}_0, \mathbf{Q}_i(\cdot)) + O(\eta^2)\,,\end{aligned} \tag{5.71}$$

where $i = 0, 1, 2$. Therefore, the following proposition holds:

PROPOSITION 5.6 ***Equation of small motions around a stable equilibrium position.*** *The differential equation in* (5.70) *can be written in terms of* $\boldsymbol{p}(t, \boldsymbol{p}_0, \dot{\boldsymbol{p}}_0, \boldsymbol{Q}_i(\cdot))$ *as*

$$\boldsymbol{K}^*\boldsymbol{p} + \boldsymbol{A}^*\ddot{\boldsymbol{p}} = \boldsymbol{Q}_0(t) + \boldsymbol{Q}_1(t)\boldsymbol{p} + \boldsymbol{Q}_2(t)\dot{\boldsymbol{p}}\,, \tag{5.72}$$

where the matrix $\boldsymbol{A}^*$ *describes the kinetic energy valued in* $\boldsymbol{q}^*$*, and the matrix* $\boldsymbol{K}^*$ *is the stiffness of the system S and can be related to the potential energy by*

$$K^*_{hk} = \left.\frac{\partial^2 U}{\partial q_h \partial q_k}\right|_{\boldsymbol{q}^*}. \tag{5.73}$$

Moreover, in order to verify the second of Eqs. (5.70), the following relations hold:

$$\boldsymbol{p}(t_0, \boldsymbol{p}_0, \dot{\boldsymbol{p}}_0, \boldsymbol{Q}_i(\cdot)) = \boldsymbol{p}_0, \quad \dot{\boldsymbol{p}}(t_0, \boldsymbol{p}_0, \dot{\boldsymbol{p}}_0, \boldsymbol{Q}_i(\cdot) = \dot{\boldsymbol{p}}_0\,. \tag{5.74}$$

Proof Since $\mathbf{q}^*$ is an equilibrium configuration and performing the Taylor series expansion with initial point $\mathbf{q}^*$ where it is required, we have the equalities:

$$\frac{\partial U(\mathbf{q})}{\partial q_h} = \left.\frac{\partial U}{\partial q_h}\right|_{\mathbf{q}^*} + \sum_{k=1}^{n} \left.\frac{\partial^2 U}{\partial q_h \partial q_k}\right|_{\mathbf{q}^*} \left(q_k - q_k^*\right) + O(\eta^2) = \eta \sum_{k=1}^{n} K^*_{hk} p_k + O(\eta^2), \tag{5.75}$$

$$\frac{\partial T(\mathbf{q})}{\partial q_r} = \frac{\partial}{\partial q_r}\left(\frac{1}{2}\sum_{h=1}^{n}\sum_{k=1}^{n} a_{hk}(\mathbf{q})\dot{q}_h\dot{q}_k\right) = \frac{1}{2}\sum_{h=1}^{n}\sum_{k=1}^{n}\frac{\partial a_{hk}(\mathbf{q})}{\partial q_r}\dot{q}_h\dot{q}_k + O(\eta^2), \tag{5.76}$$

$$a_{hk}(\mathbf{q}) = a_{hk}(\mathbf{q}^*) + \sum_{j=1}^{n} \left.\frac{\partial a_{hk}}{\partial q_j}\right|_{\mathbf{q}^*} \left(q_j - q_j^*\right) + O(\eta^2) \Rightarrow \mathbf{A}(\mathbf{q}) = \mathbf{A}^* + O(\eta), \tag{5.77}$$

$$\frac{\mathrm{d}}{\mathrm{d}t}\left(\frac{\partial T}{\partial \dot{\mathbf{q}}}\right) = \frac{\mathrm{d}}{\mathrm{d}t}\left[\mathbf{A}(\mathbf{q})\dot{\mathbf{q}}\right] = \mathbf{A}(\mathbf{q})\ddot{\mathbf{q}} + \dot{\mathbf{q}}^{\mathrm{T}}\frac{\partial \mathbf{A}(\mathbf{q})}{\partial \mathbf{q}}\dot{\mathbf{q}} = \eta\mathbf{A}^*\ddot{\mathbf{p}} + O(\eta^2). \tag{5.78}$$

Recalling (5.61), substituting the expansions found in the right-hand side of the first equation in (5.70) and considering the linear (in η) coefficient, we get (5.72).[8] □

[8] The computation of $\dfrac{\partial T}{\partial \dot{\mathbf{q}}}$ is simple (we recall that $a_{hk}(\mathbf{q})$ is symmetric):

$$\begin{aligned}\frac{\partial T}{\partial \dot{q}_l} &= \frac{1}{2}\sum_{h,k=1}^{n} a_{hk}(\mathbf{q})\frac{\partial}{\partial \dot{q}_l}\left(\dot{q}_h\dot{q}_k\right) = \frac{1}{2}\sum_{h,k=1}^{n} a_{hk}(\mathbf{q})\left(\frac{\partial \dot{q}_h}{\partial \dot{q}_l}\dot{q}_k + \dot{q}_h\frac{\partial \dot{q}_k}{\partial \dot{q}_l}\right)\\ &= \frac{1}{2}\sum_{h,k=1}^{n} a_{hk}(\mathbf{q})\left(\delta_{hl}\dot{q}_k + \dot{q}_h\delta_{kl}\right) = \frac{1}{2}\sum_{k=1}^{n}\left(a_{lk}(\mathbf{q})\dot{q}_k + a_{hl}(\mathbf{q})\dot{q}_h\right) = \sum_{k=1}^{n} a_{lk}(\mathbf{q})\dot{q}_k.\end{aligned}$$

Clearly, in the above proposition we did not prove (and it is not a trivial task) that the solution to the problem (5.70), can be well approximated by the solution of (5.72) for small values of η.

Note that one has to require that $\mathbf{q}^*$ is a stable equilibrium configuration in order to prove that the approximating function converges to the exact solution. The main reason is that, otherwise, even a small perturbation of the applied forces or of the initial data may make this analysis meaningless by moving the configuration of the system indefinitely far away from $\mathbf{q}^*$ the configuration of the system.

The linear system of equations (5.72) is an n-dimensional generalization of the harmonic oscillator equation. We will show now that, by requiring $\mathbf{q}^*$ to be a strict minimum point for the potential energy, $Q_1(t)$ to be symmetric, positive definite, independent of time, and $Q_2(t) = 0$, to solve Eq. (5.72) we have to solve a set of n uncoupled harmonic oscillators.

To simplify the notation, let us indicate

$$\text{Diag}\{\lambda_1, \lambda_2, \ldots, \lambda_n\} := \text{Diag}\{\lambda_i\} = \begin{pmatrix} \lambda_1 & 0 & \ldots & 0 \\ 0 & \lambda_2 & \ldots & 0 \\ \vdots & \vdots & \ddots & \vdots \\ 0 & 0 & \ldots & \lambda_n \end{pmatrix}, \tag{5.79}$$

where $\{\lambda_1, \lambda_2, \ldots, \lambda_n\}$ is an $n$tuple of scalar quantities. Let us observe that:

1. the matrix kinetic energy $\mathbf{A}^*$ valued in $\mathbf{q}^*$ is positive and, therefore, invertible;
2. $\mathbf{q}^*$ being a strict minimum of U, the matrix $\mathbf{K}^*$ is symmetric and positive;
3. the following proposition holds:

PROPOSITION 5.7 *A real matrix $\boldsymbol{C}$ is diagonalizable if it can be written as the product of two symmetric real matrices $\boldsymbol{A}$ and $\boldsymbol{B}^{-1}$, where is $\boldsymbol{B}$ positive definite.*

Proof Positive definiteness of $\mathbf{B}$ implies the existence of an orthogonal matrix $\mathbf{R}$ and of $n$tuple numbers $\left\{\beta_i^2\right\}$ such that

$$\mathbf{B} = \mathbf{R}^{\mathrm{T}} \left[\text{DIAG}\left\{\beta_i^2\right\}\right] \mathbf{R}.$$

To further lighten notation, we use the following definitions

$$\mathbf{D}^2 := \text{DIAG}\left\{\beta_i^2\right\}, \qquad \mathbf{D} := \text{DIAG}\left\{\beta_i\right\}.$$

As a consequence, we have

$$\mathbf{A} - \lambda\mathbf{B} = \mathbf{RD}\left(\mathbf{D}^{-1}\mathbf{R}^{\mathrm{T}}\mathbf{ARD}^{-1} - \lambda\mathbf{I}\right)\mathbf{DR}^{\mathrm{T}},$$

($\mathbf{I}$ being the identity matrix). By computing the determinant, we get

$$\det\left(\mathbf{A} - \lambda\mathbf{B}\right) = \left(\det\mathbf{R}\right)^2 \left(\det\mathbf{D}\right)^2 \det\left(\mathbf{P} - \lambda\mathbf{I}\right),$$

where we have introduced the symmetric matrix $\mathbf{P} := \mathbf{D}^{-1}\mathbf{R}^{\mathrm{T}}\mathbf{A}\mathbf{R}\mathbf{D}^{-1}$. Since

$$(\det \mathbf{R})^2 = 1, \qquad (\det \mathbf{D})^2 = \prod_{i=1}^{n} \beta_i^2, \tag{5.80}$$

the roots of the characteristic polynomial $\det(\mathbf{A} - \lambda\mathbf{B})$ coincide with those of the characteristic polynomial $\det(\mathbf{P} - \lambda\mathbf{I})$. Since the matrix $\mathbf{B}$ is invertible, those roots coincide also with those of the characteristic polynomial $\det\left(\mathbf{B}^{-1}\mathbf{A} - \lambda\mathbf{I}\right)$. Using again the theorem on the diagonalization of symmetric matrices, we infer that there exist exactly n real eigenvalues λ_i for the matrix $\mathbf{P}$ and each one of them is associated with an eigenvector $\mathbf{z}_i$, in such a way that the set $\{\mathbf{z}_i\}$ is a basis. Since we have

$$\mathbf{P}\mathbf{z}_i = \left(\mathbf{D}^{-1}\mathbf{R}^{\mathrm{T}}\mathbf{A}\mathbf{R}\mathbf{D}^{-1}\right)\mathbf{z}_i = \lambda_i \mathbf{z}_i,$$

it is easy to verify that

$$\mathbf{A}\left(\mathbf{R}\mathbf{D}^{-1}\mathbf{z}_i\right) = \lambda_i \mathbf{R}\mathbf{D}\mathbf{z}_i = \lambda_i \mathbf{R}\mathbf{D}\left(\mathbf{D}\mathbf{R}^{\mathrm{T}}\mathbf{R}\mathbf{D}^{-1}\right)\mathbf{z}_i = \lambda_i \mathbf{B}\left(\mathbf{R}\mathbf{D}^{-1}\mathbf{z}_i\right). \tag{5.81}$$

Therefore, we can conclude that the set $\{\lambda_i\}$ is the set of eigenvalues of the matrix $\mathbf{C} := \mathbf{B}^{-1}\mathbf{A}$ and that the eigenvectors associated with them are the vectors $\mathbf{x}_i := \mathbf{R}\mathbf{D}^{-1}\mathbf{z}_i$, respectively. Note that, the vector $\mathbf{z}_i$ being orthogonal and $\mathbf{R}\mathbf{D}^{-1}$ a nonsingular matrix, the set $\{\mathbf{x}_i\}$ is a basis. Clearly, the matrix $\mathbf{X}$, defined as the matrix whose columns are the eigenvectors $\mathbf{x}_i$, is nonsingular and it diagonalizes $\mathbf{C}$. Indeed, by (5.81), it is straightforward:

$$\mathbf{X}^{-1}\mathbf{C}\mathbf{X} = \textsc{Diag}\{\lambda_i\}.$$

In general, the matrix $\mathbf{X}$ is not orthogonal. Indeed, by the chain of equalities (where the symbol "$\cdot$" denotes the Euclidean inner product in $\mathbb{R}^n$)

$$0 = \mathbf{z}_i \cdot \mathbf{z}_j = \left(\mathbf{D}\mathbf{R}^{\mathrm{T}}\mathbf{x}_i\right) \cdot \left(\mathbf{D}\mathbf{R}^{\mathrm{T}}\mathbf{x}_j\right) = \mathbf{x}_i \cdot \mathbf{R}\mathbf{D}^2\mathbf{R}^{\mathrm{T}}\mathbf{x}_j = \mathbf{x}_i \cdot \mathbf{B}\mathbf{x}_j,$$

we deduce that the vectors of the basis $\{\mathbf{x}_i\}$ are orthogonal with respect to the inner product defined by

$$(\mathbf{x}, \mathbf{y}) = \mathbf{x} \cdot \mathbf{B}\mathbf{y}.$$

Finally, since the following equalities hold

$$\mathbf{A}\mathbf{x}_i = \lambda_i \mathbf{B}\mathbf{x}_i \Rightarrow \mathbf{x}_i \cdot \mathbf{A}\mathbf{x}_i = \lambda_i \mathbf{x}_i \cdot \mathbf{B}\mathbf{x}_i, \tag{5.82}$$

we notice that the function $\mathbf{A}$ is positive definite and, hence, all its eigenvalues λ_i are positive. □

Then, if we multiply Eq. (5.72) from the left by $(\mathbf{A}^*)^{-1}$, we get

$$\ddot{\mathbf{p}} = -(\mathbf{A}^*)^{-1}(\mathbf{K}^* + \mathbf{Q}_1)\mathbf{p} + (\mathbf{A}^*)^{-1}(\mathbf{Q}_0(t) + \mathbf{Q}_2(t)\dot{\mathbf{p}}), \tag{5.83}$$

which is in normal form. Let us denote $\mathbf{C} := (\mathbf{A}^*)^{-1}(\mathbf{Q}_1 + \mathbf{K}^*)$, and let us call $\mathbf{P}$ the matrix which diagonalizes $\mathbf{C}$, i.e. $\mathbf{P}^{-1}\mathbf{C}\mathbf{P} = \Lambda$, where $\Lambda = \mathrm{Diag}\{\lambda_i\}$ is a diagonal

matrix. We define the *system of modal coordinates for* $\mathbf{C}$ as the system obtained by the following transformation:

$$\zeta = \mathbf{P}^{-1}\mathbf{p}\,. \tag{5.84}$$

The existence of such a system of coordinates is ensured by the previous proposition. Indeed, the entries of Λ are the eigenvalues of $\mathbf{C}$, and the columns $\mathbf{u}_i$ of $\mathbf{P}$ are the corresponding eigenvectors. We note that $\mathbf{C}$ being positive definite, it has all positive eigenvalues. In the polar coordinate system, Eq. (5.83) can be recast as

$$\ddot{\zeta} = -\mathbf{P}^{-1}(\mathbf{A}^*)^{-1}(\mathbf{K}^* + \mathbf{Q}_1)\mathbf{P}\zeta + \mathbf{P}^{-1}(\mathbf{A}^*)^{-1}\left(\mathbf{Q}_0(t) + \mathbf{Q}_2(t)\mathbf{P}\dot{\zeta}\right), \tag{5.85}$$

that, when $\mathbf{Q}_2(t) = 0$, gives rise to n uncoupled equations

$$\ddot{\zeta}_i = -\lambda_i\zeta_i + \mathbf{f}_i(t)\,, \tag{5.86}$$

where $\mathbf{f}_i(t)$ represents the vector $\mathbf{P}^{-1}(\mathbf{A}^*)^{-1}\mathbf{Q}_0(t)$ components, which must be flanked with the initial data

$$\mathbf{P}^{-1}\mathbf{p}_0 = \zeta(t_0), \quad \mathbf{P}^{-1}\dot{\mathbf{p}}_0 = \mathbf{P}\dot{\zeta}(t_0)\,. \tag{5.87}$$

Hence, the eigenvectors of $\mathbf{C}$ will form the column of the matrix $\mathbf{P}$ and the pulsations of the set of harmonic oscillator (5.86) can be expressed in terms of its eigenvalues λ_i as

$$\sqrt{\lambda_1}, \ldots, \sqrt{\lambda_n}\,, \tag{5.88}$$

and are called *natural pulsations* of the system (5.83). The resulting solutions, written in terms of the modal coordinates, can be recast in terms of $\mathbf{p}(t)$ by means of Eq. (5.84). When a frequency related to one of the λ_i appears in the Fourier transform of $\mathbf{f}_i(t)$, both equations (5.86) show resonance phenomena: therefore, even for small (w.r.t. the parameter η) amplitude and if it acts for a sufficient time, the forcing term $\mathbf{Q}_0(t)$ will give rise to indefinitely large oscillations.

Let us end this section by remarking that, during the design phase of a structure which is subject to stationary loads, one should ensure that:

- it is in stable equilibrium configuration under operating conditions;
- the expected amplitude of the perturbation of the loads is sufficiently small, so that one can guarantee the effectiveness of the applied constraints;
- its natural frequencies are far from the expected frequencies of the perturbation.

5.3 Continuous and Discrete Modeling in Modern Mechanics

As anticipated in the previous section, it is possible to extend the aforementioned methods to continuous systems, namely systems described in terms of an infinite number of Lagrangian coordinates. A natural example is the description of the deformation of a material body which is assumed to be continuously distributed in a certain region of space. Roughly speaking, this assumption can be justified only if the description of the phenomenon is made "from far away enough" or, more rigorously, if the length-scale

of the phenomenon which we want to describe is larger than the (intrinsic) discrete nature of the body. Historically, from the beginning of the nineteenth century, continuum mechanics was probably developed as a powerful computational tool. Indeed, an "atomistic" (and in principle highly accurate) description of a complex system will often give rise to a huge number of (ordinary differential) equations of motion which, at that time, would need more than one life of the universe to be solved. On the other hand, one of the main advantages of a continuous description is that it furnishes a small set of partial differential equations which (hopefully) may be efficiently solved by using the tools of mathematical analysis. Within this paradigm, physics, mathematics, and engineering science were able to produce astonishing results, enhancing the technological possibilities open to humankind. However, by looking for the mathematical description of more complex systems, some limits of continuum modeling started to appear, mainly due to the limitations on solutions in a closed form (i.e. as combinations of known functions). Actually, the subsequent technological advancements were possible mainly thanks to the support of the (discrete) numerical methods which the Von Neumann machines were able to perform. Discrete models again became a useful tool.

The recent development of the field of metamaterials has again fueled interest in the relationship between continuous and discrete modeling. A metamaterial[9] is a dynamical system engineered to show exotic behaviors. It is characterized by a multi-scale description given in terms of (at least) two different length-scales: one which characterizes a (often periodic) discrete microstructure and one which describes its macroscopic (continuous) behavior. Its unusual macroscopic behavior is originated by the particular arrangement of the microstructure and, mathematically, it can be forecast by means of the so-called *homogenization procedures* (see [78–84] for relevant examples) which relate the behavior of the microstructure, described in terms of a discrete Lagrangian system, to the macroscopic description of the metamaterial, given in terms of a infinite dimensional Lagrangian system. Usually, these procedures are based on the following steps:

1. A discrete Lagrangian model is introduced to describe the microstructure of the metamaterial. It amounts to choosing a finite set of suitable Lagrangian coordinates (see the previous section);
2. By applying the principle of virtual work, the variation of a suitable energy functional is performed;
3. Suitable macroscopic Lagrangian coordinates describing the continuous model have to be introduced;
4. A micro–macro correspondence between the Lagrangian coordinates of the microstructure and of the continuous model has to be introduced;[10]
5. By assuming the equivalence between microscopic and macroscopic virtual works, the constitutive equations given in terms of the macroscopic Lagrangian coordinates are obtained.

[9] In this work, we refer to the so-called *mechanical metamaterials*, namely those metamaterials characterized by a microstructure made of mechanical elements like springs, bars, beams, pivots, etc.

[10] This step is known as *Piola's ansatz*.

Usually, since the continuous models arising from a microstructure often have a high level of complexity, it is not possible to solve the associated Euler–Lagrange equations by means of the tools of mathematical analysis, i.e. it is not possible to find a closed form of the solution of such partial differential equations. One of the main reasons is that, for partial differential equations, existence and uniqueness cannot be investigated by means of general theorems like Picard's theorem for ordinary differential equations. Therefore, the solutions are sought by means of numerical tools, which necessarily require a new discretization of the problem. This last step can hide some dangers. Indeed, very often, discrete models resulting by applying the finite element method (FEM) or finite difference method (FDM) to the homogenized model are able to contain only partially the information about the underlying microstructure. The main risk of such a loss of control is that it may induce the modeler to misunderstand the results of the discretization.

A natural question, therefore, arises: *is the homogenization step needed?* If we look at the homogenized continuum model of a complex microstructure as a *tool* to forecast the behavior of the system, it is clear that very often it is not able to provide us with any solution. Moreover, it requires an additional step (FEM or FDM) which may be (at least partially) irrespective of the actual discrete nature of the system. Of course, on the other hand, it is not computationally convenient to apply numerical methods directly at the level of the microstructure.

Here we review some approaches which start *ab initio* with a judiciously chosen discrete model, inspired by the mechanical features of the microstructure, which can be described in terms of a reasonable (from the computational point of view) number of Lagrangian coordinates. This *mesoscopic* model may produce efficient and robust algorithms, able to forecast equilibrium configurations of complex mechanical systems under large deformations. Indeed, the theory of discrete Lagrangian systems that we have introduced in the previous section provides us with well-posed ordinary differential equation problems which can be efficiently solved by means of numerical methods.

In the next sections we will discuss two successful examples of such a proposed paradigm: the Piola–Hencky discrete model for pantographic metamaterials and the Piola–Hencky model for the three-dimensional *Elastica*.

5.4 Hencky-Type Model for Pantographic Metamaterials

In this section, we present a Lagrangian discrete model for a pantographic metamaterial (more information can be found in [86–90, 93]). In particular, we analyze the case of a planar pantographic sheet, made of a lattice consisting of two arrays of fibers, oriented at angles $\pi/4$, $\pi/3$, and $\pi/6$ with respect to the horizontal axis, where the longer side of the pantograph lies (see Fig. 5.1).

The two arrays lie on different (but relatively close) planes and they are connected in their intersection points by means of a set of pivots (see Fig. 5.2).

In his Ph.D thesis, Hencky [91] proposed a discrete model for *Elasticae* in terms of rotational springs and rigid bars. Following the spirit of his approach and the discussion of the previous section, the discrete Lagrangian models that we are going to present

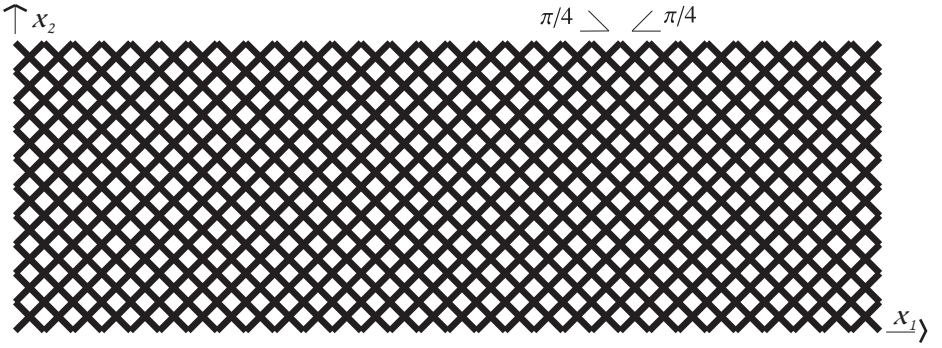

Figure 5.1 A pantographic lattice for fibers oriented at angle $\pi/4$.

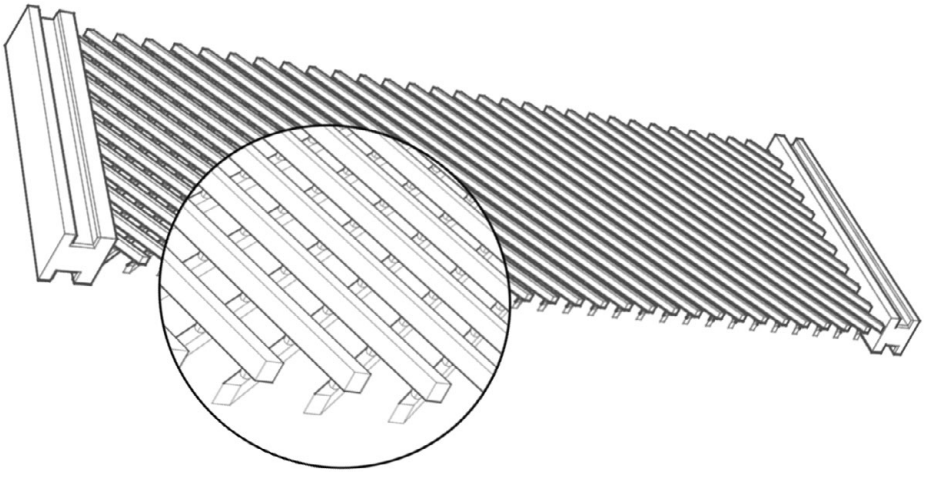

Figure 5.2 The microstructure of a pantographic structure.

are directly inspired by the pantograph's microstructure. We firstly discuss the models for different arrangements of the microstructure, then we present numerical and experimental results aiming to validate the models. In the next section, in contrast, another example of the Hencky model for three-dimensional *Elasticae* will be presented.

5.4.1 Discrete Hencky-type Model for a Planar Pantographic Sheet

In the first model that we present, we consider a pantographic sheet as a rectangular lattice made of square cells. The cells, whose side length is ϵ, are formed by two orthogonal arrays of fibers. We will call array 1 and array 2 the arrays forming a $\pi/4$ and a $-\pi/4$ angle with respect to the (horizontal) x_1 axis (see Fig. 5.1), respectively. The discrete Lagrangian system that we want to introduce to describe the pantographic sheet is made up of a finite number N of material particles occupying the intersection points of the two arrays of fibers. These particles are linked one to another by means of

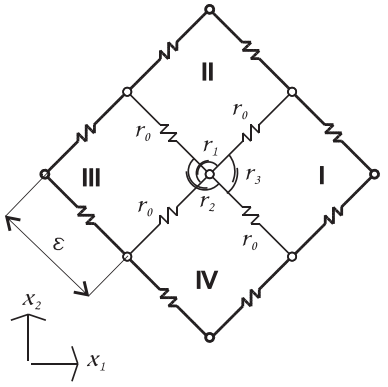

Figure 5.3 Discrete Hencky-type mechanical model for the pantographic lattice.

extensional and rotational springs, whose arrangement is sketched in Fig. 5.3. Note that this arrangement allows both pair-wise and triple-particle interactions. With respect to a *reference configuration*, for instance one can consider the pantographic sheet without any imposed displacement or any force acting on it,[11] the position of the ith particle is indicated by a vector P_i. The Lagrangian coordinates of this system are, therefore, the actual positions of the particles after a deformation, which we denote with the lowercase letter p. Hence, if we limit the kinematics of the system to planar motions, one just needs to introduce $2N$ Lagrangian coordinates to describe the system.

Once the kinematics of the system has been defined, according to the second section of this chapter, we have to find a Lagrangian function for this mechanical system such that, by imposing that the first variation of the associated functional vanishes, one can obtain the equilibrium configurations of the system. Since we are interested in equilibrium configurations, or in other words, we want to study the *statics* of the structure,[12] the Lagrangian function will contain only the potential energy part, i.e. the contribution associated with the relevant deformation. As we have already discussed in Section 5.2, this choice is not unique. We will show that our conjecture on the analytical form of the deformation energies will also lead to accurate predictions of the structural response of the pantographic sheet in the presence of large deformations.

Our ansatz is that the total energy of the pantographic sheet can be expressed as

$$W(\mathbf{d}) = W_{\text{int}} - L_{\text{ext}} = \sum_{e} \big(w_0 + w_1 + w_2 + w_3\big) - L_{\text{ext}}\,, \tag{5.89}$$

where $\mathbf{d}$ is the vector collecting all the particles' displacements, e is an index labelling the springs of the system and ranging over all of them (we refer to Fig. 5.3 and Fig. 5.4), L_{ext} is the work done by external loads and

[11] Although this is a customary choice, it not mandatory to select such a reference configuration. In Section 5.5 we discuss the case of a generic curved reference configuration of a 3D beam.

[12] In Section 5.5 we discuss an example of dynamical evolution of a 3D beam discussed in terms of a Hencky-type model.

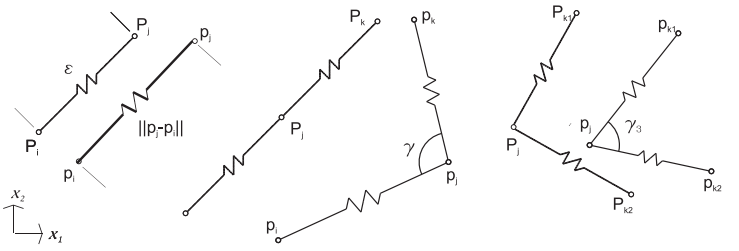

Figure 5.4 The extensional, bending and shear springs kinematics.

- w_0 is the *deformation energy for axial springs*, defined as

$$w_0 = \frac{1}{2} r_0 (\parallel p_j - p_i \parallel - \varepsilon)^2 , \tag{5.90}$$

where p_i and p_j are the actual positions of the particles i and j, respectively, and r_0 is the rigidity of the extensional spring;

- $w_{1,2}$ are the *deformation energies for bending springs* along array 1 and 2 respectively. They read

$$w_{1,2} = r_{1,2}(\cos \gamma_{1,2} + 1) , \tag{5.91}$$

where the angle γ can be written in terms of the Lagrangian coordinates as

$$\cos\gamma_{1,2} = \frac{\parallel p_{j_{1,2}} - p_{i_{1,2}} \parallel^2 + \parallel p_{k_{1,2}} - p_{j_{1,2}} \parallel^2 - \parallel p_{k_{1,2}} - p_{i_{1,2}} \parallel^2}{2 \parallel p_{j_{1,2}} - p_{i_{1,2}} \parallel^2 \parallel p_{k_{1,2}} - p_{j_{1,2}} \parallel^2} , \tag{5.92}$$

$r_{1,2}$ are the rigidities of the rotational springs involving array 1 and 2, respectively, and $p_{i_{1,2}}$, $p_{j_{1,2}}$, and $p_{k_{1,2}}$ are the actual positions of three particles aligned along array 1 or 2;

- w_3 is the *deformation energy for shear springs*, defined as

$$w_3 = \frac{1}{2} r_3 \left(\gamma_3 - \frac{\pi}{2} \right)^2 , \tag{5.93}$$

where

$$\cos \gamma_3 = \frac{\parallel p_{j_1} - p_{k_2} \parallel^2 + \parallel p_{k_1} - p_{j_1} \parallel^2 - \parallel p_{k_1} - p_{k_2} \parallel^2}{2 \parallel p_{j_1} - p_{k_2} \parallel^2 \parallel p_{k_1} - p_{j_1} \parallel^2} , \tag{5.94}$$

and r_3 is the rigidity of the rotational springs which connect the two arrays, and p_{k_1}, p_{k_2}, and p_{j_1} are the Lagrangian coordinates of the particles involved. One such shear spring will appear in all the quadrants of Fig. 5.3.

Note that the last two deformation energies involve three-particle interactions. Moreover, if we impose certain displacements on some particles, the associated deformation energies will need the specification of suitable boundary conditions. More specifically, if we assume that the short sides of the lattice are fixed to two rigid bodies and the bending springs are connected with material segments of these bodies, then from the previous expressions we can deduce the conditions required as

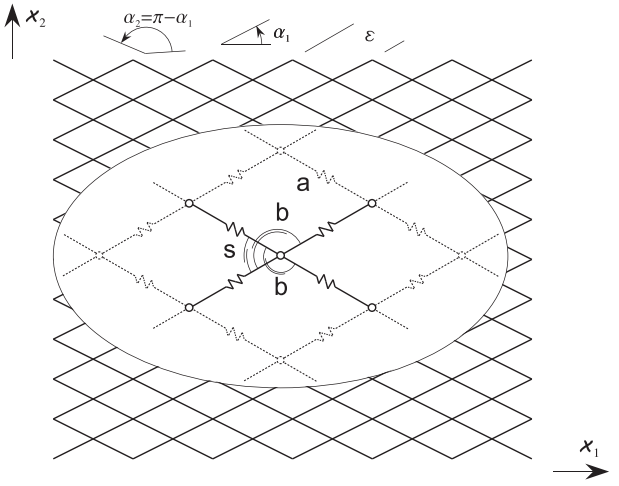

Figure 5.5 Discrete Hencky-type mechanical model for the pantographic lattice in the case of non-orthogonal fibers.

$$p_{i_{1,2}} = P_{i_{1,2}} + R_{i_{1,2}}\,, \tag{5.95}$$

if (see Fig. 5.4) with respect to the constrained j particle, there is no preceding particle i in the interior of the lattice, or as

$$p_{k_{1,2}} = P_{k_{1,2}} + R_{k_{1,2}}\,, \tag{5.96}$$

if there is no subsequent particle k in the interior of the lattice with respect to the constrained particle j, and we have indicated the corresponding rigid displacements by $R_{i_{1,2}}$ and $R_{k_{1,2}}$, respectively.

It is possible to generalize the previous model to the case of non-orthogonal fibers by distinguishing the springs along the directions α_1 and $\alpha_2 = \pi - \alpha_1$ depicted in Fig. 5.5. In the orthogonal case, these two angles reduce to $\pm\pi/4$ leading again to the expression (5.89), while in this more general case the total energy reads:[13]

$$\begin{aligned} W(\mathbf{d}) = &\frac{1}{2}\sum_{i,j} a_{i,j}^{(\alpha_1)}(\parallel p_{i+1,j} - p_{i,j} \parallel - \varepsilon)^2 \\ &+ \sum_{i,j} a_{i,j}^{(\alpha_2)}(\parallel p_{i,j+1} - p_{i,j} \parallel - \varepsilon)^2 \\ &+ \sum_{i,j} b_{i,j}^{(\alpha_1)}\left(\cos\beta_{i,j}^{(\alpha_1)} + 1\right) \\ &+ \sum_{i,j} b_{i,j}^{(\alpha_2)}\left(\cos\beta_{i,j}^{(\alpha_2)} + 1\right) \\ &+ \frac{1}{2}\sum_{q}\sum_{i,j} s_{i,j}^{(q)}\left(\theta_{i,j}^{(q)} - \bar{\theta}_{i,j}^{(q)}\right)^2\,, \end{aligned} \tag{5.97}$$

[13] The names of the rigidities have been modified with respect to Eq. (5.89) in order to lighten the notation.

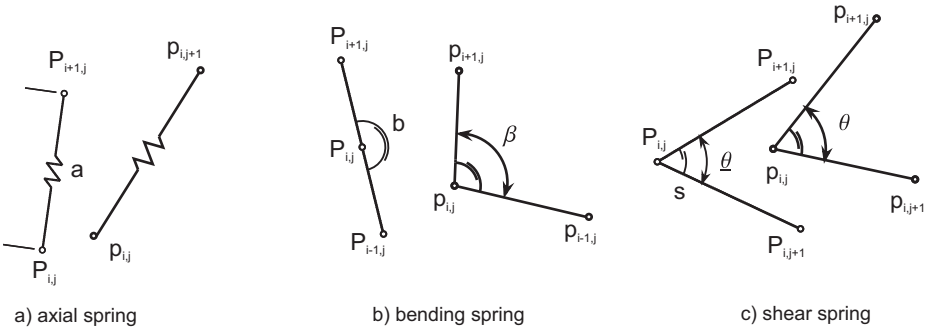

Figure 5.6 The extensional, bending and shear spring kinematics in the case of non-orthogonal fibers.

where $a_{i,j}^{(\alpha_m)}$, $b_{i,j}^{(\alpha_m)}$, and $s_{i,j}^{(q)}$ $(m = 1, 2)$ are the rigidities of the axial, bending, and shear springs respectively, which connect the particles i and j. The index q runs over the four quadrants around the particle $P_{i,j}$. Finally, the angles $\beta_{i,j}^{(\alpha_m)}$ $(m = 1, 2)$, $\theta_{i,j}^{(q)}$, and $\bar{\theta}_{i,j}^{(q)}$ are the angles shown in Fig. 5.6.

Since the discrete Lagrangian model for pantographic sheet has been introduced, it is natural to compare it with the corresponding (homogenized) continuum model. In [92] it is shown that, once a regular field χ called *placement* has been introduced satisfying the property[14]

$$\chi(P_{i,j}) = p_{i,j}\,, \tag{5.98}$$

it is possible to define the following Lagrangian energy:

$$\begin{aligned} W(\chi) = &\frac{1}{2}\int_\Omega \sum_{\alpha_m} A^{(\alpha_m)}(\parallel \mathbf{F}\mathbf{d}_{\alpha_m} \parallel -1)^2\, d\Omega \\ &+ \frac{1}{2}\int_\Omega \sum_{\alpha_m} B^{(\alpha_m)}\left(\frac{\nabla\mathbf{F}|\mathbf{d}_{\alpha_m}\otimes\mathbf{d}_{\alpha_m}\cdot\nabla\mathbf{F}|\mathbf{d}_{\alpha_m}\otimes\mathbf{d}_{\alpha_m}}{\parallel \mathbf{F}\mathbf{d}_{\alpha_m} \parallel^2}\right. \\ &\left. - \left(\frac{\mathbf{F}\mathbf{d}_{\alpha_m}}{\parallel \mathbf{F}\mathbf{d}_{\alpha_m} \parallel}\cdot\frac{\nabla\mathbf{F}|\mathbf{d}_{\alpha_m}\otimes\mathbf{d}_{\alpha_m}}{\parallel \mathbf{F}\mathbf{d}_{\alpha_m} \parallel}\right)^2\right) d\Omega \\ &+ \frac{1}{2}\int_\Omega S\left(\arccos\left(\frac{\mathbf{F}\mathbf{d}_{\alpha_1}}{\parallel \mathbf{F}\mathbf{d}_{\alpha_1} \parallel}\cdot\frac{\mathbf{F}\mathbf{d}_{\alpha_2}}{\parallel \mathbf{F}\mathbf{d}_{\alpha_2} \parallel}\right) - \bar{\theta}\right)^2 d\Omega\,, \end{aligned} \tag{5.99}$$

where the gradient of the placement field has been indicated by $\mathbf{F} = \nabla\chi$, and the stiffness parameters $A^{(\alpha_m)}$, $B^{(\alpha_m)}$, and S are related to the spring rigidities of Eq. (5.97). Note that since in the expression of the energy (5.99) all the components of the gradient of $\mathbf{F}$ appear, one refers to this model as a *second gradient* (of the displacement field) *theory* [93–95]. By comparing the different contributions of the energies (5.97) and (5.99) versus non-dimensional displacements (normalized on the longest side of the pantographic sheet) as shown in Fig. 5.7, it is apparent that they

[14] This is the aforementioned Piola's Ansatz.

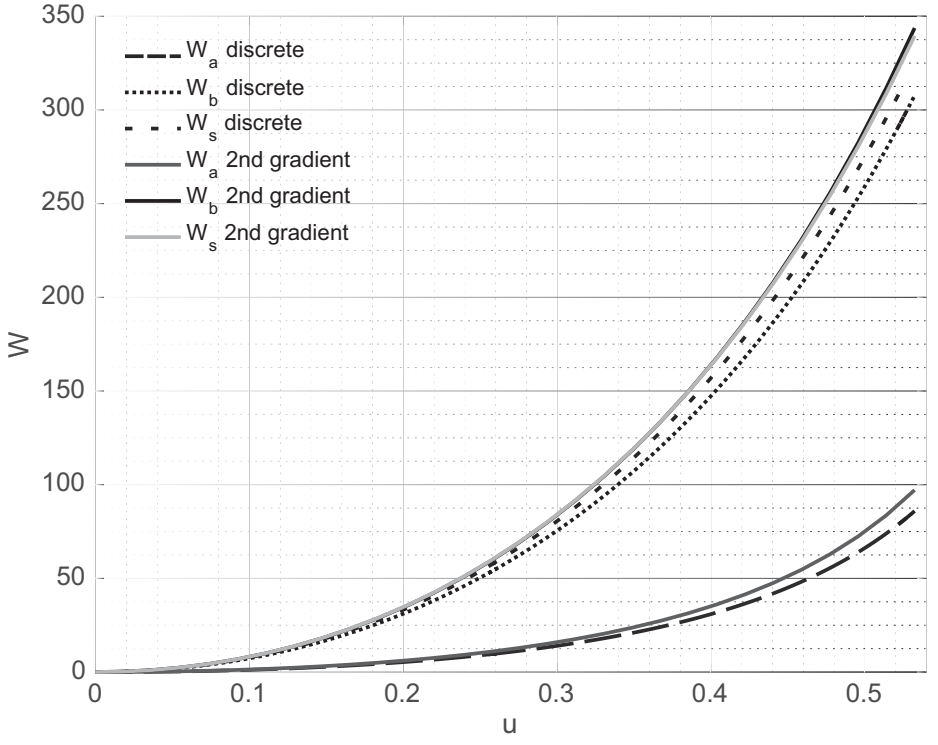

Figure 5.7 Strain energy *vs* normalized displacement. Discrete model is indicated with dashed/dotted lines, the second gradient model with continuous lines.

show a very similar behavior. In Section 5.4.3, we compare these two models with experimental measurements.

5.4.2 The Solution Algorithm

Once the Lagrangian function (5.89) has been introduced, one has to solve the associated Euler–Lagrange problem in order to determine the equilibrium configurations relative to certain boundary conditions. In other words, one has to find the particular vector $\mathbf{d}$ which minimizes the first variation of (5.89). In this subsection, we will discuss the numerical algorithm presented in [48, 49] aimed to solve this non-linear problem.

In general, one can look for equilibrium configurations of a pantographic sheet when some displacements are imposed on a set of particles and a conservative force is applied on the remaining system. Let us reorder the vector $\mathbf{d}$ as

$$\mathbf{d} = (\mathbf{u}, \mathbf{u}_a), \tag{5.100}$$

where $\mathbf{u}$ are the free displacements, $\mathbf{u}_a$ are the imposed displacements and we assume that L_{ext} depends only on $\mathbf{u}$.

By requiring that the first variation of (5.89) vanishes, one obtains

$$\mathbf{s}(\mathbf{u}) - \mathbf{p}(\mathbf{u}) = 0, \tag{5.101}$$

which is a non-linear equation in the unknown $\mathbf{u}$ and where

$$\mathbf{s}(\mathbf{u}) = \frac{dW_{\text{int}}}{d\mathbf{u}}, \quad \mathbf{p}(\mathbf{u}) = \frac{dL_{\text{ext}}}{d\mathbf{u}} \tag{5.102}$$

are the internal forces (also known as *structural reaction*) and the external forces vectors, respectively. Let us introduce a parameter λ to describe the imposed displacements and a parameter μ to describe the potential of the external load. In this case, Eq. (5.101) reads:

$$\mathbf{r}(\boldsymbol{\lambda}, \boldsymbol{\mu}, \mathbf{u}) := \mathbf{s}(\mathbf{u}, \mathbf{u}_a(\boldsymbol{\lambda})) - \mathbf{p}(\boldsymbol{\mu}, \mathbf{u}) = 0\,. \tag{5.103}$$

A configuration of equilibrium relative to the parameters λ and μ is given by that vector $\mathbf{u}(\lambda, \mu)$ which satisfies:

$$\mathbf{r}\big(\boldsymbol{\lambda}, \boldsymbol{\mu}, \mathbf{u}(\boldsymbol{\lambda}, \boldsymbol{\mu})\big) = 0\,. \tag{5.104}$$

Let us consider as external force a dead load. In this case $\mathbf{p}$ will not depend on $\mathbf{u}$ and, by assuming a linear dependence on μ, it can be written as:

$$\mathbf{p}(\mu) = \mathbf{p}_0 + \mu\hat{\mathbf{p}}\,. \tag{5.105}$$

Note that, by linearizing Eq. (5.101) around the solution $\mathbf{u}_0$ such that $\mathbf{s}(\mathbf{u}_0) - \mathbf{p}_0 = 0$, and by defining $\Delta\mathbf{u} := (\mathbf{u} - \mathbf{u}_0)$ we can write

$$0 = \mathbf{s}(\mathbf{u}(\boldsymbol{\mu})) - \mathbf{p}_0 - \boldsymbol{\mu}\hat{\mathbf{p}} \approx \mathbf{s}(\mathbf{u}_0) - \mathbf{p}_0 + \mathbf{K}_T(\mathbf{u}_0)\boldsymbol{\Delta}\mathbf{u} - \boldsymbol{\mu}\hat{\mathbf{p}} = \mathbf{K}_T(\mathbf{u}_0) - \boldsymbol{\mu}\hat{\mathbf{p}}, \tag{5.106}$$

where we have defined the tangent stiffness matrix $\mathbf{K}_T$ as

$$\mathbf{K}_T(\mathbf{u}) = \frac{d\mathbf{s}}{d\mathbf{u}} = \frac{d^2W_{\text{int}}}{d\mathbf{u}^2}\,. \tag{5.107}$$

From Eq. (5.106) we can deduce the relation

$$\Delta\mathbf{u} = \mu(\mathbf{K}_T(\mathbf{u}_0))^{-1}\hat{\mathbf{p}}, \tag{5.108}$$

which will be useful in the following discussion.

Let us now sketch the main steps of the Newton–Raphson algorithm used to solve the non-linear problem (5.103). For simplicity, we will consider as boundary conditions only imposed displacements. They will depend on a parameter λ and, by mimicking a quasi-static state, we can divide the whole displacement into a finite number of steps such that for the $(j+1)$th one, the parameter λ will be $\lambda_{j+1} = \lambda_j + \Delta\lambda$, where the step $\Delta\lambda$ is fixed. Let us start from an estimated equilibrium configuration $(\lambda_j, \mathbf{u}_j)$ for the jth step satisfying

$$\| \mathbf{r}(\lambda_j, \mathbf{u}_j) \| \leq \eta\,, \tag{5.109}$$

where $\eta > 0$. It means that the configuration $(\lambda_j, \mathbf{u}_j)$ solves the problem (5.103) in an η-approximation. Of course, most likely, for the subsequent $(j+1)$th displacement

step, the configuration $\mathbf{u}_j$ will not satisfy the requirement (5.109) anymore. Therefore, for any step of the displacement, we have to calculate the increment vector $\Delta\mathbf{u}_j$ such that the couple

$$(\lambda_j + \Delta\lambda_j, \mathbf{u}_j + \Delta\mathbf{u}_j) = (\lambda_{j+1}, \mathbf{u}_{j+1}) \tag{5.110}$$

satisfies Eq. (5.109). We proceed in the following way:

1. With respect to the $(j+1)$th displacement step, we compute the so-called *residual nodal forces*:

$$\mathbf{r}(\lambda_j + \Delta\lambda, \mathbf{u}_j) = \mathbf{r}(\lambda_{j+1}, \mathbf{u}_j) =: \mathbf{p}_{j,0}\,, \tag{5.111}$$

   which is, roughly speaking, the residual due to the new imposed displacement.
2. Once the hth approximation of the increment $\Delta\mathbf{u}_j$ has been computed (in the following, we will discuss the corresponding sub-routine), the residual will be:

$$\mathbf{r}\left(\mathbf{u}_j + \sum_{m=0}^{h} \Delta\mathbf{u}_{j,m}(\lambda_{j+1}, (\mathbf{u}_j, \lambda_j))\right) = \mathbf{p}_{j,h}\,. \tag{5.112}$$

3. If the condition

$$\| \mathbf{p}_{j,h} \| > \eta \tag{5.113}$$

   is satisfied then, by assuming $\mu = -1$ and according to Eq. (5.108), we set

$$\Delta\mathbf{u}_{j,h+1} = -\left(\frac{\partial\mathbf{r}(\lambda_{j+1}, \mathbf{u}_j + \sum_{m=1}^{h} \Delta\mathbf{u}_{j,m}(\lambda_j, \mathbf{u}_j))}{\partial\mathbf{u}}\right)^{-1} \mathbf{p}_{j,h}\,, \tag{5.114}$$

   and the iteration continues. We note that, because μ is the parameter which describes the external forces, the condition $\mu = -1$, is equivalent to imposing a fictitious external dead load aimed to compensate the value of the residual.
4. If, instead, the condition

$$\| \mathbf{p}_{j,h} \| \leq \eta \tag{5.115}$$

   is satisfied, then the increment vector will be

$$\Delta\mathbf{u}_j = \sum_{m=0}^{h} \Delta\mathbf{u}_{j,m}(\lambda_j, \mathbf{u}_j)\,, \tag{5.116}$$

   and the couple $(\lambda_{j+1}, \mathbf{u}_j + \Delta\mathbf{u}_j) = (\lambda_{j+1}, \Delta\mathbf{u}_{j+1})$ describes the equilibrium configuration of the structure relative to the $(j+1)$th step of the displacement.

Let us conclude this section by explicitly describing how to compute the $(h+1)$-th approximation of the increment vector $\Delta\mathbf{u}_j$ in the simplified case in which no external forces act on the system. The basic algorithm will be the following:

```
set
   exit := false
   K:= K (u_j)
   Δu := Δλū      (ū = 0  for free nodes and ū = u_a for the assigned
                  ones)
```

```
while (loop < maxloop) and (exit=false)
   s := s(u_j + Δu)
   u̇ := K^(−1)s
   if ||u̇|| > η
        Δu := Δu − u̇
        K := K(u_j + Δu)
    else
        exit := true
    end
save
    λ_j + 1 := λ_j + Δλ
    u_j + 1 := u_j + Δu
```

We note that, since $\mathbf{u}_{j+1,h} = \mathbf{u}_j + \Delta\mathbf{u}_{j,h}$, condition (5.113) reduces to

$$\| \mathbf{s}(\lambda_{j+1}, \mathbf{u}_{j+1,h}) \| > \eta. \tag{5.117}$$

According to Eq. (5.106), we have that, by requiring

$$0 = \mathbf{s}(\lambda_{j+1}, \mathbf{u}_{j+1,h+1}) = \mathbf{s}(\lambda_{j+1}, \mathbf{u}_{j+1,h}) + \mathbf{K}_T(\lambda_{j+1}, \mathbf{u}_{j+1,h})\dot{\mathbf{u}}\,, \tag{5.118}$$

the Newton step will be

$$\dot{\mathbf{u}} = -\mathbf{K}_T^{-1}\mathbf{s}(\lambda_{j+1}, \mathbf{u}_{j+1,h}). \tag{5.119}$$

If the condition $||\dot{\mathbf{u}}|| < \eta$ is satisfied, then the $(h+1)$th approximation of the increment vector will be $\Delta\mathbf{u}_{j,h+1} = \Delta\mathbf{u}_{j,h} + \dot{\mathbf{u}}$, otherwise the routine will continue.

5.4.3 Experimental Evidence and Numerical Simulations

In this section we present some experimental results referring to pantographic lattices. Apart from standard bias extension tests which have been widely discussed in previous chapters, here we focus also on different experimental setups, and all the results will be compared with numerical simulations based on the discrete and continuous models described in the previous sections. As an aid to clarity, this section is divided into smaller subsections referring to the various settings.

Pantographic Lattices with Non-orthogonal Fibers

In this subsection we deal with some experimental and numerical results relating to bias extension tests referring to pantographic sheets with non-orthogonal fibers. As already presented in previous chapters, a pantographic lattice is a bi-dimensional fabric made up of two families of parallel fibers interconnected by small cylinders called pivots. In the reference configuration, the angle between the two arrays of fibers is constant. Here we will consider two different regimes: in one case this angle is bigger than $\frac{\pi}{2}$, whereas in the other it is smaller. As we will see, the resulting mechanical properties are deeply affected by this quantity.

A possibility for building pantographic lattices is using 3D-printing. In this subsection we consider specimens in PA 2200 polyamide, realized via SLS Formiga P100. Referring to Fig. 5.8, all the fibers of the specimen have rectangular cross section, 2.25 mm $\times$ 1.6 mm whereas the pivots are cylinders with height $h = 1$ mm and base

Table 5.1 Stiffnesses for the discrete model used in the simulations presented in Section 5.4.3.

a (N/mm)	b_1(N mm)	b_2(N mm)	s(N mm)
165.6	148.9	148.9	0.977

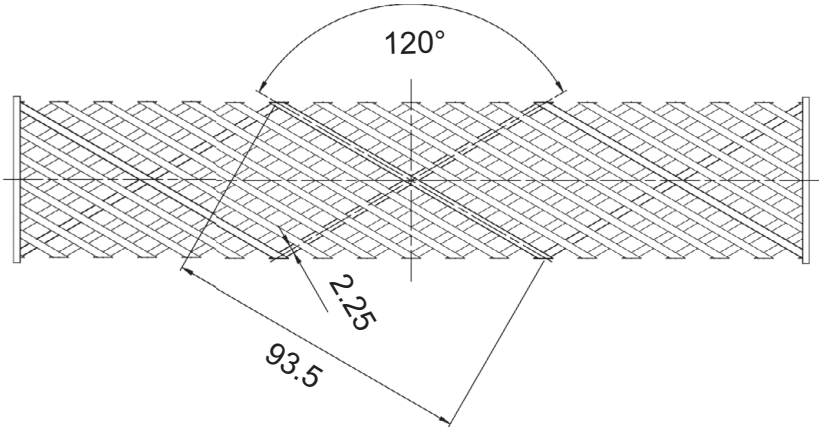

Figure 5.8 Design of the pantographic lattice with $\bar{\theta} = \frac{2\pi}{3}$ used in the experimental setup described in the first paragraph of Section 5.4.3.

diameter $D = 0.9$ mm. If we call $\bar{\theta}$ the angle between the two fibers, the first sample is characterized by $\bar{\theta} = \frac{2\pi}{3}$ while the other has $\bar{\theta} = \frac{\pi}{3}$. These specimens have been subject to a standard bias extension test along the direction of the longer side of the sheet: one side of the sample has been clamped while a prescribed displacement has been imposed at the other end. All the experiments have been performed by the MTS Bionix system strength machine, with an elongation rate of 5 mm/min. This system has an error of ± 1 N for the forces and 0.1 mm for the displacements.

Fabric with $\bar{\theta} = \frac{2\pi}{3}$

Let us start with the specimen characterized by $\bar{\theta} = \frac{2\pi}{3}$. The maximum elongation which has been selected is $u_{d1} = 23.7$ mm. In Fig. 5.9 there is a plot of the global reaction forces. For a more direct comparison with the data coming from the other sample, the non-dimensional displacement $\tilde{u} = \frac{u}{L_1}$ has been chosen as independent variable, where L_1 is the length of the longer side of the sheet.

The experimental data are then compared with numerical simulations obtained by means of both the aforementioned continuous and discrete models. The parameters used for the simulations were chosen according to the identification procedure described in [51], which produced the values listed in Table 5.1.

The results for the discrete model were obtained via the algorithm discussed in Section 5.4.2, whereas the second gradient continuum model was implemented on the software Comsol Multiphysics using the Weak Form package which makes it possible

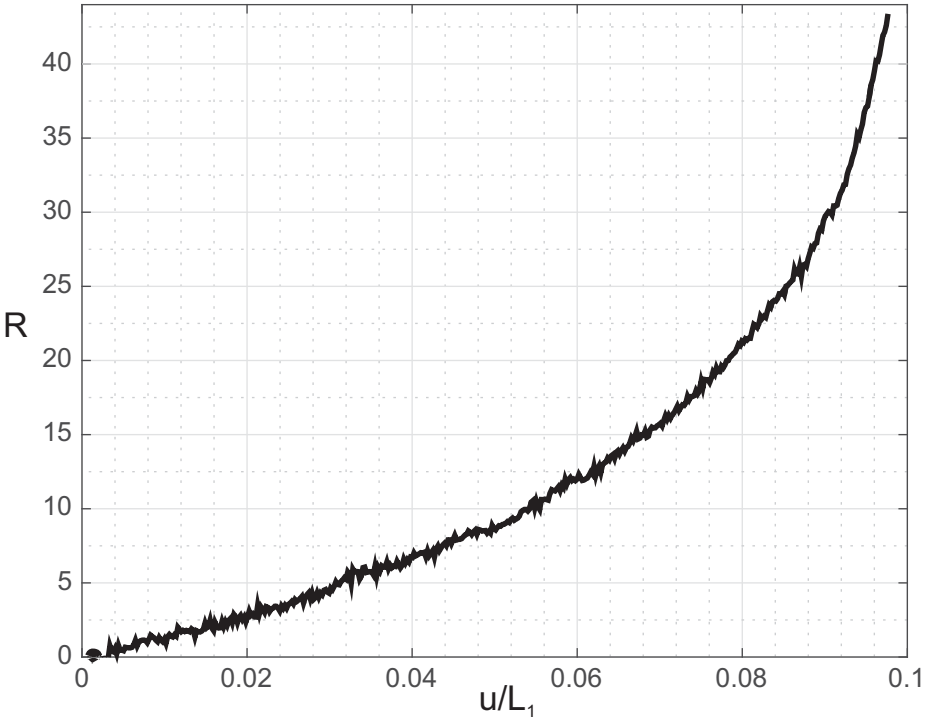

Figure 5.9 Reaction force measured on the specimen with $\bar{\theta} = \frac{2\pi}{3}$ versus the variable $\tilde{u}$. (ordinate newtons)

to minimize a given functional. Because of the non-orthogonality of the fibers, the stiffnesses of the continuous model have been derived from the values in Table 5.1 through the following formulas:

$$K_e = \frac{a}{\sin\bar{\theta}}, \tag{5.120}$$

$$K_b = \frac{b}{\sin\bar{\theta}}, \tag{5.121}$$

$$K_s = \frac{s}{\epsilon^2 \sin\bar{\theta}}, \tag{5.122}$$

where ϵ is the distance between two adjacent pivots along a fiber.

For the simulation of the continuous model a finite element scheme was chosen which employs cubic Hermitian polynomials and 3250 quadrilateral elements, for a total of 232388 degrees of freedom.

The graph in Fig. 5.10 illustrates the reaction force versus $\tilde{u}$. In particular, the global reaction force is plotted for both discrete and second gradient simulations and compared with the experimental data. It is noticeable that the results from the two simulations are very similar and the agreement with the experimental data is good, since the curves obtained via the simulations almost overlap the experimental plot.

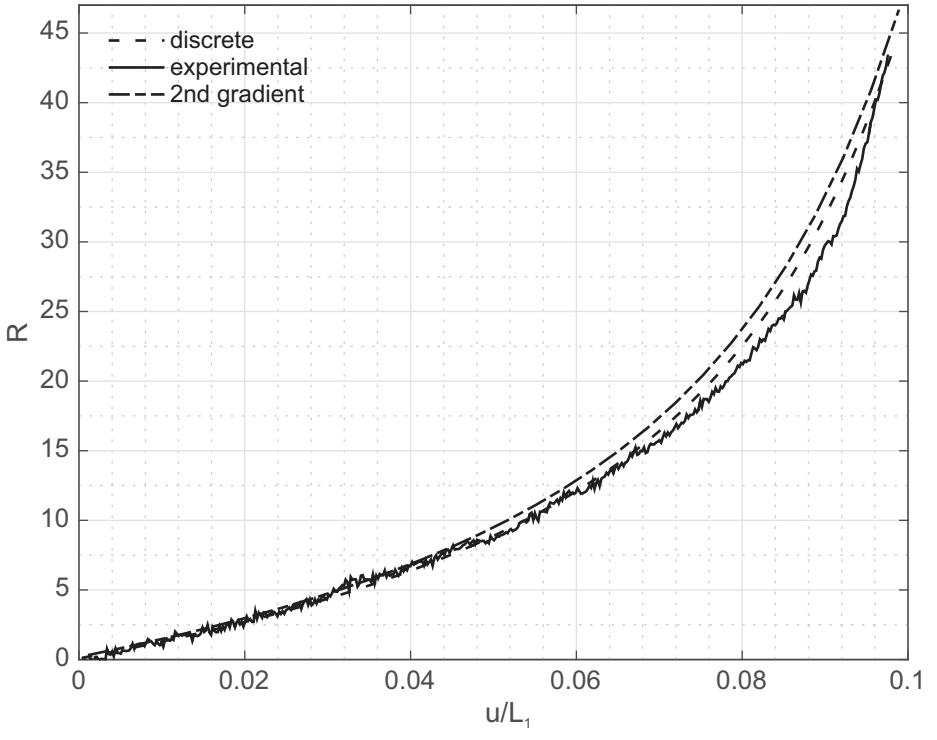

Figure 5.10 A plot of the reaction force versus the variable $\tilde{u}$ for the continuous (second gradient) model (dot-dashed line) and the discrete model (dotted line) compared with the experimental data (continuous line). The specimen is characterized by $\bar{\theta} = \frac{2\pi}{3}$ (ordinate newtons).

In Fig. 5.11 the density of the reaction force along the clamped shorter side is shown: the two densities correspond to the two components of the force. Although we are plotting only the data obtained via the discrete algorithm, similar results have been derived from the continuous model. Note that, notwithstanding the traction test, there are negative values of the reaction force around the centre of the shorter side.

Finally, Fig. 5.12 illustrates how deformation and energy density change while $\tilde{u}$ increases. In particular, the four parts of Fig. 5.12 correspond to simulations performed via the discrete algorithm imposing elongations $\frac{u}{u_{d1}} = 0.25, 0.5, 0.75, 1$, respectively. In order to show the predictive power of the modeling, in Fig. 5.13 the deformation obtained via the discrete model for the maximal elongation $u = u_d$ is overlaid on the picture captured at the final stage of the experiment. From this analysis it is apparent that the model is actually able to reproduce the observed behavior.

Fabric with $\bar{\theta} = \frac{\pi}{3}$

The second experiment is again a bias extension test, performed on a sample characterized by an angle between the fibers of $\bar{\theta} = \frac{\pi}{3}$ (see Fig. 5.14). The maximum imposed

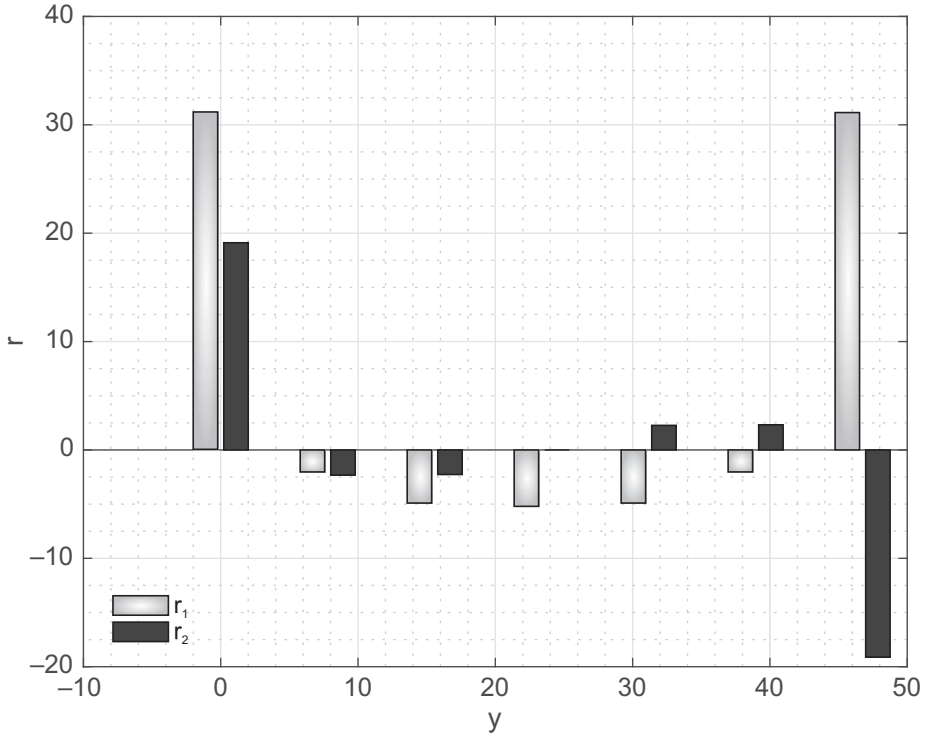

Figure 5.11 Reaction force density (newtons) along the shorter side of the specimen with $\bar{\theta} = \frac{2\pi}{3}$. Grey and black indicate the two different components.

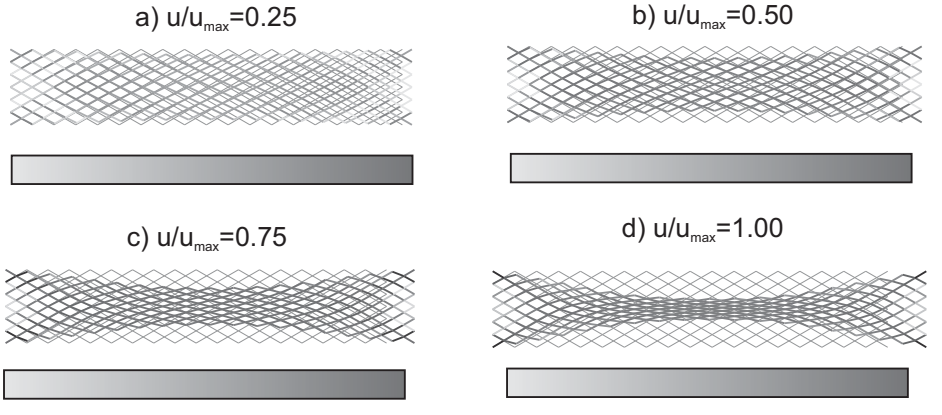

Figure 5.12 Deformation and energy density for different values of the imposed displacement, $\frac{u}{u_{d1}} = 0.25, 0.5, 0.75, 1$. The gray-levels correspond to the strain energy density for the specimen with $\bar{\theta} = \frac{2\pi}{3}$.

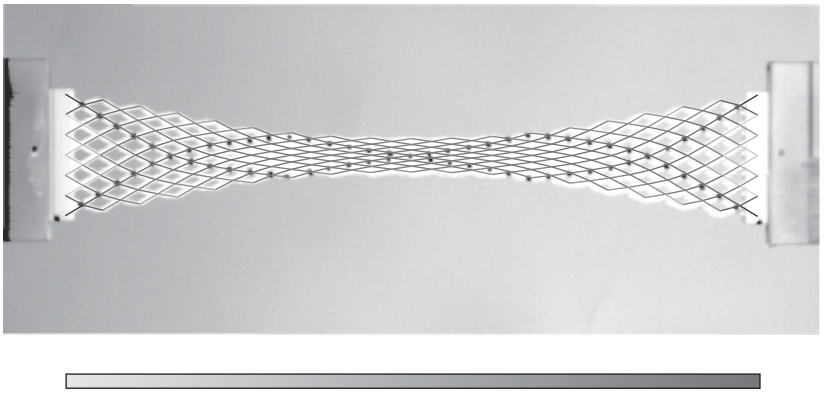

Figure 5.13 Overlap of the experimental results and the numerical simulation based on the discrete Hencky model. The specimen has $\bar{\theta} = \frac{2\pi}{3}$.

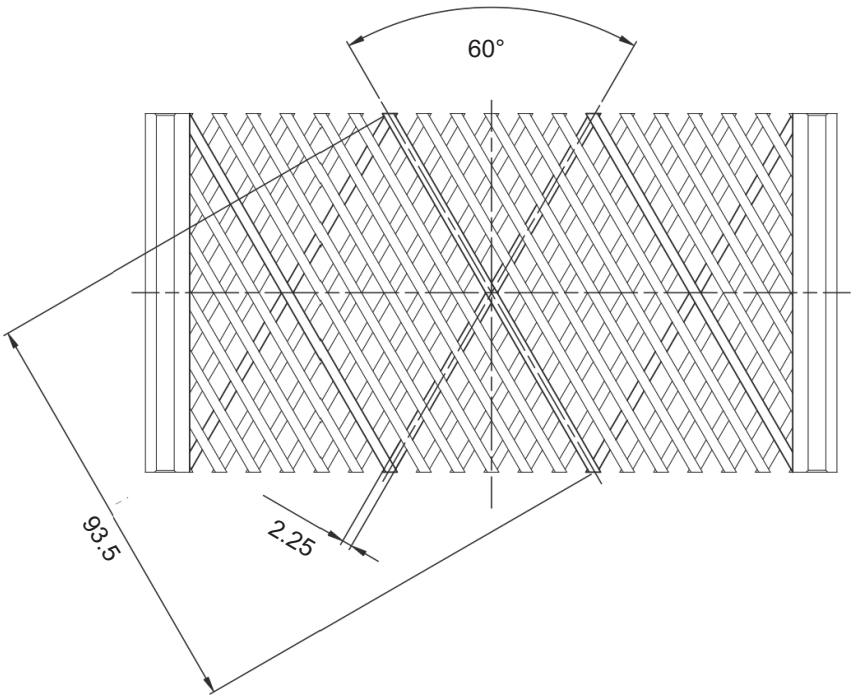

Figure 5.14 Design of the pantographic lattice with $\bar{\theta} = \frac{\pi}{3}$ used in the experimental setup described in the second paragraph of Section 5.4.3.

displacement is $u_{d2} = 74.7\,\text{mm}$. In Fig. 5.15 the global reaction force measured via the Bionix system is plotted against the relative displacement $\hat{u} = \frac{u}{L_2}$, where L_2 is the length of the longer side of the sheet.

As discussed in the previous paragraph, the experimental data are compared with simulations obtained from both continuous and discrete models. As far as the continuum

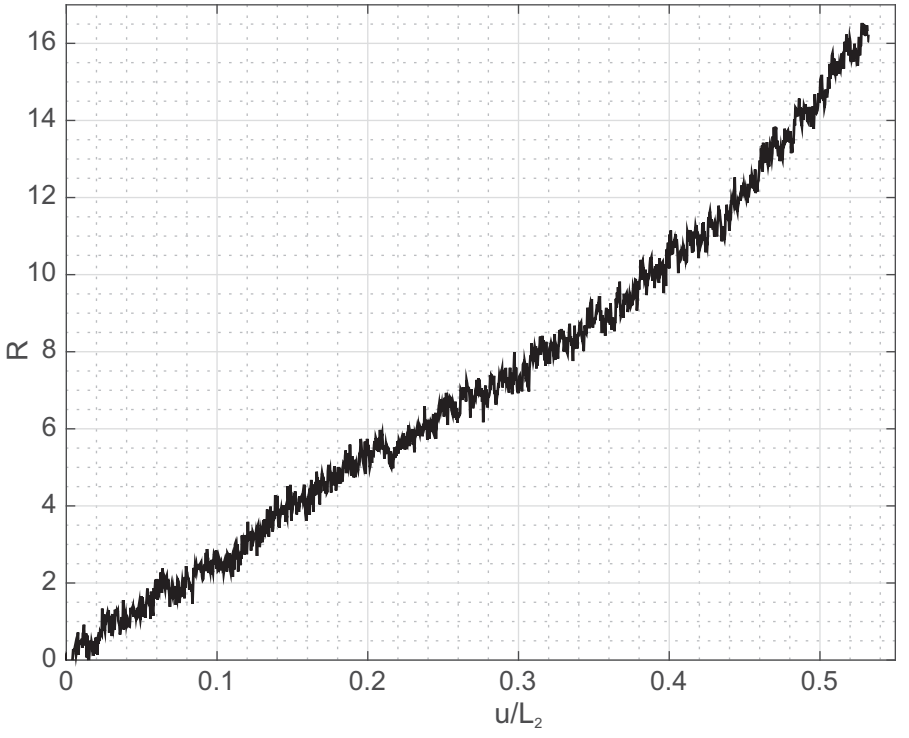

Figure 5.15 Reaction force (newtons) measured on the specimen with $\bar{\theta} = \frac{\pi}{3}$ versus the variable $\hat{u}$.

case is concerned, the parameters of the model have been obtained by using formulas (5.120)–(5.122). The model has been simulated on Comsol Multiphysics with a finite element scheme based on cubic hermitian polynomials, 2800 quadrilateral elements, for a total of 199 658 degrees of freedom.

Analogously to the analysis performed in the previous paragraph, in Fig. 5.16 a plot of the global reaction force versus the relative displacement $\hat{u}$ is presented. In particular, the reaction curves obtained via the continuous model and the discrete model with the experimental data are compared. Note once more that the results obtained using the two models are close and that the agreement with the experimental curve is good up to $\hat{u} = 0.2$.

In Fig. 5.17 we present the density of the reaction force along the shorter side, plotting both of its components. We observe the same behavior as shown by the other sample, with a negative reaction density in the central area of the clamped side. As in the previous case, the plotted results have been obtained by means of the discrete algorithm but they have been confirmed by simulations performed via the continuous model.

Finally, in Fig. 5.18 we illustrate the evolution of deformation and energy density as $\hat{u}$ increases. In particular the four pictures correspond to numerical simulations of the discrete model imposing elongations $\frac{u}{u_{d2}} = 0.25,\ 0.5,\ 0.75,\ 1$.

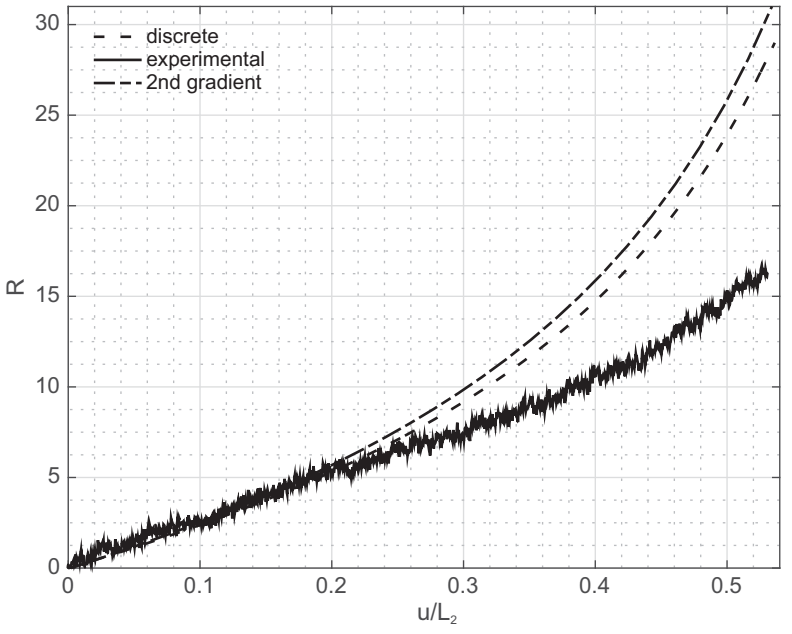

Figure 5.16 The reaction force versus the variable $\tilde{u}$ for the continuous model (dot-dashed line) and the discrete model (dotted line) compared with the experimental data (continuous line). The specimen is characterized by $\bar{\theta} = \frac{\pi}{3}$.

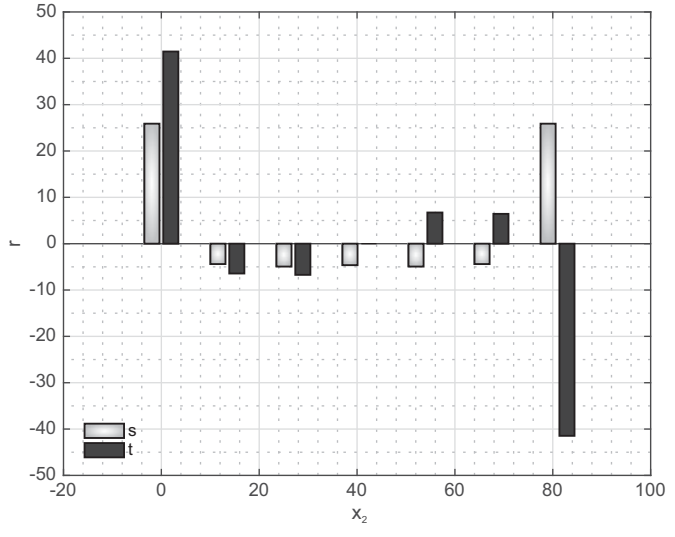

Figure 5.17 Reaction force density along the shorter side of the specimen with $\bar{\theta} = \frac{\pi}{3}$. Black and gray bars indicate the two different components.

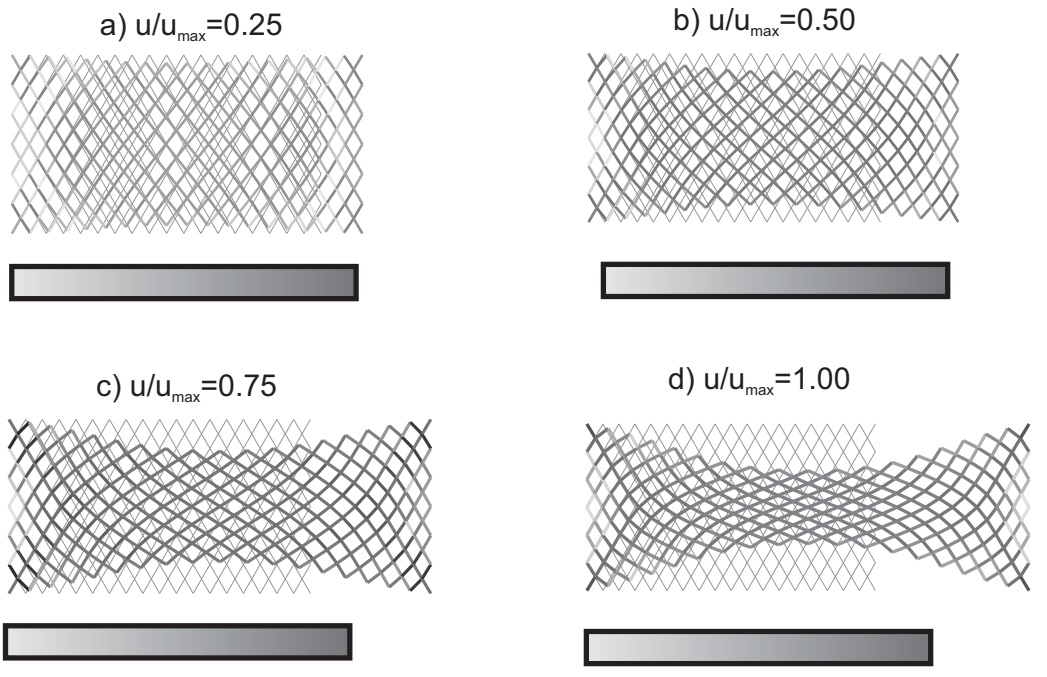

Figure 5.18 Deformation and energy density for different values of the imposed displacement, $\frac{u}{u_{d2}} = 0.25, 0.5, 0.75, 1$. The colors correspond to the strain energy density for the specimen with $\bar{\theta} = \frac{\pi}{3}$.

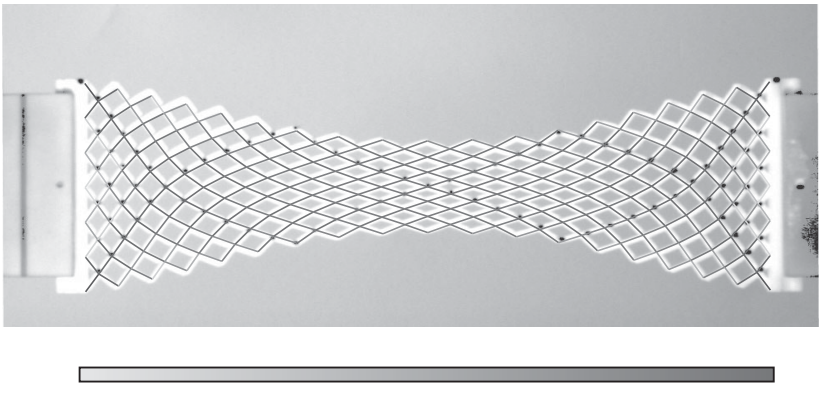

Figure 5.19 Overlap of the experimental results and the numerical simulation based on the discrete Hencky model. The specimen has $\bar{\theta} = \frac{\pi}{3}$.

The model's capability to describe the behavior of the sample can be appreciated in Fig. 5.19, where the deformation obtained by means of the discrete algorithm overlaps the experimental picture taken at the final stage of the process.

By a direct comparison of the two samples we can conclude that the orientation of the fibers in a pantographic sheet deeply affects the mechanical properties of the sample.

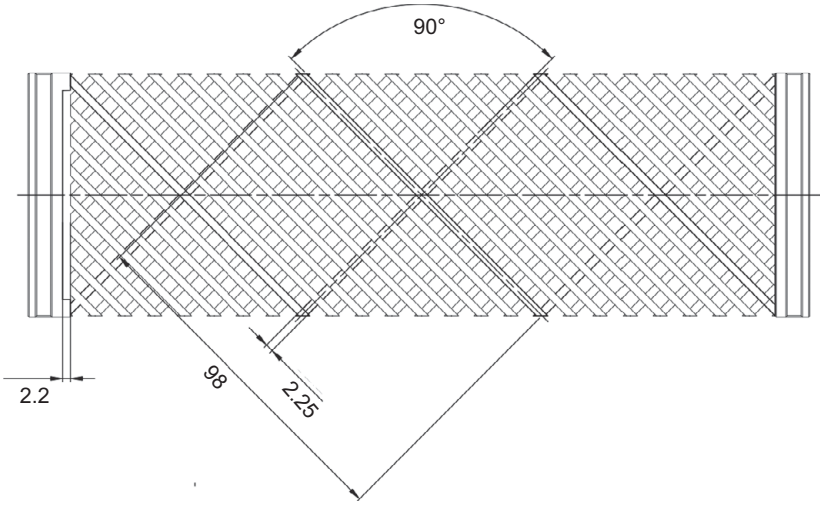

Figure 5.20 Design of the pantographic lattice with orthogonal fibers used in the experimental setup described in Section 5.4.3.

In particular the specimen with a bigger angle $\bar{\theta}$ is more stiff and can absorb less energy in the elastic regime. Indeed, the lattice characterized by $\bar{\theta} = \frac{\pi}{3}$ reached a maximal elongation $\frac{u_{d2}}{L_2} = 0.54$ much bigger than $\frac{u_{d1}}{L_1} = 0.1$ corresponding to the other specimen.

Fiber Push-out Test

In this subsection we consider an experimental setup, described as a fiber push-out test, on a pantographic lattice with an orthogonal arrays of fibers. The specimen tested has been realized by the same 3D printer and in the same material as the previous one. The characteristics of the fibers and pivots are illustrated in Fig. 5.20: the cross-sections of the fibers are rectangles, 2.25 mm $\times$ 1.6 mm, whereas the pivots are cylinders with height $h = 1$mm and base diameter $D = 0.9$ mm.

The sample has been clamped at one end and then a prescribed displacement has been applied to two fibers on the opposite side, up to a maximum value u_m. The test was performed by a MTS Bionix system mechanical testing machine, with an elongation rate of 5 mm/min. In order to apply the prescribed displacement only to two fibers, a specific design was developed: a bridge connecting the two relevant fibers was printed. A magnified view of the printed specimen is shown in Fig. 5.21, a small gap of 2.2 mm between the free fibers and the bridge is required because of the effect which is illustrated in the same picture.

The experimental data have been compared with a numerical simulation of the same test obtained via the discrete algorithm described in the previous section. The parameters used are shown in Table 5.2.

The first row of values has been obtained according to the procedure outlined in [51] with an elastic Young's modulus $E = 1.6$ GPa.[15] The global reaction force

[15] The estimated range for the Young's modulus is 1.5–1.7 GPa, according to the rules of EN ISO 527 and EN ISO 178.

Table 5.2 Stiffnesses for the discrete model obtained by means of an identification procedure and used for the numerical simulations presented in Section 5.4.3.

E (GPa)	a (N/mm)	b_1(N mm)	b_2(N mm)	s(N mm)
1.6	265.6	238.2	238.2	0.9739
1.2	198.8	178.7	148.9	0.7304

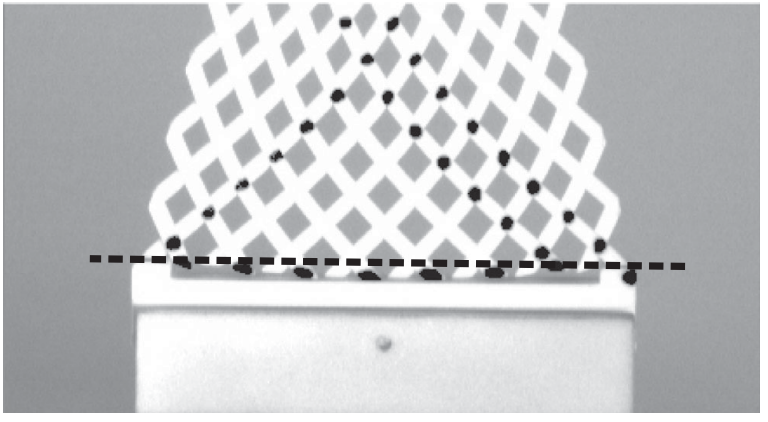

Figure 5.21 Magnified view the elongated specimen at one end. The free fibers tend to touch the bridge.

corresponding to a simulation performed with these parameters is plotted in Fig. 5.22 versus the relative elongation $\lambda = \frac{u}{u_m}$ and compared with the experimental curve.

On the other hand, because of uncertainty in knowledge of the exact Young's modulus as well as the important effect of this value on all the parameters, we have looked for a different value of E to get a better fit with the experimental curve. The results of a simulation performed using the values in the second row of Table 5.2 are presented in Figs. 5.23–5.25. The diagram in Fig. 5.23 shows the global reaction force versus λ whereas the other two charts present the strain energy, separated into its three contributions, and the density of the components of the reaction force along the shorter clamped side. It is noteworthy that, notwithstanding the extension of the specimen, the reaction density is negative in a region around the centre of the side.

Finally Fig. 5.26 shows the evolution of the deformation pattern and energy density as λ increases. In particular the four pictures refer to values of $\lambda = 0.25, 0.5, 0.75, 1$. Note also that in the simulation we observe the same effect as reported in Fig. 5.21, as illustrated by the simulation's results shown in Fig. 5.27.

Even if the agreement with the experimental reaction curve is satisfactory using the second row of parameters in Table 5.2, the deformation pattern is different from the experimental one, since the central region is less contracted in the simulation with respect to the detected one. Probably a more precise choice of the stiffnesses could improve the match with the experimental data.

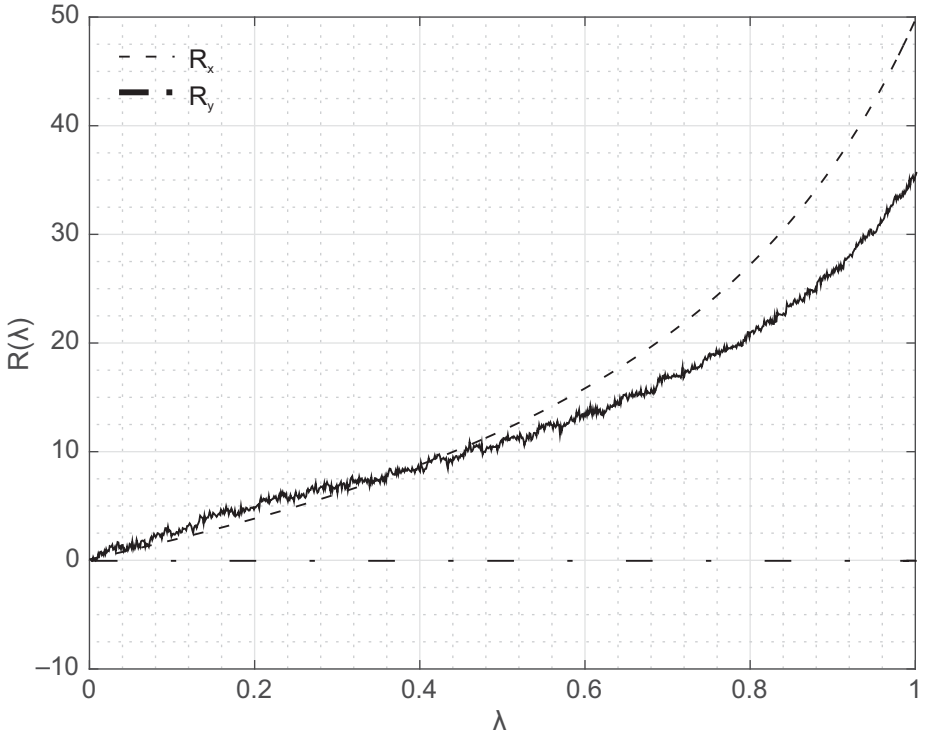

Figure 5.22 The reaction force versus the relative displacement λ for the parameters in the first row of Table 2.

Extraction Tests

In this last subsection we will consider another two experimental setups which will be denoted as T_1 and T_2 tests. Let us consider a pantographic lattice printed in polyamide as were the previous ones. The sample is made up of two orthogonal arrays of fibers with rectangular cross-sections, 2.25 mm $\times$ 1.6 mm, separated by small cylinders, with base diameter $D = 0.9$ mm and height $h = 1$mm (see Fig. 5.20).

With these characteristics, one can compute the stiffnesses appearing in the discrete model, obtaining the values reported in Table 5.3.

Both the experiments which we discuss in this subsection have been performed using a MTS Bionix system mechanical testing machine with an elongation rate of 5 mm/min. During the T_1-test, the specimen has undergone a displacement along one of its diagonals: one fiber at one short side is pinned whereas at the opposite corner a prescribed displacement is applied up to a maximal value, $u_{m1} = 75.3$ mm.

As already mentioned, a numerical simulation of the test has been performed using the discrete algorithm presented in the previous sections. In Fig. 5.28 the global reaction force is plotted versus the relative displacement $\lambda = \frac{u}{u_{m1}}$ and the curve resulting from the simulation is compared with the one measured in laboratory. Note that there is a good agreement between the two curves up to the value $\lambda = 0.7$.

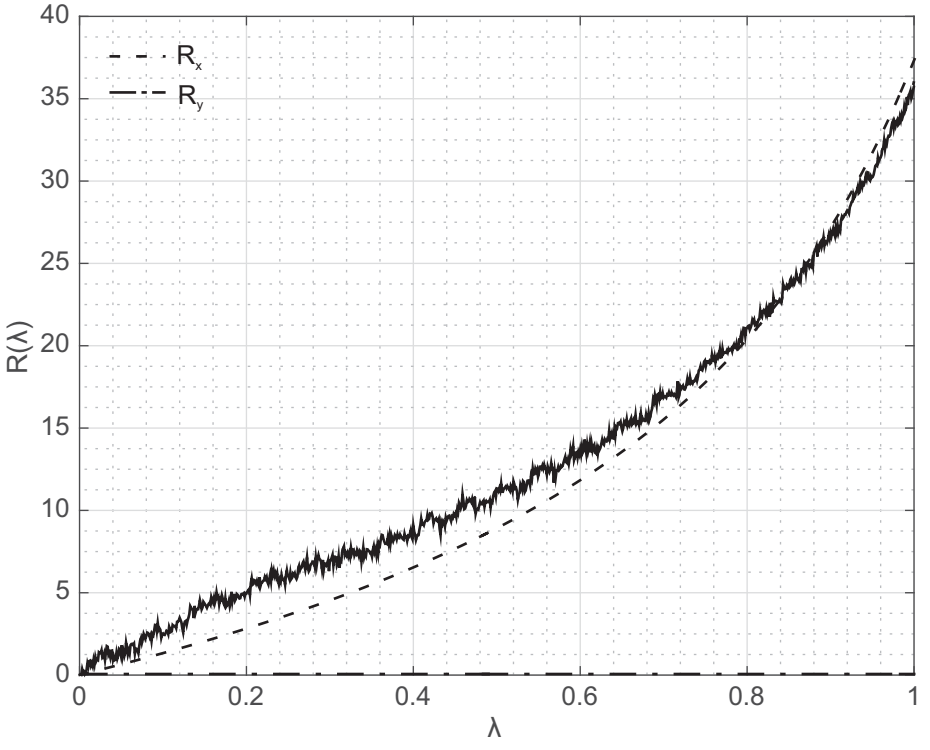

Figure 5.23 The reaction force versus the relative displacement λ for the parameters in the second row of Table 2.

In contrast Fig. 5.29, illustrates the evolution of deformation and axial force as the variable λ increases. In particular the colors refer to the level of axial force on the extensional springs. Two pictures are shown, corresponding to $\lambda = 0.5$ and $\lambda = 1$.

The second test, namely the T_2-test, consists in the application of a vertical displacement, along the longer side of the sheet, on the end of a fiber, in this specific example the sixth from the top. The bottom shorter side, instead, is clamped. The test is stopped at the maximum displacement, $u_{m2} = 40.7$ mm.

Also in this case we are going to compare the results with those obtained via a numerical simulation of the same test based on the discrete Hencky model previously introduced. In Fig. 5.30 a plot of the reaction force versus the relative displacement $\lambda = \frac{u}{u_{m2}}$ is compared with the experimental curve: a good agreement can be noticed up to $\lambda = 0.6$.

The two pictures in Fig. 5.31 show the deformation of the simulated pantographic lattice for the values $\lambda = 0.5$ and $\lambda = 1$, respectively. The colors refer to the intensity of the axial force on the elongation springs.

Let us conclude this subsection by remarking that, apart from the values of the stiffnesses, different power laws could also be used to define the strain energy. In particular, the quadratic law used for the shear contribution, could be modified to get a better fit with experimental data, as already suggested in [51].

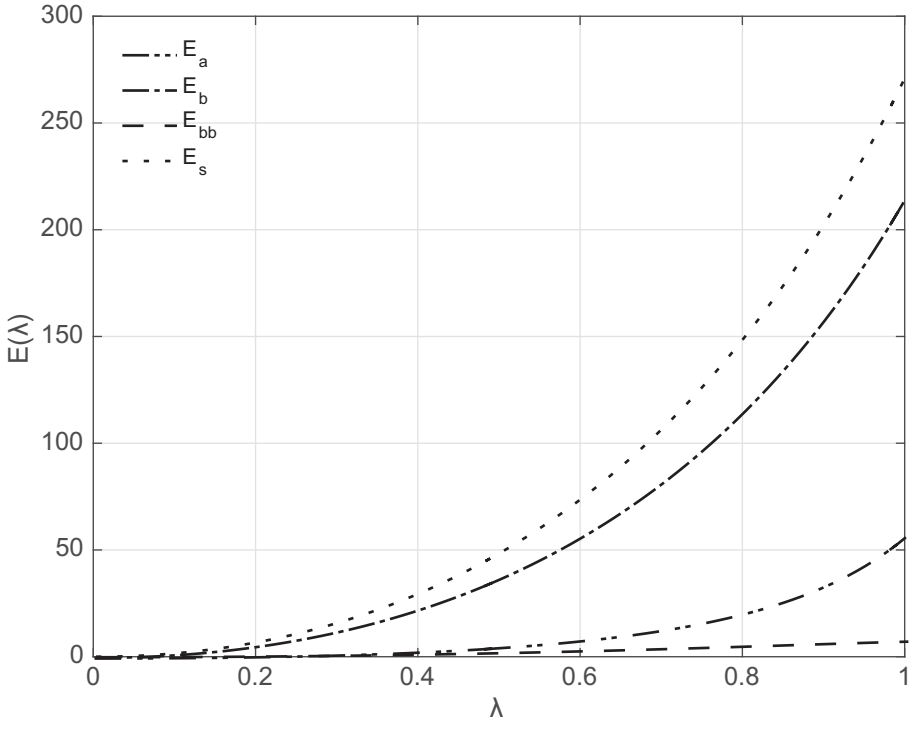

Figure 5.24 Contributions to the energy as the relative displacement λ increases.

5.4.4 King Post Truss Motif for Pantographic Fabrics

In [96], the king post truss motif (see Figs. 5.32 and 5.33) has been exploited at the microscopic level in order to show the advantageous behavior which can be obtained at the macro-level. In particular, the structure is made up by "pantographic beams" (i.e. two orthogonal families of hinge–truss systems – referred to as beams – depicted in black), by "king post rods" (in in dashed and dot-dashed lines) conferring a bending stiffness to each pantographic beam, and the "auxiliary rods" (in gray lines), which prevent rigid body motions of the lattice. We note that the king post rod configuration is completely described by means of two parameters, i.e. (ξ_1,η_1) and (ξ_2,η_2), see Fig. 5.32b.

We note that, in [96], only two-dimensional sheet structures, and only their in-plane motion, have been considered. This should not be considered as a limitation, as these sheets can possibly be further combined to form multi-layered laminates or other 3D structures. We further note that in an analogous manner to what has been done in [50, 97], the results presented in [96] for the case of orthogonal pantographic beams can be extended to the case of non-orthogonal pantographic beams, so that also considering orthogonal pantographic beams is not to be deemed as a limitation.

By analogy with the model presented in Section 5.4.1, a quite natural description of a king post pantographic lattice can be given by using a set of Lagrangian parameters which indicate the position of nodes, which can be divided in two categories: those

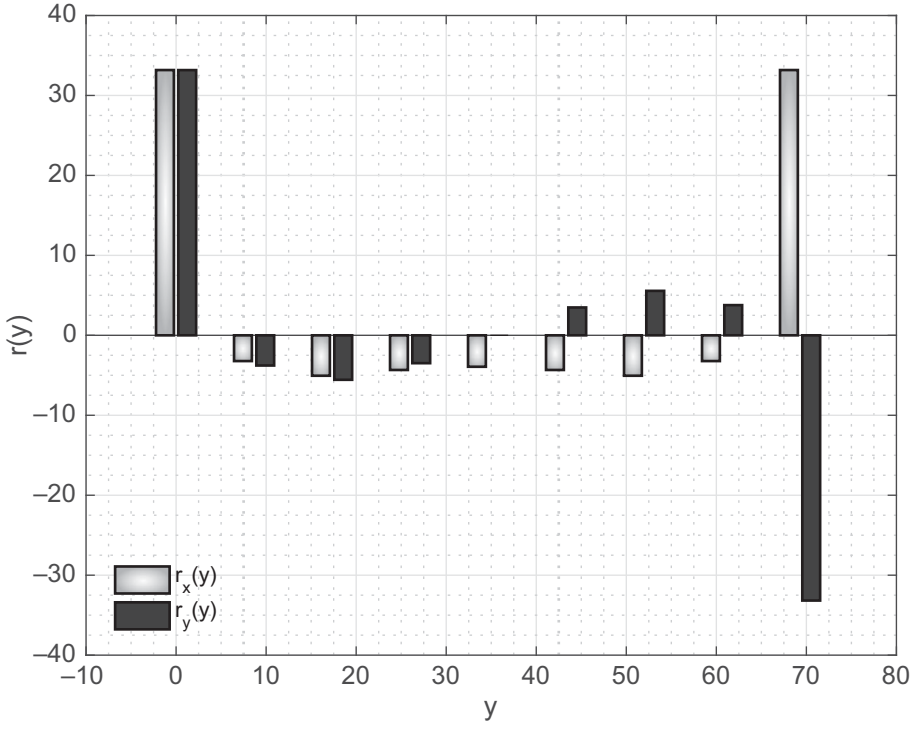

Figure 5.25 The reaction force density along the shorter side of the rectangular sheet.

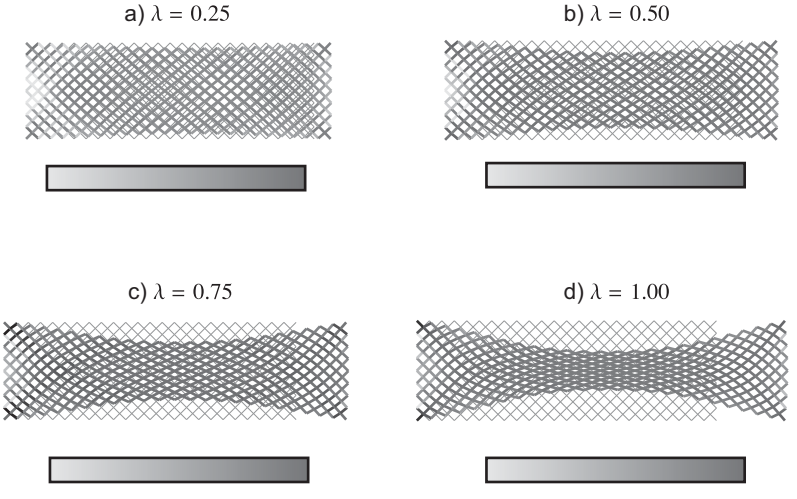

Figure 5.26 Deformation of the specimen for four different values of the variable $\lambda = 0.25, 0.5, 0.75, 1$. The colors refer to the level of the strain energy density.

Table 5.3 Stiffnesses for the discrete model obtained by means of an identification procedure.

a (N/mm)	b_1(N mm)	b_2(N mm)	s(N mm)
265.6	238.2	238.2	0.9739

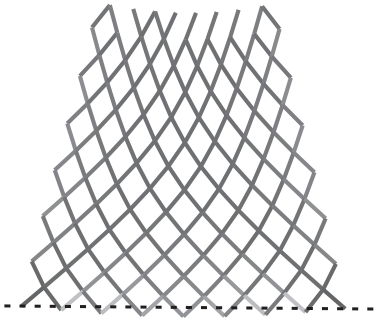

Figure 5.27 Magnification of the numerical simulation close to the boundary with a prescribed displacement. Note the same effect as illustrated in Fig. 5.21.

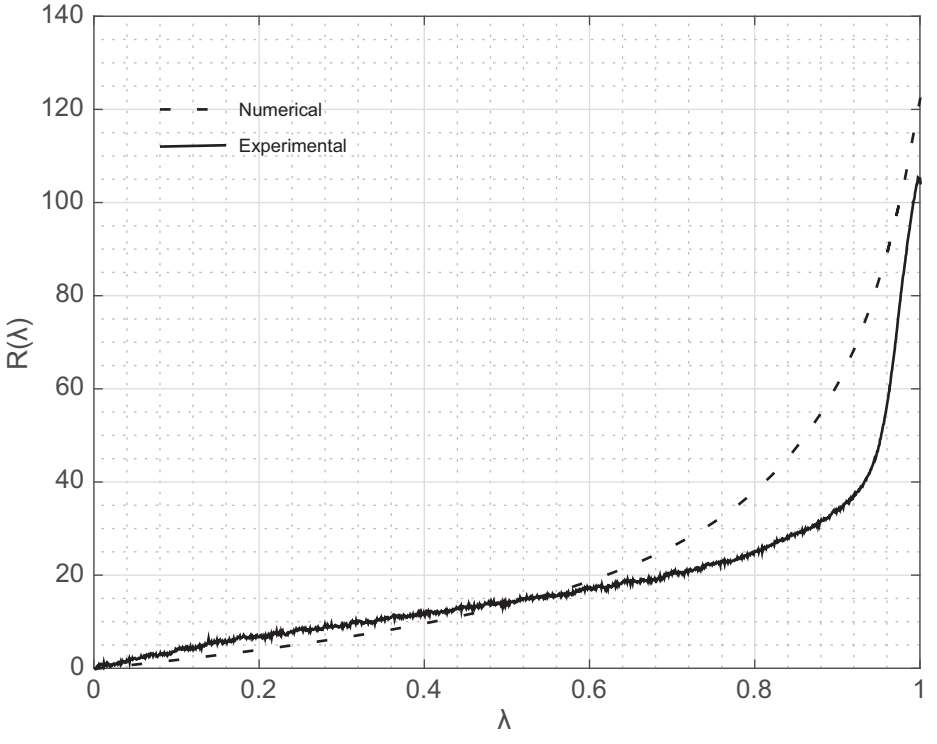

Figure 5.28 The reaction force versus the relative displacement λ for the T1-test. Dotted line indicates the numerical simulation whereas continuous line refers to experimental data.

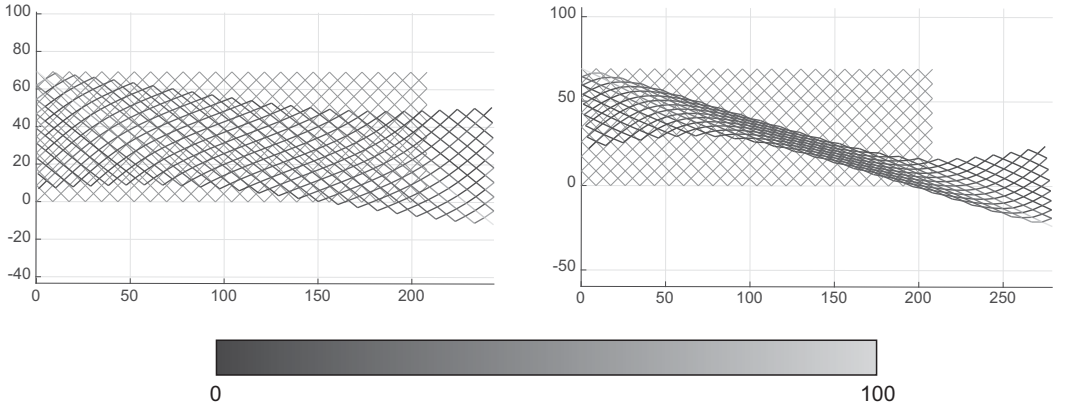

Figure 5.29 Simulation of the T1-test obtained via the discrete Hencky model. Deformations correspond to the values $\lambda = 0.5$ on the left and $\lambda = 1$ on the right. The colors refer to the level of the axial force on the extensional springs.

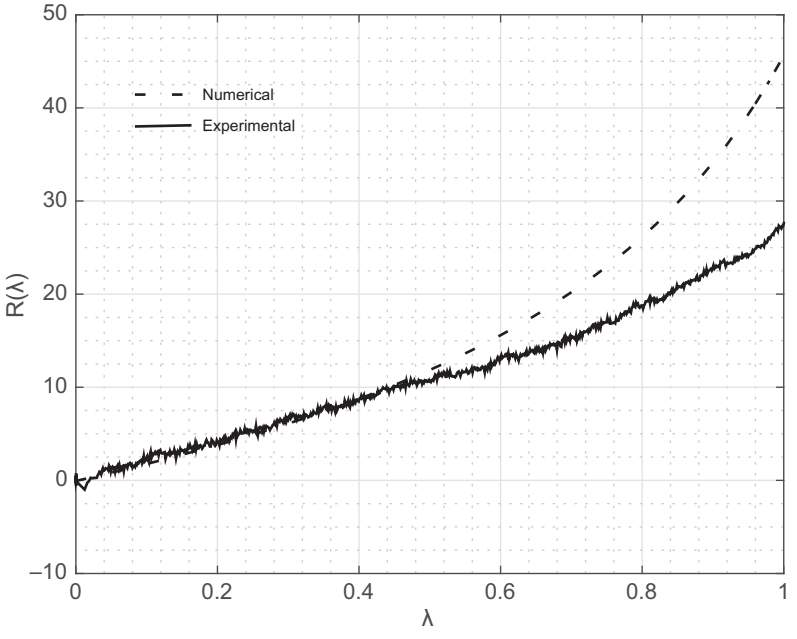

Figure 5.30 The reaction force versus the relative displacement λ for the T2-test. Dotted line indicates the numerical simulation whereas continuous line refers to experimental data.

at the intersection of two pantographic bars and those at the intersection of king post bars. Note that, as we are now concentrating on planar motions, a set of $2n$ (with n being the number of nodes) coordinates is sufficient. The position of the generic node in the undeformed configuration is labeled as P_i, while its position in the deformed configuration is denoted p_i. We now turn to the definition of the strain energy of such a

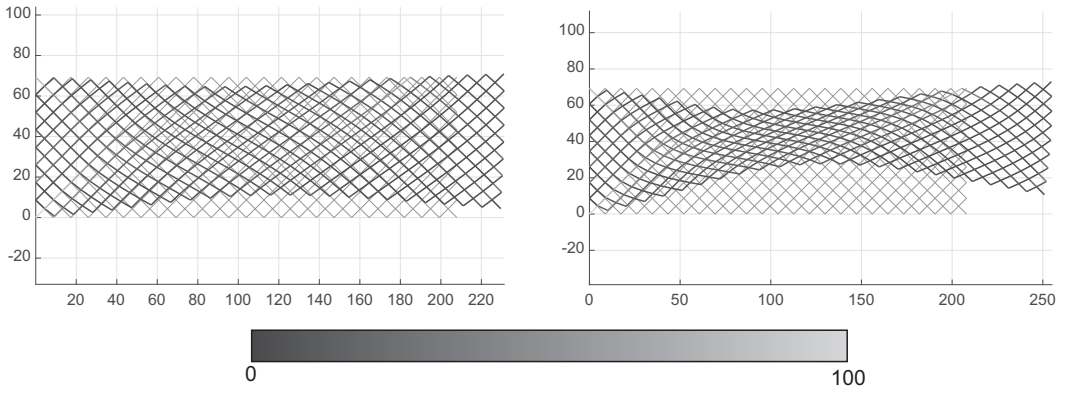

Figure 5.31 Simulation of the T2-test obtained via the discrete Hencky model. Deformations corresponding to the values $\lambda = 0.5$ on the left and $\lambda = 1$ on the right. The colors refer to the level of the axial force on the extensional springs.

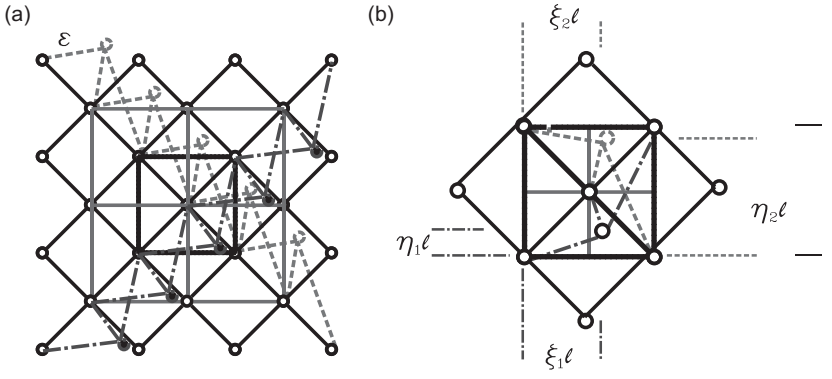

Figure 5.32 Pantographic king post lattice: king post rods (dashed and dot-dashed lines), pantographic rods (black solid lines), and auxiliary rods (grey lines) (a) and geometric parameters of a king post cell (b).

system. In [96], as all the slender elements in Fig. 5.32a and Fig. 5.32b are considered to be standard elastic trusses, the following form of the discrete Lagrangian deformation energy W_{int}, written in terms of the Lagrangian coordinates p_i is postulated:

$$W_{\text{int}}(\mathbf{d}) = \sum_{e=1}^{n_e} \frac{1}{2} a_e \left(\| p_{j_e} - p_{i_e} \| - \| P_{j_e} - P_{i_e} \| \right)^2, \tag{5.123}$$

where the vector $\mathbf{d}$ contains the nodal displacements of the lattice, the index e ranging over all the n_e bars, and a_e is the axial stiffness of the eth bar (the stiffnesses of the rods are not all the same, see Fig. 5.33).

Numerical and Experimental Results

In [96], numerical simulations of extension, shear and bending tests have been presented. The equilibrium configurations of the structure obtained by imposing a vanishing

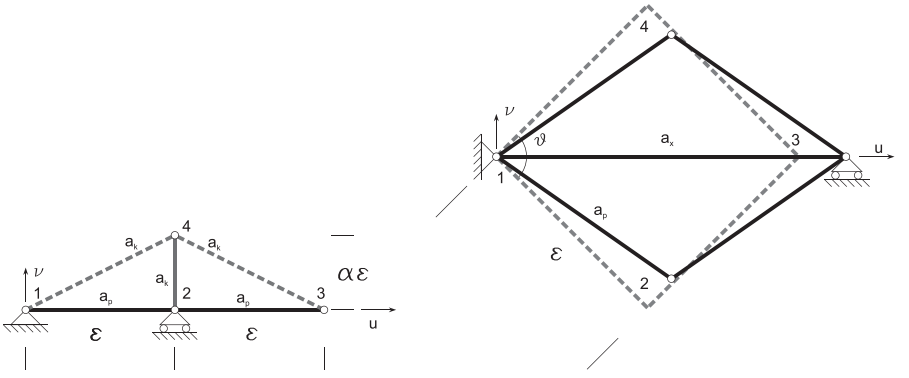

Figure 5.33 King post truss. Rod stiffnesses and geometry (left). Single pantographic square with an auxiliary rod. Geometry and rod stiffnesses (right).

first variation of the Lagrangian function (5.123) have been numerically computed using the algorithm discussed in Section 5.4.2.

The following data have been used for the quantities introduced in Fig. 5.32:

1. geometry: $L = 66.114$; $\dfrac{L}{\varepsilon} = 4\sqrt{2}$; $\xi_1 = 0.75$; $\eta_1 = 0,25$; $\xi_2 = 0,75$; $\eta_2 = 0,75$;
2. mechanical properties: $a_p = 1$; $\dfrac{a_x}{a_p} = 10^{-5}$.

The following values of the displacements have been assumed for the three numerical simulations:

1. extension test $u_1(0, x_2) = u_1(0, x_2) = u_2(3L, x_2) = 0$ and $u_1(3L, x_2) = u_1^{\max} = 75$;
2. shear test $u_1(0, x_2) = u_2(0, x_2) = u_1(3L, x_2) = 0$ and $u_2(3L, x_2) = u_2^{\max} = 75$;
3. bending test $u_1(0, x_2) = u_2(0, x_2) = 0$ and $u_2(3L, x_2) = u_1^{\max}\left(1 - 2(\dfrac{x_2}{L})\right)$, $u_1^{\max} = 35$.

In Fig. 5.34 the non-dimensional structural reaction in the x-direction $R/(3L^2 a_p)$ (Figs. 5.34a and 5.34e) and the y-direction $R/(3L^2 a_p)$ (Fig. 5.34c) and non-dimensional global strain energy $W/(3L^2 a_p)$ evolution (Figs. 5.34b, 5.34d, and 5.34f) with varying $a = a_k/a_p$ are plotted. Figures 5.34a and 5.34b refer to the extension test; Figs. 5.34c and 5.34d refer to the shear test; Figs. 5.34e and 5.34f refer to the bending test. In these plots, the black triangles give an indication of the slope of the reactions linear law (λ) and of the strain energies quadratic law (λ^2).

In [96], on the basis of these plots, it is argued that, notwithstanding its simple constituents, the king post motif applied to pantographic fabrics gives a highly non-linear non-standard elastic behavior. It is remarkable that for critical extension and bending, a reversible phase transition from a linear, relatively soft material to a hardening and stiff one happens, while retaining a classical behaviour in shear. Indeed, in the extension test (Figs. 5.34a and 5.34b), the system exhibits a linear (quadratic in energy) behavior up to $\lambda \approx 0.4$. After this point, hardening begins and this deviation from linearity in

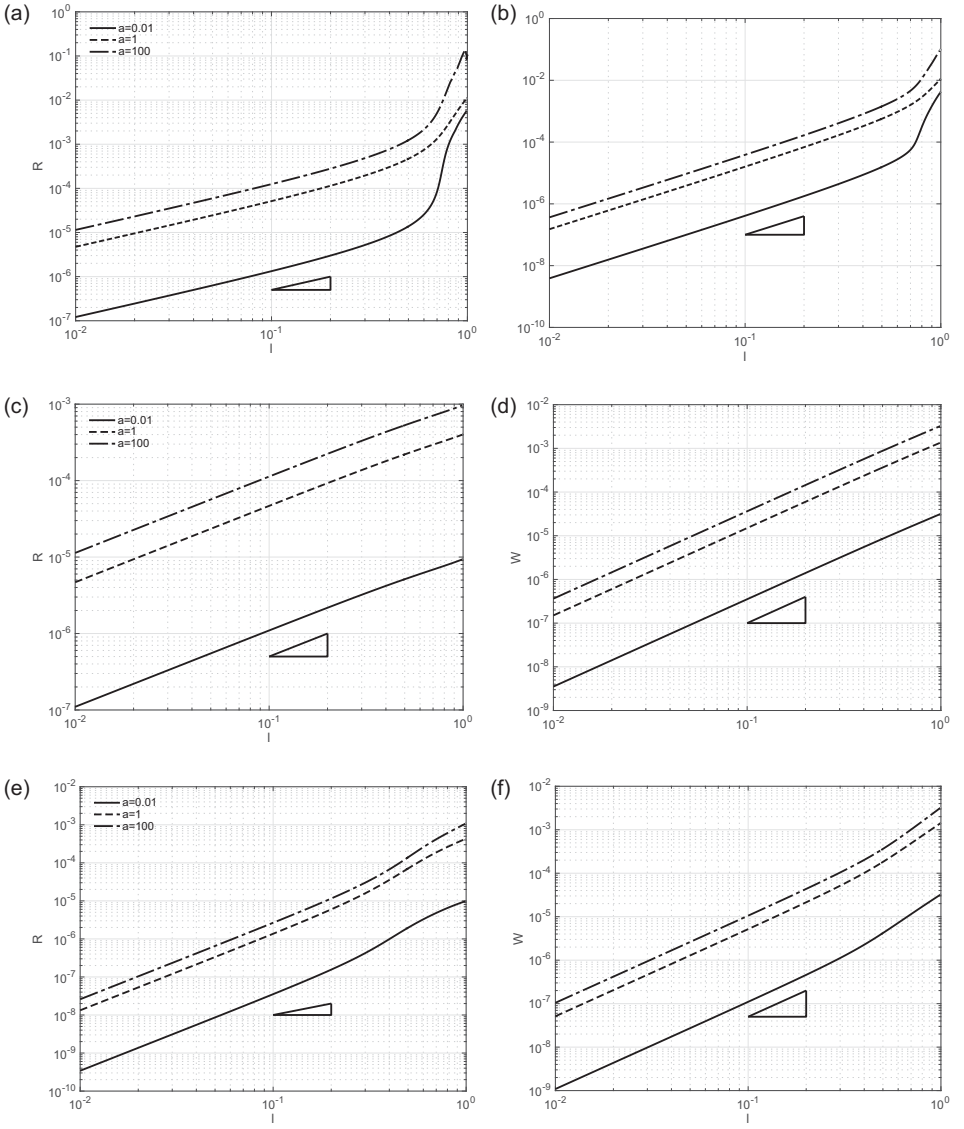

Figure 5.34 Extension, shear and bending tests: non-dimensional structural reaction in the x-direction $\frac{R}{3L^2a_p}$ (a,e) and the y-direction $\frac{R}{3L^2a_p}$ (c) and non-dimensional global strain energy $\frac{W}{3L^2a_p}$ evolution (b,d,f) varying $a = \frac{a_k}{a_p}$ and taking $u_1^{\max} = 75$ for the extension test (a,b), $u_2^{\max} = 75$ for the shear test (c,d) and $u_1^{\max} = 35$ for the bending test (the triangle indicates the slope of the structural reaction linear law for the strain energy quadratic law.).

the reaction is especially evident for $a = 0.01$. In the case of bending (Figs. 5.34c and 5.34d), a similar transition from a softer to a stiffer system is observable. However, in the case of shear (Figs. 5.34e and 5.34f), the material system retains a classical linear response (quadratic in energy) within the deformation range considered. It is possible

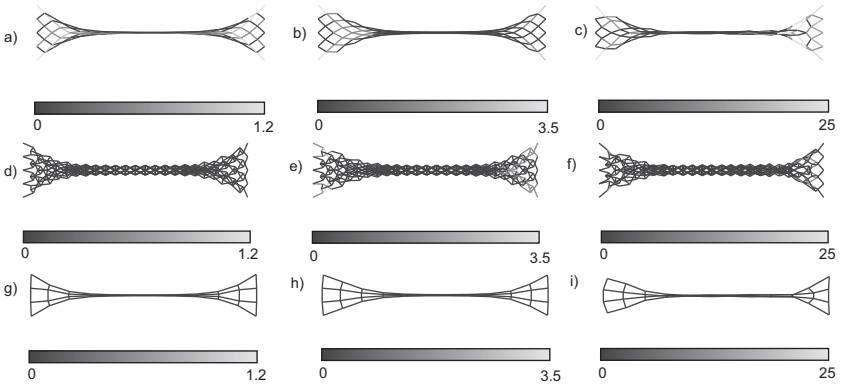

Figure 5.35 Extension test: levels of deformation and strain-energy (from the top, respectively, for pantographic, king post and auxiliary rods) for $\lambda = 1$ varying $a = \frac{a_k}{a_p}$: $a = 0, 01$ (a,d,g), $a = 1$ (b,e,h), $a = 100$ (c,f,i).

to argue that these phase transitions occurring in selected deformation modes might open the way to some new interesting applications. Pantographic structures exhibit, both locally and globally, deformation modes entailing a null deformation energy.

In [96] there is discussion that beyond some thresholds, since the surface of floppy modes has a boundary, the pantographic sheet becomes locally a standard plate, and this phase transition entails the otherwise soft system becoming much stiffer. To give an insight into the macroscopic behaviors of king post pantographic structure, in Figs. 5.35–5.38 some deformed shapes (colors representing the strain-energy level) obtained at the end of the corresponding test (extension, shear, bending) are shown for varying stiffness parameter $a = \frac{a_k}{a_p}$. For clarity, we have plotted separately the deformed shapes of pantographic, king post and auxiliary rods. In the extension case (see Fig. 5.35), the auxiliary rods contribute only negligibly to the strain energy, while the pantographic rods contribute the most for the adopted stiffness parameter a. In the shear and bending cases (Figs. 5.37 and 5.38, respectively), the king post rods and the pantographic rods contribute most to the strain energy; however, the energy distribution depends on the stiffness parameter a. For $a < 1$, the king post rods make the largest contribution to the strain energy, while for $a > 1$ the pantographic rods make the largest contribution to the strain energy. Finally, in Fig. 5.36 the structural reaction density on the left-hand side for various values of a is plotted.

5.5 Towards 3D Models: Hencky-Type Model for *Elastica*

In this section, we briefly describe the basic tools for defining a simple model, first introduced in a systematic way by Hencky (see [91]) and already outlined in the works of Piola (see [98, 99]), which is able to forecast the behavior in dynamics of the *Elastica* in the three-dimensional space. The model sketched below was initially presented in

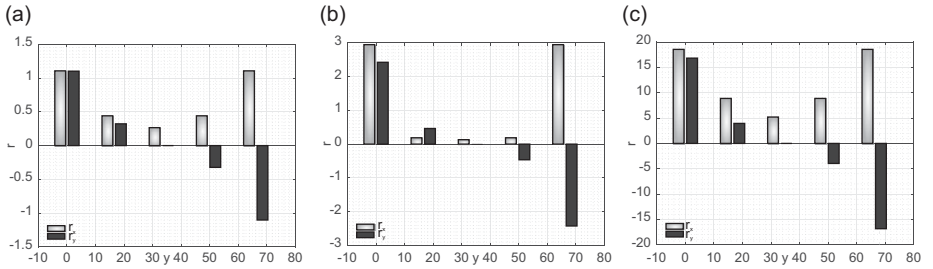

Figure 5.36 Extension test: structural reaction density r on the left-hand side ($x = 0$) for $\lambda = 1$ and varying $a = \frac{a_k}{a_p}$: $a = 0.01$ (a), $a = 1$ (b) and $a = 100$ (c).

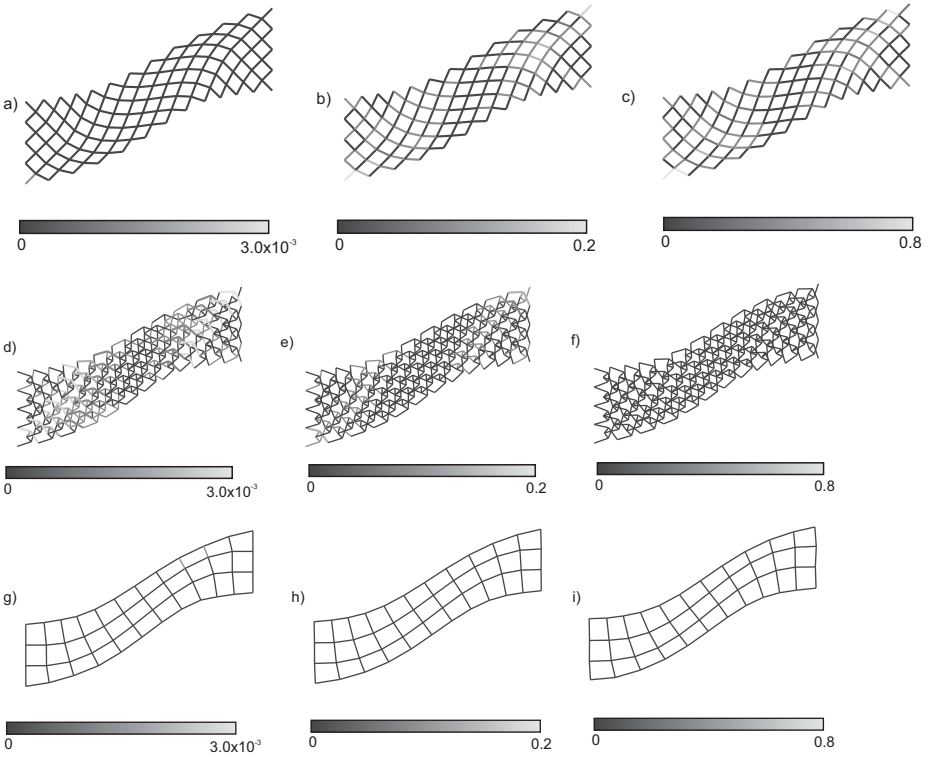

Figure 5.37 Shear test: levels of deformation and strain-energy (from the top, respectively, for pantographic, king post and auxiliary rods) for $\lambda = 1$ varying $a = \frac{a_k}{a_p}$: $a = 0.01$ (a,d,g), $a = 1$ (b,e,h), $a = 100$ (c,f ,i).

the static case for straight beams, see [100], revealing its ability to predict equilibrium paths parameterized by (one or more) load parameters in a large displacements regime. Following the spirit of Lagrangian mechanics, we introduce the main hypotheses of the model and, successively, the external load energy contributions, and the elementary contributions to the strain and kinetic energy in addition to describe the load contributions.

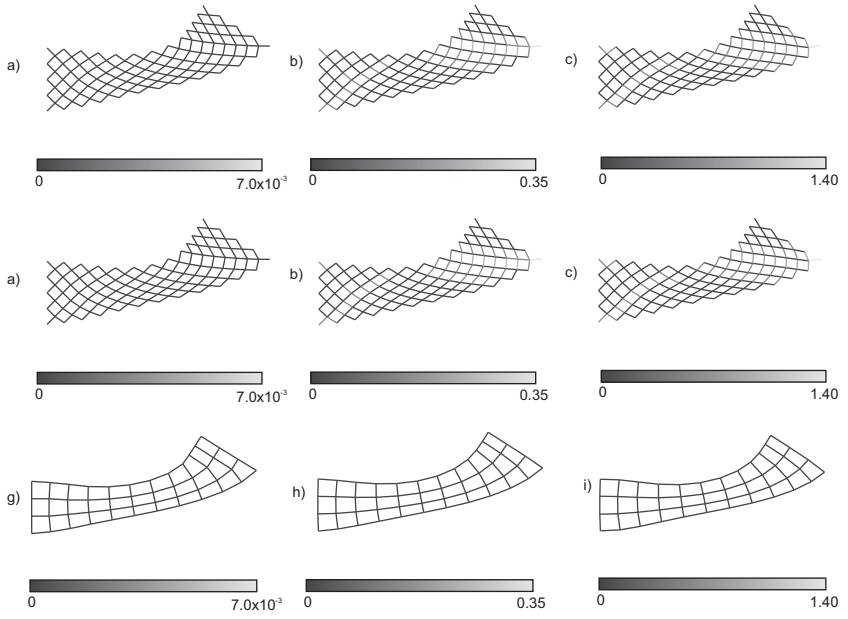

Figure 5.38 Bending test: levels of deformation and strain-energy (from the top, respectively, for pantographic, king post and auxiliary rods) for $\lambda = 1$ varying $a = \frac{a_k}{a_p}$: $a = 0.01$ (a,d,g), $a = 1$ (b,e,h), $a = 100$ (c,f ,i).

Let us consider in the three-dimensional Euclidean space $\mathbb{E}^3$ an inextensible beam and let us suppose that the mechanical behavior of the beam can be described by a sequence of rigid and rectilinear links, of the same length ℓ[16] connected by point bending elastic joints. The position of an arbitrary point of the lth link is described by the vectors $\mathbf{R}_l$ and $\mathbf{r}_l$ which define its reference and current configurations, respectively. The orientation of each link, instead, can be completely described by the unit vectors $\mathbf{D}_{3l}$ and $\mathbf{d}_{3l}$ in the reference and current configurations, respectively. The local reference system is completed by the unit vectors $\mathbf{D}_{1l}$ and $\mathbf{D}_{2l}$ which are relative to the reference configuration, whereas we have indicated with the unit vectors $\mathbf{d}_{1l}$ and $\mathbf{d}_{2l}$ the corresponding description of the current configuration. For each rigid link, for the reference and current configuration, respectively, we have

$$\begin{aligned} \mathbf{R}_{l+1} &= \mathbf{R}_l + \ell\, \mathbf{D}_{3l}\,, \\ \mathbf{r}_{l+1} &= \mathbf{r}_l + \ell\, \mathbf{Q}_l \mathbf{D}_{3l}\,, \end{aligned} \tag{5.124}$$

where $\mathbf{Q}_l$ is a rotation matrix which, by means of the Rodrigues' formula,[17]

$$\mathbf{Q}_l = \cos\varphi_l\, \mathbf{I} + (1 - \cos\varphi_l)\, \mathbf{e}_l \otimes \mathbf{e}_l + \sin\varphi_l\, \mathbf{E}_l\,, \tag{5.125}$$

where φ_l is the rotation angle, $\mathbf{e}_l$ the unit vector which defines the axis of rotation, and the tensor $\mathbf{E}_l$ is defined by $\mathbf{E}_l\mathbf{u} = \mathbf{e}_l \times \mathbf{u}$ for any vector $\mathbf{u}$.

[16] This hypothesis can easily be relaxed.
[17] In Euler's paper [101] it is possible to find this representation, as reported in [102].

The rotation angle φ_l relative to the axis $\mathbf{e}_l$ can be expressed in terms of the rotation tensor $\mathbf{Q}_l$ as

$$\begin{aligned} 2\cos\varphi_l &= \operatorname{tr}\mathbf{Q}_l - 1\,, \\ 2\sin\varphi_l\,\mathbf{e}_l &= \mathbf{Q}_{l\times}\,, \end{aligned} \tag{5.126}$$

where $\mathbf{Q}_{l\times}$ is the vectorial invariant of $\mathbf{Q}_l$ and with $\operatorname{tr}(\cdot)$ we have indicated the trace operator. The finite rotation vector[18] associated with $\mathbf{Q}_l$ can be defined as

$$\boldsymbol{\theta}_l = 2\tan\frac{\varphi_l}{2}\mathbf{e}_l\,, \tag{5.127}$$

so that, as a consequence, each $\mathbf{Q}_l$ can be written as [104]

$$\mathbf{Q}_l = \frac{1}{4+\vartheta_l^2}\left((4-\vartheta_l^2)\mathbf{I} + 2\boldsymbol{\theta}_l\otimes\boldsymbol{\theta}_l + 4\vartheta_l\mathbf{E}_l\right)\,, \tag{5.128}$$

where $\vartheta_l^2 = \boldsymbol{\theta}_l\cdot\boldsymbol{\theta}_l$. The use of a vector in place of a tensor for defining a rotation represents the main advantage of Eq. (5.128). This not only simplifies the definition of the strain energy, but it is also convenient computationally.

Having defined the kinematics of the motion for each rigid link, we need a suitable measure for the strain of elastic joints. For the joint between the lth and the $(l+1)$th link, the relative rotation tensor $\mathbf{P}_{l+1}$ is defined in the following way:

$$\mathbf{P}_{l+1} = \mathbf{Q}_l^T\mathbf{Q}_{l+1}\,, \tag{5.129}$$

whereas the vector $\boldsymbol{\phi}_{l+1}$ of the finite rotations, or, alternatively, the angle ϕ_{l+1} of relative rotation and the vector $\mathbf{e}_{l+1}$, are defined by Eq. (5.126).

Finally, by using the finite relative rotation vector $\boldsymbol{\phi}_{l+1}$ just introduced we can define the strain energy. The simplest form is

$$2E_{l+1} = \boldsymbol{\phi}_{l+1}\cdot\mathbf{B}\,\boldsymbol{\phi}_{l+1}\,, \tag{5.130}$$

where the matrix $\mathbf{B}$ collects the stiffness parameters. If we choose a diagonal form for $\mathbf{B}$, the three stiffnesses are related to bending (two terms), and torsion (one term). From Eq. (5.130), it is possible to derive the structural reaction, the gradient, and the tangent stiffness matrix (the Hessian) related to the pair of links sharing the same elastic joints.

In order to complete the description of the discrete model introduced in the spirit of Hencky, we need the definition of the kinetic energy of each rigid link involved in the modelling of the beam. The lth rigid link can be viewed as a rigid body and, therefore, the current position of each single material point is described (see [104] for a concise introduction to the dynamics of rigid bodies and [102, 105] for an extended one), by

$$\mathbf{r}_l(t) = \mathbf{R}_{lO} + \mathbf{u}_l(t) + \mathbf{Q}_l(t)\mathbf{Z}_l\,, \tag{5.131}$$

where $\mathbf{R}_{lO}$ is the position in the reference configuration of an arbitrary point of the lth link chosen as pole, $\mathbf{u}_l$ the displacement of the pole O, and $\mathbf{Z}_l$ the position of an arbitrary material point in the reference configuration.

[18] Apart from an irrelevant factor 2, expression (5.127) can also be found in O'Reilly [102] and is called the Rodrigues vector. In the authors' opinion, Eq. (5.127) was initially written to exploit its suitability for small displacement analysis.

Deriving Eq. (5.130) with respect to time, we can compute the velocity

$$\dot{\mathbf{r}}_l(t) = \dot{\mathbf{u}}_l(t) + \dot{\mathbf{Q}}_l(t)\mathbf{Z}_l \,, \tag{5.132}$$

where dots indicate time derivatives. Since $\mathbf{Q}_l$ is a proper orthogonal tensor, then

$$\dot{\mathbf{Q}}_l = \dot{\mathbf{Q}}_l \mathbf{Q}_l^T \mathbf{Q}_l \,, \tag{5.133}$$

and, furthermore, we note that $\dot{\mathbf{Q}}_l \mathbf{Q}_l^T$ is a skew-symmetric tensor. Therefore, by using the angular velocity vector $\boldsymbol{\omega}_l$ defined as

$$\boldsymbol{\omega}_l = -\frac{1}{2}\left(\dot{\mathbf{Q}}_l \mathbf{Q}_l^T\right)_\times \,, \tag{5.134}$$

we can rewrite Eq. (5.132) as

$$\dot{\mathbf{u}}_l(t) = \dot{\mathbf{u}}_{lO}(t) + \boldsymbol{\omega}_l(t) \times \mathbf{Q}_l(t)\mathbf{Z}_l \,, \tag{5.135}$$

where it is possible to distinguish between translation and rotation velocities.

In order to work with handy formulas, it is convenient to choose as pole O the mass center of the link, which is defined as

$$\int_{v_l} \rho(\mathbf{r}_l - \mathbf{r}_{lO}) dv \,, \tag{5.136}$$

where ρ is the mass density, in such a way that the kinetic energy can be expressed as

$$E_c = \frac{1}{2}\left(m_l \dot{\mathbf{u}}_{lO} \cdot \dot{\mathbf{u}}_{lO} + \boldsymbol{\omega}_l \cdot \mathbf{J}_l \boldsymbol{\omega}_l\right) \,, \tag{5.137}$$

where the inertia tensor $\mathbf{J}_l$ can be evaluated as

$$\mathbf{J}_l = \mathbf{Q}_l \left(\int_{V_l} \rho_l \left((\mathbf{Z}_l \cdot \mathbf{Z}_l)\, \mathbf{I} - \mathbf{Z}_l \otimes \mathbf{Z}_l \right) dV \right) \mathbf{Q}_l^T \,. \tag{5.138}$$

Some further specifications are still needed to obtain the vector of generalized external forces.[19]

For example, a torque $\mathbf{m}_l$ on the lth link gives a contribution W_c to the external work which is equal to

$$W_c = \frac{2 \arctan \dfrac{\|\boldsymbol{\theta}_l\|}{2}}{\|\boldsymbol{\theta}_l\|} \mathbf{m}_l \cdot \boldsymbol{\theta}_l \,, \tag{5.139}$$

taking into account the change of variables defined in Eq. (5.127). Similarly, the contribution to the external work of an external force $\mathbf{f}_l$ acting on the position $\alpha\ell$ from the left end of the lth link can be computed:

$$W_f = \mathbf{f} \cdot \left((\mathbf{r}_1 - \mathbf{R}_1) + \ell \sum_{k=1}^{l-1} (\mathbf{Q}_k - \mathbf{I})\, \mathbf{D}_{3k} + \alpha\ell\, (\mathbf{Q}_l - \mathbf{I})\, \mathbf{D}_{3l} \right) \,. \tag{5.140}$$

Analogously, it is possible to compute the contributions to the external work of distributed axial and shear loads and distributed torques.

[19] We emphasize that in this section all the generalised external forces are dead loads.

5.6 Conclusions and Perspectives

In this chapter, we have reviewed a method proposed in [48] to model complex mechanical systems in terms of a discrete Lagrangian model directly inspired by the microstructure of the system. Two examples have been analyzed in detail, namely the pantographic sheet and the three dimensional *Elastica*. A good agreement with both homogenized second gradient continuum theory and experimental data has been obtained, including when the structure under analysis undergoes large deformations [92]. Higher gradient continua are those continua in which different length scales play an important role at macro-level (see for instance [36, 40, 80, 93] and the chapters about pantographic structures, and [46, 124]) In order to make the discussion self-consistent, a review of the main ideas and tools of the Lagrangian formulation of mechanics was presented at the beginning of the chapter.

Starting from the results presented, several interesting research lines can be considered. For instance, one may look for a generalization of the discrete model for the pantographic sheet to out-of-plane deformations (preliminary studies can be found in [92, 106, 108, 109]). To this end, the analysis performed in the last section can be considered as a preparatory stage. Another interesting possibility is to study wave-propagation phenomena in a pantographic sheet [28, 110–113], by implementing the kinetic energy part in the Lagrangian function also, following the methods discussed in Section 5.5 for the three-dimensional *Elastica*. The feasibility of the description of non-ordered microstructure by means of the methods presented can also be analyzed. Finally, the analysis of fiber rupture is of great interest for engineering applications [114–123].

The hope of the authors is that the discussions herein have brought out the importance of the Lagrangian formalism in modern mechanics, in particular when it is wished to exploit the relation between discrete and continuous models.

Bibliography

[1] S. Caprino, R. Esposito, R. Marra, and M. Pulvirenti. Hydrodynamic limits of the Vlasov equation. *Communications in Partial Differential Equations*, 18(5):805–820, 1993.

[2] A. De Masi and S. Olla. Quasi-static hydrodynamic limits. *Journal of Statistical Physics*, 161(5):1037–1058, Dec 2015.

[3] A. De Masi, A. Galves, E. Löcherbach, and E. Presutti. Hydrodynamic limit for interacting neurons. *Journal of Statistical Physics*, 158(4):866–902, Feb 2015.

[4] Gioia Carinci, A. De Masi, C. Giardinà, and E. Presutti. Super-hydrodynamic limit in interacting particle systems. *Journal of Statistical Physics*, 155(5):867–887, Jun 2014.

[5] G. Carinci, A. De Masi, C. Giardinà, and Errico Presutti. Hydrodynamic limit in a particle system with topological interactions. *Arabian Journal of Mathematics*, 3(4):381–417, Dec 2014.

[6] R. Esposito and M. Pulvirenti. From particles to fluids. *Handbook of Mathematical Fluid Dynamics*, Vol. III, eds. S. Friedlander and D. Serre, pp. 1–82, North Holland, Amsterdam, 2004.

[7] M. Pulvirenti. *Kinetic Limits for Stochastic Particle Systems*. Lecture Notes in Mathematics- Springer-Verlag, 1996.

[8] Francesco dell'Isola, David Steigmann, and Alessandro Della Corte. Synthesis of fibrous complex structures: Designing microstructure to deliver targeted macroscale response. *Applied Mechanics Reviews*, 67(6):21pages, 2016.

[9] N.A. Fleck, V.S. Deshpande, and M.F. Ashby. Micro-architectured materials: Past, present and future. In *Proceedings of the Royal Society of London A: Mathematical, Physical and Engineering Sciences*, 466(2121): 2495–2516, 2010.

[10] Emilio Barchiesi, Francesco dell'Isola, Marco Laudato, Luca Placidi, and Pierre Seppecher. A 1D continuum model for beams with pantographic microstructure: Asymptotic micro-macro identification and numerical results. In *Advances in Mechanics of Microstructured Media and Structures*, pages 43–74. Springer, 2018.

[11] D. Del Vescovo and I. Giorgio. Dynamic problems for metamaterials: Review of existing models and ideas for further research. *International Journal of Engineering Science*, 80:153–172, 2014.

[12] A. Rinaldi and L. Placidi. A microscale second gradient approximation of the damage parameter of quasi-brittle heterogeneous lattices. *ZAMM - Zeitschrift für Angewandte Mathematik und Mechanik/Journal of Applied Mathematics and Mechanics*, 2013.

[13] Marco Laudato and Fabio Di Cosmo. Euromech 579 arpino 3–8 April 2017: Generalized and microstructured continua: New ideas in modeling and/or applications to structures with (nearly)inextensible fibers—a review of presentations and discussions. *Continuum Mechanics and Thermodynamics*, 2018.

[14] David J. Steigmann and Francesco dell'Isola. Mechanical response of fabric sheets to three-dimensional bending, twisting, and stretching. *Acta Mechanica Sinica*, DOI:10.1007/s10409-015-0413-x.

[15] Ivan Giorgio, Roman Grygoruk, Francesco dell'Isola, and David J. Steigmann. Pattern formation in the three-dimensional deformations of fibered sheets. *Mechanics Research Communications*, 69:164–171, 2015.

[16] Emilio Barchiesi, Mario Spagnuolo, and Luca Placidi. Mechanical metamaterials: A state of the art. *Mathematics and Mechanics of Solids*, page 1081286517735695, 2018.

[17] E. Turco, K. Barcz, and N.L. Rizzi. Non-standard coupled extensional and bending bias tests for planar pantographic lattices. Part II: Comparison with experimental evidence. *Zeitschrift fur Angewandte Mathematik und Physik*, 67(5), 2016.

[18] Francesco dell'Isola and David Steigmann. A two-dimensional gradient-elasticity theory for woven fabrics. *Journal of Elasticity*, 118(1):113–125, 2015.

[19] Francesco dell'Isola, Sara Bucci, and Antonio Battista. Against the fragmentation of knowledge: The power of multidisciplinary research for the design of metamaterials. In *Advanced Methods of Continuum Mechanics for Materials and Structures*, pages 523–545. Springer, 2016.

[20] J. Clerk Maxwell. On the calculation of the equilibrium and stiffness of frames. *The London, Edinburgh, and Dublin Philosophical Magazine and Journal of Science*, 27(182):294–299, 1864.

[21] Fabio di Cosmo, Marco Laudato, and Mario Spagnuolo. Acoustic metamaterials based on local resonances: Homogenization, optimization and applications. In *Generalized Models and Non-classical Approaches in Complex Materials 1*, pages 247–274. Springer, 2018.

[22] A. Cazzani and M. Rovati. Sensitivity analysis and optimum design of elastic-plastic structural systems. *Meccanica*, 26(2–3):173–178, 1991.

[23] U. Andreaus, M. Colloca, D. Iacoviello, and M. Pignataro. Optimal-tuning PID control of adaptive materials for structural efficiency. *Structural and Multidisciplinary Optimization*, 43(1):43–59, 2011.

[24] Duy Khanh Trinh, Ralf Janicke, Nicolas Auffray, Stefan Diebels, and Samuel Forest. Evaluation of generalized continuum substitution models for heterogeneous materials. *International Journal for Multiscale Computational Engineering*, 10(6), 2012.

[25] T. Lekszycki. Optimality conditions in modelling of bone adaptation phenomenon. *Journal of Theoretical and Applied Mechanics*, pages 607–623, 1999.

[26] T. Lekszycki. Modelling of bone adaptation based on an optimal response hypothesis. *Meccanica*, 37(4):343–354, 2002.

[27] T. Lekszycki. Functional adaptation of bone as an optimal control problem. *Journal of Theoretical and Applied Mechanics*, 43(3):555–574, 2005.

[28] Francesco dell'Isola, Ivan Giorgio, and Ugo Andreaus. Elastic pantographic 2D lattices: a numerical analysis on static response and wave propagation. *Proceedings of the Estonian Academy of Sciences*, 2015.

[29] Angelo Luongo, Daniele Zulli, and Giuseppe Piccardo. Analytical and numerical approaches to nonlinear galloping of internally resonant suspended cables. *Journal of Sound and Vibration*, 315(3):375–393, 2008.

[30] A. Javili, A. McBride, and P. Steinmann. Numerical modelling of thermomechanical solids with mechanically energetic (generalised) Kapitza interfaces. *Computational Materials Science*, 65:542–551, 2012.

[31] E. Turco and P. Caracciolo. Elasto-plastic analysis of Kirchhoff plates by high simplicity finite elements. *Computer Methods in Applied Mechanics and Engineering*, 190(5–7):691–706, 2000.

[32] Antonio Cazzani, Marcello Malagù, and Emilio Turco. Isogeometric analysis: A powerful numerical tool for the elastic analysis of historical masonry arches. *Continuum Mechanics and Thermodynamics*, pages 1–18, 2014.

[33] Antonio Cazzani, Marcello Malagù, Emilio Turco, and Flavio Stochino. Constitutive models for strongly curved beams in the frame of isogeometric analysis. *Mathematics and Mechanics of Solids*, page 1081286515577043, 2015.

[34] U. Andreaus, F. dell'Isola, I. Giorgio, *et al.* Numerical simulations of classical problems in two-dimensional (non) linear second gradient elasticity. *International Journal of Engineering Science*, 108:34–50, 2016.

[35] F. dell'Isola, P. Seppecher, and A. Della Corte. The postulations à la d'Alembert and à la Cauchy for higher gradient continuum theories are equivalent: A review of existing results. *Proc. R. Soc. A*, 471(2183):20150415, 2015.

[36] Catherine Pideri and Pierre Seppecher. A second gradient material resulting from the homogenization of an heterogeneous linear elastic medium. *Continuum Mechanics and Thermodynamics*, 9(5):241–257, 1997.

[37] I. Giorgio. Numerical identification procedure between a micro-Cauchy model and a macro-second gradient model for planar pantographic structures. *Zeitschrift fur Angewandte Mathematik und Physik*, 67(4), 2016.

[38] L. Placidi, U. Andreaus, A. Della Corte, and T. Lekszycki. Gedanken experiments for the determination of two-dimensional linear second gradient elasticity coefficients. *Zeitschrift für angewandte Mathematik und Physik*, 66(6):3699–3725, 2015.

[39] Manuel Ferretti, Angela Madeo, Francesco dell'Isola, and Philippe Boisse. Modeling the onset of shear boundary layers in fibrous composite reinforcements by second-gradient theory. *Zeitschrift für angewandte Mathematik und Physik*, 65(3):587–612, 2014.

[40] Jean-Jacques Alibert, Pierre Seppecher, and Francesco dell'Isola. Truss modular beams with deformation energy depending on higher displacement gradients. *Mathematics and Mechanics of Solids*, 8(1):51–73, 2003.

[41] P. Seppecher. Second-gradient theory: Application to Cahn–Hilliard fluids. In *Continuum Thermomechanics*, pages 379–388. Springer, 2002.

[42] Victor A. Eremeyev and Holm Altenbach. Equilibrium of a second-gradient fluid and an elastic solid with surface stresses. *Meccanica*, 49(11):2635–2643, 2014.

[43] N. Auffray, Francesco dell'Isola, V.A. Eremeyev, A. Madeo, and Giuseppe Rosi. Analytical continuum mechanics à la Hamilton–Piola least action principle for second gradient continua and capillary fluids. *Mathematics and Mechanics of Solids*, 20(4):375–417, 2015.

[44] Francesco dell'Isola, Ugo Andreaus, and Luca Placidi. At the origins and in the vanguard of peridynamics, non-local and higher-gradient continuum mechanics: An underestimated and still topical contribution of Gabrio Piola. *Mathematics and Mechanics of Solids*, page 1081286513509811, 2014.

[45] Antonio Carcaterra, F. dell'Isola, R. Esposito, and M. Pulvirenti. Macroscopic description of microscopically strongly inhomogenous systems: A mathematical basis for the synthesis of higher gradients metamaterials. *Archive for Rational Mechanics and Analysis*, pages 1–24, 2015.

[46] Anil Misra and Payam Poorsolhjouy. Identification of higher-order elastic constants for grain assemblies based upon granular micromechanics. *Math. Mech. Complex Syst*, 3(3):285–308, 2015.

[47] Albrecht Bertram and Rainer Glüge. Gradient materials with internal constraints. *Mathematics and Mechanics of Complex Systems*, 4(1):1–15, 2016.

[48] E. Turco, F. dell'Isola, A. Cazzani, and N.L. Rizzi. Hencky-type discrete model for pantographic structures: Numerical comparison with second gradient continuum models. *Zeitschrift fur Angewandte Mathematik und Physik*, 67(4):1–28, 2016.

[49] Emilio Turco, Maciej Golaszewski, Ivan Giorgio, and Luca Placidi. Can a Hencky-type model predict the mechanical behaviour of pantographic lattices? In *Mathematical Modelling in Solid Mechanics*, pages 285–311. Springer, 2017.

[50] Emilio Turco, Maciej Golaszewski, Ivan Giorgio, and Francesco D'Annibale. Pantographic lattices with non-orthogonal fibres: Experiments and their numerical simulations. *Composites Part B: Engineering*, 118:1–14, 2017.

[51] Emilio Turco, Maciej Golaszewski, Antonio Cazzani, and Nicola Luigi Rizzi. Large deformations induced in planar pantographic sheets by loads applied on fibers: Experimental validation of a discrete Lagrangian model. *Mechanics Research Communications*, 76:51–56, 2016.

[52] Lucio Russo. *The Forgotten Revolution. How Science Was Born in 300 BC and Why It Had to be Reinvented.* Translated from the Italian of Silvio Levy. Springer, Berlin, 2004.

[53] Joseph Louis Lagrange. *Mécanique analytique*, volume 1. Mallet-Bachelier, 1853.

[54] Angela Madeo, Tomasz Lekszycki, *et al.* A continuum model for the bio-mechanical interactions between living tissue and bio-resorbable graft after bone reconstructive surgery. *Comptes Rendus Mécanique*, 339(10):625–640, 2011.

[55] Ugo Andreaus, Francesco dell'Isola, and Maurizio Porfiri. Piezoelectric passive distributed controllers for beam flexural vibrations. *Journal of Vibration and Control*, 10(5):625–659, 2004.

[56] Angela Madeo, D. George, T. Lekszycki, Mathieu Nierenberger, and Yves Rémond. A second gradient continuum model accounting for some effects of micro-structure on reconstructed bone remodelling. *Comptes Rendus Mécanique*, 340(8):575–589, 2012.

[57] U. Andreaus, I. Giorgio, and T. Lekszycki. A 2-D continuum model of a mixture of bone tissue and bio-resorbable material for simulating mass density redistribution under load slowly variable in time. *ZAMM - Zeitschrift für Angewandte Mathematik und Mechanik / Journal of Applied Mathematics and Mechanics*, 94(12):978–1000, 2014.

[58] I. Giorgio, U. Andreaus, T. Lekszycki, and A. Della Corte. The influence of different geometries of matrix/scaffold on the remodeling process of a bone and bioresorbable material mixture with voids. *Mathematics and Mechanics of Solids*, page 1081286515616052, 2015.

[59] Corrado Maurini, Joël Pouget, and Francesco dell'Isola. On a model of layered piezoelectric beams including transverse stress effect. *International Journal of Solids and Structures*, 41(16):4473–4502, 2004.

[60] Corrado Maurini, Joël Pouget, and Francesco dell'Isola. Extension of the Euler–Bernoulli model of piezoelectric laminates to include 3D effects via a mixed approach. *Computers & Structures*, 84(22):1438–1458, 2006.

[61] L. Dietrich, T. Lekszycki, and K. Turski. Problems of identification of mechanical characteristics of viscoelastic composites. *Acta Mechanica*, 126(1):153–167, 1998.

[62] Francesco dell'Isola, Corrado Maurini, and Maurizio Porfiri. Passive damping of beam vibrations through distributed electric networks and piezoelectric transducers: Prototype design and experimental validation. *Smart Materials and Structures*, 13(2):299, 2004.

[63] Jong-Gu Park, Qiang Ye, Elizabeth M Topp, *et al.* Dynamic mechanical analysis and esterase degradation of dentin adhesives containing a branched methacrylate. *Journal of Biomedical Materials Research Part B: Applied Biomaterials*, 91(1):61–70, 2009.

[64] A. Misra and Y. Yang. Micromechanical model for cohesive materials based upon pseudo-granular structure. *International Journal of Solids and Structures*, 47:2970–2981, 2010.

[65] J-F Ganghoffer. Spatial and material stress tensors in continuum mechanics of growing solid bodies. *Mathematics and Mechanics of Complex Systems*, 3(4):341–363, 2015.

[66] Anil Misra, Paulette Spencer, Orestes Marangos, Yong Wang, and J. Lawrence Katz. Parametric study of the effect of phase anisotropy on the micromechanical behaviour of dentin–adhesive interfaces. *Journal of The Royal Society Interface*, 2(3):145–157, 2005.

[67] Paulette Spencer, Qiang Ye, Jonggu Park, *et al.* Adhesive/dentin interface: The weak link in the composite restoration. *Annals of Biomedical Engineering*, 38(6):1989–2003, 2010.

[68] Qiang Ye, Paulette Spencer, Yong Wang, and Anil Misra. Relationship of solvent to the photopolymerization process, properties, and structure in model dentin adhesives. *Journal of Biomedical Materials Research Part A*, 80(2):342–350, 2007.

[69] Lev Davidovich Landau. *The Classical Theory of Fields*, Volume 2. Elsevier, 2013.

[70] Vladimir Igorevich Arnold. *Mathematical Methods of Classical Mechanics*, Volume 60. Springer Science & Business Media, 1989.

[71] Francesco dell'Isola and Luca Placidi. Variational principles are a powerful tool also for formulating field theories. In *Variational Models and Methods in Solid and Fluid Mechanics*. Springer Science & Business Media, 2012.

[72] Jacobo Riccati. Animadversiones in aequationes differentiales secundi gradus. *Actorum Eruditorum Supplementa*, 8(1724):66–73, 1724.

[73] Sophus Lie. *Vorlesungen über continuierliche Gruppen mit geometrischen und anderen Anwendungen*. BG Teubner, 1893.

[74] Florio Maria Ciaglia, Fabio Di Cosmo, Marco Laudato, and Giuseppe Marmo. Differential calculus on manifolds with boundary applications. *International Journal of Geometric Methods in Modern Physics*, 14(08):1740003, 2017.

[75] Florio M. Ciaglia, Fabio Di Cosmo, Alberto Ibort, Marco Laudato, and Giuseppe Marmo. Dynamical vector fields on the manifold of quantum states. *Open Systems & Information Dynamics*, 24(03):1740003, 2017.

[76] Ward Cheney. *Analysis for Applied Mathematics*, Volume 208. Springer Science & Business Media, 2013.

[77] Hermann von Helmholtz. Ueber die physikalische bedeutung des princips der kleinsten wirkung. *Journal für die reine und angewandte Mathematik*, 100:137–166, 1887.

[78] A. Alù. First-principles homogenization theory for periodic metamaterials. *Physical Review B*, 84(7):075153, 2011.

[79] A. Javili, G. Chatzigeorgiou, and P. Steinmann. Computational homogenization in magneto-mechanics. *International Journal of Solids and Structures*, 50(25):4197–4216, 2013.

[80] Y. Rahali, I. Giorgio, J.F. Ganghoffer, and F. dell'Isola. Homogenization à la Piola produces second gradient continuum models for linear pantographic lattices. *International Journal of Engineering Science*, 97:148–172, 2015.

[81] A. Cecchi and N. Rizzi. Heterogeneous elastic solids: A mixed homogenization-rigidification technique. *International Journal of Solids and Structures*, 38(1):29–36, 2001.

[82] S. Saeb, P. Steinmann, and A. Javili. Aspects of computational homogenization at finite deformations: A unifying review from Reuss' to Voigt's bound. *Applied Mechanics Reviews*, 68(5):050801, 2016.

[83] G. Chatzigeorgiou, A. Javili, and P. Steinmann. Unified magnetomechanical homogenization framework with application to magnetorheological elastomers. *Mathematics and Mechanics of Solids*, 19(2):193–211, 2014.

[84] A. Javili, A. McBride, J. Mergheim, P. Steinmann, and U. Schmidt. Micro-to-macro transitions for continua with surface structure at the microscale. *International Journal of Solids and Structures*, 50(16):2561–2572, 2013.

[85] E. Barchiesi and L. Placidi. A review on models for the 3D statics and 2D dynamics of pantographic fabrics. In *Wave Dynamics and Composite Mechanics for Microstructured Materials and Metamaterials*, pages 239–258. Springer, 2017.

[86] F. dell'Isola, M. Cuomo, L. Greco, and A. Della Corte. Bias extension test for pantographic sheets: numerical simulations based on second gradient shear energies. *Journal of Engineering Mathematics*, pages 1–31, 2016.

[87] L. Placidi, U. Andreaus, and I. Giorgio. Identification of two-dimensional pantographic structure via a linear d4 orthotropic second gradient elastic model. *Journal of Engineering Mathematics*, pages 1–21, 2016.

[88] Francesco dell'Isola, Tomasz Lekszycki, Marek Pawlikowski, Roman Grygoruk, and Leopoldo Greco. Designing a light fabric metamaterial being highly macroscopically tough under directional extension: first experimental evidence. *Zeitschrift für angewandte Mathematik und Physik*, 66(6):3473–3498, 2015.

[89] G. Ganzosch, F. dell'Isola, E. Turco, T. Lekszycki, and W.H. Müller. Shearing tests applied to pantographic structures. *Acta Polytechnica CTU Proceedings*, 7:1–6, 2016.

[90] D. Scerrato, I. Zhurba Eremeeva, T. Lekszycki, and N. Rizzi. On the effect of shear stiffness on the plane deformation of linear second gradient pantographic sheets. *ZAMM-Journal of Applied Mathematics and Mechanics/Zeitschrift für Angewandte Mathematik und Mechanik*, 2016.

[91] Heinrich Hencky. *Über die angenäherte Lösung von Stabilitätsproblemen im Raum mittels der elastischen Gelenkkette*. PhD thesis, Engelmann, 1921.

[92] F. dell'Isola, I. Giorgio, M. Pawlikowski, and N.L. Rizzi. Large deformations of planar extensible beams and pantographic lattices: Heuristic homogenization, experimental and numerical examples of equilibrium. *Proceedings of the Royal Society A: Mathematical, Physical and Engineering Sciences*, 472(2185), 2016.

[93] J. J. Alibert and A. Della Corte. Second-gradient continua as homogenized limit of pantographic microstructured plates: a rigorous proof. *Zeitschrift für angewandte Mathematik und Physik DOI: 10.1007/s00033-015-0526-x*, 2015.

[94] Victor A. Eremeyev, Francesco dell'Isola, Claude Boutin, and David Steigmann. Linear pantographic sheets: existence and uniqueness of weak solutions. *Journal of Elasticity*, pages 1–22, 2017.

[95] Claude Boutin, Ivan Giorgio, Luca Placidi, *et al.* Linear pantographic sheets: Asymptotic micro-macro models identification. *Mathematics and Mechanics of Complex Systems*, 5(2):127–162, 2017.

[96] Emilio Turco, Ivan Giorgio, Anil Misra, and Francesco dell'Isola. King post truss as a motif for internal structure of (meta) material with controlled elastic properties. *Royal Society Open Science*, 4(10):171153, 2017.

[97] D. Scerrato, I. Giorgio, and N.L. Rizzi. Three-dimensional instabilities of pantographic sheets with parabolic lattices: numerical investigations. *Zeitschrift fur Angewandte Mathematik und Physik*, 67(3), 2016.

[98] Francesco Dell'Isola, Giulio Maier, Umberto Perego, *et al. The Complete Works of Gabrio Piola*: Volume I. Cham, Switzerland: Springer, 2014.

[99] Francesco Dell'Isola, Giulio Maier, Umberto Perego, *et al. The Complete Works of Gabrio Piola*: Volume II. Cham, Switzerland: Springer, 2019.

[100] Emilio Turco. Discrete is it enough? The revival of Piola–Hencky keynotes to analyze three-dimensional elastica. *Continuum Mechanics and Thermodynamics*, Apr 2018.

[101] L. Euler. Nova methodus motum corporum rigidorum determinandi. *Novi Commentari Academiae Scientiarum Imperalis Petropolitanae*, 20:208–238, 1775.

[102] O. M. O'Reilly. *Intermediate Dynamics for Engineers: A Unified Treatment of Newton–Euler and Lagrangian Mechanics*. Cambridge University Press, 2008.

[103] O. Rodrigues. Des lois géométriques qui régissent les déplacements d'un système solide dans l'espace, et de la variation des coordonnées provenant de ces déplacements considérés indépendamment des causes qui peuvent les produire. *Journal de Mathématiques Pure et Appliquées*, 1(5):380–440, 1840.

[104] A. Eremeyev and H. Altenbach. *Shell-like Structures*. Springer International Publishing, 2017.

[105] A. I. Lurie. *Analytical Mechanics*. Springer-Verlag Berlin Heidelberg, 2002.

[106] Ivan Giorgio, Alessandro Della Corte, Francesco dell'Isola, and David J. Steigmann. Buckling modes in pantographic lattices. *Comptes rendus Mecanique*, 344(7):487–501, 2016.

[107] Emilio Barchiesi, Gregor Ganzosch, Christian Liebold, *et al.* Out-of-plane buckling of pantographic fabrics in displacement-controlled shear tests: Experimental results and model validation. *Continuum Mechanics and Thermodynamics*, pages 1–13, 2018.

[108] Angelo Luongo. Mode localization in dynamics and buckling of linear imperfect continuous structures. *Nonlinear Dynamics*, 25(1-3):133–156, 2001.

[109] N.L. Rizzi, V. Varano, and S. Gabriele. Initial postbuckling behavior of thin-walled frames under mode interaction. *Thin-Walled Structures*, 68:124–134, 2013.

[110] L. Placidi, G. Rosi, I. Giorgio, and A. Madeo. Reflection and transmission of plane waves at surfaces carrying material properties and embedded in second-gradient materials. *Mathematics and Mechanics of Solids*, 19(5):555–578, 2014.

[111] Angela Madeo, Patrizio Neff, Ionel-Dumitrel Ghiba, Luca Placidi, and Giuseppe Rosi. Wave propagation in relaxed micromorphic continua: modeling metamaterials with frequency band-gaps. *Continuum Mechanics and Thermodynamics*, pages 1–20, 2013.

[112] A. Madeo, A. Della Corte, L. Greco, and P. Neff. Wave propagation in pantographic 2D lattices with internal discontinuities. *Proceedings of the Estonian Academy of Sciences*, 64(3S):325–330, 2015. doi: 10.3176/proc.2015.3S.01 Available online at "http://www.eap.ee/proceedings" www.eap.ee/proceedings.

[113] Arkadi Berezovski, Ivan Giorgio, and Alessandro Della Corte. Interfaces in micromorphic materials: Wave transmission and reflection with numerical simulations. *Mathematics and Mechanics of Solids*, page 1081286515572244, 2015.

[114] E. Turco, F. dell'Isola, N.L. Rizzi, *et al.* Fiber rupture in sheared planar pantographic sheets: Numerical and experimental evidence. *Mechanics Research Communications*, 76:86–90, 2016.

[115] Luca Placidi and Emilio Barchiesi. Energy approach to brittle fracture in strain-gradient modelling. *Proc. Roy. Soc. A*, 474(2210):20170878, 2018.

[116] A. Battista, L. Rosa, R. dell'Erba, and L. Greco. Numerical investigation of a particle system compared with first and second gradient continua: Deformation and fracture phenomena. *Mathematics and Mechanics of Solids*, page 1081286516657889, 2016.

[117] L. Placidi. A variational approach for a nonlinear one-dimensional damage-elasto-plastic second-gradient continuum model. *Continuum Mechanics and Thermodynamics*, Published online 23 December 2014. DOI: 10.1007/s00161-014-0405-2.

[118] A. Misra and V. Singh. Micromechanical model for viscoelastic-materials undergoing damage. *Continuum Mechanics and Thermodynamics*, 25:1–16, 2013.

[119] L. Placidi. A variational approach for a nonlinear 1-dimensional second gradient continuum damage model. *Continuum Mechanics and Thermodynamics*, Published online 20 February 2014. DOI: 10.1007/s00161-014-0338-9.

[120] Yang Yang and Anil Misra. Micromechanics based second gradient continuum theory for shear band modeling in cohesive granular materials following damage elasticity. *International Journal of Solids and Structures*, 49(18):2500–2514, 2012.

[121] Yang Yang, W.Y. Ching, and Anil Misra. Higher-order continuum theory applied to fracture simulation of nanoscale intergranular glassy film. *Journal of Nanomechanics and Micromechanics*, 1(2):60–71, 2011.

[122] Loredana Contrafatto, Massimo Cuomo, and Francesco Fazio. An enriched finite element for crack opening and rebar slip in reinforced concrete members. *International Journal of Fracture*, 178(1-2):33–50, 2012.

[123] Daniela Ciancio, Ignacio Carol, and Massimo Cuomo. Crack opening conditions at 'corner nodes' in FE analysis with cracking along mesh lines. *Engineering Fracture Mechanics*, 74(13):1963–1982, 2007.

[124] Anil Misra and Payam Poorsolhjouy. Grain-and macro-scale kinematics for granular micromechanics based small deformation micromorphic continuum model. *Mechanics Research Communications*, 81:1–6, 2017.

6 Experimental Methods in Pantographic Structures

F. dell'Isola, T. Lekszycki, M. Spagnuolo, P. Peyre, C. Dupuy, F. Hild, A. Misra, E. Barchiesi, E. Turco, J. Dirrenberger

6.1 Introduction

Experiments are integral to the development of physical theories. They serve the critical role of verifying and validating the principles and assumptions that form the basis of theoretical developments. The predictive ability of a physical theory must be tested against experiments to establish its applicability and credibility. This chapter focuses upon experimental approaches and measurements that aim to test the theoretical principles and tools employed to develop and design the novel pantographic metamaterials. Undoubtedly these metamaterials are endowed with exotic properties as shown through theoretical analyses, such that at their macroscopic scale, that is at the specimen size with as many pantographic sub-units as possible, they may be considered as a second gradient continuum material [1–7, 64]. However, such pantographic structures do not appear ordinarily in materials formed by currently extant manufacturing or natural processes. Clearly, before attempting to devise a suitable experimental program that can establish their second gradient continuum nature, it is necessary to address the ability to realize such a metamaterial. Indeed, only in the last few years attempts to synthesize physical specimens of pantographic materials have been successful, see Fig. 6.1.

In the discussion that follows, we give an account of the steps undertaken to validate the development of pantographic metamaterials from their theoretical conception to their physical realization. These steps span computer-aided design for the manufacture of different variants of the structure up to a suite of mechanical tests performed to determine the essence of their behavioral characteristics. Since these materials also exhibit resilience under large deformation, we also discuss experimental evidence related to their damage and failure. Specifically, we have divided the subsequent exposition into four macro-categories: (i) design and manufacture, (ii) experimental measurements, (iii) failure and damage analysis, and (iv) digital image correlation (DIC) analysis.

6.2 Design and Manufacturing

In the recent past, computer-aided manufacturing with the advent of 3D printing technology has been having a transforming impact in the field of mechanics. With this technology it is possible to manufacture specimens whose geometrical structure can be controlled with precision and reliability. The possibility to specify a design

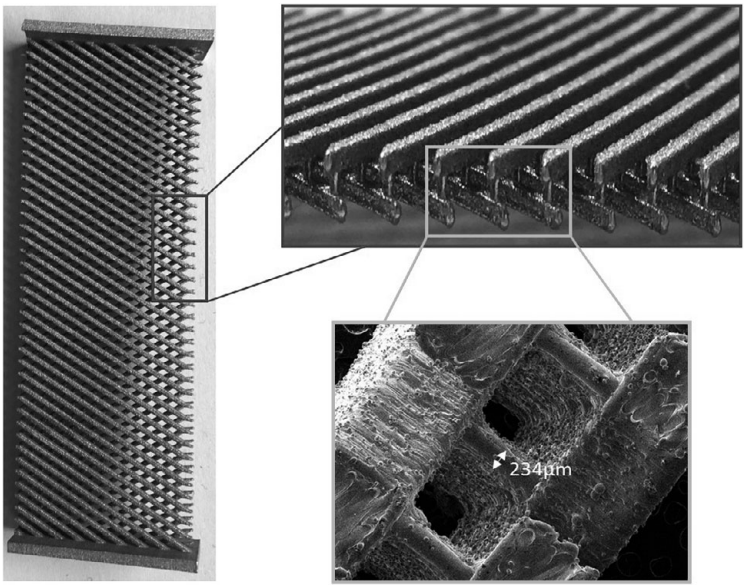

Figure 6.1 Different views of a steel pantographic structure at three length scales: (left) natural size, (top right) view of the interconnecting pivots, (bottom right) magnification $\times 40$.

and manufacture an object by means of software has far reaching consequences for experimental as well as numerical investigations. The microstructure of a sample can be more complex and better controlled as opposed to traditional manufacturing methods. The clear implication is that experimental results will be more reliable, repeatable and less affected by several sources of variability usually encountered in mechanical testing. From the viewpoint of analysis, there is no need for abstractions of geometrical features, particularly with respect to boundary conditions, that need to be commonly employed when usual sample preparation methods are used. Thus there is promise of more reliable evaluation of the theoretical concepts with the ensuing experimental data. The conceived pantographic structure described in Chapter 2 was manufactured by means of 3D printing technology. The production process consisted of two steps: (i) computer-aided design, and (ii) additive manufacturing. The samples have been produced with different geometrical properties, as well as with different base materials, e.g. polyamide, steel, aluminum, etc. The production of a wide range of samples was possible due to an extended network of collaborations across the world.

6.2.1 Design of Pantographic Structures

An appealing feature of the computer aided design and additive manufacturing route is that exactly the same geometry can be used for both manufacturing and full-scale 3D numerical simulations. This point is well illustrated in Fig. 6.2, which provides a resume of the complete processing history of a particular pantographic structure beginning from its theoretical conception up to its actual production.

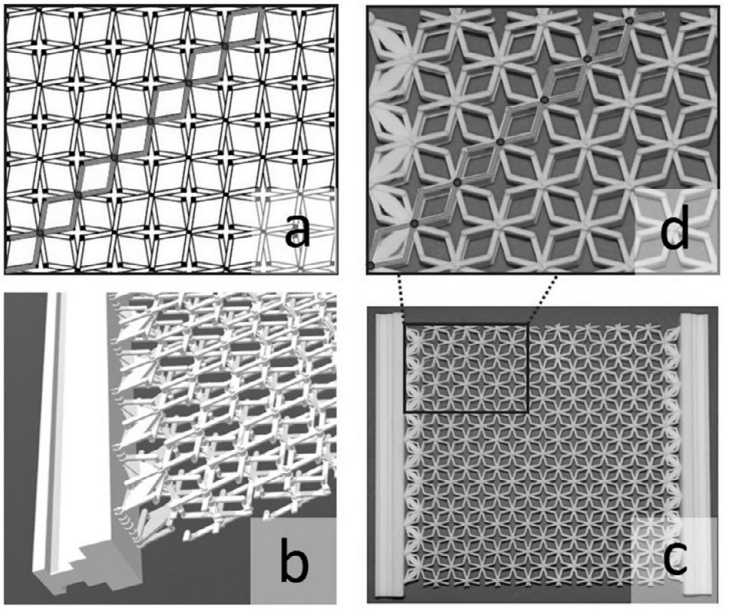

Figure 6.2 Processing history of a newly conceived pantographic structure, whose fibers are in turn pantographic beams: (a) proof-of-concept; (b) CAD model; (c) final printed polyamide structure; (d) zoomed detail of the printed specimen.

In Figs. 6.3–6.5, additional examples of CAD models for the design of different pantographic structures are shown. In Fig. 6.3, a pantographic structure with so-called "perfect" pivots is shown. The adjective "perfect" applies because the pivots function as true hinges (or pin joints) such that negligible (neglecting minor frictional interactions) rotational energy is stored in these pivots. Unlike "standard" pivots, which are deformable small cylinders (subject to torsional and shear actions), the "perfect" pivot ensures that the intersecting fibers undergo the same displacement while allowing only for arbitrary relative rotations.

Specimen with "perfect" pivots, in contrast to those with standard ones, afford the possibility of isolating the contribution of fiber bending to the global deformation energy of the pantographic structure, particularly under a deformation range within which the fiber elongation has a non-negligible contribution, which covers a wide range of compressive and extensive deformation regimes. Indeed, in [25–27] it has been shown that when the fibers are behaving like small-strain extensible Euler beams, the second gradient contribution to the deformation energy of an equivalent elastic small-strain continuum model describing the mechanical behavior of pantographic fabrics is given by the bending energy of such fibers.

Further, Fig. 6.4, shows the design of a "millimetric" pantographic sub-structure, whose dimensions are approximately 1 cm $\times$ 3 cm. The realisation of such a sub-structure, composed of a few basic units, presents the possibility of exploring with greater detail the local behavior of more complex structures made up of a larger numbers

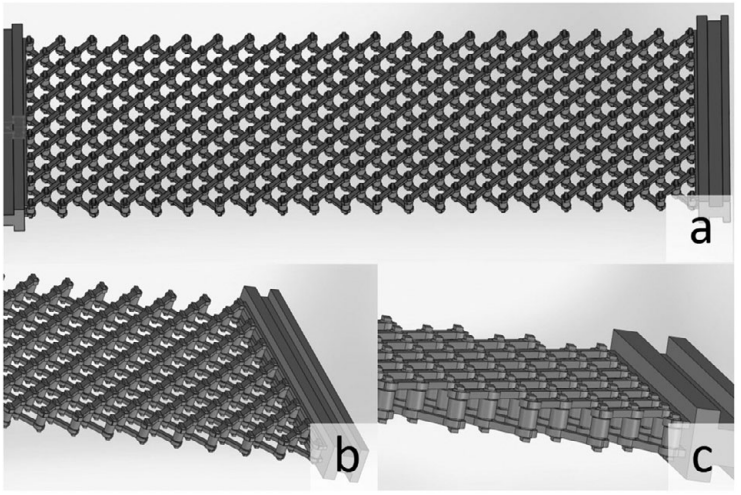

Figure 6.3 Design of a pantographic structure with perfect pivots. The stl file can be used both for numerical simulations and for manufacturing a specimen.

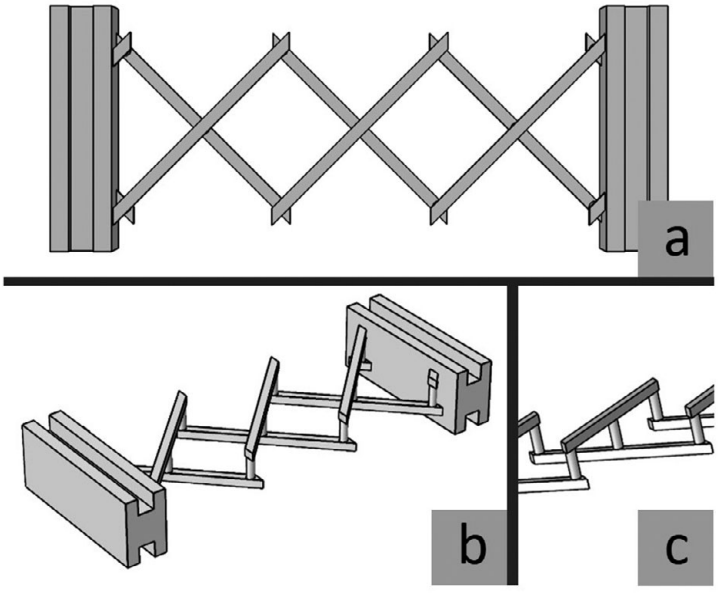

Figure 6.4 CAD modeling of a so-called millimetric pantographic structure.

of primitive cells. Finally, a third example of manufacturing of pantographic structures is shown in Fig. 6.5. This kind of pantographic structure is not a sheet-like material as those which have been presented so far. Instead, it is made up of many layers, so that its depth cannot be neglected. With this design choice it is possible to suppress the undesirable out-of-plane motions when performing certain mechanical tests to determine in-plane deformability properties (like the three-point bending test in the figure).

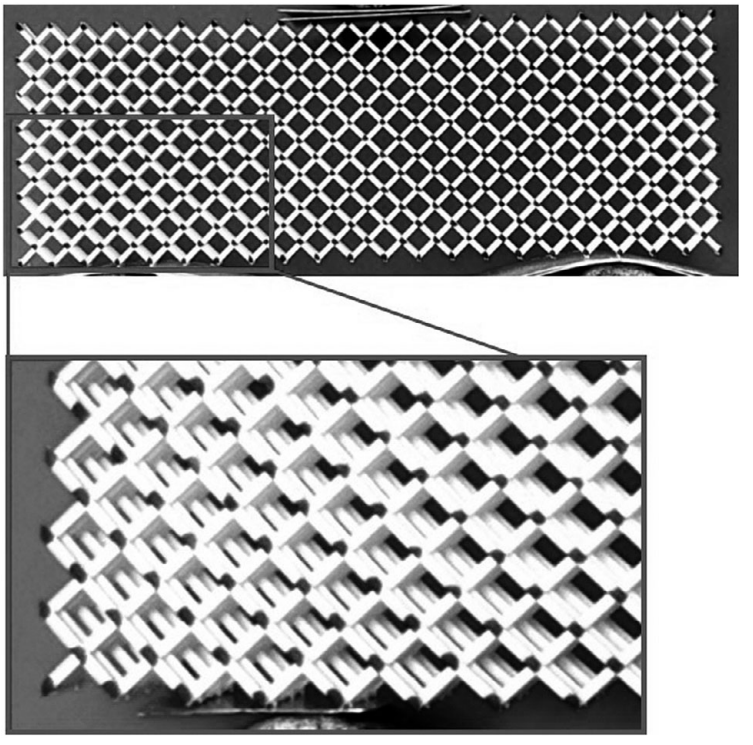

Figure 6.5 A multi-layers pantographic structure.

6.2.2 Additive Manufacturing

General Trends in AM and SLM Processes

Additive manufacturing (AM) provides new and valuable solutions for generating complex metallic or polymer shapes, mainly through the interaction of an energy source with a wire or powder material. The main application, and major advantage, of this technique is to generate simultaneously the shape and the constitutive material in a single step. The basics steps of AM are as follows: 3D parts, discretized by triangles and their normal vector, are generated in the form of a STL file utilizing CAD software. This file is used as input data for specific AM software where the 3D part is virtually sliced into thin layers, positioned on the building platform of the 3D printing machine and connected to the plateau with dedicated supports that combines two functions: (1) dissipating heat, (2) avoiding thermal distortions and clamping of parts on the plate. For AM metal processes, specific care is also given to the minimization of overhanging areas where overheating zones usually occur and cause a deterioration of surface roughness. Among AM techniques, the selective laser melting (SLM) process, also called laser beam melting (LBM), provides spatial resolution, due to the small size of the laser beam (usually in-between 50 and 100 μm), and the height of the powder layers (20 to 50 μm).

This process, including electron beam melting (EBM), is one of the so-called powder bed processes and is certainly the most promising one for combining complex geometries with satisfactory metallurgical and mechanical behaviors, usually as a compromise between cast and wrought alloys. Basically, the SLM process is based upon the laser melting and resulting consolidation of a powder bed layer, using dedicated first order process parameters (laser power, scan speed, beam diameter, hatch distance) and follows a scanning strategy initially determined in the AM software file. This strategy includes more-or-less complex contour (for the outer surface volume) and hatching (for the inner volume) steps with the global objective of achieving dense matter while limiting heat concentration areas. As a whole, a SLM part is obtained by the overlap of hundreds of meters of welding beads (approximately 500 m of bead/cm^3), performed in an inert gas atmosphere (Ar, N^2), each of them having dimensions of approximately 200–300 μm in width and in depth. Usually, after a preliminary optimization step, very low porosity rates (less than 0.2 %) can be obtained in most metallic parts. In a final step, such porosities can be suppressed by post-SLM hot isostatic pressing (HIP), resulting in almostfully-dense metallic alloys. The generation of architectured materials with unusual combinations of properties is certainly one of the most promising features of the AM process [11]. A number of recent publications on a large range of materials (titanium, steels, aluminum-base, nickel-base, Ti-Ni shape memory alloys) have already demonstrated the feasibility of SLM or EBM manufacturing applied to lattice structures. This technique has been chosen to manufacture some special shapes of lattice structures also called pantographic fabrics from an STL file.

Experimental Work

- *SLM equipment*

  In this survey, an SLM125HL set-up from SLM solutions has been used. This machine is equipped with a 400W YAG laser (YLR-400-WC) at a wavelength of 1070 nm. The scanning speed range is between 400 and 1500 mm/s. The minimum diameter of the laser at the focus point is about 70 μm. Layer thickness can vary from 30 to 100 μm.

- *Powder material*

  Gas atomized powder of 316L stainless steel has been used to create the pantographic structure. This powder has been characterized by SEM and by particle size analyzer (CILAS 920). Other kinds of powder materials can be used in fabricating pantographic structures. Here the case of stainless steel is described, but already existing results have been found in the case of aluminum. If other materials are used, it could be useful to study the microscopic and macroscopic mechanisms involved in the deformation process, as has been done in [31] for aluminum and in [32] for titanium.

  As seen in Fig. 6.6, powder have particles have a spherical shape. The mean diameter of the volume distribution of the particle size is 37 μm. Its composition is shown in Table 6.1. To prevent oxidation of the powder the process takes place under shielding gas (argon) with less than 500 ppm O_2.

Table 6.1 Composition of the 316L stainless steel

Element	Fe	C	Si	Mn	P	P	S	Cr	Ni	N
wt%	Balance	0.01	0.65	1.19	0.023	0.005	17.17	10.99	2.47	0.1

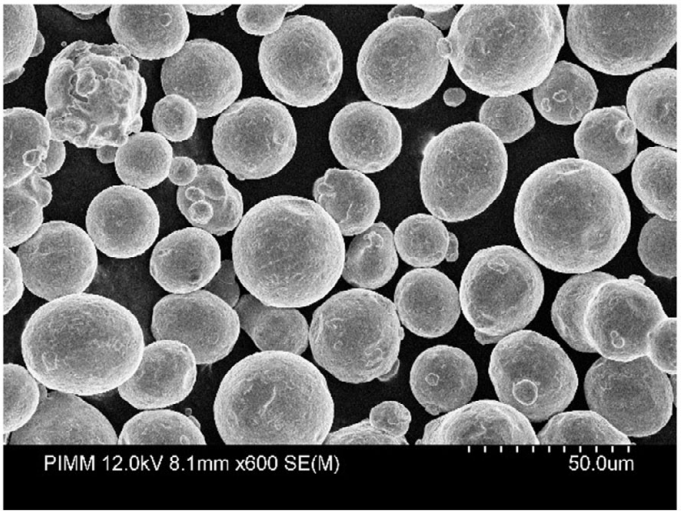

Figure 6.6 SEM image of 316L powder.

- *File preparation for 3D printing*

  Once the 3D drawing of the pantographic structures was done, it was converted to stl format so that it could be prepared for manufacturing using the MAGICS – Materialize software. The samples were positioned perpendicularly to the plate, as shown in Fig. 6.7, to maintain a similar geometry on both sides of the sample even though a 45° tilt of the sample would have been preferable for the realization of the pivots. The samples, above the plate, are positioned on 4 mm-height supports in order to facilitate their removal after manufacturing and to favor heat dissipation.
- *Laser parameters*

  In order to limit thermal deformations, volume energy distribution was lowered by a small amount compared to the standard machine parameters. The parameters used were as follows: P = 175 W V = 800 mm/s, hatch distance = 100 μm. Figure 6.8 shows the samples manufactured on their build platform. No heat treatment has been applied to the samples either before their removal or after.
- *Post-mechanical testing analysis of SLM samples*

  The samples were then subjected to static tensile testing. Images of the pivots taken after tensile tests highlight a rotation of the pivots at the ends of the samples with or without fracture, while in the center of the samples pivots do not seem to have moved as shown in Fig. 6.9.

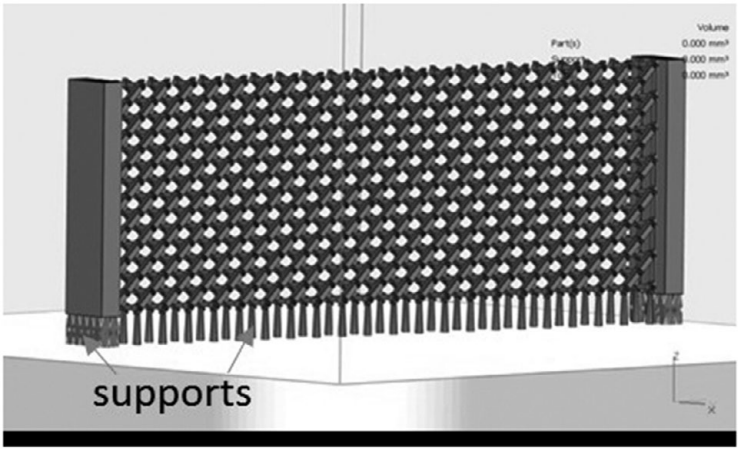

Figure 6.7 Visualization of the supports created between the sample and the platen.

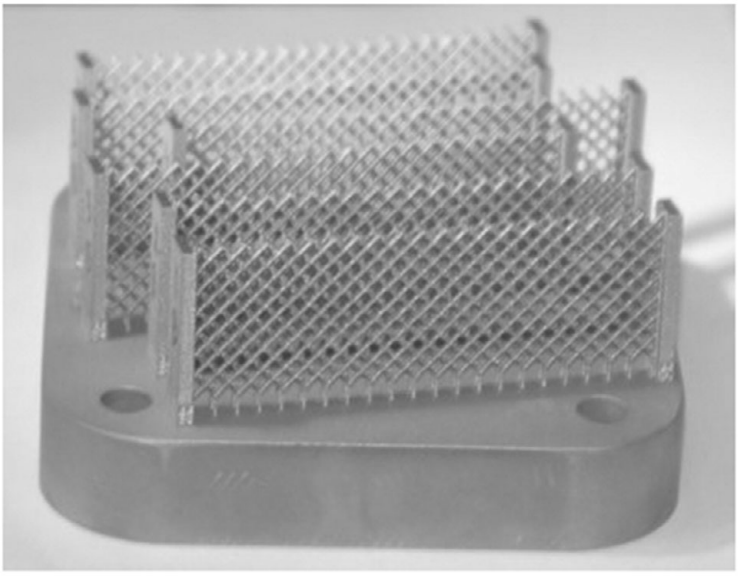

Figure 6.8 Manufactured samples.

SLS for Polyamide Specimens

Selective laser sintering (SLS) was used to fabricate polyamide specimens. Figure 6.10 shows an example of a polyamide printed pantographic structure. The SLS 3D printing process requires the specification of a number of parameters, which include, among others, the pre-heating temperature, the laser power, and the bed cooling time. Also a careful choice of the arrangement of prototypes in the virtual printing chamber is required. A misorientation of the model, especially when the model includes multiple moving parts (as in the case of hinges in "perfect" pantographic fabrics), can affect functionality or render a specimen completely useless. After printing, especially in

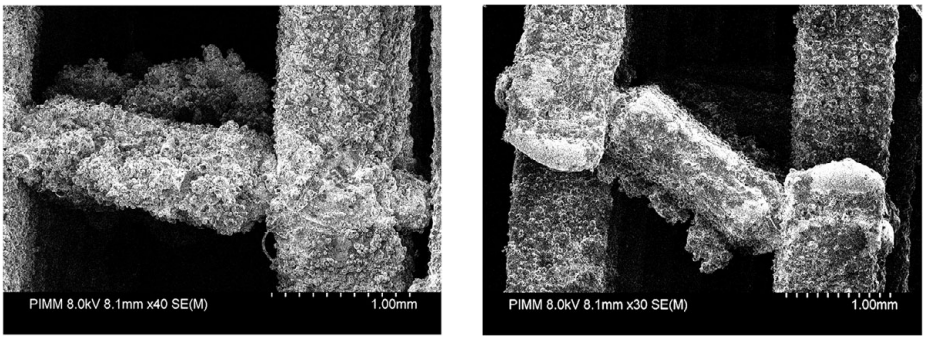

Figure 6.9 SEM top view of the beam-pivot connection at the middle of the sample after tensile testing (left). SEM top view of a beam-pivot connection at the end of the sample after tensile testing (right).

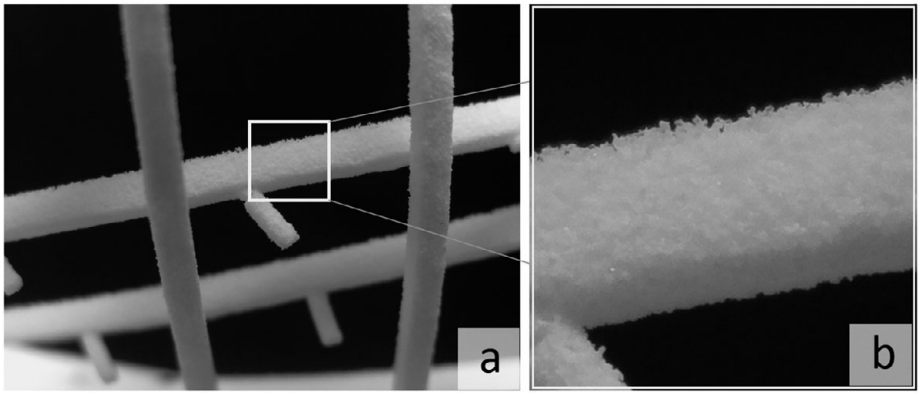

Figure 6.10 Top view of the beam-pivot connection at the middle of the polyamide sample after tensile test (a). A detail showing the granular nature of the material (b).

SLS technology, it is necessary to wait until all the objects are cooled down in order to reduce material contractions. Inadequate cooling procedures could lead to internal differential pre-stresses in the material, entailing impaired performances or even rupture of the printed specimen. As a final step of the fabrication, the fabricated specimen is subjected to a cleaning process. Either pressurized air, abrasive blasting or ultrasonic washers may be used to clean the unsintered powder from void spaces of the specimen. Before finalizing a SLS protocol for a given specimen, test runs are executed in order to determine the optimal setting for specimen manufacturing and the optimal geometric properties of the CAD model.

6.2.3 Tomographic Analyses

Preliminary tomographic analyses have been carried out on a stainless steel pantographic structure. This type of analysis will be used in the future for the understanding of microscopic mechanisms of damage and failure. The acquisition was conducted at

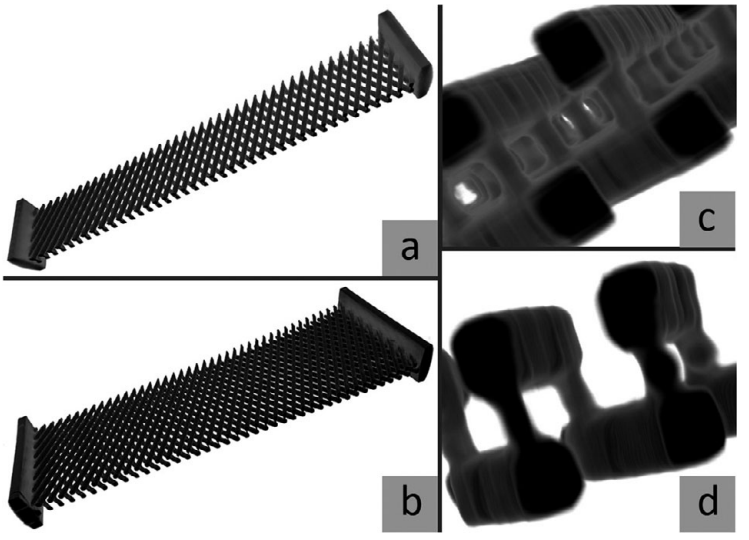

Figure 6.11 3D rendering of a steel pantographic structure at macroscale and mesoscales.

low resolution inside a North Star Imaging X50+ tomograph, using a source setting of 170 kV, 600 μA and a 1536 $\times$ 1944 pixel panel detector. The physical voxel size is 69.5 μm in order to image the whole sample. 800 radiographs were acquired over the 360° of rotation with a frame average equal to 10. The acquisition frequency was 10 fps. The total duration of a single acquisition was approximately 30 minutes. A 0.5 mm thick copper filter was used. Figure 6.11(left) shows the 3D rendering of a steel pantograph, and Fig. 6.11(right) a close-up view of a section showing the mesostructure.

6.3 Comparison between Experimental Measurements and Numerical Simulations

The pantographic structures realized using AM techniques were tested under a variety of loading conditions to experimentally verify and validate the theoretical basis of their development. The testing program particularly focused upon their wide elastic deformation range and their high resiliency. In the subsequent discussion, we will present results from the following tests: (i) bias extension of steel specimens with standard and quasi-perfect pivots, (ii) bias extension of millimetric pantographic structures, (iii) torsion of aluminum specimens, and (iv) three-point bending of polyamide multi-layer pantographic lattices.

6.3.1 Extension Tests of Steel Pantographic Structures

In Fig. 6.12 a force-displacement diagram is shown for a pantographic structure with standard pivots, and in Fig. 6.13 the corresponding deformed shapes for different

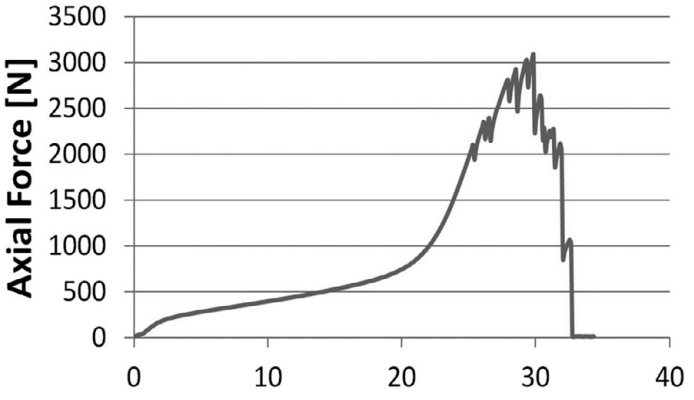

Figure 6.12 Axial force vs imposed displacement for a BIAS extension test performed on a steel printed pantographic structure.

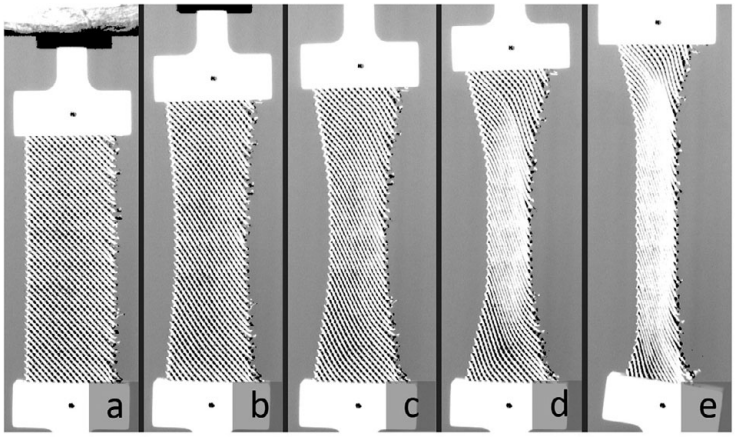

Figure 6.13 Deformed shapes of a steel pantographic structure.

values of prescribed displacement are presented. It is instructive to compare the force-displacement curve in Fig. 6.12 with that in Fig. 6.14, which gives measured behavior for a structure with "perfect" pivots. Remarkably, the measured force for the case of a specimen with "perfect" pivots is an order of magnitude smaller than that for a specimen with standard pivots over the range of the imposed displacement. It is notable, though that in these steel specimens, there is strong evidence that the "perfect" pivots are not ideal hinges [28]. Indeed, at the considered length-scale, the 3D-printing manufacturing process is still not able to ensure that the hinge is ideally frictionless. Finally, in Fig. 6.15, deformed shapes for different values of prescribed displacement for the structure with "perfect" pivots are reported.

Resiliency of Pantographic Structures

The measured behavior under BIAS experiments also shows that the damage tolerance (resiliency) of pantographic structures is rather noteworthy. This aspect is clear from the

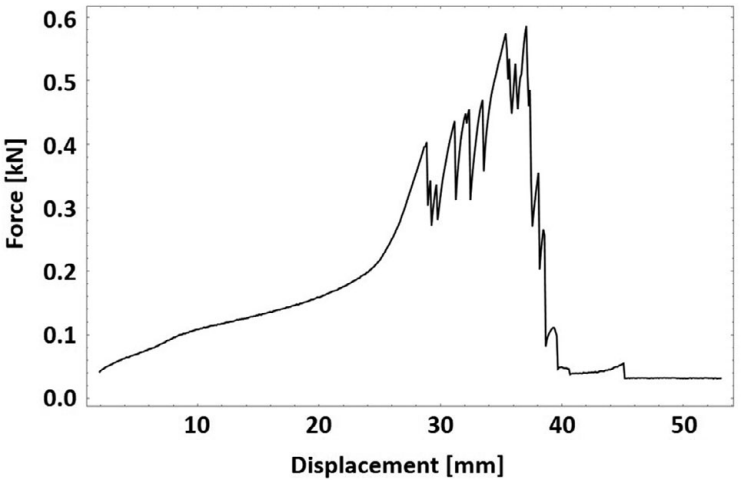

Figure 6.14 Axial force vs imposed displacement for a BIAS extension test performed on a steel printed pantographic structure with (theoretically) perfect pivots.

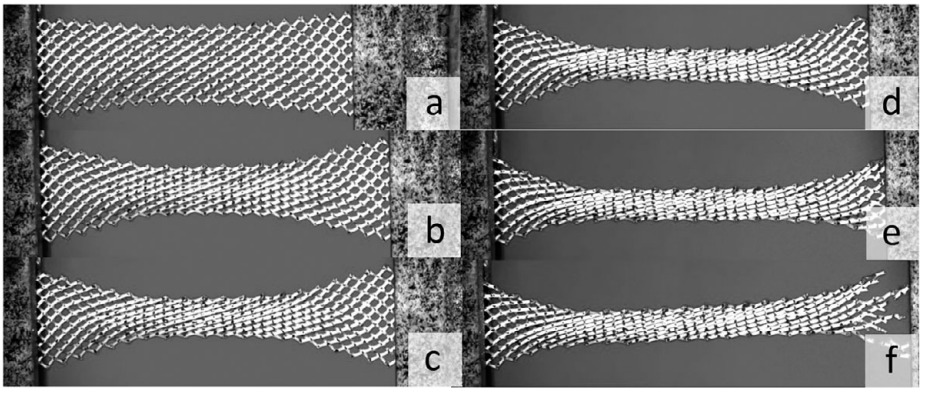

Figure 6.15 Deformed shapes of a pantographic structure with perfect pivots.

force-displacement plots discussed earlier as well as that shown in Fig. 6.16 (the figures refer to a specimen 3D printed in stainless steel, with quasi-perfect pivots). The force-displacement diagram for pantographic fabrics customarily exhibits a peak at the end of the stiffening stage. After the peak, the structure undergoes sequential rupture of its sub-components, typically the shearing of pivots, resulting in a cascade type softening. The gradual cascading softening leading to failure suggests that the topology of the structure and the deformability properties of its members are such that, when a sub-component rupture occurs, load can be redistributed in a mitigating manner that prevents simultaneous catastrophic rupture. In fact such resiliency is also exhibited by the pantographic structure when failure of its sub-components occurs before the peak load, as seen in Figs. 6.16 and 6.17. Similar observations across several specimens clearly demonstrate the resiliency of pantographic structures. Further theoretical investigations in these aspects

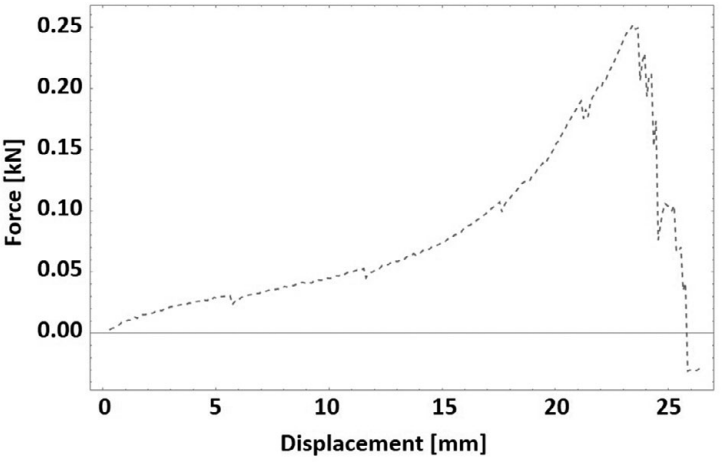

Figure 6.16 Force vs displacement diagram for a pantographic structure with perfect pivots. In this test, the structure has undergone the subsequent rupture of several pivots. The main rupture events are apparent from the small bumps before irreversible collapse of the structure.

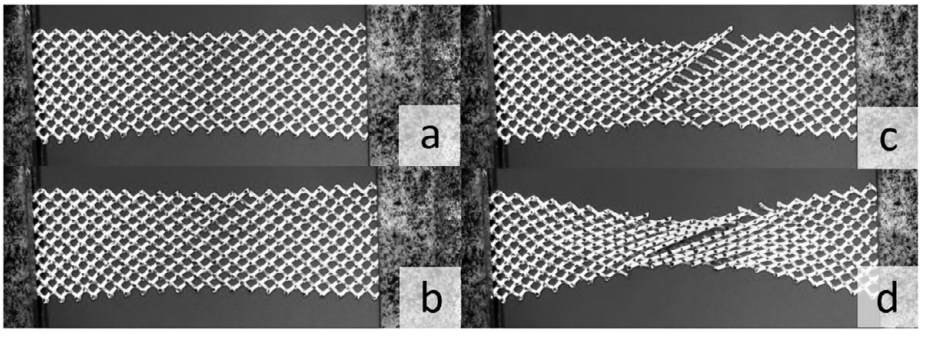

Figure 6.17 Deformed shapes of a pantographic structure with perfect pivots: subsequent rupture of several pivots.

are currently underway as this is a promising line of research for applications related to performance engineering.

6.3.2 Millimetric Pantographic Structures

We refer below to the specimen of the type shown in Fig. 6.4 as a *millimetric pantographic structure.* In Fig. 6.18 selected experimental measurements on these types of specimen are compared with the theoretical predictions based upon the enhanced Piola–Hencky model described in [19]. By means of this model it is possible to obtain good agreement with the experimental data. In Fig. 6.19 the computed deformed shapes are compared to the measured ones.

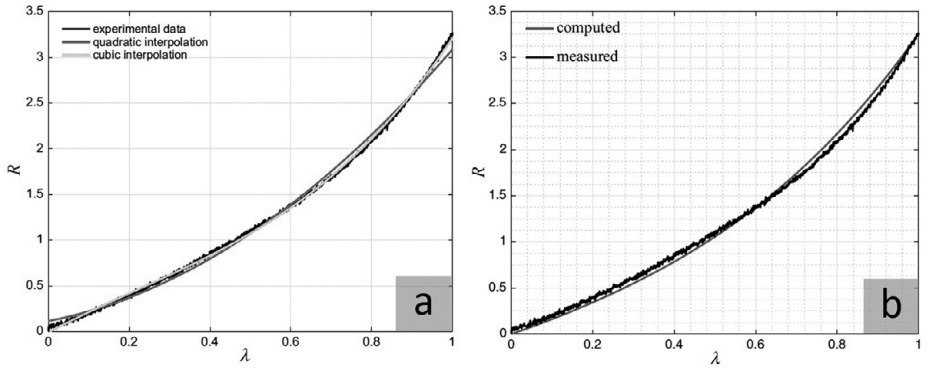

Figure 6.18 Force-displacement diagram for a millimetric pantographic structure. Comparison between experimental data and predictions based on the enhanced Piola–Hencky model. The displacement is expressed in terms of the adimensional ratio $\lambda = \frac{\Delta L}{L_0}$.

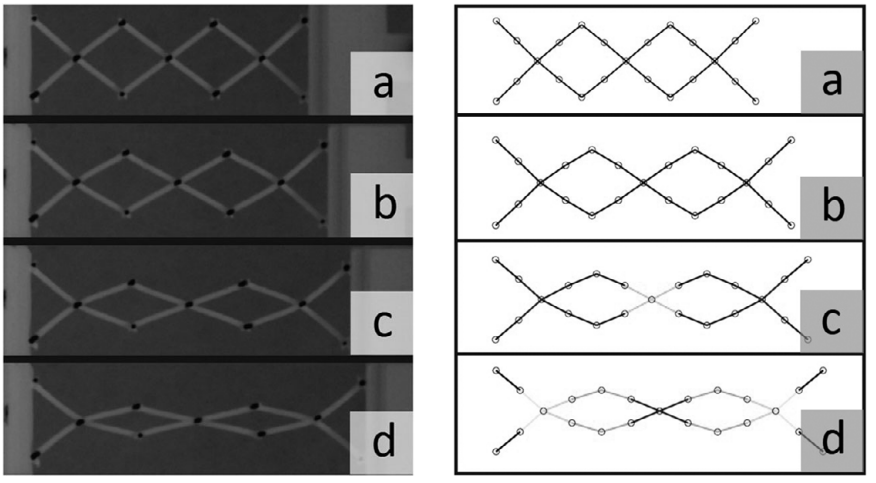

Figure 6.19 Deformed shapes of a millimetric pantographic structure for different values of the prescribed displacement (a) and comparison with numerical simulations (b).

6.3.3 Torsion Tests and Emerging of Atypical Poynting Effect Reversal in Aluminum Pantographic Structures

Due to their unique distribution of deformation energy within beams and pivots, pantographic structures exhibit interesting behaviors under torsional loading. These behaviors are influenced by the competition of the emerging geometrical properties and the response of the material composing the structure. One of the effects that has emerged recently in pantographic structures is the nonlinear Poynting effect as reported in [24].

Poynting Effect and Reverse Poynting Effect

The Poynting effect is a phenomenon observed in elastic materials. From a geometric point of view, it comes from the fact that the deformation of any square element of

an elastic material is the most important in its diagonals. That phenomenon may be observed during the torsion of a beam as an axial effect: although there are no axial loads, the length of the beam changes. Alternatively, if the beam has fixed extremities, an axial reaction force appears. Under such a load, if the beam tends to increase its length, the Poynting effect is said to be positive. On the contrary, if the beam tends to shrink, then it is a negative or reverse Poynting effect. While the usual materials where this phenomenon may be observed present a linear relation between the reaction force and the squared angle of rotation, the focus of the article [24] is on a certain material which shows a non-linear Poynting effect. That is to say not only is the above-mentioned relation not linear, but the phenomenon may also be reversed, so that increasing the rotation angle decreases the reaction once a certain critical angle is reached.

Studied Pantographic-structured Metamaterial

In order to study the causes of the nonlinear Poynting effect, several objects with such a structure were built, with varying dimensions and relative stiffness between the pivot and the beams. To measure the Poynting effects during the torsion, each specimen was fixed at the bottom end, while the other end was twisted progressively. The vertical elongation at the upper end was constrained so that the Poynting effect could be quantified by measuring the upper axial reaction force (see Fig. 6.20).

Results of the Torsion Tests

The evolution of the axial reaction force during the torsion for each specimen is represented in Fig. 6.21. The resulting behaviors were clearly not linear: while every studied object showed a positive Poynting effect at first, the increase of reaction force for a fixed increase in rotation angle decreased progressively. Most of the specimens

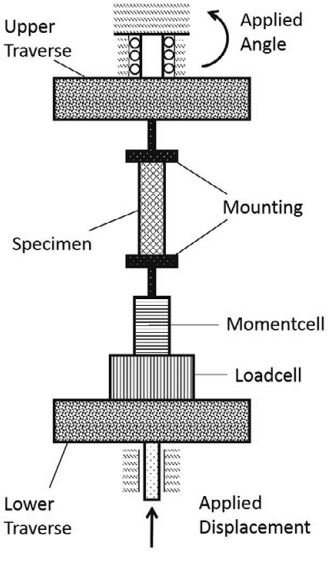

Figure 6.20 Torsion test.

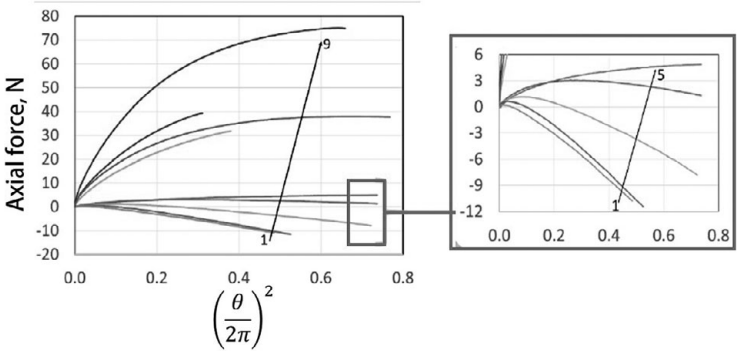

Figure 6.21 Torsion tests results: axial reaction force versus rotation angle. Usual Poynting effect would be represented by a linear function.

showed the reversal of the Poynting phenomenon, reached when the slope (of the curves in Fig. 6.21) reduced to zero. After that point, the reaction force decreased, to the extent that it became negative for the first three specimens, showing an inverse Poynting phenomenon.

Interpretation and Modeling

- *Competing deformation mechanisms*

  The differences in experimental behavior may be accounted for as resulting from two competing mechanisms: the bending of the beams on the one hand, and the shearing of the pivots on the other. The influence of each mechanism may be explained by the original geometrical aspect of the Poynting effect. Among the relevant parameters characterizing the material, the relative deformation of the beams and the pivots is here the most important one. Indeed, the squares making up the initial lattice are sheared during the torsion test, so that the direction of the elongated diagonal determines whether the material as a whole is elongated or compressed. Consequently, when the pivots are weaker, they will allow a change in the angle of the lattice while the beams keep their length, resulting in a reverse Poynting effect. On the contrary, if the beams are the less stiff, they will be bent during the torsion test, while the stiff pivots will fix the angles; this makes the deformed shape extend itself in the direction orthogonal to the twist axis, and results in a positive Poynting effect (see Fig. 6.22). As for the reversal phenomenon, it appears if the more deformed parts are the beams at first, and then the pivots, where the relative deformations are quantified by the ratio between their respective deformation energies.
- *Mathematical modeling*

  It should be noted that, to model macroscopically the behavior that was geometrically justified above, one has to use a generalised continuum model, as the double-scale of the problem cannot be fully taken into account by a classical Cauchy elastic material. More specifically, in [24], the authors used a

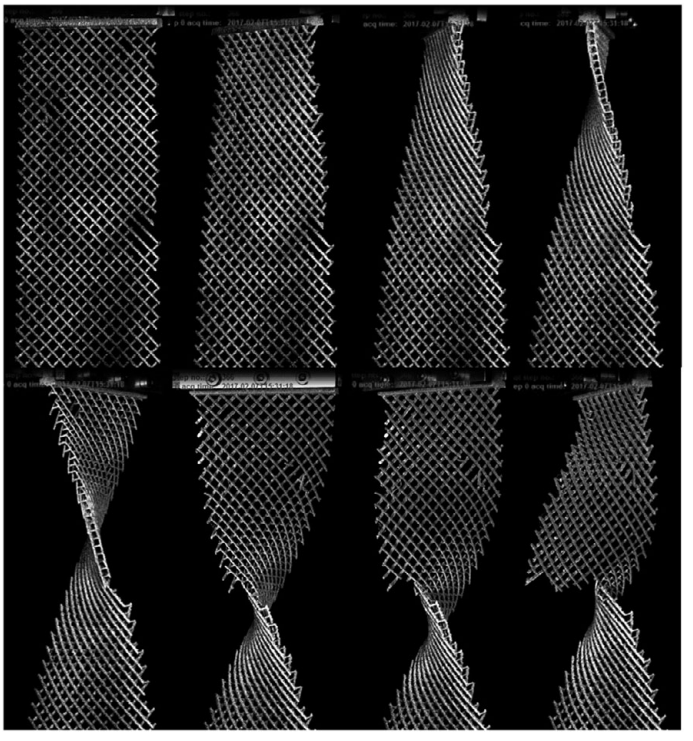

Figure 6.22 Torsion of an aluminum pantographic structure showing the Poynting effect reversal.

bidimensional second-gradient continuum model: second-order phenomena were taken into account by the second gradient of the displacement, that is to say the strain gradient. Several characteristic stiffnesses were then identified to build a proper macroscopic continuous model of the studied material, which led to its numerical modeling and simulation.

6.4 Damage and Failure in Pantographic Fabrics

The resiliency of pantographic structures is clear from the extension test measurements discussed earlier. Here we further discuss the issue of damage and failure in pantographic structures [13, 14]. The ensuing discussions are based upon experimental data published in [9, 15].

6.4.1 Mechanisms of Rupture

Experimentally, three different mechanisms of rupture have been observed: one concerning the fibers and two related to the pivots. The fiber rupture occurs when the maximum elongation is reached related to the geometrical and material features of

the fiber in a considered sample. On the other hand, the pivots can experience failure depending on two different mechanisms: (i) the shear of the pivot, and (ii) its torsion. Needless to say, failure occurs when reaching certain thresholds, in shear (i) or torsion (ii) of the pivot. As a qualitative observation, it is possible to forecast which of these mechanisms will prevail by considering the shape ratio of the pivots: for "slim" pivots it has been observed that the *shear mechanism* prevails, while for "stubby" pivots the *torsion mechanism* plays the fundamental role.

In the following sections we quantitatively analyze the aforementioned mechanisms.

Fiber Elongation Mechanism

From a quantitative viewpoint for characterizing rupture, the discrete quasi-static Hencky spring model described in the previous chapter can be modified by considering a simple irreversible rupture mechanism for the extensional springs, as discussed in [13]. An extensional spring fails if its deformation level exceeds a certain threshold. Experimental data for a displacement-controlled bias extension test (Fig. 6.23) are provided in [9]. The first fiber failure is observed at the corners of the specimen, where the elongation of fibers attains its maximum, as also predicted by the second gradient continuum model discussed in the previous chapter.

This predicted failure initiation has also been confirmed by a displacement-controlled shear test [13] (see Figs. 6.24 and 6.25). It was also observed that in this case the elongation of fibers attains its maximum at the corners of the specimen. We note that in the proposed second gradient model, the assumed damage mechanism was that of the fibers due to their elongation.

Pivot Shear Mechanism

In [14], a pivot damage mechanism due to shearing of pivots, i.e. fibers detaching due to relative sliding in correspondence of pivots, is taken into account, allowing sliding between the two layers (families) of fibers. Thus, the non-linear homogenized quasi-static model for the discrete system discussed in the previous chapter is modified by introducing, in the spirit of mixture theory, two independent placement functions χ^1 and

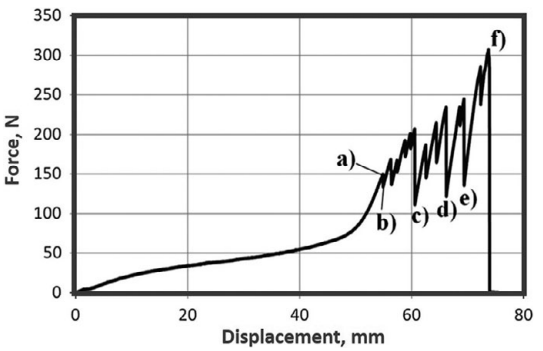

Figure 6.23 Force versus prescribed displacement for a bias extension test. (a) Sample before first beam breakage (i.e. breakdown onset); (b) upper-left corner beam breakage; (c)-(f) further fiber breakages.

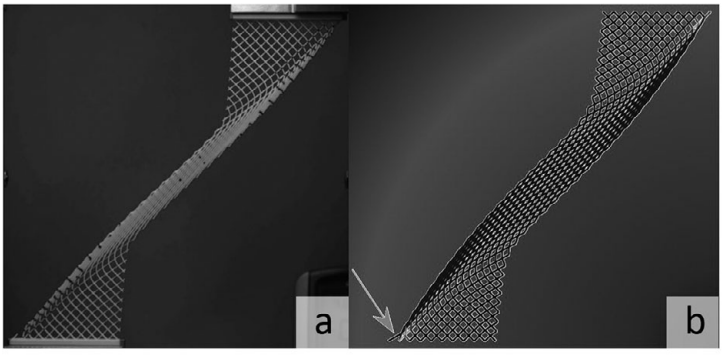

Figure 6.24 (a) Damage onset ($\lambda = 0.976$) of a shear test. (b) The broken fiber is in black and it is indicated by the arrow.

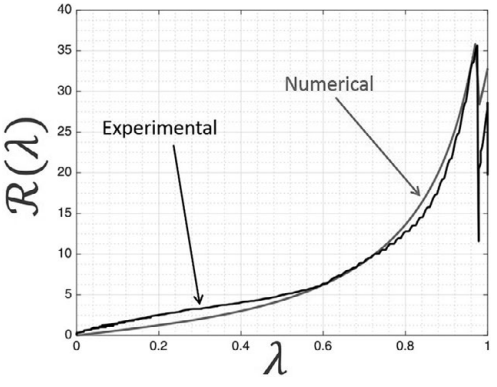

Figure 6.25 Force (N) vs non-dimensional displacement for shear test of a pantographic sheet up to the onset of fiber breakage.

χ^2 (the placement functions of body points belonging to horizontal and vertical fibers, respectively) defined on the same reference domain and, accordingly, considering the following nonlinear (elastic) strain energy to be minimized:

$$\int_{\mathcal{B}_0} \underbrace{\sum_{\alpha=1,2} \frac{K_e^\alpha}{2} \|F^\alpha \hat{e}_\alpha - 1\|^2}_{\text{extension of horiz. and vert. fibers}} + \int_{\mathcal{B}_0} \underbrace{\frac{K_p}{2} \left| \arccos\left(\frac{F^1\hat{e}_1 \cdot F^2\hat{e}_2}{\|F^1\hat{e}_1\| \cdot \|F^2\hat{e}_2\|} \right) - \frac{\pi}{2} \right|^\xi}_{\text{shear (pivots torsion) contribution}}$$
$$+ \int_{\mathcal{B}_0} \underbrace{\sum_{\alpha=1,2} \frac{K_b^\alpha}{2} \left[\frac{\|\nabla F^\alpha |\hat{e}_\alpha \otimes \hat{e}_\alpha\|^2}{\|F^\alpha \hat{e}_\alpha\|^2} - \left(\frac{F^\alpha \hat{e}_\alpha \cdot \nabla F^\alpha |\hat{e}_\alpha \otimes \hat{e}_\alpha}{\|F^\alpha \hat{e}_\alpha\|^2} \right)^2 \right]}_{\text{bending of horiz. and vert. fibers}} \tag{6.1}$$
$$+ \int_{\mathcal{B}_0} \underbrace{\frac{K_{\text{int}}}{2} \|\chi^1 - \chi^2\|^2}_{\text{relative sliding of the two layers}}.$$

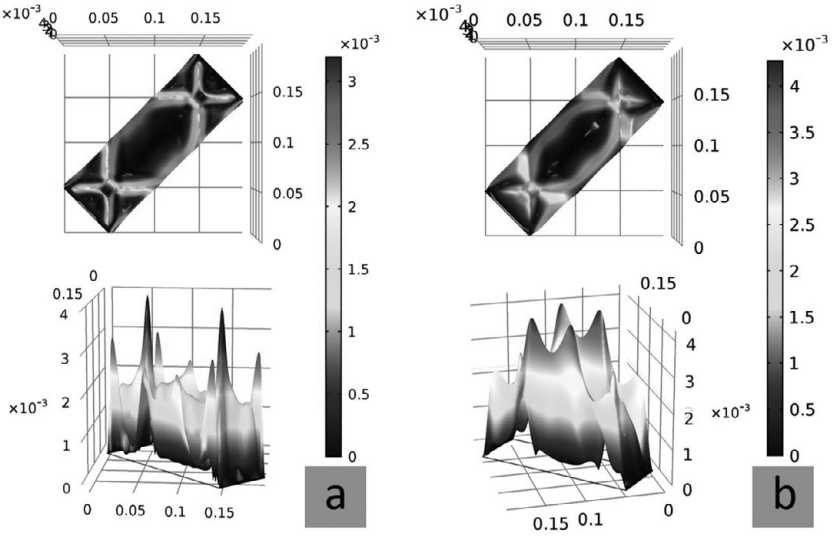

Figure 6.26 Depending on the geometrical features of the considered pantographic structure, one can predict a relative displacement between the fibers in the corner of the rigid triangles near the short sides of the structure (a) or on the long sides of the sheet (b).

where K_{int} (resistance to the relative sliding of the two layers) evolves following a criterion based on thresholds for the relative distance $\delta = \|\chi^1 - \chi^2\|$ between χ^1 and χ^2. Depending on the geometrical features of the considered pantographic structure, one can then predict a relative displacement between the fibers in the corner of the rigid triangles near the short side of the structure or on the long sides of the sheet (see Figs. 6.26 and 6.27).

One can then qualitatively forecast the development of fracture in the pantographic sheet by allowing the beams to slide with respect to one another with correspondence of the pivots as introduced in [14] and [16]. Indeed, the algorithm developed in [16] is able to forecast the onset of fracture, by considering a *mechanism* based on a threshold of the relative displacement (corresponding to the shear of the pivot, as experimentally observed). We note that in this algorithm, the model used is based on the non-linear Euler–Bernoulli beam theory and the pivots are modeled as extensional springs whose elastic constant corresponds to the K_{int} of the homogenised model.

In Fig. 6.28 it is possible to observe the relative displacement between beams as a 3D bar graph, plotted on the shape of the pantographic sheet. A noteworthy aspect related to the introduction of the cubic factor in the *sliding* energetic term is the breaking of symmetry in the plot of relative displacement seen in Fig. 6.28. From the viewpoint of fracture initiation, it is clear from the figure that there are two maxima which correspond to two precise pivots. One of them will undergo the first rupture, due to a flexural/shear stress. This numerical prediction is validated in Fig. 6.29, where an illuminating sequence showing the load step when the first fracture occurs is presented: the broken pivot is precisely the one predicted by the model.

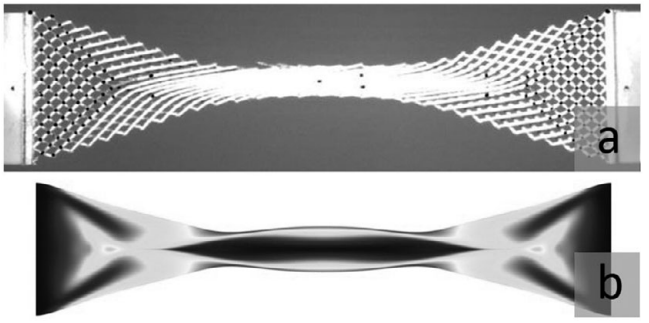

Figure 6.27 Comparison between experimental emerging of the first rupture in an aluminum pantographic structure (a) and numerical prediction (b) of the maximum of the relative displacement between the fibers (relative displacement in colour scale).

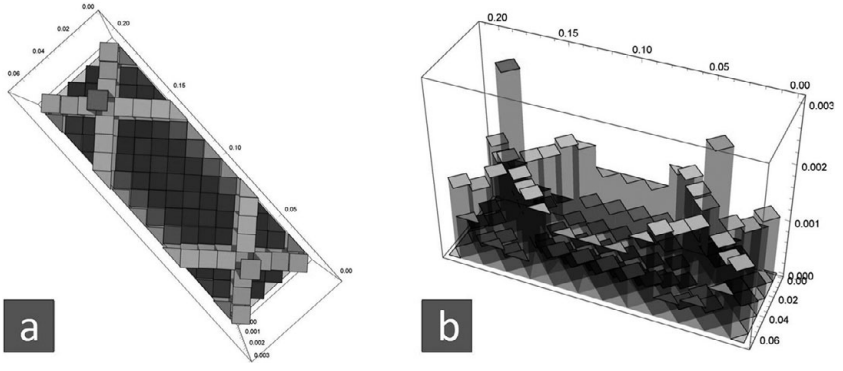

Figure 6.28 Plot of the relative displacement of the shape of the pantographic sheet in the framework of the nonlinear Euler–Bernoulli beam meso-model.

A dissipation problem could be suitably adapted to the relative displacement description. In this case, it would need a preliminary analysis on the friction mechanisms, such as the one presented in [76].

Pivot Torsion Mechanism

Finally, we consider a rupture criterion based on computation of the shear angle[1] (see Fig. 6.30). One can relate the torsion of the pivots to the shear angle. For certain specimens endowed with a particular set of geometrical parameters, the rupturing development is controlled (and initiated) by excessive shear deformation (or torsion) of the pivots (Fig. 6.30). In the displacement-controlled shear test in Fig. 6.24, the shear attains its maximum near the two internal vertices of the quasi-rigidly deforming triangles. The results of numerical modeling incorporating this type of rupturing

[1] We refer here to the shear of the whole pantographic structure, different from the aforementioned shear of the pivot.

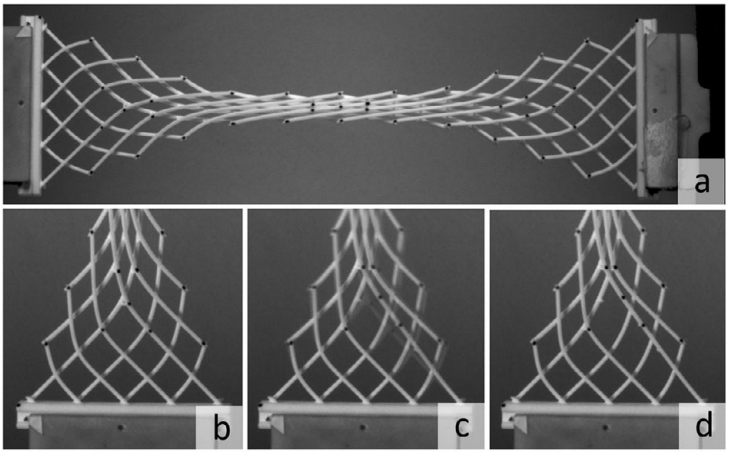

Figure 6.29 A clear explanatory sequence which shows the moment of the first fracture, in the pivot forecast by the model.

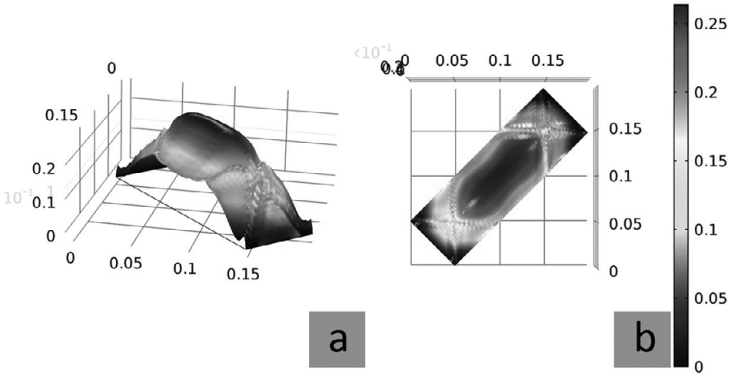

Figure 6.30 Plot of the shear angle. It is possible to use it for defining a rupture criterion based on the pivot torsion.

mechanism also agree well with the measured force-displacement curve up to the onset of fiber rupture (see Fig. 6.25).

Other methods useful to study damage occurring in pantographic structures can be found in [60, 61].

6.4.2 Further Research: Optimization in Pantographic Structures

Utilizing the models developed in the previous chapter, we are able to forecast the exact point of failure initiation within the pantographic structure. It is also possible to postulate certain heuristic criteria to characterize the emergence and evolution of damage, such as the relative displacement between two fibers of the two families in correspondence of a pivot, torsion of the pivot, elongation of a fiber, and flexion of a

fiber. These models and damage postulates can be combined to develop strategies for optimizing the pantographic structure by changing some of its structural members and their mechanical properties. Useful results in the field of optimization are reported in [54, 55, 62, 63].

6.5 Validations via Image Correlation

Digital image correlation (DIC [17, 18]) can be used to quantify evolution of a displacement field at the prescribed resolution of a deformed specimen. Recently, this technique has been applied to extract the displacement fields as the pantograph is deformed in experimental tests [19, 22]. For the pantographic structures, displacement fields can be derived at macroscopic and mesoscopic scales. These displacement fields can then be compared with those predicted via numerical simulations. By this comparison it is possible to validate the constitutive model being considered.

6.5.1 Principle of Digital Image Correlation

DIC is based upon the analysis of digital images of surfaces at different stages of deformation in experiments which aim to obtain a precise estimation of the deformations. One of the limits of DIC comes from its ill-posedness. Generally, only limited information is available from gray level images. For this reason, it is not possible to measure displacement fluctuations beyond certain spatial resolution. Consequently, it is necessary to find a compromise between the uncertainty level and the spatial resolution [23]. Unrefined descriptions of displacement fields based on discretizations coarser than the scale of pixels are usually required. Additional information is necessary to achieve finer resolutions. For example, it is possible to consider continuous displacement fields and decompose them on convenient kinematic bases (e.g. finite element shape functions). The calculation time is increased in this global approach, but the uncertainties can be lowered [23].

Global DIC

The registration of two gray level images in the reference (f) and deformed (g) configurations is based on the conservation of gray levels:

$$f(\boldsymbol{x}) = g(\boldsymbol{x} + \boldsymbol{u}(\boldsymbol{x})), \tag{6.2}$$

where $\boldsymbol{u}$ is the (unknown) displacement field to be measured and $\boldsymbol{x}$ the position of pixels. The sought displacement field minimizes the sum of squared differences Φ_c^2 over the region of interest (ROI),

$$\Phi_c^2 = \sum_{\text{ROI}} \varphi_c^2(\boldsymbol{x}), \tag{6.3}$$

where φ_c defines the gray level residuals $\varphi_c(x) = f(\boldsymbol{x}) - g(\boldsymbol{x} + \boldsymbol{u}(\boldsymbol{x}))$ that are computed at each pixel position $\boldsymbol{x}$ of the ROI. The minimization of Φ_c^2 is a nonlinear and

ill-posed problem. This is the reason for considering a weak formulation in which the displacement field is expressed over a chosen kinematic basis,

$$\boldsymbol{u}(\boldsymbol{x}) = \sum_n \boldsymbol{u}_n \boldsymbol{\psi}_n(\boldsymbol{x}), \tag{6.4}$$

where $\boldsymbol{\psi}_n$ are vector fields and u_n the associated degrees of freedom, which are gathered in the column vector $\boldsymbol{u}$. Thus the measurement problem consists in the minimization of Φ_c^2 with respect to the unknown vector $\boldsymbol{u}$. This problem is nonlinear and to obtain a solution Newton's iterative scheme can be implemented.

In the following analyses, the vector fields correspond to the shape functions of 3-noded triangular elements (i.e. T3 elements). Consequently, the unknown degrees of freedom are the nodal displacements of the T3 elements.

Regularized DIC

The previous approach can be penalized when the image contrast is not sufficient to achieve low spatial resolutions. This is, for instance, the case in the analyses reported hereafter. Regularization techniques can then be selected [21]. They consist of adding to the global correlation functional Φ_c^2 penalty terms. In the following, a first penalty, which is based on the local equilibrium gap, is added for the inner nodes of the finite element mesh and those belonging to the free edges:

$$\Phi_m^2 = \{\mathbf{u}\}^\top [\mathbf{K}]^\top [\mathbf{K}] \{\mathbf{u}\}, \tag{6.5}$$

where $[\mathbf{K}]$ is the rectangular stiffness matrix restricted to the considered nodes. For the other edges, a similar penalization is considered,

$$\Phi_b^2 = \{\mathbf{u}\}^\top [\mathbf{L}]^\top [\mathbf{L}] \{\mathbf{u}\}, \tag{6.6}$$

where $[\mathbf{L}]$ is a second operator acting on the nodal displacements of the boundaries that are not traction-free [21].

The global residual to minimize then consists of the weighted sum of the previous three functionals (i.e. Φ_c^2,Φ_m^2, and Φ_b^2). Because the dimensions of the first functional are different from the other two, they need to be made dimensionless. It follows that the penalization weights acting on Φ_m^2 and Φ_b^2 are proportional to a regularization length raised to the power 4 [21]. The larger the regularization length, the more weight is put on the penalty terms. This penalization acts as a low-pass mechanical filter, namely, all high frequency components of the displacement field that are not mechanically admissible are filtered out. Similarly, for low-contrast areas mechanical regularization provides the displacement interpolation. The following analyses illustrate the benefit of using DIC to measure displacement fields at the macroscopic and mesoscopic scales.

6.5.2 DIC Applied to Pantographic Structures

As an example of the application of DIC to a pantographic structure, we discuss here the analysis of a BIAS extension test presented earlier in this section (see Fig. 6.15). A series of 55 images were analyzed for the deformation range in which no damage

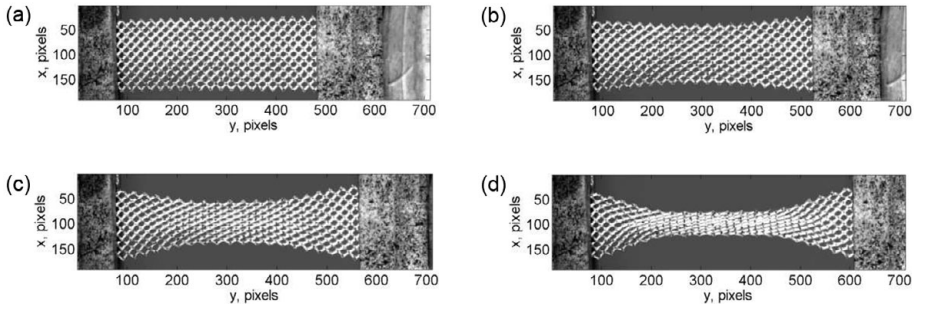

Figure 6.31 Gray level images of the pantograph in the reference configuration (a), 17th (b), 34th (c) and 51st (d) loading steps

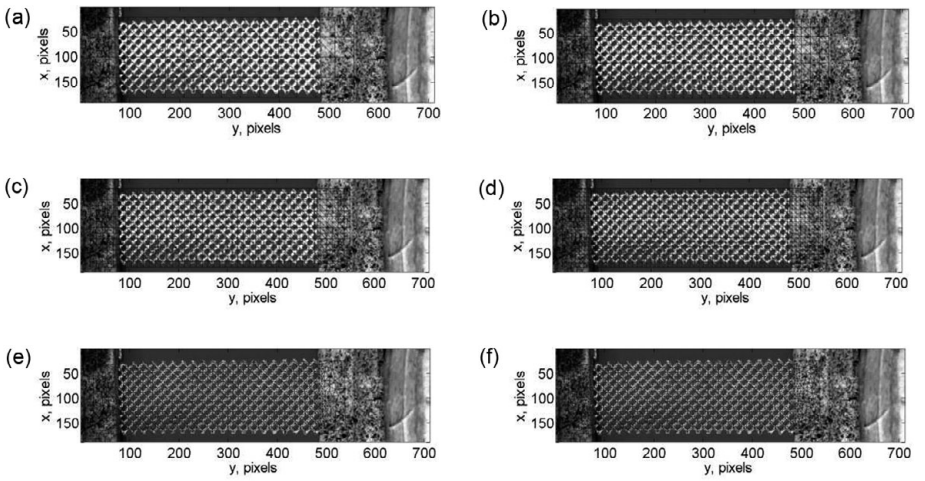

Figure 6.32 Finite element meshes overlaid with the gray level picture of the reference configuration.

was observed. Figure 6.31 shows the images of the initial configuration, and three loaded configurations corresponding to the 17th, 34th, and 51st studied steps. In the present case, the pivots of the pantograph were marked in black, and a random pattern was created by spraying black and white paint on the grips. The fact that the grips were patterned contributes to the convergence of the DIC code even though very large displacement levels occur during the experiment.

Macro- and meso-scale analyses are reported below. For macroscale analyses, the rectangular region of interest was meshed with T3 elements independently of the underlying mesostructure. Four different mesh densities are considered (Fig. 6.32a–d). The characteristic mesh size, which is defined as the square root of the average element surface, is equal to 28 pixels for the first mesh, 13 pixels for the second one, 8 pixels for the third one, and 6 pixels for the last. These four meshes are utilized for convergence analyses of the DIC results at the macroscale.

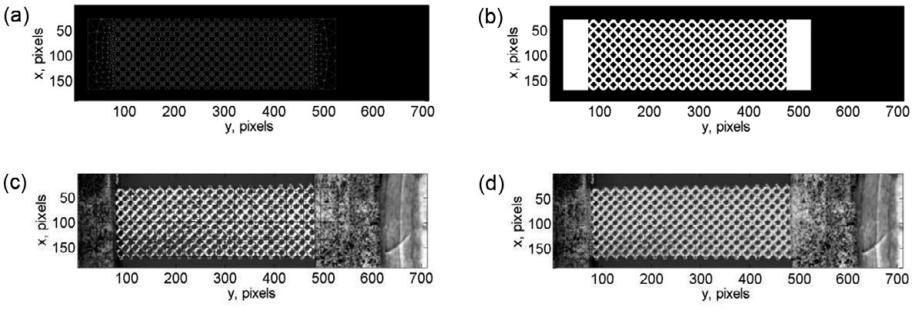

Figure 6.33 The back-tracking procedure. Initial mesh (a) and corresponding mask (b). (c) Reference picture and mesh used to register the mask. (d) Overlay of back-tracked mesh and reference picture.

Two additional meshes are tailored to the pantograph mesostructure (Fig. 6.32 e and f)). The starting point is the nominal geometry of the pantograph, which would be used, say, in FE simulations. From this information, the mesh has been created with Gmsh [20] (Fig. 6.33a) and a picture of the corresponding mask (Fig. 6.33b). A DIC analysis was performed between the reference picture and the mask to deform it so that the mesh can be backtracked onto the actual pantograph surface. In such an analysis, an auxiliary (coarse) mesh has been used (Fig. 6.33c). Once the DIC analysis converged, the original mesh was consistent with the actual geometry of the pantograph (Fig. 6.33d).

This back-tracking procedure has been applied to two meshes (Fig. 6.33a–d). The corresponding characteristic mesh size is equal to 3.7 and 3.6 pixels, respectively. It is worth noting that such discretizations can only be considered as a consequence of regularization techniques since the correlation length of the pantographic structure is of the order of 10 pixels.

In global DIC, the registration quality is assessed with gray level residual fields, which correspond to the pixel-wise gray level difference between the picture in the reference configuration and the picture in the deformed configuration corrected by the measured displacement. The quantity to be minimized is the L2-norm of the gray level residuals over the region of interest [18]. The root mean square (RMS) level is reported in Fig. 6.34 for all six meshes considered herein. The first general tendency is that the registration quality degrades as more steps are analyzed, thereby signaling that the measured fields become increasingly complex as the loading progresses (Fig. 6.31). Second, there is a significant difference between the first four meshes and the last two. This proves that meshes tailored to the actual pantograph surface better capture the kinematics of the test, even with the same regularization length as for coarser meshes. Third, in both cases, a converged solution is obtained in terms of mesh density with respect to the chosen regularization length. More precisely, meshes 3 and 4 at the macroscale, meshes 5 and 6 at the mesoscale have the same residual levels. Consequently, there is no need to further refine the discretization with the chosen regularization length.

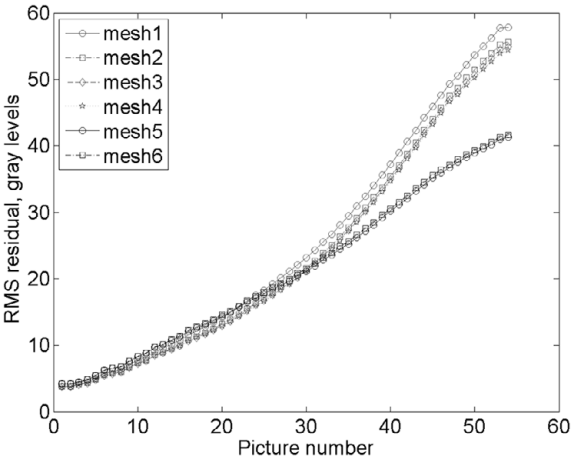

Figure 6.34 RMS gray level residual as functions of the picture number for the six meshes shown in Fig. 6.32.

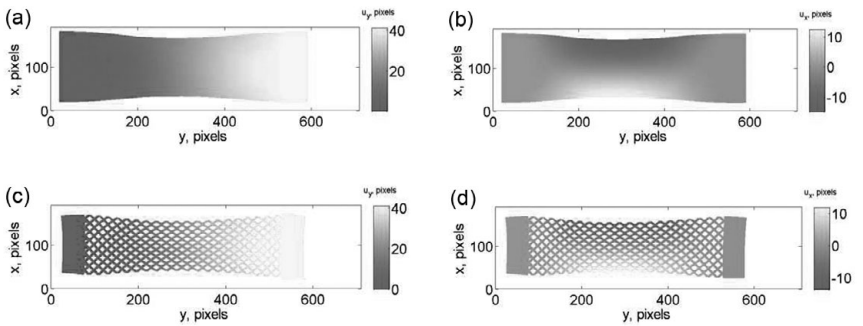

Figure 6.35 Longitudinal (a-c) and transverse (b-d) displacement fields measured with meshes 4 (a-b) and 6 (c-d) for the 14th picture. The fields are shown on the deformed configuration.

In the following discussion, only two sets of results are reported, namely, those of meshes 4 (at the macroscale) and 6 (at the mesoscale). Figure 6.35 shows the longitudinal and transverse displacements measured for the 14th picture. The transverse displacement field u_x shows a very important contraction, which is of the same order of magnitude as the longitudinal motions u_y. Since the width of the sample is one third of its length, the transverse deformations are much more important than the longitudinal component. This observation applies to both scales. In the present case, both measurements have approximately the same quality in terms of overall registration residuals (Fig. 6.34).

In Fig. 6.36 the same fields are shown for the 34th picture. The main features of the transverse and longitudinal displacement fields are identical to the previous step, yet with higher overall levels. The displacement ranges are still of the same order of magnitude for the longitudinal and transverse displacements. Consequently the central

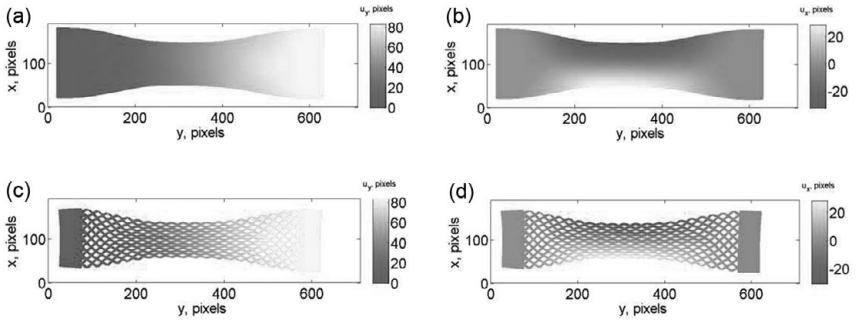

Figure 6.36 Longitudinal (a-c) and transverse (b-d) displacement fields measured with meshes 3 (a-b) and 4 (c-d) for the 34th picture. The fields are shown on the deformed configuration.

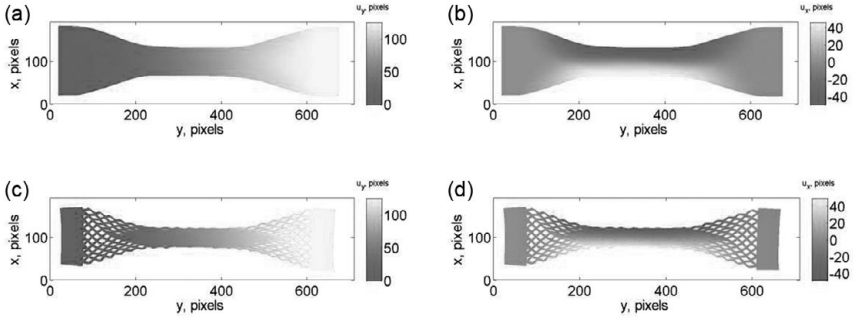

Figure 6.37 Longitudinal (a-c) and transverse (b-d) displacement fields measured with meshes 3 (a-b) and 4 (c-d) for the 51st picture. The fields are shown on the deformed configuration.

part of the sample is thinner. The deformed shapes are very close for both meshes, which translates into the same levels of registration residuals (Fig. 6.34).

One of the last steps is reported in Fig. 6.37. In this case the gray level residuals (Fig. 6.34) are significantly higher for mesh 4 (at the macroscopic scale) in comparison with mesh 6 (at the mesoscopic scale). There is a clear difference in the deformed shape whose width is lower for the mesoscopic analysis in comparison with the macroscopic result. The highly deformed region has grown toward both ends of the pantographic sheet, which can be understood by the fact that when struts touch each other, the deformation mechanisms can be completely altered and the consequent behavior changes in a dramatic manner.

The results reported herein confirm that DIC analyses can be applied to pantographic structures at macroscopic scales [19] and mesoscopic levels with regularized DIC on very fine meshes (i.e. down to 3.6 pixel elements). Important gains were observed in terms of registration quality by moving from the macroscopic to the mesoscopic scale (i.e. more than a factor of one and a half at the end of the picture series). The final gray level residuals indicate that even more advanced approaches should be adopted. It must be remarked here though that due to the nature of DIC, which relies only upon images

from the surface of the object, the effect of pivots, which are subsurface and hidden in the images, upon the kinematics cannot be directly evaluated.

6.6 Conclusion

Pantographic metamaterial is a concept that is founded upon a physical theory. To verify and validate the physical theory it is essential to realize the predicted structure and subject it to experimental tests. This chapter has dealt with experimental evidence and technological challenges regarding pantographic metamaterials. Such issues are forerunners of those that must be confronted by all types of metamaterials regardless of their working principles [29, 30, 69, 70]. It is clear that a transdisciplinary approach must be employed to address these challenges successfully. Indeed, robust experimental verification of theoretical predictions has been possible only due to the diligent efforts in coordinating the different aspects of the investigations. It has been shown that CAD modeling and 3D printing are not only powerful tools for rapid prototyping, but indispensable for metamaterial development, as are the predictive theories. Moreover, an important improvement in developing and validating theories is to be researched in numerical simulations. Finite element methods nowadays make it possible to clarify the modelized phenomena and to calibrate the mechanical tests needed to validate the models involved. Some useful examples of numerical tools developed for metamaterials are reported in [33–41, 79, 80]. Theoretical models have guided the design of experiments and they have led to clear conclusions about further changes to be adopted in order to improve the gap between modeling and reality. In particular, pantographic Metamaterial constitutes the most clear and simple example of a second gradient material. Some homogenization procedures useful in finding a continuum model describing it can be found in [42, 42, 44–47, 56–59]. More general mathemathical methods useful in this context are reported in [71–75, 77, 78]. DIC techniques have proved useful in measuring deformation fields inexpensively as a post-processing step. A possible new challenge to face in the study of pantographic metamaterial consists in developing models to describe a composite fiber reinforced material, whose fibers are arranged in a pantographic-like network. Preliminary results about alignments of fibers embedded in a softer matrix are reported in [48, 53]. Many results about the different homogenisation techniques needed to develop similar models can be found in [49–52]. Pantographic structures show large deformations also remaining in the elastic stage. Another challenging problem is to study the effect of the pantographic microstructure (and its large deformations) coupled with some exotic material properties. For example, an interesting coupling could be arranged with memory alloys, whose mechanical properties are reported in [65–68]. Material science has played an important role as well in understanding how the manufacturing process affects the crystalline and granular properties of printed aluminum, polyamide and steel. The results of these last investigations will guide the choice of the manufacturing process parameters like bed temperature, laser temperature, specimen arrangement inside the bed, powder composition, powder treatment, cooling time, etc. In conclusion, experimental investigation of pantographic metamaterials is an

active area of research which will involve ever more specialists, resulting in a general advancement of all the disciplines involved. Such research output will certainly have a relevant impact also in the testing and manufacturing of current metamaterials as well as of those which have not been invented yet.

Acknowledgments

Mario Spagnuolo has received funding from the European Union's Horizon 2020 research and innovation programme under the Marie Skłodowska-Curie grant agreement No 665850. Anil Misra is funded by United States National Science Foundation (NSF) grant CMMI-1727433.

Bibliography

[1] B. E. Abali, W. H. Müller, and F. dell'Isola. Theory and computation of higher gradient elasticity theories based on action principles. *Archive of Applied Mechanics*, 87(9):1–4, 2015.

[2] B. E. Abali, W. H. Müller, and V. A. Eremeyev. Strain gradient elasticity with geometric nonlinearities and its computational evaluation. *Mechanics of Advanced Materials and Modern Processes*, 1(1):4, 2015.

[3] C. Pideri and P. Seppecher. A second gradient material resulting from the homogenization of an heterogeneous linear elastic medium. *Continuum Mechanics and Thermodynamics*, 9(5):241–257, 1997.

[4] P. Seppecher. Second-gradient theory: application to Cahn–Hilliard fluids. In *Continuum Thermomechanics*, 379–388, 2000, Springer.

[5] C. Pideri and P. Seppecher. Asymptotics of a non-planar rod in non-linear elasticity. *Asymptotic Analysis*, 48(1,2):33–54, 2006.

[6] C. Pideri and P. Seppecher. A homogenization result for elastic material reinforced periodically with high rigidity elastic fibres. *Comptes Rendus de l'Academie des Sciences Series IIB Mechanics Physics Chemistry Astronomy*, 8(324):475–481, 1997.

[7] H. Abdoul-Anziz and P. Seppecher. Strain gradient and generalized continua obtained by homogenizing frame lattices. *Mathematics and Mechanics of Complex Systems*, 6(3):213–250, 2018.

[8] F. dell'Isola, I. Giorgio, M. Pawlikowski, and N. L. Rizzi. Large deformations of planar extensible beams and pantographic lattices: Heuristic homogenization, experimental and numerical examples of equilibrium. *Proc. R. Soc. A*, 472 (2185), 20150790, 2016.

[9] F. dell'Isola, T. Lekszycki, M. Pawlikowski, R. Grygoruk, and L. Greco. Designing a light fabric metamaterial being highly macroscopically tough under directional extension: First experimental evidence. *Zeitschrift för angewandte Mathematik und Physik*, 66(6):3473–3498, 2015.

[10] F. dell'Isola, M. Cuomo, L. Greco, and A. Della Corte. Bias extension test for pantographic sheets: Numerical simulations based on second gradient shear energies. *Journal of Engineering Mathematics*, 103(1):127–157, 2017.

[11] Y. Brechet and J. D. Embury. Architectured materials: Expanding materials space. *Scripta Materialia*, 68:1–3, 2013.

[12] F. dell'Isola, M. Spagnuolo, P. Peyre, *et al*. Quasi-perfect pivots in inox printed pantographic structures: First approaches to dissipative mechanisms. *to appear*, 2018.

[13] E. Turco, F. dell'Isola, N. Rizzi, *et al*. Fiber rupture in sheared planar pantographic sheets: Numerical and experimental evidence. *Mechanics Research Communications*, 76:86–90, 2016.

[14] M. Spagnuolo, K. Barcz, A. Pfaff, F. dell'Isola, and P. Franciosi. Qualitative pivot damage analysis in aluminum printed pantographic sheets: Numerics and experiments. *Mechanics Research Communications*, 83:47–52, 2017.

[15] G. Ganzosch, F. dell'Isola, E. Turco, T. Lekszycki, and W. H. Müller. Shearing tests applied to pantographic structures. *Acta Polytechnica CTU Proceedings*, 7:1-6, 2016.

[16] U. Andreaus, M. Spagnuolo, T. Lekszycki, and S. R. Eugster. A Ritz approach for the static analysis of planar pantographic structures modeled with nonlinear Euler–Bernoulli beams. *Continuum Mechanics and Thermodynamics*, 1-21, 2018.

[17] M.A. Sutton, J.J. Orteu, and H. Schreier. *Image Correlation for Shape, Motion and Deformation Measurements: Basic Concepts, Theory and Applications*. Springer Science & Business Media, 2009.

[18] F. Hild and S. Roux. Digital image correlation, in Rastogi, P. and Hack, E., ed., *Optical Methods for Solid Mechanics. A Full-Field Approach*. Weinheim (Germany): Wiley-VCH, pp. 183–228, 2012.

[19] E. Turco, A. Misra, M. Pawlikowski, F. dell'Isola, and F. Hild. Enhanced Piola–Hencky discrete models for pantographic sheets with pivots without deformation energy: Numerics and experiments, *International Journal of Solids and Structures*. 147:94–109, 2018.

[20] C. Geuzaine and J.-F. Remacle. Gmsh: A 3-D finite element mesh generator with built-in pre- and post-processing facilities, *International Journal for Numerical Methods in Engineering* 79(11): 1309–1331, 2009.

[21] Z. Tomičević, F. Hild, and S. Roux. Mechanics-aided digital image correlation. *The Journal of Strain Analysis for Engineering Design*, 48(5):330–343, 2013.

[22] F. dell'Isola. Pantographic metamaterials: an example of mathematically driven design and of its technological challenges. *Continuum Mechanics and Thermodynamics*, 13:1–34, 2018.

[23] F. Hild and S. Roux. Comparison of local and global approaches to digital image correlation. *Experimental Mechanics*, 52(9):1503–1519, 2012.

[24] A. Misra, T. Lekszycki, I. Giorgio, *et al.* Pantographic metamaterials show atypical Poynting effect reversal. *Mechanics Research Communications*, 89:6–10, 2018.

[25] L. Placidi, U. Andreaus, and I. Giorgio. Identification of two-dimensional pantographic structure via a linear D4 orthotropic second gradient elastic model. *Journal of Engineering Mathematics*, 103(1):1–21, 2017.

[26] L. Placidi, E. Barchiesi, and A. Della Corte. Identification of two-dimensional pantographic structures with a linear D4 orthotropic second gradient elastic model accounting for external bulk double forces. In *Mathematical Modelling in Solid Mechanics* pp. 211–232. Springer, Singapore, 2017.

[27] L. Placidi, E. Barchiesi, and A. Battista. An inverse method to get further analytical solutions for a class of metamaterials aimed to validate numerical integrations. In *Mathematical Modelling in Solid Mechanics* pp. 193–210. Springer, Singapore, 2017.

[28] M. Golaszewski, R. Grygoruk, I. Giorgio, M. Laudato, and F. Di Cosmo. Metamaterials with relative displacements in their microstructure: Technological challenges in 3D printing,

experiments and numerical predictions. *Continuum Mechanics and Thermodynamics*, 1–20, 2018.

[29] M. Laudato and F. Di Cosmo. Euromech 579 Arpino 3–8 April 2017: Generalized and microstructured continua: New ideas in modeling and/or applications to structures with (nearly) inextensible fibers—a review of presentations and discussions. *Continuum Mechanics and Thermodynamics*, 1–15, 2018.

[30] F. di Cosmo, M. Laudato, and M. Spagnuolo. Acoustic metamaterials based on local resonances: Homogenization, optimization and applications. In *Generalized Models and Non-classical Approaches in Complex Materials 1* pp. 247–274. Springer, Cham, 2018.

[31] S. Billard, J.P. Fondere, B. Bacroix, and G.F. Dirras. Macroscopic and microscopic aspects of the deformation and fracture mechanisms of ultrafine-grained aluminum processed by hot isostatic pressing. *Acta Materialia*, 54(2):411–421, 2006.

[32] M. Wronski, Krzysztof Wierzbanowski, S. Wronski, Brigitte Bacroix, and P. Lipinski. Texture variation in asymmetrically rolled titanium. Study by finite element method with implemented crystalline model. *International Journal of Mechanical Sciences*, 87:258–267, 2014.

[33] Leopoldo Greco and Massimo Cuomo. B-spline interpolation of Kirchhoff–Love space rods. *Computer Methods in Applied Mechanics and Engineering*, 256:251–269, 2013.

[34] Leopoldo Greco, Ivan Giorgio, and Antonio Battista. In plane shear and bending for first gradient inextensible pantographic sheets: Numerical study of deformed shapes and global constraint reactions. *Mathematics and Mechanics of Solids*, 22(10):1950–1975, 2017.

[35] Leopoldo Greco, Nicola Impollonia, and Massimo Cuomo. A procedure for the static analysis of cable structures following elastic catenary theory. *International Journal of Solids and Structures*, 51(7-8):1521–1533, 2014.

[36] Franco Buffa, Andrea Causin, Antonio Cazzani, *et al.* The Sardinia radio telescope: A comparison between close-range photogrammetry and finite element models. *Mathematics and Mechanics of Solids*, 22(5):1005–1026, 2017.

[37] Antonio Cazzani, Marcello Malagù, Emilio Turco, and Flavio Stochino. Constitutive models for strongly curved beams in the frame of isogeometric analysis. *Mathematics and Mechanics of Solids*, 21(2):182–209, 2016.

[38] Antonio Cazzani, Marcello Malagù, and Emilio Turco. Isogeometric analysis of plane-curved beams. *Mathematics and Mechanics of Solids*, 21(5):562–577, 2016.

[39] J. Austin Cottrell, Alessandro Reali, Yuri Bazilevs, and Thomas J. R. Hughes. Isogeometric analysis of structural vibrations. *Computer Methods in Applied Mechanics and Engineering*, 195(41–43):5257–5296, 2006.

[40] Thomas J. R. Hughes, Alessandro Reali, and Giancarlo Sangalli. Efficient quadrature for nurbs-based isogeometric analysis. *Computer Methods in Applied Mechanics and Engineering*, 199(5-8):301–313, 2010.

[41] Josef Kiendl, Ferdinando Auricchio, and Alessandro Reali. A displacement-free formulation for the Timoshenko beam problem and a corresponding isogeometric collocation approach. *Meccanica*, 53(6):1403–1413, 2018.

[42] Claude Boutin. Microstructural effects in elastic composites. *International Journal of Solids and Structures*, 33(7):1023–105, 1996.

[43] Claude Boutin and Christian Geindreau. Periodic homogenization and consistent estimates of transport parameters through sphere and polyhedron packings in the whole porosity range. *Physical Review E*, 82(3):036313, 2010.

[44] Claude Boutin and Stéphane Hans. Homogenisation of periodic discrete medium: Application to dynamics of framed structures. *Computers and Geotechnics*, 30(4):303–320, 2003.

[45] Nicolas Auffray, Regis Bouchet, and Y Brechet. Strain gradient elastic homogenization of bidimensional cellular media. *International Journal of Solids and Structures*, 47(13):1698–1710, 2010.

[46] Francisco Chinesta, Amine Ammar, François Lemarchand, Pierre Beauchene, and Fabrice Boust. Alleviating mesh constraints: Model reduction, parallel time integration and high resolution homogenization. *Computer Methods in Applied Mechanics and Engineering*, 197(5):400–413, 2008.

[47] Margherita Solci. Double-porosity homogenization for perimeter functionals. *Mathematical Methods in the Applied Sciences*, 32(15):1971–2002, 2009.

[48] P. Franciosi. A decomposition method for obtaining global mean Green operators of inclusions patterns. Application to parallel infinite beams in at least transversally isotropic media. *International Journal of Solids and Structures*, 147:1–19, 2018.

[49] Patrick Franciosi. On the modified Green operator integral for polygonal, polyhedral and other non-ellipsoidal inclusions. *International Journal of Solids and Structures*, 42(11–12):3509–3531, 2005.

[50] Patrick Franciosi, Renald Brenner, and Abderrahim El Omri. Effective property estimates for heterogeneous materials with cocontinuous phases. *Journal of Mechanics of Materials and Structures*, 6(5):729–763, 2011.

[51] Patrick Franciosi and Yann Charles. Mean Green operators and Eshelby tensors for hemispherical inclusions and hemisphere interactions in spheres. Application to bi-material spherical inclusions in isotropic spaces. *Mechanics Research Communications*, 75:57–66, 2016.

[52] Patrick Franciosi and Gérard Lormand. Using the radon transform to solve inclusion problems in elasticity. *International Journal of Solids and Structures*, 41(3-4):585–606, 2004.

[53] Patrick Franciosi, Mario Spagnuolo, and Oguz Umut Salman. Mean Green operators of deformable fiber networks embedded in a compliant matrix and property estimates. *Continuum Mechanics and Thermodynamics*, pages 1–32.

[54] Boris Desmorat and Rodrigue Desmorat. Topology optimization in damage governed low cycle fatigue. *Comptes Rendus Mecanique*, 336(5):448–453, 2008.

[55] Boris Desmorat and Georges Duvaut. Optimization of the reinforcement of a 3D medium with thin composite plates. *Structural and Multidisciplinary Optimization*, 28(6):407–415, 2004.

[56] Samuel Forest. Micromorphic approach for gradient elasticity, viscoplasticity, and damage. *Journal of Engineering Mechanics*, 135(3):117–131, 2009.

[57] Samuel Forest and Rainer Sievert. Elastoviscoplastic constitutive frameworks for generalized continua. *Acta Mechanica*, 160(1-2):71–111, 2003.

[58] Nicolas Auffray, Regis Bouchet, and Yves Brechet. Derivation of anisotropic matrix for bi-dimensional strain-gradient elasticity behavior. *International Journal of Solids and Structures*, 46(2):440–454, 2009.

[59] Nicolas Auffray, Justin Dirrenberger, and Giuseppe Rosi. A complete description of bi-dimensional anisotropic strain-gradient elasticity. *International Journal of Solids and Structures*, 69:195–206, 2015.

[60] Loredana Contrafatto and Massimo Cuomo. A framework of elastic–plastic damaging model for concrete under multiaxial stress states. *International Journal of Plasticity*, 22(12):2272–2300, 2006.

[61] Loredana Contrafatto, Massimo Cuomo, and Salvatore Gazzo. A concrete homogenisation technique at meso-scale level accounting for damaging behaviour of cement paste and aggregates. *Computers & Structures*, 173:1–18, 2016.

[62] Anita Catapano, Boris Desmorat, and Paolo Vannucci. Stiffness and strength optimization of the anisotropy distribution for laminated structures. *Journal of Optimization Theory and Applications*, 167(1):118–146, 2015.

[63] A. Jibawy, Boris Desmorat, and Angela Vincenti. Structural rigidity optimization of thin laminated shells. *Composite Structures*, 95:35–43, 2013.

[64] Giuseppe Rosi, Luca Placidi, and Nicolas Auffray. On the validity range of strain-gradient elasticity: A mixed static-dynamic identification procedure. *European Journal of Mechanics-A/Solids*, 69:179–191, 2018.

[65] Mohammad Reza Karamooz Ravari, Mahmoud Kadkhodaei, and Abbas Ghaei. Effects of asymmetric material response on the mechanical behavior of porous shape memory alloys. *Journal of Intelligent Material Systems and Structures*, 27(12):1687–1701, 2016.

[66] M. R. Karamooz Ravari and M. Kadkhodaei. A computationally efficient modeling approach for predicting mechanical behavior of cellular lattice structures. *Journal of Materials Engineering and Performance*, 24(1):245–252, 2015.

[67] M. R. Karamooz Ravari, M. Kadkhodaei, M. Badrossamay, and R. Rezaei. Numerical investigation on mechanical properties of cellular lattice structures fabricated by fused deposition modeling. *International Journal of Mechanical Sciences*, 88:154–161, 2014.

[68] Hojjat Rezaei, Mahmoud Kadkhodaei, and Hassan Nahvi. Analysis of nonlinear free vibration and damping of a clamped–clamped beam with embedded prestrained shape memory alloy wires. *Journal of Intelligent Material Systems and Structures*, 23(10):1107–1117, 2012.

[69] Ben Nadler, Panayiotis Papadopoulos, and David J Steigmann. Multiscale constitutive modeling and numerical simulation of fabric material. *International Journal of Solids and Structures*, 43(2):206–221, 2006.

[70] Jian Cao, Remko Akkerman, Philippe Boisse, *et al*. Characterization of mechanical behavior of woven fabrics: experimental methods and benchmark results. *Composites Part A: Applied Science and Manufacturing*, 39(6):1037–1053, 2008.

[71] Giulio Alfano, Fabio De Angelis, and Luciano Rosati. General solution procedures in elasto/viscoplasticity. *Computer Methods in Applied Mechanics and Engineering*, 190(39):5123–5147, 2001.

[72] Brice Bognet, Adrien Leygue, and Francisco Chinesta. Separated representations of 3D elastic solutions in shell geometries. *Advanced Modeling and Simulation in Engineering Sciences*, 1(1):4, 2014.

[73] Andrea Braides, Maria Colombo, Massimo Gobbino, and Margherita Solci. Minimizing movements along a sequence of functionals and curves of maximal slope. *Comptes Rendus Mathematique*, 354(7):685–689, 2016.

[74] G. Piccardo, F. Tubino, and A. Luongo. A shear–shear torsional beam model for nonlinear aeroelastic analysis of tower buildings. *Zeitschrift für angewandte Mathematik und Physik*, 66(4):1895–1913, 2015.

[75] Giovanni Romano, Luciano Rosati, and Marina Diaco. Well-posedness of mixed formulations in elasticity. *ZAMM-Journal of Applied Mathematics and Mechanics/Zeitschrift für*

Angewandte Mathematik und Mechanik: Applied Mathematics and Mechanics, 79(7):435–454, 1999.

[76] Simon R. Eugster and Ch. Glocker. Constraints in structural and rigid body mechanics: a frictional contact problem. *Annals of Solid and Structural Mechanics*, 5(1-2):1–13, 2013.

[77] Simon R. Eugster and Christoph Glocker. On the notion of stress in classical continuum mechanics. *Mathematics and Mechanics of Complex Systems*, page 299, 2017.

[78] S. R. Eugster, C. Hesch, P. Betsch, and Ch. Glocker. Director-based beam finite elements relying on the geometrically exact beam theory formulated in skew coordinates. *International Journal for Numerical Methods in Engineering*, 97(2):111–129, 2014.

[79] Ramiro dell'Erba. Position-based dynamic of a particle system: A configurable algorithm to describe complex behaviour of continuum material starting from swarm robotics. *Continuum Mechanics and Thermodynamics*, pages 1–22, 2018.

[80] Ramiro dell'Erba. Swarm robotics and complex behaviour of continuum material. *Continuum Mechanics and Thermodynamics*, pages 1–26, 2018.

7 Variational Methods as Versatile Tools in Multidisciplinary Modeling and Computation

U. Andreaus, I. Giorgio

7.1 Variational Principles: A Powerful Tool

Variational approaches have proven successful in the analysis of many systems, e.g. economic, engineering, social, biological, as well as being elegant from a theoretical point of view [1–8].

Variational methods and principles, after their birth in the Hellenistic age and their subsequent developments by Euler and Lagrange, are experiencing a sort of revival thanks to the new developments of numerical techniques based on stationarity principles, like the finite element method (FEM) [83–89]. Such techniques benefit from a variational formulation of the model to be solved: energy methods, beyond their wide use in obtaining estimates and bounds aimed at proving well-posedness for a broad class of PDEs and in formulating field theories [9], are thus of major practical importance as they also allow for an effective numerics.

On the other hand, variational principles are sometimes considered by numerical analysts working in FEM as nothing but an efficient tool, rather than a fundamental concept in model formulation: a common approach is to derive the weak form, the one giving, after a sort of discretization of the field variables, the algebraic system to be finally solved, starting from the strong form, i.e. the PDEs. In this regard, it is noteworthy that there is no reason why one should believe that models are more 'naturally' (whatever this means) formulated using PDEs rather than in terms of an action functional. Very often, by means of an energy principle, it is possible to derive the same weak form obtained starting from the strong form PDEs. Usually, when this is not possible, the theory could be affected by serious problems. Furthermore, the availability of rigorous theorems about existence and, possibly, uniqueness of a weak solution makes it possible to establish convergence of the finite element method to the solution. Hence, it not unreasonable to state that sound numerics can be done when well-posedness results are available, in order not to proceed blindly in a sort of *terra incognita*. It is clear that, without resorting to a (well-behaving) energy functional, it is unlikely (and generally false) that a well-posedness result can be achieved. When a weak form is derived without an underlying energy functional, by means of more or less licit integrations by parts, it is of course possible to obtain some results: unfortunately, often, they are meaningless or, at least, controversial ones.

The modeller usually faces challenges coming from the description of phenomena which involve a great variety of features: elastic macroscopic deformations related

to microscopic complex mechanisms, dissipation due to damaging, plasticity, friction, electro-mechanical or other multi-physical couplings. A good part of the efforts involved in the modelling of these phenomena, which should not be considered inclusive of all the physical situations which can be addressed by the method we are going to present, can be effectively exemplified by referring to recent approaches to three-different branches of applied sciences, in which the use of variational methods has proven useful. We are referring to: a) some applications in the field of biomechanics, where a relevant problem which needs to be addressed is the one of studying and describing the functional adaptation of bone tissue interacting with a graft of bio-resorbable artificial material under mechanical loading; b) the problem of modelling dissipation of mechanical energy, addressed by considering some kind of internal friction mechanism; and c) the problem of vibration damping, which can be addressed by coupling a lightweight structural element with a multi-terminal electrical network by means of piezoelectric transducers.

7.2 Applications in Biomechanics

In order to address the problem of studying the interaction between living bone tissue and a tissue which has been reconstructed by means of an artificial bio-resorbable material, we consider a body which is made up of a mixture composed of three phases: the binary solid porous matrix of bone and bio-resorbable material, and the fluid phase that fills the connected pores of the solid matrix, i.e. bone marrow, blood and interstitial fluid. At an initial stage, there are two distinct zones characterized, respectively, by the presence of bone tissue and bio-material only (see e.g. Fig. 7.1). Afterwards, the remodelling process, which is driven by an external mechanical excitation, promotes the bone growth inside the graft. Indeed, it is only in the graft region that the three-phase mixture can be found, while in the bone area a simpler two-phase mixture is present because, clearly, the bio-resorbable material remains confined in the initial zone and, possibly, it is resorbed. The shape of the body in its undeformed reference configuration

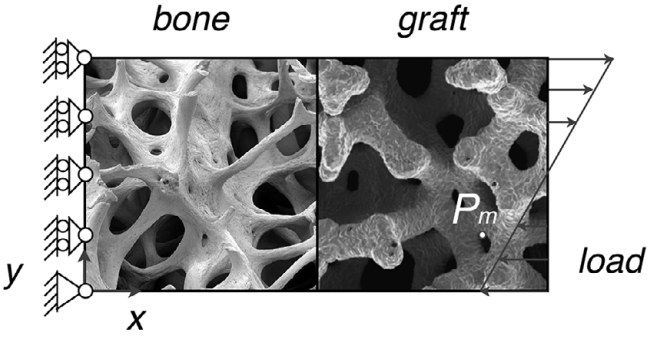

Figure 7.1 Representation of a bone sample reconstructed with a graft of bio-resorbable material in its initial configuration under a cyclic lineal load with a linear distribution.

is represented by the subset $\mathcal{B}_0$ of a Euclidean space $\mathcal{E}$. We are not going to make use of a so-called mixture model in a strict sense, since we are not going to consider as independent kinematical descriptors of the model placement functions for each component of the mixture. The only displacement field $\boldsymbol{u}(\boldsymbol{X},t)$, with $\boldsymbol{\chi}(\boldsymbol{X}) = \boldsymbol{X} + \boldsymbol{u}(\boldsymbol{X})$ being the corresponding placement function, which we consider as an independent Lagrangian kinematic variable, is assumed to be the displacement of the barycenter $\boldsymbol{X}$ of the representative elementary volume (REV) of the solid binary mixture. Nevertheless, in order to take into account the porous nature of the system, we introduce a further micro-kinematical descriptor ϕ, which is the Lagrangian representation of the porosity of the body in the current configuration, while ϕ^* is the porosity of the body in the reference configuration.

Clearly, when approaching the description of a real system, it is of crucial importance to decide the physical observed quantities and the observed length scale as, according to these choices, the same system can be modelled in many different ways. In order to stress this fact we will present three different possible continuum mechanics approaches to bone mechanics and remodelling. The reason why we decided to present these examples will be self-explanatory: variational principles allow us to deal synthetically with different models within the same conceptual framework.

We start by describing the first approach. It is based upon the energy density proposed by Biot, which is classical in poromechanics. In order to do so, we introduce the deformation measures of the model. Specifically, for the solid phase we define the strain tensor $\varepsilon_{\mathrm{ij}}(\boldsymbol{X},t)$ as follows

$$\varepsilon_{\mathrm{ij}}(\mathbf{X},t) = \frac{1}{2}\left(u_{\mathrm{i,j}} + u_{\mathrm{j,i}}\right). \tag{7.1}$$

The micro-deformation of pores is described by means of the change, between the reference and the current configurations, of the effective volume of the fluid content per unit volume of the body. In algebraic expressions, we have

$$\zeta(\boldsymbol{X},t) = \phi(\chi(\boldsymbol{X},t),t) - \phi^*(\boldsymbol{X},t). \tag{7.2}$$

According to mixture theory, these porosities can be expressed as

$$\phi = 1 - (\rho_{\mathrm{b}}/\hat{\rho}_{\mathrm{b}} + \rho_{\mathrm{m}}/\hat{\rho}_{\mathrm{m}}), \quad \phi^* = 1 - (\rho^*_{\mathrm{b}}/\hat{\rho}_{\mathrm{b}} + \rho^*_{\mathrm{m}}/\hat{\rho}_{\mathrm{m}}), \tag{7.3}$$

where ρ_{b} and ρ_{m} are the apparent mass densities of bone tissue and artificial material, respectively; the hat symbol denotes the true densities, while the superscript * indicates all quantities in the reference configuration.

Following the classical papers [10, 11], one of the simplest choices for the potential energy-density is the following purely quadratic function of the deformation measures[12]:

$$\mathscr{W}_B = \frac{1}{2}\lambda\,\varepsilon_{\mathrm{hh}}\varepsilon_{\mathrm{kk}} + \mu\,\varepsilon_{\mathrm{ij}}\varepsilon_{\mathrm{ij}} + \frac{1}{2}K_1\zeta^2 + \frac{1}{2}K_2\zeta_{,\mathrm{i}}\zeta_{,\mathrm{i}} - K_3\,\zeta\,\varepsilon_{\mathrm{ii}}, \tag{7.4}$$

where λ and μ are the Lamé parameters and the coupling between the two sets of state variables is given by the mixed term $K_3\,\zeta\,\varepsilon_{\mathrm{ii}}$. Note that the potential energy density in Eq. (7.4) depends upon the first gradient of the internal variable representing the

porosity. Resulting from this, relying on a variational framework, we are able to encode into the model external actions on pores at the boundary, e.g. fluid pressure, by means of Dirichlet boundary conditions and/or their dual contributions. We postulate the following dependencies for the Lamé parameters:

$$\lambda = \frac{\nu\, Y(\rho_{\mathrm{b}}^*, \rho_{\mathrm{m}}^*)}{(1+\nu)(1-2\nu)}, \qquad \mu = \frac{Y(\rho_{\mathrm{b}}^*, \rho_{\mathrm{m}}^*)}{2(1+\nu)}, \tag{7.5}$$

and we assume the Young's modulus of the mixture to be given by

$$Y = Y_{\mathrm{b}}^{\mathrm{Max}}\big(\rho_{\mathrm{b}}^*/\hat{\rho}_{\mathrm{b}}\big)^2 + Y_{\mathrm{m}}^{\mathrm{Max}}\big(\rho_{\mathrm{m}}^*/\hat{\rho}_{\mathrm{m}}\big)^2, \tag{7.6}$$

$Y_{\mathrm{b}}^{\mathrm{Max}}$ and $Y_{\mathrm{m}}^{\mathrm{Max}}$ being the maximal elastic moduli of bone tissue and of the resorbable material, respectively. In a first analysis, it is reasonable to assume Poisson's ratio ν to be not dependent upon the volume fractions of mixture constituents in the reference configuration. We relate the coefficient K_1, which is a measure of the compressibility of bone marrow inside the pores, with the stiffness of marrow K_{f} and with the bulk modulus of the drained porous matrix $K_{\mathrm{dr}} = Y/(3(1-2\nu))$. Thus, we assume that

$$K_1 = \left(\frac{\phi^*}{K_{\mathrm{f}}} + \frac{(\alpha_B - \phi^*)(1-\alpha_B)}{K_{\mathrm{dr}}}\right)^{-1}, \tag{7.7}$$

where α_B is the Biot–Willis coefficient. The parameter K_2 is a stiffness related to the gradient of porosity and, hence, to interaction phenomena among neighboring pores. With regard to the stiffness related to the contribution coupling the microstructure and the solid bulk, we assumed that

$$K_3 = \sqrt{\hat{g}(\phi^*)\,\lambda\, K_1}, \quad \hat{g}(\phi^*) \in [0,1), \tag{7.8}$$

where the weight

$$\hat{g}(\phi^*) = \frac{A_0}{\pi}\left\{\mathrm{atan}\left[s_0\left(\phi^* - \frac{1}{2}\right)\right] + \mathrm{atan}\left(\frac{s_0}{2}\right)\right\} \tag{7.9}$$

is a monotonically increasing function depending on the reference porosity which modulates the micro–macro coupling. The choice of (7.8) is motivated by a well-known result in consolidation theory. It is indeed possible to prove that [13], unlike the second Lamé parameter, the effective first Lamé parameter λ_{eq} of the porous medium is affected by the porosity and is expressed as

$$\lambda_{\mathrm{eq}} = \left[\lambda - \frac{(K_3)^2}{K_1}\right] = \lambda - \lambda_v. \tag{7.10}$$

Indeed, thermodynamics rules that the effective first Lamé parameter must be less than the one related to the homogeneous material and, thus, it is possible to express it as in Eq. (7.8).

In order to handle dissipation inside the body, we adopt a Rayleigh–Hamilton generalized virtual work principle and, accordingly, we introduce the following dissipation functions aimed at describing the main different phenomena occurring. Solid-fluid

friction is to be modelled by means of a dissipation function including so-called Darcy's and Brinkman's contributions [14]:

$$2\mathcal{D}_{DB}(\dot{\boldsymbol{w}}, \nabla\dot{\boldsymbol{w}}) = K_D\dot{\boldsymbol{w}}\cdot\dot{\boldsymbol{w}} + \mathbb{K}_B\nabla\dot{\boldsymbol{w}} : \nabla\dot{\boldsymbol{w}}, \tag{7.11}$$

with $\boldsymbol{w} = \phi(\boldsymbol{U} - \boldsymbol{u})$ being $\boldsymbol{U}$ the average fluid displacement, i.e. the volume flow vector of the fluid relative to the solid, K_D and $\mathbb{K}_B$ are, respectively, the Darcy second order and the Brinkman fourth order permeability tensors. For the particular case of an isotropic medium, these two tensors are reduced to two positive scalar constants. Specifically, the vector $\boldsymbol{w}$ is assumed to be the gradient of a scalar function ξ and, therefore, it is given by the mass balance for nonhomogeneous porosity as follows:

$$\zeta = -\nabla\cdot\boldsymbol{w} = -\nabla\cdot(\nabla\xi). \tag{7.12}$$

We assume the following Neumann boundary condition,

$$\boldsymbol{w}\cdot\boldsymbol{n} = a(\boldsymbol{X}, t) \quad \text{ on } \partial\mathcal{B}, \tag{7.13}$$

where $\boldsymbol{n}$ denotes the unit normal vector to the boundary $\partial\mathcal{B}$ and, therefore, a is the normal component of $\boldsymbol{w}$ prescribed on the same boundary. In addition, a Rayleigh dissipation function related to the solid-matrix macroscopic strain rate is given by

$$2\mathcal{D}_s(\dot{\varepsilon}_{\mathrm{ij}}) = 2\mu^v\left(\dot{\varepsilon}_{\mathrm{ij}}\dot{\varepsilon}_{\mathrm{ij}} - \frac{1}{3}\dot{\varepsilon}_{\mathrm{ii}}\dot{\varepsilon}_{\mathrm{jj}}\right) + \kappa^v\,\dot{\varepsilon}_{\mathrm{ii}}\dot{\varepsilon}_{\mathrm{jj}}, \tag{7.14}$$

with κ^v and μ^v being the bulk and shear viscosity coefficients, respectively. Moreover, the dissipative potential related to the micro-deformation ζ can be introduced as

$$2\mathcal{D}_\zeta(\dot{\zeta}) = K_\zeta\dot{\zeta}^2, \tag{7.15}$$

where K_ζ is a positive damping coefficient. The extended Rayleigh–Hamilton principle of virtual work, including dissipation effects and neglecting inertia terms, states that, for arbitrary variations δu_{i} and $\delta\zeta$

$$-\int_{\mathcal{B}}\delta\mathscr{W}_B + \int_{\mathcal{B}}\delta\mathscr{W}^{\mathrm{ext}} = \int_{\mathcal{B}}\left(\frac{\partial\mathcal{D}_s}{\partial\dot{\varepsilon}_{\mathrm{ij}}}\delta\varepsilon_{\mathrm{ij}} + \frac{\partial\mathcal{D}_\zeta}{\partial\dot{\zeta}}\delta\zeta + \frac{\partial\mathcal{D}_{DB}}{\partial\dot{\xi}_{,\mathrm{k}}}\delta\xi_{,\mathrm{k}} + \frac{\partial\mathcal{D}_{DB}}{\partial\dot{\xi}_{,\mathrm{ki}}}\delta\xi_{,\mathrm{ki}}\right), \tag{7.16}$$

where $\delta\mathscr{W}^{\mathrm{ext}}$ is the first variation of the work done by external actions on kinematically admissible variations, i.e.,

$$\delta\mathscr{W}^{\mathrm{ext}} = \int_{\partial_\tau\mathcal{B}}\tau_{\mathrm{i}}\delta u_{\mathrm{i}}\mathrm{d}\mathcal{S} + \int_{\partial\mathcal{B}}Z\,\delta\zeta\mathrm{d}\mathcal{S}, \tag{7.17}$$

where τ_{i} is the surface traction on the boundary, and Z is a microstructural action which describes the local dilational behaviour of a porous material induced by pore opening and capillary interaction phenomena among neighbouring pores.

We now turn to the presentation of another approach to bone remodelling within the variational setting employed in this chapter [15–18]. We consider a Cosserat continuum, which, in the words of the notable mechanician R. D. Mindlin is characterized by the property that: *At each point of a Cosserat continuum there is a micro-structure which*

can rotate with respect to the surrounding medium [19]. This entails that a Cosserat continuum possesses an augmented kinematics as, in addition to the standard placement function of each material point of the body, it is endowed with a micro-rotation described by a skew-symmetric tensor. As we are considering a material which shows a phenomenology strongly related to its porosity, another kinematic parameter, the porosity, must be added as before. In the elastic case, the potential energy density is expressed as a quadratic function of the strain measures. In the framework of the small strain hypothesis, we define the coupling strain measure γ_{ij} as follows:

$$\gamma_{ij}(\mathbf{X}, t) = u_{[j,i]} - \psi_{ij}, \tag{7.18}$$

with ψ_{ij} being the skew-symmetric micro-structure rotation tensor and $u_{[j,i]}$ the linearized macro-rotation in the polar decomposition of the deformation gradient

$$u_{[j,i]} = \frac{1}{2}\left(u_{j,i} - u_{i,j}\right). \tag{7.19}$$

We now introduce the micro-rotation gradient

$$\kappa_{i[jk]}(\mathbf{X}, t) = \psi_{jk,i}. \tag{7.20}$$

Hence, the potential energy-density reads as

$$\begin{aligned}\mathscr{W}_C = &\frac{1}{2}\lambda\,\varepsilon_{hh}\varepsilon_{kk} + \mu\,\varepsilon_{ij}\varepsilon_{ij} + \beta\gamma_{ij}\gamma_{ij} + \alpha_1\,\kappa_{i[ik]}\kappa_{j[kj]} + \alpha_2\,\kappa_{i[jk]}\kappa_{i[jk]} + \alpha_3\,\kappa_{i[jk]}\kappa_{j[ki]} \\ &+ \frac{1}{2}K_1\zeta^2 + \frac{1}{2}K_2\zeta_{,i}\zeta_{,i} - K_3\,\zeta\,\varepsilon_{ii},\end{aligned} \tag{7.21}$$

while the dissipation energy function is assumed to be the same as that in Eqs. (7.11), (7.14) and (7.15). The external virtual work is given by:

$$\delta\mathscr{W}^{\text{ext}} = \int_{\partial_\tau\mathcal{B}} \tau_i\delta u_i \mathrm{d}\mathcal{S} + \int_{\partial_\tau\mathcal{B}} \Psi_{jk}\delta\psi_{jk}\mathrm{d}\mathcal{S} + \int_{\partial\mathcal{B}} Z\,\delta\zeta\mathrm{d}\mathcal{S}. \tag{7.22}$$

We notice that Ψ_{jk} in the second term of Eq. (7.22) can be interpreted as a micro-couple. The extended Rayleigh–Hamilton principle of virtual work in this case is also given by Eq. (7.16).

As we mentioned before, it is well-understood that, at a certain length scale ($\sim 200\ \mu$m), bone tissue can be schematized as a three-dimensional porous network of interconnected trabeculae (cancellous bone). It is for this reason that, previously, we dealt with the modelling of bone tissue by endowing nodes of such a network with rotational degrees of freedom by using Cosserat theory. Nevertheless, it is possible to look at bone tissue at the same length scale as a quasi-periodic system of cylindroid structures, i.e. osteons (cortical bone), characterized by a marked contrast in mechanical properties between bending and extension. On the basis of this observation and noting that local bending in micro-structured materials can be modelled macroscopically by means of strain gradient theories [20, 91–93, 97], it is possible to model bone tissue mechanics by complementing the classical framework of poromechanics [10] and [11] by means of the theory of the second gradient continua developed by [21] and [22]). In the simplest case a potential energy-density (potential energy per unit of macro-volume)

which is homogeneous, quadratic in the variables ε, $\nabla\varepsilon$, ζ and $\nabla\zeta$ [20, 23, 24] can be written as

$$\begin{aligned}\mathscr{W}_{II} = &\frac{1}{2}\lambda\,\varepsilon_{\mathrm{ii}}\varepsilon_{\mathrm{jj}} + \mu\,\varepsilon_{\mathrm{ij}}\varepsilon_{\mathrm{ij}} \\ &+ 4\,\alpha_1\varepsilon_{\mathrm{ii,j}}\varepsilon_{\mathrm{jk,k}} + \alpha_2\varepsilon_{\mathrm{ii,j}}\varepsilon_{\mathrm{kk,j}} + 4\,\alpha_3\varepsilon_{\mathrm{ij,i}}\varepsilon_{\mathrm{kj,k}} + 2\,\alpha_4\varepsilon_{\mathrm{ij,k}}\varepsilon_{\mathrm{ij,k}} + 4\,\alpha_5\varepsilon_{\mathrm{ij,k}}\varepsilon_{\mathrm{ik,j}} \\ &+ \frac{1}{2}K_1\zeta^2 + \frac{1}{2}K_2\zeta_{,\mathrm{i}}\zeta_{,\mathrm{i}} - K_3\,\zeta\,\varepsilon_{\mathrm{ii}}.\end{aligned} \tag{7.23}$$

The second gradient stiffness coefficients are assumed to be:

$$\begin{aligned}&\alpha_1 = \alpha_2 = \alpha_4 = Y(\rho_{\mathrm{b}}^*, \rho_{\mathrm{m}}^*)\ell^2,\ \alpha_3 = 2\,Y(\rho_{\mathrm{b}}^*, \rho_{\mathrm{m}}^*)\ell^2, \\ &\alpha_5 = 1/2\,Y(\rho_{\mathrm{b}}^*, \rho_{\mathrm{m}}^*)\ell^2,\end{aligned} \tag{7.24}$$

where ℓ is a suitable scale length of the microstructure, which is related to the diameter of trabeculae or osteons.

In this framework, the virtual external work is given by

$$\delta\mathscr{W}^{\mathrm{ext}} = \int_{\partial_\tau\mathcal{B}} \tau_{\mathrm{i}}\delta u_{\mathrm{i}}\mathrm{d}\mathcal{S} + \int_{\partial_\tau\mathcal{B}} T_\alpha\delta u_{\alpha,\mathrm{j}}n_{\mathrm{j}}\mathrm{d}\mathcal{S} + \int_{\partial\mathcal{B}} Z\,\delta\zeta\mathrm{d}\mathcal{S}, \tag{7.25}$$

where T_α is the external double force field which is acting on the boundary of the body.

At the interface between two jointed regions, for all the models we have considered so far, the following extra boundary terms are added to the energy density (7.23):

$$\mathscr{E}_{\mathrm{int}} = \frac{1}{2}K_\zeta\,[\![\zeta]\!]^2 + \frac{1}{2}K_u\,[\![\boldsymbol{u}]\!]\cdot[\![\boldsymbol{u}]\!], \tag{7.26}$$

where K_ζ and K_u, respectively, define elastic interactions due to the jump in the fields of ζ and $\boldsymbol{u}$ for the two different jointed regions. The symbol $[\![\cdot]\!]$ stands for the jump of any field $f(\boldsymbol{X})$ through the interface, i.e. $[\![f]\!] = (f^+ - f^-)$.

The evolution of the apparent mass densities is given by the distributed system of ordinary differential equations [13, 25]:

$$\begin{cases}\dot{\rho}_{\mathrm{b}}^* = A_{\mathrm{b}}\,(S)\ H\,(\phi) & \text{with } 0 < \rho_{\mathrm{b}}^* \leqslant \hat{\rho}_{\mathrm{b}} \\ \dot{\rho}_{\mathrm{m}}^* = A_{\mathrm{m}}\,(S)\ H\,(\phi) & \text{with } 0 < \rho_{\mathrm{m}}^* \leqslant \rho_{\mathrm{m}}^*(\boldsymbol{X}, 0).\end{cases} \tag{7.27}$$

We note that the right-hand side of (7.27) depends upon the mechanical stimulus S resulting from an external applied load and the current porosity ϕ, while the functions A_{b} and A_{m} are taken to be

$$A_{\{\mathrm{b,m}\}}\,(S) = \begin{cases} s_{\{\mathrm{b,m}\}}S & \text{for } S \geq 0 \\ r_{\{\mathrm{b,m}\}}S & \text{for } S < 0,\end{cases} \tag{7.28}$$

with different constant rates for synthesis (s_{b} and $s_{\mathrm{m}} = 0$) and for resorption (r_{b} and r_{m}). The weight function H modulates the efficiency of the remodelling process in accordance with experimental evidence, which suggests considering a $\cap$-like shape for H, which attains its maximum in a neighbourhood of $\phi = 0.5$. In the definition of the stimulus, the presence of a lazy zone, bounded by two thresholds ($P_{\mathrm{ref}}^{\mathrm{s}}$ and $P_{\mathrm{ref}}^{\mathrm{r}}$ for

synthesis and for resorption, respectively), is taken into account, as in the lazy zone the osteoregulatory balance of the bone is kept. Algebraically, we have

$$S(\boldsymbol{X},t)=\begin{cases}P(\boldsymbol{X},t)-P^{\mathrm{s}}_{\mathrm{ref}} & \text{for } P(\boldsymbol{X},t)>P^{\mathrm{s}}_{\mathrm{ref}}\\ 0 & \text{for } P^{\mathrm{r}}_{\mathrm{ref}}\leqslant P(\boldsymbol{X},t)\leqslant P^{\mathrm{s}}_{\mathrm{ref}}\\ P(\boldsymbol{X},t)-P^{\mathrm{r}}_{\mathrm{ref}} & \text{for } P(\boldsymbol{X},t)<P^{\mathrm{r}}_{\mathrm{ref}},\end{cases} \tag{7.29}$$

where the signal P is related to the sensor cells activity, assumed to be transmitted instantaneously and to be expressed by means of the following convolution integral [12]:

$$P\,(\boldsymbol{X},t)=\frac{\int_{\mathcal{B}}\left(a\;\mathscr{E}_s(\boldsymbol{X}_0)\;+b\;\mathcal{D}_s(\boldsymbol{X}_0)\right)\varpi\left(\rho^*_{\mathrm{b}}(\boldsymbol{X}_0)\right)\;e^{-\frac{\|\boldsymbol{X}-\boldsymbol{X}_0\|^2}{2D^2}}\,\mathrm{d}\boldsymbol{X}_0}{\int_{\mathcal{B}}e^{-\frac{\|\boldsymbol{X}-\boldsymbol{X}_0\|^2}{2D^2}}\,\mathrm{d}\boldsymbol{X}_0} \tag{7.30}$$

characterized by a reference length D, which is a cut-off of the range of influence of the biological processes. The quantity $\mathscr{E}_s$ is the density of strain energy of the solid matrix and ϖ is the density of active sensor cells (osteocytes), which are assumed to be present only in living bone tissue. The functional dependence of ϖ upon ρ^*_{b} is assumed to be:

$$\varpi\left(\rho^*_{\mathrm{b}}\right)=\eta\tanh(\xi\,\rho^*_{\mathrm{b}})\quad 0<\eta\leqslant 1, \tag{7.31}$$

where the hyperbolic tangent function is used to consider saturation of the living bone matrix. Note that the quantity ϖ can be interpreted, in the framework of feedback control theory [26, 27], as a gain for the actual mechanical stimulus, i.e. 'the actuating signal', that takes the real activities of the osteocytes into account [28]. For a similar approach in modelling the stimulus see e.g. [29, 30]. The remodelling process can change dramatically depending on the mechanical properties of the microstructure of the bone tissue and of the artificial graft. Indeed, considering the very simple case sketched in Fig. 7.1 and using the extended Rayleigh–Hamilton principle of virtual work involving the constitutive Eq. (7.23) combined with the evolutionary rules (7.27), it is clear from Fig. 7.2 how the characteristic length ℓ affects the time evolution and consequently the final distribution of both the mass density of bone and of bio-material [31]. We also note that, when ℓ is zero, the second gradient model used turns out to be a Biot's model, which can be considered, roughly speaking, as a sort of reference model. All the models that we have considered so far can describe a particular behaviour in the remodelling process of bone tissue, possibly reconstructed with an implant made up of bio-resorbable material. Therefore, the wise judgment of the researcher should always guide their choice case by case, depending on the particular architecture and geometry of the microstructure. For example, if the thickness of the trabeculae is too large with respect to their length, the elastic energy stored in their bending deformation is negligible and, hence, a Biot's model is suitable for a proper description. On the other hand, if the slenderness ratio of the trabeculae is high, the amount of elastic energy needed for their bending is significant and, for this reason, a second gradient model should be employed. Moreover, if the nodes in which trabeculae connect are very thick, they can be considered in a first approximation as rigid objects surrounded by a medium which can store elastic energy. In this last case, a Cosserat's model could be more appropriate.

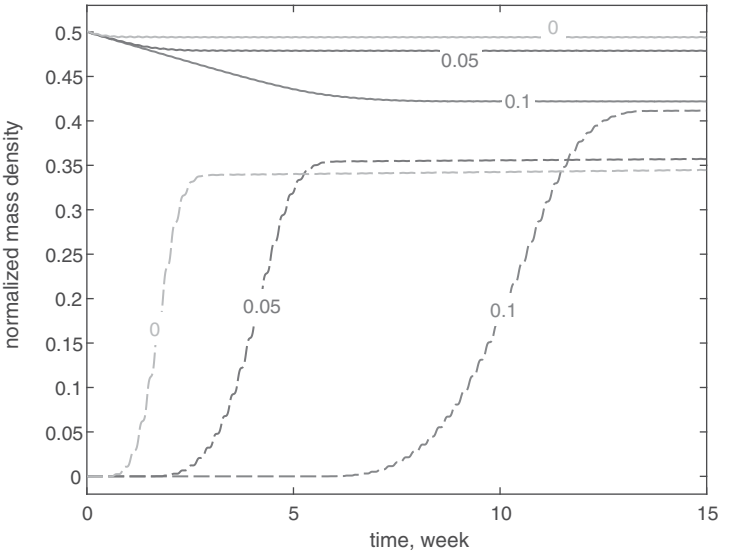

Figure 7.2 History of the mass densities of bone tissue (dashed line) and bio-resorbable material (solid line) in the probe point P_m for different values of the characteristic length ℓ normalized with respect to the length of the sample, i.e. $\ell = 0, 0.05, 0.1$.

7.3 Applications in Materials Science

The variational approach proved to be useful also in improving the damping performance of materials with penny-shaped cracks, like concrete (with or without additives [32, 33]). Here, we present a modelling approach which is aimed at describing the mechanism of internal dissipation associated with Coulomb friction in brittle materials, which are naturally characterized by a network of micro-cracks. Other dissipation mechanisms, as might be expected, can be approached with a variational framework, and for the sake of completeness, we mention here [34, 35, 94–96, 98] to cover visco-plastic models. As a Coulomb friction approach, similarly to the others presented in this chapter, is based on continuum mechanics, kinematic descriptors representing the displacement of a REV are considered. We now address the description of microstructural properties of such materials. When no relevant damage phenomena occur at the macroscopic level, and the statistical distribution of micro-crack orientation in a REV can be satisfactorily considered to be uniform, the effect of such micro-cracks can be accounted for effectively by introducing the micro-kinematical variable φ, which stands, roughly speaking, for an average sliding (relative) displacement between the opposite faces of the micro-cracks coming into contact [36, 37]. Note that, for isotropy reasons, the variable φ is a scalar quantity. As the kinematic variables have been defined, we now turn to the definition of the volume strain energy density Ψ. It is postulated to have the following form:

$$\Psi(\boldsymbol{E},\varphi) = \frac{1}{2}\left(2\mu\,\boldsymbol{E}\cdot\boldsymbol{E} + \lambda\,(\mathrm{tr}\,\boldsymbol{E})^2\right) + \frac{1}{2}\alpha\left(\sqrt{I_2^{(d)}} - \varphi\right)^2 + \frac{1}{2}k_1\varphi^2 + \frac{1}{3}k_2\varphi^3 + \frac{1}{4}k_3\varphi^4, \tag{7.32}$$

where λ and μ are the Lamé parameters for linearly elastic isotropic materials, $\boldsymbol{E}$ is the small strain tensor and the scalar $I_2^{(d)}$ is the second invariant of the deviatoric strain tensor $\mathrm{dev}\,\boldsymbol{E} = \boldsymbol{E} - \frac{1}{3}\mathrm{tr}\,\boldsymbol{E}\,\mathbb{1}$, defined as $I_2^{(d)} = \frac{1}{2}\,\mathrm{tr}\,(\mathrm{dev}\,\boldsymbol{E}\;\mathrm{dev}\boldsymbol{E})$. The dependence in (7.32) of the volume strain energy density upon the micro-kinematic parameter φ has been assumed to be non-quadratic [38]. This choice can be justified on the basis of experimental evidence. The kinetic energy density is defined by

$$\mathcal{K} = \frac{1}{2}\,\rho\,\dot{\boldsymbol{u}}^2 + \frac{1}{2}\,\rho_\varphi\,\dot{\varphi}^2, \tag{7.33}$$

where ρ is the mass density of bulk material and ρ_φ is an effective macroscopic mass density linked to the microstructural variable φ. In this context, a Rayleigh potential $\mathcal{R}$, aimed at describing a regularized Coulomb-type friction dissipation is introduced as follows:

$$\mathcal{R} = \zeta\,\mathrm{tr}\boldsymbol{E}\,\frac{1}{\eta}\,\ln(\cosh(\,\eta\,\dot{\varphi}\,)), \tag{7.34}$$

where ζ and η are constitutive constants. The virtual work due to internal dissipation is

$$\delta W^{(\mathrm{Dis})}(\boldsymbol{E},\varphi,\dot{\varphi}) = \int_0^T\int_V\left(\frac{\partial\mathcal{R}}{\partial\dot{\varphi}}\,\delta\varphi\right)\mathrm{d}V = \int_0^T\int_V \zeta\,\mathrm{tr}\,\boldsymbol{E}\,\tanh(\,\eta\,\dot{\varphi}\,)\,\delta\varphi\,\mathrm{d}V,$$

where $[0,T]$ is the time interval considered. It is worth noting that the term $\zeta\,\mathrm{tr}\,\boldsymbol{E}\,\tanh(\,\eta\,\dot{\varphi}\,)$ can be interpreted as an internal friction force density, which is proportional to the normal contact action σ_n. Hence, we can express $\zeta\,\mathrm{tr}\,\boldsymbol{E}$ as $\varpi\mu_k\sigma_n$, assuming $\zeta = \varpi\mu_k K$. Indeed, σ_n can be evaluated as $K\,\mathrm{tr}\,\boldsymbol{E}$, where K is the bulk modulus, μ_k the friction coefficient and ϖ the surface area of microcracks per unit volume of concrete. The function $\tanh(\cdot)$, instead of the usual sign function, is introduced to smooth the term at low velocity range. The parameter η, being the slope of the hyperbolic tangent at zero, can be used to modulate the extension of the smoothed zone. The weak form equation governing the evolution of the system is the following:

$$-\int_0^T\int_V \delta\Psi\,\mathrm{d}V + \int_0^T\int_V \delta\mathcal{K}\,\mathrm{d}V + \int_0^T\int_S \boldsymbol{\tau}^{\mathrm{ext}}\cdot\delta\boldsymbol{u}\,\mathrm{d}S = \delta W^{(\mathrm{Dis})}, \tag{7.35}$$

where $\boldsymbol{\tau}^{\mathrm{ext}}$ are the externally applied forces per unit area. Note that there is a good agreement between the results of experimental tests and those of numerical simulations. This is clear when, for instance, a dissipation loop obtained with a cyclic external load at a frequency of 1 Hz is considered for the experimental setup (see [39] and Figs. 7.3 and 7.4). Note that the composition of concrete strongly affects its dissipative behaviour. Indeed, after a suitable optimisation of the additives (shape, quantity and mechanical properties), the area of the region included within the loops in Figs. 7.3 and 7.4 related to the enriched concrete samples approximately doubles with respect to the corresponding area of that for standard concrete.

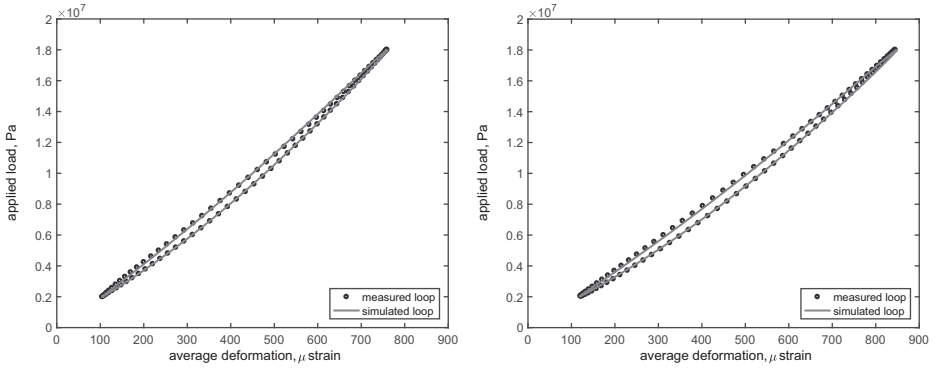

Figure 7.3 Dissipation loops for M32 grade concrete: standard (left); enriched (right).

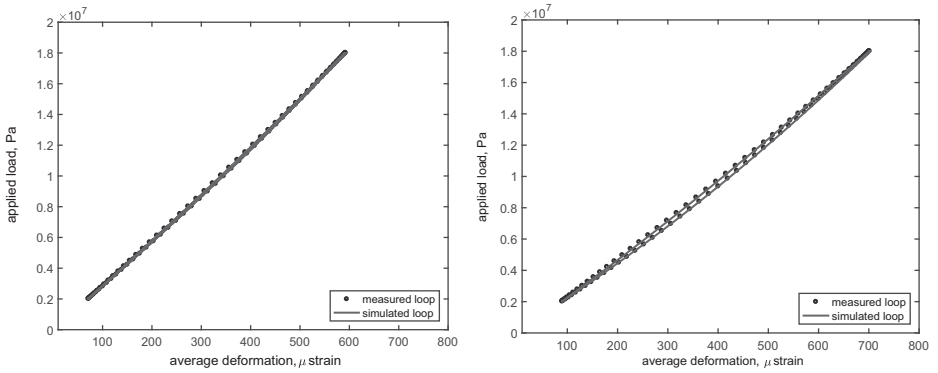

Figure 7.4 Dissipation loops for M52 grade concrete: standard (left); enriched (right).

7.4 Applications in Vibration Damping

In many engineering applications, the employment of increasingly thin structures has given rise to several issues regarding vibration and noise emission. Therefore, a critical problem has emerged, which is the design of mechanical systems endowed with an efficient means of controlling structural vibrations, in order to ensure reliability, by reducing fatigue loads, crack propagation and damage. In this context, the use of piezoelectric transducers appears to be an attractive opportunity. Indeed, many 'smart' devices (or materials) incorporating these special materials as sensing and actuating mechanisms are being studied in literature. For example, the use of piezoelectric materials has expanded greatly in the field of structural control and health monitoring (on this topic the literature is huge, see, e.g. [40–42] for an overview, [43–46, 82, 90] for some applications on beams, [47–50] on plates, [51–54] for some aspects of modelling). This is primarily due to the desirable piezoelectric properties, but also to the growing availability of more efficient piezoelectric ceramics.

Mechanical thin structures such as beams or shells equipped with piezoelectric transducers can be regarded as *metamaterials* [55] whose configuration is described by a displacement field and an additional kinematic variable, which is usually an electric quantity, like charge or voltage. Generally, a metamaterial can be conceived as a material designed in order to exhibit some tailored exotic features. To this end, it is characterized by a microstructure or other features – here the piezoelectric elements – which determine a non-standard behaviour. In other words, such materials can be described by means of generalized continua. The basic working principle of materials fitted with piezoelectric transducers is very simple. Indeed, the piezoelectric transducers transform mechanical into electrical energy, which is then conveyed to an electric device, whose properties are designed to attain a desired behaviour. For instance, the system could be designed to have as its main purpose the reduction of vibration or noise emission at the maximum possible rate (see e.g. [56–59]).

Here, we consider a beam with a rectangular cross-section of height h and width b, and having length L. Let $\mathcal{C}^*$ be the reference configuration of a piezoelectric beam, a reference frame (O, x_1, x_2) is chosen so that $\mathcal{C}^*$ is coincident with the segment x_1, such that $0 \leqslant x_1 \leqslant L$ and the origin O is at the centre of the cross-section. Repetitions of pairs of piezoelectric patches are arranged such that two piezoelectric elements belonging to the same pair are bonded on the beam to implement the proposed control technique. For the sake of simplicity, we locate only one pair of piezoelectric patches of width b – the same as the beam – and thickness h_p between the endpoints $x_{1,i}$ and $x_{1,f}$. This pair of piezoelectric transducers is made up of two identical thin slices glued symmetrically onto two opposite faces, i.e. upper and lower (see Fig. 7.8), of the host beam and connected in parallel; they are bonded with inverted polarisation directions, in order to produce opposite elongation and, thus, to induce pure bending deformations.

In this way, the actual configuration can be described, from a mechanical point of view, by the transverse displacement $v(x_1, t)$, while the descriptor for the electric behaviour is the electric field vector $\boldsymbol{E}$. Hence, following the approach of [60], to describe the piezoelectric beam we assume the Lagrangian function per unit length to be [61, 62]

$$\mathscr{L} = \frac{1}{2}\rho \dot{v}^2 - \mathscr{H}(S_{ij},\, E_i), \tag{7.36}$$

where $\mathscr{H}$ is the electric enthalpy density [63], which depends on the small strain tensor S_{ij} and the electric field E_i. In particular, it can be expressed as

$$\mathscr{H}(S_{11},\, E_2) = \frac{1}{2}k_m^E S_{11}^2 - k_{me} S_{11} E_2 - \frac{1}{2}k_e^S E_2^2. \tag{7.37}$$

The constitutive parameters in (7.37) are

$$k_m^E = Y_p^E, \qquad k_{me} = Y_p^E d_{21}, \qquad k_e^S = \epsilon_2^S = \epsilon_2^T - Y_p^E d_{21}^2, \tag{7.38}$$

where Y_p^E is the Young's modulus of the piezoelectric material under short circuit condition (refer to the superscript E), d_{21} the piezoelectric constant with polarisation along

the x_2-direction and ϵ_2^S the dielectric constant for the null deformation. Furthermore, the parameter ϵ_2^T is the dielectric constant under free stress conditions (refer to the superscript T). It is possible to consider more refined models; for instance, one can consider the piezoelectric material to exhibit anisotropic behaviour [64, 65], non-linear effects due to hysteresis or memory effects [66–68]. The constitutive relations for the only significant components of the stress tensor $\boldsymbol{T}$ and the electric displacement vector $\boldsymbol{D}$, from Eq. (7.37), are given by

$$T_{11} = \frac{\partial \mathscr{H}}{\partial S_{11}} = k_m^E S_{11} - k_{me} E_2, \tag{7.39}$$

$$D_2 = -\frac{\partial \mathscr{H}}{\partial E_2} = k_{me} S_{11} + k_e^S E_2, \tag{7.40}$$

In the framework of the linear theory of piezoelectricity, considering linear elastic deformations and the quasi-static electric field approximation, we have

$$S_{11} = -x_2 v'', \qquad E_2 = -\phi_{,2}, \tag{7.41}$$

where ϕ is the electric potential. By substituting these assumptions (7.41) in Eq. (7.36), the Lagrangian $\mathcal{L}$ can be computed as

$$\begin{aligned}\mathcal{L}(v,\,\phi) = {} & b\int_0^L \int_{-\frac{h}{2}}^{\frac{h}{2}} \frac{1}{2}\rho_b \dot{v}^2 \mathrm{d}x_1 \mathrm{d}x_2 + 2b \int_{x_{1,i}}^{x_{1,f}} \int_{\frac{h}{2}}^{\frac{h}{2}+h_p} \frac{1}{2}\rho_p \dot{v}^2 \mathrm{d}x_1 \mathrm{d}x_2 \\ & - b\int_0^L \int_{-\frac{h}{2}}^{\frac{h}{2}} \frac{1}{2} Y_b \left(x_2 v''\right)^2 \mathrm{d}x_1 \mathrm{d}x_2 - 2b \int_{x_{1,i}}^{x_{1,f}} \int_{\frac{h}{2}}^{\frac{h}{2}+h_p} \frac{1}{2} k_m^E \left(x_2 v''\right)^2 \mathrm{d}x_1 \mathrm{d}x_2 \\ & + 2b \int_{x_{1,i}}^{x_{1,f}} \int_{\frac{h}{2}}^{\frac{h}{2}+h_p} \left[k_{me} x_2 \phi_{,2} v'' + \frac{1}{2} k_e^S \left(\phi_{,2}\right)^2\right] \mathrm{d}x_1 \mathrm{d}x_2. \end{aligned} \tag{7.42}$$

By computing the first variation of the last term of Eq. (7.42), we obtain the electrostatic equation for an insulator

$$\frac{\partial D_2}{\partial x_2} = -k_{me} v'' - k_e^S \frac{\partial^2 \phi}{\partial x_2^2} = 0, \tag{7.43}$$

and then, through a simple double integration, we obtain the electric potential

$$\phi(x_1, x_2) = -\frac{1}{2}\frac{k_{me}}{k_e^S} x_2^2 v'' + a_1 x_2 + a_0. \tag{7.44}$$

By imposing the electrode voltage V

$$\Delta\phi = \phi(x_1,\, h/2 + h_p) - \phi(x_1,\, h/2) = V, \tag{7.45}$$

we can evaluate the parameter a_1

$$a_1 = \frac{1}{2}\frac{k_{me}}{k_e^S}(h + h_p) v'' + \frac{V}{h_p}. \tag{7.46}$$

The electric field can then be expressed in terms of the displacement $v(x_1, t)$ and the electrode voltage $V(t)$ as

$$E_2 = \frac{k_{me}}{k_e^S} x_2 v'' - \frac{1}{2}\frac{k_{me}}{k_e^S}(h + h_p)v'' - \frac{V}{h_p}. \tag{7.47}$$

At this point, since the voltage is an easily measurable electric quantity, it is appropriate to use it as a state variable, and rearranging the terms of the Lagrangian (7.42), we can obtain an equivalent expression in terms of v and V:

$$\begin{aligned}\mathcal{L}(v,\, V) = &\int_0^L \frac{1}{2}\rho_{lb}\dot{v}^2 \mathrm{d}x_1 + \int_{x_{1,i}}^{x_{1,f}} \frac{1}{2}\rho_{lp}\dot{v}^2 \mathrm{d}x_1 \\ &- \int_0^L \frac{1}{2} K_{mb}\,(v'')^2 \mathrm{d}x_1 - \int_{x_{1,i}}^{x_{1,f}} \frac{1}{2} K_{mp}\,(v'')^2 \mathrm{d}x_1 \\ &- \int_{x_{1,i}}^{x_{1,f}} \left(-K_{me} v'' V - \frac{1}{2} K_e V^2\right) \mathrm{d}x_1,\end{aligned} \tag{7.48}$$

where the meaning of the parameters used is defined below. The linear mass density of the host beam ρ_{lb} and of the piezoelectric pair ρ_{lp} are

$$\rho_{lb} = b \int_{-\frac{h}{2}}^{\frac{h}{2}} \rho_b \mathrm{d}x_2, \qquad \rho_{lp} = 2b \int_{\frac{h}{2}}^{\frac{h}{2}+h_p} \rho_p \mathrm{d}x_2. \tag{7.49}$$

Analogously, the host beam stiffness K_{mb} and the piezoelectric stiffness K_{mp} are

$$K_{mb} = b \int_{-\frac{h}{2}}^{\frac{h}{2}} Y_b\, x_2^2 \mathrm{d}x_2 = Y_b\, \frac{bh^3}{12}, \tag{7.50}$$

$$\begin{aligned}K_{mp} &= 2b \int_{\frac{h}{2}}^{\frac{h}{2}+h_p} \left\{ k_m^E\, x_2^2 + \frac{k_{me}^2}{k_e^S}\left[x_2^2 - \frac{1}{2}\left(h + h_p\right) x_2\right] \right. \\ &\qquad \left. - \frac{1}{2}\frac{k_{me}^2}{k_e^S}\left[\frac{1}{4}\left(h + h_p - 2\,x_2\right)^2\right]\right\} \mathrm{d}x_2 \\ &= 2b\, k_m^E \left(\frac{h^2 h_p}{4} + \frac{h h_p^2}{2} + \frac{h_p^3}{3}\right) + b\frac{k_{me}^2}{k_e^S}\frac{h_p^3}{12}.\end{aligned} \tag{7.51}$$

The electro-mechanical coupling parameter K_{me} is

$$K_{me} = 2b \int_{\frac{h}{2}}^{\frac{h}{2}+h_p} \frac{k_{me}}{h_p}\, x_2 \mathrm{d}x_2 = b\, k_{me}\left(h + h_p\right). \tag{7.52}$$

Finally, the electric parameter K_e is

$$K_e = 2b \int_{\frac{h}{2}}^{\frac{h}{2}+h_p} \frac{k_e^S}{h_p^2}\, x_2 \mathrm{d}x_2 = 2b\, \frac{k_e^S}{h_p}. \tag{7.53}$$

By including the mechanical and electrical work done by, respectively, the linear force density f and the applied charge density q, and equating to zero the variation of the

introduced action, we obtain the governing equations of the piezoelectric system in terms of the mechanical and electrical degrees of freedom:

$$\int_{t_0}^{t_1} \delta\mathcal{L}\mathrm{d}t + \int_{t_0}^{t_1}\int_0^L f\delta v \,\mathrm{d}x_1\mathrm{d}t - \int_{t_0}^{t_1}\int_{x_{1,1}}^{x1,f} 2q\delta V \,\mathrm{d}x_1\mathrm{d}t = 0. \tag{7.54}$$

The governing equations of the piezoelectric composite beam can be deduced from Eq. (7.54) and (7.48):

$$\begin{cases} \rho_l \ddot{v}(x_1,t) + \left(K_m v''(x_1,t)\right)'' = \left[\delta'(x_1 - x_{1,i}) - \delta'(x_1 - x_{1,f})\right] K_{me} V(t) + f(x_1,t) \\ C_e V(t) + K_{me} v'(x_1,t)|_{x_{1,i}}^{x_{1,f}} = Q(t). \end{cases} \tag{7.55}$$

For the sake of conciseness, we introduce the total linear mass density

$$\rho_l = \rho_{lb} + \rho_{lp}\left[H(x_1 - x_{1,i}) - H(x_1 - x_{1,f})\right]$$

and the total stiffness

$$K_m = K_{mb} + K_{mp}\left[H(x_1 - x_{1,i}) - H(x_1 - x_{1,f})\right],$$

in which H is the Heaviside step function. The constant

$$C_e = 2\frac{k_e^S b}{h_p}\left(x_{1,f} - x_{1,i}\right) \tag{7.56}$$

is the whole capacitance and Q is the total applied charge. In Eq. (7.55) the mechanical action of the piezoelectric patches is represented by the derivative of the Dirac delta δ', since these transducers act on the beam with concentrated moments at the endpoints $x_{1,i}$ and $x_{1,f}$.

Recalling that the terminal voltage V is the time derivative of the flux linkage $\dot{\psi}$, in order to simplify the theoretical analysis, a generalized flux linkage χ and a normalised current ι are introduced,

$$\chi = \sqrt{C_e}\psi, \qquad \iota = \frac{i}{\sqrt{C_e}}. \tag{7.57}$$

Therefore, by differentiating the second equation of Eq. (7.55) with respect to time, and plugging it into the relations (7.57), we obtain

$$\begin{cases} \rho_l \ddot{v}(x_1,t) + \left(K_m v''(x_1,t)\right)'' - \left[\delta'(x_1 - x_{1,i}) - \delta'(x_1 - x_{1,f})\right]\gamma\dot{\chi}(t) = f(x_1,t) \\ \ddot{\chi}(t) + \gamma\, \dot{v}'(x_1,t)|_{x_{1,i}}^{x_{1,f}} = \iota(t), \end{cases} \tag{7.58}$$

where the coupling coefficient γ is equal to $K_{me}/\sqrt{C_e}$. The space discretisation of equations (7.58) is nowadays undertaken by means of finite element discretisation. In this regard, very recently an approach based on non-uniform rational B-splines (NURBS) has proved to be successful in the treatment of bending structural elements, see e.g. [69–73]. In order to derive the governing equations of the system considered in a form convenient for designing a control to suppress undesired vibration modes of the host

beam, the governing equations (7.58) have been expressed in the frequency domain by means of a modal analysis. Thus, the displacement v of the system is expanded as

$$v(x_1,t) = \sum_i W_i(x_1)\eta_i(t), \tag{7.59}$$

where $W_i(x_1)$ is the mode shape of the ith normal mode of the system, obtained by removing the excitation f, and under short circuit condition $\dot{\chi} = 0$. The coefficient $\eta_i(t)$ is the generalized coordinate describing the response of the ith normal mode. In order to make the decomposition unique, the mode shapes are normalised to a unitary value. Hence, the governing equations of the electro-mechanical beam can be expressed in the frequency domain as follows [74]:

$$\begin{cases} \ddot{\eta}_i(t) + \omega_i^2\eta_i(t) - \omega_i g_i \dot{\chi}(t) = f_i(t) \quad \text{with } i = 1,2,... \\ \ddot{\chi}(t) + \sum_i \omega_i g_i \dot{\eta}_i(t) = \iota(t), \end{cases} \tag{7.60}$$

where $f_i(t) = \int_0^L W_i(x_1)\, f(x_1,t)\mathrm{d}x_1$ represents the ith mode force. We define the unit-frequency normalised coupling coefficient g_i as

$$g_i = \gamma\ W_i'\big|_{x_{1,i}}^{x_{1,f}} /\omega_i. \tag{7.61}$$

Then, assuming low modal coupling and the mechanical load to have a frequency content in a range close to the jth mode frequency, we can simplify Eq. (7.60) by neglecting the effects of the other modes,

$$\begin{cases} \ddot{\eta}_j(t) + \omega_j^2\eta_j(t) - \omega_j g_h \dot{\chi}(t) = f_h(t) \\ \ddot{\chi}(t) + \omega_j g_h \dot{\eta}_j(t) = \iota(t). \end{cases} \tag{7.62}$$

The system (7.62) is characterized by a single mechanical degree of freedom with a single piezoelectric transducer having a unit inherent capacitance and a gyroscopic coupling [75]. In order to address the problem of vibration control of the mode of the beam under consideration with a single piezoelectric transducer, we can complete this system with an external shunt circuit consisting of an electrical impedance, or admittance. The key idea is to use the piezoelectric transducer as a device which allows exchange of the mechanical energy with the electric circuit. Indeed, as the base structure vibrates, the piezoelectric transducer will be subjected to a voltage, which, in turn, causes a flow of electric current through the shunted admittance. A strictly passive admittance involves a loss of vibration energy. Firstly, in [76] and in [77], a passive shunt circuit made up of a resistor and an inductor connected in series or in parallel, respectively, is proposed. It has been shown that with proper design of these components, an electrical damper can be obtained (see also [74, 78, 79]).

In the case of a shunt circuit with a resistor, r, and an inductor, ℓ, connected in parallel (see Fig. 7.5), the total admittance is associated with a normalised current given by

$$\iota(t) = -\frac{1}{r}\dot{\chi}(t) - \frac{1}{\ell}\chi(t). \tag{7.63}$$

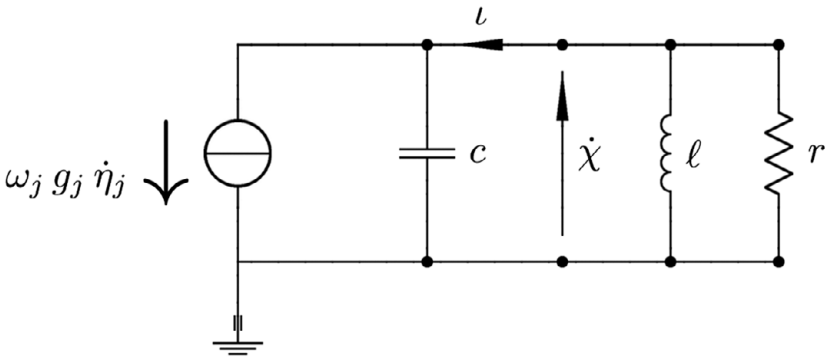

Figure 7.5 Equivalent circuit for a shunted circuit with a resistor and an inductor connected in parallel.

Introducing the notation

$$\frac{1}{\ell} = \varpi_j^2, \quad \frac{1}{r} = 2\,\varpi_j \zeta_j \quad \text{and} \quad \beta_j = \frac{\varpi_j}{\omega_j}, \tag{7.64}$$

the equations involving the control action of the shunt admittance can be written as follows:

$$\begin{cases} \ddot{\eta}_j(t) + \omega_j^2\, \eta_j(t) - \omega_j\, g_j\, \dot{\chi}\,(t) = f_j(t) \\ \ddot{\chi}\,(t) + 2\,\varpi_j \zeta_j \dot{\chi}(t) + \varpi_j^2 \chi(t) + \omega_j\, g_j\, \dot{\eta}_j(t) = 0. \end{cases} \tag{7.65}$$

The second equation of (7.65) can be interpreted as the electric subsystem constituted by the parallel of r, ℓ and the unit capacitance related to the piezoelectric patch, and whose eigenfrequency is ϖ_j, and loss factor is ζ_j. In order to set the optimal values of the external resistor and inductance, namely the natural circular frequency, ϖ_j, and the damping ratio, ζ_j, the fixed points method, developed in [80], can be employed (see Fig. 7.6),

$$\varpi_j^{\text{opt}} = \omega_j, \qquad \zeta_j^{\text{opt}} = \frac{\sqrt{6}}{4}\, g_j. \tag{7.66}$$

Up to now, the piezoelectric beam has been characterized by means of two Lagrangian descriptors: the displacement field and the voltage of each pair of piezoelectric patches. Nevertheless, as we mentioned before, in addition to the displacement variable, the system which we are considering can be characterized also in terms of charge. Thus, in that situation, the current configuration can be described, from a mechanical point of view, by the transverse displacement $v(x_1, t)$, while the descriptor for the electric behaviour is assumed to be the electric displacement $\boldsymbol{D}$. Hence, in order to describe the piezoelectric beam we assume the density of the Lagrangian function [81] to be as follows:

$$\mathscr{L} = \frac{1}{2}\rho \dot{v}^2 - \mathscr{U}(S_{ij},\, D_i), \tag{7.67}$$

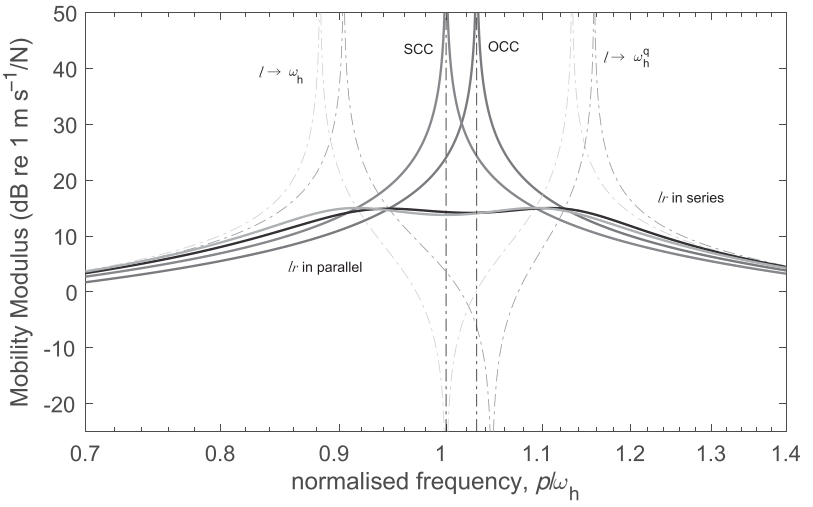

Figure 7.6 Mobility functions of a piezoelectric pair with a coupling coefficient, $g_h = 0.25$ on a beam for: i) an open circuit condition (OCC); ii) a shunted inductor tuned in the neighbourhood of the open circuit frequency ω_h^q ($\ell \to \omega_h^q$); iii) a short circuit condition (SCC); iv) a shunted inductor tuned around the short circuit frequency ω_h ($\ell \to \omega_h$); v) an optimal shunt circuit of a resistor and an inductor connected in series; vi) an optimal shunt circuit of a resistor and an inductor connected in parallel.

where $\mathscr{U}$ is the stored energy density [63], which depends on the small strain tensor S_{ij} and the electric displacement D_i. In particular, the stored energy density $\mathscr{U}$ can be expressed as

$$\mathscr{U}(S_{11},\, D_2) = \frac{1}{2}\tilde{k}_m^D\, S_{11}^2 - \tilde{k}_{me} S_{11} D_2 + \frac{1}{2}\tilde{k}_e^S D_2^2, \tag{7.68}$$

where only the significant components of S and $\boldsymbol{D}$ have been taken into account. The constitutive parameters appearing in Eq. (7.68) are defined as:

$$\tilde{k}_m^D = Y_p^D, \qquad \tilde{k}_{me} = h_{21} = Y_p^D\, g_{21}, \qquad \tilde{k}_e^S = \beta_{22}^S = \frac{1}{\epsilon_{22}^S}, \tag{7.69}$$

where Y_p^D is the Young's modulus in the x_1-direction (perpendicular to the direction in which the piezoelectric element is polarised) and under open circuit conditions (refer to the superscript D), h_{21} or g_{21} are piezoelectric constants with polarisation along the x_2-direction and ϵ_{22}^S is the dielectric constant for the null deformation. Equivalently, the parameters (7.69) can be expressed as follows

$$\tilde{k}_m^D = Y_p^E + \frac{\left(Y_p^E\, d_{21}\right)^2}{\epsilon_{22}^T - Y_p^E\, d_{21}^2}, \qquad \tilde{k}_{me} = \frac{Y_p^E\, d_{21}}{\epsilon_{22}^T - Y_p^E\, d_{21}^2}, \qquad \tilde{k}_e^S = \frac{1}{\epsilon_{22}^T - Y_p^E\, d_{21}^2}, \tag{7.70}$$

in terms of Y_p^E, i.e. the Young's modulus under short circuit conditions, the piezoelectric constant d_{21} and ϵ_{22}^T, namely the dielectric constant under free stress conditions. Note

that, as is clear from Eqs. (7.69) and (7.70), the Young's modulus with short circuited electrodes is lower than the Young's modulus with the open circuited electrodes. By means of some simple thermodynamical arguments it is possible to show that the following relation between the enthalpy $\mathscr{H}$ and the stored energy $\mathscr{U}$ holds:

$$\mathscr{U}(S_{11},\, D_2) = \mathscr{H}(S_{11},\, E_2(D_2)) + E_2 D_2. \tag{7.71}$$

The constitutive relations for the only significant components of the stress tensor $\boldsymbol{T}$ and the electric field vector $\boldsymbol{E}$, from Eq. (7.68), are given by

$$T_{11} = \frac{\partial \mathscr{U}}{\partial S_{11}} = \tilde{k}_m^D\, S_{11} - \tilde{k}_{me}\, D_2, \tag{7.72}$$

$$E_2 = \frac{\partial \mathscr{U}}{\partial D_2} = -\tilde{k}_{me}\, S_{11} + \tilde{k}_e^S\, D_2. \tag{7.73}$$

In the framework of the linear theory of piezoelectricity, considering linear elastic deformations and the quasi-electro-static approximation, by denoting the free charge density per unit surface with q, we have

$$S_{11} = -x_2 v'', \qquad \boldsymbol{D}\cdot\mathbf{n} = D_2 = -q. \tag{7.74}$$

By substituting the assumptions (7.74) in Eq. (7.67), the Lagrangian function $\mathcal{L}$ can be computed as

$$\begin{aligned}\mathcal{L}(v,\, q) = {} & b\int_0^L \int_{-\frac{h}{2}}^{\frac{h}{2}} \frac{1}{2}\rho_b \dot{v}^2 \mathrm{d}x_1\mathrm{d}x_2 + 2b\int_{x_{1,i}}^{x_{1,f}} \int_{\frac{h}{2}}^{\frac{h}{2}+h_p} \frac{1}{2}\rho_p \dot{v}^2 \mathrm{d}x_1\mathrm{d}x_2 \\ & - b\int_0^L \int_{-\frac{h}{2}}^{\frac{h}{2}} \frac{1}{2} Y_b\,(x_2 v'')^2 \mathrm{d}x_1\mathrm{d}x_2 - 2b\int_{x_{1,i}}^{x_{1,f}} \int_{\frac{h}{2}}^{\frac{h}{2}+h_p} \frac{1}{2}\tilde{k}_m^D\,(x_2 v'')^2 \mathrm{d}x_1\mathrm{d}x_2 \\ & + 2b\int_{x_{1,i}}^{x_{1,f}} \int_{\frac{h}{2}}^{\frac{h}{2}+h_p} \left[\tilde{k}_{me}\, x_2\, q\, v'' - \frac{1}{2}\tilde{k}_e^S\, q^2\right] \mathrm{d}x_1\mathrm{d}x_2. \end{aligned} \tag{7.75}$$

By performing integrations with respect to the variable x_2, we obtain

$$\begin{aligned}\mathcal{L}(v,\, q) = {} & \int_0^L \frac{1}{2}\rho_{lb}\dot{v}^2 \mathrm{d}x_1 + \int_{x_{1,i}}^{x_{1,f}} \frac{1}{2}\rho_{lp}\dot{v}^2 \mathrm{d}x_1 \\ & - \int_0^L \frac{1}{2} K_{mb}\,(v'')^2 \mathrm{d}x_1 - \int_{x_{1,i}}^{x_{1,f}} \frac{1}{2}\tilde{K}_{mp}\,(v'')^2 \mathrm{d}x_1 \\ & + \int_{x_{1,i}}^{x_{1,f}} \left(\tilde{K}_{me} v'' q - \tilde{K}_e\, q^2\right) \mathrm{d}x_1, \end{aligned} \tag{7.76}$$

where the meanings of the material parameters are defined in the following way. The lineal mass densities of the host beam ρ_{lb} and of the piezoelectric pair ρ_{lp} are

$$\rho_{lb} = b\int_{-\frac{h}{2}}^{\frac{h}{2}} \rho_b \mathrm{d}x_2, \qquad \rho_{lp} = 2b\int_{\frac{h}{2}}^{\frac{h}{2}+h_p} \rho_p \mathrm{d}x_2. \tag{7.77}$$

The host beam stiffness K_{mb} and the piezoelectric stiffness $\tilde{K}_{mp}$ are given by

$$K_{mb} = b \int_{-\frac{h}{2}}^{\frac{h}{2}} Y_b \, x_2^2 \mathrm{d}x_2 = Y_b \, \frac{bh^3}{12} \tag{7.78}$$

and

$$\tilde{K}_{mp} = 2b \int_{\frac{h}{2}}^{\frac{h}{2}+h_p} \tilde{k}_m^D \, x_2^2 \mathrm{d}x_2 = 2b \, \tilde{k}_m^D \left(\frac{h^2 h_p}{4} + \frac{h h_p^2}{2} + \frac{h_p^3}{3} \right). \tag{7.79}$$

The electro-mechanical coupling parameter $\tilde{K}_{me}$ is

$$\tilde{K}_{me} = 2b \int_{\frac{h}{2}}^{\frac{h}{2}+h_p} \tilde{k}_{me} \, x_2 \, \mathrm{d}x_2 = b \, \tilde{k}_{me} h_p \left(h + h_p \right), \tag{7.80}$$

and, finally, the electric parameter $\tilde{K}_e$ is

$$\tilde{K}_e = 2b \int_{\frac{h}{2}}^{\frac{h}{2}+h_p} \frac{\tilde{k}_e^S}{2} \, \mathrm{d}x_2 = b \, \tilde{k}_e^S h_p. \tag{7.81}$$

By including the mechanical and electrical work done, respectively, by the force density per unit line f and the applied voltage V, and equating to zero the variation of the introduced action, we obtain the governing equations of the piezoelectric system in terms of the mechanical v and electric q degrees of freedom:

$$\int_{t_0}^{t_1} \delta \mathcal{L} \mathrm{d}t + \int_{t_0}^{t_1} \int_0^L f \, \delta v \, \mathrm{d}x_1 \mathrm{d}t + 2b \int_{t_0}^{t_1} \int_{x_{1,1}}^{x_{1,f}} V \, \delta q \, \mathrm{d}x_1 \mathrm{d}t = 0. \tag{7.82}$$

Therefore, the governing equations of the piezoelectric composite beam can be deduced from Eq. (7.82) and (7.76):

$$\begin{cases} \rho_l \ddot{v}(x_1, t) + \left(\tilde{K}_m v''(x_1, t) \right)'' = \left[\delta'(x_1 - x_{1,i}) - \delta'(x_1 - x_{1,f}) \right] \Re_{me} Q(t) + f(x_1, t) \\ \dfrac{1}{\tilde{C}_e} Q(t) - \Re_{me} v'(x_1, t) \big|_{x_{1,i}}^{x_{1,f}} = V(t), \end{cases} \tag{7.83}$$

where Q is the total free charge and, for the sake of conciseness, we introduce the total lineal mass density

$$\rho_l = \rho_{lb} + \rho_{lp} \left[H(x_1 - x_{1,i}) - H(x_1 - x_{1,f}) \right], \tag{7.84}$$

the total stiffness

$$\tilde{K}_m = K_{mb} + \tilde{K}_{mp} \left[H(x_1 - x_{1,i}) - H(x_1 - x_{1,f}) \right], \tag{7.85}$$

in which $H(\cdot)$ is the Heaviside step function, and the constants

$$\Re_{me} = \frac{\tilde{K}_{me}}{x_{1,f} - x_{1,i}}, \qquad \tilde{C}_e = 2 \frac{b \left(x_{1,f} - x_{1,i} \right)}{\left(\tilde{k}_e^S h_p \right)}, \tag{7.86}$$

which represent, respectively, a coupling coefficient and the whole capacitance. Since the derivative of the Dirac delta δ' is involved, in Eq. (7.83) the mechanical actions of the piezoelectric patches can be interpreted as concentrated moments at the endpoints $x_{1,i}$ and $x_{1,f}$. The second equation of Eqs. (7.83) can be interpreted as corresponding to the equivalent electrical circuit of the piezoelectric patches. Indeed, according to Thévenin's theorem, such an equation represents a strain dependent voltage source in series connection with a capacitance.

In order to simplify the theoretical analysis, a normalised total free charge θ and a generalized voltage κ are introduced:

$$\theta(t) = \frac{Q(t)}{\sqrt{\tilde{C}_e}}, \qquad \kappa(t) = \sqrt{\tilde{C}_e} V(t). \tag{7.87}$$

Therefore, substituting the relations (7.87) in Eq. (7.83), we obtain

$$\begin{cases} \rho_l \ddot{v}(x_1,t) + \left(\tilde{K}_m v''(x_1,t)\right)'' - \left[\delta'(x_1 - x_{1,i}) - \delta'(x_1 - x_{1,f})\right] \tilde{\gamma}\, \theta(t) = f(x_1,t) \\ \theta(t) - \tilde{\gamma}\, v'(x_1,t)\big|_{x_{1,i}}^{x_{1,f}} = \kappa(t), \end{cases} \tag{7.88}$$

where now $\tilde{\gamma} = \mathfrak{K}_{me}\sqrt{\tilde{C}_e}$ denotes the generalized coupling coefficient. As before, the governing equations employed to control an undesired vibration mode of the beam have been obtained by performing a modal analysis. The displacement v of the system considered may be expanded in series as

$$v(x_1,t) = \sum_i W_i(x_1)\eta_i(t), \tag{7.89}$$

where $W_i(x_1)$ is the mode shape of the ith normal mode of the system when the excitation f is removed and under open circuit condition ($\theta = 0$), the coefficients $\eta_i(t)$ are the generalized coordinates describing the response of the ith normal mode. In order to make the decomposition unique, the mode shapes are normalised to the unitary value. Therefore, the governing equations for the piezo-electro-mechanical beam can be summarised as

$$\begin{cases} \ddot{\eta}_i(t) + (\omega_i^q)^2\, \eta(t) - \omega_i^q\, \tilde{g}_i \theta(t) = f_i(t) \quad \text{with } i = 1, 2, ... \\ \theta(t) - \sum_i \omega_i^q\, \tilde{g}_i \eta_i(t) = \kappa(t), \end{cases} \tag{7.90}$$

in which $f_i(t) = \int_0^L W_i(x_1)\, f(x_1,t)\mathrm{d}x_1$ represents the ith mode force and the following definition has been used for the unit-frequency normalised coupling coefficient $\tilde{g}_i$:

$$\tilde{g}_i = \tilde{\gamma}\; W_i'\big|_{x_{1,i}}^{x_{1,f}} / \omega_i^q. \tag{7.91}$$

Then, assuming low modal coupling and the mechanical load having a frequency content in a range close to the hth mode frequency, we can simplify Eq. (7.90) neglecting the effects of the other modes,

$$\begin{cases} \ddot{\eta}_h(t) + (\omega_h^q)^2\, \eta(t) - \omega_h^q\, \tilde{g}_h \theta(t) = f_h(t) \\ \theta(t) - \omega_h^q\, \tilde{g}_h \eta_h(t) = \kappa(t). \end{cases} \tag{7.92}$$

It is noteworthy that relations between ω_h and ω_h^q can be easily deduced analysing the relevant conditions of a short circuit condition and an open circuit condition, both from Eqs. (7.62) and (7.92), as follows

$$(\omega_h^q)^2 = \omega_h^2\,(1+g^2) \quad \text{or} \quad \omega_h^2 = (\omega_h^q)^2\,(1-\tilde{g}^2), \tag{7.93}$$

respectively. Consequently, the relationship between the coupling coefficient g and $\tilde{g}$ reads as

$$\tilde{g}^2 = \frac{g^2}{1+g^2}. \tag{7.94}$$

In the same spirit of [76], we can consider a vibration control shunting the piezoelectric transducer with an electric circuit. Specifically, in the case of a shunt circuit with a resistor, r, and an inductor, ℓ, connected in series (see Fig. 7.7), the generalized voltage is given by

$$\kappa(t) = -r\dot{\theta}(t) - \ell\ddot{\theta}(t). \tag{7.95}$$

Introducing the notation

$$\frac{1}{\ell} = \varpi_h^2, \quad \frac{r}{\ell} = 2\,\varpi_h\zeta_h \quad \text{and} \quad \alpha_h = \frac{\varpi_h}{\omega_h^q}, \tag{7.96}$$

the closed-loop equations are written as follows:

$$\begin{cases} \ddot{\eta}_h(t) + (\omega_h^q)^2\,\eta_h(t) - \omega_h^q\,\tilde{g}_h\theta(t) = f_h(t) \\ \ddot{\theta}\,(t) + 2\,\varpi_h\zeta_h\dot{\theta}(t) + \varpi_h^2\theta(t) - \omega_h^q\,\tilde{g}_h\,\varpi_h^2\,\eta_h(t) = 0. \end{cases} \tag{7.97}$$

The optimal values of the external resistor and inductance, related to the natural circular frequency, ϖ_j, and the damping ratio, ζ_j, obtained by means of the fixed points method [80] are (see Fig. 7.6):

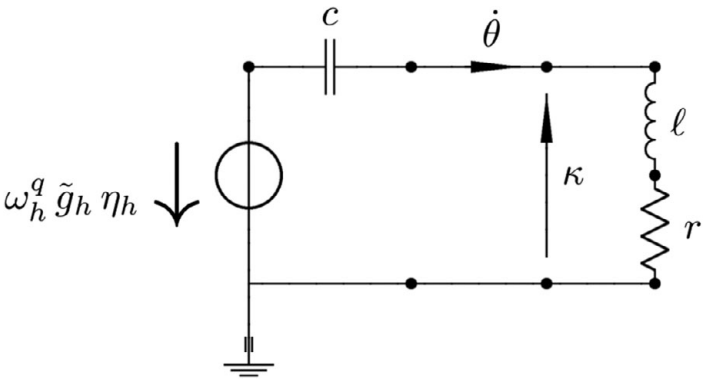

Figure 7.7 Equivalent circuit for a shunted circuit with a resistor and an inductor connected in series.

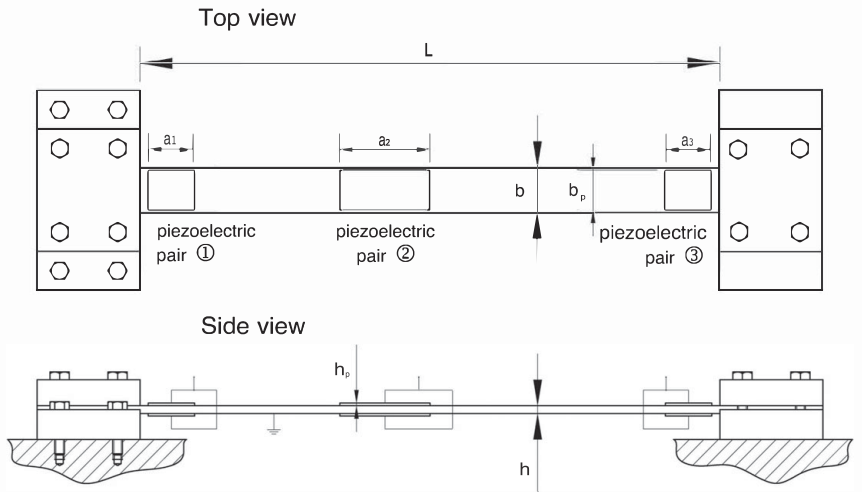

Figure 7.8 Piezoelectric beam.

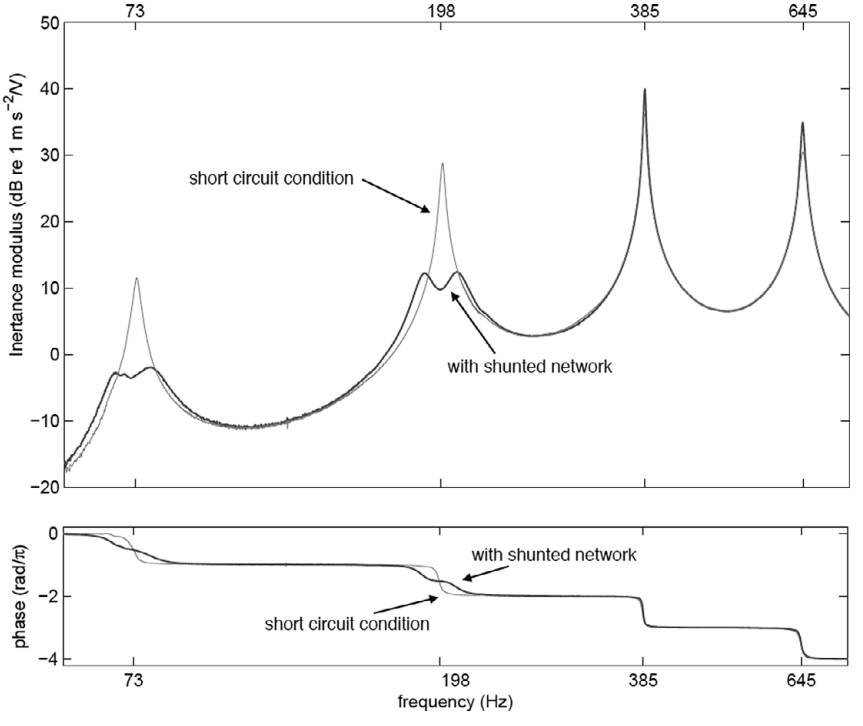

Figure 7.9 Inertance functions of the piezoelectric beam in Fig. 7.8 shunted with a multiterminal network and in a short circuit condition.

$$\varpi_h^{\text{opt}} = \frac{\sqrt{2}}{\sqrt{2-\tilde{g}_h^2}}\,\omega_h^q, \qquad \zeta_h^{\text{opt}} = 0.6465\,\tilde{g}_h. \tag{7.98}$$

Finally, using the models sketched in this section, it is possible to generalize the vibration control for many vibration modes of a beam or a plate equipped with many piezoelectric patches as reported in [74] and shown in Fig. 7.9 with measured inertance functions on a real beam in which one piezoelectric pair is used to impose a vibration and the other two are shunted with an electrical multiterminal network to damp such a vibration.

Bibliography

[1] Paul Germain. The method of virtual power in continuum mechanics. Part 2: Microstructure. *SIAM Journal on Applied Mathematics*, 25(3):556–575, 1973.

[2] L.D. Landau and E.M. Lifshitz. Mechanics: Volume 1 (course of theoretical physics), 3rd edition, Butterworth-Heinemann, 1976.

[3] Jerrold E. Marsden, Sergey Pekarsky, Steve Shkoller, and Matthew West. Variational methods, multisymplectic geometry and continuum mechanics. *Journal of Geometry and Physics*, 38(3):253–284, 2001.

[4] Victor Berdichevsky. *Variational Principles of Continuum Mechanics: I. Fundamentals*. Springer Science & Business Media, 2009.

[5] Gérard A. Maugin. The principle of virtual power: from eliminating metaphysical forces to providing an efficient modelling tool. *Continuum Mechanics and Thermodynamics*, 25(2-4):127–146, 2013.

[6] Simon R. Eugster and Francesco dell'Isola. Exegesis of the introduction and sect. I from *Fundamentals of the Mechanics of Continua* by E. Hellinger. *ZAMM-Zeitschrift für Angewandte Mathematik und Mechanik*, 97(4):477–506, 2017.

[7] Simon R. Eugster and Francesco dell'Isola. Exegesis of sect. II and III. A from *Fundamentals of the mechanics of continua* by E. Hellinger. *ZAMM- Zeitschrift für Angewandte Mathematik und Mechanik*, 98(1):31–68, 2018.

[8] Simon R. Eugster and Francesco dell'Isola. Exegesis of sect. III. B from *Fundamentals of the mechanics of continua* by E. Hellinger. *ZAMM-Zeitschrift für Angewandte Mathematik und Mechanik*, 98(1):69–105, 2018.

[9] Francesco dell'Isola and Luca Placidi. Variational principles are a powerful tool also for formulating field theories. In *Variational Models and Methods in Solid and Fluid Mechanics*, pages 1–15. Springer, 2011.

[10] M. A. Biot. Mechanics of deformation and acoustic propagation in porous media. *J. Appl. Phys.*, 33(4):1482–1498, 1962.

[11] S. C. Cowin. Bone poroelasticity. *J. Biomech.*, 32(3):217–238, 1999.

[12] I. Giorgio, U. Andreaus, D. Scerrato, and F. dell'Isola. A visco-poroelastic model of functional adaptation in bones reconstructed with bio-resorbable materials. *Biomech. Model. Mechanobiol.*, 15(5):1325–1343, 2016.

[13] U. Andreaus, I. Giorgio, and A. Madeo. Modeling of the interaction between bone tissue and resorbable biomaterial as linear elastic materials with voids. *Z. Angew. Math. Phys.*, 66(1):209–237, 2015.

[14] H. C. Brinkman. On the permeability of media consisting of closely packed porous particles. *Flow, Turbulence and Combustion*, 1(1):81, 1949.

[15] Hyo Sub Yoon and J. Lawrence Katz. Is bone a Cosserat solid? *Journal of Materials Science*, 18(5):1297–1305, 1983.

[16] H.C. Park and R.S. Lakes. Cosserat micromechanics of human bone: Strain redistribution by a hydration sensitive constituent. *Journal of Biomechanics*, 19(5):385–397, 1986.

[17] Holm Altenbach and Victor A. Eremeyev. On the constitutive equations of viscoelastic micropolar plates and shells of differential type. *Mathematics and Mechanics of Complex Systems*, 3(3):273–283, 2015.

[18] Jean-François Ganghoffer and Ibrahim Goda. Micropolar models of trabecular bone. In Jean-François Ganghoffer, editor, *Multiscale Biomechanics*, pages 263–316. Elsevier, 2018.

[19] R. D. Mindlin. Stress functions for a Cosserat continuum. *International Journal of Solids and Structures*, 1(3):265–271, 1965.

[20] L. Placidi, U. Andreaus, A. Della Corte, and T. Lekszycki. Gedanken experiments for the determination of two-dimensional linear second gradient elasticity coefficients. *Z. Angew. Math. Phys.*, 66(6):3699–3725, 2015.

[21] R. D. Mindlin. Micro-structure in linear elasticity. *Arch. Rational Mech. Anal.*, 16(1):51–78, 1964.

[22] R. A. Toupin. Elastic materials with couple-stresses. *Arch. Rational Mech. Anal.*, 11(1): 385–414, 1962.

[23] F. dell'Isola, G. Sciarra, and S. Vidoli. Generalized Hooke's law for isotropic second gradient materials. *Proc. R. Soc. A*, 465:2177–2196, 2009.

[24] F. dell'Isola, P. Seppecher, and A. Della Corte. The postulations á la D'Alembert and á la Cauchy for higher gradient continuum theories are equivalent: A review of existing results. *Proc. R. Soc. A*, 471(2183):20150415, 2015.

[25] T. Lekszycki and F. dell'Isola. A mixture model with evolving mass densities for describing synthesis and resorption phenomena in bones reconstructed with bio-resorbable materials. *Z. Angew. Math. Mech*, 92(6):426–444, 2012.

[26] Harold M. Frost. Bone "mass" and the "mechanostat": A proposal. *The Anatomical Record*, 219(1):1–9, 1987.

[27] Charles H. Turner. Homeostatic control of bone structure: an application of feedback theory. *Bone*, 12(3):203–217, 1991.

[28] Ivan Giorgio, Ugo Andreaus, Daria Scerrato, and Piero Braidotti. Modeling of a non-local stimulus for bone remodeling process under cyclic load: Application to a dental implant using a bioresorbable porous material. *Mathematics and Mechanics of Solids*, 22(9): 1790–1805, 2017.

[29] Daniel George, Camille Spingarn, Caroline Dissaux, *et al*. Examples of multiscale and multiphysics numerical modeling of biological tissues. *Bio-medical Materials and Engineering*, 28(s1):S15–S27, 2017.

[30] D. George, R. Allena, and Y. Rémond. Mechanobiological stimuli for bone remodeling: mechanical energy, cell nutriments and mobility. *Computer Methods in Biomechanics and Biomedical Engineering*, 20(sup1):91–92, 2017.

[31] Ivan Giorgio, Ugo Andreaus, Francesco dell'Isola, and Tomasz Lekszycki. Viscous second gradient porous materials for bones reconstructed with bio-resorbable grafts. *Extreme Mechanics Letters*, 13:141–147, 2017.

[32] Adam G. Bowland, Richard E. Weyers, Finley A. Charney, *et al*. Effect of vibration amplitude on concrete with damping additives. *ACI Materials Journal*, 109(3), 2012.

[33] Anil Misra. Stabilization characteristics of clays using class C fly ash. *Transportation Research Record: Journal of the Transportation Research Board*, 1611(1):46–54, 1998.

[34] Massimo Cuomo. Forms of the dissipation function for a class of viscoplastic models. *Mathematics and Mechanics of Complex Systems*, 5(3):217–237, 2017.

[35] Luca Placidi and Emilio Barchiesi. Energy approach to brittle fracture in strain-gradient modelling. *Proc. R. Soc. A*, 474, 2018.

[36] D. Scerrato, I. Giorgio, A. Madeo, A. Limam, and F. Darve. A simple non-linear model for internal friction in modified concrete. *International Journal of Engineering Science*, 80:136–152, 2014.

[37] Ivan Giorgio and Daria Scerrato. Multi-scale concrete model with rate-dependent internal friction. *European Journal of Environmental and Civil Engineering*, 21(7–8):821–839, 2017.

[38] G. Oliveto and M. Cuomo. Incremental analysis of plane frames with geometric and material nonlinearities. *Engineering Structures*, 10(1):2–12, 1988.

[39] D. Scerrato, I. Giorgio, A. Della Corte, *et al*. Towards the design of an enriched concrete with enhanced dissipation performances. *Cement and Concrete Research*, 84:48–61, 2016.

[40] Silvio Alessandroni, Francesco dell'Isola, and Maurizio Porfiri. A revival of electric analogs for vibrating mechanical systems aimed to their efficient control by pzt actuators. *International Journal of Solids and Structures*, 39(20):5295–5324, 2002.

[41] Ivan Giorgio, Luca Galantucci, Alessandro Della Corte, and Dionisio Del Vescovo. Piezo-electromechanical smart materials with distributed arrays of piezoelectric transducers: Current and upcoming applications. *International Journal of Applied Electromagnetics and Mechanics*, 47(4):1051–1084, 2015.

[42] Francesco dell'Isola, Fabrizio Vestroni, and Stefano Vidoli. Structural-damage detection by distributed piezoelectric transducers and tuned electric circuits. *Research in Nondestructive Evaluation*, 16(3):101–118, 2005.

[43] Francesco dell'Isola and Stefano Vidoli. Damping of bending waves in truss beams by electrical transmission lines with pzt actuators. *Archive of Applied Mechanics*, 68(9): 626–636, 1998.

[44] Ugo Andreaus, Francesco dell'Isola, and Maurizio Porfiri. Piezoelectric passive distributed controllers for beam flexural vibrations. *Modal Analysis*, 10(5):625–659, 2004.

[45] Francesco dell'Isola, Corrado Maurini, and Maurizio Porfiri. Passive damping of beam vibrations through distributed electric networks and piezoelectric transducers: Prototype design and experimental validation. *Smart Materials and Structures*, 13(2):299, 2004.

[46] Romesh C. Batra, Francesco dell'Isola, Stefano Vidoli, and D. Vigilante. Multimode vibration suppression with passive two-terminal distributed network incorporating piezoceramic transducers. *International Journal of Solids and Structures*, 42(11–12):3115–3132, 2005.

[47] Silvio Alessandroni, Ugo Andreaus, Francesco dell'Isola, and Maurizio Porfiri. Piezo-electromechanical (PEM) Kirchhoff–Love plates. *European Journal of Mechanics-A/Solids*, 23(4):689–702, 2004.

[48] Silvio Alessandroni, Ugo Andreaus, Francesco dell'Isola, and Maurizio Porfiri. A passive electric controller for multimodal vibrations of thin plates. *Computers & structures*, 83(15–16):1236–1250, 2005.

[49] Giuseppe Rosi, Joël Pouget, and Francesco dell'Isola. Control of sound radiation and transmission by a piezoelectric plate with an optimized resistive electrode. *European Journal of Mechanics-A/Solids*, 29(5):859–870, 2010.

[50] B. Lossouarn, J.F. Deü, M. Aucejo, and K.A. Cunefare. Multimodal vibration damping of a plate by piezoelectric coupling to its analogous electrical network. *Smart Materials and Structures*, 25(11):115042, 2016.

[51] Corrado Maurini, Joël Pouget, and Francesco dell'Isola. On a model of layered piezoelectric beams including transverse stress effect. *International Journal of Solids and Structures*, 41(16–17):4473–4502, 2004.

[52] Francesco D'Annibale, Giuseppe Rosi, and Angelo Luongo. Linear stability of piezoelectric-controlled discrete mechanical systems under nonconservative positional forces. *Meccanica*, 50(3):825–839, 2015.

[53] Valerii P. Matveenko, E.P. Kligman, M.A. Yurlov, and N.A. Yurlova. Simulation and optimization of dynamic characteristics of piezoelectric smart structures. *Physical Mesomechanics*, 15(3-4):190–199, 2012.

[54] V.P. Matvvenko, D.A. Oshmarin, N.V. Sevodina, and N.A. Iurlova. Natural vibration problem for electroviscoelastic body with external electric circuits and finite-element relations for its numerical implementation. *Computational Continuum Mechanics*, 9(4):476–485, 2016.

[55] Emilio Barchiesi, Mario Spagnuolo, and Luca Placidi. Mechanical metamaterials: a state of the art. *Mathematics and Mechanics of Solids*, page doi: 10.1177/1081286517735695, 2018.

[56] Dionisio Del Vescovo and Ivan Giorgio. Dynamic problems for metamaterials: Review of existing models and ideas for further research. *International Journal of Engineering Science*, 80:153–172, 2014.

[57] Giuseppe Rosi, Roberto Paccapeli, François Ollivier, and Joël Pouget. Optimization of piezoelectric patch positioning for passive sound radiation control of plates. *Journal of Vibration and Control*, 19(5):658–673, 2013.

[58] Holm Altenbach and Victor A. Eremeyev. Analysis of the viscoelastic behavior of plates made of functionally graded materials. *ZAMM-Zeitschrift für Angewandte Mathematik und Mechanik*, 88(5):332–341, 2008.

[59] Victor A. Eremeyev, Leonid P. Lebedev, and Michael J. Cloud. The Rayleigh and Courant variational principles in the six-parameter shell theory. *Mathematics and Mechanics of Solids*, 20(7):806–822, 2015.

[60] H.F. Tiersten. Hamilton's principle for linear piezoelectric media. *Proceedings of the IEEE*, 55(8):1523–1524, 1967.

[61] Gérard A Maugin. *Nonlinear Electromechanical Effects and Applications*, Volume 1. World Scientific Publishing Company, 1986.

[62] J.A. Mitchell and J.N. Reddy. A refined hybrid plate theory for composite laminates with piezoelectric laminae. *International Journal of Solids and Structures*, 32(16):2345–2367, 1995.

[63] A.W.W.A.H. Meitzler, H.F. Tiersten, A.W. Warner, *et al*. IEEE Standard on Piezoelectricity, 1988.

[64] Luca Placidi and Kolumban Hutter. An anisotropic flow law for incompressible polycrystalline materials. *Zeitschrift für angewandte Mathematik und Physik ZAMP*, 57(1):160–181, 2005.

[65] Luca Placidi and Kolumban Hutter. Thermodynamics of polycrystalline materials treated by the theory of mixtures with continuous diversity. *Continuum Mechanics and Thermodynamics*, 17(6):409, 2006.

[66] H.J.M.T.S. Adriaens, Willem L. De Koning, and Reinder Banning. Modeling piezoelectric actuators. *IEEE/ASME Transactions on Mechatronics*, 5(4):331–341, 2000.

[67] S.-H. Lee and T.J. Royston. Modeling piezoceramic transducer hysteresis in the structural vibration control problem. *The Journal of the Acoustical Society of America*, 108(6): 2843–2855, 2000.

[68] K. Frischmuth, W. Kosiéski, and T. Lekszycki. Free vibrations of finite-memory material beams. *International Journal of Engineering Science*, 31(3):385–395, 1993.

[69] Robin Bouclier, Thomas Elguedj, and Alain Combescure. Locking free isogeometric formulations of curved thick beams. *Computer Methods in Applied Mechanics and Engineering*, 245:144–162, 2012.

[70] Leopoldo Greco and Massimo Cuomo. B-spline interpolation of Kirchhoff–Love space rods. *Computer Methods in Applied Mechanics and Engineering*, 256:251–269, 2013.

[71] Antonio Cazzani, Marcello Malagù, and Emilio Turco. Isogeometric analysis: A powerful numerical tool for the elastic analysis of historical masonry arches. *Continuum Mechanics and Thermodynamics*, 28(1-2):139–156, 2016.

[72] Viacheslav Balobanov, Sergei Khakalo, and Jarkko Niiranen. Isogeometric analysis of gradient-elastic 1D and 2D problems. In *Generalized Continua as Models for Classical and Advanced Materials*, pages 37–45. Springer, 2016.

[73] L. Greco, M. Cuomo, L. Contrafatto, and S. Gazzo. An efficient blended mixed b-spline formulation for removing membrane locking in plane curved Kirchhoff rods. *Computer Methods in Applied Mechanics and Engineering*, 324:476–511, 2017.

[74] Ivan Giorgio, Antonio Culla, and Dionisio Del Vescovo. Multimode vibration control using several piezoelectric transducers shunted with a multiterminal network. *Archive of Applied Mechanics*, 79(9):859–879, 2009.

[75] A Bloch. XXXVIII. A new approach to the dynamics of systems with gyroscopic coupling terms. *The London, Edinburgh, and Dublin Philosophical Magazine and Journal of Science*, 35(244):315–334, 1944.

[76] Nesbitt W. Hagood and Andreas von Flotow. Damping of structural vibrations with piezoelectric materials and passive electrical networks. *Journal of Sound and Vibration*, 146(2):243–268, 1991.

[77] Shu-yau Wu. Piezoelectric shunts with a parallel RL circuit for structural damping and vibration control. In *Smart Structures and Materials 1996: Passive Damping and Isolation*, volume 2720, pages 259–270. International Society for Optics and Photonics, 1996.

[78] Ivan Giorgio. *Multimode Collocated Vibration Control with Multiple Piezoelectric Transducers*. PhD thesis, Università degli studi di Roma "La Sapienza," 2008.

[79] Boris Lossouarn, M. Aucejo, J.-F. Deü, and B. Multon. Design of inductors with high inductance values for resonant piezoelectric damping. *Sensors and Actuators A: Physical*, 259:68–76, 2017.

[80] J. P. Den Hartog. *Mechanical Vibrations*. McGraw-Hill Book Company, Inc., New York, NY,, 1956.

[81] R.C. Batra and J.S. Yang. Saint-Venant's principle in linear piezoelectricity. *Journal of Elasticity*, 38(2):209–218, 1995.

[82] Mircea Bîrsan, Holm Altenbach, Tomasz Sadowski, VA Eremeyev, and Daniel Pietras. Deformation analysis of functionally graded beams by the direct approach. *Composites Part B: Engineering*, 43(3):1315–1328, 2012.

[83] T. Lekszycki. Application of variational methods in analysis and synthesis of viscoelastic continuous systems. *Journal of Structural Mechanics*, 19(2):163–192, 1991.

[84] T. Lekszycki and Z. Mróz. Variational principles in analysis and synthesis of elastic systems with damping. *Solid Mech. Arch*, 14(3-4):181–201, 1989.

[85] Jarkko Niiranen, Viacheslav Balobanov, Josef Kiendl, and S.B. Hosseini. Variational formulations, model comparisons and numerical methods for Euler–Bernoulli micro-and nano-beam models. *Mathematics and Mechanics of Solids*, page 1081286517739669, 2017.

[86] Jarkko Niiranen, Josef Kiendl, Antti H. Niemi, and Alessandro Reali. Isogeometric analysis for sixth-order boundary value problems of gradient-elastic Kirchhoff plates. *Computer Methods in Applied Mechanics and Engineering*, 316:328–348, 2017.

[87] Siamak Niroomandi, Iciar Alfaro, Elias Cueto, and Francisco Chinesta. Model order reduction for hyperelastic materials. *International Journal for Numerical Methods in Engineering*, 81(9):1180–1206, 2010.

[88] David Steigmann, Eveline Baesu, Robert E. Rudd, Jim Belak, and Mike McElfresh. On the variational theory of cell-membrane equilibria. *Interfaces and Free Boundaries*, 5(4): 357–366, 2003.

[89] David J. Steigmann and Allen C. Pipkin. Equilibrium of elastic nets. *Phil. Trans. R. Soc. Lond. A*, 335(1639):419–454, 1991.

[90] E. Barchiesi, M. Laudato, and F. Di Cosmo. Wave dispersion in non-linear pantographic beams. *Mechanics Research Communications*, 2018.

[91] Emilio Barchiesi, Francesco dell'Isola, Marco Laudato, Luca Placidi, and Pierre Seppecher. A 1D continuum model for beams with pantographic microstructure: Asymptotic micro-macro identification and numerical results. In *Advances in Mechanics of Microstructured Media and Structures*, pages 43–74. Springer, 2018.

[92] Emilio Barchiesi, Gregor Ganzosch, Christian Liebold, *et al*. Out-of-plane buckling of pantographic fabrics in displacement-controlled shear tests: Experimental results and model validation. *Continuum Mechanics and Thermodynamics*, pages 1–13, 2018.

[93] Emilio Barchiesi and Luca Placidi. A review on models for the 3D statics and 2D dynamics of pantographic fabrics. In *Wave Dynamics and Composite Mechanics for Microstructured Materials and Metamaterials*, pages 239–258. Springer, 2017.

[94] Luca Placidi, Emilio Barchiesi, and Anil Misra. A strain gradient variational approach to damage: a comparison with damage gradient models and numerical results. *Mathematics and Mechanics of Complex Systems*, 6(2):77–100, 2018.

[95] Luca Placidi, Anil Misra, and Emilio Barchiesi. Simulation results for damage with evolving microstructure and growing strain gradient moduli. *Continuum Mechanics and Thermodynamics*, pages 1–21, 2018.

[96] Luca Placidi, Anil Misra, and Emilio Barchiesi. Two-dimensional strain gradient damage modeling: a variational approach. *Zeitschrift für angewandte Mathematik und Physik*, 69(3):56, 2018.

[97] Luca Placidi, Emilio Barchiesi, Emilio Turco, and Nicola Luigi Rizzi. A review on 2D models for the description of pantographic fabrics. *Zeitschrift für angewandte Mathematik und Physik*, 67(5):121, 2016.

[98] Yang Yang and Anil Misra. Higher-order stress-strain theory for damage modeling implemented in an element-free Galerkin formulation. *CMES-Computer Modeling in Engineering & Sciences*, 64(1):1–36, 2010.

8 Least Action and Virtual Work Principles for the Formulation of Generalized Continuum Models

F. dell'Isola, P. Seppecher, L. Placidi, E. Barchiesi, A. Misra

8.1 Introduction and Historical Background

Although the principle of virtual velocities is rooted deep in time, the study of its historical development, as well as studies of its variations and transformations that have been presented at various times, are surprisingly meagre. In this rather sparingly explored field we have found especially interesting the work [36], and particularly modern and still topical the presentations by Lagrange and Piola ([15, 30],[24, 25, 27–29]). A presentation of the history of mechanics cataloguing the main contributions to mechanical sciences on the basis of their postulation scheme is, in our opinion, a worthy endeavor that deserves the exemplary efforts of modern mechanicians. It is clear that the great majority of formulations of novel branches of mechanics, and more generally of physics, has been obtained via a basic unifying variational principle (see e.g. [1, 11, 16, 18, 26, 32–35]). In his works Jean Le Rond D'Alembert has been one of the bravest champions of this point of view: we refer to [10] for a due tribute to his contribution to mechanical sciences. The D'Alembertian point of view is shared, among many other scholars, by Hellinger ([38]), Landau ([17]), Feynman [11], Germain [13], Cosserat brothers [6], Lagrange [30], Piola [29], Sedov, Mindlin and Toupin [28], and Winter [23].

8.1.1 Ancient Occurrences of the Principle of Virtual Velocities

It is accepted, nearly unanimously, by scholars in Greek science that the first formulations of mechanics, that reached us via the texts of the Hellenistic school, are based upon the principle of virtual velocities (see again [23]). A careful analysis of ancient texts (see e.g. [2, 5, 22]) will lead to the assessment that the law of the lever was formulated starting from precisely such a principle. Thomas Winter arrives at a conclusion to attribute, in a brilliant way, to Archytas of Tarentum the pseudo-Aristotelian text *Mechanical Problems*, where the first known formulation of the principle of virtual velocities can be found. Archytas was believed by ancient sources (for instance by Vitruvius, see also e.g. [40]) to be the founder of "mathematical" mechanics and was credited with having an "algebraic" approach to mathematics (see [39]). The reader will agree that the program of transforming mechanics into an algebra-based physical theory, which abandons the support of geometrical techniques, is exactly the cultural project successfully started by Lagrange (see Chapter 4 where the Lagrangian introduction to analytical mechanics is translated).

To illustrate the depth and breadth of Hellenistic science, we have found a quote by an Epicurean scholar which gives a clue to the advanced understanding of mathematics and physics of his era. The Hellenistic effort to produce a predictive science seems to have been continuous and determinate: we refrain here from the necessarily longer arguments needed to present this case, and we refer to the precise and rigorous discussion presented in [21] by Lucio Russo. The Epicurean philosopher and scientist to whom we refer is Metrodoron, and we believe that the following sentence attributed to him can be regarded as one among the first statements at the basis of "modern" epistemology (see also [41]):

Always remember that you were born mortal and such is your nature and you were given a limited time: but by means of your reasonings about Nature you could rise to infinity and to eternity and you indeed contemplate ***"the things that were, and that were to be, and that had been before***."

Gnomologium Epicureum Vaticanum X (fr.37 Alfred Körte, Metrodori Epicurei Fragmenta, *Jahrböcher för classiche Philologie*, Suppl. XVII, 1890, p. 557).

From what we know about him, Metrodoron may have formulated some epistemological concepts leading him to claim that science (i.e. reasonings about Nature) allows for the prediction of future events. By stating this old concept in modern terms (even if many scholars would claim that we are considering the Hellenistic science too modern!) he states that by using a mathematical model one can manage to predict the future evolution of physical systems. The educated classical scholar has probably recognized that the bold sentence in the previous quotation is a quotation inside a quotation: it is from Iliad Vol.I line 70. One can claim that in Hellenistic culture there was no distinction between (with a later terminology) humanistic and scientific culture: the interested reader can refer to [21] for a detailed discussion of this point.

8.2 Why Look for the Historical Roots of Variational Principles and Calculus of Variation?

The most efficient way to learn how to formulate new mathematical models apt to describe physical reality consists in carefully studying how the most successful models were first formulated by their inventors. For this reason we believe that it is important to understand ***how, when, and by whom*** a model was formulated the first time: we need to be inspired by the creative acts of our predecessors if we want to follow in their foot steps.[1] Archimedes was aware of this need. In his *On the The Method* (as translated by Heath from the Latin translation by Heiberg (see [42] pp. 12–14)) we can read:[2]

Archimedes to Eratosthenes greeting. I sent you on a former occasion some of the theorems discovered by me, merely writing out the enunciations and inviting you to discover the proofs, which at the moment I did not give. The enunciations of the theorems which I sent were as follows. . . . The proofs then of these theorems I have written in this

[1] We believe that all the other motivations involving the establishment of priority are not relevant except, maybe, for the vainglory of some scholars.

[2] This quotation seems to us so important that we decided to reproduce it completely.

book and now send to you. Seeing moreover in you, as I say, an earnest student, a man of considerable eminence in philosophy, and an admirer [of mathematical inquiry], I thought fit to write out for you and explain in detail in the same book the peculiarity of a certain method, by which it will be possible for you to get a start to enable you to investigate some of the problems in mathematics by means of mechanics. This procedure is, I am persuaded, no less useful even for the proof of the theorems themselves; for certain things first became clear to me by a mechanical method, although they had to be demonstrated by geometry afterwards because their investigation by the said method did not furnish an actual demonstration. But it is of course easier, when we have previously acquired, by the method, some knowledge of the questions, to supply the proof than it is to find it without any previous knowledge. This is a reason why, in the case of the theorems the proof of which Eudoxus was the first to discover, namely that the cone is a third part of the cylinder, and the pyramid of the prism, having the same base and equal height, we should give no small share of the credit to Democritus who was the first to make the assertion with regard to the said figure though he did not prove it. I am myself in the position of having first made the discovery of the theorem now to be published [by the method indicated], and I deem it necessary to expound the method partly because I have already spoken of it and I do not want to be thought to have uttered vain words, but equally because I am persuaded that it will be of no little service to mathematics; for I apprehend that some, either of my contemporaries or of my successors, will, by means of the method when once established, be able to discover other theorems in addition, which have not yet occurred to me. First then I will set out the very first theorem which became known to me by means of mechanics, namely that: Any segment of a section of a right-angled cone (i.e. a parabola) is four-thirds of the triangle which has the same base and equal height, and after this I will give each of the other theorems investigated by the same method. Then, at the end of the book, I will give the geometrical [proofs of the propositions]. . ..

To the benefit of his successors, Archimedes not only writes down the formal proof of the theorem he managed to demonstrate, but he also discloses the heuristic procedure which allowed him to reach his formal result. Indeed, he is aware of the importance of letting all scholars know not only about the mathematical result by itself, but also how it has been conjectured.

Heiberg's palimpsest, lost after its first modern rediscovery by Heiberg [19], has more recently been rediscovered: its careful analysis is allowing us to understand better and better the scientific vision of Archimedes. For instance (see [20] for more details) in his *On Floating Bodies* he solves (by using a variational principle and variational techniques), the problem of determining the shape of a hull which optimizes its floating performances. In [21] it is shown that this is not an episodic application of optimization techniques in Hellenistic science: such techniques were already very well known in that époque. For instance, we have evidence that some Hellenistic scholars were able to find which regular polygon encloses the maximal area (see [39] and [43] for more details about this and some other optimization problems). We have tried carefully to find in the literature some precise references about the famous Dido's isoperimetric problem: it seems to us that the only trace of its ancient formulation remains in Virgil's Aeneid.

Without doubt variational principles and methods were developed within Hellenistic science and, since then, they have often been used in many fields of physics. The variational formulation leading to the evolution equations of a system has always been considered a very important challenge in mechanical sciences and mathematics, as it seems to make the study of their well-posedness easier. Moreover, variational methods are very effective for proving stability results, and they allow for an effective and immediate application of numerical solution strategies.

It is also clear that the majority of mechanical models have been formulated at first by means of variational principles (this statement is discussed or supported by many authors: see for a detailed discussion of this point e.g. [1–3, 5, 6, 11, 15–18, 22, 24, 25, 27–30, 32–34, 37, 38, 41]). More generally the principle of virtual work must be regarded as the most effective foundation of all models in physics, and also as the most effective tool to solving them. Finally, it is very useful to establish the needed relationships between micro and macro models, as they can be employed to deduce approximate homogenized asymptotic models.[3]

It seems to us that the principle of virtual work and the principle of least action have roots much deeper than many scientists believe (see again Vailati [22]). Even if some authors refer to a theorem of the principle of virtual work (which seems to us to be rather an oxymoron), it appears clear from the available sources that the first formulations of the majority of mathematical models for physical phenomena were obtained by assuming it as the most fundamental postulate. Such models were then, eventually, reformulated in terms of balance laws.

Moreover, most likely, the principle of least action, i.e. a "geometric" formulation of its laws, was used by the scientists of the Hellenistic period to establish mechanics as a hypothetico-deductive theory.[4] Most of the epigones of Hellenistic science, especially during Middle Age, could not master the arguments leading from variational principles to the solution of "practical" exercises useful in the applications. However, they could grasp the "a posteriori" interpretations of the necessary minimality or stationarity conditions[5] deduced by their predecessors, which were, therefore, assumed sometimes as a starting point (i.e. as postulates) on the basis of not so clear "physical" arguments.

Therefore, a group of epigones of Hellenistic scientists decided to start from a postulation of mechanics based on balance laws and to consider the conservation of energy and, eventually, the validity of the principle of virtual work as some sophisticated and sometimes too abstract mathematical tools, without any "physical" meaning, to be reserved for some very particular mathematical considerations and applications.[6]

[3] The most ancient sources presenting this kind of result which we managed to find are [24, 27, 29], as discussed in [25, 28].

[4] This point of view is also shared, among others, by Colonnetti [5] and by Netz and Noel [19].

[5] i.e. the necessary conditions which are deduced from the variational principles and are equivalent to those which are now called Euler–Lagrange equations and boundary conditions, naming them after the modern champions of variational methods.

[6] The reader will note that Truesdell treated variational principles as a kind of (unimportant) appendix in the work which he co-authored with R. Toupin. In this appendix Truesdell criticized bitterly the work and the opinions expressed by Hellinger [32–35], who may be considered as the main German champion of variational principles of his generation. The more sophisticated technique of *damnatio memoriae* has been

This process of erasing ancient theories together with the fundamental assumptions on which they were based and their reformulation in what are called "more modern presentations" occur frequently in the history of science (see e.g. [21**?**]). We recall here, as an example, the story of the formulations (and reformulations) of the Euler–Bernoulli Beam theory (see [2] for more details). Its discovery, as far as we can reconstruct it with the available sources, can be summarised as follows: i) Euler postulated that the *Elastica* "chooses" the stable equilibrium configurations by minimizing its deformation energy; ii) Euler and Bernoulli decided that the most suitable deformation energy density had to be chosen as a quadratic function of the *Elastica* curvature; iii) Lagrange managed to calculate the stationarity condition for the energy postulated by Euler and Bernoulli and, therefore, he could get the well-known differential equation and boundary conditions for the transverse displacement beams (i.e. the equations for the equilibrium of the *Elastica*); iv) Navier, in his lectures, needed to use the equation of the *Elastica* and wanted to present it without using the calculus of variations. He therefore obtained the equilibrium equation starting from the principle of balance of forces and couples, and imposed "ad hoc" boundary conditions based on "physical" assumptions.[7] Because of the success of this teaching approach, many engineering courses based the whole of continuum mechanics on postulations starting from balance principles and a wrong idea spread among scholars: i.e. the beam equations were obtained by Euler starting from balance of forces and moments. This belief induced a wrong understanding of the process of invention of new models in mechanics and, more generally, in physics.

We recall here that: i) Navier did try to get the equilibrium equations for a three-dimensional continuous body via an averaging procedure starting from molecular dynamics, and his results were very partial and rather defective (see [2] where the presence of a unique Poisson ratio in the Navier model is discussed); ii) Piola, instead, had already found the correct equations for generalized continua in his work [27], starting from a postulation of mechanics based on the principle of virtual work.

The point of view accepted by Navier persisted until numerical simulations became necessary. In order to formulate numerical codes variational "principles" are indispensable, as finite differences procedures are not effective in the study of partial differential equations. Unfortunately, instead of coming back to the origins of postulation in mechanics, variational principles were recovered as theorems as, simply for some sociological reasons, the "balance postulates" are considered to be more "physically" understandable.

Variational principles were therefore regarded simply as computational and mathematical[8] tools and their heuristic power was often forgotten, especially in some parts of the scientific milieux of the scholars in continuum mechanics. This attitude has not been modified by these scholars even when it was observed that (see e.g. [28, 51, 96])

applied in [45]: in this textbook there is absolutely no mention of variational principles and techniques, as if they were not an important part of mechanics.

[7] Note that, instead, when using the principle of minimum energy the correct boundary conditions are deduced, by means of a process of integration by parts.

[8] Therefore too abstract to be understandable.

the majority[9] of the advancements in mechanics were made possible by the wise use of some variational principles. It is ironic that many of the said scholars, in the presence of the unavoidable difficulties arising when using balance laws postulations, invoke the use of the "physical sense." While many declare to know the essence of such a "mythological phoenix,"[10] nobody can teach what it is or, at least, how to use it. Physical sense is declared as a necessary tool to choose the right "balance principles" when one wants to invent new models. However, nearly all creative theoretical physicists refrain from using balance laws and systematically base their reasonings on minimization postulates: for instance, quantum mechanics and general relativity have been developed firmly based on a variational principle (see e.g. Landau [17], Feynman [11], Lagrange [15, 30], Lanczos [16]).

We list here some additional historical examples, beyond the study of equilibrium of the lever:

i) Lagrange, Sophie Germain and Kirchhoff based their investigations aimed at determining the equations of plates on the basis of deformation energy minimization, and found the (right!) natural boundary conditions without any physical intuition (see e.g. [2]);
ii) Cosserat brothers, in order to generalize Cauchy-first gradient continuum mechanics, needed to "rediscover" the principle of least action (see [6]);
iii) also nonconservative phenomena can be described by means of variational principles: the case of fracture is exemplary (see [4, 12]).

We underscore that our interest is not to engender disputes regarding the priority in discoveries. We simply try to make clear our opinion about the logical frame which is more suitable for inventing novel mechanical models, entailing the following advice to the modeler: always avoid trying to formulate new models using "ad hoc" modifications of already existing theories, but try always to understand which is the most suitable action functional. When you have found it: simply minimize it!

8.3 Pluralitas non est ponenda sine necessitate (John Duns Scoto 1265–1308)

Very often, in order to be able to transmit knowledge, scholars have used slogans, and some of them have been learnt by heart by generations of students.[11] The word (slogan) which is nowadays used in all languages has a relatively recent etymology.[12] However, the concept was known and the technique was used systematically in every educational system based on the classical Greek and Latin culture. Mnemonics techniques are based

[9] We may want to say: all. However such a general statement is impossible to prove.
[10] "E' la fede degli amanti come l'araba fenice, che vi sia, ciascun lo dice, dove sia nessun lo sa. Se tu sai dov'ha ricetto, dove muore e torna in vita, me l'addita . . ." which may be translated as follows: "Is the fidelity of the lovers like the phoenix: that it exists everybody says, but where it is nobody knows. If you know where his shelter is, where it dies and comes back to life, please indicate this place to me" Metastasio, *Demetrio,* II.3 (1731)
[11] Slogan: a short and striking or memorable phrase used in advertising. (Oxford Dictionary definition).
[12] It is an Anglicisation of the Scottish Gaelic and Irish word sluagh-ghairm (sluagh "army", + gairm "cry").

on a careful choice of slogans, which are repeated again and again with the intention to leave a trace of their meaning in the mind of all scholars.[13]

Of course slogans can be misunderstood. Therefore, memory must be supported by a strong conceptual and logical structure. When interpreting slogans one has to be coherent with a general epistemological vision having very sound bases (see Chapter 4).

8.3.1 What Does It Mean?

The statement which we wish to consider is: "Pluralitas non est ponenda sine necessitate": i.e. "Plurality is not to be posited without necessity." This is a slogan or a mantra used to fix in the mind of scholars some basic principles of epistemology. We refer to the beautiful entry [46] of the Stanford *Encyclopedia of Philosophy* for a clear and deep examination of the genesis, transmission and transformations, in Hellenistic, Middle Ages and Modern Western civilization of all the concepts related to it.

We simply recall here that it is considered one of the most popular formulations of the so called Occam's razor, also known in Latin: *lex parsimoniae* ("law of parsimony"). Occam's razor is a principle to be followed in formulating a mathematical theory aiming to describe efficiently a class of physical phenomena. This principle states that, when the modeler is comparing competing hypothetical assumptions which may be placed at the basis of the theoretical analysis of a problem, then *ceteris paribus* (i.e. when all logical conditions and results are equivalent) the model which makes the least number of assumptions must be selected.

Occam's razor must be regarded as a way to help in the formulation and the development of theoretical models. Needless to say, it is not an algorithm capable of selecting among candidate models. Unfortunately, we are not yet able to formulate a meta-theory able to teach us precisely how to formulate lower order[14] theories (see Chapter 3). Therefore, Occam's razor cannot be regarded either as an "irrefutable principle of logic," or as a kind of scientific result based on experience (as sometimes we have found written in textbooks based on some naive epistemology). However, the falsifiability criterion (see Chapter 3 and [47]) dictates a precise preference for "simplicity in the formulation" of mathematical models for physical phenomena.

Actually, given a phenomenon, one can find an extremely large number of possible alternative models explaining it: as argued, among others, by Duhem (see [48]) there is

[13] The eldest author has learnt by heart the slogan attributed to Duns Scoto, while a high school student at least forty years ago, and he had forgotten it until he needed such a statement in a debate: suddenly the sentence and its meaning appeared in his mind, apparently out of the blue. He learnt in his subsequent studies that a statement with a very similar meaning can be attributed to Aristotle: however, in his mind only the one attributed to Duns Scoto, which he has learnt in a young age, remains printed permanently.

[14] There are theories (first order theories) which are directly describing phenomena, while there are higher order meta-theories which describe how to construct lower order theories. For instance, the theory of rings in abstract algebra studies how to build and use those sets of objects in which two algebraic operations, with particular properties, are defined. The rings of real numbers and complex numbers (actually they are special rings: i.e. algebraic fields) are particular objects among those studied by the theory of rings. The theory of real numbers is a theory describing physical quantities (i.e. it is a first order theory), while the theory of rings describes the behavior of a large class of theories, which share some specific common features, and it is a second order theory.

a clear "underdetermination" of any scientific theory. Actually, via a logical argument or via a selection operated using experimental evidence one cannot discriminate among all these theories, which might appear to be equivalent. Therefore, one must choose, among all the equivalent models, the simplest one. Indeed, as it is possible to avoid any realistic falsification of a scientific theory with ad hoc hypotheses, one should prefer "simpler theories" to "complex theories," because experimental tests and control of theoretical details are clearly more feasible and reliable (for more details in this context see again [46]).

Regarding this fact, we mention that in modern mechanics it has been recently observed (see e.g. [49]) that there is a proliferation of basic assumptions in the formulation of continuum theories. Generalized continuum models have been produced based on those which appear to be too many hypotheses (more details in the subsequent Section 8.4). Indeed, one often finds the postulation of too many ad hoc balance laws: one balance law for each of the needed kinematical descriptors. Truesdell (see e.g. [28, 41, 44]) was aware of this dangerous proliferation of basic assumptions. His response was to reject[15] the kind of continuum models which could not be encompassed in the postulation scheme based only on the balance of force and momentum.

Truesdell, therefore, opposed firmly those scholars who, having i) accepted considering models whose kinematics could not be limited to the placement field or whose deformation energy was depending on second (or higher) gradients of the kinematical descriptors, and ii) based their postulation scheme on the concept of balance laws, were obliged to introduce more and more complex ad hoc fluxes and sources, and correspondingly to postulate ad hoc balance laws. Truesdell was right in remarking that this process (see e.g. [49]) resembles very much that which was adopted by Ptolemy and his followers: to overcome possible falsifications of their model aimed at describing the motion of planets, they added ad hoc (and without any unifying rationale) more epicycles.

The reader will discover in the next sections[16] how elegant is the postulation presented by Paul Germain, who postulates a unique basic principle: the principle of virtual work. On the contrary, in order to keep using the concept of force, some scholars have attempted its generalization: for instance by formulating the concept of configurational force (see e.g. [50, 51]). We doubt that such an effort can really lead to a conceptual scheme which can produce novel models and a deeper understanding of physical phenomenology, unless it is reduced to a rephrasing of the principle of virtual work.

To make our opinion clear, in this context, we believe it is enough to quote a statement by D'Alembert:

forces relative to bodies in motion are obscure and methaphysical entities which can only spread shadows on a science which, otherwise, is crystal clear in itself

(D'Alembert, *Traité de dynamique* (1743) p.XVI)

[15] This refusal was based on the (doubtful) persuasion that generalized continuum models were not logically consistent with the second principle of thermodynamics (see [55], and for a detailed discussion on this subject [32–35]).

[16] And carefully studying the work [56].

8.3.2 Occam's Razor Originated in Hellenistic Science

Here, we make a small digression. The principle of virtual work is not the only scientific principle which has its roots in Hellenistic science. We briefly refer here to what is argued in greater detail in [46].

Aristotle (in his *Posterior Analytics* [52]) writes

We may assume the superiority, ceteris paribus [other things being equal], of the demonstration which derives from fewer postulates or hypotheses.

While Ptolemy stated (see [53]),

We consider it a good principle to explain the phenomena by the simplest hypothesis possible.

Then, the Hellenistic tradition was simply transmitted by John Duns Scotus (1265–1308), Robert Grosseteste (1175–1253), and Maimonides (Moses ben-Maimon, 1138–1204) to modern scientists. Again in [53], one finds the sources which allowed Duns Scotus to state that: "Phrases such as 'It is vain to do with more what can be done with fewer' and 'A plurality is not to be posited without necessity' were commonplace in 13th-century scholastic writing."

8.3.3 What It Does not Mean?

However, slogans can be misunderstood and misinterpreted. In the history of science it has been observed that some scholars can even manage to completely twist the original meaning of slogans to convey the opposite idea. For this reason, a slogan must be intended to be a kind of "abstract" of a fully developed corpus of knowledge, which has to be taught and understood in its completeness. In the context of the theory of generalized continua, there is a tendency towards a very limited interpretation of the slogan *Pluralitas non est ponenda sine necessitate* which must be discussed.

For instance, the considered class of deformation energies in the literature have been drastically limited. Such limitations cannot be dismissed a priori, since the excercise of examining which of the possible performances of materials belong to a specific particular class could be inherently interesting. However, it is not possible to invoke the principle of parsimony for stating that complex constitutive equations are useless or, worse, that the use of too many constitutive parameters is like adding epicycles (see Chapter 3).[17]

The principle of parsimony must be applied to the choice of the fundamental postulates of a theory, but not for limiting a priori the number of materials parameters. Limiting this number is appropriate only when dealing with certain subclasses of materials. In general it is not possible to limit the number of parameters which one has to use for an arbitrary material. (This is even more clear when considering the so-called metamaterials, where constitutive equations are decided by the modeler)!

[17] Obviously the experimental characterization of the material benefits from the reduced number of constitutive parameters (see e.g. [94]). The drawback of this reduction is a more likely poorer description of diverse experiments.

Why should there be a restriction for modeling complex phenomena with oversimplified models? This wish is bound to remain a vain hope, as the intrinsic complexity of a physical system cannot be ignored when looking for a mathematical model suitable to predict its behavior. While the number of parameters reflects the richness of possible behaviors, this richness cannot be simplified if one wants to describe reality. On the contrary the number of basic principles to be used when formulating a model must be reduced to a minimum. Unfortunately, the misguided champions of simplicity, instead of appropriately using Occam's razor for reducing the number of basic assumptions,[18] assume that it is possible to use it for (arbitrarily!) reducing the number of needed parameters. They want to impose this reduction simply because these parameters need new theoretical and experimental efforts for being determined. It is as if, after having discovered that the Poisson's ratio was not the one predicted by Navier micro-macro identification (see e.g. [2]), instead of proceeding with the Green–Lamé reasonings and the Saint-Venant solutions for determining Young's modulus and Poisson's ratio with the needed experimental measurements, the scholars of the nineteenth century had decided to ignore "superfluous" theoretical information and to continue surviving with its only available value, as other values were difficult to determine.

One cannot decide to give up the complexity needed to model complex systems simply because with the available theoretical analysis and experimental evidence it is not possible or too difficult to determine the needed parameters. The described extravagant attitude has a cause: many objections to generalized continua theory were raised by those who believed that simplicity means a small number of constitutive parameters and, therefore, the extravagant scholars chose to study those generalized continua which are characterized by few non-classical elastic moduli. Why should we be ready to accept 21 first gradient elasticity parameters and be afraid of many second gradient ones? If we want to capture complex internal interactions, such a richness is unavoidable. On the contrary, one must find a postulation scheme which equally applies in formulating models for both first and second gradient continua, and also all kinds of generalized continua (see [24, 25, 27–29]). The principle of virtual work gives a unique and efficient conceptual scheme for all mechanical theories without involving any thermodynamical concept (this point is discussed also by Piola, when dealing with Fourier heat theory, see [24]) and without needing any ad hoc adaptation.

In the history of mechanics we can find a clear example of a similar dispute. While looking for a model aimed at the description of planetary motion, Ptolemaic aproaches introduced for every planet: eccentrics, equants and epicycles. All these ad hoc concepts were introduced to simplify the calculation procedures, as ancient analog computers were based on controlled circular motions. The Jesuits opposing Galileo and Copernicus

[18] And this can be done very elegantly by postulating a form of the principle of virtual work instead of postulating many balance laws or, worse, by postulating some ad hoc modifications of already known equations, basing these modifications on "physical sense" or "physical intuition." This is what seems to have been done often in generalized continua theory: the reader is referred e.g. to the controversy described in [92–94].

claimed to prefer Ptolemaic models as "they needed fewer parameters" i.e. physical constants and degrees of freedom.[19]

Instead, Laplace's approach for the description of the solar system involved complex coupled interactions,[20] used $3N$ degrees of freedom (with N the number of considered planets), and the mass of each planet, together with the universal constant of gravitation. However, the Laplacian system is based on one basic principle only. It does not need any ad hoc adaptation and it is applied systematically to deduce all the predictions about the motion of planets.

Galileo could not fully rebut the objections of Jesuits, as his model was not as sophisticated as the one later put forward by Laplace, and his appeal to Occam's razor was considered inappropriate by many of his opponents. The final success of the Laplacian planetary model was established when it allowed for the discovery of not yet observed planets. On the other hand, the ad hoc Ptolemaic model could only describe the already observed motion of a known planet and, by no means, could it predict the existence of a not yet observed planet. Moreover eccentrics, equants and epicycles of a new planet must be found by trial and error, and cannot be forecast a priori based on some fundamental principles.

Do we need an economy of thought or an economy of parameters? We must avoid the wrong application of Occam's razor also in formulating generalized continua theories.

8.4 Lex parsimoniae: "Law of Parsimony." Balance Laws or Variational Principles for Generalized Continua?

The beautiful encyclopedia article by Hellinger (see [38]) is based on a precise objective: to show how to use the principle of virtual work to get a unifying vision of all field theories. Hellinger manages to describe (in 1913!), among others, the concept of higher gradient continuum models. In a few pages, exploiting the elegance and effectiveness of this principle, he gathers the most important and relevant results available in his époque (see [32–35]). In [44] Truesdell, having been induced by his co-author to discuss variational principles,[21] writes negative evaluations of Hellinger's effort, and states that, in general, the variational principles should be avoided in the postulation process of continuum mechanics. It is ironic, however, that many scholars learned about such a variational principle while reading such negative comments. In the later treatise [45], there is absolutely no mention of any form of variational principles.

Let us make our point of view clearer. Our aim here is to discuss more technically the meta-problem of determining the procedure for formulating mathematical models designed to describe natural phenomena and to predict their evolution. We look for an epistemological criterion guiding us in this formulation.

[19] The Ptolemaic model, as many modern computation softwares, was used too often without knowing the fundamental theory on which it had been based: each planet was studied independently of the others.

[20] Our knowledge of Hipparchus' contributions to the subject is too fragmentary for considering him as the founder of this theory (see [21]).

[21] Also the choice of the title of their treatise was influenced by Hellinger's title, see [54].

8.4.1 La Cin'ematique d'Abord!

As discussed in more detail in the Chapter 3, one must keep in mind that the ontological status of mathematical entities is very different from that of physical objects. With a slogan: the equations of *Elastica* are not a physical beam![22]

One finds equations when one models phenomena exhibited by physical systems. These equations determine and characterize mathematical objects. Once the equations obtained by means of a model are solved, then one has to translate these solutions into predictions which forecast the behavior of the described physical system. If the predictions correspond to the evolution which is observed in experiments, then the model can be deemed reliable. An important warning needs to be reasserted here: a model can describe only a limited set of phenomena. A model focuses only on a specific class of physical objects and only a specific class of their possible evolutionary behaviors.

A first step in the above-mentioned (and needed) focusing process consists in establishing the postulated kinematics for the considered model.

As we have remarked before, in the literature dealing with continuum mechanics one finds two competing postulation schemes, which we will describe below. The first postulation scheme is based on balance laws, the second on variational principles. For both postulation schemes, a modeling procedure is needed for defining the (described) kinematics of deformable bodies.[23] In order to compare the two approaches, let us assume here that in both the postulations[24] the same kinematics concepts are introduced as a first step in the modeling procedure.

Then, let us assume that the set of fields $\Psi = \left\{\Psi_\sigma(x_\mu); \sigma = 1, ..n, \mu = 1, 2, 3, 4\right\}$ constituted by n tensor fields defined on $\mathbb{B} \times [t_0, t_f]$, is specified and the physical interpretation of these fields is clearly characterized (see Chapter 3) we denote a suitably regular subset of the Euclidean three-dimensional space $\mathbb{E}^3$ which models a reference shape of the considered physical body, while the deformation phenomenon is observed in the time interval $[t_0, t_f]$.

In a formal mathematical way it is possible to state that the **space of configurations** used to model the set of possible states of the considered physical system is thus specified precisely. The space of configurations is the set of all Ψ which are considered admissible.

8.4.2 Balance Approach

The generic admissible configuration Ψ is a collection of fields which includes the placement field and other fields whose determination is needed for specifying the state

[22] This is an important warning as sometimes scholars confuse a physical object with the mathematical model used for describing it.

[23] However, some textbooks are based on the extremist idea (possibly due to Cauchy, see [57]) that the balance of force is even more fundamental than the kinematical description of a mechanical system. In these textbooks one finds that the concept of stress is defined before the concept of strain. Such an approach in a variational postulation is simply inconceivable.

[24] Incidentally, in [49] the presented postulation is based on balance laws, but the kinematics is studied before these laws. Therefore one cannot criticize our showing a biased version of the postulation scheme which we oppose.

of the considered system. The physical interpretation of each of these fields must be specified when the continuum model is formulated.

In some mechanics schools (see e.g. [49]) one postulates, in order to find the evolution equation pertinent to the field Ψ_σ, a balance law for the generic physical quantity σ in the form:

$$\int_{\partial S} D_\sigma \cdot N_{\partial S} + \int_S d_\sigma = 0, \tag{8.1}$$

which is assumed to be valid at very time instant, and for every sub-body $S \subset B$ having a sufficiently regular boundary ∂S with normal $N_{\partial S}$. In the balance law (8.1), D_σ and d_σ are, respectively, the surface flux and volume production of σ, which are to be chosen via suitable constitutive equations, given in terms of the local values of the whole set of the kinematic fields Ψ.

The previous balance equation is usually formulated in the so-called Eulerian description, i.e. in the actual configuration of the considered continuum. However, with a simple change of variable in the involved integrals one can reformulate it in the Lagrangian, or referential, description.

By a standard localization procedure one finds the associated partial differential equations valid, at every time instant, in the interior of B:

$$\mathrm{Div} D_\sigma + d_\sigma = 0. \tag{8.2}$$

On the boundary of B one must assume applying an external interaction per unit area D_σ^{ext}, extracting out or pumping in the physical quantity σ: D_σ^{ext} is assumed to be known as a function of the local values of the fields Ψ. This assumption, via a standard continuity argument, produces the boundary condition

$$D_\sigma^{\mathrm{ext}} = D_\sigma. \tag{8.3}$$

Very often one reads that, in order to formulate correct boundary conditions one needs a "physical insight" of the problem, and that they are dictated by the studied phenomenology. This is clearly a way for stating that also boundary conditions are to be postulated, independently of the other assumptions made.[25]

In [58] the equations (8.2) are postulated directly, one by one, together with the corresponding boundary conditions (8.3). Finally, we note that d_σ includes all kinds of inertia forces to be attributed to the quantity σ.

Clearly, the set of equations (8.2) and (8.3) (or equivalently (8.1), which must be postulated for every regular sub-body $S \subseteq B$) is not sufficient to determine well-posed mathematical problems. Therefore the postulation based on balance laws must be completed by assuming a set of constitutive equations. Of course, this choice cannot be completely arbitrary. As a consequence, even in the study of purely mechanical models, the entropy inequality is introduced [45], which is considered as a tool for selecting among constitutive equations those which are physically admissible. Such an approach was criticized from an epistemological point of view by Gabrio Piola (see [24]), who

[25] It is a constant response of every scholar who assumes the balance postulation to ask about the physical basis and meaning of boundary conditions, when one deduces them from variational principles.

stated that it would be preferable to base the study of mechanical phenomena on principles which do not involve other extraneous phenomena. It seems to us that, while formulating the basic equations of continuum mechanics, Piola systematically invokes the need for using the Occam's razor.

8.4.3 Principle of Least Action

We describe now the most fundamental variational postulation scheme which can be found in the literature. Some scholars simply refuse to consider it because, they claim, it cannot describe dissipative phenomena. We ask the reader to be patient and to allow us to show how this postulation scheme has been conceived and then we will demonstrate how it can be suitably generalized and/or adapted to include dissipative phenomena.

A synthetic flow chart sketching the procedure to be followed is as follows:

1. To choose a set of mathematical objects which seems the most suitable for specifying the state of the considered physical systems: this is the chosen set of kinematical descriptors used, also called **the space of configurations**.
2. To limit attention only to those **motions which are physically admissible**, i.e. to determine the set of regular functions mapping time instants into the set of configurations which are postulated to be capable of describing the evolution of the studied phenomena.
3. To postulate the form of an ***action functional***. This functional has to be minimized in the set of admissible motions, in order to find the mathematical predictions that are capable of forecasting experimental evidence.

In other words: the formulation of a mathematical model has to begin with a determination of the space of configurations, then one considers time sequences of configurations: i.e. motions; finally, one conjectures that there is a quantity which Nature wants to minimize. This is done by choosing the action functional which seems the most suitable. More formally:

- We denote the set of **possible configurations** by C, and a generic **motion** is a smooth function having values in C defined on the time interval $\left[t_0, t_f\right]$.
- Not all of these motions are admissible as, for instance, the presence of some constraints will make in admissible some elements from the set of possible motions: we will denote the set of all **admissible motions** by M_A.
- An **action** is a real-valued functional, having as domain M_A, which we assume to be capable of telling us the "preferences" of Nature. Indeed, we assume that the motion to be considered in order to predict the evolution of the modeled system is a minimizer of the chosen action.
- It is clear that, in order to define precisely the concept of minimizer of a functional, one has to specify the domain in which this minimizer must be looked for. Following Lagrange (see also Chapter 4), in the principle of least action we choose to minimize the action functional in the set of admissible motions which are also **isochronous**. In other words, we assume that the action has to be

minimized among motions starting at the instant t_0 from a specified configuration Ψ_0 and arriving at the instant t_f at another specified configuration Ψ_f. We will denote by $M_A(\Psi_0, \Psi_f)$ the set of isochronous admissible motions.

It is possible, having suitable computing tools, to stop the theoretical development of the model at this stage. Indeed, after having postulated an "effective" action functional, one simply needs to find its minima: and such a search is made possible by means of modern computers using suitable numerical codes.

Actually one has only to decide, by considering the specific postulated action functional, which is the numerical integration scheme more suitable to get those previsions which are essential to supply a reliable theoretical guide for every experimental, technological or engineering activity. However, when more qualitative and theoretical general properties of the formulated models are investigated (and when modern computing tools are not available), it is possible to proceed further in the analysis of the model as follows:

1. one can impose **a stationarity condition** on the action functional, and therefore determine its **associated Euler–Lagrange conditions**, which include boundary conditions and some local conditions on the kinematical fields, which are usually partial differential equations (PDEs); these stationarity conditions mean that the first variation of action must vanish for every small variation of motion, which starting from a physically admissible motion leads to a varied motion which is still physically admissible (we also call such variations of motions **physically admissible);**
2. one can try to find an interpretation of the thus found Euler–Lagrange condition which accomodates physical intuition: such an interpretation may lead us to recognize them as a form of **balance laws in which suitable constitutive equations are replaced**;[26]
3. one can try to find analytical solutions for initial and boundary problems for the determined PDEs.

Clearly, in the époques in which computational tools were not very well developed,[27] the only reliable method for getting predictions was the analytical one, and many scientists invested all their intelligence into pushing the frontiers of mathematical knowledge forward to get as many closed form solutions as possible.[28]

The advent of modern and effective Von Neumann machines has very often made the second group of three steps above redundant. It is somehow surprising that one of the

[26] The reader is however warned that higher gradient action functionals, see e.g. [10, 26], may lead to more boundary conditions for the same bulk equation. In this case, if one really needs to interpret Euler–Lagrange equations as balance laws, then one has to accept that the same balance law may associate with its localized (differential) form many boundary balances. This will induce another proliferation of ad hoc assumptions.

[27] Note, however, that analog computers have already been developed and used by the Hellenistic scholars, as Ptolemaic systems of moving circles must be regarded as one of the first analog computers, see [21].

[28] Exemplary efforts in this direction were performed by the Soviet school. For instance, the textbook by Muskhelishvili is one of the most famous sources of analytical solutions in the theory of elasticity (see [59]). Note that these solutions are very useful as benchmarks for testing numerical codes.

most passionate champions[29] of non-linear continuum mechanics could not forecast the impact that these machines could have in the growth of its applications to real world problems. All these applications are simply inconceivable if one decides to use exclusively closed form solutions.

8.4.4 How Can We Include Dissipation in the Modelling? The Rayleigh–Hamilton Dissipation Functional

Even if one can model some dissipative phenomena by using a least action principle (see for some interesting examples [64]), it is debatable if this principle is general enough for formulating all the models which are needed in mechanics. Since, at least, in the works by Lagrange and Piola (see [15, 27, 29, 30]) the possible controversies have been avoided by formulating a weaker version of it, i.e. the principle of virtual velocities, later called the principle of virtual work. The beautiful postulation of continuum mechanics by Paul Germain (see [13, 56]), is very similar to those used by Sedov, Toupin, Mindlin and Rivlin, among many others (see [28]), and is exactly based on the principle of virtual velocity (or virtual work). Note that this principle, in its modern form, was proposed by D'Alembert exactly to try avoiding the mentioned debates.

To include dissipative phenomena in the picture it is possible to proceed as follows (following Lagrange and D'Alembert):

1. describe only the conservative part of a phenomenon by an action functional;
2. then, calculate the first variation of the postulated action, which is interpreted as the Lagrangian[30] part of the virtual work expended on admissible variations of motion superimposed on the real motion;
3. together with the thus found first variation, additional linear[31] functionals must be postulated, which are defined on the same set of virtual velocities: **these functionals are conceived to model dissipative phenomena** by introducing the virtual work which they dissipate on every admissible variation of motion; they are suitable definite positive functionals and are called **Rayleigh dissipation functionals**;
4. the sum of the Lagrangian virtual work and of the dissipative virtual work is postulated to be vanishing for every physically admissible variation of motion (**Hamilton–Rayleigh Principle).**

We will mathematically formulate the just discussed postulation procedure in the following sections, and we will present it in a rather general way in the Section 8.6 of this chapter. A careful inquiry into the historical development of continuum mechanics (see e.g. again [28, 29, 61, 62]) shows that this procedure is exactly the one which has been followed in the pioneering work by Lagrange, Piola, Hamilton and Rayleigh.

[29] See [60]: it is, however, worthwhile in this context, to repeat that Truesdell did not consider variational principles as an important subject in continuum mechanics.

[30] Which is not necessarily conservative, as, for instance, the Lagrangian density of action could be time dependent.

[31] Some scholars objected that in this way one is not considering nonlinear systems (sic!).

The logical connection between the principle of least action and the principle of virtual velocities clearly justifies the choice of classifying this last principle in the set of variational principles.

The procedure of integration by parts which produces mathematically the required consistent boundary conditions is applicable in exactly the same way for models formulated by using either the principle of least action or the principle of virtual velocities.

The following remarks are appropriate here:

- Although we have already discussed the subsequent issue in many places, we feel a reiteration here is warranted for emphasis and clarity. Indeed, the opponents of generalized continuum theories sometimes state not only that these theories lack logical consistency with the second principle of thermodynamics (see the literature originated by [55]) but also claim at the same time that the boundary conditions to be chosen for generalized continua are physically meaningless and are mathematically inconsistent. Their statement is related to the mistaken belief that Cauchy treatment is universally valid for all materials, and not to the fact that the treatment of boundary conditions due to Cauchy is not universally valid and applies only to a particular constitutive class of materials.
- As a matter of fact, (this is a point of view elegantly presented by Hellinger, see [32–35, 38], but also in [62]) variational principles, as a heuristic tool for effectively finding the most predictive mathematical models present many advantages. Among others, preeminent is their capability to deduce the boundary conditions which are most appropriate for a given constitutive class of materials. What happens is that if one does not want to use a variational principle, it can be nearly impossible[32] to determine the class of boundary conditions logically consistent with those bulk evolution equations which it was decided to postulate independently (see *Pluralitas non est ponenda sine necessitate*, Section 8.3). Instead, purely on logical bases, variational principles lead systematically to well-posed mathematical problems, if the postulated functionals are well-behaving.
- Let us now call Lagrangian systems those systems whose evolution is governed by a least action principle. Obviously (see the characterization given by Helmholtz conditions as discussed e.g. in [63]), not every system of ordinary differential equations or of partial differential equations (with appropriate boundary conditions) can be regarded as a stationarity condition for an action functional. This circumstance has led many scholars to conclude that dissipation phenomena cannot be described by means of a least action principle. In some ways this is, in a strict sense, true. However, it has been conjectured that a dissipative system of evolution equations can always be regarded as a system which is approximating and/or simplifying another one which is Lagrangian. This is still a controversial question, and here we will simply give some conjectural hints concerning the solution of the related mathematical problems. One could obtain a non-Lagrangian system starting from a Lagrangian one by using, at least, two specific procedures: i) by neglecting some terms in the original Lagrangian action functional, thus

[32] Unless the correct result, which has been obtained using other methods, is already known.

obtaining an "approximation" which is not Lagrangian,[33] ii) by noting that the non-Lagrangian system actually is a subsystem of a larger system which has many more degrees of freedom and is itself Lagrangian. Dissipative phenomena may in this case only be apparent (see [1]), as the energy which is apparently dissipated may be trapped in the hidden degrees of freedom and return to the visible degrees of freedom only after the elapse of the Poincaré time, which may be very large.

We finally note that the statement: "a variational principle can be used only for non-dissipative systems" has frequently been disproved in the literature: we cite here for instance [12], dealing with crack opening phenomena. As in the literature it is not clearly established if the least action principle can or cannot encompass all "non-conservative" phenomena, to make this presentation expedient, **we assume a postulation based on the Hamilton–Rayleigh principle**, which allows for a unified treatment of dissipative and non-dissipative systems. We consider it appropriate to classify the Hamilton–Rayleigh principle as a variational principle, although in the literature this choice is sometimes disputed. We will follow what seems to us the preference of those who appear to be the most authoritative scholars. Therefore, it is appropriate to describe as "variational" the postulation schemes based upon the principle of virtual work or on the Hamilton–Rayleigh principle, and not limit the use of this adjective to the models based exclusively on the least action principle.

8.5 More about Action Functionals

Lagrange was one of the first to give, in his *Mécanique Analytique*, some historical remarks about theoretical mechanics preceding a technically complex and deep textbook. As a consequence, the great majority of textbooks in calculus of variations and/or in variational and energy principles in applied sciences (see e.g. the beautiful text by Lanczos [16]), begin and/or are concluded with some historical considerations and discussions. In the present text[34] we have followed this tradition, interweaving the historical reconstructions throughout the discussions in a diffused manner while presenting the subject.

We believe that the fundamental idea underlying the principle of least action is very old and, possibly, dates back to Hellenistic science (see [21]). We have found (see [41]) a quote from some fragments of an Epicurean philosopher:

For this would be agreed by all: that Nature does nothing in vain nor labours in vain.
Olympiodorus in Commentary on Aristotle's Meteora
as translated by Ivor Thomas in the Greek Mathematical Works Loeb Classical Library;

[33] A typical example is given by the Cattaneo equation for heat propagation which, after some approximation, becomes the classical Fourier equation for diffusion (see again [64]).
[34] Hopefully the reader will not be too averse to this choice!

which could be one of the ancient sources of the famous other quote:

La nature, dans la production de ses effets, agit toujours par les voies les plus simples.
Pierre de Fermat. [35]

As the second quote has been used to justify from a higher philosophical viewpoint the formulation of variational principles, and as the Epicurean school is known to have produced important scientific contributions in theoretical mechanics, we conjecture that Olympiodorus (see his quote above) formulated a version of the least action principle.

8.5.1 Lagrangian Action as a Measure of Simplicity in Nature

The structure of the least action principle needs to be clarified, as all other variational principles are formulated by generalizing its formal structure. We, therefore, must describe at first how, based on the principle, a stationarity condition was found, and how it was used to solve specific problems, thus formulating the equations to forecast "real motions."

In the entries [98], the formal definitions required to present the modern structure of the corresponding mathematical theory are presented in a precise and concise way. There, it is seen that the space of configurations is a topological space further endowed with the structure of a manifold with charts in Banach spaces.[36] However, in the following pages we prefer to present a generalization of Lagrange's and Piola's results without invoking such mentioned sophisticated concepts. Indeed, in order to be correct from a historical point of view, it has to be stated explicitly that Banach (or Fréchet) spaces were invented long after the masterpieces by Lagrange and Piola were written. Therefore, in these masterpieces the concepts of Fréchet and Gateaux derivatives in Banach spaces were applied long before their explicit formulation. As Lagrange and Piola could master and use the underlying basic concepts and successfully proceed in their investigations we will follow their steps.

Simplicity of the Nature action means that: "the motion minimizes the Lagrangian action."

In the discussion up to now, neither has a mathematical structure been assumed for $M_A(\Psi_0, \Psi_f)$ nor the form of the action functional been specified. On the other hand, in order to produce predictions, it is necessary to calculate the solutions of the minimization problem for the postulated action. Therefore, some further elaborations about the action functional are clearly needed. To proceed further, similarly to what is done in [17] and [18], we follow Lagrange [15, 30], and we limit our attention to a particular class of functionals defined on $M_A(\Psi_0, \Psi_f)$. More precisely, we assume that a Lagrangian action density function (see the following formula (8.4)) is defined and that action can be calculated as its space-time integral (see the following

[35] For a detailed analysis of the sources of this quote (*Nature, in the production of its effects, always acts in the simplest ways*.) and also for a very lucid analysis of the history of the calculus of variations we refer to the beautiful book by Freguglia and Giaquinta [66].

[36] Although even more abstract settings have been conceived, which may be useful in some applications, we can content ourselves with this degree of generality.

formula (8.5)).[37] Such particular action functionals are usually called Lagrangian functionals.

Let $\Psi_\sigma(x_\mu)$ be any set of n tensor fields defined on $\mathbb{R}^m$, with $\sigma = 1, \dots n$ and $\mu = 1, 2, \dots, m$. As the reasoning which will be developed holds for fields defined in higher dimension spaces, we will not immediately limit our considerations to the case $m = 4$.

The **Lagrangian action density** is a function of the form:[38]

$$\mathfrak{L}\left(x_\mu, \Psi_\sigma, \frac{\partial \Psi_\sigma}{\partial x_\mu}\right), \tag{8.4}$$

and the corresponding **Lagrangian action functional** has the form:

$$\mathfrak{A}(\Psi_\sigma(\cdot)) = \int_T \mathfrak{L}\left(x_\mu, \Psi_\sigma, \frac{\partial \Psi_\sigma}{\partial x_\mu}\right) dV, \tag{8.5}$$

where $T \subset \mathbb{R}^m$, dV is the Lebesgue measure, and the coordinates x_μ are used to label the generic point x in T.

- We will assume below that T is compact and that its boundary is suitably regular: Lipschitz continuous, for instance. In this case one is assured that i) the set $C^\infty(T)$ of infinitely differentiable functions defined in T can be endowed with the Fréchet metric (see e.g. [67, 68]), and ii) it is possible to define the trace of the functions belonging to Sobolev spaces (see e.g. [69]).

Following tradition we denote the dependence of the action functional $\mathfrak{A}$ on the fields Ψ_σ by introducing the symbol $\mathfrak{A}(\Psi_\sigma(\cdot))$, which indicates that its value depends on the whole fields and not on their values at a specific point x having coordinates x_μ.

To use differential calculus in order to define continuity of the Lagrange action functional, it is obviously necessary to introduce a topological structure in M_A: this is equivalent to specifying mathematically the meaning of the expression: "two motions are close". Moreover, it is necessary to calculate minima of the introduced functional, typically, by calculating its first variation and by imposing that this variation is vanishing. Further, the following mathematical concepts:

- finite variation of the independent variable;
- first variation of a functional;
- order of infinitesimals for remainders in Taylor expansions for a functional and the consequent concept of infinitesimal variations;

introduced in classical mathematical analysis (dealing with functions defined in a subset of $\mathbb{R}^k$), can be generalized to the present context, where the domain of the action functional is the set of motions M_A.

[37] In order to compare the discrete and continuous cases see Chapter 4

[38] The case in which higher gradients of fields appear in the Lagrangian action density will be considered later.

8.5.2 Variation of the Action Functional

A necessary condition for a motion to be a minimizer of the action is that the first variation of the action, as calculated in correspondence of the motion, is vanishing. It is therefore necessary to define and calculate the first variation of Lagrangian functional.

A motion minimizing the action has to be searched for among the motions for which the first variation of the action vanishes.

The method for finding the necessary conditions to be fulfilled by a motion in order for it to be a minimizer of a Lagrangian functional was conceived by Lagrange when he was only 19 years old, and it was used systematically in all his long scientific career (see [2] and the last chapters of [30]). These necessary conditions consist in a system of differential equations complemented by some boundary conditions.[39] They are called **Euler–Lagrange conditions** relative to the considered action functional.

We may assume that the set of functions M_A in which we are seeking the minimizers of action is such that its constituting functions have an assigned value on a part $\partial_d T \subseteq \partial T$ of the boundary of T. These boundary conditions are called "essential" boundary conditions, as they are assigned a priori in the formulation of the minimization problem.

We now consider the variations $\varepsilon\eta_\sigma(x)$ of the considered fields $\Psi_\sigma(x)$ (ε will be assumed soon to be small):

$$\tilde{\Psi}_\sigma(x) = \Psi_\sigma(x) + \varepsilon\eta_\sigma(x), \tag{8.6}$$

where the functions $\eta_\sigma(x)$ are called **virtual variations** of the fields $\Psi_\sigma(x)$: they must be such that both $\Psi_\sigma(x)$ and $\tilde{\Psi}_\sigma(x)$ belong to the set M_A of admissible fields. In addition, virtual variations must be vanishing on $\partial_d T$. These are the only restrictions to be assumed for the virtual variations, which are otherwise completely arbitrary.

Many scholars have shown a certain resistance to the concept of virtual variations.[40] Again, they claim that this is an unphysical concept. In [22], the reader will find a beautiful presentation of the Hellenistic roots of this concept, and will surely appreciate its physical content, as understood already by Archimedes.

Instead of referring to any kind of physical understanding, we can here remark that, in order to verify that a given motion is a (possibly local) minimizer of the action, the value of the action must increase if another motion, close to the minimizer, is considered. If the minimizer is $\Psi_\sigma(x)$, then for every $\tilde{\Psi}_\sigma(x)$ obtained, varying it with whatever variation $\varepsilon\eta_\sigma(x)$ (ε being small enough), we have that

$$\mathfrak{A}(\Psi_\sigma(\cdot)) \leq \mathfrak{A}(\tilde{\Psi}_\sigma(\cdot)).$$

[39] The derived conditions are ordinary differential equations for discrete systems and partial differential equations for continuous systems. Obviously boundary conditions are obtained only for continuous systems.

[40] The choice of the word "virtual" may have induced these scholars to believe that these variations are not "real," therefore "not physical." We will investigate the sources of the presented theory to try to discover who first introduced this nomenclature and how he justified it.

Therefore, for the considered varied fields, the finite variation of the action functional must fulfil the inequality:

$$\Delta\mathfrak{A} = \int_T \mathfrak{L}\left(x_\mu, \tilde{\Psi}_\sigma, \frac{\partial\tilde{\Psi}_\sigma}{\partial x_\mu}\right) - \int_T \mathfrak{L}\left(x_\mu, \Psi_\sigma, \frac{\partial\Psi_\sigma}{\partial x_\mu}\right) \geq 0. \tag{8.7}$$

The definition of first variation of the Action functional is given by

$$\Delta\mathfrak{A} =: \delta\mathfrak{A} + O\left(\varepsilon^2\right), \tag{8.8}$$

where we assume that $\delta\mathfrak{A}$ depends linearly on the variations $\varepsilon\eta_\sigma(x_\mu)$, and therefore

$$\delta\mathfrak{A} = O(\varepsilon).$$

By expanding the Lagrangian action density into the integral in (8.7), we get

$$\delta\mathfrak{A}(\eta_\sigma(\cdot)) = \varepsilon \int_T \sum\nolimits_\sigma \left(\frac{\partial\mathfrak{L}}{\partial\Psi_\sigma}\eta_\sigma + \sum_{\mu=1}^{m} \frac{\partial\mathfrak{L}}{\partial\left(\partial\Psi_\sigma/\partial x_\mu\right)}\frac{\partial\eta_\sigma}{\partial x_\mu}\right). \tag{8.9}$$

- The functional $\delta\mathfrak{A}$ is defined in terms of the set of admissible variations, and it is usually assumed to be a continuous functional in this variable. Using the language of functional analysis, the functional $\mathfrak{A}$ is continuous and Fréchet differentiable.[41]
- We will assume that the set of infinitely differentiable functions $C^\infty(T)$ is included in the set of admissible variations.
- Moreover, we will assume that its inclusion in the space of admissible variations, when $C^\infty(T)$ is endowed with the Fréchet metric d_F, is continuous. This request implies that the functional defined in (8.9), once restricted to the metric space $(C^\infty(T), d_F)$, defines a distribution in the sense of Schwartz (see [70]).
- Following the definition given by Schwartz, Eq. (8.9) defines a distribution of order 1: i.e. a distribution which can be represented as the first derivative of a measure. Theorem XXVII on page 91 in [70] states that, for a generic distribution D with compact support, there exists a finite natural number N such that D is an Nth order derivative of a measure. This circumstance strongly motivates the introduction of field theories in which the Lagrangian depends on Nth order field gradients (see [7, 8, 10] for more details).

Now, we assume that the Lagrangian density $\mathfrak{L}$ and the fields which are minimizing the action are regular enough to perform integration by parts of the RHS of (8.9). The reader aware of the basic ideas of the theory of distributions will recall that it is always possible to calculate the (weak) derivative of a distribution, and therefore that integration by parts in the sense of distributions is always possible. This circumstance will be exploited below, and will render the use of space of distributions the most appropriate choice for framing the study of the properties of action functionals.

[41] If the space of configurations is a Fréchet manifold, then continuity of the functional $\mathfrak{A}$ can be defined as there is a topology defined in it. Also its derivative is defined because of the local topological vector space structure. The interested reader is referred to [67, 68].

Proceeding as if we were apparently unaware of the existence of the concept of distribution, and therefore following the steps of Lagrange, we integrate by parts the RHS of Eq. (8.9) and use the fact that η_σ is vanishing on $\partial_d T$, so obtaining:

$$\delta\mathfrak{A} = \varepsilon \int_T \sum\nolimits_\sigma \eta_\sigma \left(\frac{\partial \mathfrak{L}}{\partial \Psi_\sigma} - \sum_{\mu=1}^{m} \frac{\partial}{\partial x_\mu} \left(\frac{\partial \mathfrak{L}}{\partial \left(\partial \Psi_\sigma / \partial x_\mu \right)} \right) \right) + \varepsilon \int_{\partial T / \partial_d T} \sum\nolimits_\sigma \eta_\sigma \sum_{\mu=1}^{m} \frac{\partial \mathfrak{L}}{\partial \left(\partial \Psi_\sigma / \partial x_\mu \right)} N_\mu, \tag{8.10}$$

where $\partial T / \partial_d T$ is the set difference between ∂T and $\partial_d T$, and where the vector field N_μ denotes, at every point, the external unit normal of $\partial T / \partial_d T$.

It is now necessary to remark that, as a consequence of (8.7), of (8.8) and of the linearity of the functional $\delta\mathfrak{A}$, we obtain that

$$(\forall \eta_\sigma(\cdot))\, (\delta\mathfrak{A}(\eta_\sigma(\cdot)) \geq 0) \Rightarrow (\forall \eta_\sigma(\cdot))\, (\delta\mathfrak{A}(\eta_\sigma(\cdot)) = 0)\,. \tag{8.11}$$

Because of the arbitrariness of η_σ in the obtained stationarity condition, one can deduce that for all values of σ:

$$\frac{\partial \mathfrak{L}}{\partial \Psi_\sigma} - \sum_{\mu=1}^{m} \frac{\partial}{\partial x_\mu} \left(\frac{\partial \mathfrak{L}}{\partial \left(\partial \Psi_\sigma / \partial x_\mu \right)} \right) = 0, \quad \forall x \in T, \tag{8.12}$$

$$\sum_{\mu=1}^{m} \frac{\partial \mathfrak{L}}{\partial \left(\partial \Psi_\sigma / \partial x_\mu \right)} N_\mu = 0, \quad \forall x \in \partial T / \partial_d T. \tag{8.13}$$

The boundary conditions (8.13) obtained as a consequence of stationarity of action functional are sometimes called "natural" boundary conditions.[42]

When inside the domain T there is a discontinuity oriented material surface Σ (whose unit normal field is denoted N_μ) for the derivatives of the fields $\frac{\partial \mathfrak{L}}{\partial (\partial \Psi_\sigma / \partial x_\mu)}$ then, by performing integration by parts on both sides of such a discontinuity, we get

$$\sum_{\mu=1}^{m} \left[\left| \frac{\partial \mathfrak{L}}{\partial \left(\partial \Psi_\sigma / \partial x_\mu \right)} \right| \right] N_\mu = 0, \quad \forall x \in \Sigma, \tag{8.14}$$

where $[|\,(\cdot)\,|]$ is the jump of $(\cdot)$ across the surface Σ. These conditions produce so called "moving boundary conditions" for the considered minimization problem. Some difficulties arise when one wants to get "free moving boundary conditions," and we postpone the presentation of a general treatment which is able to include them.

8.5.3 The Case of Minimizing Motions: Fields Depending on Space–Time ($m = 4$)

The formulas in the previous subsection are valid in the more general case of fields Ψ defined on $\mathbb{R}^{\gtrdot}$. While it is possible to consider, more generally, fields defined on smooth manifolds embedded in $\mathbb{R}^{\gtrdot}$, this generalization does not need any major additional effort, and will, therefore, not be considered explicitly here for simplicity.

[42] Again, we believe that the historical roots of this nomenclature should be investigated.

Let us consider the case $m = 4$, where the kinematic fields depend on the reference space and time coordinates $x = (x_\mu) = (X^1, X^2, X^3, t)$ of each material particle constituting the considered continuum. For the sake of simplicity we assume that the domain T is a 4-dimensional space–time, whose 3D-volume section V is the same for each time instant $t \in [t_0, t_f]$. From now on, we systematically use the notation presented in [26]: in particular, we use capital letters for denoting the coordinates in the reference configuration, and for the indices used to label vector and tensor quantities in the reference configuration. We believe Levi-Civita tensor notation to be indispensable for the clarity of presentation. Clearly, none among the other possible notations which were tried to avoid some of the most cumbersome aspects is efficient enough to deal with the most complicated tensor fields needed in the theory of generalized continua.

In what follows, the set of kinematical descriptors Ψ must include (but in general it does not reduce to!) the placement field χ, which maps the material point $X = (X^1, X^2, X^3)$ into the position $x = (x^1, x^2, x^3)$ which it is occupying at every instant t.

Strong and weak formulations of action stationarity conditions

If we consider isochronous motions as admissible motions, then the **admissible virtual variations of motion** must fulfil on the time boundary the conditions

$$\eta_\sigma(X^1, X^2, X^3, t_0) = \eta_\sigma(X^1, X^2, X^3, t_f) = 0.$$

Also on $\partial_d V$, i.e. on the subset of the boundary ∂V of V, where the essential space-boundary conditions are assigned, we have that

$$\eta_\sigma(X^1, X^2, X^3, t) = 0, \quad \forall (X^1, X^2, X^3) \in \partial_d V, \quad \forall t \in [t_0, t_f].$$

Particularizing to the case of fields depending on space and time, and by using the Fubini Theorem for decomposing space–time integrals (we note again that V is a subdomain of the reference frame and does not depend upon time, thus fulfilling the decomposition hypothesis of the Fubini Theorem), we find that (8.9) becomes

$$\delta\mathfrak{A}(\eta_\sigma(\cdot)) = \varepsilon \int_{t_0}^{t_f} dt \int_V \left(\frac{\partial \mathfrak{L}}{\partial \Psi_\sigma} \eta_\sigma + \sum_{A=1}^{3} \frac{\partial \mathfrak{L}}{\partial \left(\partial \Psi_\sigma / \partial X^A\right)} \frac{\partial \eta_\sigma}{\partial X^A} + \frac{\partial \mathfrak{L}}{\partial \left(\partial \Psi_\sigma / \partial t\right)} \frac{\partial \eta_\sigma}{\partial t} \right) dV. \tag{8.15}$$

- In the case under study, the quantity $\mathfrak{L}$ has the dimensions of an energy per unit volume and, therefore, $\mathfrak{A}(\Psi_\sigma(\cdot))$ is assumed to have the dimensions of [energy][time] or [momentum][length].
- The quantity $\delta\mathfrak{A}(\eta_\sigma(\cdot))$ can be interpreted as the **virtual variation of action** needed for passing from a motion $\Psi_\sigma(\cdot)$ to its varied motion $\Psi_\sigma(\cdot) + \eta_\sigma(\cdot)$.

As a consequence of the statement (8.11), from the principle of least action it is possible to deduce the following **weak condition of stationarity of the action functional.**

For every admissible variation of motion the first variation of action is zero, expressed as:

$$(\forall \eta_\sigma(\cdot)) \quad \delta\mathfrak{A}(\eta_\sigma(\cdot)) = \int_{t_0}^{t_f} dt \int_V \left(\frac{\partial \mathfrak{L}}{\partial \Psi_\sigma} \eta_\sigma + \sum_{A=1}^{3} \frac{\partial \mathfrak{L}}{\partial \left(\partial \Psi_\sigma / \partial X^A \right)} \frac{\partial \eta_\sigma}{\partial X^A} + \frac{\partial \mathfrak{L}}{\partial \left(\partial \Psi_\sigma / \partial t \right)} \frac{\partial \eta_\sigma}{\partial t} \right) dV = 0. \quad (8.16)$$

By simply particularizing the local conditions (8.12), (8.13) and (8.14) we get the following set of local conditions (the index σ is varying in the set $\{1, 2, \ldots, n\}$):

$$\frac{\partial \mathfrak{L}}{\partial \Psi_\sigma} - \sum_{A=1}^{3} \frac{\partial}{\partial X^A} \left(\frac{\partial \mathfrak{L}}{\partial \left(\partial \Psi_\sigma / \partial X^A \right)} \right) - \frac{\partial}{\partial t} \left(\frac{\partial \mathfrak{L}}{\partial \left(\partial \Psi_\sigma / \partial t \right)} \right) = 0, \quad \forall X \in V, \qquad \forall t \in \left[t_0, t_f \right] \quad (8.17)$$

$$\sum_{A=1}^{3} \frac{\partial \mathfrak{L}}{\partial \left(\partial \Psi_\sigma / \partial X^A \right)} N_A = 0, \quad \forall X \in \partial V / \partial_d V, \quad \forall t \in \left[t_0, t_f \right] \quad (8.18)$$

$$\sum_{A=1}^{3} \left[\left| \frac{\partial \mathfrak{L}}{\partial \left(\partial \Psi_\sigma / \partial X^A \right)} \right| \right] N_A = 0, \quad \forall X \in \Sigma. \quad \forall t \in \left[t_0, t_f \right] \quad (8.19)$$

These last conditions are a set of partial differential equations which are verified by sufficiently regular minimizers of action. They represent the set of Euler–Lagrange conditions for stationarity of the action.

Note that:

- The search for solutions to the set of Eqs. (8.17), (8.18), (8.19) verifying the initial and the essential boundary conditions represents the **existence problem of mathematical physics**, as described for instance in [71]. This classical problem is often called the **strong form of initial and boundary conditions problem for partial differential equations**. The adjective ***strong*** is used referring to the fact that, in order to formulate it, the existence of derivatives of unknown fields is required.
- In the strong form of the existence problem of mathematical physics a space divergence operator and a time derivative appear, suggesting that it may represent a law of conservation of a certain quantity. This quantity is sometimes called **the dual in energy** of the physical quantity expressed by the field Ψ_σ. For instance, if the field Ψ_σ coincides with placement, then its dual in energy is what is called *force*, as the product of force with the variation of placement (i.e. displacement) is a work.
- The postulation of mechanics based on Balance Equations starts by assuming a set of conservation laws either in their strong form or in an integral form derived by integrating them and applying to the divergence theorem.

- Many closed form solutions have been obtained for several of such problems. However, the most effective framework in which one can discuss the existence problem of mathematical physics is represented by what is called its **weak form**. Actually, it is possible to prove well-posedness problems for the weak form given in (8.16), while it is sometimes much more arduous to prove similar results while dealing with well-posedness problems in the strong form.
- The last remark suggests another conceptual weak point of the choice of basing postulations of mechanics on balance laws. Even when one starts from such postulations, there is a need to move to a weak form of balance laws, i.e. to a form of variational principle. Therefore, Occam's razor indicates that postulations based on variational principles are preferable.
- Numerical integration methods are based upon the weak form of the existence problem in mathematical physics, further underlining the significance of variational principles. Notably, numerical analysts, generally, view mathematical physics as an interesting source of variational principles.

A condition deduced from the action stationarity condition useful for formulating more general variational principles

The least action principle must be extended if one wants to model dissipative phenomena. We have already outlined (see the previous discussion about this point in Section 4.4) the possibilities which have been explored in the literature. In this section and in the following ones we want to substantiate the previous considerations with some technical details. In order to generalize the least action principle we first investigate some of its equivalent formulations that reveal possible directions towards the desired aim.

We begin by manipulating the term including the time derivative appearing on the RHS of (8.15) by sequentially applying the Fubini Theorem and integration by parts, and considering isochronous variations to find that

$$\begin{aligned}
&\int_{t_0}^{t_f}\int_V \left(\frac{\partial \mathfrak{L}}{\partial\left(\partial\Psi_\sigma/\partial t\right)}\frac{\partial \eta_\sigma}{\partial t}\right) dtdV = \int_V \int_{t_0}^{t_f} \left(\frac{\partial \mathfrak{L}}{\partial\left(\partial\Psi_\sigma/\partial t\right)}\frac{\partial \eta_\sigma}{\partial t}\right) dtdV \\
&= -\int_V \int_{t_0}^{t_f} \frac{\partial}{\partial t}\left(\frac{\partial \mathfrak{L}}{\partial\left(\partial\Psi_\sigma/\partial t\right)}\right)\eta_\sigma dtdV \; + \; \int_V \left[\frac{\partial \mathfrak{L}}{\partial\left(\partial\Psi_\sigma/\partial t\right)}\eta_\sigma\right]_{t_0}^{t_f} dtdV \\
&= -\int_{t_0}^{t_f}\int_V \frac{\partial}{\partial t}\left(\frac{\partial \mathfrak{L}}{\partial\left(\partial\Psi_\sigma/\partial t\right)}\right)\eta_\sigma dtdV\,.
\end{aligned}$$

As a consequence, Eq. (8.15) becomes

$$\begin{aligned}
\delta\mathfrak{A}(\eta_\sigma(\cdot)) = \varepsilon \int_{t_0}^{t_f} dt \int_V \Bigg(\Bigg(\frac{\partial \mathfrak{L}}{\partial \Psi_\sigma} - \frac{\partial}{\partial t}\left(\frac{\partial \mathfrak{L}}{\partial\left(\partial\Psi_\sigma/\partial t\right)}\right)\Bigg)\eta_\sigma \\
+ \sum_{A=1}^{3} \frac{\partial \mathfrak{L}}{\partial\left(\partial\Psi_\sigma/\partial X^A\right)}\frac{\partial \eta_\sigma}{\partial X^A}\Bigg) dV. \qquad (8.20)
\end{aligned}$$

It is useful now to introduce the quantity (with obvious notation)

$$\delta\mathfrak{W}(\eta_\sigma(\cdot,t);t) := \int_V \left(\left(\frac{\partial \mathfrak{L}}{\partial \Psi_\sigma} - \frac{\partial}{\partial t} \left(\frac{\partial \mathfrak{L}}{\partial \left(\partial \Psi_\sigma / \partial t\right)} \right) \right) \eta_\sigma + \sum_{A=1}^{3} \frac{\partial \mathfrak{L}}{\partial \left(\partial \Psi_\sigma / \partial X^A\right)} \frac{\partial \eta_\sigma}{\partial X^A} \right) dV. \tag{8.21}$$

The dimensions of this introduced quantity are those of work. It is expedient to label the quantity as the **"virtual variation of work"** or, shortly, the **"virtual work"** needed at instant t for passing from a motion $\Psi_\sigma(\cdot)$ to its varied motion $\Psi_\sigma(\cdot)+\eta_\sigma(\cdot)$. Needless to say, the virtual variation of work depends linearly on the variation of motion.[43] It has to be explicitly remarked that the **virtual work functional maps virtual displacements** depending on space variables only**,** obtained by blocking the time variable in the virtual variation of motion, **into real numbers**. However, because of its definition, the virtual work functional depends explicitly on the time variable, that is, at different instants we have different functionals. For this reason, in the symbol $\delta\mathfrak{W}(\eta_\sigma(\cdot,t);t)$ the time variable appears twice. By using the definition just introduced, the virtual variation of action can be written in the symbolic form of Lagrange:

$$\delta\mathfrak{A}(\eta_\sigma(\cdot)) = \varepsilon \int_{t_0}^{t_f} \delta\mathfrak{W}(\eta_\sigma(\cdot;t))dt. \tag{8.22}$$

Let us now consider an interesting **consequence of the stationarity condition**

$$\delta\mathfrak{A}(\eta_\sigma(\cdot)) = 0\,, \tag{8.23}$$

which is valid for every admissible isochronous virtual variation η_σ. To do so, we must recall a localization argument which was first developed by Lagrange. This argument has been exploited much beyond the initial intentions which had motivated Lagrange, as it became the conceptual basis of finite element theory and method. It is based on the concept of a *mollifier* which we briefly introduce here for the sake of self-consistency.

(Positive) Mollifiers in the time variable. A function $\zeta(t)$ having as compact support the interval $[-\alpha,\alpha]$ is a mollifier if it is such that

- i) $\zeta(t)$ is infinitely differentiable with respect to the variable t,
- ii) $\int_{\mathbb{R}} \zeta(t) = 1$,
- iii) $(\forall t)\ (\zeta(t) \geq 0)$,
- iv) $\lim\limits_{\alpha\to 0}\ \alpha^{-1}\zeta(t\alpha^{-1}) = \delta_D(t,0)$.

In point iv) of the above definitions, the symbol $\delta_D(t,0)$ denotes the Dirac delta centered in 0, and the limit is in the sense of distributions. The interested reader is referred to [73] for more details.

[43] We want to make this point clear to the supporters of balance postulations, who remain skeptical about variational principles. Obviously, the virtual variation of work DOES NOT depend linearly on the motion, as it depends linearly on the variation of motion. Therefore, the objection that the principle of virtual work, as will be formulated later, seems to be valid only for linear systems is very naive.

By using time mollifiers it is possible to prove that:

If the stationarity condition (8.23) holds then, in every time instant, the **virtual work** vanishes for every admissible (in particular vanishing on $\partial_d V$) variation ξ_σ **(virtual displacement)** which depends on space variables only. Thus, we can state that (8.23) implies:

$$\left(\forall t \in \left[t_0, t_f\right]\right)\left(\forall \xi_\sigma(X^1, X^2, X^3)\right)\left(\delta \mathfrak{W}(\xi_\sigma; t) = 0\right). \tag{8.24}$$

The principle of virtual work (or virtual displacements) states that the motion of a system is characterized by imposing that (8.24) holds.

The principle of virtual velocities is a reformulation of the **principle of virtual work**. The generic virtual displacement is given by $\xi_\sigma = v_\sigma dt$, using the generic virtual velocity field v_σ. If, instead, the virtual velocity is used directly in the linear functional δW, then the formulation of the **principle of virtual powers** is obtained.

With the introduced nomenclature we can state that:

If the virtual work is given by (8.21)**, the principle of least action implies the principle of virtual work.**

The proof of this statement can be easily obtained. Let us consider the following admissible virtual variations of motion constructed by multiplying a mollifier with an admissible virtual displacement:

$$\eta_\sigma(X^1, X^2, X^3, t) = \alpha^{-1}\zeta(\left(t - \bar{t}\right)\alpha^{-1})\xi_\sigma(X^1, X^2, X^3). \tag{8.25}$$

For every $\bar{t}$ we have

$$\begin{aligned} 0 = \delta\mathfrak{A}(\eta_\sigma(\cdot)) &= \varepsilon \int_{t_0}^{t_f} \delta\mathfrak{W}(\alpha^{-1}\zeta(\left(t - \bar{t}\right)\alpha^{-1})\xi_\sigma(X^1, X^2, X^3); t)dt \\ &= \varepsilon \int_{t_0}^{t_f} \alpha^{-1}\zeta(\left(t - \bar{t}\right)\alpha^{-1})\delta\mathfrak{W}(\xi_\sigma(X^1, X^2, X^3); t)dt, \end{aligned}$$

where the second equality holds because the function ζ depends only upon the time variable, and the **virtual work functional is defined for virtual displacements** that depend only upon space variables, such that the linearity of the functional $\delta\mathfrak{W}$ can be exploited. To conclude the proof it is enough to calculate the limit for α tending to zero in the previous equality, and recalling the definition of the Dirac delta:

$$0 = \lim_{\alpha \to 0} \int_{t_0}^{t_f} \alpha^{-1}\zeta(\left(t - \bar{t}\right)\alpha^{-1})\delta\mathfrak{W}(\xi_\sigma(X^1, X^2, X^3); t)dt = \delta\mathfrak{W}(\xi_\sigma(X^1, X^2, X^3); \bar{t}).$$

8.6 The Principle of Virtual Work

In the previous section we have noted that starting from the principle of least action, and using a time-localization argument, a necessary condition to be verified by motions minimizing the action can be found.

Such a necessary condition is the statement given by (8.24). Although the statement has been proven as a theorem starting from the condition of stationarity of action, we call it "**the principle of virtual work**."

Calling the thesis of a theorem seems rather paradoxical, and we must clarify this apparent paradox. The theorem which we have proven is based on the assumption that the virtual work is given by the expression (8.21), which is a specific expression derived starting from a Lagrangian density function and by calculating the first variation of the corresponding action functional. The result described in the previous section supplies a heuristic guide to finding the postulation process on more general basis. Indeed, as already discussed, there are some unsolved difficulties to be confronted in order to eventually apply the least action principle to model dissipative systems.

8.6.1 General Statement

Therefore, as already done by Lagrange and by Piola, one can, being inspired by the structure of the virtual work functional as obtained in the particular case of systems governed by the minimization of action, postulate a more general expression than the one given by (8.21) and ask that at every instant and for every virtual displacement the total virtual work expended on the virtual displacement must vanish. The papers [13, 56, 65] by Paul Germain are very clear and manage to present this idea in a comprehensive way.

We assume that, in general, the virtual work functional can be split into three distinct functionals.
These functionals are:

- The inertial virtual work $\delta\mathfrak{W}^{iner}(\xi_\sigma; t)$,
- the internal virtual work $\delta\mathfrak{W}^{int}(\xi_\sigma; t)$, and
- the external virtual work $\delta\mathfrak{W}^{ext}(\xi_\sigma; t)$.

A specific continuum model is formulated by choosing the specific forms of these three functionals.

An important warning on the symbol $\delta\mathfrak{W}$.
A symbol denoting any kind of virtual work has traditionally included the symbol δ. This notation is suggestive of the process which originally led D'Alembert and Lagrange to introduce the concept. If the system is Lagrangian, i.e. if its evolution is governed by a least action principle, then the virtual work functional is obtained by considering the first variation of action. This means that the linear functional expressing virtual work is, in some sense, an exact differential. The precise sense to be given to the expression "exact differential" in this context is the following:

- there exists a Lagrangian density of action such that the virtual work functional is given by (8.21), which derives from the first variation of action given by equation (8.20). In this case, the virtual work functional has to be defined in terms of displacement variations which do not depend on time. Therefore, the time-integration-by-parts transforming (8.20) into (8.21) is needed.

Of course we do not want to restrict ourselves to the case of virtual work functionals which are "exact," i.e. can be derived from a Lagrangian.
Indeed we want to consider, in general, systems for which the virtual work functional cannot be expressed in terms of a variation of an action. Therefore, in general, the inclusion of the symbol δ in the expression $\delta\mathfrak{W}$ is an abuse of notation, which can be

misleading. In reality, the symbol δ has to be understood as referring only to the "small" variation of the argument of the work functional.

Roughly speaking the functional $\delta\mathfrak{W}$ gives the expended work of all active interactions in correspondence with the virtual displacements ξ_σ. This functional depends linearly on the virtual displacements and, in general, nonlinearly on the actual configuration of the system, in a way which must be specified by means of constitutive equations.

In the case of Lagrangian systems, i.e. when the expression of virtual work derives from the action functional expressed in terms of a Lagrangian density $\mathfrak{L}$, we assume the following identifications for the virtual work functionals:

$$\begin{cases} \delta\mathfrak{W}^{\text{iner}}(\xi_\sigma;t) = \displaystyle\int_V \left(-\frac{\partial}{\partial t}\left(\frac{\partial \mathfrak{L}}{\partial\left(\partial\Psi_\sigma/\partial t\right)}\right)\right)\xi_\sigma dV. \\ \delta\mathfrak{W}^{\text{int}}(\xi_\sigma;t) = \displaystyle\int_V \left(\sum_{A=1}^{3}\frac{\partial \mathfrak{L}}{\partial\left(\partial\Psi_\sigma/\partial X^A\right)}\frac{\partial\xi_\sigma}{\partial X^A}\right)dV. \\ \delta\mathfrak{W}^{\text{ext}}(\xi_\sigma;t) = \displaystyle\int_V \left(\frac{\partial \mathfrak{L}}{\partial\Psi_\sigma}\xi_\sigma\right)dV. \end{cases} \tag{8.26}$$

By further particularizing the Lagrangian density $\mathfrak{L}$, i.e. by regarding it as the sum of a kinetic energy plus an external potential energy plus an internal energy, as done by Hamilton, one can make the previous identifications even more transparent.[44]

The reader is invited to consider the previous formula (8.26) only as the most simple (and maybe the most useful) example of virtual work functionals.

Being inspired by and generalizing the action stationarity condition we can now formulate the

PRINCIPLE OF VIRTUAL WORK

The evolution of a mechanical system is determined by:

1. Choosing its space of configurations;
2. Postulating the form of inertial, internal and external virtual work functionals ***without necessarily assuming that there exists a Lagrangian*** which allows for the representation given by (8.26).
3. Assuming that, at any time instant, the total virtual work vanishes for every admissible virtual displacement, expressed as

$$\begin{aligned} &\left(\forall t \in \left[t_0, t_f\right]\right)\left(\forall\xi_\sigma(X^1,X^2,X^3)\right)\Big(\delta\mathfrak{W}^{\text{TOT}}(\xi_\sigma;t) \\ &\quad = \delta\mathfrak{W}^{\text{iner}}(\xi_\sigma;t) - \delta\mathfrak{W}^{\text{int}}(\xi_\sigma;t) + \delta\mathfrak{W}^{\text{ext}}(\xi_\sigma;t) = 0\Big). \end{aligned} \tag{8.27}$$

8.6.2 Principle of Hamilton–Rayleigh

In the previous sections we have seen that the range of applicability of the principle of least action is somehow limited. This circumstance was understood, among others, by Lagrange and Piola. This was the reason why they preferred to base their postulation schemes on the principle of virtual work.

[44] Maybe actually these identifications simply become more familiar.

In order to get a description of the dissipative phenomena occurring in systems to be modeled, it is possible to postulate the existence of a Rayleigh dissipation functional $\mathcal{R}$. This functional is a map which associates, at every instant t, a positive real number with every ordered set of space-fields $\left(\Psi_\sigma(\cdot;t), \frac{\partial\Psi_\sigma(\cdot;t)}{\partial X^A}, \frac{\partial\Psi_\sigma(\cdot;t)}{\partial t}, \frac{\partial}{\partial X^A}\left(\frac{\partial\Psi_\sigma(\cdot;t)}{\partial t}\right)\right)$. Using the symbols introduced in (8.21) with the same meaning, we write:

$$\mathcal{R}\left(\Psi_\sigma(\cdot;t), \frac{\partial\Psi_\sigma(\cdot;t)}{\partial X^A}, \frac{\partial\Psi_\sigma(\cdot;t)}{\partial t}, \frac{\partial}{\partial X^A}\left(\frac{\partial\Psi_\sigma(\cdot;t)}{\partial t}\right);t\right) \in \mathbb{R}^+.$$

We assume that the first variation $\delta_v\mathcal{R}$ of $\mathcal{R}$ with respect to the variations of the field $\partial\Psi_\sigma/\partial t$ can be obtained keeping the fields $(\Psi_\sigma, \partial\Psi_\sigma/\partial x_k)$ and the time instant t fixed. Now the stationarity condition for the action functional is modified as follows:

PRINCIPLE OF HAMILTON–RAYLEIGH

$$\left(\left(\forall t \in [t_0, t_f]\right)\left(\forall\xi_\sigma(X^1, X^2, X^3)\right)\left(\delta\mathfrak{W}(\xi_\sigma;t) = \delta_v\mathcal{R}\left(\xi_\sigma;t\right)\right)\right). \tag{8.28}$$

As an example, we consider the following dissipation functional, which has a similar space structure to the action functional:

$$\begin{aligned}&\mathcal{R}\left(\Psi_\sigma(\cdot;t), \frac{\partial\Psi_\sigma(\cdot;t)}{\partial x_k}, \frac{\partial\Psi_\sigma(\cdot;t)}{\partial t}, \frac{\partial}{\partial x_k}\left(\frac{\partial\Psi_\sigma(\cdot;t)}{\partial t}\right);t\right)\\ &\quad= \int_V \mathfrak{R}\left(X^1, X^2, X^3; t, \Psi_\sigma(x;t), \frac{\partial\Psi_\sigma(x;t)}{\partial X^A}, \frac{\partial\Psi_\sigma(x;t)}{\partial t}, \frac{\partial}{\partial X^A}\left(\frac{\partial\Psi_\sigma(\cdot;t)}{\partial t}\right)\right) dV,\end{aligned} \tag{8.29}$$

where $\mathfrak{R}$ is the volume density of energy dissipation. Its first variation $\delta_v\mathcal{R}$ can be calculated as follows:

$$\delta_v\mathcal{R}\left(\xi_\sigma;t\right) = \int_V \left(\frac{\partial\mathfrak{R}}{\partial\left(\partial\Psi_\sigma/\partial t\right)}\xi_\sigma + \sum_{A=1}^{3}\frac{\partial\mathfrak{R}}{\partial\left(\partial^2\Psi_\sigma/\partial t\partial X^A\right)}\frac{\partial\xi_\sigma}{\partial X^A}\right) dV\,,$$

so that, after integration by parts, we get

$$\begin{aligned}\delta_v\mathcal{R}\left(\xi_\sigma;t\right) = &\int_V \left(\frac{\partial\mathfrak{R}}{\partial\left(\partial\Psi_\sigma/\partial t\right)} - \sum_{A=1}^{3}\frac{\partial}{\partial X^A}\left(\frac{\partial\mathfrak{R}}{\partial\left(\partial^2\Psi_\sigma/\partial t\partial X^A\right)}\right)\right)\xi_\sigma dV\\ &+ \int_{\partial V}\left(\sum_{A=1}^{3}\left(\frac{\partial\mathfrak{R}}{\partial\left(\partial^2\Psi_\sigma/\partial t\partial X^A\right)}\right)N_A\xi_\sigma\right)dA.\end{aligned}$$

As a consequence, we have that the strong form PDEs and boundary conditions of the weak conditions (8.28) are

$$\begin{aligned}&\frac{\partial\mathfrak{L}}{\partial\Psi_\sigma} - \sum_{k=1}^{3}\frac{\partial}{\partial X^A}\left(\frac{\partial\mathfrak{L}}{\partial\left(\partial\Psi_\sigma/\partial X^A\right)}\right) - \frac{\partial}{\partial t}\left(\frac{\partial\mathfrak{L}}{\partial\left(\partial\Psi_\sigma/\partial t\right)}\right)\\ &\qquad\qquad\qquad\qquad\qquad\qquad\qquad\qquad\qquad\qquad\qquad\qquad\forall X \in V, \forall t \in [t_0, t_f]\\ &\quad= \frac{\partial\mathfrak{R}}{\partial\left(\partial\Psi_\sigma/\partial t\right)} - \sum_{A=1}^{3}\frac{\partial}{\partial X^A}\left(\frac{\partial\mathfrak{R}}{\partial\left(\partial^2\Psi_\sigma/\partial t\partial X^A\right)}\right),\end{aligned} \tag{8.30}$$

$$\sum_{k=1}^{3}\left(\frac{\partial \mathfrak{L}}{\partial\left(\partial \Psi_\sigma/\partial X^A\right)}-\frac{\partial \mathfrak{R}}{\partial\left(\partial^2 \Psi_\sigma/\partial t \partial X^A\right)}\right) N_k=0, \quad \forall X \in \partial V/\partial_d V, \forall t \in \left[t_0, t_f\right] \tag{8.31}$$

$$\sum_{k=1}^{3}\left[\left|\frac{\partial \mathfrak{L}}{\partial\left(\partial \Psi_\sigma/\partial X^A\right)}-\frac{\partial \mathfrak{R}}{\partial\left(\partial^2 \Psi_\sigma/\partial t \partial X^A\right)}\right|\right] N_k=0, \quad \forall X \in \Sigma. \forall t \in \left[t_0, t_f\right] \tag{8.32}$$

where, as in the previous sections, discontinuities of the derivatives of the fields

$$\frac{\partial \mathfrak{L}}{\partial\left(\partial \Psi_\sigma/\partial X^A\right)}, \qquad \frac{\partial \mathfrak{R}}{\partial\left(\partial^2 \Psi_\sigma/\partial t \partial X^A\right)},$$

may be concentrated on the surface Σ. Let us conclude by remarking that, when using the Hamilton–Rayleigh principle, we just make use of a particular instance of the principle of virtual work by assuming that

$$\delta \mathfrak{W}^{\mathrm{TOT}}\left(\xi_\sigma ; t\right)=\delta \mathfrak{W}\left(\xi_\sigma ; t\right)-\delta_v \mathcal{R}\left(\xi_\sigma ; t\right).$$

This assumption can be interpreted by stating that in the total work we distinguish a Lagrangian part (which could describe the conservative[45] interactions occurring in the considered system) and a dissipative part, obtained with the Rayleigh functional.

Also, the Rayleigh functional may be split into an internal and an external part. Consequently we can write,

$$\delta_v \mathcal{R}^{\mathfrak{ext}}\left(\xi_\sigma ; t\right)=\int_V\left(\frac{\partial \mathfrak{R}}{\partial\left(\partial \Psi_\sigma/\partial t\right)} \xi_\sigma\right) dV$$

$$\delta_v \mathcal{R}^{\mathrm{int}}\left(\xi_\sigma ; t\right)=\int_V\left(\sum_{A=1}^{3} \frac{\partial \mathfrak{R}}{\partial\left(\partial^2 \Psi_\sigma/\partial t \partial X^A\right)} \frac{\partial \xi_\sigma}{\partial X^A}\right) dV .$$

For a more detailed heuristic and physical insight into the Hamilton–Rayleigh principle, the interested reader is referred to [98].

8.6.3 The Principle of Virtual Work as a Powerful Heuristic Tool: Lagrange, Cauchy and Generalized Continua

Gabrio Piola, in his works (the first of which dates to 1824, see [24, 25, 27–29]), gave himself the obligation to "continue the work which had been left unfinished by our Schoolmaster [i.e. Lagrange] when death stopped his genius." Indeed, Piola notes that, in the last pages[46] of the last edition ([15]) of the *Mécanique Analytique*, Lagrange had established clearly the path to be followed for determining all equations of mathematical physics starting from the principle of virtual work. The opinion of Piola is shared by the editors of the mentioned edition of Lagrange's works: in their foreword they

[45] We repeat again here that non-conservative phenomena can also be included in some particular Lagrangians.

[46] NOTE II. Sur le mouvement de rotation, page 357.

write: "In this work ... Lagrange developed the law of virtual work, from which single principle the whole of solid and fluid mechanics can be derived."

In the already cited "NOTE II. Sur le mouvement de rotation, page 357" Lagrange introduces those quantities which, once regrouped to form a tensor, have been called Piola Stress. Piola in [27] develops the ideas of Lagrange, to such an extent that only contemporary literature has managed to parallel it (see [25]). Indeed Piola introduces the basic equations of what has been called in the present century "peri-dynamics," which he then particularizes to get the Nth gradient continua (see [10]). Finally, in his work dated 1845–48 ([27]), Piola proves that the results obtained by Cauchy in 1822–1828 (see [75]) are more easily and elegantly obtained by using the methods devised by Lagrange.

In any case, we believe that in the aforementioned note by Lagrange all the ideas and methods, so deeply and masterfully presented by Piola, were already clearly present. Unfortunately Cauchy did not realise the importance of that note. For sure its title is somehow misleading: moreover Lagrange seems to have sketched it literally only a few months before dying and it resembles rather a set of formulas with comments of only few words. Instead of following Lagrange's approach, Cauchy formulated his continuum model basing his postulation on the balance of forces, by including contact forces and by developing the celebrated tetrahedron argument. This argument proves, from the postulated balance of forces, the existence of the Cauchy stress tensor field. Note that this stress field is defined in the actual configuration, where balance of forces is more naturally formulated: in this way Cauchy treatment of the concept of stress departs from the natural surrounding framework of variational principles, which are preferably formulated in the reference (sometimes called Lagrangian) configuration.

The ingenious procedure conceived by Cauchy has been the reason for which generalized continua were not considered in the main flow of research in continuum mechanics for a long period. Even if the tetrahedron argument can somehow be generalized (for instance to the case of higher gradient theories, see [76–78]), the postulation scheme based on balances of force and angular momentum is not the most suitable tool for formulating models more general than those developed by Cauchy. This fact was perfectly clear to Piola, who presented clear arguments to support this point of view in his work published in 1848.

The principle of virtual work is, indeed, suitable to formulate continuum models which are much more general than those conceived by Cauchy. On the other hand, Cauchy models have been considered nearly exclusively in the literature and, for this reason, those models developed by relaxing one or another of his restricting assumptions very often have been called generalized continua. We will prove below that the most expeditious and efficient way to formulate these more general models is to use the principle of virtual work and the related postulation scheme.

On the other hand, an accurate reading of the aforementioned note by Lagrange indicates that Cauchy continua were also first invented in this way, and that Cauchy simply found an equivalent way for formulating them. As this equivalence can be established only in the particular case developed by Cauchy, we claim that the principle of virtual work has to be preferred in any case.

8.6.4 The Case of Cauchy Continua

As an illustration, we first discuss the most simple classical continuum model among those which were introduced to study the deformation of bodies. Nobody should expect that such a model, and similarly every other model, can include the description of **all possible deformation phenomena**. Unfortunately, a group of scholars contributed to propagating a belief to the contrary. Consequently, many mechanicians have adopted the belief that the continua whose deformation energy depends only on the first gradient of deformation (otherwise called Cauchy[47] continua) are the only ones which may exist, in the sense that they are the only continua which are logically consistent with the second principle of thermodynamics. This belief had already been rebutted by Piola in his *Memoir* of 1848.

Hamel–Noll theorem

We refrain here from presenting the tetrahedron argument developed by Cauchy. The importance of this argument has been overestimated in continuum mechanics (this overestimation is evident in [57] and in the various comments found in [45]). Interestingly, the overestimation has been based upon the apparently very general result which was called the Hamel–Noll[48] theorem in [79].

The theorem, remarkably, has been misinterpreted by Noll himself. He stated that, in general, every contact force must be a force per unit area, and that this force depends only on the normal of the contact surface. For reasons that remain obscure, this theorem has been considered as the final justification of the non-existence of contact forces concentrated on lines or on points. Needless to say, as with every other theorem, the Hamel–Noll theorem is also based on some hypotheses. If these hypotheses are not verified then, obviously, the theorem, as set out below, is not necessarily true:[49]

THEOREM IV (stress principle): There is a vector valued function $s(x,n)$*, where* $x \in \theta_t(\mathfrak{B})$ *and where* n *is a unit vector, such that*

$$s(c;x) = s(x,n), \tag{5.11}$$

whenever $\theta_t(c)$ *has the unit normal* n *at* $x \in \theta_t(c)$*, directed towards the positive side of the oriented surface* $\theta_t(c)$*, the orientation of* $\theta_t(c)$ *being induced by the orientation of* c*.*

To this theorem the following footnote is added as commentary:

The assertion of this theorem appears in all of the past literature as an assumption. It has been proposed occasionally that one should weaken this assumption and allow the stress to depend not only on the tangent plane at x, but also on the curvature of the

[47] An issue of terminology arises here: why did scholars add the qualifier "Cauchy" if all continua are Cauchy continua?

[48] Truesdell cared to underline that the proof of Hamel was "imperfect."

[49] Unfortunately, in [80] the starting hypotheses of the Hamel–Noll theorem are assumed to be the basis of every conceivable continuum theory and, therefore, they are not explicitly repeated in its statement. This state of facts induced many scholars to believe that these assumptions must be accepted always. This attitude is to be deprecated but is unfortunately not new and can also be recognized in many scholastic philosophers.

surface c at x. The theorem given here shows that such dependence on the curvature, or on any other local property of the surface at x, is impossible.[50]

While carefully reading the assumptions made by Noll in the pages preceding the theorem statement and the following proof, one discovers that he accepts rather immediately the assumption that in the considered continua both line and point contact forces are vanishing. This point has been carefully discussed in [76–78]. It is therefore clear that, in the framework of Noll's treatment of contact actions, only surface contact actions are possible. Moreover (see [76, 78]), contact line forces are possible if and only if surface contact forces depend on curvature of the contact surface. The statement written in the cited footnote by Noll is clearly false, and the great influence exerted by Noll in continuum mechanics explains in part why the development of higher gradient theories has lagged to the detriment of progress in mechanical sciences.

In conclusion, the Hamel–Noll theorem shows an interesting result valid for a specific class of continua, which have been characterized by Piola in [27].

Cauchy continua: characterizations

There are several equivalent ways to characterize the particular constitutive[51] class of continua studied by Cauchy. First of all, for Cauchy continua the set of kinematical fields Ψ reduces to only the placement field χ. By introducing a vector basis and an origin in the actual configuration, the placement field is given by its component fields $\chi^i(X)$. It can be proven (see e.g. [10, 77, 78]) that the two following statements are equivalent:

1. **Piola's characterization of Cauchy continua**. The internal work $\delta\mathfrak{W}^{int}(\xi;t)$ functional has the following form:

$$\int_V P(X;t) : \nabla_X \xi \, dV = \int_V P_i^A(X;t) \frac{\partial \xi^i}{\partial X^A} \, dV \,,$$

   where the tensor field P is called Piola stress (note that, in every point X, the tensor P is defined as a linear function mapping vectors in the reference configuration into displacements in the actual configuration. The symbol : denotes the saturation between tensors of the same order (see [26] for more details about the introduced index notations). As in the previous expression of virtual work only the first gradient of virtual displacement appears, we can call the corresponding class of continua also **first gradient continua.**
2. **Cauchy definition of continua.** Contact interactions reduce to forces per unit area of (suitably regular) contact surfaces, and the surface vector field representing this force per unit area (so-called Cauchy vector) depends (linearly) only on the normal of contact surface.

[50] It has to be said that Richard Toupin[54] never believed that the mentioned theorem had the said presumed enormous range of applications. In his papers Toupin systematically applied variational principles, and for this reason he was always at odds with Noll.

[51] If one agrees that contact actions may depend in general on the shape of the contact surface, then those continua for which the Hamel–Noll theorem holds are a particular class in a most general set of continua.

If the expression for the internal work can be deduced from a stored deformation energy, then (we omit the indices when this will not cause ambiguities: this notation is already present in the works by Piola)

$$P = \frac{\partial \mathfrak{L}}{\partial \left(\partial \chi / \partial X\right)}.$$

If dissipation phenomena are also included via a Rayleigh potential, then

$$P = \frac{\partial \mathfrak{L}}{\partial \left(\partial \chi / \partial x\right)} - \frac{\partial \mathfrak{R}}{\partial \left(\partial^2 \chi / \partial t \partial x\right)}.$$

Existence of Cauchy stress and corresponding balance equations as deduced by Piola from the principle of virtual work

In [27] Piola discusses the postulation of mechanics based on the principle of virtual work, and shows that using this postulation scheme:

1. the tetrahedron argument becomes superfluous;
2. the concept of Cauchy stress can be easily deduced from a simple Piola's transport of Piola's stress;
3. the concept of contact force becomes a simple consequence of the concept of virtual work;
4. the statement of the balance of forces is equivalent to the principle of virtual work for Cauchy continua.[52]

We show now, in modern notation, how Piola proceeds.

a) He starts from the principle of virtual work in the formulation (8.27).

b) Then he calls **Cauchy–Lagrange continua** those for which:

b1) the internal work is expressed in terms of the first gradient of the virtual displacement only; and

b2) inertial forces are given in terms of the second time derivative of placement field and of a scalar field ϱ (**volume mass density**).

As equations point b) above reads as

$$\begin{cases} \delta \mathfrak{W}^{\mathrm{int}}(\xi; t) = \displaystyle\int_V P(X;t) : \nabla_X \xi \, dV = \int_V P_i^A(X;t) \frac{\partial \xi^i}{\partial X^A} \, dV, \\ \\ \delta \mathfrak{W}^{\mathrm{iner}}(\xi_\sigma; t) = \displaystyle\int_V -\varrho \frac{\partial^2 \chi}{\partial t^2} \cdot \xi dV. \end{cases} \tag{8.33}$$

Then, using integration by parts, he proves that:

c) the principle of virtual work together with the assumed structure for $\delta \mathfrak{W}^{\mathrm{int}}$ and $\delta \mathfrak{W}^{\mathrm{iner}}$, implies that for $\delta \mathfrak{W}^{\mathrm{ext}}(\xi_\sigma; t)$ a specific representation is possible:[53]

[52] A crystal clear modern version of the proof of this equivalence can be found in [81].

[53] This point will be commented on in more detail in what follows. Piola explicitly remarks that this circumstance should not surprise anybody who had studied the theory of Euler fluids. Indeed, for these fluids it is assumed a priori that the deformation energy depends on the actual mass density only, and as a consequence it is proven that they cannot support shear forces on their boundaries. It is therefore logically

indeed, there must exist two vector fields b^V and $b^{\partial V}$ (**external surface and volume forces**), eventually depending on the field χ, such that (the dot denotes the inner product between vectors)[54]

$$\delta\mathfrak{W}^{\mathfrak{ext}}(\xi_\sigma;t)=\int_V b^V\cdot\xi_\sigma dV+\int_{\partial V} b^{\partial V}\cdot\xi_\sigma d\Sigma. \tag{8.34}$$

d) The following local Euler–Lagrange conditions hold (we use here for compactness the Einstein convention which assumes summations over repeated indices):

$$\begin{cases} \frac{\partial P_i^A}{\partial X^A}+b_i^V=\varrho\frac{\partial^2\chi_i}{\partial t^2} & \forall X\in V \\ \\ P_i^A N_A=b_i^{\partial V} & \forall X\in\partial V_i. \end{cases} \tag{8.35}$$

e) Subsequently, Piola obtains the transformation formulas from through reference to the actual configurations for normals to surfaces and for the divergence operator.[55] These expressions (obviously Piola did not use the modern tensorial or matrix notation, see [26] and [25]) are

$$\begin{aligned} J^{-1}F_A^i n_i da&=N_A dA,\\ \frac{\partial P_i^A}{\partial X^A}&=J\frac{\partial}{\partial x^j}\left(J^{-1}P_i^B F_B^j\right), \end{aligned} \tag{8.36}$$

where we take the reference surface, Σ, as having normal N at the point X and Hausdorff measure dA, the surface $\sigma=\chi(\Sigma)$, as having normal n at the point $x=\chi(X)$ and Hausdorff measure da, the matrix $F=\left[F_A^i\right]:=\left[\frac{\partial\chi^i}{\partial X^A}\right]$ (we assume that in both the reference and actual configurations one orthonormal global basis is chosen), and we have defined $J=\det F$.

f) As a final step, Piola replaces (8.36) inside (8.35) and obtains

$$\begin{cases} \frac{\partial}{\partial x^j}\left(J^{-1}P_i^B F_B^j\right)+J^{-1}b_i^V=0 & \forall x\in\chi(V) \\ \\ \left(J^{-1}P_i^A F_A^j\right)n_j=b_i^{\partial V}\frac{dA}{da} & \forall x\in\chi(\partial V). \end{cases} \tag{8.37}$$

These equations, when introducing the definition

$$T_i^j:=J^{-1}P_i^A F_A^j \tag{8.38}$$

reduce to the balance of force, in local form, as obtained in the Cauchy postulation scheme.

clear and already generally accepted that the assumptions made on the structure of internal work limit the capacity of a continuum to support external forces. In other words: in continuum theories, the admissible expression for external forces applicable to a continuum depends on the postulated material properties.

54 In the language of measure theory, we can say that the external work is the sum of a volume measure absolutely continuous with respect to a Lebesgue measure plus a surface measure absolutely continuous with respect to a bi-dimensional Hausdorff measure.

55 The works by Piola were never lost, they were always available in libraries all over the world: Italian is not a lost language and the notations of mathematical analysis are universal. Moreover, Edward John Nanson was born the same year that Piola died. How it was possible to attribute to Nanson the aforementioned formula of transformations of normals is not clear.

The reader will recall that, in the Cauchy postulation scheme, the balance of force in integral form and the existence of only contact surface forces are postulated, while the linear dependence of contact forces (as given by the second equation in (8.37)), i.e. the existence of the Cauchy stress tensor, and the first equation in (8.37) are deduced as consequences.

The Cauchy proof is based on a tetrahedron argument, which has been considered by Truesdell the most fundamental argument in continuum mechanics (see [57]; moreover in [44], while discussing variational principles, it is stated that the concept of Cauchy stress is not deduced using a variational postulation, unless one starts from a least action principle). The procedure illustrated above, already used by Piola in 1848, shows that, on the contrary, all continuum mechanics studied by Truesdell and Noll can be based on the principle of virtual work. The initial statements from 1 to 3 are thus proven. The proof of statement 4 is simply completed by using, for instance, the results presented by Antman in [81].

8.6.5 Generalized Continua and Their Relevance in the Theory of Metamaterials

We want to consider several generalizations of Cauchy continuum and, among these, in particular the model which was proposed by Gabrio Piola in his (unfortunately widely neglected) *Memoir* of 1848. We will not delve into the mathematical and physical motivations which led Piola to propose this formulation. We will limit ourselves to presenting the general structure of the theory, basing it on the principle of virtual work, and to noting that Piola clearly pointed out the reasons why the Cauchy model could not be the most general one. We will also underline that it seems very difficult to formulate Piola's continuum models in the framework of postulation schemes based on Balance Laws.

Because of the predominance of the Cauchy postulation and model, many specific aspects of the first gradient continua have been believed to have a universal validity in continuum mechanics. Unfortunately, this is not the case. Here we try to make clearer the conceptual situation, and to point out how the various concepts formulated in the framework of first gradient can be generalized.

Moreover, it has to be remarked that, when one wants to design new metamaterials, the clear intent is to exploit at best all the possible effects and phenomena which may occur during the deformation of bodies. Therefore, when designing metamaterials, one has to try to use the widest possible family of mathematical models, trying to avoid overly restricting their range of application. The two chapters of this book dedicated to pantographic metamaterials give a specific example of how the application of the principle of virtual work to its full potential can lead to the conception and subsequent design of materials whose behavior is really unexpected.

The concepts which can be easily extended, without immediately incurring logical contradictions, from first gradient continua to higher gradient continua include (see e.g. [13, 56]):

- the action functional;
- the virtual work functional.

Instead, the following concepts need a more complex elaboration to be generalized:

- Stress and stress tensor;
- Measure of deformation, strain;
- Contact interactions.

It has to be explicitly stated that it is not possible to base the study of higher gradient continua on using as primitive the concepts of force and couple alone.

Instead, we can easily extend to a wider class of continua the action functional and the virtual work functional.

8.6.6 Second Gradient Continua

We call second gradient continua those continua for which the internal virtual work functional is given by the following expression:

$$\begin{aligned}\delta\mathfrak{W}^{\mathrm{int}}(\xi;t) &= \int_V P_1(X;t) : \nabla_X \xi \, dV + P_2(X;t) : \nabla_X^2 \xi \, dV \\ &= \int_V P_{1i}^A(X;t)\frac{\partial \xi^i}{\partial X^A}\, dV + \int_V P_{2i}^{AB}(X;t)\frac{\partial^2 \xi^i}{\partial X^A \partial X^B}\, dV\,,\end{aligned} \tag{8.39}$$

where we will call the tensors P_1 and P_2, the first gradient and the second gradient **Piola stress tensors**, respectively.

A **Lagrangian second gradient continuum** has an action functional given by (we use the notations of the previous formula (8.5)):

$$\mathfrak{A}(\Psi_\sigma(\cdot)) = \int_T \mathfrak{L}\left(x_\mu, \Psi_\sigma, \frac{\partial \Psi_\sigma}{\partial x_\mu}, \frac{\partial \Psi_\sigma^2}{\partial x_\mu \partial x_\nu}\right) dV\,. \tag{8.40}$$

By recalling the methods used in the previous sections, it is easy to represent first gradient and second gradient Piola tensors in terms of the Lagrangian density function, *when such a function exists*.

The example of second gradient continua shows that, while the attempt to base the postulation of continuum mechanics on the primitive concept of contact interaction has been successful (see [7, 8, 10]), on the contrary, ***by using contact forces and contact couples alone, it is not possible to describe all possible kinds of interactions between parts of a deformable body***.

Indeed, even if it is more difficult to get this generalization, one can always introduce the concept of virtual work of contact interactions, defining it as a linear and continuous functional on the set of displacements concentrated on contact surfaces. However, such a linear functional cannot be, in general, so simple as the one considered by Cauchy.

To be precise (see [10, 77]): let us consider the functional of virtual work of contact interactions $\delta\mathfrak{W}^{\mathrm{cont}}$. This functional can be regarded as the functional describing the interactions between two parts of a deformable body as localized on their surface of

contact. Obviously, when one considers a part of a deformable body P, then the remaining part of the same deformable body is a part of the external world with respect to P. Therefore $\delta\mathfrak{W}^{\mathtt{cont}}$ is the part of the functional of external work for P representing those interactions with the external world which are concentrated on ∂P.

Now, let us denote by ξ the virtual displacement of the material contact surface Σ, with N_Σ the field of normals to Σ, which is assumed to exist except on a finite number of curves. We moreover assume that we can determine, for every $\alpha = 1, \ldots, N$, the set Γ_α of curves on Σ where the fields $\nabla^\beta N_\Sigma$ (with $0 \leq \beta < \alpha$) are continuous and the fields $\nabla^\alpha N_\Sigma$ have discontinuities of the first kind.[56] We assume that the surface Σ and all curves Γ_α are as regular as needed in our reasoning.

Representation theorem for virtual work of contact interactions in first and second gradient continua.
We can now state a very important result:

If for every sub-body P of the considered continuum:

- the part of the external work functional representing long-range interactions on P is absolutely continuous with respect to the Lebesgue measure;
- the same is true of the inertial virtual work functional; and
- the principle of virtual work holds;

then the structures of contact interaction functionals are given:

- in Cauchy continua by[57]

$$\delta\mathfrak{W}^{\mathtt{cont}} = \int_\Sigma b_\Sigma^{\mathrm{cont}}(N_\Sigma) \cdot \xi d\Sigma$$

- in second gradient continua by [58]

$$\delta\mathfrak{W}^{\mathtt{cont}} = \int_\Sigma b_{\Sigma,0}^{\mathrm{cont}}(N_\Sigma, \nabla N_\Sigma) \cdot \xi d\Sigma + \int_\Sigma b_{\Sigma,1}^{\mathrm{cont}}(N_\Sigma) \cdot \frac{d\xi}{dN_\Sigma} d\Sigma + \int_{\Gamma_0} b_{\Gamma_0,0}^{\mathrm{cont}}(N_\Sigma^{\pm}, N_{\Sigma\Gamma_0}^{\pm}) \cdot \xi d\Sigma,$$

where

- the contact force per unit area $b_\Sigma^{\mathrm{cont}}(N_\Sigma)$ depends linearly on its argument and the following representation holds:

$$b_\Sigma^{\mathrm{cont}}(N_\Sigma) = P N_\Sigma, \tag{8.41}$$

which allows for the representation of contact forces in terms of Piola stress and the normal of the contact surface;

[56] A discontinuity of the first kind, or jump discontinuity of a field on a curve embedded in a surface, occurs when the considered field has continuous limits on both sides of the curve along the surface, but these limits are not equal. Obviously, $\nabla^0 N_\Sigma = N_\Sigma$.

[57] This has been shown by proving the previous point c) and Eq. (8.34).

[58] See [13] for a very elegant deduction of this statement, but also [26].

- the contact force per unit area $b^{\text{cont}}_{\Sigma,0}(N_\Sigma, \nabla N_\Sigma)$ depends linearly on its arguments, and the following representation holds

$$b^{\text{cont}}_{\Sigma,0}(N_\Sigma, \nabla N_\Sigma) = (P_1 - \nabla \cdot P_2)\, N_\Sigma + \nabla_\Sigma \cdot ((I - N_\Sigma \otimes N_\Sigma)\, P_2 N_\Sigma)\,, \tag{8.42}$$

  where $\nabla_\Sigma \cdot$, $\nabla \cdot$ denote surface and volume divergence operators, $I - N_\Sigma \otimes N_\Sigma$ denotes the projector on the tangent plane of Σ. The formula above allows for the representation of surface contact force in terms of first and second gradient Piola stresses: however, both curvature and normal of the contact surface are involved:
- the contact double force per unit area[59] $b^{\text{cont}}_{\Sigma,1}(N_\Sigma \otimes N_\Sigma)$ depends linearly on $N_\Sigma \otimes N_\Sigma$, and the following representation holds

$$b^{\text{cont}}_{\Sigma,1}(N_\Sigma \otimes N_\Sigma) = P_2(N_\Sigma \otimes N_\Sigma), \tag{8.43}$$

  which allows for the representation of contact double forces in terms of the second gradient Piola stress and of the normal of the contact surface;
- the edge contact force per unit line $b^{\text{cont}}_{\Gamma_0,0}(N^{\pm}_\Sigma, N^{\pm}_{\Sigma\Gamma_0})$ depends linearly on the tensors $N^{+}_\Sigma \otimes N^{+}_{\Sigma\Gamma_0}, N^{-}_\Sigma \otimes N^{-}_{\Sigma\Gamma_0}$, where $N^{\pm}_\Sigma$ are the limits from both faces $\Sigma^{\pm}$ of Σ concurring in Γ_0 of the outer normal fields to Σ, and are defined by $N^{\pm}_{\Sigma\Gamma_0} = N^{\pm}_\Sigma \times T_{\Gamma_0}$, with T_{Γ_0} being the chosen unit tangent vector to the curve Γ_0.[60] The following representation holds:

$$b^{\text{cont}}_{\Gamma_0,0}(N^{\pm}_\Sigma, N^{\pm}_{\Sigma\Gamma_0}) = P_2\left(N^{+}_\Sigma \otimes N^{+}_{\Sigma\Gamma_0}\right) + P_2\left(N^{-}_\Sigma \otimes N^{-}_{\Sigma\Gamma_0}\right), \tag{8.44}$$

  which allows for the representation of contact forces in terms of the second gradient Piola stress and of the normals to the contact line and surface.

We postpone to a following subsection the description of contact forces in higher gradient continua, as already the example of second gradient continua can be used to show the peculiarities of higher gradient theories and the difficulties which one meets when generalizing some concepts in a more inclusive context.

8.6.7 Peculiarity of Higher Gradient Theories

In higher gradient continua contact interactions need to be represented by many stress tensors of different order.

The most simple and immediate way for generalizing first gradient models consists in simply adding higher order stress tensors in the functional of internal work, as duals of higher gradients of virtual displacements. If, instead of generalizing the functional of

[59] Here we use the nomenclature of Germain [13]. Contact double forces are defined as those quantities which in the expression of virtual work are the factors of the derivatives of virtual displacement along the normal to the contact surface. A possible physical interpretation of double forces is given in [83].

[60] The vectors $N^{\pm}_{\Sigma\Gamma_0}$ are the outward pointing normal unit vectors to the curve Γ_0 when it is regarded as a boundary respectively of the faces Σ^{+} and Σ^{-}. The vectors $N^{\pm}_{\Sigma\Gamma_0}$ are tangent to Σ and play a crucial role in the process of integration by parts on the surface Σ, when the surface divergence theorem is applied.

internal work, the desire is to generalize the formula (8.41) for contact interactions, then one must deduce the complicated formulas (8.42), (8.43) and (8.44). This has been done in [7, 8], where a rather involved procedure was conceived to obtain the representation formulas noted above from so-called ***quasi-balance of work***[61] and without postulating the form of internal work functional.

Higher gradient continua are those continua in which different length scales play an important role at macro-level (see for instance [83–86] and Chapters 3 and 6 about pantographic structures). In these continua complex types of contact interactions may arise, and the geometrical properties of contact surfaces play a greater role in the determination of contact interactions.

The Hamel–Noll theorem does not encompass such general interactions, as it is based in a hidden way, on the assumption that all contact forces are distributed on surfaces.

Instead, Eq. (8.44) shows that line contact forces are possible. Moreover, together with (8.42), the aforementioned edge force representation shows that the existence of edge forces is strongly related to the dependence of contact surface forces on the curvature of the contact surface. Also one cannot have edge force without having double forces (see again [7, 8]).

A simple argument of continuity (see again [8]) clearly shows that without edge forces one cannot have surface forces depending on curvature, and viceversa. In fact, an edge can be approached in the limit by a family of smoothed surfaces having higher and higher curvature in correspondence *i*th the approximated edge.

In the following we will see that in third gradient continua one can also have wedge contact forces, in points where curves of discontinuity meet. Finally, in general, one can have *k*th forces (i.e. dual quantities in work of *k*th order orthogonal derivatives, both concentrated on edges and on wedges). In [83] and [87] it is shown, via a homogenization procedure, how this kind of interaction may arise at macro-level due to complex microstructures and micro-mechanisms.

Higher gradient models have been criticized for their complexity, which has often been used as an argument for refusing their use, their development and their importance. In facts as high gradient continua are intended to model complexity, to complain of their complex formal structure is nothing but perverse.

Obviously, we do not need complexity per se: we must use Cauchy models when they suffice but we should not believe that their structure and the cultural paradigm developed by some scholars for describing them are the most general conceivable, useful and possible.

If there is a paradigm developed for considering Cauchy continua as the unique continuum model for describing the deformation of bodies, then we must change the paradigm.

8.6.8 Virtual Work Functionals: General Structure

Clearly, there is no reason for limiting our attention only to the expression of internal work which is valid for Cauchy continua. The need to design exotic metamaterial is

[61] An assumption which generalizes the principle of virtual work.

a strong motivation for searching for more general models, as by means of them one can conceive and design more general materials. On the other hand, based on clear and sound logical reasons, Piola had already underlined the possibility to observe in Nature materials whose description could not fall within the scope of Cauchy models.

We describe in what follows an adaptation of Piola's reasoning, in the spirit of work by Germain [13, 56].

Given a generic sub-body D (i.e. a suitably smooth[62] subset of material particles in the chosen reference configuration) of the continuous body B we must specify, for every configuration of the body B, the set $\mathcal{A}$ of all virtual displacements for D which are admissible. This means that the placement obtained by adding any admissible displacement to an admissible placement is still admissible. Admissible placements are allowed by the kinematical constraints imposed to the body.

We will assume that the subset $\mathcal{D}_{\mathcal{A}}$ of so called "test functions" (i.e. infinitely differentiable functions having compact support) verifying the imposed constraints is included in $\mathcal{A}$. Roughly speaking, we assume that, even if the body can have a rich set of admissible placements and displacements, very regular displacements are always allowed for.[63]

Finally we must specify what we mean for virtual work expended on virtual displacements by the internal or external or inertial interaction involving the sub-body D. We assume that all kinds of virtual work interactions can be represented by linear and continuous functionals when restricted to the set of test functions $\mathcal{D}_{\mathcal{A}}$. The set of test functions is clearly a vector space. We assume that, in addition, it is endowed with the structure given by Fréchet topology ([67]). In other words:

We assume that the virtual work functionals of every interaction relative to a sub-body D are distributions (in the sense of Schwartz [70]***) concentrated on $\overline{D}$.***[64]

Given the previous assumption, all the theorems and definitions of the theory of distributions become the conceptual basis of continuum mechanics. Here we accept the point of view presented in [65], which is a natural evolution of the ideas developed in [24].[65]

As we need it again, we recall here once more the following fundamental representation theorem for distributions (see [70]):

LS1. every distribution having compact support K can be represented as the sum of a finite number of derivatives of measures all having their support included in K.[66]

[62] See [10] for some useful smoothness requirements.

[63] If one wants to allow for non-smooth displacements but restrain the body from smooth displacements for some reason, then clearly the following theory must be modified correspondingly.

[64] We have denoted by $\overline{D}$ the topological closure of the set D.

[65] The reader will note that while Germain in [13, 56, 65] bases his postulation scheme on the mathematical tool supplied by the results by Schwartz in [70], Piola in [24] bases his postulation on the results presented by his Maestro Vincenzo Brunacci in his *Corso di Matematica Sublime*.

[66] This theorem was recalled before in a previous section. As a consequence we have that the following definition is well-posed: ***a distribution has order smaller than or equal to k if it is the sum of derivatives of order $h \leq k$ of measures.***

Because of LS1 we can conclude that if the virtual work functionals $\delta\mathfrak{W}$ to be introduced for every sub-body $D \subseteq B$ can be regarded as a distribution when restricted to test functions, then it can be represented as follows:

$$\delta\mathfrak{W}(D,\xi) = \sum_{i=1}^{N_D} \int_{\overline{D}} (\nabla^i \xi) \mid dT_{i,D}, \quad \forall \xi \in \mathcal{D} \tag{8.45}$$

where the symbol $\mid$ is introduced to denote the total saturation of contravariant and covariant tensor indices, N_D and $dT_{i,D}$ $(i = 1, \dots N_D)$ are, respectively, integer and tensor valued measures which depend upon the considered sub-body $D \subseteq B$. We will call **Piola stress measures** (or Piola stresses) the measures $dT_{i,D}$ $(i = 1, \dots N_D)$.

Classes of constitutive equations for deformable bodies

Obviously different constitutive descriptions will be selected when specifying the properties of the set of measures $dT_{i,D}$ $(i = 1, \dots N_D)$ to be used for internal virtual work.

For instance:

- **Cauchy first gradient continua** are such that their internal virtual work functional has $N_D = 1$ for all sub-bodies and the measure $dT_{1,D}$ is absolutely continuous with respect to the Lebesgue measure;
- **Second gradient continua** are defined in [13] as those continua for which $N_D = 2$ for all sub-bodies and the measures $dT_{1,D}$ and $dT_{2,D}$ are absolutely continuous with respect to the Lebesgue measure (see previous formula (8.39));
- **Lagrangian *N*th gradient continua** are those continua whose total work functional is obtained by calculating the first variation of the action functional given by (we use the notations of the previous formula (8.5)):

$$\mathfrak{A}(\Psi_\sigma(\cdot)) = \int_T \mathfrak{L}\left(x_\mu, \Psi_\sigma, \frac{\partial \Psi_\sigma}{\partial x_\mu}, \dots, \frac{\partial^N \Psi_\sigma}{\partial x_{\mu_1} \dots \partial x_{\mu_N}}\right) dV. \tag{8.46}$$

- In all the discussion below we assume that the order N_D and the measures $dT_{i,D}$ $(i = 1, \dots N_D)$ are not depending on the considered sub-body D of the body B. We call this the **condition of localization of Piola stresses**.
- We call ***N*th gradient Piola's continua** those for which: i) the condition of localization of Piola stress measures is verified; ii) the measures $dT_i = T_i\, dV$ are absolutely continuous with respect to the Lebesgue measure; iii) inertial work[67] is given by

$$\delta\mathfrak{W}^{\text{iner}}(\xi_\sigma; t) = \int_V -\varrho \frac{\partial^2 \chi}{\partial t^2} \cdot \xi dV;$$

iv) the internal work is given by

$$\delta\mathfrak{W}^{\text{int}}(D,\xi) = \sum_{i=1}^{N} \int_D (\nabla^i \xi) \mid T_i\, dV, \quad \forall \xi \in \mathcal{D}_A, \tag{8.47}$$

[67] We note that the micro-inertial terms have not been included (see for example Polizzotto [88] for other possible choices).

where the Piola stresses T_i are smooth enough (suitably differentiable in the sense of distributions) to allow for the integration by parts which we will perform in the subsequent section on contact forces.

An important remark about Piola stress measures and the functional space of admissible virtual displacement

There is an important mathematical problem which is related to the virtual work functionals and Piola stress measures which we need to highlight.

Piola stress measures are defined as distributions and their domain is therefore, by definition, the subset of test functions $\mathcal{D}_{\mathcal{A}}$ verifying some constraint or some initial or boundary conditions. Now there are **two dual extension problems** to be solved in order to frame in the correct functional space the problem of determination of the motion of considered continua:

1. Having specified the Piola stress measures defining the internal work distribution in the set $\mathcal{D}_{\mathcal{A}}$ to find the maximal set of functions including $\mathcal{D}_{\mathcal{A}}$ and a suitable topology on this set (which we will identify with the set previously called $\mathcal{A}$) such that the internal work distribution can be extended into a continuous linear functional on $\mathcal{A}$.
2. Having specified the set $\mathcal{A}$ including $\mathcal{D}_{\mathcal{A}}$ defining the set of virtual admissible displacements and endowed with its topology to find the set of all Piola stress measures for which the duality formula (8.45) defines a linear and continuous functional in $\mathcal{A}$.

The postulation process of continuum mechanics based on the principle of virtual work supplies a clear set of mathematical problems formulated in the framework of functional analysis and the theory of distributions.

8.6.9 Deformation Measures in Lagrangian *N*th Gradient Continua

In [25] the problem of finding the right deformation measure in the case of Nth gradient continua is addressed from a historical point of view.We refer to the analysis which has been developed there for all the technical details. The interested reader can also see how in [26] the case of second gradient continua can be addressed. We limit ourselves here to recalling some of the results presented in the literature which are relevant in the present context.

Piola, in our opinion correctly, bases his analysis on finite deformation analysis at first and it is only subsequently that he eventually linearizes the deformation measures obtained. The reason that this is the most correct approach is that experience of infinitesimal deformations and placements is, in general, lacking. Rigid placements are preserving distances and their representation is easily obtained by means of translations and rotations, i.e. affine transformations whose linear part is orthogonal. It is only after the process of linearization, which is valid for small displacements and deformations, that skew symmetric linear transformations play a (limited!) role.

By underlining this circumstance and point of view, Piola introduces the tensors

$$F = \nabla\chi, \qquad C = F^T F,$$

and, with simple arguments, concludes that if the placement is rigid then

$$C = I.$$

Therefore one can conclude that the field $C - I$ must be non-vanishing when there is a deformation phenomenon.

Next Piola considers a generic placement and also a very general class of internal interactions, which in general involve long distance interactions between the material particles which constitute the body. To be precise, Piola assumes that at a micro-level the relevant body consists of a discrete system of particles and considers a pairwise interaction depending on the particle distance as a decreasing function. Clearly this kind of interactions is objective: i.e. they do not depend on the observer. In the particular case of Lagrangian continuous bodies, Piola's interactions include the case in which deformation energy depends on all the variations of the distances between any pair of material particles between the reference and the actual configurations.

With ingenious reasoning he:

i) introduces a homogenized continuum, equivalent to the discrete system at large length scales;

ii) shows that, in order to recover his class of interactions, and when the particle interaction is smooth, in general one may need all gradients of C;

iii) as a particular case he considers the class of Lagrangian continua whose deformation energy depends on all the gradients of C up to the Nth order.

Actually Piola's arguments were very general and led him to determine the most general set of fields which may describe locally the state of deformation of continua whose kinematics is described by their placement. To this end he finds the following important equation (for more details see again [25], where the relationship between this statement and the Riemann condition of flatness is established):

$$\nabla^k F = F^{-1} M(C, \ldots . \nabla^k C),$$

where M is a suitable function which depends linearly on its arguments.

Then Piola exploits this relationship to conclude that[68] the maximal list of quantities which are invariant under rigid rotations and can be obtained from the list $\left\{F, \nabla F, \ldots . \nabla^k F\right\}$ is

$$C, \nabla C, \ldots \nabla^k C.$$

Therefore if we want to generalize the definition of first gradient continua by considering deformation energies depending on higher gradients of placement by imposing the objectivity of this dependence we are led to consider C and all its gradients up to the Nth gradient as the appropriate deformation measure.

[68] Here we use the modern nomenclature; the interested reader can peruse [25] to explore Piola's original notations and reasoning.

8.6.10 Consequences of the Principle of Virtual Work on the Structure of Contact Interactions in *N*th Gradient Continua

The structures of the internal work functionals, external work functionals (contact work functionals are a particular case of external work functional, as we have already remarked) and inertial work functionals are not independent.

Indeed, it is obvious that:

the principle of virtual work implies a relationship between the work functionals involved.

For instance, if the structures of internal work functional and inertial work functional are chosen via a constitutive choice (as was done e.g. when we introduced Piola *N*th gradient continua), then stipulating that their sum plus the external virtual work functional has to vanish for every admissible virtual displacement (which is the statement of the principle of virtual work) implies a limitation to the possible admissible choices for external work functionals. In other words:

The assumption of the constitutive equations for internal work and inertial virtual work imposes a specific structure to the possible contact interactions involving the given body.

This point has been extensively commented upon in the previous sections, but we want to go further. Piola proceeded to formulate the previous considerations and rebutted possible objections (or those objections which he knew were frequently cited in opposition) by remarking that one should not be surprised by their consequences, as nobody is surprised by the observation that Euler fluids, whose internal energy depends only on Eulerian mass density, cannot interact at their boundaries with shear contact surface forces.

Further considerations of methodological nature are required here: Physical intuition?

In the postulation approach based on balance of forces and torques, the different assumptions are not logically connected one with another as they are formulated separately. The list of independent assumptions is long: i) form of local (or global) balance equations; ii) constitutive equations for every flux and source term; and iii) constitutive equation for external interactions, which are intended to supply boundary conditions for the balance equations already postulated. It has been remarked by the scholars preferring postulation based on balance laws that it is rather difficult to choose constitutive equations for external interactions which are logically compatible with the other postulated relationships. Therefore, very often, it is claimed that boundary conditions need guidance: physical intuition and evidence. Like naive inductivists, these scholars need to deduce directly from experiments some postulates of their model. Why this point of view must be discarded is discussed at length in Chapter 4.

This inductivist attitude has been extended further. Indeed, in order to establish the needed logical restrictions on (and relationships among) postulated constitutive

equations, it was necessary to invoke physical evidence once more: in this case the entropy inequality (see e.g. [45, 79, 80]).

Why one should introduce entropy (and heat production and balance of total energy) in a purely mechanical context is not clear. Moreover, the Lex Parsimoniae and the Occam's Razor approaches require that the minimum possible assumptions be used while formulating theories.

This is another argument which must be considered for preferring postulations based on the principle of virtual work.

A particular class of external interactions and contact interactions

We explicitly limit ourselves now to considering a particular class of continua. For these continua the external interactions involving every regular sub-body D are described by a **virtual external work functional** which we assume **can be split** into the sum of two addends.

- The first addend models long range external interactions between $D \subseteq B$ and the world external to D. This external interaction functional is assumed to be represented by a distribution which coincides with an integrable function (in the sense of Lebesgue). The inertial virtual work is assumed to be of this last type.
- The second addend corresponds to contact actions. Contact interactions are those particular interactions which are assumed to be distributions concentrated on the boundaries of D and are conceived to account for the localized external interactions involving D .

Some needed results form the theory of distributions and differential geometry

In this context, it is relevant to consider the following results obtained by Laurent Schwartz (see [70]):

LS2 Given a distribution whose support is included in a regular embedded submanifold[69] $M \subset \mathbb{R}^m$ it is possible to represent it uniquely as a finite sum of transverse derivatives of extensions of distributions defined on M.[70]

Obviously, we will want to consider sub-bodies having as boundaries polyhedra or surfaces which are diffeomorphic up to a certain degree to polyhedral surfaces. Therefore the representation theorem by Schwartz must be generalized, even if it gives a useful starting point for our investigations.

With the aim of establishing the structure of contact interactions in Piola's continua it is necessary to study the structure of a distribution $\mathfrak{D}$:

- whose support is included in a compact piece-with-boundary manifold M[71] suitably regular and embedded in $\mathbb{R}^3$,

[69] We explicitly note that the submanifolds considered by Schwartz do not have boundaries. In Schwartz nomenclature regularity means smoothness and absence of boundaries.

[70] A distribution defined on a submanifold M can always be extended to a distribution whose support is included in an open set including M.

[71] For a precise definition see [89]. In a three-dimensional space one can embed curves or surfaces. Roughly speaking we consider here the surfaces which include curves where normals and gradients of normal fields may have first kind discontinuities or curves which include a finite set of points where the tangent

- for which the following representation formula holds

$$\mathfrak{D}_M^N(\xi) = \int_M S \mid \nabla^N \xi \, d\mathcal{H}_M, \tag{8.48}$$

where S and $d\mathcal{H}_M$ denote a suitably regular N-times contravariant tensor field defined on M and the Hausdorff measure relative to M, respectively and the symbol $\mid$ denotes the complete saturation of contravariant and covariant components.

The key results of this study are included in the appendix which concludes the present chapter, and leads us to the following:

The distribution given by the previous formula (8.48) can be represented as follows

$$\mathfrak{D}_M^N(\xi) = \mathfrak{D}_{\perp M}^N(\xi) + \mathfrak{D}_L^{N-1}(\xi) + \mathfrak{D}_{\partial M}^{N-1}(\xi),$$

where

$$\mathfrak{D}_{\perp M}^N(\xi) := \sum_{J=0}^{N} (-1)^{N-J} \int_M \left(\mathrm{div}_{\not\perp M}^{N-J}(S) \right) \mid \left(\nabla^J \xi \right)_\perp$$

$$\mathfrak{D}_L^{N-1}(\xi) := \sum_{J=0}^{N-1} (-1)^{N-1-J} \int_L \left(\left(\mathbb{P}(\mathrm{div}_{\not\perp M}^{N-1-J}(S)) \cdot \nu \right)^+ + \left(\mathbb{P}(\mathrm{div}_{\not\perp M}^{N-1-J}(S)) \cdot \nu \right)^- \right) \mid \nabla^J \xi$$

$$\mathfrak{D}_{\partial M}^{N-1}(\xi) := \sum_{L=0}^{N-1} (-1)^{N-1-L} \int_{\partial M} \mathbb{P}(\mathrm{div}_{\not\perp M}^{N-1-L}(S)) \cdot \nu \mid \nabla^L \xi.$$

In other words:

A distribution $\mathfrak{D}_M^N$ of order N concentrated on an embedded manifold M can be represented as the sum of: i) a distribution $\mathfrak{D}_{\perp M}^N$ of order N concentrated on M and totally orthogonal to M; ii) a distribution $\mathfrak{D}_L^{N-1}$ of order $N-1$ concentrated on L, i.e. the union of submanifolds embedded in M where either the field S or the normal fields to M or the gradients of these normal fields up to the order $N-1$ are jumping; iii) a distribution $\mathfrak{D}_{\partial M}^{N-1}$ of order $N-1$ concentrated on ∂M, i.e. on the boundary (or border) of M.

The structure of contact interactions in Nth gradient continua

Here we want simply to show the complexity of the structure of contact interactions which may arise in Nth gradient continua. Therefore, we postpone the most general possible representation formulas to more technical works and **we assume tha**t:

Piola stresses and all gradients of the normal fields are continuous on the boundary ∂B.

Therefore, the only non-smooth curves embedded in ∂B which we consider are those where the normals to ∂B suffer discontinuities of the first kind. This is the case studied in [10]. Referring to it for more details we describe here the main results found there.

unit vector suffers first kind discontinuities. For more details the reader is referred to the appendix to this chapter.

External virtual work functional for Nth gradient continua Let us consider an Nth gradient continuum B. Let D be a sub-body of B whose topological boundary is a compact piece-with-boundary suitably smooth manifold. Under the assumptions specified in the previous paragraph, the principle of virtual work implies that the external virtual work functional can be additively decomposed in terms of:

i) a functional concentrated on the union of faces $\mathcal{S}_D$ of the boundary of D; this functional, once regarded as a distribution, is totally orthogonal, absolutely continuous with respect to the Hausdorff $\mathcal{H}^2$ measure and its order is smaller or equal to $N-1$,

ii) a functional concentrated on the edges $\mathcal{E}_D$ of the boundary of D; this functional, once regarded as a distribution, is totally orthogonal, absolutely continuous with respect to the Hausdorff $\mathcal{H}^1$ measure and its order is smaller than or equal to $N-2$,

iii) a functional concentrated on the wedges $\mathcal{W}_D$ of the boundary of D. This functional is simply a discrete distribution whose order is smaller than or equal to $N-3$,

iv) a functional absolutely continuous with respect to the Lebesgue measure of D.

In algebraic form:[72]

$$\delta\mathfrak{W}^{\mathfrak{ext}}(D,\xi) = \int_{\mathcal{D}} E\xi\, d\mathcal{H}^3 + \sum_{\Delta=0}^{N-1}\int_{\mathcal{S}_D} F_\Delta \mid \left(\nabla^\Delta \xi\right)_\perp d\mathcal{H}^2 + \sum_{\Delta=0}^{N-2}\int_{\mathcal{E}_D} G_\Delta \mid \left(\nabla^\Delta \xi\right)_\perp d\mathcal{H}^1 + \sum_{\Delta=0}^{N-3}\int_{\mathcal{W}_D} H_\Delta \mid \nabla_\perp^\Delta \xi\, d\mathcal{H}^0. \quad (8.49)$$

where the symbol $_\perp$ has a meaning which depends on the context as it indicates the totally transverse derivation operator with respect to the relevant embedded manifold.

All fields E, F, G, and H are sometimes called dual quantities (with respect to the work functional) of the corresponding virtual displacement or gradient of displacement. We can also call

$$E,\ F_0,\ G_0,\ H_0$$

volume, surface, line or point external forces, respectively, and

$$F_\Delta,\ G_\Delta,\ H_\Delta\ ; \Delta = 1, \ldots N-1$$

the surface, line or point external $(\Delta+1)-$forces (in this last case we follow the nomenclature of Paul Germain), respectively.

[72] In [10] it is attempted to define the "higher powers of border operator" ∂D, $\partial\partial D$ and $\partial\partial\partial D$ of the subbody D. This attempt will make sense completely only when it is framed in the theory of integration of differential forms defined on differential manifolds (for the theory which is presently available we believe that [1] is still the best reference)

In the present context ∂D coincides with $\mathcal{S}_D$ when oriented with the normal field outward pointing with respect to D. For what concerns $\partial\partial D$ and $\partial\partial\partial D$ one has to remark that an edge in $\mathcal{E}_D$ must be regarded as the union of the borders of the two faces in $\mathcal{S}_D$ coming together to form it. Each of these faces has, on this edge, its own external tangent normal ν (for more details see the appendix). Finally, concerning wedges one must consider that several edges can meet in them. Therefore, the shape of any wedge is determined by all tangent-to-edge external vectors coming together, normal to faces externally pointing vectors and external tangent normal vectors.

Representation of contact forces in terms of Piola stresses
Applying the process of integration by parts presented in the appendix (or in [10]) we can show that $\delta\mathfrak{W}^{ext}$ has the same structure appearing in the RHS of (8.49) and determine all quantities dual to virtual displacement or gradients of virtual displacement in terms of Piola stresses T_Λ.

In order to use a systematic notation we start by introducing the following:

$$T(D,\Lambda) := T_\Lambda.$$

The notation refers to $D-$**volume** $\Lambda-$**stresses**. They are the dual of $\Lambda-$gradients of displacement in the distribution representing volume virtual internal work.

We are then obviously led to call **volume internal (1-)force** the quantity

$$F(D,0) := \sum_{\Lambda=0}^{N} (-1)^{\Lambda}\,\mathrm{div}^{\Lambda}(T_\Lambda), \tag{8.50}$$

which manifestly depends linearly on the set of Piola stresses $\{T_\Lambda\}$.

- The notation just introduced is better justified when noting that the zero in (8.50) indicates the order of the distribution which it defines.
- The dependence on D indicates that the introduced fields are used to calculate the images of corresponding distributions via a volume integral.
- One can define only the volume internal $(1-)$force as there are no transverse derivatives in the volume D. The manifold D is a three-dimensional manifold embedded in the three-dimensional Euclidean space $\mathbf{E}^3$.

Next introduce the $\partial D-$**surface** $\Delta-$**stresses**:

$$T(\partial D,\Delta) := \sum_{\Lambda=\Delta+1}^{N} (-1)^{\Lambda-1-\Delta}(\mathrm{div}^{\Lambda-1-\Delta}T_\Lambda)\cdot n, \tag{8.51}$$

where n represents the normal unit vector to the faces of ∂D.

The $\partial D-$**surface** $\Delta-$**stresses** are the dual of $\Delta-$gradients of displacement in the distribution representing virtual internal work concentrated on ∂D.

Using a systematic notation, we can then introduce the **surface density of 1-force** as follows

$$F\,(\partial D,0) := \sum_{L=0}^{N-1}(-1)^{L}\,(\mathrm{div}_{\not\perp\partial D})^{L}\,T(\partial D,L). \tag{8.52}$$

The careful reader will remark immediately that this formula, together with (8.51), contradicts the so-called Cauchy postulate, as dependence on $\nabla n, ..., \nabla^{N-1}n$ appears in it.

We can therefore conclude that the choice of the dependence of contact surface force is NOT a postulate, in the sense made clear by our considerations in Chapter 4, but simply a constitutive assumption. Indeed, the Cauchy postulate is characteristic of first Gradient Piola continua.

Similarly, for $J > 0$, **the surface contact** $(J+1)$**-forces** are given by

$$F\,(\partial D, J) := \left(\sum_{L=J}^{N-1} (-1)^{L-J}\, (\mathrm{div}_{\not\partial D})^{L-J}\, T(\partial D, L) \right)_{\perp \partial D}. \tag{8.53}$$

Obviously, surface contact $(J+1)$-forces depend linearly on the family of stresses $\{T_\Lambda\}$. They also depend on $\nabla n, \ldots, \nabla^{N-1-J} n$.

Continuing the process of integration by parts, we arrive at 1-dimensional embedded manifolds, i.e. curves constituting the second boundary of D.

The $\partial\partial D-$**line** $J-$**stresses** are defined as follows:

$$T(\partial\partial D, J) := \sum_{L=J+1}^{N-1} (-1)^{L-1-J} \left(\mathbb{P}_{\partial D}((\mathrm{div}_{\not\partial D})^{L-1-J}\, T(\partial D, L)) \cdot \nu \right)^{\pm}, \tag{8.54}$$

where $\mathbb{P}_{\partial D}$ denotes the projection operator on the tangent planes of the faces constituting ∂D, and the symbol $()^{\pm}$ denotes the sum of the values in the brackets on the $+$ and on the $-$ side of the edge $\partial\partial D$.

- These stresses are defined only for Nth gradient continua with $N \geq 2$.
- They are the dual of $\Delta-$gradients of displacement in the distribution representing virtual internal work concentrated on $\partial\partial D$.
- The integration by parts along the edges will reduce $\partial\partial D-$**line** $J-$**stresses** to edge forces.

The rationale of our definitions being now manifest, we introduce for $J \geq 0$ and $H \geq 0$ the **line densities of** $(J+1)-$ **forces** $F\,(\partial\partial D, J)$ and **the** $(H+1)$**–forces concentrated on wedges** by setting

$$F(\partial\partial D, 0) := \sum_{L=0}^{N-2} (-1)^{L}\, (\mathrm{div}_{\not\partial\partial D})^{L}\, T(\partial\partial D, L) \tag{8.55}$$

and, for $J > 0$ and $H \geq 0$,

$$F(\partial\partial D, J) := \left(\sum_{L=J}^{N-2} (-1)^{L-J}\, (\mathrm{div}_{\not\partial\partial D})^{L-J}\, T(\partial\partial D, L) \right)_{\perp \delta\delta D} \tag{8.56}$$

$$F(\partial\partial\partial D, H) = T(\partial\partial\partial D, H)$$

$$:= \sum_{L=H+1}^{N-2} (-1)^{L-1-H} \mathbb{P}_{\partial\partial D}((\mathrm{div}_{\not\partial\partial D})^{L-1-H}\, T(\partial\partial D, L)) \cdot t_{\partial\partial D}. \tag{8.57}$$

The reader will note that in the case of wedges, the concepts of wedge-forces and wedge-stresses coincide. This is not surprising, as all vectors applied to a wedge are orthogonal to the plane tangent to a wedge, which degenerates to the singleton of the null vector. Also, note that, when starting with the three-dimensional manifold D embedded in $\mathbf{E}^3$, then the orthogonal space is empty and, therefore, there are no transverse derivatives, and the only volume forces are 1-forces.

Balance of $\Delta-$forces and external forces concentrated on wedges and edges
We conclude this section by remarking that one can easily get the balance laws of $\Delta-$forces by simply equating the just calculated volume and contact forces (all denoted with the symbol $F(\ldots)$) with the externally applied

$$F_\Delta,\ G_\Delta,\ H_\Delta\ ; \Delta = 0, \ldots N-1,$$

i.e. the external surface, line or point $(\Delta+1)$-forces.

It is difficult to conceive how the believers of balance laws may directly postulate these laws, basing them on physical intuition or evidence.

The analysis developed in the appendix shows that it is possible to apply external line and point forces also in curves and points which are not edges or wedges, i.e. manifolds of discontinuity of normal fields to the contact surface. In this case the corresponding stresses will become singular on the application curve or point.

8.6.11 Some Hints on the Relationship between First and Higher Gradient Micro-Structured Continua and the Theory of Lagrange Multipliers

We now also give indications of some easy-to-conceive generalizations of what has been presented so far. One could indeed introduce continua whose kinematics is richer than in the case of Piola continua. For example, a set of further kinematical descriptors may be introduced.

A typical example is given by Cosserat continua, whose kinematics is characterized by an additional field of rotations. This field of rotations is different from the rotation obtained by decomposing $\nabla\chi$ into its symmetric and orthogonal parts (so called Cauchy polar decomposition).

In these generalizations, a difficult task has to be confronted. Indeed, one has to introduce suitably generalized deformation measures in which placement and placement gradients are mixed with the other kinematical descriptors.

However, as already remarked in [10], once the kinematical descriptors are introduced, the postulate of virtual work naturally introduces all relevant stresses and balance laws, once one has postulated what seems to be the most suitable form for inertial and internal virtual work functionals.

The analysis of constrained continua appears to be more delicate, however. In such a case, suitable Lagrange multipliers can be introduced to account for the contact actions induced by the introduced constraints. This analysis becomes rather delicate and needs some advanced arguments from functional analysis. The interested reader is referred to [98] on Lagrange multipliers.

In these entries the work by [91] is extended and formulated by using the most recent results in the theory of constrained optimization in Banach spaces.

8.6.12 How to Implement a Variational Principle Dealing with Initial Conditions

Antman and Osborn (see [82]) faced the problem of formulating a variational principle which is at least as general as the principle of virtual work, and which has the capability

to include the imposition of initial conditions together with boundary conditions. The motivation for such a conceptual effort is not only imposed by a requirement of logical consistence and elegance, but also by the need of having a powerful tool to be exploited in applications.

Their formulation is very elegant and effective, and can, possibly, be extended to higher gradient continua. We discuss below, by retaining the notations employed up to now, which are slightly different from those used by Antman, the statement of the principle of virtual work as formulated at page 445 of [81].

The motion of a Cauchy continuum, i.e. the function $\chi : V \times [0, \infty] \to E^3$ which fulfils the imposed boundary conditions and such that $\chi(X, t_0) = \chi_0(X)$, where χ_0 is the initial placement, is determined by imposing the verification of the following condition:

$$\int_{t_0}^{\infty} dt \int_V \left[P : \nabla_X \eta - b^V \eta - \varrho \frac{\partial \chi}{\partial t} \cdot \frac{\partial \eta}{\partial t} \right] dV - \int_V \varrho v_0 \eta dV$$

$$\forall \eta \in Adm \quad (8.58)$$

$$- \int_{t_0}^{\infty} dt \int_{\partial V / \partial_d V} b^{\partial V} \eta dA = 0,$$

where the set $Adm \subset C^{\infty}(\bar{V}) \times [0, \infty]$ [73] is the set of infinitely differential functions which have compact support included in $\bar{V}$ and are vanishing on $\partial_d V$ and for $t = t_0$, where the field v_0 is the initial velocity of the body, and where the Piola tensor P has to be determined by some constitutive equations in terms of the motion.

The theory of constitutive equations to be used when the Piola tensor depends locally only on the value of the first gradient of placement is fully developed in [81], where, however, the theory of higher gradient continua is simply evoked without making clear that, in order to develop it, a major improvement of the modeling procedure is needed.

Note that (8.58) is simply the reformulation of Eq. (8.22) with a work functional $\delta \mathfrak{W}(\eta(\cdot; t))$ given as the sum of the functionals in (8.33) and (8.34) where, instead of the virtual displacement $\xi(X)$, the virtual variation of motion function $\eta(X; t)$ has to be considered.

By considering a reformulation of Eq. (8.22), considering the work functional used to formulate the principle of virtual work for higher gradient micro-structured continua, it is easy to generalize the condition (8.58) to this more complex (and wide) family of continua.

Clearly, this ease of development justifies fully the preference for the postulations based on the principle of virtual work.

8.6.13 Some Final Considerations about Nominalism: On the Nature of Forces

Forces and stresses are concepts which are introduced on the basis of the analysis of the mathematical structure of considered models. They are concepts whose abstract nature places them very far from physical reality. In Chapter 4 we have tried to understand and enlarge upon how it could happen that, simply for contingent reasons, the ontological status of "real objects" was assigned to these abstract concepts. Although no force or

[73] With $\bar{V}$ we denote the topological closure of V.

stress has ever been measured directly, as only displacements, elongations or deformations can be really measured, they were regarded as the most fundamental concepts in the theory of deformable bodies. Moreover, because the naive inductivism tends to find experimental evidence to support abstract concepts, directly basing on it any kind of postulate, the balance of force and torque has been attributed an exaggerated importance (see for instance [45, 57]).

Such a naive inductivism is too much rooted into the tradition of mechanical science: even in otherwise remarkable work [74] Hellenistic science is criticized because it is considered to be based on a "series of pure abstract assumptions" without "any experimental support", which the authors believe is an approach that has been introduced, as a solid foundation of physical theories, only (sic!) during the Middle Ages, as "Greek scientists were not interested in experiments" but only "abstract theory".

The author of [74] seems, therefore, to be unaware of the enormous technological achievements of Hellenistic science (see [21]) and also underestimates the importance, with respect to technological advancements, of the formulation of hypothetico-deductive models.[74]

In this chapter we have focused our attention on the description of what we believe to be the best postulation scheme to be used in the formulation of models for innovative metamaterials. In this context, we have remarked that the nineteenth century concepts of stress and strain must be generalized, if exotic materials have to be described, conceived and designed. We believe that there is no possibility to understand, with physical intuition and/or experimental evidence only, the complex and abstract concepts of force and stress, and their more modern generalizations.

Even if reading some of the statements of D'Alembert one could believe the contrary, D'Alembert did use the concept of force, but as a derived concept.[75] The concept of force is an abstract logical construction, invented by the human mind, whose role may be important to develop a conjectural theory to be tested with experiments[76] Forces, in the postulations based on the principle of virtual work, are derived concepts. ***Once the primitive concept of work, or action, has been introduced, then forces and stresses are defined as the dual in the expended virtual work of displacement and strain, respectively.***

In this definition, which is nominalistic[77] in nature, and only in this definition, consists the true nature of forces and stresses. Indeed

"In Nomina est Natura Rerum". Anonymous (*In the names is the nature of things*).

[74] We repeat here that we are aware, as W.V. Quine among many others states, that "all theories (and the propositions derived from them) are under-determined by empirical data" and that "although some theories are not justifiable, failing to fit with the data or being unworkably complex, there are many equally justifiable alternatives."

[75] We do not believe that "force" is a "non-referring name" as described by Quine.

[76] In [21] it is proven that such concepts were already used in Hellenistic science. The presumed incapacity of Hellenistic science to achieve technological progress is, in reality, simply the result of the failure of many modern scholars to understand the conjectural nature of scientific theories. The ontology of names is clear since Hellenistic science: their existence is based on their precisely assigned meaning. Either this meaning is given by a system of axioms (then they are primitive concepts) or it is given by a set of definitions (then they are derived concepts).

[77] As J. S. Mill, echoing Auguste Comte, had the occasion to state "there is nothing general except names."

The above statement, whose more ancient sources have been lost, probably originated in Middle Age epistemology during the debate about ancient logics and science and their meaning. We interpret it as a slogan invented to underline the importance of mathematical formalism. The sentence claims that the nature of things (i.e. phenomena, experimental evidence and our experience of the world) is given by the names (i.e. the definitions) used to talk about them.

In the present context we claim that one cannot specify the meaning of the action and its variation without definitions. If one cannot write integrals on T, calculate derivatives, impose boundary conditions, define the set of admissible variations and so on then one cannot transmit the capacity of describing the nature of things. Precise names given to things are needed to proceed in our investigation of the world in which we are living. We may add that our models are constructed by means of particular names: constructed with symbols and formulas.

The interaction between theories and experimental evidence is a complex interplay, based on motivations, **a priori** assumptions and experimental feedback. To underline this circumstance, and therefore the role which evidence must play when building a theory, the classical scientific tradition developed other slogans.[78]

"Nomina sunt Consequentia Rerum." Iustinianus, Institutiones Liber II,7,3
(The names are consequences of the things).

The indication is that we should not use an empty nominalism,[79] otherwise we will develop empty mathematical models, full of non-referring names.[80]

Mathematical models must describe reality. In order to do this, the exchange between the phenomena, and their mathematical description must be continuous. Therefore, the names are to be molded in order to somehow reflect the object or the concept which they are intended to designate. The classical example is the word "trapezoid" coming from the Greek word "τραπεζοειζή," which means stool or small table.[81] A whole mathematical theory must be consciously molded on the basis of what we expect that it should describe.

In doing so, variational principles can be of great use: Nature seems to minimize everything and works in a very efficient way.

8.7 Appendix

In this appendix we extend some of the results presented in [10] in a slightly more general context.

[78] Iustinianus used this slogan in a juridic context. However, J.S. Mill's work proves how close are philosophy of science and political theory.

[79] Here again the work of Quine seems precious to recover and develop the ancient Archimedean spirit.

[80] Some negative drifts of modern mechanics lead some scholars to an empty nominalism which either tells absolutely trivial things in a complex way or tells absolutely nothing, always in a extremely complex way.

[81] The reader should think of "a single seat on legs or a pedestal without arms or a back," as defined in Dictionary.com. If one had the opportunity to see ancient Roman seats or small tables, one would recognize the geometrical figure (see [21] for a more detailed discussion of this point).

8.7.1 Piecewise Regular Surfaces Embedded in E^3

We identify the reference configuration of the body with a subset B of the Euclidean three-dimensional affine space $\mathbf{E}^3$. The set of sub-bodies on whose boundary we will consider contact interactions are the closure of open subsets of B having a topological boundary which is a piecewise regular surface of the type defined below.

To describe contact interactions we need some concepts of Gaussian differential geometry and follow closely the notation used in [90]. Indeed, the relevant topological boundaries, when regarded as embedded submanifolds in $\mathbf{E}^3$, are an example of compact piece-with-boundary smooth manifolds (see [89]). These surfaces are an example of "shape" as defined in [7, 8].

We say that Σ is a **piecewise regular (orientable and rectifiable) surface embedded in $\mathbf{E}^3$** when there exists a finite collection $(A = 0, ...M)$

$$\Gamma_A := \left\{\gamma_{i,A} \subset \Sigma, i = 1, \dots K_A\right\}$$

of C^1 curves (which we call ***A-edges***) whose union is called Γ and a finite set of points (which we call ***wedges***)

$$W := \{W_i \in \Sigma, i = 1, \dots, H\}$$

such that all the following conditions are verified:

- Every $p \in \Sigma - (W \cup \Gamma)$ is **a regular point of** Σ: this means that there exists a neighbourhood of p on Σ for which there exists a local $C^{M+1}-$diffeomorphism r defined in $\mathbb{R}^2$. Each one of these local diffeomorphisms is called **an internal chart** of Σ. We assume that for every internal chart r the set $r(\mathbb{R}^2)$ is a rectifiable surface.
- In every $p \in \Sigma - (W \cup \Gamma)$ there exists a normal vector $n(p)$ to the surface Σ.
- The field n is assumed to have a discontinuity of the first kind on the curves belonging to Γ_0. The boundary of the surface Σ is assumed to belong to Γ_0 and is denoted with the symbol $\gamma_{1,0}$,
- The field $\nabla^A n$ is assumed to have a discontinuity of the first kind on the curves belonging to Γ_A $(A = 1, ...M)$, and in the following $\nabla^0 n = n$.
- For every $p \in \gamma_{i,A}$ there exist two **boundary (or border[82]) charts,** i.e. bijective and smooth functions

$$r^{\pm} : [0, \infty[\times \mathbb{R} \to I^{\pm} \subset \Sigma \tag{8.59}$$

such that

$$r^{\pm}(0, 0) = p, \qquad r^{\pm}(0, \mathbb{R}) = \gamma_{i,A} \cap I^{\pm}, \tag{8.60}$$

$$(\forall y \in]0, \infty[\times \mathbb{R}) \left(r^{\pm}(y) \in \Sigma - (W \cup \Gamma)\right), \tag{8.61}$$

and both the following limits exist

$$\lim_{x \to (0,0)} \nabla^A n(r^{\pm}(x)) := \nabla^A n^{\pm}(p).$$

[82] We believe that the generally accepted nomenclature should be modified to avoid the confusion between the topological boundary and border as defined here.

- Every curve $\gamma_{i,A}$ is the boundary of two regular faces $\Sigma^{\pm}_{i,A}$ one of which is called side $+$ and the other side $-$ relative to $\gamma_{i,A}$. The unit outward pointing normal vectors to $\gamma_{i,A}$ in the tangent plane to $\Sigma^{\pm}_{i,A}$ will be denoted respectively with the symbols $\nu^{\pm}_{i,A}$.
- Every curve $\gamma_{i,A}$ (whose length will be $l_{i,A}$) can be globally parameterized by the C^1 chart $r_{i,A}$

$$r_{i,A} : s \in \left[0, l_{i,A}\right] \mapsto p \in S$$

such that [83]

$$\left\| \frac{dr_{i,A}}{ds} \right\| = 1, \qquad \frac{dr_{i,A}}{ds} \cdot n^{\pm} = 0.$$

We will assume that

$$\frac{dr_{i,A}}{ds} \times n^{\pm} = \pm \nu^{\pm}_{i,A}.$$

- Every wedge $W_j \in W$ is the initial or final endpoint for a curve $\gamma_{i,A}$. In equation form:

$$r_{i,A}(0) = W_j \ \text{ or } \ r_{i,A}(l_{i,A}) = W_j.$$

- We call the **face of** Σ a maximal connected subset of regular points; each face Σ_α ($\alpha = 1, \ldots . \Phi$) is a manifold with boundary, its boundary being the finite union of some curves in the set $\left\{\gamma_{i,A}\right\}$ and some wedges.

On the basis of the previous definition, one can say that piecewise regular orientable and rectifiable surfaces, are surfaces embedded in $\mathbf{E}^3$ having a finite set of curves where the normal vector field is jumping, and a finite set of curves where $\nabla^A n$ is jumping. Moreover, these curves are coming together in a finite set of wedges, and for all these curves a tangent vector is always defined while both the gradients $\nabla^A n^{\pm}$ of the two faces coming together on the edge are defined.

8.7.2 Gauss Divergence Theorem for Embedded Riemannian Manifolds

From now on we will assume that we have fixed a global orthonormal basis $(E_A, A = 1, 2, 3)$ in $\mathbf{E}^3$, and all needed tensor fields will be represented using their components in such a basis. As the differential geometric objects forming the piecewise regular surfaces Σ which we are considering as contact surfaces are either surfaces with boundary (the faces of Σ) or curves (the edges of Σ), in this section we will recall in a comprehensive way some results which hold for a generic embedded piece-with-boundary manifold M in $\mathbf{E}^3$, be it a regular curve or a surface with boundaries.

Due to our regularity assumptions, it is possible (see [97]) to prove the existence of Gaussian coordinate systems for such embedded manifolds.[84] As a consequence there is a neighborhood of these embedded manifolds in which the projection operator fields

[83] Note that when $A > 0$ then $n^+ = n^-$.

[84] These coordinates are such that: i) the considered surface is a coordinate surface (or the considered curve is a coordinate curve); and ii) the remaining coordinate curves are tangent to the normal fields.

P (projection on their tangent space) and Q (projection on their normal bundle) can be defined. These projection operators will be used to represent the needed divergence operators on the embedded manifolds. Using this representation, Germain obtained in an expeditious way, in the case of second gradient materials, the representation formulas which were sought for contact interactions.

Obviously we have

$$\begin{gathered}\delta_A^B = P_A^B + Q_A^B, \quad P_A^B P_B^C = P_A^C, \\ Q_A^B Q_B^C = Q_A^C, \quad P_A^B Q_B^C = 0.\end{gathered} \tag{8.62}$$

We consider a set $\mathcal{F}$ of fields defined on M: one of these fields will be the field of unit normals in the case of surfaces, and the field of unit tangents in the case of curves. We assume that M includes a finite set of lower dimension manifolds whose union is denoted by L,[85] where the fields in $\mathcal{F}$ (or their gradients up to the maximal order considered) may suffer discontinuities of the first kind. The points in M which do not belong to L are called **regular points**. In these points, the manifold and all considered fields have the maximal regularity required. The maximal connected sets of regular points, in short **maximal regularity sets,** are called **faces** if M is a surface or **arcs** if M is a curve. We assume that there is a finite number Φ of maximal regularity sets: we will denote each of them M_σ, with $\sigma = 1, \dots \Phi$. Every element L_β, where $\beta = 1, \dots, \Psi$, in L has on each of its two sides a maximal regularity set, which, when needed, will be called ${M_\beta}^{\pm}$. The unit external normal to the boundary ∂M tangent to M will be denoted by ν, while, for every element L_β, the unit external normal to L_β tangent to ${M_\beta}^{\pm}$, the tangent and orthogonal projectors to ${M_\beta}^{\pm}$ will be denoted respectively $\nu_\beta^{\pm}$, $P_\beta^{\pm}$ and $Q_\beta^{\pm}$. The limits of every considered field on each side of L_β will equally be followed by the corresponding $\overset{\pm}{\beta}$ apices and indices.

- Let us consider a vector field W in the set $\mathcal{F}$: W (or one of its derivatives) is possibly suffering discontinuities of the first kind on the set of lower dimension manifolds L.[86] Moreover, we assume that W is regular enough to allow us to apply the Gauss divergence theorem to every maximal regularity set M_σ. The divergence theorem applied to the manifold M and the field W reads (see e.g. [97]):

$$\begin{aligned}\int_M (P_B^A W^B)_{,C} P_A^C &= \sum_{\sigma=1}^{\Phi} \int_{M_\sigma} (P_B^A W^B)_{,C} P_A^C \\ &= \int_{\partial M} W^A P_A^C \nu_C + \sum_{\beta=1}^{\Psi} \int_{L_\beta} \left[\left(W^A P_A^C \nu_C \right)_\beta^+ + \left(W^A P_A^C \nu_C \right)_\beta^- \right] \\ &= \int_{\partial M} W^A P_A^C \nu_C + \int_L \left[\left(W^A P_A^C \nu_C \right)^+ + \left(W^A P_A^C \nu_C \right)^- \right].\end{aligned} \tag{8.63}$$

[85] In the case of surfaces we have a finite number of discontinuity curves, in the case of curves we have a finite number of discontinuity points.

[86] We repeat that in L are included the curves where the normal fields to M, or their gradients up to the maximal order considered, are discontinuous.

- We can rewrite the previous formula in a compact form. To this end, let div_M denote the divergence operator on M: it maps any tangent vector field $W_\parallel$, having components $P^A_B W^B$ into the scalar field (denoted $\mathrm{div}_M W_\parallel$) which has as components $(P^A_B W^B)_{,C} P^C_A$:

$$\begin{aligned}\int_M \mathrm{div}_M W_\parallel &= \sum_{\sigma=1}^{\Phi} \int_{M_\sigma} \mathrm{div}_M W_\parallel = \\ &= \int_{\partial M} \left(W_\parallel \cdot \nu\right) + \sum_{\beta=1}^{\Psi} \int_{L_\beta} \left[\left(W_\parallel \cdot \nu\right)^+_\beta + \left(W_\parallel \cdot \nu\right)^-_\beta\right] \\ &= \int_{\partial M} \left(W_\parallel \cdot \nu\right) + \int_L \left[\left(\left(W_\parallel \cdot \nu\right)\right)^+ + \left(\left(W_\parallel \cdot \nu\right)\right)^-\right]\end{aligned} \tag{8.64}$$

  where the dot product stands for the saturation of contravariant and covariant indices.
- The previous definition of divergence operator on M can be easily extended to an Nth order tensor field T by applying the derivation and projection to a specific coordinate. As a consequence, $\mathrm{div}_M T$ is a $(N-1-\mathrm{th})$-order tensor.

8.7.3 Projections of Tensor Fields Defined on Embedded Manifolds

We are interested in studying the structure of distributions concentrated on embedded manifolds. The main result on which we base our analysis is the representation formula (8.48), where the totally symmetric tensor $\nabla^N \xi$ is saturated with a tensor S. Clearly, this last tensor can be naturally assumed to be totally symmetric. Moreover, as the Nth gradient operator is defined as a covariant tensor, S is naturally regarded as a contravariant Nth order tensor.

Therefore, in what follows, we will consider Nth order totally symmetric tensors and we will represent their contravariant and covariant components with the upper ${}^{i_1 i_2 \dots i_N}$ and lower ${}_{j_1 \dots j_N}$ indices notations, respectively.

For any totally symmetric tensor field S of order N defined on M, the following projected tensors fields can be defined:

$$S^{j_1 \cdots j_N}_\perp := S^{i_1 i_2 \dots i_N} Q^{j_1}_{i_1} Q^{j_2}_{i_2} \dots Q^{j_N}_{i_N} \tag{8.65}$$

$$\mathbb{P}(S)^{j_1 \cdots j_N} := \underset{j_1 \cdots j_{N-1}}{Sym} \left(\sum_{\alpha=0}^{N-1} C^\alpha_N S^{i_1 i_2 \dots i_N} Q^{j_1}_{i_1} \dots Q^{j_\alpha}_{i_\alpha} P^{j_{\alpha+1}}_{i_{\alpha+1}} \dots P^{j_{N-1}}_{i_{N-1}} \right) P^{j_N}_{i_N}, \tag{8.66}$$

where C^α_N denote the binomial coefficients.

The field $S_\perp$ is the field obtained projecting all components of S in the normal bundle of M. Instead, the field $\mathbb{P}(S)$ is obtained by extracting at its last component a projector in the tangent space of M and calculating the total symmetric part of its factor.

The obvious identity

$$S^{j_1 \dots j_N} = S^{i_1 \dots i_N} (P^{j_1}_{i_1} + Q^{j_1}_{i_1}) \dots (P^{j_N}_{i_N} + Q^{j_N}_{i_N})$$

implies that

$$\underset{j_1\dots j_N}{Sym}\ \mathbb{P}(S)^{j_1\dots j_N} = (S - S_\perp)^{j_1\dots j_N}. \tag{8.67}$$

To write the integration by parts formula which follows in a more compact way we use the composed operator $\mathrm{div}_{\not\sim M}$ and its iterates $\mathrm{div}^{\alpha}_{\not\sim M}$ defined as follows:

$$\mathrm{div}_{\not\sim M}(T) := \mathrm{div}_M\,(\mathbb{P}(T)) \tag{8.68}$$

$$\mathrm{div}^0_{\not\sim M} T := T \quad \text{and} \quad \mathrm{div}^{\alpha}_{\not\sim M}(T) := \mathrm{div}_{\not\sim M}(\mathrm{div}^{\alpha-1}_{\not\sim M}(T)). \tag{8.69}$$

First integration by parts formula:
Let T be a totally symmetric Nth order tensor field and let V be a scalar field, both defined on M.

If they are suitably regular then the following equality holds:

$$\begin{aligned}\int_M T \mid \nabla^N V = \int_M T_\perp \mid \left(\nabla^N V\right)_\perp - \int_M \mathrm{div}_{\not\sim M}(T) \mid \nabla^{N-1} V \\ + \int_L \left((\mathbb{P}(T)\cdot\nu)^+ + (\mathbb{P}(T)\cdot\nu)^-\right) \mid \nabla^{N-1} V + \int_{\partial M} \mathbb{P}(T)\cdot\nu \mid \nabla^{N-1} V,\end{aligned} \tag{8.70}$$

where the symbol $\mid$ denotes the saturation of contravariant and covariant indices of the tensors involved.

Note that it is only because all these tensors are totally symmetric that the notation used is not ambiguous. Moreover, it was only to avoid ambiguities that we introduced the symbol $\mathbb{P}(T)\cdot\nu$ denoting the saturation of the last contravariant index of $\mathbb{P}(T)$ with the covariant index of ν.

In the less ambiguous component representation Eq. (8.70) reads

$$\begin{aligned}\int_M T^{i_1 i_2\dots i_N} V_{,i_1 i_2\dots i_N} = \int_M T^{i_1 i_2\dots i_N} Q^{j_1}_{i_1} Q^{j_2}_{i_2}\dots Q^{j_N}_{i_N} V_{,j_1 j_2\dots j_N} \\ - \int_M \left(\left(\mathbb{P}(T)^{j_1\dots j_N}\right)_{,l} P^l_{j_N}\right) V_{,j_1 j_2\dots j_{N-1}} \\ + \int_L \left(\left(\mathbb{P}(T)^{j_1\dots j_N}\nu_{j_N}\right)^+ + \left(\mathbb{P}(T)^{j_1\dots j_N}\nu_{j_N}\right)^-\right) V_{,j_1 j_2\dots j_{N-1}} \\ + \int_{\partial M} \left(\mathbb{P}(T)^{j_1\dots j_N}\nu_{j_N}\right) V_{,j_1 j_2\dots j_{N-1}}.\end{aligned} \tag{8.71}$$

Proof of the first integration by parts formula
The tensors $\mathbb{P}(T)$ and $(T - T_\perp)$ have been defined to have the same totally symmetric part. Therefore:

$$\int_M T^{i_1 i_2\dots i_N} V_{,i_1 i_2\dots i_N} = \int_M T^{i_1\dots i_N} Q^{j_1}_{i_1}\dots Q^{j_N}_{i_N} V_{,j_1\dots j_N} + \int_M \mathbb{P}(T)^{j_1\dots j_N} V_{,j_1\dots j_N}.$$

Moreover we have that $\mathbb{P}(T)^{j_1\dots j_{N-1}j_N} = \mathbb{P}(T)^{j_1\dots j_{N-1}l}P_l^{j_N}$. By using the divergence theorem (see 8.63):

$$\begin{aligned}\int_M T^{i_1\dots i_N}V_{,i_1\dots i_N} &= \int_M T^{i_1\dots i_N}Q_{i_1}^{j_1}\dots Q_{i_N}^{j_N}V_{,j_1j_2\dots j_N} + \int_M \mathbb{P}(T)^{j_1\dots j_{N-1}l}V_{,j_1\dots j_{N-1}j_N}P_l^{j_N}\\ &= \int_M T_\perp^{j_1\dots j_N}V_{,j_1\dots j_N} - \int_M \left(\mathbb{P}(T)^{j_1\dots j_{N-1}l}\right)_{,j_N}P_l^{j_N}V_{,j_1\dots j_{N-1}}\\ &\qquad + \int_M \left(\mathbb{P}(T)^{j_1\dots j_{N-1}l}V_{,j_1\dots j_{N-1}}\right)_{,j_N}P_l^{j_N}\\ &= \int_M T_\perp^{j_1\dots j_N}V_{,j_1\dots j_N} - \int_M \left(\left(\mathbb{P}(T)^{j_1\dots j_{N-1}l}\right)_{,j_N}P_l^{j_N}\right)V_{,j_1j_2\dots j_{N-1}}\\ &\quad + \int_L \left(\left(\mathbb{P}(T)^{j_1\dots j_{N-1}j_N}\nu_{j_N}\right)^+ + \left(\mathbb{P}(T)^{j_1\dots j_{N-1}j_N}\nu_{j_N}\right)^-\right)V_{,j_1j_2\dots j_{N-1}}\\ &\quad + \int_{\partial M}\mathbb{P}(T)^{j_1\dots j_{N-1}l}V_{,j_1j_2\dots j_{N-1}}P_l^{j_N}\nu_{j_N},\end{aligned}$$

the proof is concluded.

Complete integration by parts formula

It is possible to apply exactly N times the formula of integration by parts that we have just found.

Let T be a suitably regular totally symmetric tensor field of order N defined on M. We have:

$$\begin{aligned}\int_M T \mid \nabla^N V &= \sum_{J=0}^{N}(-1)^{N-J}\int_M \left(\mathrm{div}_{\not\subset M}^{N-J}(T)\right) \mid \left(\nabla^J V\right)_\perp\\ &\quad + \sum_{L=0}^{N-1}(-1)^{N-1-L}\int_L \left(\left(\mathbb{P}(\mathrm{div}_{\not\subset M}^{N-1-L}(T))\cdot\nu\right)^+\right.\\ &\qquad\qquad \left. + \left(\mathbb{P}(\mathrm{div}_{\not\subset M}^{N-1-L}(T))\cdot\nu\right)^-\right) \mid \nabla^L V. \qquad (8.72)\\ &\quad + \sum_{L=0}^{N-1}(-1)^{N-1-L}\int_{\partial M}\mathbb{P}(\mathrm{div}_{\not\subset M}^{N-1-L}(T))\cdot\nu \mid \nabla^L V.\end{aligned}$$

Proof by induction

When $N = 1$ the formula has already been proven.

In the inductive step we start by assuming that (8.72) holds for a generic N.

Then, we consider the LHS of Eq. (8.72) when the order of T is $N+1$. By integrating by parts we get

$$\begin{aligned}\int_M T \mid \nabla^{N+1}V &= \int_M T \mid \left(\nabla^{N+1}V\right)_\perp +\\ &\quad - \int_M \mathrm{div}_{\not\subset M}T \mid \nabla^N V + \int_L \left((\mathbb{P}(T)\cdot\nu)^+ + (\mathbb{P}(T)\cdot\nu)^-\right) \mid \nabla^N V\\ &\quad + \int_{\partial M}\mathbb{P}(T)\cdot\nu \mid \nabla^N V.\end{aligned}$$

Afterwards, we apply the induction hypothesis to the LHS. We note that the Nth order tensor for which we apply (8.72) is now $\mathrm{div}_{\not\vdash M} T$. With simple calculations we get:

$$\begin{aligned}\int_M T \mid \nabla^{N+1} V = &\int_M T \mid \left(\nabla^{N+1} V\right)_\perp \\ &- \sum_{J=0}^{N} (-1)^{N-J} \int_M \left(\mathrm{div}_{\not\vdash M}^{N-J}(\mathrm{div}_{\not\vdash M} T)\right) \mid \left(\nabla^J V\right)_\perp \\ &- \sum_{L=0}^{N-1} (-1)^{N-1-L} \int_L \Big(\left(\mathbb{P}(\mathrm{div}_{\not\vdash M}^{N-1-L}(\mathrm{div}_{\not\vdash M} T)) \cdot \nu\right)^+ \\ &\qquad + \left(\mathbb{P}(\mathrm{div}_{\not\vdash M}^{N-1-L}(\mathrm{div}_{\not\vdash M} T)) \cdot \nu\right)^- \Big) \mid \nabla^L V \\ &+ \int_L \left((\mathbb{P}(T) \cdot \nu)^+ + (\mathbb{P}(T) \cdot \nu)^-\right) \mid \nabla^N V \\ &- \sum_{L=0}^{N-1} (-1)^{N-1-L} \int_{\partial M} \mathbb{P}(\mathrm{div}_{\not\vdash M}^{N-1-L}(\mathrm{div}_{\not\vdash M} T)) \cdot \nu \mid \nabla^L V \\ &+ \int_{\partial M} \mathbb{P}(T) \cdot \nu \mid \nabla^N V \,,\end{aligned}$$

which can be seen to prove our statement by extending the first summation range up to $N + 1$, and the following summations range up to N.

It is clear that the formula just determined can be used to decompose any regular distribution of order N on M in a transverse regular distribution of the same order on M and a distribution of order $N - 1$ concentrated on $L \cup \partial M$. In this way, we generalize the previously mentioned result LS2 found by Schwartz.

Bibliography

[1] Arnold, V.I., *Mathematical Methods of Classical Mechanics*, Springer, 2nd edition, 1989.

[2] Benvenuto, E., *La scienza delle costruzioni e il suo sviluppo storico*, Sansoni, Firenze, 1981.

[3] Berdichevsky V., *Variational Principles of Continuum Mechanics*, Springer, 2009.

[4] Bourdin, B., Francfort, G.A., and Marigo, J.-J., The variational approach to fracture, *J. Elasticity*, 91, 1–3, 1–148, 2008. (The paper also appeared as a Springer book: ISBN: 978-1-4020-6394-7).

[5] Colonnetti, G., *Scienza delle costruzioni*, Torino, Edizioni Scientifiche Einaudi, 3rd ed., 1953–57.

[6] Cosserat, E., and Cosserat, F., Sur la Théorie des Corps Déformables, Herman, Paris, 1909.

[7] dell'Isola, F., and Seppecher, P., The relationship between edge contact forces, double force and interstitial working allowed by the principle of virtual power. *Comptes Rendus de l'Academie de Sciences - Serie IIb: Mécanique, Physique, Chimie, Astronomie*, 321: 303–308, 1995.

[8] dell'Isola, F., and Seppecher, P., Edge Contact Forces and Quasi-Balanced Power. *Meccanica*, 32: 33–52, 1997.

[9] dell'Isola, F., Madeo, A., and Seppecher, P., Boundary Conditions in Porous Media: A Variational Approach. *Int. Journal of Solids and Structures*, 46: 3150–3164, 2009.

[10] dell'Isola, Francesco, Pierre Seppecher, and Angela Madeo. How contact interactions may depend on the shape of Cauchy cuts in Nth gradient continua: Approach "à la D'Alembert." *Zeitschrift für angewandte Mathematik und Physik* 63.6: 1119–1141, 2012.

[11] Feynman, R.P., Leighton, R., and Sands, M., *The Feynman Lectures on Physics: The Definitive and Extended Edition*, (Feynman, Leighton, Sands), 3 vv., Addison Wesley, Reading (MA) 2^{nd} ed., 2005.

[12] Bourdin B. and Francfort, G.A., "Fracture" in dell'Isola, Francesco, and Sergey Gavrilyuk, eds. Variational Models and Methods in Solid and Fluid Mechanics. Vol. 535. Springer Science & Business Media, 2012.

[13] Germain, P., La méthode des puissances virtuelles en mécanique des milieux continus. Première partie. Théorie du second gradient, *J. Mécanique*, 12: 235–274, 1973.

[14] Homer. *The Iliad*. Translated by Murray, A. T., Loeb Classical Library Volumes1. Cambridge, MA, Harvard University Press; London,William Heinemann Ltd., 1924.

[15] Lagrange, J.L., *Mécanique Analytique*, Editions Jaques Gabay, Sceaux,- Cambridge Library Collection 1788-1815-2009.

[16] Lanczos, C., *The Variational Principles of Mechanics*. Toronto: University of Toronto, 1970.

[17] Landau, L.D., and Lifshitz, E.M., *Quantum Mechanics: Non-Relativistic Theory*. Vol. 3 (3rd ed.), Pergamon Press, 1977.

[18] Moiseiwitsch, B.L., *Variational Principles*, Dover, 1966.

[19] Netz, R., and Noel., W., *The Archimedes Codex: How a Medieval Prayer Book Is Revealing the True Genius of Antiquity's Greatest Scientist*, Da Capo Press, 2009. See also the website http://www.archimedespalimpsest.org/

[20] Rorres, C., Completing Book II of Archimedes's *On Floating Bodies, The Mathematical Intelligencer*, 26(3): 32–42, 2004.

[21] Russo, L., *The Forgotten Revolution*, Springer Verlag, 2003.

[22] Vailati, G., Il principio dei lavori virtuali da Aristotele a Erone d'Alessandria, Scritti (Bologna, Forni, 1987), vol. II, pp. 113–128. Atti della R. Accademia delle Scienze di Torino, vol. XXXII, adunanza del 13 giugno 1897, quaderno IG (091) 75 I - III. 1987.

[23] Winter T.N. The mechanical problems in the corpus of Aristotle, vol 68. Faculty Publications, Classics and Religious Studies Department, Lincoln (2007)

[24] dell'Isola, F., Maier, G., Perego, U., *et al*. *The Complete Works of Gabrio Piola*: Volume I. Cham, Switzerland: Springer, 2014.

[25] dell'Isola, F., Andreaus, U., and Placidi, L. At the origins and in the vanguard of peridynamics, non-local and higher-gradient continuum mechanics: An underestimated and still topical contribution of Gabrio Piola. *Mathematics and Mechanics of Solids*, 20(8): 887–928, 2015.

[26] Auffray, N., dell'Isola, F., Eremeyev, V. A., Madeo, A., and Rosi, G.. Analytical continuum mechanics à la Hamilton–Piola least action principle for second gradient continua and capillary fluids. *Mathematics and Mechanics of Solids*, 20(4): 375–417, 2015.

[27] dell'Isola, F., Andreaus, U., Placidi, L., and Scerrato, D. Intorno alle equazioni fondamentali del movimento di corpi qualsivogliono, considerati secondo la naturale loro forma e costituzione. In *The Complete Works of Gabrio Piola*: Volume I (pp. 1–370). Springer, Cham, 2014.

[28] dell'Isola, Francesco, Alessandro Della Corte, and Ivan Giorgio. Higher-gradient continua: The legacy of Piola, Mindlin, Sedov and Toupin and some future research perspectives. *Mathematics and Mechanics of Solids* 22(4): 852–872, 2017.

[29] Piola, Gabrio. Sull'applicazione de'principj della meccanica analitica del Lagrange ai principali problemi. Memoria di Gabrio Piola presentata al concorso del premio e coronata dall'IR Istituto di Scienze, ecc. nella solennitá del giorno 4 ottobre 1824. dall'Imp. Regia stamperia, 1825.

[30] Lagrange, Joseph Louis. Analytical Mechanics. Vol. 191. Springer Science & Business Media, 2013.

[31] dell'Isola, F., Della Corte, A., Esposito, R., and Russo, L. Some cases of unrecognized transmission of scientific knowledge: from antiquity to Gabrio Piola's peridynamics and generalized continuum theories. In *Generalized Continua as Models for Classical and Advanced Materials* pp. 77–128. Springer, Cham.

[32] S. R. Eugster and F. dell'Isola. Exegesis of the Introduction and Sect. I from "Fundamentals of the Mechanics of Continua" by E. Hellinger, *ZAMM – Zeitschrift für Angewandte Mathematik und Mechanik.*, 97(4):477–506, 2017. (First Published 17 November 2016). (DOI: 10.1002/zamm.201600108). D

[33] S. R. Eugster and F. dell'Isola. Exegesis of Sect. II and III.A from "Fundamentals of the Mechanics of Continua" by E. Hellinger, *ZAMM – Journal of Applied Mathematics and Mechanics / Zeitschrift für Angewandte Mathematik und Mechanik*, pp. 1–38, 2017. (DOI: 10.1002/zamm.201600293).

[34] S. R. Eugster and F. dell'Isola. Exegesis of Sect. III.B from "Fundamentals of the Mechanics of Continua" by E. Hellinger, *ZAMM – Journal of Applied Mathematics and Mechanics / Zeitschrift für Angewandte Mathematik und Mechanik*, 98(1):69–105, 2017.

[35] S. R. Eugster and F. dell'Isola. An ignored source in the foundations of continuum physics "Die Allgemeinen Ansätze der Mechanik der Kontinua" by E. Hellinger, *Proceedings in Applied Mathematics and Mechanics*, 22 May 2017, 2 pages.

[36] Capecchi, Danilo. On the logical status of the virtual work law. *Meccanica* 39(2):159–173, 2004.

[37] Baldacci, Riccardo. *Scienza delle costruzioni*. Utet, 1970.

[38] Hellinger, E. Die allgemeinen Ansätze der Mechanik der Kontinua Encyklopädie der mathematischen Wissenschaften. Bd. IV-4, Hft 5 (1913).

[39] Morris Kline, *Mathematical Thought from Ancient to Modern Times*. Oxford University Press, 1972

[40] Laërtius, Diogenes. "*Pythagoreans: Archytas." Lives of the Eminent Philosophers. 2:8*. Translated by Hicks, Robert Drew (Two volume ed.). Loeb Classical Library (1925).

[41] dell'Isola, Francesco, and Luca Placidi. Variational principles are a powerful tool also for formulating field theories. pp. 1–15, in dell'Isola, Francesco, and Sergey Gavrilyuk, eds. *Variational Models and Methods in Solid and Fluid Mechanics*. Vol. 535. Springer Science & Business Media, 2012.

[42] T. L. Heath, *The Method of Archimedes, Recently Discovered by Heiberg: A Supplement to the Works of Archimedes* (Cambridge: at the University Press, London, 1912).

[43] Loeb Classical Library. *Greek Mathematical Works* Vol.I, II. Translated by Ivor Thomas 1939–1991.

[44] Truesdell, Clifford, and Richard Toupin. *The Classical Field Theories. Principles of Classical Mechanics and Field Theory/Prinzipien der Klassischen Mechanik und Feldtheorie*. Springer, Berlin, Heidelberg, 1960. 226–858.

[45] Truesdell, Clifford, and Walter Noll. *The Non-linear Field Theories of Mechanics.* Springer, Berlin, Heidelberg, 2004. 1–579.

[46] Baker, Alan. "Simplicity," The Stanford Encyclopedia of Philosophy (Winter 2016 Edition), Edward N. Zalta (ed.), URL = https://plato.stanford.edu/archives/win2016/entries/simplicity/.

[47] Hansson, Sven Ove, "Science and Pseudo-Science," The Stanford Encyclopedia of Philosophy (Summer 2017 Edition), Edward N. Zalta (ed.), URL = https://plato.stanford.edu/archives/sum2017/entries/pseudo-science/.

[48] Stanford, Kyle. Underdetermination of Scientific Theory, The Stanford Encyclopedia of Philosophy (Winter 2017 Edition), Edward N. Zalta (ed.), URL = https://plato.stanford.edu/archives/win2017/entries/scientific-underdetermination/.

[49] Eringen, A. Cemal. *Microcontinuum Field Theories: I. Foundations and Solids*. Springer Science & Business Media, 2012.

[50] Gurtin, Morton E. The nature of configurational forces. *Archive for Rational Mechanics and Analysis* 131(1):67–100, 1995.

[51] Maugin, Gérard A. *Configurational Forces: Thermomechanics, Physics, Mathematics, and Numerics*. CRC Press, 2016.

[52] Richard McKeon (tr.) *Aristotle's Posterior Analytics*, p. 150, Clarendon Press, 1963.

[53] Franklin, James. *The Science of Conjecture: Evidence and Probability before Pascal*. The Johns Hopkins University Press. Chap 9. p. 241, 2001.

[54] Toupin, Richard. Private Communication

[55] M. E. Gurtin, Thermodynamics and the possibility of spatial interaction in elastic materials. *Arch. Ration. Mech. An*. 19(5): 339–352, 1965.

[56] P. Germain, The method of virtual power in continuum mechanics. Part 2: Microstructure. *SIAM J. Appl. Math*. 25: 556–575, 1973.

[57] Truesdell, Clifford A. Cauchy and the modern mechanics of continua. *Revue d'histoire des sciences* (1992): 5–24.

[58] Capriz, G. *Continua with Microstructure*. Springer 1989

[59] Muskhelishvili, Nikolaĭ Ivanovich. *Some Basic Problems of the Mathematical Theory of Elasticity*. Springer Science & Business Media, 2013.

[60] Truesdell, C. *The Computer: Ruin of Science and Threat to Mankind (1980/1982). An Idiot's Fugitive Essays on Science*. Springer, New York, NY, 1984. 594–631

[61] Sedov, L.I., Models of continuous media with internal degrees of freedom. *Journal of Applied Mathematics and Mechanics*, 32: 803–819, 1972.

[62] Sedov, L.I., *Variational Methods of Constructing Models of Continuous Media. Irreversible Aspects of Continuum Mechanics and Transfer of Physical Characteristics in Moving Fluids*. Springer Vienna, 346–358, 1968.

[63] Santilli, R., *Foundations of Theoretical Mechanics*. Vol. I *The Inverse Problem in Newtonian Mechanics*, (1978). Vol.II *Birkhoffian Generalization of Hamiltonian Mechanics*. Springer, (1982).

[64] Vujanovic, B.D. and Jones S.E., *Variational Methods in Nonconservative Phenomena*. Academic Press, 1989.

[65] Germain, Paul. Functional concepts in continuum mechanics. *Meccanica* 33(5):433–444, 1998.

[66] Freguglia, Paolo, and Mariano Giaquinta. *The Early Period of the Calculus of Variations*. Basel: Birkhäuser, 2016.

[67] Rudin, Walter. *Functional Analysis*. McGraw-Hill Science/Engineering/Math,ISBN 978-0-07-054236-5, 1991.

[68] Lang, Serge. *Differential and Riemannian Manifolds*. Springer, ISBN 0-387-94338-2, 1995.

[69] Adams, Robert A.; Fournier, John J.F. *Sobolev Spaces*. Academic Press, 2003.

[70] Schwartz, L., Institut de Mathématique (Strasbourg). (1957). *Théorie des distributions* (Vol. 2). Paris: Hermann.

[71] Tikhonov, Andreĭ Nikolaevich, and Aleksandr Andreevich Samarskii. *Equations of Mathematical Physics*. Courier Corporation, 2013.

[72] Rudin, Walter. *Real and Complex Analysis* (3rd ed.). New York: McGraw-Hill. ISBN 0-07-054234-1, 1987.

[73] Giusti, Enrico. *Direct Methods in the Calculus of Variations*. World Scientific, 2003.

[74] Usher, Abbott Payson. *A History of Mechanical Inventions*: revised edition. Courier Corporation, 2013.

[75] Maugin, Gérard A. *What Happened on September 30, 1822, and What Were its Implications for the Future of Continuum Mechanics?. Continuum Mechanics Through the Eighteenth and Nineteenth Centuries*. Springer, Cham, 2014. 33–54.

[76] dell'Isola, Francesco, and Pierre Seppecher. Edge contact forces and quasi-balanced power. *Meccanica*, 32(1):33–52, 1997.

[77] dell'Isola, F., P. Seppecher, and A. Della Corte. The postulations á la D'Alembert and á la Cauchy for higher gradient continuum theories are equivalent: A review of existing results. *Proc. R. Soc. A* 471.2183 (2015): 20150415.

[78] dell'Isola, Francesco, Angela Madeo, and Pierre Seppecher. Cauchy tetrahedron argument applied to higher contact interactions. *Archive for Rational Mechanics and Analysis*, 219(3):1305–1341, 2016.

[79] Truesdell, Clifford A. *A First Course in Rational Continuum Mechanics*. Vol. 1. Academic Press, 1992.

[80] Noll, W., *The Foundations of Classical Mechanics in the Light of Recent Advances in Continuum Mechanics. The Axiomatic Method, with Special Reference to Geometry and Physics.* North-Holland Company: Amsterdam, 266–281 (1959).

[81] Antman, Stuart. *Nonlinear Problems of Elasticity*. Vol. 107. Springer Science & Business Media, 2013.

[82] Antman, Stuart S., and John E. Osborn. The principle of virtual work and integral laws of motion. *Archive for Rational Mechanics and Analysis* 69(3):231–262, 1979.

[83] Alibert, J.J., Seppecher, P. and dell'Isola, F., Truss modular beams with deformation energy depending on higher displacement gradients. *Mathematics and Mechanics of Solids*, 8:51–73, 2003.

[84] Alibert, Jean-Jacques, and Alessandro Della Corte. Second-gradient continua as homogenized limit of pantographic microstructured plates: a rigorous proof. *Zeitschrift für angewandte Mathematik und Physik*, 66(5):2855–2870, 2015.

[85] Rahali, Y., Giorgio, I., Ganghoffer, J. F., and dell'Isola, F. Homogenization á la Piola produces second gradient continuum models for linear pantographic lattices. *International Journal of Engineering Science*, 97: 148–172, 2015.

[86] Pideri, Catherine, and Pierre Seppecher. A second gradient material resulting from the homogenization of an heterogeneous linear elastic medium. *Continuum Mechanics and Thermodynamics* 9(5):241–257, 1997.

[87] Seppecher, Pierre, Jean-Jacques Alibert, and Francesco dell'Isola. Linear elastic trusses leading to continua with exotic mechanical interactions. *Journal of Physics*: Conference Series. Vol. 319. No. 1. IOP Publishing, 2011.

[88] Polizzotto, Castrenze. A second strain gradient elasticity theory with second velocity gradient inertia–Part II: Dynamic behavior. *International Journal of Solids and Structures* 50(24):3766–3777, 2013.

[89] J.H. Hubbard, B.B. Hubbard, *Vector Calculus, Linear Algebra and Differential Forms, a Unified Approach*. Prentice Hall ed., (2009).

[90] R. Abraham, J.E. Marsden, and T. Ratiu, *Manifolds,Tensor Analysis, and Applications*. Applied Mathematical Sciences, 75, Springer Verlag, (1988).

[91] Bleustein, Jeffrey L. A note on the boundary conditions of Toupin's strain-gradient theory. *International Journal of Solids and Structures*, 3(6):1053–1057, 1967.

[92] Lazar, Markus, Eleni Agiasofitou, and Demosthenes Polyzos. On gradient enriched elasticity theories: A reply to "Comment on 'On non-singular crack fields in Helmholtz type enriched elasticity theories'" and important theoretical aspects. arXiv preprint arXiv:1504.00869 (2015).

[93] Lazar, Markus, and Demosthenes Polyzos. On non-singular crack fields in Helmholtz type enriched elasticity theories. *International Journal of Solids and Structures*, 62:1–7, 2015.

[94] Iman Karimipour and Ali Reza Fotuhi Anti-plane analysis of an infinite plane with multiple cracks based on strain gradient theory. *Acta Mech*, 228:1793–1817, 2017. DOI 10.1007/s00707-016-1793-0

[95] Gérard A. Maugin. *Non-Classical Continuum Mechanics. A Dictionary*. Springer Nature Singapore Pte Ltd, 2017.

[96] M. Spivak. *A Comprehensive Introduction to Differential Geometry*, Vol. I and II. Second edition. Publish or Perish, Inc., Wilmington, Del., 1979.

[97] H. Goldstein. *Classical Mechanics*. Second edition. Addison-Wesley, Reading, MA, 1980.

[98] F. dell'Isola, E. Barchiesi, and L. Placidi, Finite Dimensional Lagrangian Systems, H. Altenbach, A. Ochsner (eds.), *Encyclopedia of Continuum, Mechanics*, Springer-Verlag GmbH, Germany, 2018.

Index